

THE UNIVERSITY OF CHICAGO

HYDROGEN BOND MEDIATED [3+3] CYCLOADDITION REACTIONS OF OXYALLYL
CATIONS WITH NITRONES

AND

TOTAL SYNTHESSES OF PENTACYCLIC AMBIGUINE NATURAL PRODUCTS

A DISSERTATION SUBMITTED TO
THE FACULTY OF THE DIVISION OF THE PHYSICAL SCIENCES
IN CANDIDACY FOR THE DEGREE OF
DOCTOR OF PHILOSOPHY

DEPARTMENT OF CHEMISTRY

BY

LINGBOWEI HU

CHICAGO, ILLINOIS

AUGUST 2021

For my family

Table of Contents

LIST OF SCHEMES.....	vii
LIST OF TABLES	xi
LIST OF FIGURES	xii
LIST OF ABBREVIATIONS.....	xx
Acknowledgements.....	xxiii
Chapter 1. Introduction to Oxyallyl Cations: Generations and Reactivities	1
1.1 Generation of Oxyallyl Cations.....	1
1.2 Reactivities of Oxyallyl Cations	5
1.3 Hydrogen Bond Catalysis Involving Oxyallyl Cations.....	8
Chapter 2. A Novel [3+3] Cycloaddition Reaction Involving Oxyallyl Cations and Catalysis of the Reaction with Hydrogen-Bond donors	11
2.1 Discovery of a Novel [3+3] Cycloaddition Reaction Between Oxyallyl Cations and Nitrones	11
2.2 Substrate Scope of the [3+3] Cycloaddition Reaction	16
2.3 Catalysis of the [3+3] Cycloaddition Reaction with Hydrogen-Bond Donors	20
2.4 Conclusion.....	23
Chapter 3. Introduction to the Ambiguine Natural Products.....	25
3.1 Isolation of Ambiguine Natural Products and Their Bioactivities	25
3.2 Biogenesis of Ambiguine Natural Products	27

3.3 Chemical Synthesis of Ambiguine Natural Products	31
3.3.1 Sarpong's Synthesis of Ambiguine P	31
3.3.2 Our First-Generation Synthesis of Ambiguine P.....	34
3.3.3 Our Attempted Synthesis of Ambiguine Q.....	36
Chapter 4. Synthesis Towards Pentacyclic ambiguines: The Cyclohexanone Fragment.....	38
4.1 First-Generation Synthesis of the Cyclohexanone 4.1	38
4.2 Initial Attempts of the Synthesis of the Cyclohexanone 4.1 with Higher Efficiency	39
4.3 Enantioselective Synthesis of the Cyclohexanone 4.1	42
4.4 The Development of a Novel Hypervalent Organobismuth Based Vinylation Reagent	44
4.4.1 Reactivities Between Hypervalent Organobismuth Compounds and Carbonyl Derived Nucleophiles	45
4.4.2 Synthesis of A Novel Vinylbismuth Reagent.....	48
4.4.3 Synthesis of Ketone 4.37 with the Vinylbismuth Reagent.....	50
4.5 Conclusion.....	51
Chapter 5. Total Syntheses of Ambiguine P and Ambiguine Q Within Nine-steps From Carvone	52
5.1 Second-Generation Synthesis of Ambiguine P	52
5.2 Third-Generation Synthesis of Ambiguine P: A 6-step Synthesis of Ambiguine P From (R)-Carvone.....	55
5.3 Synthesis of Ambiguine Q from Ambiguine P	59

5.4 Structural Revision of Ambiguine P	62
5.5 Conclusion.....	63
Chapter 6. Total Synthesis of Ambiguine G	65
6.1 Attempted Synthesis of Chloroketone 6.1 with the Vinylbismuth Reagent	65
6.2 Synthesis of Chloroketone 6.1 Using Directed Vinyl Grignard Addition	67
6.3 Synthesis of Ambiguine G	70
6.4 Conclusion.....	73
Chapter 7. Synthetic Efforts Towards Ambiguine L.....	75
7.1 C-N Bond Formation Through Sigmatropic Rearrangement.....	75
7.2 Functionalization of 7.5 for Intramolecular Cyclization Reactions	77
7.3 Electrophilic Amination	79
7.4 Photocatalytic Azidation of the Pentacyclic Scaffold.....	82
7.4.1 Unexpected Reactivity.....	82
7.4.2 Proposed Mechanism for the Formation of Different Products	85
7.5 Synthesis Towards Ambiguine L Utilizing the Photocatalytic Reaction.....	88
7.6 Conclusion.....	88
Chapter 8. Experimental Procedures and Characterization Data	90
8.1 General Information	90
8.2 Experimental Procedures and Characterization Data for Chapter 2	92
8.2.1. Synthetic Procedures and Characterization Data for nitrones	92

8.2.2. Synthetic Procedures and Characterization Data for α -tosyloxy ketones	94
8.2.3. General Procedure for the [3+3] Cycloaddition Reaction	96
8.2.3.1 General Procedure A: [3+3] Cycloaddition Reaction in HFIP: xylenes Mixed Solvent	96
8.2.3.2 General Procedure B: [3+3] Cycloaddition Reaction Catalyzed by 4-Nitrophenol	97
8.2.4. Characterization of [3+3] Cycloaddition Products	98
8.2.5 Derivatization of the [3+3] Cycloaddition Product	118
8.3 Experimental Procedures and Characterization Data for Chapter 4	122
8.4 Experimental Procedures and Characterization Data for Chapter 5	132
8.5 Experimental Procedures and Characterization Data for Chapter 6	151
8.6 Experimental Procedures and Characterization Data for Chapter 7	164
Appendix	172

LIST OF SCHEMES

Scheme 1.1. Oxyallyl cations.	1
Scheme 1.2. Early reports of reactions involving oxyallyl cations.	3
Scheme 1.3. Generation of oxyallyl cation from preformed enol precursors.	4
Scheme 1.4. Oxyallyl cation generation through Nazarov cyclization.	5
Scheme 1.5. Reactivities of oxyallyl cations: [4+3] cycloaddition and S _N 1 type substitution.	6
Scheme 1.6. [3+2] Cycloaddition reaction involving oxyallyl cations.	7
Scheme 1.7. Porco's report of TADDOL catalyzed enantioselective cycloaddition involving oxyallyl cations.	9
Scheme 1.8. Enantioselective catalysis involving oxyallyl cations with substoichiometric amount of hydrogen bond donor.	10
Scheme 2.1. Initial results from the screening of 1,3-dipoles as the 4 π component.	13
Scheme 2.2. Nitron scope for the [3+3] cycloaddition reaction of 2-tosyloxycyclohexanone. .	17
Scheme 2.3. Scope of [3+3] cycloaddition of cyclic α -tosyloxy ketones.	18
Scheme 2.4. Scope of [3+3] cycloaddition of acyclic α -tosyloxy ketones.	19
Scheme 2.5. Derivatization of the 1,2-oxazinane products.	20
Scheme 2.6. [3+3] Cycloaddition of selected substrates from scheme 2.2 promoted by 4-nitrophenol as a hydrogen-bond donor catalyst.	23
Scheme 3.1. Ambiguine natural products.	26
Scheme 3.2. Representative natural products in the hapalindole, fischerindole and welwitindolinone families.	27
Scheme 3.3. Hapalindole biogenesis.	29

Scheme 3.4. Stereocontrol in the biogenesis of hapalindoles.	29
Scheme 3.5. Biogenesis of ambiguine A from hapalindole G through dimethylallyltransferase mediated isoprenylation.	30
Scheme 3.6. Biogenesis of chlorinated hapalindoles via non-heme iron-dependent halogenase mediated late-stage chlorination.	30
Scheme 3.7. Sarpong's synthesis of ambiguine P.	33
Scheme 3.8. Rawal's first-generation synthesis of ambiguine P.	35
Scheme 3.9. Rawal's previous attempts of halogenation at C23 of 3.54 and 3.67	37
Scheme 4.1. Baran's synthesis of 4.1	39
Scheme 4.2. Synthesis of 4.1 through cyclopropanation of 4.9	40
Scheme 4.3. Synthesis of 4.1 via selenoaldehyde 4.14	41
Scheme 4.4. Enantioselective synthesis of ketone 4.1	43
Scheme 4.5. A better solution: vinylation using a vinyl cation equivalent	45
Scheme 4.6. Barton's early exploration of hypervalent organobismuth chemistry.	46
Scheme 4.7. Matano's study of triaryl-monoalkenylbismuth compounds.	47
Scheme 4.8. Synthesis of the vinylbismuth reagent 4.35	49
Scheme 4.9. One-step vinylation of TMS silyl enol ether.	50
Scheme 4.10. One-step synthesis of ketone 4.38 from (<i>R</i>)-carvone.	51
Scheme 5.1. Second-generation synthesis of ambiguine P.	54
Scheme 5.2. Serendipitous findings of unexpected generation of ambiguine P.	56
Scheme 5.3. Conversion of the mixture of dienens 5.13 and 5.16 into ambiguine P through controlled air oxidation.	57
Scheme 5.4. Third-generation synthesis of ambiguine P: 6 steps from (<i>R</i>)-carvone.	59

Scheme 5.5. Unsuccessful attempts towards ambiguine Q from ambiguine P.	60
Scheme 5.6. Synthesis of ambiguine Q from ambiguine P.	62
Scheme 5.7. Structural revision of ambiguine P.	63
Scheme 6.1. Ketones suitable for the synthesis of ambiguine G.....	65
Scheme 6.2. Fukuyama's synthesis of chloroketone 6.1	66
Scheme 6.3. Attempted synthesis of ketone 6.3 with the vinylbismuth reagent.	67
Scheme 6.4. Directed α -functionalization of α -epoxy <i>N</i> -sulfonyl hydrazones developed by Coltart and co-workers.....	68
Scheme 6.5. Problems with the synthesis of 6.19	69
Scheme 6.6. First-generation synthesis of 6.3	69
Scheme 6.7. Two-step synthesis of chloroketone 6.1	70
Scheme 6.8. Synthesis and isolation of ethoxy diene 6.24	72
Scheme 6.9. Total synthesis of ambiguine G.	73
Scheme 7.1. Attempted thiocyanate rearrangement.	77
Scheme 7.2. A possible intramolecular cyclization reaction to form the desired C-N bond.	77
Scheme 7.3. Unsuccessful carbamate formation.....	78
Scheme 7.4. Unsuccessful hemiaminal formation.	79
Scheme 7.5. Unsuccessful electrophilic aminations.....	80
Scheme 7.6. Unexpected reactivity with PTAD.....	81
Scheme 7.7. Attempts of derivatizing 7.14 led to decomposition.....	82
Scheme 7.8. Seminal works reported by Lu and co-workers as well as Nicewicz and co-workers.	83
Scheme 7.9. Initial attempts of azidation of 7.26	83

Scheme 7.10. Unexpected products observed in the photocatalysis conditions.....	84
Scheme 7.11. Proposed mechanism of the generation of 7.28 and 7.29	87
Scheme 7.12. Synthesis of 7.36 : a potential intermediate towards ambiguines L, I and J.....	88

LIST OF TABLES

Table 2.1. Effect of temperature on reaction yield.....	14
Table 2.2. Selected examples of organic bases screened	14
Table 2.3. Selected examples of inorganic bases screened	15
Table 2.4. Selected examples of co-solvents screened.....	15
Table 2.5. [3+3] Cycloaddition promoted by hydrogen-bond donor molecules.....	21

LIST OF FIGURES

Figure 1. ^1H NMR spectrum of 8.2.3 (500 MHz, CDCl_3).....	173
Figure 2. ^{13}C NMR spectrum of 8.2.3 (125 MHz, CDCl_3).....	174
Figure 3. ^1H NMR spectrum of 8.2.5 (500 MHz, CDCl_3).....	175
Figure 4. ^{13}C NMR spectrum of 8.2.5 (125 MHz, CDCl_3).....	176
Figure 5. ^1H NMR spectrum of 8.2.9 (500 MHz, CDCl_3).....	177
Figure 6. ^{13}C NMR spectrum of 8.2.9 (125 MHz, CDCl_3).....	178
Figure 7. ^1H NMR spectrum of 2.23 (500 MHz, CDCl_3).....	179
Figure 8. ^{13}C NMR spectrum of 2.23 (125 MHz, CDCl_3).....	180
Figure 9. ^1H NMR spectrum of 2.25 (500 MHz, CDCl_3).....	181
Figure 10. ^{13}C NMR spectrum of 2.25 (125 MHz, CDCl_3).....	182
Figure 11. ^1H NMR spectrum of 2.29 (500 MHz, CDCl_3).....	183
Figure 12. ^{13}C NMR spectrum of 2.29 (125 MHz, CDCl_3).....	184
Figure 13. ^1H NMR spectrum of 2.7 (500 MHz, CDCl_3).....	185
Figure 14. ^{13}C NMR spectrum of 2.7 (125 MHz, CDCl_3).....	186
Figure 15. ^1H NMR spectrum of 2.7' (500 MHz, CDCl_3).....	187
Figure 16. ^{13}C NMR spectrum of 2.7' (125 MHz, CDCl_3).....	188
Figure 17. ^1H NMR spectrum of 2.9 (500 MHz, CDCl_3).....	189
Figure 18. ^{13}C NMR spectrum of 2.9 (125 MHz, CDCl_3).....	190
Figure 19. ^1H NMR spectrum of 2.9' (500 MHz, CDCl_3).....	191
Figure 20. ^{13}C NMR spectrum of 2.9' (125 MHz, CDCl_3).....	192
Figure 21. ^1H NMR spectrum of 2.10 (500 MHz, CDCl_3).....	193

Figure 22. ^{13}C NMR spectrum of 2.10 (125 MHz, CDCl_3).....	194
Figure 23. ^1H NMR spectrum of 2.11 (500 MHz, CDCl_3).....	195
Figure 24. ^{13}C NMR spectrum of 2.11 (125 MHz, CDCl_3).....	196
Figure 25. ^1H NMR spectrum of 2.12 (500 MHz, CDCl_3).....	197
Figure 26. ^{13}C NMR spectrum of 2.12 (125 MHz, CDCl_3).....	198
Figure 27. ^1H NMR spectrum of 2.13 (500 MHz, CDCl_3).....	199
Figure 28. ^{13}C NMR spectrum of 2.13 (125 MHz, CDCl_3).....	200
Figure 29. ^1H NMR spectrum of 2.14 (500 MHz, CDCl_3).....	201
Figure 30. ^{13}C NMR spectrum of 2.14 (125 MHz, CDCl_3).....	202
Figure 31. ^1H NMR spectrum of 2.15 (500 MHz, CDCl_3).....	203
Figure 32. ^{13}C NMR spectrum of 2.15 (125 MHz, CDCl_3).....	204
Figure 33. ^1H NMR spectrum of 2.16 (500 MHz, CDCl_3).....	205
Figure 34. ^{13}C NMR spectrum of 2.16 (125 MHz, CDCl_3).....	206
Figure 35. ^1H NMR spectrum of 2.17 (500 MHz, CDCl_3).....	207
Figure 36. ^{13}C NMR spectrum of 2.17 (125 MHz, CDCl_3).....	208
Figure 37. ^1H NMR spectrum of 2.17' (500 MHz, CDCl_3).....	209
Figure 38. ^{13}C NMR spectrum of 2.17' (125 MHz, CDCl_3).....	210
Figure 39. ^1H NMR spectrum of 2.18 (500 MHz, CDCl_3).....	211
Figure 40. ^{13}C NMR spectrum of 2.18 (125 MHz, CDCl_3).....	212
Figure 41. ^1H NMR spectrum of 2.19 (500 MHz, CDCl_3).....	213
Figure 42. ^{13}C NMR spectrum of 2.19 (125 MHz, CDCl_3).....	214
Figure 43. ^1H NMR spectrum of 2.20 (500 MHz, CD_2Cl_2).....	215
Figure 44. ^{13}C NMR spectrum of 2.20 (125 MHz, CD_2Cl_2).....	216

Figure 45. ^1H NMR spectrum of 2.22 (500 MHz, CDCl_3).....	217
Figure 46. ^{13}C NMR spectrum of 2.22 (125 MHz, CDCl_3).....	218
Figure 47. ^1H NMR spectrum of 2.24 (500 MHz, CDCl_3).....	219
Figure 48. ^{13}C NMR spectrum of 2.24 (125 MHz, CDCl_3).....	220
Figure 49. ^1H NMR spectrum of 2.24' (500 MHz, CDCl_3).	221
Figure 50. ^{13}C NMR spectrum of 2.24' (125 MHz, CDCl_3).	222
Figure 51. ^1H NMR spectrum of 2.26 (500 MHz, CDCl_3).....	223
Figure 52. ^{13}C NMR spectrum of 2.26 (125 MHz, CDCl_3).....	224
Figure 53. ^1H NMR spectrum of 2.3 (500 MHz, CDCl_3).....	225
Figure 54. ^{13}C NMR spectrum of 2.3 (125 MHz, CDCl_3).....	226
Figure 55. ^1H NMR spectrum of 2.28 (500 MHz, CDCl_3).....	227
Figure 56. ^{13}C NMR spectrum of 2.28 (125 MHz, CDCl_3).....	228
Figure 57. ^1H NMR spectrum of 2.5 (500 MHz, CDCl_3).....	229
Figure 58. ^1H NMR spectrum of 2.5 (500 MHz, CDCl_3).....	230
Figure 59. ^{13}C NMR spectrum of 2.5 (125 MHz, CDCl_3).....	231
Figure 60. ^1H NMR spectrum of 2.30 (500 MHz, CDCl_3).....	232
Figure 61. ^1H NMR spectrum of 2.30 (500 MHz, CDCl_3).....	233
Figure 62. ^{13}C NMR spectrum of 2.30 (125 MHz, CDCl_3).....	234
Figure 63. ^{13}C NMR spectrum of 2.30 (125 MHz, CDCl_3).....	235
Figure 64. ^1H NMR spectrum of 2.32 (500 MHz, CDCl_3).....	236
Figure 65. ^{13}C NMR spectrum of 2.32 (125 MHz, CDCl_3).....	237
Figure 66. ^1H NMR spectrum of 2.34 (500 MHz, CDCl_3).....	238
Figure 67. ^{13}C NMR spectrum of 2.34 (125 MHz, CDCl_3).....	239

Figure 68. ^1H NMR spectrum of 2.36 (500 MHz, CDCl_3).....	240
Figure 69. ^{13}C NMR spectrum of 2.36 (125 MHz, CDCl_3).....	241
Figure 70. ^1H NMR spectrum of 2.38 (500 MHz, CDCl_3).....	242
Figure 71. ^{13}C NMR spectrum of 2.38 (125 MHz, CDCl_3).....	243
Figure 72. ^1H NMR spectrum of 2.38' (500 MHz, CDCl_3).....	244
Figure 73. ^{13}C NMR spectrum of 2.38' (125 MHz, CDCl_3).....	245
Figure 74. ^1H NMR spectrum of 2.39 (500 MHz, CDCl_3).....	246
Figure 75. ^{13}C NMR spectrum of 2.39 (125 MHz, CDCl_3).....	247
Figure 76. ^1H NMR spectrum of 2.40 (500 MHz, CDCl_3).....	248
Figure 77. ^{13}C NMR spectrum of 2.40 (125 MHz, CDCl_3).....	249
Figure 78. ^1H NMR spectrum of 2.41 (500 MHz, CDCl_3).	250
Figure 79. ^{13}C NMR spectrum of 2.41 (125 MHz, CDCl_3).....	251
Figure 80. ^1H NMR spectrum of 2.42 (500 MHz, CDCl_3).....	252
Figure 81. ^{13}C NMR spectrum of 2.42 (125 MHz, CDCl_3).....	253
Figure 82. ^1H NMR spectrum of 4.18 (500 MHz, CDCl_3).....	254
Figure 83. ^{13}C NMR spectrum of 4.18 (125 MHz, CDCl_3).....	255
Figure 84. ^1H NMR spectrum of 8.3.1 (500 MHz, CDCl_3).....	256
Figure 85. ^{13}C NMR spectrum of 8.3.1 (125 MHz, CDCl_3).....	257
Figure 86. ^1H NMR spectrum of 4.29 (500 MHz, CDCl_3).....	258
Figure 87. ^{13}C NMR spectrum of 2.42 (125 MHz, CDCl_3).....	259
Figure 88. ^1H NMR spectrum of 4.35 (400 MHz, $\text{DMSO}-d_6$).	260
Figure 89. ^{13}C NMR spectrum of 4.35 (125 MHz, $\text{DMSO}-d_6$).....	261
Figure 90. ^1H NMR spectrum of 4.38 (500 MHz, CDCl_3).....	262

Figure 91. ^{13}C NMR spectrum of 4.38 (125 MHz, CDCl_3).....	263
Figure 92. ^1H NMR spectrum of 5.4 (500 MHz, CDCl_3).....	264
Figure 93. ^{13}C NMR spectrum of 5.4 (125 MHz, CDCl_3).....	265
Figure 94. ^1H NMR spectrum of 5.5 (500 MHz, C_6D_6).....	266
Figure 95. ^{13}C NMR spectrum of 5.5 (125 MHz, C_6D_6).....	267
Figure 96. ^1H NMR spectrum of 5.6 (500 MHz, CDCl_3).....	268
Figure 97. ^{13}C NMR spectrum of 5.6 (125 MHz, CDCl_3).....	269
Figure 98. ^1H NMR spectrum of 5.7 (500 MHz, CDCl_3).....	270
Figure 99. ^{13}C NMR spectrum of 5.7 (125 MHz, CDCl_3).....	271
Figure 100. ^1H NMR spectrum of 5.8 (500 MHz, CDCl_3).....	272
Figure 101. ^1H NMR spectrum of 5.10 (500 MHz, CDCl_3).....	273
Figure 102. ^{13}C NMR spectrum of 5.10 (125 MHz, CDCl_3).....	274
Figure 103. ^1H NMR spectrum of 5.11 (500 MHz, CDCl_3).....	275
Figure 104. ^{13}C NMR spectrum of 5.11 (125 MHz, CDCl_3).....	276
Figure 105. NOESY spectrum of 5.11 (CDCl_3).....	277
Figure 106. ^1H NMR spectrum of 5.13 (500 MHz, C_6D_6).....	278
Figure 107. ^{13}C NMR spectrum of 5.13 (125 MHz, C_6D_6).....	279
Figure 108. ^1H NMR spectrum of 5.9 (500 MHz, CDCl_3).....	280
Figure 109. ^{13}C NMR spectrum of 5.9 (125 MHz, CDCl_3).....	281
Figure 110. ^1H NMR spectrum of ambiguine P (500 MHz, CD_3OD).	282
Figure 111. ^{13}C NMR spectrum of ambiguine P (125 MHz, CD_3OD).	283
Figure 112. ^1H NMR spectrum of 15- <i>epi</i> -ambiguine P (500 MHz, CD_3OD).....	284
Figure 113. ^{13}C NMR spectrum of 15- <i>epi</i> -ambiguine P (125 MHz, CD_3OD).....	285

Figure 114. ^1H NMR spectrum of 5.26 (500 MHz, CDCl_3).....	286
Figure 115. ^{13}C NMR spectrum of 5.26 (125 MHz, CDCl_3).....	287
Figure 116. ^1H NMR spectrum of 5.24 (500 MHz, CDCl_3).....	288
Figure 117. ^{13}C NMR spectrum of 5.24 (125 MHz, CDCl_3).....	289
Figure 118. ^1H NMR spectrum of ambiguine Q (500 MHz, CD_3OD).	290
Figure 119. ^{13}C NMR spectrum of ambiguine Q (125 MHz, CD_3OD).....	291
Figure 120. ^1H NMR spectrum of 15- <i>epi</i> -ambiguine Q (500 MHz, CD_3OD).	292
Figure 121. ^{13}C NMR spectrum of 15- <i>epi</i> -ambiguine Q (125 MHz, CD_3OD).....	293
Figure 122. ^1H NMR spectrum of 6.3 (500 MHz, CDCl_3).....	294
Figure 123. ^{13}C NMR spectrum of 6.3 (125 MHz, CDCl_3).....	295
Figure 124. ^1H NMR spectrum of 6.1 (500 MHz, CDCl_3).....	296
Figure 125. ^{13}C NMR spectrum of 6.1 (125 MHz, CDCl_3).....	297
Figure 126. ^1H NMR spectrum of 6.23 (500 MHz, CDCl_3).....	298
Figure 127. ^{13}C NMR spectrum of 6.23 (125 MHz, CDCl_3).....	299
Figure 128. NOESY spectrum of 6.23 (CDCl_3).....	300
Figure 129. ^1H NMR spectrum of 6.24 (500 MHz, C_6D_6).....	301
Figure 130. ^{13}C NMR spectrum of 6.24 (125 MHz, C_6D_6).....	302
Figure 131. ^1H NMR spectrum of 6.26 (500 MHz, CDCl_3).....	303
Figure 132. ^{13}C NMR spectrum of 6.26 (125 MHz, CDCl_3).....	304
Figure 133. ^1H NMR spectrum of 6.27 (500 MHz, CDCl_3).....	305
Figure 134. ^{13}C NMR spectrum of 6.27 (125 MHz, CDCl_3).....	306
Figure 135. ^1H NMR spectrum of 6.28 (500 MHz, CDCl_3).....	307
Figure 136. ^{13}C NMR spectrum of 6.28 (125 MHz, CDCl_3).....	308

Figure 137. ^1H NMR spectrum of 6.29 (500 MHz, CDCl_3).....	309
Figure 138. ^{13}C NMR spectrum of 6.29 (125 MHz, CDCl_3).....	310
Figure 139. ^1H NMR spectrum of 6.30 (500 MHz, CDCl_3).....	311
Figure 140. ^{13}C NMR spectrum of 6.30 (125 MHz, CDCl_3).....	312
Figure 141. ^1H NMR spectrum of ambiguine G (500 MHz, CDCl_3).....	313
Figure 142. ^{13}C NMR spectrum of ambiguine G (125 MHz, CDCl_3).....	314
Figure 143. ^1H NMR spectrum of 7.3 (400 MHz, CDCl_3).....	315
Figure 144. ^1H NMR spectrum of 8.6.3 (500 MHz, CDCl_3).....	316
Figure 145. ^1H NMR spectrum of 7.14 (400 MHz, CDCl_3).....	317
Figure 146. ^1H NMR spectrum of 8.6.5 (500 MHz, CD_2Cl_2).....	318
Figure 147. ^{13}C NMR spectrum of 8.6.5 (125 MHz, CD_2Cl_2).....	319
Figure 148. HMBC spectrum of 8.6.5 (CD_2Cl_2).....	320
Figure 149. HSQC spectrum of 8.6.5 (CD_2Cl_2).....	321
Figure 150. ^1H NMR spectrum of 7.14' (500 MHz, CDCl_3).....	322
Figure 151. ^1H NMR spectrum of 7.28 (500 MHz, C_6D_6).....	323
Figure 152. ^{13}C NMR spectrum of 7.28 (100 MHz, C_6D_6).....	324
Figure 153. ^1H NMR spectrum of 7.29 (500 MHz, CDCl_3).....	325
Figure 154. ^{13}C NMR spectrum of 7.29 (100 MHz, CDCl_3).....	326
Figure 155. HMBC spectrum of 7.29 (CDCl_3).....	327
Figure 156. HSQC spectrum of 7.29 (CDCl_3).....	328
Figure 157. ^1H NMR spectrum of 7.30 (500 MHz, CDCl_3).....	329
Figure 158. ^{13}C NMR spectrum of 7.30 (125 MHz, CDCl_3).....	330
Figure 159. HMBC spectrum of 7.30 (CDCl_3).....	331

Figure 160. HSQC spectrum of 7.30 (CDCl ₃).	332
Figure 161. ¹ H NMR spectrum of 7.36 (500 MHz, CDCl ₃).....	333

LIST OF ABBREVIATIONS

Ac	acetyl
Acac	acetylacetonate
9-BBN	9-borabicyclo[3.3.1]nonane
Boc	<i>tert</i> -butoxycarbonyl
Bu	butyl
DBU	1,8-diazabicyclo[5.4.0]undec-7-ene
DCM	dichloromethane
DCE	dichloroethane
DDQ	2,3-dichloro-5,6-dicyano-1,4-benzoquinone
DIBAL	diisobutylaluminum hydride
DMAP	4-(dimethylamino)pyridine
DMF	<i>N,N</i> -dimethylformamide
DMSO	dimethylsulfoxide
dppf	1,1'-bis(diphenylphosphino)ferrocene
d.r.	diastereomeric ratio
ee	enantiomeric excess
Et	ethyl

GPP	geranyl pyrophosphate
HFIP	1,1,1,3,3,3-hexafluoro-2-propanol
HRMS	high resolution mass spectrometry
Hz	Hertz
IR	infrared
NaHMDS	potassium bis(trimethylsilyl)amide
Me	methyl
Ms	methanesulfonyl
NBS	<i>N</i> -bromosuccinimide
NCS	<i>N</i> -chlorosuccinimide
NMR	nuclear magnetic resonance
Ph	phenyl
PPTS	pyridinium <i>p</i> -toluenesulfonate
PTAD	4-phenyl-1,2,4-triazoline-3,5-dione
R _f	retention factor
rt	room temperature
TADDOL	$\alpha,\alpha,\alpha,\alpha$ -tetraaryl-1,3-dioxolane-4,5-dimethanol
TBAF	tetrabutylammonium fluoride

TBS	<i>tert</i> -butyldimethylsilyl
Tf	trifluoromethanesulfonyl
TFA	trifluoroacetate
TFE	2,2,2-trifluoroethanol
THF	tetrahydrofuran
TLC	thin layer chromatography
TMS	trimethylsilyl
Ts	<i>p</i> -toluenesulfonyl

Acknowledgements

I sincerely thank Professor Viresh Rawal for all his encouragement, guidance and helpful suggestions during my time at the University of Chicago. Both his desire to elucidate the mechanisms of unexpected reactivities and his ability to devise alternative explanations to seemingly straightforward reaction mechanisms have always fascinated me. Through my interactions with him in the past few years, he made me realize multiple prerequisite features that a person should have to be successful, not only at chemistry, but in any field. I am also thankful for his support in the past few years, especially during my hardest time.

I am grateful to Professor Guangbin Dong for allowing me to attend his group's weekly literature meetings since I started at the University of Chicago. I learnt numerous chemical transformations, reaction mechanisms etc. from these meetings and I have always been in amazement at how knowledgeable he is. I would also like to thank him for willing to serve on my dissertation committee.

With much gratitude, I thank Professor Scott Snyder, my other committee member, for his insightful comments and suggestions on my graduate work, during both my candidacy exam and my thesis defense. I would also like to thank Professor Mark Levin for insightful discussions and for his generous help.

In the Rawal group, I've had the privilege to work with many great people. Dr. Michael Rombola was my first bay-mate and helped me on the oxyallyl cation project. He is an exceptionally smart and funny person, with whom I have many things in common. Thanks for making my first couple years in grad school less boring through the endless and creative jokes. Dr.

Pavel Elkin sat and worked at the “most dangerous” spot of the lab. However, he always seemed so happy with chemistry that I don’t recall seeing a frustrated Pavel. Dr. Ferdinand Taenzler, the encyclopedia of trivia in the lab, was my TA-mate, with whom I TA-ed many quarters together. We were the only two TAs who were asked to record and stream the OChem undergraduate lectures in fall 2019, which was by no means our job as TAs and we hated it. Dr. Jiasu Xu (Jasper-Jason-Jiasu Xu) is a hard-working and modest person who performed the early explorations in the ambiguiene synthesis. He is the most meticulous chemist I’ve ever known in my life and his level of lab notebook keeping is unparalleled. I’ve known him since our undergraduate time, and I spent my first night at the University of Chicago in his apartment. Kyle Cassaidy is the second (approaching the most as days go by) meticulous chemist who has a strong passion for organic chemistry, especially total synthesis. I have always been surprised at the amount of time he has spent reading papers. Nathaniel Durfee is my second bay-mate with whom I spent most time in lab. He is an extraordinary smart and affable person. We had daily conversations on random topics which kept my time in grad school interesting. I appreciate him for correcting my English pronunciations and grammar, as well as for answering my questions on American culture with great patience. Dr. Sudhakar Athe is an experienced and knowledgeable chemist with outstanding insight. Jirapon Sae-Jew is my third bay-mate who has already shown talent in chemistry after a couple month working in lab.

I would like to offer my special thanks to Dr. Yang Song, one of the kindest and most easy-going people I’ve known. I would also like to thank my other friends outside the Rawal lab for their company: Jiaze Xie, Tian Qiu, Fangjie Yin etc.

I spent a few years at the University of Illinois, Urbana-Champaign before coming to University of Chicago. I am deeply grateful to Professor Martin Burke for his guidance and support. His

passion about science was always infectious and his intuition of science had always left me in awe. I learnt from him the importance of hard-work, persistence and discipline to a scientist. I owe special thanks to Dr. Stephen Davis, who taught me all my experimental skills. I would also like to thank Jiabao Zhang, Dr. Rulin Ma, Dr. Wei Liu, Dr. Jinpeng Zhao, Dr. Jun Li, Dr. Zhao Wu and other friends at Champaign.

Finally, I thank my family for their support, as I owe everything I have to my family, especially my mom.

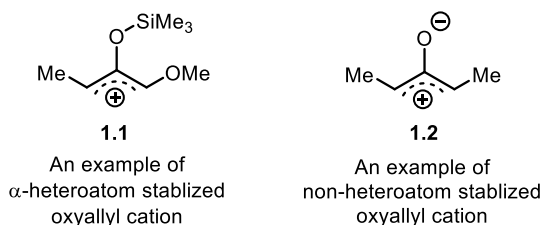
– July 22, 2021 –

Chapter 1

Introduction to Oxyallyl Cations: Generations and Reactivities

1.1 Generation of Oxyallyl Cations

Oxyallyl cations are reactive intermediates with a diverse range of applications in chemical synthesis. There are two major types of oxyallyl cation species based on their structures and reactivity: 1) oxyallyl cations that are stabilized by an α -electron-donating heteroatom such as oxygen and nitrogen (**1.1**, Scheme 1.1), and 2) oxyallyl cations that are stabilized by only carbon and hydrogen-based substituents (**1.2**). The former species are overall easier to generate and are more reactive than the latter, but the requirement of the heteroatom-based substituents limit their broad application in synthesis and therefore are not the focus of this thesis. The non-heteroatom-stabilized oxyallyl cations will be referred to as oxyallyl cations in the following discussions.¹



Scheme 1.1. Oxyallyl cations.

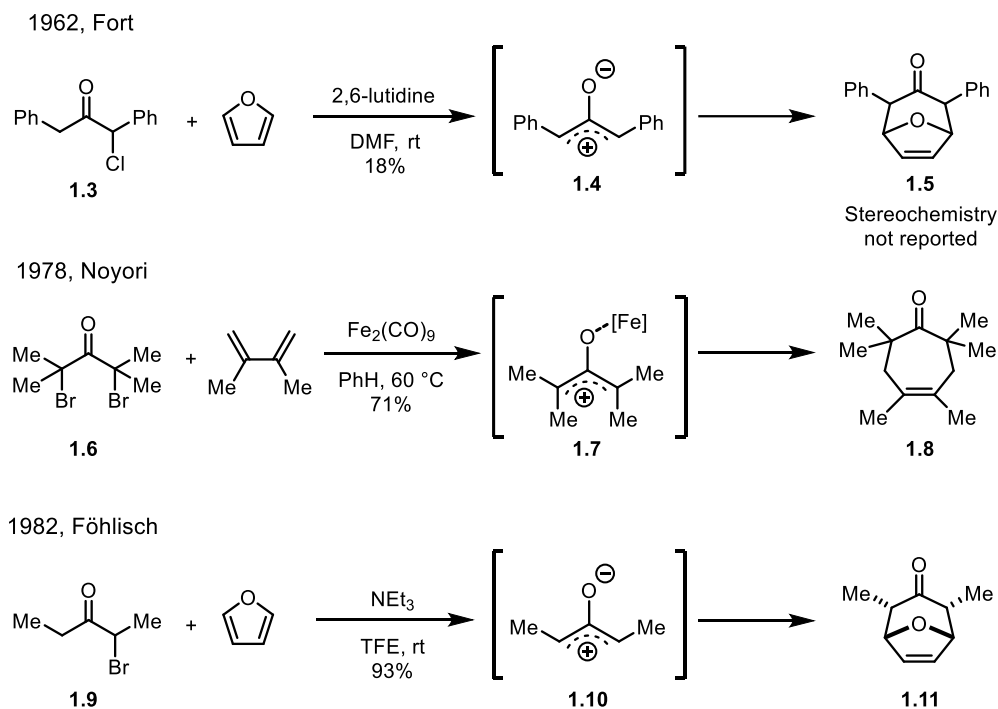
¹ For reviews and books on oxyallyl cations, see (a) Hoffmann, H. M. R. *Angew. Chem., Int. Ed. Engl.* **1984**, *23*, 1. (b) Rigby, J. H.; Pigge, F. C. [4 + 3] Cycloaddition Reactions. In *Organic Reactions*; Paquette, L. A., Eds.; John Wiley and Sons: New York, 1997; Vol. *51*, pp 351. (c) Harmata, M. *Adv. Synth. Catal.* **2006**, *348*, 2297. (d) Harmata, M. *Chem. Commun.* **2010**, *46*, 8886. (e) Harmata, M. *Chem. Commun.* **2010**, *46*, 8904. (f) Lohse, A. G.; Hsung, R. P. *Chem. - Eur. J.* **2011**, *17*, 3812.

In 1962, Fort reported the generation of oxyallyl cation from α -chloro-diphenylacetone in the presence of 2,6-lutidine with DMF as the solvent (Scheme 1.2).² However, this method was not widely applicable to non-aryl substituted ketones that lacked the stabilization effect from the α -aryl group. Later, different methods of generating oxyallyl cations from various precursors were developed. Noyori and co-workers later reported the generation of oxyallyl cations from α,α' -dibromoketones using $\text{Fe}_2(\text{CO})_9$ as a stoichiometric amount of reductant.³ The oxyallyl cations generated through this method were generally more reactive than other types of oxyallyl cations but the corresponding dibromoketones are difficult to access, which limits the application of this method. Föhlich and co-worker reported in 1982 the generation of oxyallyl cations from simple, dialkyl substituted α -chloro and α -bromoketones with solvent quantity of 2,2,2-trifluoroethanol (TFE), a method that is more useful compared to the first two methods due to the easy access to the α -halogen substituted precursors.⁴

² Fort, A. W. *J. Am. Chem. Soc.* **1962**, *84*, 4979.

³ Takaya, H.; Makino, S.; Hayakawa, Y.; Noyori, R. *J. Am. Chem. Soc.* **1978**, *100*, 1765.

⁴ Föhlich, B.; Gehrlach, E.; Herter, R. *Angew. Chem., Int. Ed.* **1982**, *21*, 137.

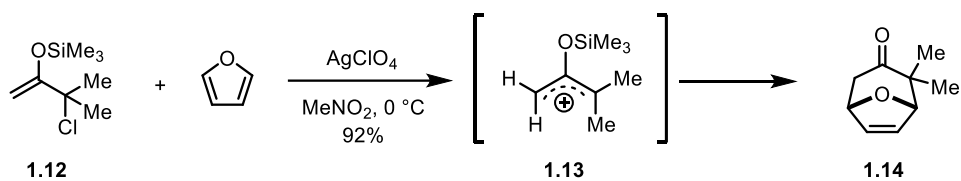


Scheme 1.2. Early reports of reactions involving oxyallyl cations.

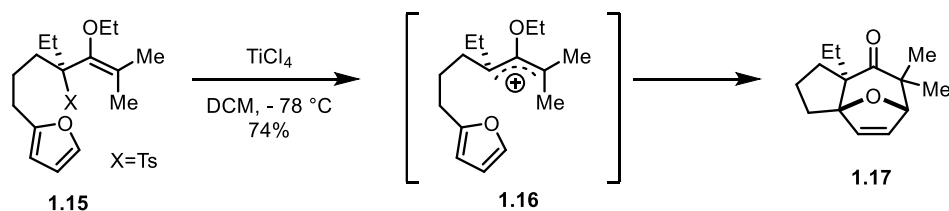
A common feature of these aforementioned methods is that an enolate was generated first, either through deprotonation or reduction. The electron rich enolate then accelerates the leaving of the α -halogen on the other α -carbon and stabilizes the resulting carbocation. It is also possible to generate oxyallyl cations from alkyl enol ethers with an α -leaving group (Scheme 1.3). The enol is preformed and addition of a Lewis acid activates the leaving group in order to generate to carbocation, which is stabilized by the existing enol.⁵ Unfortunately, the selective generation of the enol ether on the opposite side of the α -leaving group, a process that may induce the generation of oxyallyl cations as well, limits the broad application of this method.

⁵ (a) Shimizu, N.; Tanaka, M.; Tsuno, Y. *J. Am. Chem. Soc.* **1982**, *104*, 1330. (b) Harmata, M.; Gamlath, C. B. *J. Org. Chem.* **1988**, *53*, 6154.

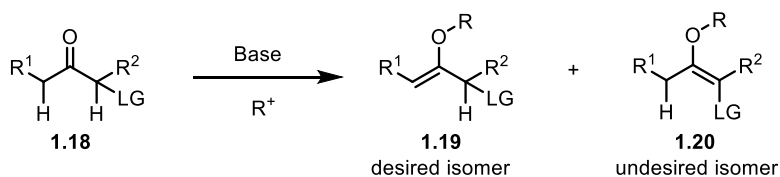
1982, Shimizu



1988, Harmata



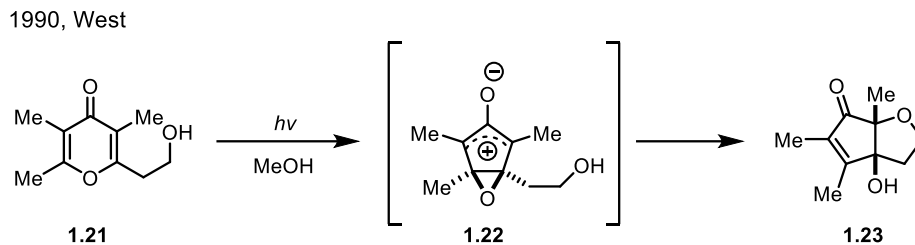
Complication with the synthesis of the oxallyl cation precursors:



Scheme 1.3. Generation of oxallyl cation from preformed enol precursors.

Oxallyl cations are also a known intermediate in the Nazarov cyclization reactions (Scheme 1.4). Such oxallyl cations can be trapped by a proper nucleophile, leading to what is referred to as an “interrupted Nazarov cyclization” product.⁶ However, the Nazarov reaction is limited to generating cyclopentanone based oxallyl cations and the substrates needs to be specially designed in order to fulfill the stereoelectronic requirements for a successful Nazarov cyclization process.

⁶ (a) West, F. G.; Fisher, P. V.; Willoughby, C. A. *J. Org. Chem.* **1990**, *55*, 5936. (b) West, F. G.; Hartke-Karger, C.; Koch, D. J.; Kuehn, C. E.; Arif, A. M. *J. Org. Chem.* **1993**, *58*, 6795. (c) Wang, Y.; Arif, A. M.; West, F. G. *J. Am. Chem. Soc.* **1999**, *121*, 876.



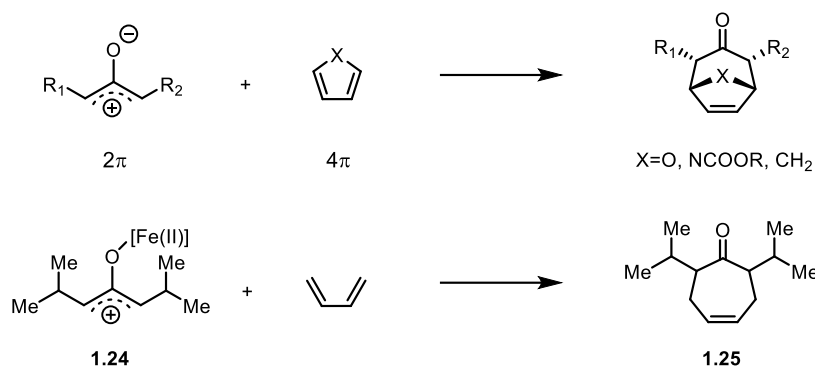
Scheme 1.4. Oxyallyl cation generation through Nazarov cyclization.

1.2 Reactivities of Oxyallyl Cations

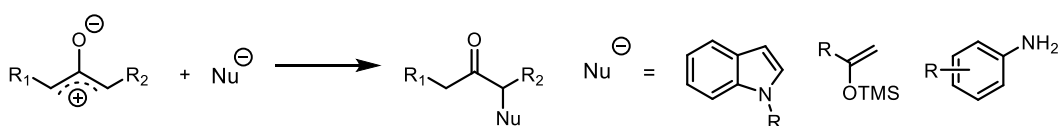
The most well-known reactivity of oxyallyl cations is their intermolecular [4+3] cycloaddition reactions with furans and *N*-protected pyrroles to form bridged cycles (Scheme 1.5).^{1c-e} The oxyallyl cations act as an electron deficient 2π system that reacts with the electron rich 4π systems through either a concerted mechanism or a stepwise mechanism, depending on the electronics and sterics of the substrates. The 4π components are usually used in large access, sometimes as a co-solvent. Cyclopentadienes are also known to participate in [4+3] cycloaddition reactions with oxyallyl cations but have been less studied.

For the less reactive 4π systems, the [4+3] reactivity highly depends on how the oxyallyl cations are generated. For example, oxyallyl cations (**1.24**) generated from α,α' -dibromoketones and $\text{Fe}_2(\text{CO})_9$ are highly reactive, probably because the Fe(II) generated from bromide reduction strongly binds to the C2 oxygen of the oxyallyl cations, enhancing its cationic feature. As a result, even butadienes can undergo cycloadditions under the reaction condition to form cycloheptanone derivatives.² In stark contrast, oxyallyl cations generated using the Föhlich method³, namely from α -haloketones in fluorinated alcohol solvents, are not reactive at all with butadienes.

[4+3] Cycloaddition reaction



S_N1 type substitution

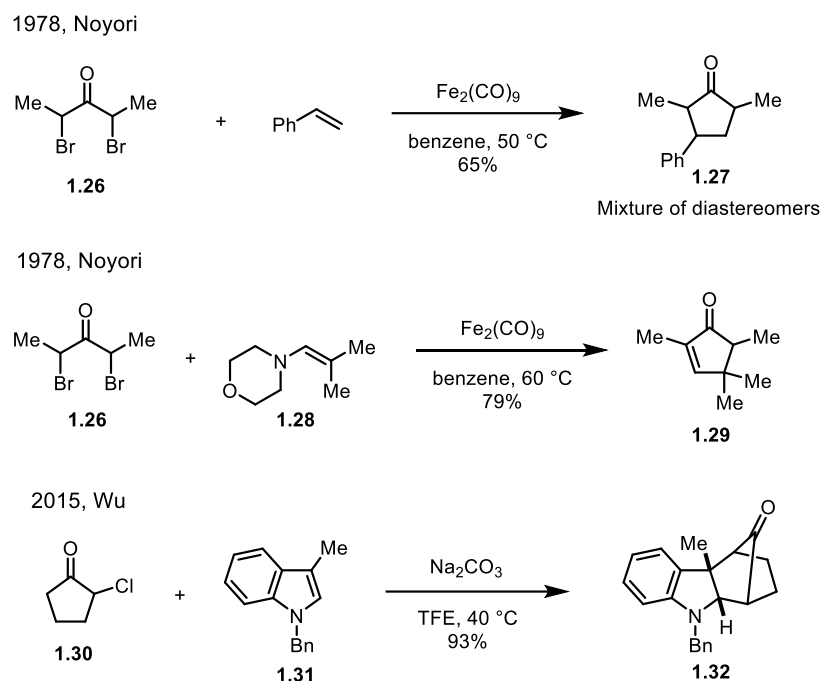


Scheme 1.5. Reactivities of oxyallyl cations: [4+3] cycloaddition and S_N1 type substitution.

Oxyallyl cations can also participate in a S_N1 type substitution reaction where the oxyallyl cations behave similarly to allyl cations. In such cases, a nucleophile attacks directly on one of the outer carbons of the oxyallyl cation, generating an α -substituted enolate which transforms into an α -substituted ketone upon aqueous workup. A variety of nucleophiles could participate in such reactions, including phenols, alcohols, indoles, silyl enol ethers etc.^{7,8} However, for asymmetric oxyallyl cations, the reaction usually generates a mixture of regioisomeric ketones resulting from the nucleophile reacting non-specifically with either end of the cation species, limiting the application of such reactions.

⁷ Noyori, R.; Hayakawa, Y.; Takaya, H.; Murai, S.; Kobayashi, R.; Sonoda, N. *J. Am. Chem. Soc.* **1978**, *100*, 1759.

⁸ (a) Vander Wal, M. N.; Dilger, A. K.; MacMillan, D. W. C. *Chem. Sci.* **2013**, *4*, 3075. (b) Liu, C.; Oblak, E. Z.; Vander Wal, M. N.; Dilger, A. K.; Almstead, D. K.; MacMillan, D. W. C. *J. Am. Chem. Soc.* **2016**, *138*, 2134.



Scheme 1.6. [3+2] Cycloaddition reaction involving oxyallyl cations.

A rare type of reaction involving oxyallyl cations is [3+2] cycloadditions (Scheme 1.6). Noyori and co-workers reported the first example with the dibromoketone and $\text{Fe}_2(\text{CO})_9$ system, where the oxyallyl cation reacted with styrenes and enamines in a [3+2] fashion, forming the cyclopentanone products in good yield.^{9,10} In 2015, Wu and co-workers showed that oxyallyl cations generated in fluorinated alcohol solvents can also undergo [3+2] cycloaddition reactions with *N*-methyl or *N*-benzyl protected indoles.¹¹

⁹ Hayakawa, Y.; Yokoyama, K.; Noyori, R. *J. Am. Chem. Soc.* **1978**, *100*, 1791.

¹⁰ Hayakawa, Y.; Yokoyama, K.; Noyori, R. *J. Am. Chem. Soc.* **1978**, *100*, 1799.

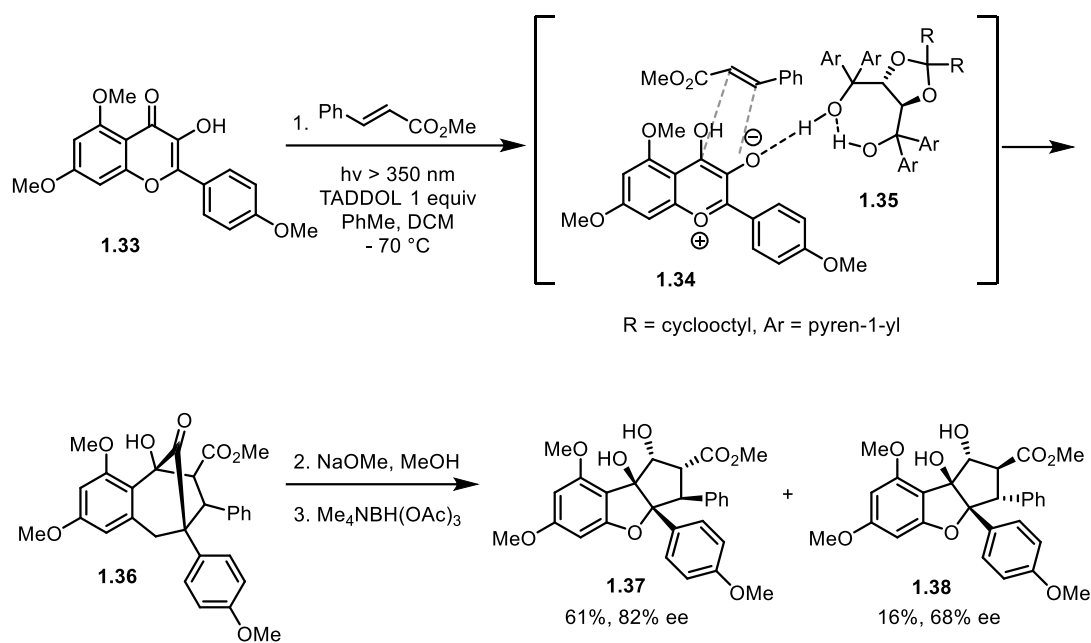
¹¹ Li, H.; Hughes, R. P.; Wu, J. *J. Am. Chem. Soc.* **2014**, *136*, 6288.

1.3 Hydrogen Bond Catalysis Involving Oxyallyl Cations

Despite the long history of the studies of different reactions involving oxyallyl cation, the catalysis of such reactions with a sub-stoichiometric catalyst has been relatively under-studied, as has the asymmetric catalysis involving oxyallyl cations. It is widely accepted that in the Föhlich system, the fluorinated alcohol solvent facilitates the formation of oxyallyl cations as well as stabilizes them through hydrogen bonding to the C2 oxygen atom. The fluorinated alcohol does not participate in the reaction as a reactant which shows the potential of performing asymmetric catalysis on oxyallyl cation species with a proper hydrogen-bond donor.

In 2006, Porco and co-workers demonstrated for the first time the induction of enantioselectivity involving oxyallyl cations with a hydrogen-bond donor (Scheme 1.7).¹² In their synthesis of Rocaglamides, a TADDOL based hydrogen-bond donor **1.35** was employed to render the key [3+2] photocycloaddition reaction between **1.33** and methyl cinnamate enantioselective. It was hypothesized that **1.35** induced enantioselectivity by binding to the enolate oxygen of **1.34** through hydrogen bond. Although high ee was only achieved with one equivalent of **1.35** (82% ee for **1.37** and 68% ee for **1.38**), this reaction still illustrated the possibility of performing asymmetric catalysis involving oxyallyl cations.

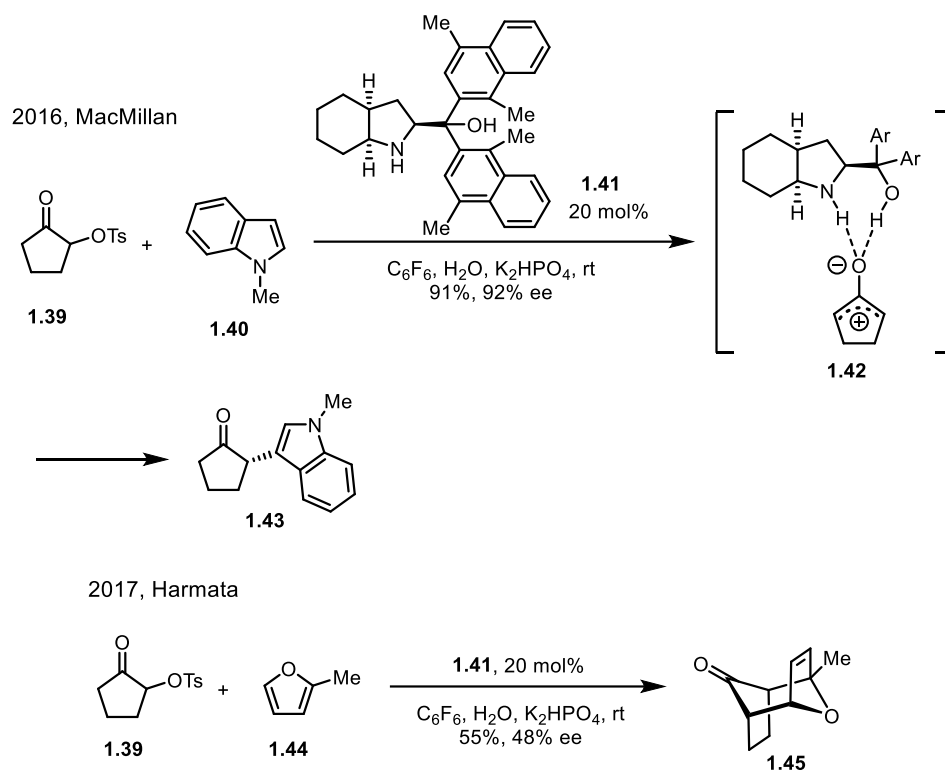
¹² Gerard, B.; Sangji, S.; O'Leary, D. J.; Rorco, J. A. Jr. *J. Am. Chem. Soc.* **2006**, *128*, 7754.



Scheme 1.7. Porco's report of TADDOL catalyzed enantioselective cycloaddition involving oxyallyl cations.

The first example of catalysis involving oxyallyl cations and a sub-stoichiometric amount of hydrogen-bond donor was reported by MacMillan and co-workers in 2016 (Scheme 1.8).^{7b} They discovered that oxyallyl cations can be generated from α -tosyloxy cyclopentanones in the presence of a 20 mol% loading of prolinol based catalysts. The oxyallyl cations thus generated then further reacted with *N*-alkyl indoles to provide α -indolyl cyclopentanones in an enantioselective manner induced by the catalyst. High ee values were obtained with a modified prolinol based catalyst **1.41**. Preliminary mechanistic studies showed that the reaction has a first-order dependence in both the ketone substrate and the catalyst and it was proposed that the catalyst binds to the C2 oxygen of the oxyallyl cation through two hydrogen bonds, with both the N-H and the O-H hydrogens on the catalyst acting as hydrogen-bond donors. A drawback of this catalysis system was that it was applicable to only α -tosyloxy cyclopentanone substrates and no products were observed with α -tosyloxy cyclohexanone.

Harmata and co-workers showed later that the prolinol catalysis system can be applied to the asymmetric intermolecular [4+3] cycloadditions between oxyallyl cations and 2-substituted furans.¹³ However, α -tosyloxyl cyclopentanone was again the only oxyallyl cation precursor reported and the reaction time were unusually long (95-264 hours), showcasing the limitation of the prolinol catalysis system.



Scheme 1.8. Enantioselective catalysis involving oxyallyl cations with substoichiometric amount of hydrogen bond donor.

¹³ Topinka, M.; Zawatzky, K.; Barnes, C. L.; Welch, C. J.; Harmata, M. *Org. Lett.* **2017**, *19*, 4106.

Chapter 2

A Novel [3+3] Cycloaddition Reaction Involving Oxyallyl Cations and Catalysis of the Reaction with Hydrogen-Bond donors

2.1 Discovery of a Novel [3+3] Cycloaddition Reaction Between Oxyallyl Cations and Nitrones

As was described in Chapter 1, non-heteroatom stabilized oxyallyl cations can be generated from various types of precursors. We were interested in the Föhlisch method because the oxyallyl cation precursor under such reaction conditions are ketones with an α -leaving group, which are easily accessible from the corresponding ketone. As a result, the products of any transformation under the Föhlisch conditions are essentially mono- or di-functionalized products of the ketone precursors, making these transformations useful and desirable. Furthermore, the oxyallyl cations generated under this condition were hypothesized to be hydrogen bonded with the fluorinated alcohol solvent. Motivated by our lab's long-standing interest in hydrogen bond catalysis, we were intrigued by the possibility of catalyzing the reactions involving oxyallyl cations with a substoichiometric amount of hydrogen-bond donor catalysts.

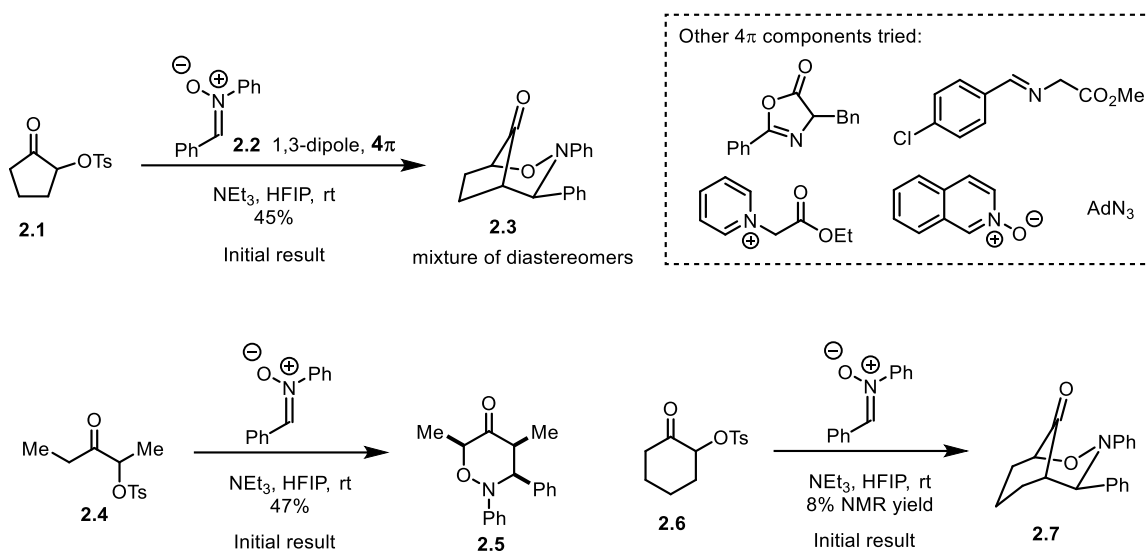
Our first task was to pick an interesting reaction to study its catalysis with hydrogen-bond donors. The reported reactions involving oxyallyl cations are mostly confined to [4+3] cycloadditions, S_N1 type substitutions and, more rarely, [3+2] cycloadditions. Being aware that oxyallyl cations are highly reactive intermediates, we decided to explore undiscovered reactivities of oxyallyl cations.¹ Realizing that the oxyallyl cations are acting as the electron deficient 3 carbon, 2π -electron systems in the [4+3] cycloaddition reactions, we reasoned that 1,3-dipolar compounds, many of which are

¹ See Chapter 1 for references.

known to engage in [3+2] reactions with a variety of 2π -electron systems, might undergo cycloaddition reactions with oxyallyl cations in a [3+3] manner.

Screening of a variety of 1,3-dipolar compounds as the 4π -electron component revealed an unreported [3+3] cycloaddition reaction between oxyallyl cations and *N*, α -diphenyl nitrene (Scheme 2.1). Upon mixing with α -tosyloxy ketones **2.1**, **2.4** and **2.6** and NEt_3 at room temperature in the solvent hexafluoro-2-propanol (HFIP), *N*, α -diphenyl nitrene (**2.2**) provided interesting 1,2-oxazinanes as the products, which were difficult to access otherwise.² Under the unoptimized conditions, moderate yields were obtained from *N*, α -diphenyl nitrene reacting with both 2-tosyloxy-3-pentanone **2.1** and 2-tosyloxycyclopentanone **2.4** (45% and 47% isolated yields, respectively). In contrast, 2-tosyloxycyclohexanone **2.6** was a substantially worse reaction partner, with the cycloaddition proceeding very slowly (8% NMR yield). Reasoning that the optimized conditions for this particular substrate should be applicable to the other α -tosyloxy ketone substrates, we proceeded the optimization of the reaction conditions with 2-tosyloxycyclohexanone and *N*, α -diphenyl nitrene.

² For an alternative method through rhodium catalysis, see: Wang, X.; Xu, X.; Zavalij, P. Y.; Doyle, M. P. *J. Am. Chem. Soc.* **2011**, *133*, 16402.

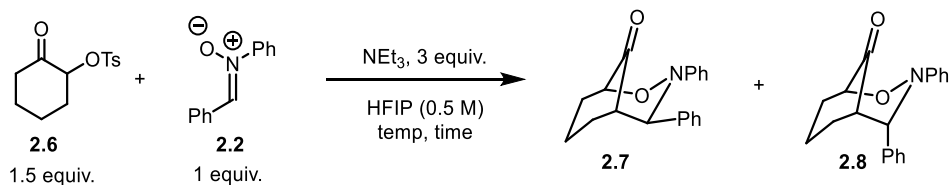


Scheme 2.1. Initial results from the screening of 1,3-dipoles as the 4π component.

The impact of the reaction temperature was first examined. As shown in Table 2.1, a 40 °C temperature led to a much faster reaction, leading to the cycloadduct in a significantly higher yield. Further raising the temperature to 58 °C (reflux) was deleterious on the yield. The temperature change had little effect on the diastereomeric ratio of the product, with a 1:1 d.r. in both cases. Shown in Table 2.2 and Table 2.3 are the selected results of an extensive base screening. The general trend found during the base screening was that weaker bases lead to higher yields, but also slower conversions. Additionally, inorganic heterogeneous bases such as K_2CO_3 and $KHCO_3$ provided higher yields than organic, homogeneous bases. NEt_3 was first chosen for the cosolvent screening due to its high solubility in different solvents. Poor hydrogen bonding cosolvents such as toluene, DCM gave higher yields of the cycloadduct compared to HFIP alone, whereas hydrogen bond acceptor solvents such as acetonitrile, THF and DMSO led to decreased yields. With this result, screening of poor hydrogen bonding cosolvents with $KHCO_3$ was performed (Table 2.4). Many of the cosolvents screened gave similar yields and xylenes were chosen as the

optimum solvent due to its slightly higher diastereomeric ratio compared to the other solvent. Further screen showed that a 1:1 ratio between HFIP and xylenes gave the highest yields.

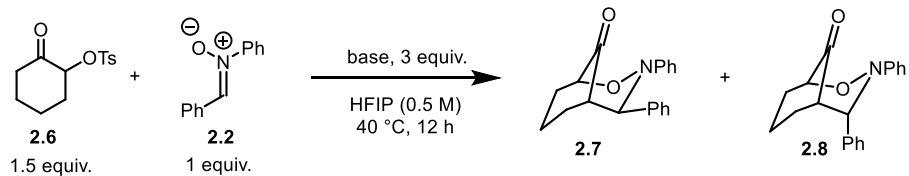
Table 2.1. Effect of temperature on reaction yield



Entry	temperature/°C	time	NMR yield (%) ^a
1	23	5 d	44
2	30	3 d	46
3	40	12 h	56
4	58	12 h	46

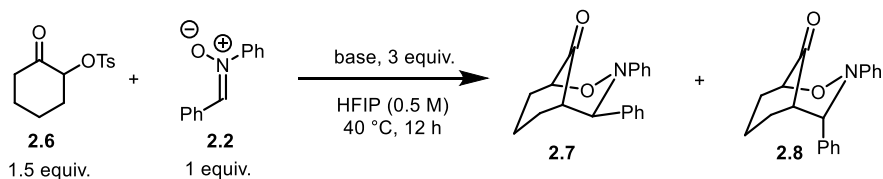
^a $\text{Cl}_2\text{CHCHCl}_2$ was used as the internal standard.

Table 2.2. Selected examples of organic bases screened



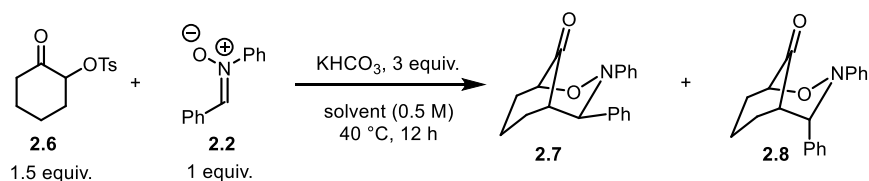
Entry	base	NMR yield (%) ^a	d.r.
1	2,6-lutidine	62	1:1
2	NEt_3	56	1:1
3	<i>N</i> -methyl morpholine	45	1:1
4	Quinuclidine	60	1:1
5	Proton sponge	57	1:1
6	DBU	16	1:1

^a $\text{Cl}_2\text{CHCHCl}_2$ was used as the internal standard.

Table 2.3. Selected examples of inorganic bases screened

Entry	base	NMR yield (%) ^a	d.r.
1	KOH	45	1:1
2	Li ₂ CO ₃	0	n.d. ^b
3	Na ₂ CO ₃	55	1:1
4	K ₂ CO ₃	67	1:1
5	Cs ₂ CO ₃	0	1:1
6	KHCO ₃	77	1:1

^aCl₂CHCHCl₂ was used as the internal standard. ^bNot determined.

Table 2.4. Selected examples of co-solvents screened

Entry	Solvent	NMR yield (%) ^a	d.r.
1	HFIP:DCE 2:1	85	1:1
2	HFIP:PhCl 2:1	75	1:1
3	HFIP:PhCF ₃ 2:1	74	1:1
4	HFIP:Hexane 2:1	62	2:1
5	HFIP:xylenes 2:1	86	1.3:1
6	HFIP:xylenes 4:1	71	1:1
7	HFIP:xylenes 1:1	90	1.7:1
8	HFIP:xylenes 1:2	85	2:1

^aCl₂CHCHCl₂ was used as the internal standard. ^bNot determined.

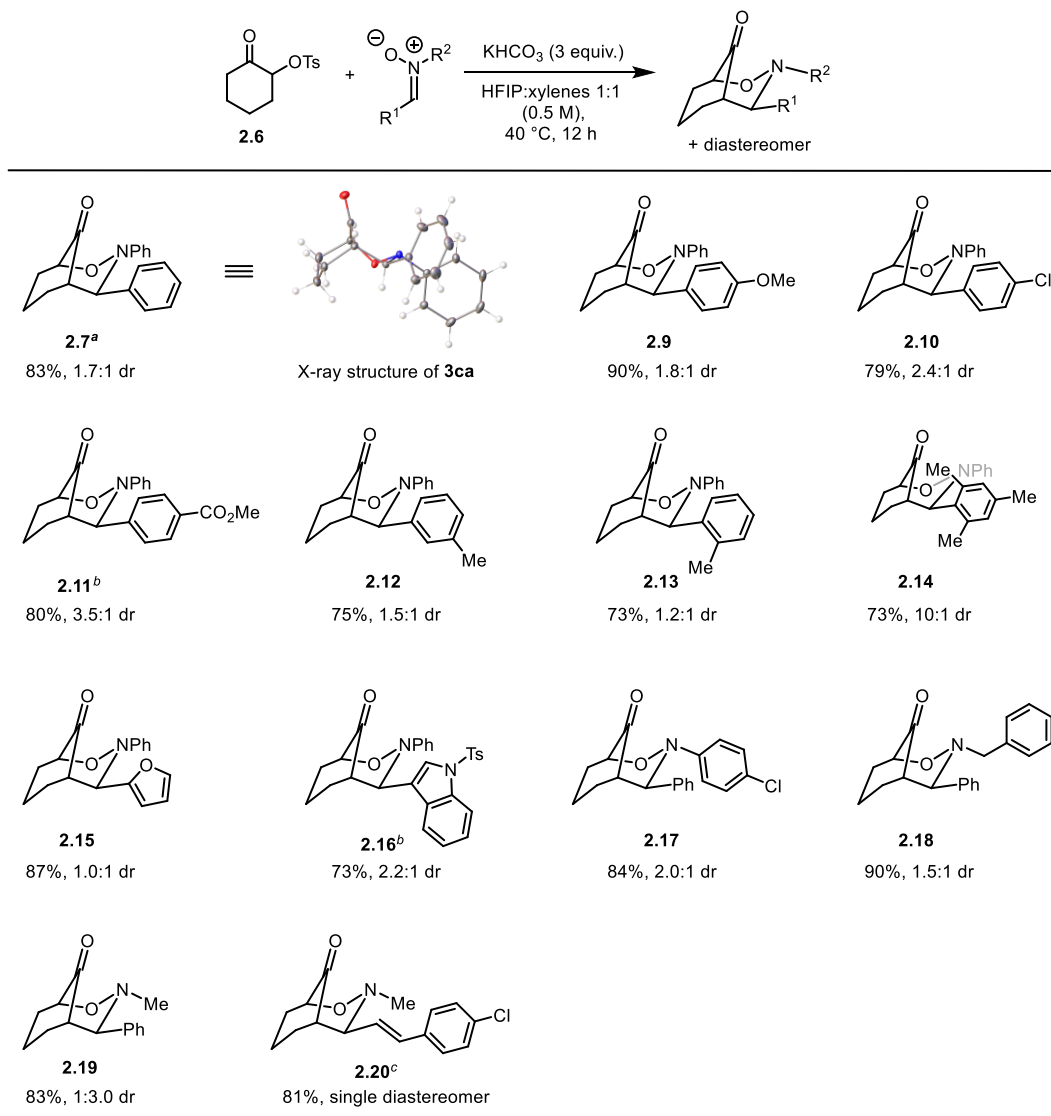
2.2 Substrate Scope of the [3+3] Cycloaddition Reaction

With the optimal reaction conditions in hand, we next examined the scope of the cycloaddition between 2-tosyloxycyclohexanone and different nitrones (Scheme 2.2).³ Nitrones containing electron-donating or electron-withdrawing groups on the α -phenyl ring of the nitron both provided the corresponding cycloadducts in good yields. Similarly, different substitution patterns on the α -Phenyl ring also gave good yields, including the sterically encumbered α -mesityl group, which curiously also afforded the products with a high d.r. α -Heterocycles were also tolerated under the reaction conditions, and in the case of **2.15**, the potential competing [4+3] cycloaddition with the furan moiety was not observed. Electron-deficient *N-p*-chlorophenyl nitron underwent the cycloaddition smoothly to afford **2.17** in high yield. Interestingly, *N-p*-methylphenyl nitron and *N-p*-methoxyphenyl nitron gave a mixture of products, possibly because the electron-rich *N*-phenyl ring of the nitron and/or the cycloadduct participated in competing Friedel-Crafts-type side reactions with the electron-deficient oxyallyl cation. Contrarily, *N*-methyl and *N*-benzyl nitrones provided the desired cycloadducts in good to high yields.

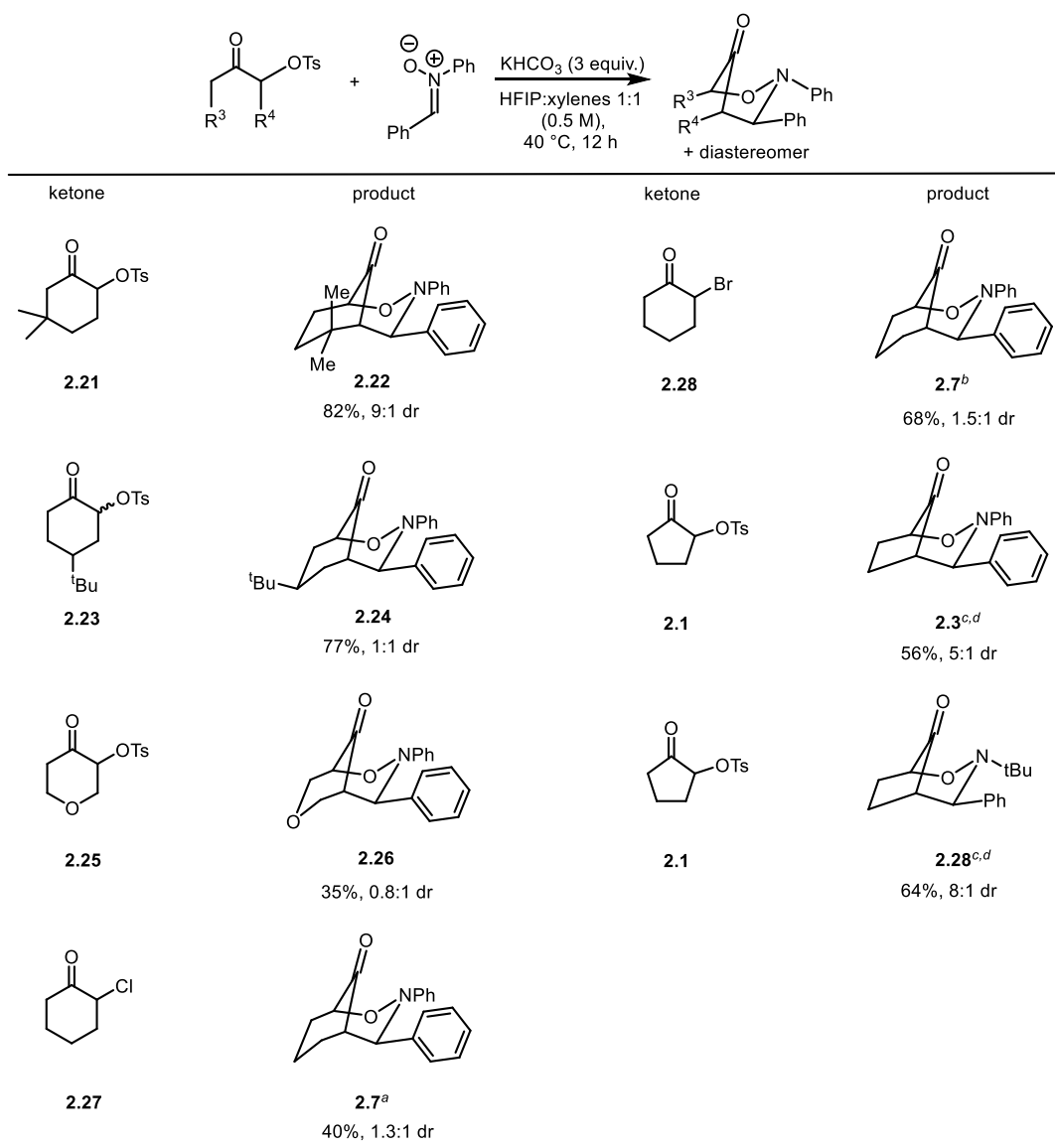
The scope of the α -tosyloxy-substituted cyclic and acyclic ketones was then explored (Scheme 2.3). The *gem*-dimethyl-substituted ketone **2.21** reacted provided the products in good yield with surprisingly high diastereoselectivity and complete regioselectivity. α -Tosyloxy ketones derived from 4-*tert*-butyl cyclohexanone and tetrahydropyran-4-one also give the cycloadducts in good yield. Furthermore, α -chloro and α -bromo ketones are also found to be suitable reaction partners. α -Tosyloxy cyclopentanone as well as acyclic ketones were also found to react well with nitrones. Ketone **2.29**, which is sterically hindered due to the presence of a tertiary carbon, reacted much

³ Hu, L.; Rombola, M.; Rawal, V. H. *Org. Lett.* **2018**, *20*, 5384.

slower and the use of a stronger base (NEt_3) was the required (Scheme 2.4). The reaction provided a mixture of diastereomers and regioisomers, in high yield. Acyclic ketones also reacted with complex nitrones such as **2.36** and **2.37** and gave the corresponding products in good yields.

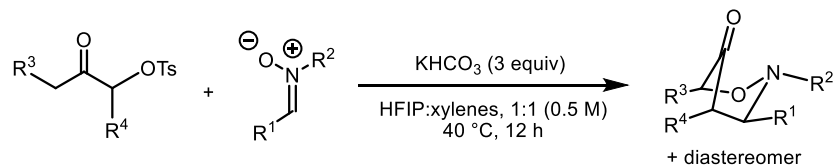


Scheme 2.2. Nitron scope for the [3+3] cycloaddition reaction of 2-tosyloxycyclohexanone.

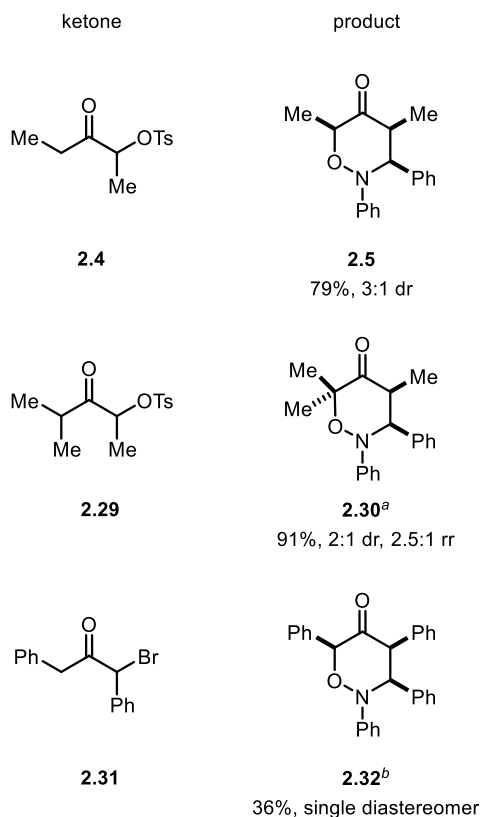


Reaction conditions: tosyloxy ketone (0.75 mmol), nitronium (0.50 mmol), K_2CO_3 (1.5 mmol), HFIP (500 μL), xylenes (500 μL), 40 °C, 12 h, isolated yields are shown. Structures assigned by analogy to that of 3ca based on ^1H NMR. ^a96 h. ^b60 h. ^cReaction run at room temperature. ^dYield of the major diastereomer.

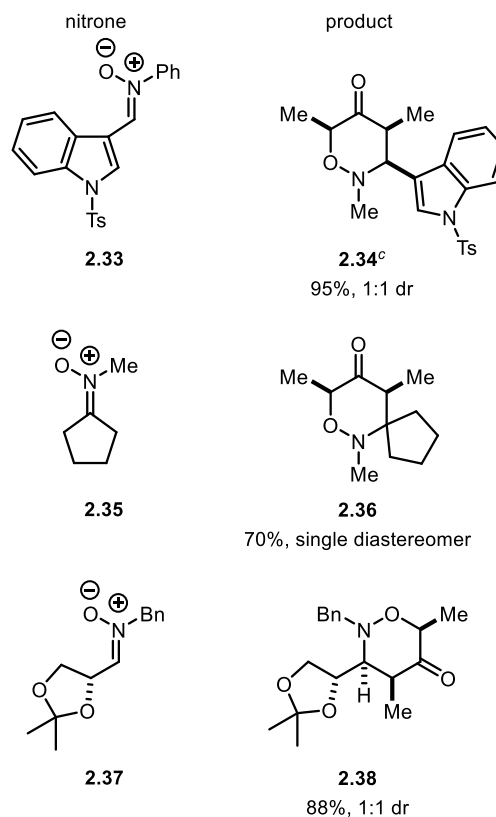
Scheme 2.3. Scope of [3+3] cycloaddition of cyclic α -tosyloxy ketones.



• Acyclic α -tosylketones with nitrone **2.2**



• α -Tosylketone **2.4** with nitrones

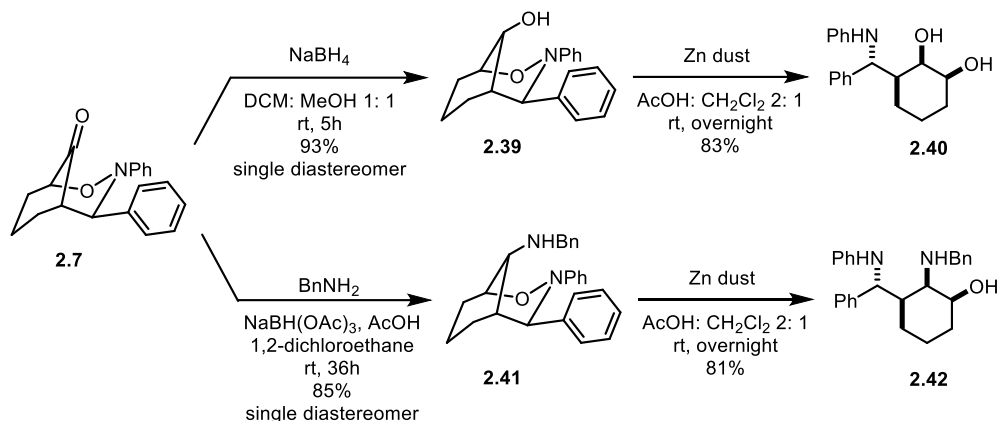


Reaction conditions: tosyloxy ketone (0.75 mmol), nitronium (0.50 mmol), KHCO_3 (1.5 mmol), HFIP (500 μL), xylenes (500 μL), 40 $^\circ\text{C}$, 12 h, isolated yields are shown. Structures assigned by analogy to that of **3ca** based on ^1H NMR. ^a NEt_3 (1.8 equiv), 60 h.. ^bReaction run at room temperature. ^c2 equiv of tosyloxy ketone was used.

Scheme 2.4. Scope of [3+3] cycloaddition of acyclic α -tosyloxy ketones.

The cycloadducts from the [3+3] reactions containing interesting chemical space and could potentially be useful for medicinal chemistry. They could also be easily transformed into different hydroxyl- and amine-functionalized derivatives. As shown in Scheme 2.5, **2.39** was obtained as a single diastereomer upon reduction of **2.7** with NaBH_4 . The subsequent reduction of the labile N-

O bond afforded the product **2.40** in good yield. The diamino product **2.42** was also obtained in a similar manner through an initial reductive amination.⁴



Scheme 2.5. Derivatization of the 1,2-oxazinane products.

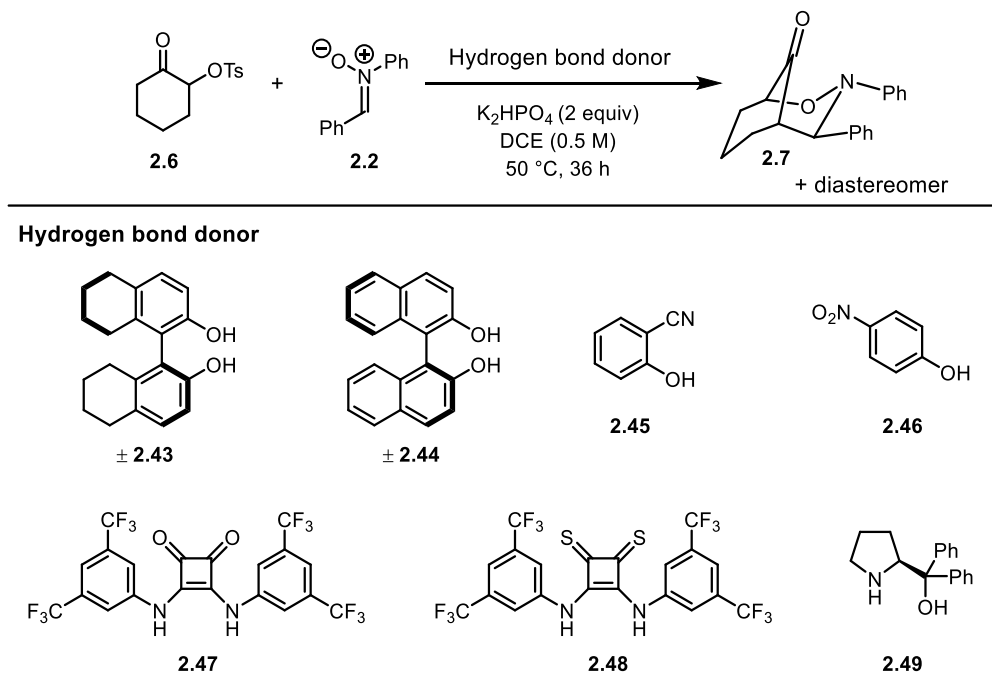
2.3 Catalysis of the [3+3] Cycloaddition Reaction with Hydrogen-Bond Donors

We discovered during the cosolvent screen that even with as little as 2 equiv of HFIP, the [3+3] cycloaddition still proceeded and afforded the desired products, although with a longer reaction time and a moderate drop in yield. In the absence of HFIP, however, no products were obtained. This result prompted us to investigate different hydrogen-bond donors as better promoters for the [3+3] cycloaddition. More than 50 different known hydrogen-bond donors were examined, with some representative examples shown in Table 2.5. The general trend observed was that the phenol-based hydrogen-bond donors gave better results than the N-H bond-based donors. For the phenols, within a certain range, the lower the *pKa*, generally the higher the yield. However, when the *pKa*

⁴ During the course of this work, Archambeau et al. reported similar chemistry focusing on acyclic α -tosyloxy ketone substrates. No studies on the possibility of performing the transformation with other hydrogen-bond donors were reported. Cordier, M.; Archambeau, A. *Org. Lett.* **2018**, *20*, 2265.

became too low, the hydrogen-bond donor would be completely quenched by the base (K_2HPO_4) and no reaction would take place. Squaramide based catalysts, which have found broad success as impactful hydrogen-bond donors, led to unsatisfying yields, with the exception of **2.47**, which provided the products in 58% yield with only 10 mol% loading. Unfortunately, due to its low solubility in the solvent used (1,2-dichloroethane), further optimization of the reaction conditions was unsuccessful. Its thiosquaramide analogue, **2.48**, with higher solubility as well as acidity, disappointingly gave no products. It's worth noting that prolinol **2.49**, which had been shown by MacMillan and co-workers to be an effective catalyst for the reaction between 2-tosyloxy cyclohexanone and *N*-methylindole, did not provide any desired cycloaddition products.⁵

Table 2.5. [3+3] Cycloaddition promoted by hydrogen-bond donor molecules

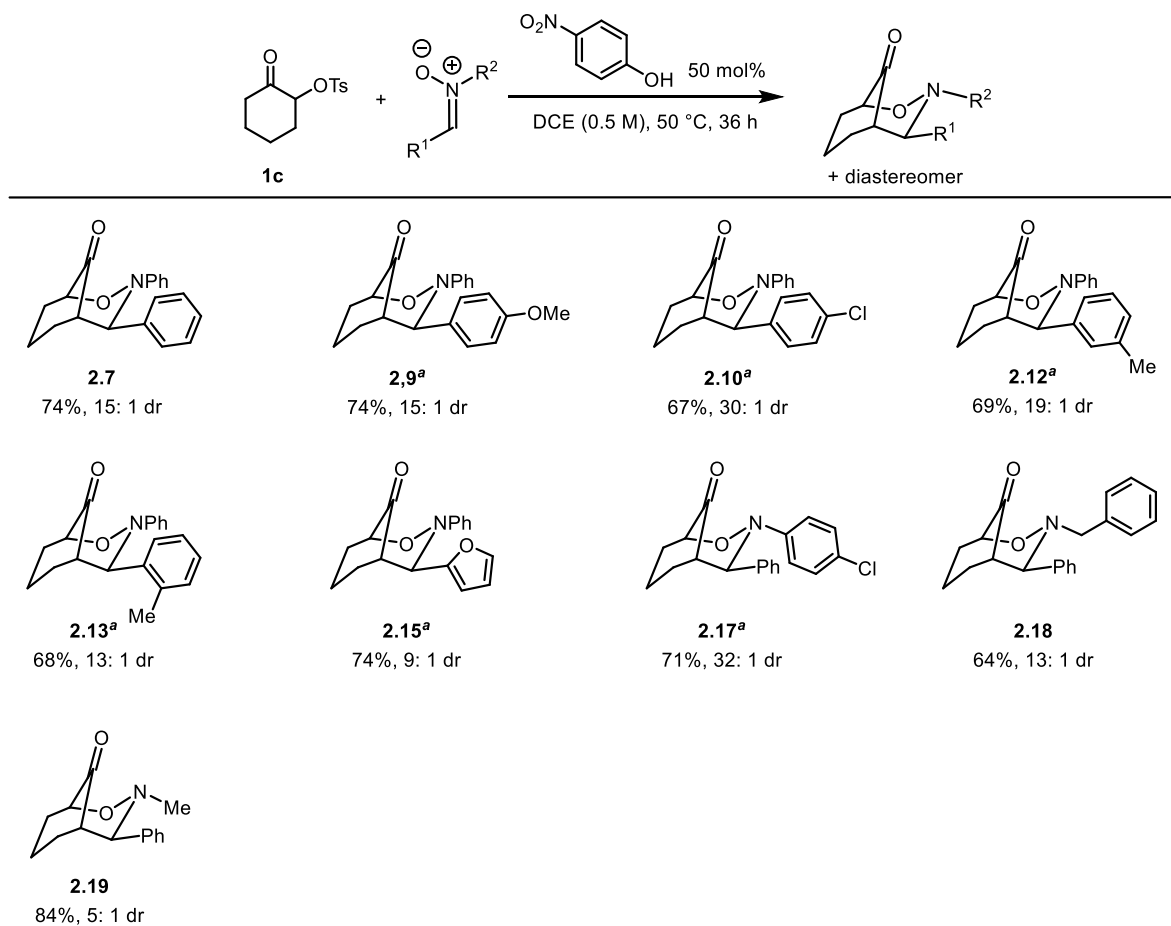


⁵ See section 1.3.

Table 2.5. Continued

entry	hydrogen bond donor	equivalents of hydrogen bond donor	Time (h)	Yield (NMR, %)	dr
1	HFIP	2	36	74	5:1
2	none	0	36	<2	n.d.
3	2.43	1	36	14	2:1
4	2.44	1	36	43	5:1
5	2.45	1	24	72	8:1
6	2.46	1	18	84	7:1
7	2.46	0.5	36	80	15:1
8	2.36	0.2	72	59	10:1
9	2.47	0.1	36	58	4:1
10	2.48	0.1	36	<2	n.d.
11	2.49	1	36	<2	n.d.

It was noticed that many of the hydrogen-bond donors examined not only provided the cycloaddition products, but also that the diastereoselectivity was dramatically improved. To assess this effect in a general sense, we selected 4-nitrophenol as the catalyst (50 mol% loading) and compared its results with that obtained under the HFIP/xylenes conditions. Gratifyingly, the 4-nitrophenol catalyst afforded the cycloadducts in comparable yields but with significantly improved diastereoselectivity. On average, the 4-nitrophenol system led to a 10-times increase in d.r.



Reaction conditions: tosyloxy ketone (0.60 mmol), nitronium (0.50 mmol), K_2HPO_4 (1.5 mmol), 4-nitrophenol (0.25 mmol), DCE (1 mL), 50 °C, 36 h, isolated yields are shown. Structures assigned by analogy to that of 3ca based on 1H NMR.

^aAn additional 50 mol% of nitrophenol was added after 24 h to shorten the reaction time.

Scheme 2.6. [3+3] Cycloaddition of selected substrates from scheme 2.2 promoted by 4-nitrophenol as a hydrogen-bond donor catalyst.

2.4 Conclusion

In summary, we have developed a novel [3+3] cycloaddition reaction between nitronium and oxyallyl cations in the fluorinated alcohol solvent HFIP and xylenes as a cosolvent. The oxyallyl cations were generated from α -tosyloxy and α -halogen ketones, which are readily accessed from the corresponding ketones. The reaction afforded 1,2-oxazinanones as the cycloadducts, heterocycles

that are otherwise difficult to obtain. Remarkably, based on the widely accepted hypothesis that HFIP facilitated the formation of oxyallyl cations and stabilized them through hydrogen-bonding to the C2 oxygen of the oxyallyl cations, we investigated the possibility of catalyzing this novel [3+3] cycloaddition reaction with other hydrogen-bond donors. We discovered that phenol-based hydrogen-bond donors provided the best results among other types of hydrogen-bond donor we tested. Eventually, we were able to perform the [3+3] cycloaddition reaction with a 50 mol% loading of 4-nitrophenol, which gave comparable yields compared to that from the HFIP/xylenes conditions, but with an average of a 10-times increase in the diastereoselectivity.

Chapter 3

Introduction to the Ambiguine Natural Products

3.1 Isolation of Ambiguine Natural Products and Their Bioactivities

The ambiguity natural products are a subset of the hapalindole family, which has more than 80 members. These secondary metabolites are isolated from the *Stigonemataceae* family of cyanobacteria, also known as blue-green algae. The first isolation of ambiguines were reported by Moore and co-workers in 1992.¹ During their examination of the fungicidal activities of the *Stigonemataceae* species, six ambiguines (A-F) were isolated and characterized (Scheme 3.1). Ambiguines A-C were tetracyclic, structurally similar to hapalindoles but with a flanking 1,1-dimethyl-2-propenyl group attached at the C2 position.² Ambiguines D-F were pentacyclic, in which case the C2 1,1-dimethyl-2-propenyl group also connected with the distal six-membered ring, forming a seven-membered ring. All six ambiguines contained a C11 isonitrile group, a functionality that is uncommonly seen in other natural products but a common feature within the hapalindole family. The same group later reported the isolation of ambiguity G, the first nitrile containing indole alkaloids isolated from *Stigonemataceae*.

Almost a decade later, Carmeli disclosed three additional members in the ambiguity family: ambiguines: H, I and J, which are the C13-dechloro analogues of three of the previously reported ambiguines.³ Later, Orjala and co-workers reported five more ambiguines (K-O), which were

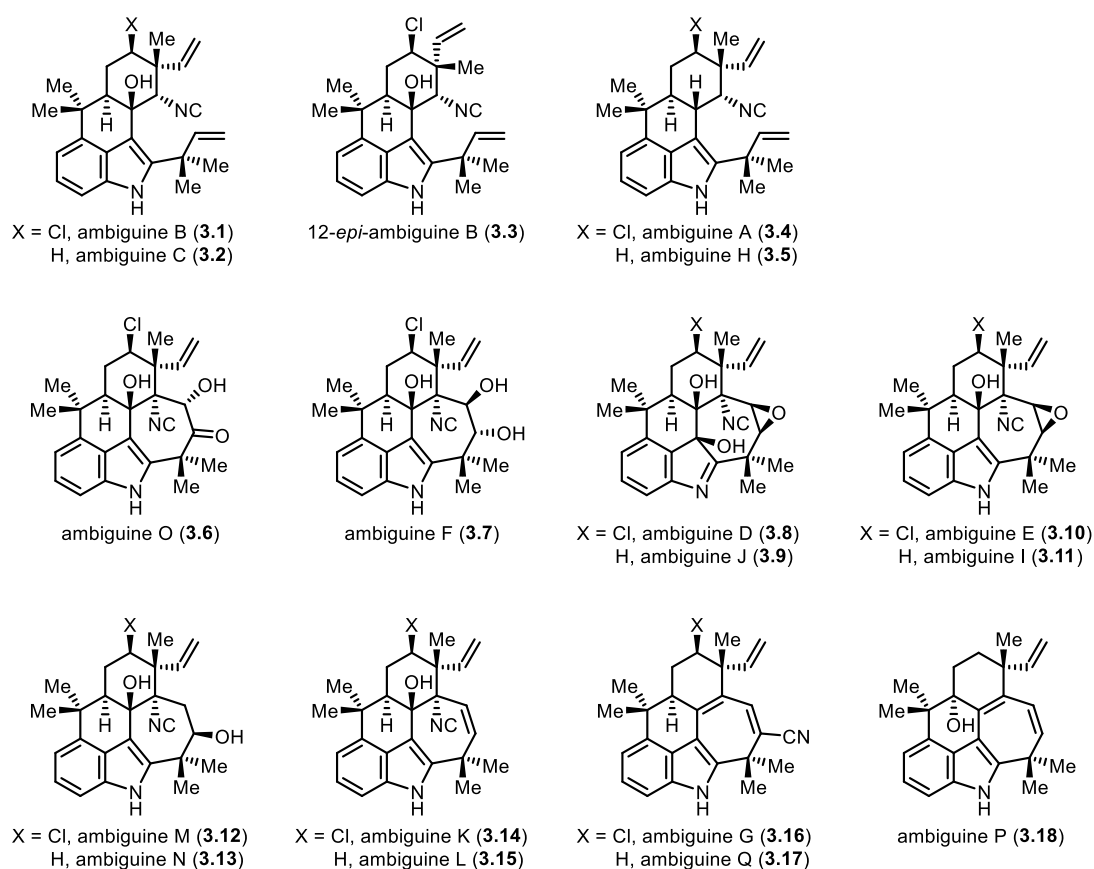
¹ Smitka, T. A.; Bonjouklian, R.; Doolin, L.; Jones, N. D.; Deeter, J. B.; Yoshida, W. Y.; Prinsep, M. R.; Moore, R. E.; Patterson, G. M. L. *J. Org. Chem.* **1992**, *57*, 857.

² Huber, U.; Moore, R. E.; Patterson, G. M. *J. Nat. Prod.* **1998**, *61*, 1304.

³ Raveh, A.; Carmeli, S. *J. Nat. Prod.* **2007**, *70*, 196.

different from the previously identified ambiguine in terms of the oxidation pattern on the C25, C26 positions.⁴ Closely following this discovery was the identification of ambiguine P, a different structured ambiguines without either isonitrile or nitrile groups, and ambiguine Q, the dechloro analogue of ambiguine G by the same group.⁵

In 2014, a new tetracyclic ambiguine, 12-*epi*-ambiguine B nitrile was identified, whose stereochemistry at the C12 position is the opposite to all other known ambiguines.⁶



Scheme 3.1. Ambiguine natural products.

⁴ Mo, S.; Kronic, A.; Chlipala, G.; Orjala, J. *J. Nat. Prod.* **2009**, *72*, 894.

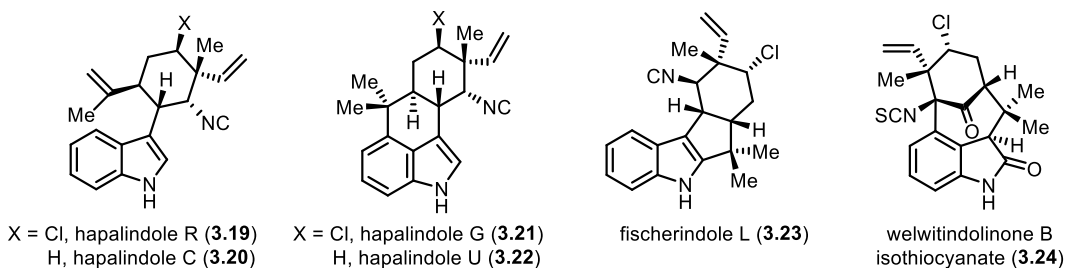
⁵ Mo, S.; Kronic, A.; Santarsiero, B. D.; Franzblau, S. G.; Orjala, J. *Phytochemistry* **2010**, *71*, 2116.

⁶ Walton, K.; Gantar, M.; Gibbs, P. D. L.; Schmale, M. C.; Berry, J. P. *Toxins* **2014**, *6*, 3568.

Some of the ambiguines have shown various promising bioactivities. Many of the ambiguines exhibited potent antifungal activities and Ambiguine I in particular, has shown strong fungicidal activity against *C. albicans* and *S. cerevisiae*, comparable to amphotericin B and puromycin respectively.³ The same compound has also shown potent inhibition of NF- κ B (IC₅₀= 30 nM), with cytotoxic activity against HT-29 colon cancer as well as MCF-7 breast cancer cell lines.⁷

3.2 Biogenesis of Ambiguine Natural Products

Ambiguines are structurally closely related to hapalindoles, fischerindoles and welwitindolinones, as distinguished by their indole moiety and a cyclohexane ring containing a methyl and vinyl substituted quaternary carbon center (Scheme 3.2). The biogenesis of the tetracyclic scaffold of these indole alkaloids was first proposed by Moore and co-workers in 1994,⁸ and later modified by Carmeli and co-workers in 2007 (Scheme 3.3).³



Scheme 3.2. Representative natural products in the hapalindole, fischerindole and welwitindolinone families.

⁷ Acuña, U. M.; Zi, J.; Orjala, J.; Carcache de Blanco, E. J. *Int. J. Cancer Res.* **2015**, *49*, 1655.

⁸ Stratmann, K.; Moore, R. E.; Bonjouklian, R.; Deeter, J. B.; Patterson, G. M. L.; Shaffer, S.; Smith, C. D.; Smitka, T. A. *J. Am. Chem. Soc.* **1994**, *116*, 9935.

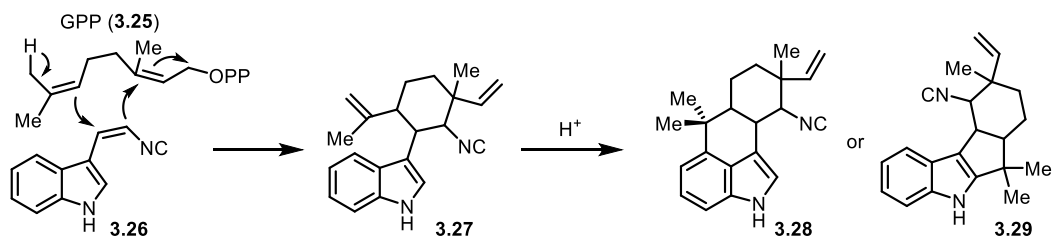
However, the actual mechanism of how the hapalindole scaffold was formed remained elusive until 2015, when Sherman and co-worker revealed the biosynthetic pathway with experimental data.⁹ It was found that the indole isonitrile core **3.26** reacted with geranyl pyrophosphate (GPP) in an intriguing manner where the C3 position of the indole first participated in the reaction with GPP, and the resulting intermediate then underwent a Cope rearrangement followed by 6-exo-trig cyclization and an electrophilic aromatic substitution reaction, leading to the tetracyclic core of hapalindoles (**3.28**). The Sherman group reported in 2020 that the rearrangement, cyclization and aromatic substitution steps take place in Stig cyclase dimers, and the nature of the combination of the subunits in these dimers control the stereo-outcome at the C10, C12 and C15 positions of the hapalindoles (Scheme 3.4).¹⁰ The installation of the isoprenyl group on the C2 position of ambiguines was achieved by a dimethylallyltransferase utilizing dimethylallyl pyrophosphate, as shown by Liu and co-workers in 2014 (Scheme 3.5).¹¹ However, the mechanism for the formation of the seven-membered ring found in most ambiguines remains unknown.

⁹ Li, S.; Lowell, A. N.; Yu, F.; Raveh, A.; Newmister, S. A.; Bair, N.; Schaub, J. M.; Williams, R. M.; Sherman, D. H. *J. Am. Chem. Soc.* **2015**, *137*, 15366.

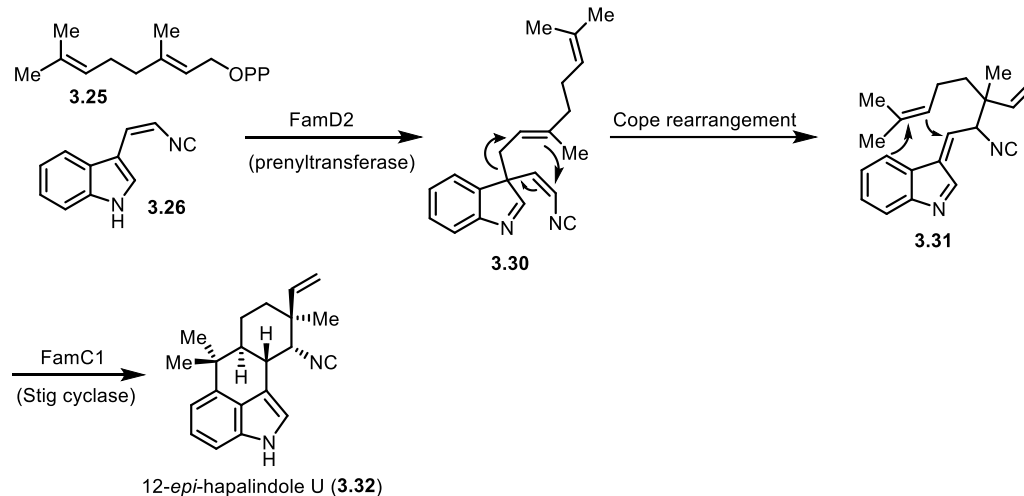
¹⁰ Li, S.; Newmister, S. A.; Lowell, A. N.; Zi, J.; Chappell, C. R.; Yu, F.; Hohlman, R. M.; Orjala, J.; Williams, R. M.; Sherman, D. H. *Angew. Chem. Int. Ed.* **2020**, *59*, 8166.

¹¹ Hillwig, M. L.; Zhu, Q.; Liu, X. *ACS Chem. Biol.* **2014**, *9*, 372.

Hapalindole biogenesis hypothesis proposed by Moore and Carmeli:

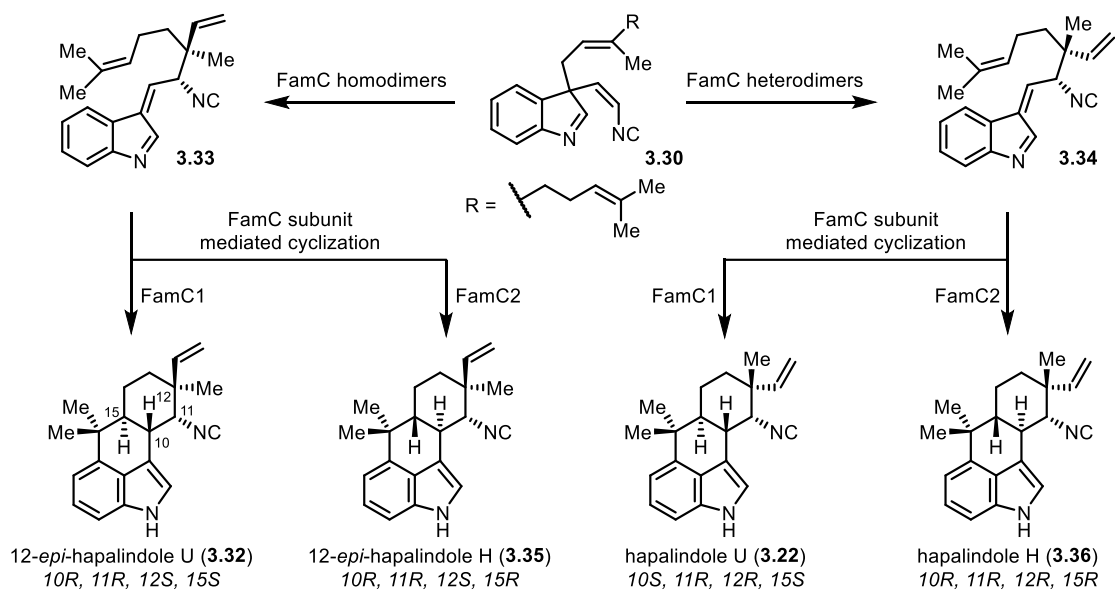


Hapalindole biogenesis revealed by Sherman and co-workers:

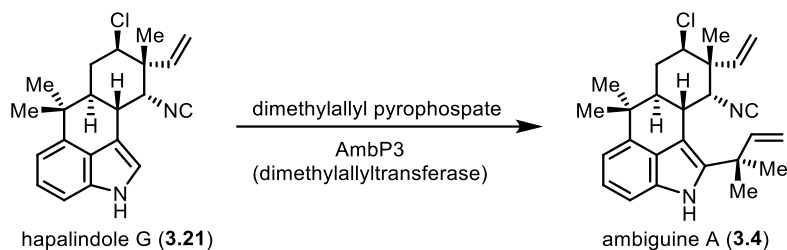


Scheme 3.3. Hapalindole biogenesis.

Stereocontrol at the C10, C11, C12 and C15 positions:

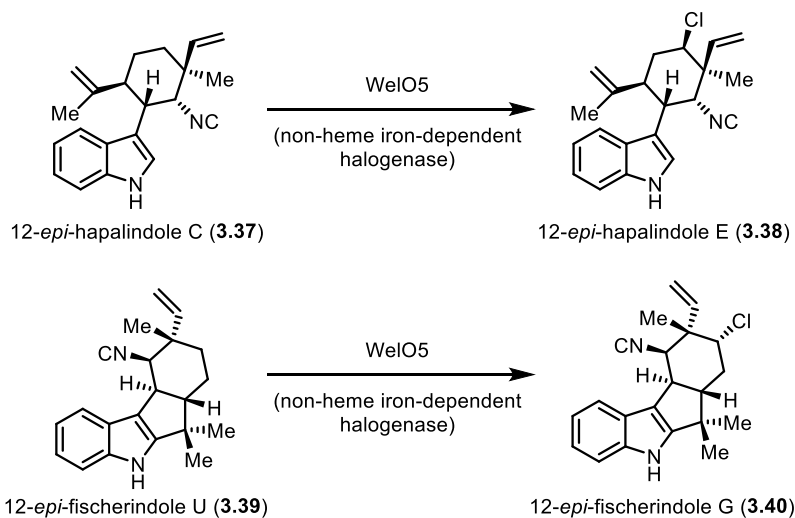


Scheme 3.4. Stereocontrol in the biogenesis of hapalindoles.



Scheme 3.5. Biogenesis of ambigaine A from hapalindole G through dimethylallyltransferase mediated isoprenylation.

More than half of the hapalindoles alkaloids also contain a C13 chlorine atom which had been originally proposed to be incorporated into the scaffold concomitantly with the installation of the geranyl group. Liu and co-workers have proved experimentally that the chlorine atom in some of the hapalindoles was installed stereospecifically at a late stage by a family of non-heme iron-dependent halogenases, and genes encoding such non-heme iron-dependent halogenases were also identified in the ambigaine biosynthetic gene cluster (Scheme 3.6).¹²



Scheme 3.6. Biogenesis of chlorinated hapalindoles via non-heme iron-dependent halogenase mediated late-stage chlorination.

¹² Hillwig, M. L.; Liu, Q. *Nat. Chem. Biol.* **2014**, *10*, 921.

3.3 Chemical Synthesis of Ambiguine Natural Products

Because of the intriguing and complex structures of ambiguines, multiple groups have devoted energy to the total syntheses of ambiguines. Baran and co-workers reported in 2007 the first total synthesis of tetracyclic ambiguityine H, and the formal total synthesis of the same compound was disclosed in 2018 by Maji and co-workers.^{13,14} There are also a myriad of unsuccessful attempts towards the total synthesis of ambiguines.¹⁵ Due to the large body of work in this field, only the syntheses targeting the pentacyclic ambiguines will be discussed in this section.

Among the eighteen known members in the ambiguityine family, thirteen share a fused pentacyclic backbone containing a seven-membered ring that connects the indole to the distal six-membered ring, a challenging scaffold to construct. These pentacyclic ambiguines also possess multiple quaternary carbon centers and most of them are densely functionalized, rendering their syntheses even more challenging. Due to these daunting structural features, only ambiguityine P has yielded to synthesis before the successful syntheses of ambiguines Q and G that will be discussed in the following chapters.

3.3.1 Sarpong's Synthesis of Ambiguine P

In 2019, Sarpong and co-worker disclosed the total synthesis of the pentacyclic ambiguityine P.¹⁶ Their overall strategy was to construct the pentacyclic scaffold through an oxidative coupling

¹³ Baran, P. S.; Maimone, T. J.; Richter J. M. *Nature* **2007**, *446*, 404.

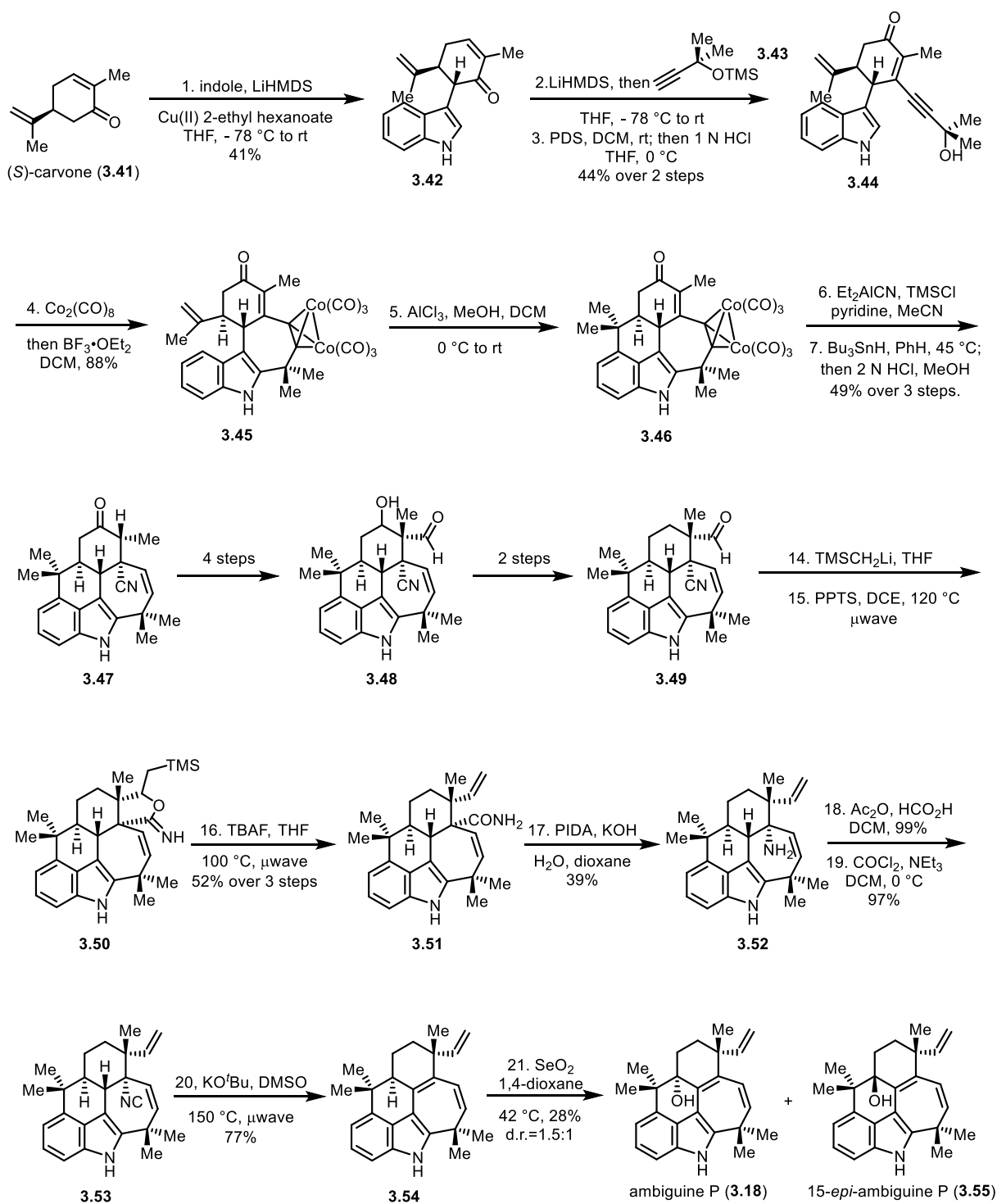
¹⁴ Sahu, S.; Das, B.; Maji, M. S. *Org. Lett.* **2018**, *20*, 6485.

¹⁵ A few selected examples: (a) Chandra, A.; Viswanathan, R.; Johnston, J. N. *Org. Lett.* **2007**, *9*, 5027. (b) Rafferty, R. J.; Williams, R. M. *Tetrahedron Lett.* **2011**, *52*, 2037. (c) Rafferty, R. J.; Williams, R. M. *Heterocycles* **2012**, *86*, 219.

¹⁶ Johnson, R. E.; Ree, H.; Hartmann, M.; Lang, L.; Sawano, S.; Sarpong, R. *J. Am. Chem. Soc.* **2019**, *141*, 2233.

between indole and carvone, a Nicholas reaction to form the seven-membered ring, and a proton induced Friedel-Crafts type cyclization. Functional group manipulation was then performed which granted the access to multiple pentacyclic intermediates that eventually led to ambiguine P. Details are shown in Scheme 3.7. The synthesis started from the oxidative coupling between indole and (*S*)-carvone based on the method developed by Baran and co-workers.¹⁷ Alkynylation followed by Babler-Dauben oxidation led to **3.44**, and the seven-membered ring was then formed via Nicholas reaction. The resulting organocobalt species, which was column isolable, was carried over the next two steps and eventually removed through tributyltin hydride reduction, leaving a carbon-carbon double bond on the seven-membered ring. After a few manipulations to install the vinyl group and to remove the C13 carbonyl, intermediate **3.52** was obtained through a Hofmann rearrangement. The amino group generated was then transformed into an isonitrile group, which was eliminated under strongly basic conditions, leading to **3.54**, which upon allylic oxidation, afforded ambiguine P and its C15 epimer in a 28% yield with a 1.5:1 diastereoselectivity, in a total of 21 steps.

¹⁷ Baran, P. S.; Richter, J. M. *J. Am. Chem. Soc.* **2004**, *126*, 7450.



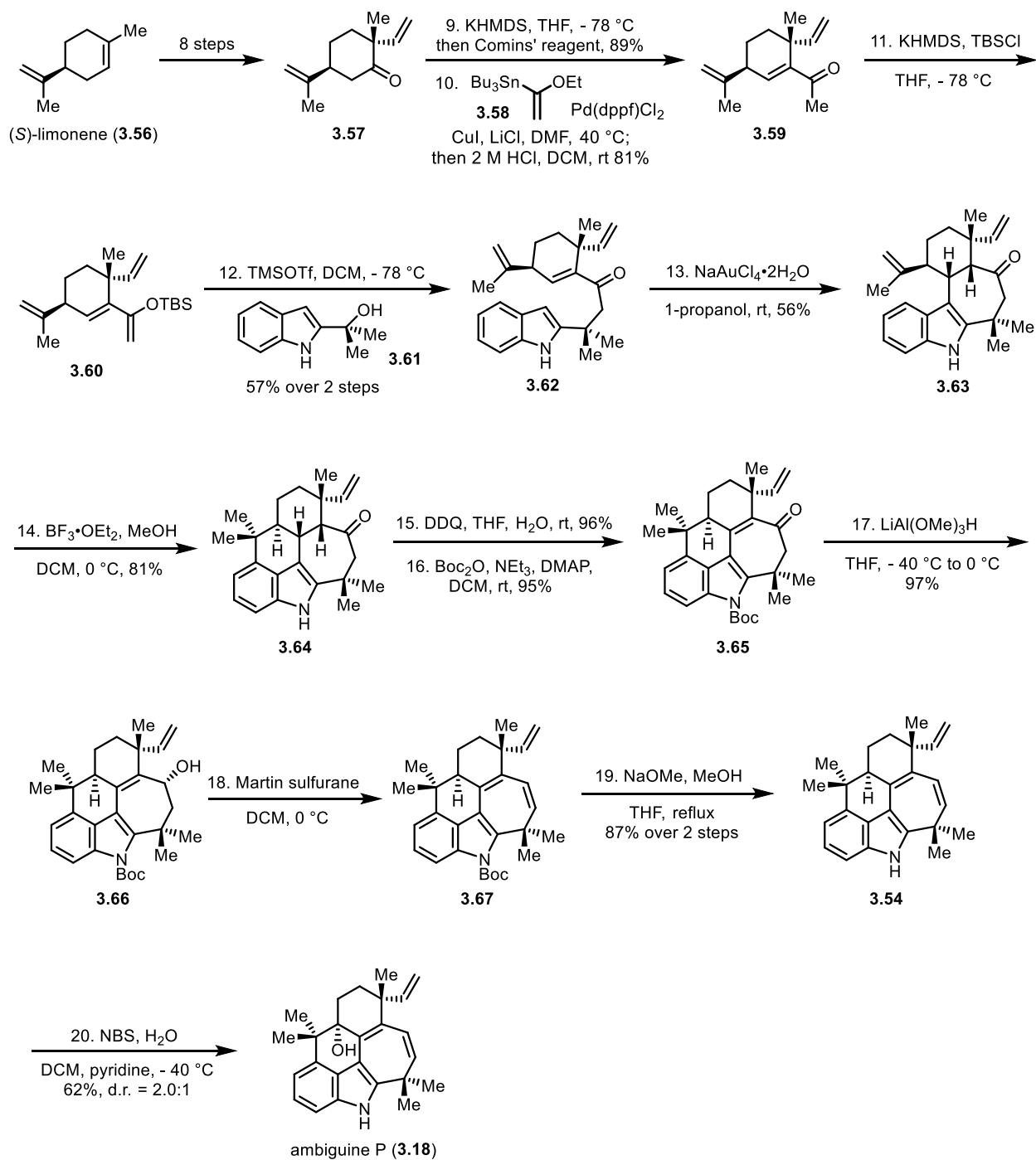
Scheme 3.7. Sarpong's synthesis of ambigaine P.

3.3.2 Our First-Generation Synthesis of Ambiguine P

Prior to the publication of the Sarpong synthesis of ambiguityne P, our group had also synthesized ambiguityne P.¹⁸ Our guiding strategy to construct the seven-membered ring was through an intermolecular [4+3] cycloaddition reaction, which enabled the synthesis of ambiguityne P by conjoining two easily accessible components with comparable sizes. Even though the seven-membered ring was ultimately formed in two steps due to unexpected interrupted [4+3] reaction between the two coupling components, we viewed the [4+3] cycloaddition as a potentially powerful strategy to construct the pentacyclic backbone of ambiguines.

Our first-generation synthesis of ambiguityne P started with the synthesis of ketone **3.57**, which was accessed in eight steps from (*S*)-limonene using a route reported by Baran and co-workers. Triflation of **3.57** followed by Stille coupling provided **3.59** upon hydrolysis, which was subsequently transformed into the corresponding TBS silyl enol ether **3.60**. The [4+3] cycloaddition between **3.60** and the indole alcohol **3.61** did not undergo the desired cycloaddition reaction and only led to the Friedel-Crafts type product **3.62**. The seven-membered ring was then constructed with an extra step by uncommon Au(III) catalyzed intramolecular Michael addition type reaction. Another Friedel-Crafts type cyclization and DDQ induced dehydrogenation led to enone **3.65**. The indole N-H was then protected as N-Boc, the reduction of which gave alcohol **3.66** as a single diastereomer. Subsequent dehydration with Martin sulfurane and Boc deprotection afforded diene **3.54**, the same intermediate that Sarpong and co-workers also had access to with their synthetic route. Eventually, ambiguityne P was obtained in 62% yield (d.r.=2.0:1) from **3.54**, and in a total of 20 steps from (*S*)-limonene.

¹⁸ Xu, J. Rawal, V. H. *J. Am. Chem. Soc.* **2019**, *141*, 4820.

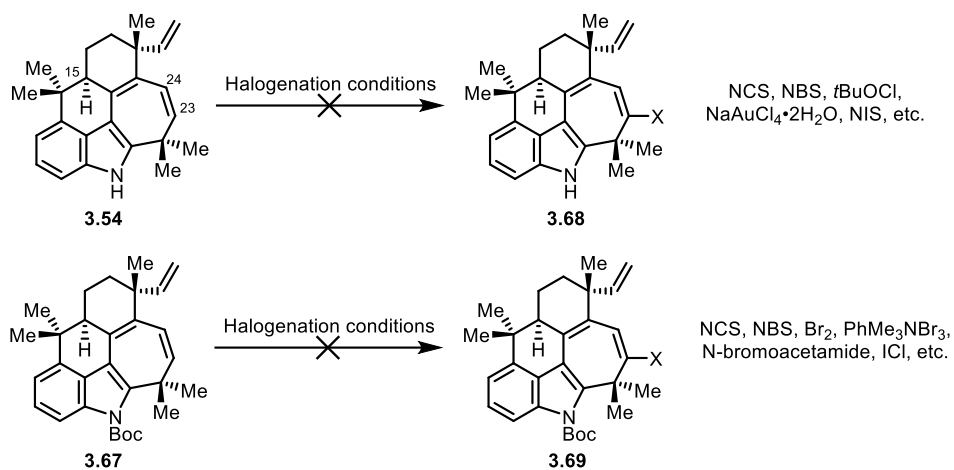


Scheme 3.8. Rawal's first-generation synthesis of ambiguine P.

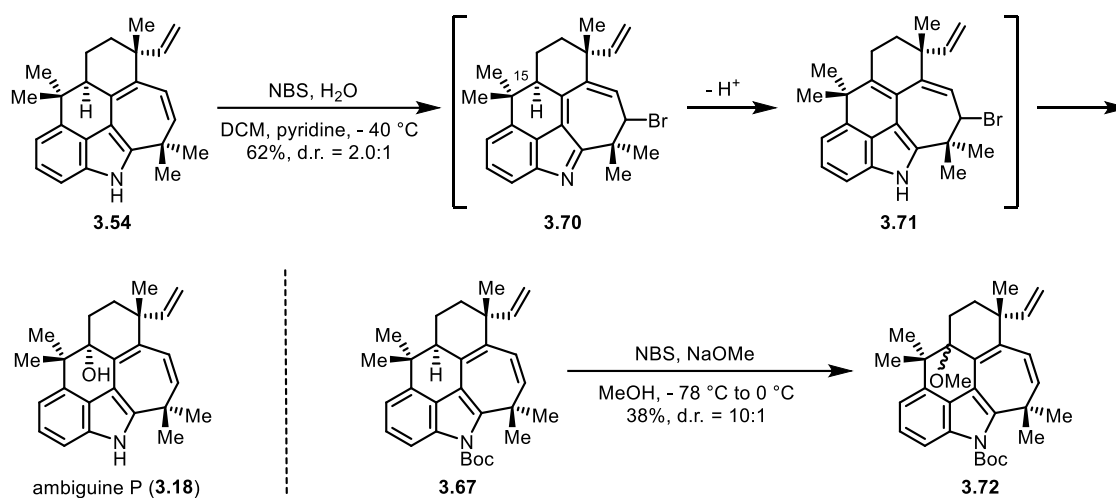
3.3.3 Our Attempted Synthesis of Ambiguine Q

With compound **3.54** obtained from our synthesis of ambiguityne P, we explored the synthesis towards ambiguityne Q from this compound.¹⁹ It was anticipated that a direct cyanation of **3.54** at the C23 position or a halogenation at the same position followed by transition metal catalyzed cyanation should provide ambiguityne Q. However, numerous cyanation and halogenation conditions were screened but without success. It was during this process that the direct transformation of **3.54** into ambiguityne P was discovered. A related reactivity was observed with **3.67** in the presence of NBS, NaOMe and MeOH. Both reactions were proposed to proceed through structurally similar intermediates, resulting from the deprotonation of the undesired C15 hydrogen upon the addition of the electrophile on the C23-C24 double bond, instead of the desired C23 hydrogen.

¹⁹ Xu, J. Synthetic studies toward ambiguityne natural products and total synthesis of (-)-ambiguine P. *Ph.D. Dissertation*, University of Chicago, Chicago, IL. 2019.



Labile C-H bond at C15 led to unsuccessful halogenations:



Scheme 3.9. Rawal's previous attempts of halogenation at C23 of **3.54** and **3.67**.

Chapter 4

Synthesis Towards Pentacyclic ambigunes: The Cyclohexanone Fragment

With the first-generation synthesis of ambigune P, we foresaw the great potential of a [4+3] cycloaddition strategy in the synthesis of other pentacyclic ambigunes. The strategy enabled us to construct the pentacyclic scaffold from two easily accessible fragments with comparable sizes, and the [4+3] cycloaddition product contained a carbonyl group as a proper handle for the further functionalization leading to the desired natural products.¹ But the conciseness of the construction of the pentacyclic scaffold through the [4+3] cycloaddition strategy was counteracted by the inefficiency of the synthesis of cyclohexanone **4.1**, which we thus decided to improve.

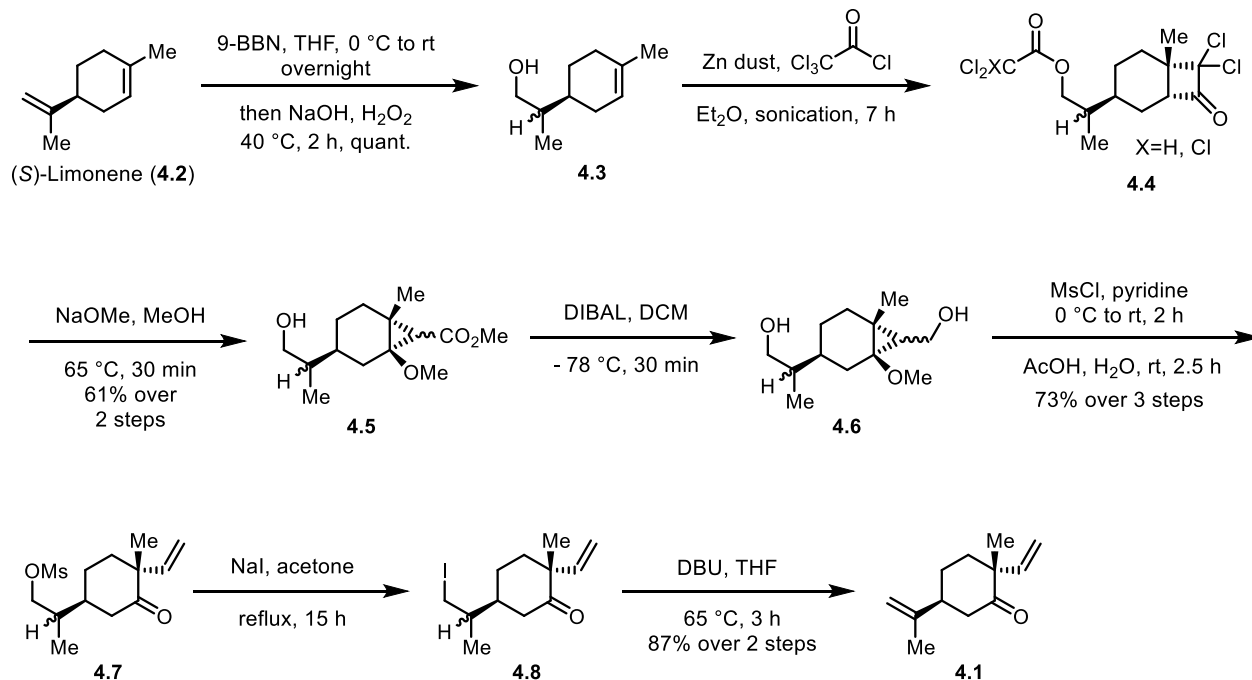
4.1 First-Generation Synthesis of the Cyclohexanone 4.1

The route towards cyclohexanone **4.1** developed by Baran and co-workers (Scheme 4.1) was applied in our previous synthesis of ambigune P as well as our attempts towards the synthesis of ambigune Q. Despite being highly innovative, the route suffers from a few drawbacks. To start with, compound **4.3**, which was used as the starting material in the original Baran report, was expensive and was therefore synthesized in an extra step from (*S*)-limonene.² The [2+2] cycloaddition step could only be operated at a maximum 7 grams scale, limited by the size of sonicator. Compounds **4.4**, **4.5** and **4.6** were obtained as a mixture of multiple diastereomers and various unknown by-products, making it difficult to assess the yields of each step. These

¹ See section 3.3 and references therein.

² Baran, P. S.; Maimone, T. J.; Richter J. M. *Nature* **2007**, *446*, 404.

drawbacks significantly lowered the efficiency of our overall route towards the pentacyclic ambiguine scaffold and necessitated the development of alternative routes towards **4.1**.



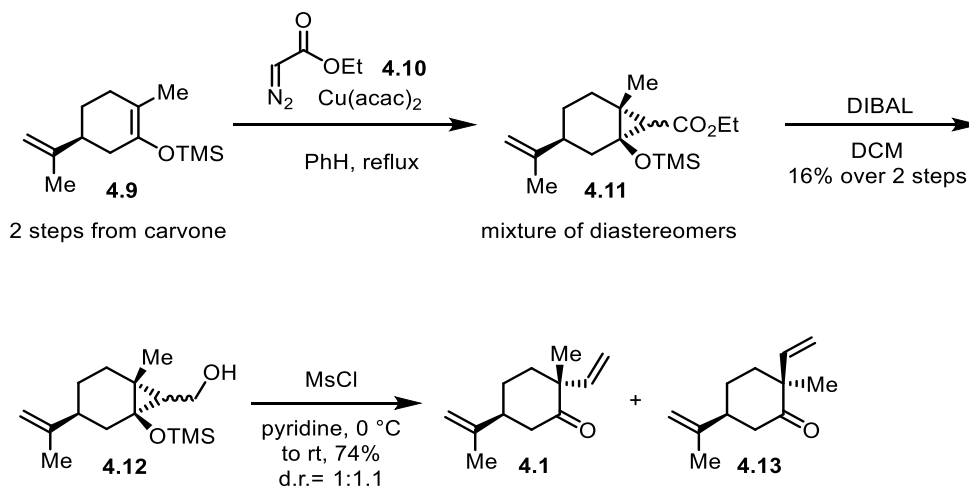
Scheme 4.1. Baran's synthesis of **4.1**.

4.2 Initial Attempts of the Synthesis of the Cyclohexanone **4.1** with Higher Efficiency

The cyclopropanation strategy shown in Scheme 4.2 was first attempted. Wenkert and co-workers reported that with ethyl diazoacetate and $\text{Cu}(\text{acac})_2$ as a catalyst, the cyclopropanation of silyl enol ethers could be achieved.³ We applied their conditions to substrate **4.9** in the hope that the silyl enol ether could be selectively cyclopropanated, due to its higher electron density compared to that of the isopropenyl double bond. Following this rationale would lead to the desired

³ Wenkert, E.; Arrhenius T. S.; Bookerser, B.; Guo, M.; Mancini, P. *J. Org. Chem.* **1990**, *55*, 1185.

adduct **4.11**, an analogue of **4.5** in the Baran synthesis. However, under the reported reaction conditions, both the silyl enol ether and the isopropenyl group were cyclopropanated, affording two regioisomers, both as a mixture of multiple diastereomers that could not be isolated from each other. The reduction of **4.11** with DIBAL provided **4.12** in only 16% yield over 2 steps. Elimination of the free alcohol of **4.12** in the presence of MsCl led to the desired product **4.1**, together with the undesired diastereomer **4.13**. The low diastereoselectivity is presumably a result of the cyclopropanation step being non-selective.

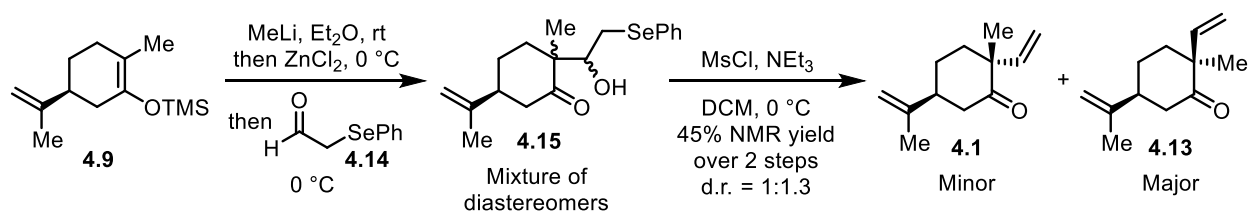


Scheme 4.2. Synthesis of **4.1** through cyclopropanation of **4.9**.

Direct functionalization of the silyl enol ether **4.9** with electrophiles was then explored. We were intrigued by the selenoaldehyde method developed by Kowalski and co-workers as well as Clive and co-workers⁴. Both groups demonstrated that the selenoaldehyde **4.14** could be used as a vinyl cation equivalent and would react with zinc enolates easily derived from silyl enol ethers. The aldol reaction product could then be transformed into a vinyl group in the presence of MsCl and NEt_3 with DCM being the solvent. The possibility of utilizing this selenoaldehyde method in our

⁴ (a) Kowalski C. J. Dung, J. J. *Am. Chem. Soc.* **1980**, *102*, 7950. (b) Clive, D. L. J.; Russell, C. G.; Suri, S. C. *J. Org. Chem.* **1982**, *47*, 1632.

system was then tested. As shown in Scheme 4.3, silyl enol ether **4.9** was converted to the corresponding lithium enolate through desilylation with MeLi, which was then transformed into zinc enolate. The addition of **4.14** into the reaction at 0 °C afforded the aldol products **4.15** as a mixture of diastereomers, both at the quaternary carbon center as well as the alcohol attaching carbon. The hydroxyl group and the selenophenyl group were then eliminated at 0 °C in DCM in a subsequent step to afford the desired vinylation products but with poor diastereoselectivity (1:1.3), favoring the undesired diastereomer. The improvement of the diastereoselectivity turned out to be challenging. The diastereoselectivity-determining aldol reaction worked well at 0 °C but gave poor yields at elevated temperature, which presumably favors the formation of the desired, minor diastereomer.



Scheme 4.3. Synthesis of **4.1** via selenoaldehyde **4.14**.

Aside from the diastereoselectivity issue, the reaction also suffered from other problems. The enolate needed to be generated from the corresponding silyl enol ether while the same enolate generated formed from 1,4-reduction of carvone using L-Selectride failed. Attempts to combine the aldol step with the elimination step were also unsuccessful, mostly because Et₂O, the solvent used in the aldol step, stalled the subsequent elimination under the MsCl/NEt₃ condition from taking place. The isolation of the final product was also complicated by the presence of an unknown selenium-based impurity, which co-eluted with the desired product and was difficult to remove without a significant loss of the desired product.

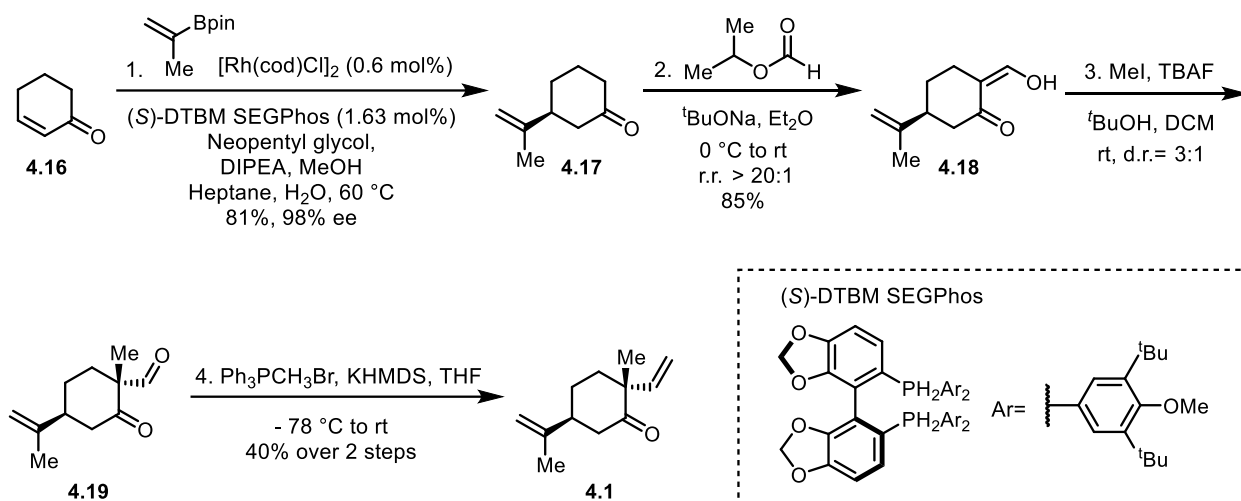
4.3 Enantioselective Synthesis of the Cyclohexanone **4.1**.

After the unsuccessful attempts of synthesizing **4.1** from a carvone based starting material, we approached the problem from a different angle. Instead of utilizing the pre-existing the isopropenyl group and the methyl group on carvone, we decided to install different substituents on a cyclohexene ring one by one, reasoning that it only takes 3-4 steps to install the isopropenyl, methyl and vinyl groups and the diastereoselectivity could be conveniently affected by the sequence of the installation of these groups. The isopropenyl group was first installed utilizing a Rhodium catalyzed asymmetric Hayashi 1,4-addition reaction developed by chemist at Bristol Myers Squibb, which was reported at 100 kg scale!⁵ Although the reactions yields we obtained were similar to reported values, we initially observed the enantiomeric excess values to be much lower compared to the reported 99.6% ee. It was later found that the oxygen level had a significant influence on the enantioselectivity, especially when the reaction was executed on a gram scale with a low, 0.3 mol% loading of [Rh(cod)Cl]₂. The diminishing enantioselectivity problem was eventually solved by doubling the loading of [Rh(cod)Cl]₂ and the ligand, as well as performing the reaction in the smallest possible reaction vessels with rigorous deoxygenation of both the solvents and the reaction vessels.

With ketone **4.17** synthesized in high yield and enantioselectivity, we then explored the methods for the installation of the methyl and vinyl groups (Scheme 4.4). Retrosynthetically, the desired product required the installation of the vinyl group before the methyl group. However, we envisioned that a direct installation of vinyl group on **4.17** would potentially lead to a mixture of

⁵ Simmons, E. M.; Mudryk, B.; Lee, A. G.; Qiu, Y.; Razler, T. M.; Hsiao, Y. *Org. Process Res. Dev.* **2017**, *21*, 1659.

the desired product and a isomerized enone product. The methylation of the latter would run into the problem of a competing side reaction where the methyl group being installed on the other α -carbon of the carbonyl group. To avoid this complication, we decided to first subject ketone **4.17** to formylation, then, methylate the resulting dicarbonyl intermediate and ultimately transform the formyl group into a vinyl group. The formation of ketone **4.17** gave a good yield with ethyl formate as the formylation reagent with a 13:1 regioselectivity, which could be improved to 26:1 by switching to isopropyl formate.



Scheme 4.4. Enantioselective synthesis of ketone **4.1**.

The methylation reaction of **4.18** turned out to be problematic. The initial reaction conditions using potassium *tert*-butoxide and *tert*-butanol provided large amounts of undesired O-methylated products and the diastereoselectivity of the C-methylation was also mediocre. Exploration of other methylation conditions showed that MeI under basic conditions gave the most promising results and further screening led us to TBAF as the best base for the transformation. It was found that alcohol co-solvents gave improved C versus O selectivity as well as diastereoselectivity. Upon

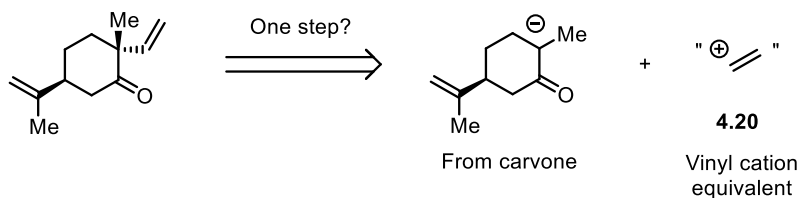
extensive screen of various co-solvents at different ratios led us to the conditions shown in Scheme 4.4, which provided the desired product **4.19** in the highest yield.

Of the two carbonyl groups on **4.19**, the aldehyde was more electrophilic and sterically more accessible. Therefore, selective methylenation of the aldehyde was achieved through Wittig reaction, affording the desired product **4.1** in only four steps enantioselectively.

4.4 The Development of a Novel Hypervalent Organobismuth Based Vinylation Reagent

Despite that a short and efficient 4-step synthesis of ketone **4.1** was achieved, we still wondered if there was an even quicker synthesis. Ideally, **4.1** could be synthesized in one step, directly from the corresponding enolate, easily generated from carvone through *in situ* 1,4-reduction, by trapping with a vinyl cation equivalent (Scheme 4.5). However, most of the known vinyl cation equivalents, such as the selenoaldehyde reagent **4.14** as discussed in section 4.2, required multiple manipulations before they were eventually transformed into a vinyl group. The only one-step vinylation of ketone enolates that could potentially meet our demand were palladium catalyzed vinylation variants, but the lack of examples of vinylation at ketone enolates to form quaternary carbon centers and the potential complication of regioselectivity were concerning.⁶ In addition, the probably incompatibility of the 1,4-reducing conditions with the palladium catalyzed protocols also made the transformation less attractive. Our strong desire for a robust vinylation reaction condition prompted us to dig into literature and the overlooked hypervalent organobismuth chemistry caught our attention.

⁶ Selected ketone alkenylation reactions catalyzed by transition metals: (a) Chieffi, A.; Kamikawa, K.; Ahman, J.; Fox, J. M.; Buchwald, S. L. *Org. Lett.* **2001**, *3*, 1897. (b) Grigalunas, M.; Ankner, T.; Norrby, P-O.; Wiest, O.; Helquist, P. *Org. Lett.* **2014**, *16*, 3970.



Scheme 4.5. A better solution: vinylation using a vinyl cation equivalent

4.4.1 Reactivities Between Hypervalent Organobismuth Compounds and Carbonyl Derived

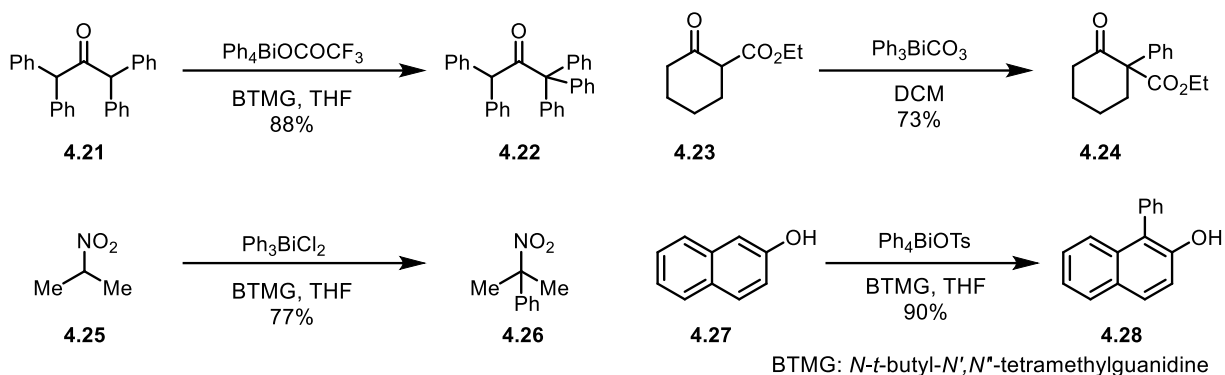
Nucleophiles

In 1978, Barton and co-workers first introduced the hypervalent organobismuth compounds into the organic community.⁷ Extensive work on these fascinating species were later performed mostly by the same group in the 1980's (Scheme 4.6).⁸ These seminal works showed that the aryl group of the hypervalent organobismuth species were good electrophiles for carbon-based nucleophiles accessed from deprotection of an acidic C-H bond, such as 1,3-dicarbonyls, α -nitroalkane, and in some cases, phenols.

⁷ Barton, D. H. R.; Kitchin, J. P.; Motherwell, W. B. *J. C. S. Chem. Comm.* **1978**, 24, 1099.

⁸ Selected examples: (a) Barton, D. H. R.; Lester, D. J.; Motherwill, W. B.; Papoula, M. T. B. *J. C. S. Chem. Comm.* **1980**, 26, 246. (b) Barton, D. H. R.; Blazejewski, J.; Charpiot, B.; Motherwell, W. B. *J. C. S. Chem. Comm.* **1981**, 27, 503. (c) Barton, D. H. R.; Charpiot, B.; Motherwell, W. B. *Tetradedron Lett.* **1982**, 23, 3365. (d) Barton, D. H. R.; Bhatnagar, N. Y.; Blazejewski, J.; Charpiot, B.; Finet, J.; Lester, D. J.; Motherwell, W. B.; Papoula, M. T. B.; Stanforth, S. P. *J. Chem. Soc. Perkin Trans. I* **1985**, 2657. (e) Barton, D. H. R.; Finet, J.; Giannotti, C.; Halley, F. J. *J. Chem. Soc. Perkin Trans. I* **1985**, 241.

1980's Barton



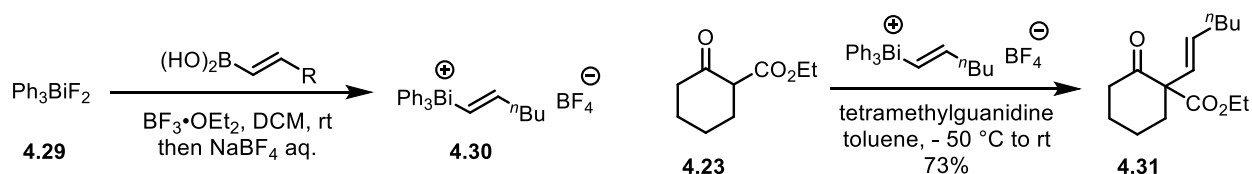
Scheme 4.6. Barton's early exploration of hypervalent organobismuth chemistry.

A few issues of the early work restricted their wide application in organic synthesis. The major problem was that the organobismuth compounds studied were mostly homoleptic, wherein all the aryl substituents, oftentimes a simple phenyl group, were the same and only one of which would eventually be transferred onto the nucleophile. The arylbismuth species after the reaction could not be recycled in most cases, which results in a low utilization rate of the aryl groups. Hence the use and practicality in synthesis has been limited, especially when the aryl group to be transferred were difficult to access. This problem was in large extent due to the lack of an efficient method of synthesizing heteroleptic organic bismuth compounds. Partly because of this reason, the chemistry of alkenyl substituted organobismuth compounds were not studied due to the stability of the trialkenylbismuth species. Furthermore, the more reactive tetrasubstituted bismuth(V) species required multiple steps to synthesize while the easier-to-access triaryl bismuth(V) dianion species (anions = Cl^- , OAc^- , CO_3^{2-} , etc.), were only reactive enough towards 1,3-dicarbonyl based nucleophiles but not particularly effective towards harder nucleophiles such as ketone enolates.

During the mid-90's and early 2000's, Matano and co-workers reported the breakthrough findings that heteroleptic organobismuth compounds could be synthesized conveniently from

triarylbismuth difluoride and organotin, organosilicon or organoboron species.⁹ Both aryl and alkenyl groups of the organo-tin, -silicon and -boron species were able to transmetalate onto the bismuth(V) center to form the tetrasubstituted, cationic organobismuth compounds that are stable to air and water. In fact, these cationic organobismuth species were isolated through aqueous workup. The same research group revealed later that the cationic, triaryl-monoalkenylbismuth compounds behaved similarly to the triarylbismuth(V) dianion species when reacting with 1,3-dicarbonyl based nucleophiles (Scheme 4.7).¹⁰ It was found that the more electron deficient alkenyl group transferred favorably over the aryl group as the electrophile.

2004, Matano



Scheme 4.7. Matano's study of triaryl-monoalkenylbismuth compounds.

Although the nucleophiles studied for the early organobismuth chemistry were majorly 1,3-dicarbonyl-based nucleophiles, Maruoka and co-worker demonstrated in 2003 that silyl enol ethers derived from ketones could also act as nucleophiles when reacting with tetraphenylbismuth monofluoride.¹¹ Particularly, a few examples were shown where *tri-p*-tolyl-styrenylbismuth monofluoride reacted with silyl enol ethers and afforded α -alkenyl ketones as the products.

⁹ (a) Matano, Y.; Yoshimune, M.; Azuma, N.; Suzuki, H. *J. Chem. Soc., Perkin Trans. 1*, **1996**, 1971. (b) Matano, Y.; Begum, S. A.; Miyamatsu, T.; Suzuki, H. *Organometallics* **1998**, *17*, 4332. (c) Matano, Y.; Begum, S. A.; Miyamatsu, T.; Suzuki, H. *Organometallics* **1999**, *18*, 5668.

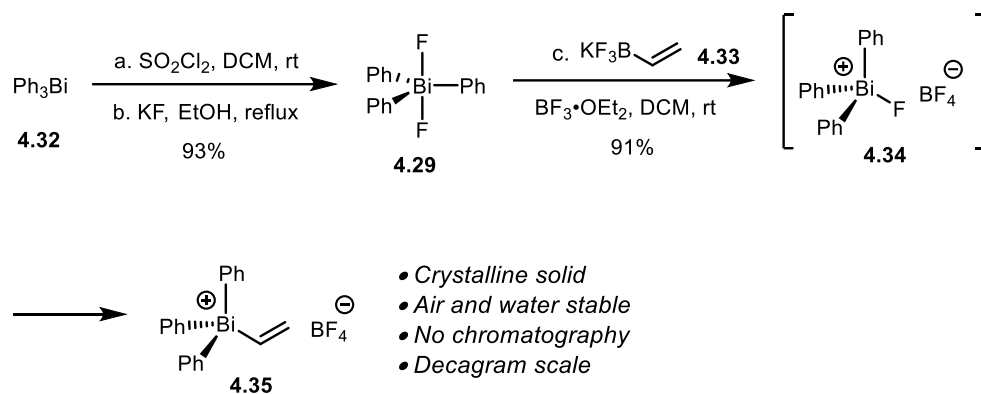
¹⁰ Matano, Y.; Imahori, H. *J. Org. Chem.* **2004**, *69*, 5505.

¹¹ Ooi, T.; Goto, R.; Maruoka, K. *J. Am. Chem. Soc.* **2003**, *125*, 10494.

4.4.2 Synthesis of A Novel Vinylbismuth Reagent

Based on the reactivities of the bismuth(V) compounds, we envisioned that a one-step vinylation reaction of a ketone enolate is feasible through a proper vinyl-containing bismuth(V) compound, but with a few underlying complications. To start with, no vinyl-containing bismuth(V) species were ever reported and no data on the stability of these species were available. Furthermore, as stated in Matano's studies on the monoalkenylbismuth compounds, the alkenyl group underwent an elimination side reaction pathway under basic conditions and forms the corresponding alkynes, which could be a problem when the more basic ketone enolates were used instead of 1,3-dicarbonyl anions. Despite these possible issues, the hypervalent organobismuth chemistry seemed rather promising as a solution for a facile one-step vinylation reaction and we decided to explore its potential.

The synthesis of triphenylvinylbismuth(V) tetrafluoroborate is shown in Scheme 4.8. Commercially available triphenylbismuth was first oxidized to triphenylbismuth dichloride by sulfuryl chloride in DCM at room temperature. The two chlorides were then displaced by fluoride in the presence of excess KF in a refluxing EtOH and water mixture. Interestingly, in the first few attempts, even though NMR of the crude reaction showed full conversion of Ph_3BiCl_2 to Ph_3BiF_2 , much Ph_3BiClF was observed after aqueous workup. It was later revealed that Ph_3BiClF arose from Ph_3BiF_2 reacting with NaCl when brine was used as the last step of the aqueous workup procedure. The simple omission of the brine wash step solved the problem. It is worth noting that Ph_3BiF_2 is also commercially available but expensive.

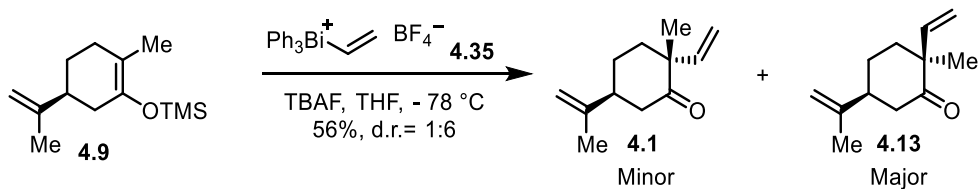


Scheme 4.8. Synthesis of the vinylbismuth reagent **4.35**.

The next step was the installation of the vinyl group onto the bismuth(V) center based on the procedure developed by the Matano group.¹⁰ One of the fluorides on Ph_3BiF_2 was pulled off by $\text{BF}_3 \cdot \text{Et}_2\text{O}$, providing intermediate **4.34**, which is an isolable, semi-stable solid that is difficult to crystallize. The tetrasubstituted intermediate **4.34** could then undergo transmetalation with vinylboronic acid at room temperature to afford the product **4.35** after an aqueous workup with saturated NaBF_4 solution, which exchanges the anion to tetrafluoroborate. Vinylboronic acid was expensive and supplied by a limited number of vendors, so we replaced it with the inexpensive, widely accessible potassium vinyltetrafluoroborate that underwent the transmetalation step with an even higher rate. The product was obtained a stable, crystalline, free-flowing solid that maintained its reactivity after a 20-month store in a fridge under air. Attempts to make triphenylvinylbismuth(V) monofluoride that is similar to the compounds reported in the Maruoka work, all failed. Triphenylbismuth(III) was the only product isolated after reacting of **4.35** with various fluoride sources.

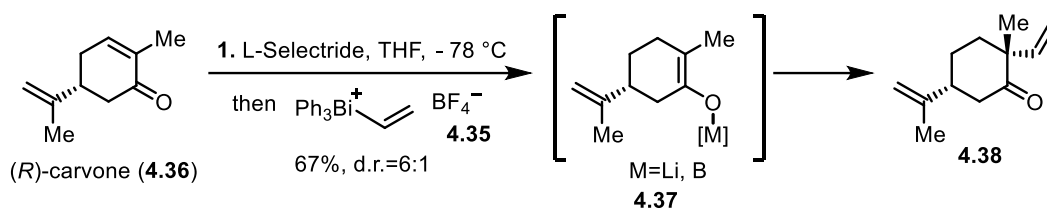
4.4.3 Synthesis of Ketone **4.37** with the Vinylbismuth Reagent

With the vinylbismuth reagent in hand, we then tested its ability of vinyllating ketone enolate **4.9**. Silyl enol ether **4.9** was first used as the enolate precursor. As shown in Scheme 4.9, the addition of TBAF to a mixture of **4.9** and the vinylation reagent **4.35** in THF at $-78\text{ }^{\circ}\text{C}$ provided the desired vinylation products in 56% yield with a 6:1 d.r. favoring **4.13**. The reaction gave a similar yield when TBAF was premixed with the silyl enol ether **4.9** at $-78\text{ }^{\circ}\text{C}$ before the addition of **4.35** as a solid.



Scheme 4.9. One-step vinylation of TMS silyl enol ether.

Although attempts of altering the inherent diastereoselectivity were unsuccessful, we reasoned that the enantiomer of the major diastereomer **4.13**, namely **4.38** (Scheme 4.10) was also a useful ketone precursor for the synthesis of some of the pentacyclic ambiguines (detailed discussion in Chapter 5). Therefore, we continued the exploration of the vinylbismuth chemistry and sought for an even more efficient synthesis of ketone **4.38**. Ultimately, we found that ketone enolate **4.37**, generated *in situ* from the 1,4-reduction of carvone with L-Selectride, also underwent vinylation to afford the products in 67% yield with the same 6:1 d.r. The borane from L-Selectride was found to be compatible with the oxidizing vinylbismuth reagent.



Scheme 4.10. One-step synthesis of ketone **4.38** from (*R*)-carvone.

4.5 Conclusion

In summary, the synthetic route towards ketone **4.1** in our first-generation synthesis of ambiguine P was lengthy and offset the high efficiency of our [4+3] cycloaddition strategy for the construction of the pentacyclic scaffold of ambiguine. The demand of a highly efficient synthesis of **4.1** prompted us to develop a 4-step enantioselective synthesis of **4.1** enabled by a rhodium-catalyzed Hayashi addition reaction. During this process, we also encountered a surprising gap in the methodology development for a one-step vinylation reaction of ketone enolates. To solve this problem, we resorted to the overlooked hypervalent organobismuth chemistry and developed a novel vinylbismuth(V) reagent that is stable, easy to handle and effective towards the vinylation of ketone enolate derived from dihydrocarvone. Enabled by this new reagent, ketone **4.38** was synthesized in merely one step from carvone through a sequential 1,4-reduction and vinylation reaction.

Chapter 5

Total Syntheses of Ambiguine P and Ambiguine Q Within Nine-steps From Carvone

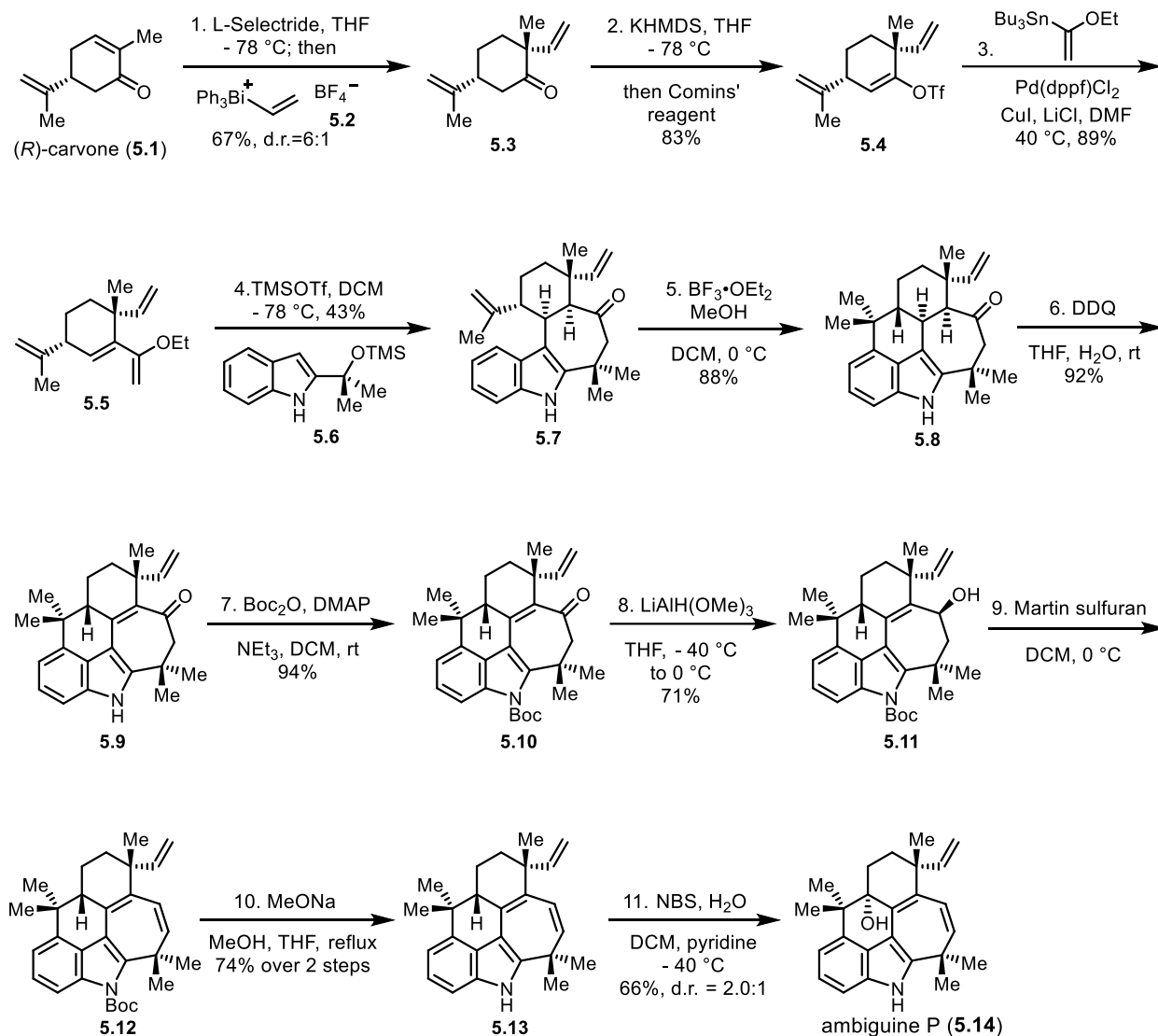
With the new and efficient syntheses of different functionalized cyclohexanones, we set out to synthesize ambiguityine Q. Our previous studies towards ambiguityine Q showed that the functionalization of the C23 π bond with electrophiles often led to the formation of by-products arising from deprotonation at C15, instead of at the desired C23 position (Section 3.3.3). A probable solution to this complication was to replace the C15 hydrogen with a heteroatom that has a low tendency to leave as a cation. Naturally, ambiguityine P, due to its C15 hydroxyl group, was deemed to be an ideal precursor for the synthesis of ambiguityine Q. But the lengthy syntheses of ambiguityine P reported previously (21 steps by Sarpong and co-workers and 20 steps by our group)¹ made this approach less appealing and practical. Therefore, the development of a new, efficient synthesis of ambiguityine P was necessary.

5.1 Second-Generation Synthesis of Ambiguine P

A key insight of our new synthesis of ambiguityine P came from our proposed mechanism of the formation of ambiguityine P from diene **3.54** through NBS oxidation (Section 3.3.2). In our previous synthesis, a cationic intermediate with much sp^2 character on C15 was proposed, and the only stereogenic center left on the molecule was the C12 quaternary center. In other words, the chirality at the C15 position of the starting material was destroyed in the reaction and the stereo-outcome

¹ See section 3.3 for references.

at the C15 position of the C-O bond forming step should be governed solely by the C12 position whose stereochemistry was pre-set. Based on this proposed mechanism, we hypothesized that both diene **3.54** and its C15 epimer **5.13** should provide ambigine P and its C15 epimer with the same ratio. As an inference of this hypothesis, both ketones **4.1** and **5.3**, despite having different chirality at the isopropenyl attaching carbon, ought both afford ambigine P with the same diastereoselectivity. While ketone **4.1** took eight operations to make, or four steps using our enantioselective route, ketone **5.3** could be accessed in merely one single step enabled by our vinylation reagent. The use of the latter route should significantly increase the efficiency of the synthesis of ambigine P and provide enough material to further explore the chemistry towards ambigine Q.



Scheme 5.1. Second-generation synthesis of ambiguine P.

Therefore, we started to develop our second-generation synthesis of ambiguine P using ketone **5.3** as the starting material, with the hope that the change of chirality at the isopropenyl position would have no deleterious effect in any of the following steps (Scheme 5.1). The triflation of **5.3** using KHMDS and Comins' reagent and subsequent Stille coupling reaction gave ethoxy diene **5.5** in a slightly higher overall yield compared to the congener obtained in our first-generation synthesis. The [4+3] cycloaddition reaction with the TMS protected indole alcohol **5.6** proceeded

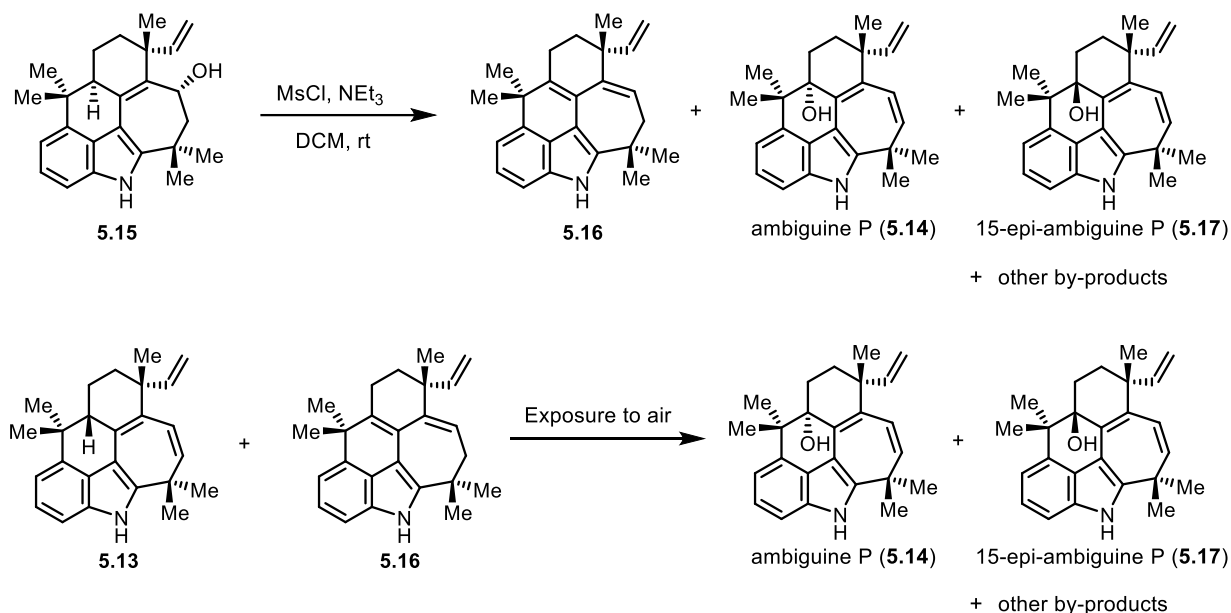
smoothly, providing the cycloadduct in 43% yield.² Proton induced Friedel-Crafts type cyclization afforded **5.8**, whose oxidation by DDQ was noticeably slower than its C15 epimer analogue. It took 6 hours instead of 2 hours for the reaction to achieve full conversion, but the isolated yields were similar. The enone product **5.9** was protected by Boc at the indole nitrogen position and then reduced to the corresponding alcohol with LiAl(OMe)₃H formed *in situ* from LiAlH₄ and MeOH. A dehydration reaction induced by Martin sulfurane and Boc deprotection under basic conditions led to the diene product **5.13**, which was oxidized with the NBS condition to give ambiguiene P and its C15 epimer with the same 2.0:1 ratio and a similar yield compared to that of our first-generation synthesis.

5.2 Third-Generation Synthesis of Ambiguiene P: A 6-step Synthesis of Ambiguiene P From (R)-Carvone

Through our second-generation synthesis, we confirmed that ketone **5.3** was a valid starting material to generate ambiguiene P and all the reactions gave similar results compared to their counterparts in our first-generation synthesis. Next, we wanted to eliminate the need of a Boc protection in the reaction sequence. The Boc protection was first introduced to the synthetic route for the synthesis of the desired diene **5.13**. Otherwise, dehydration performed on alcohol **5.15** always provided the undesired cross-conjugated diene **5.16** as the major product under all the dehydration conditions tried (Scheme 5.2). Remarkably, it was found that when dehydration was performed in the presence of MsCl and NEt₃ in DCM under air, ambiguiene P could be obtained

² For the related [4+3] cycloaddition of the C15 isomer, see: Xu, J. Synthetic studies toward ambiguiene natural products and total synthesis of (-)-ambiguiene P. *Ph.D. Dissertation*, University of Chicago, Chicago, IL. 2019.

directly. In contrast, only the dehydration products were observed when the reaction was performed under argon. Unfortunately, the reaction gave irreproducible yields on scales larger than 2 mg and optimizations of the reaction conditions failed.³

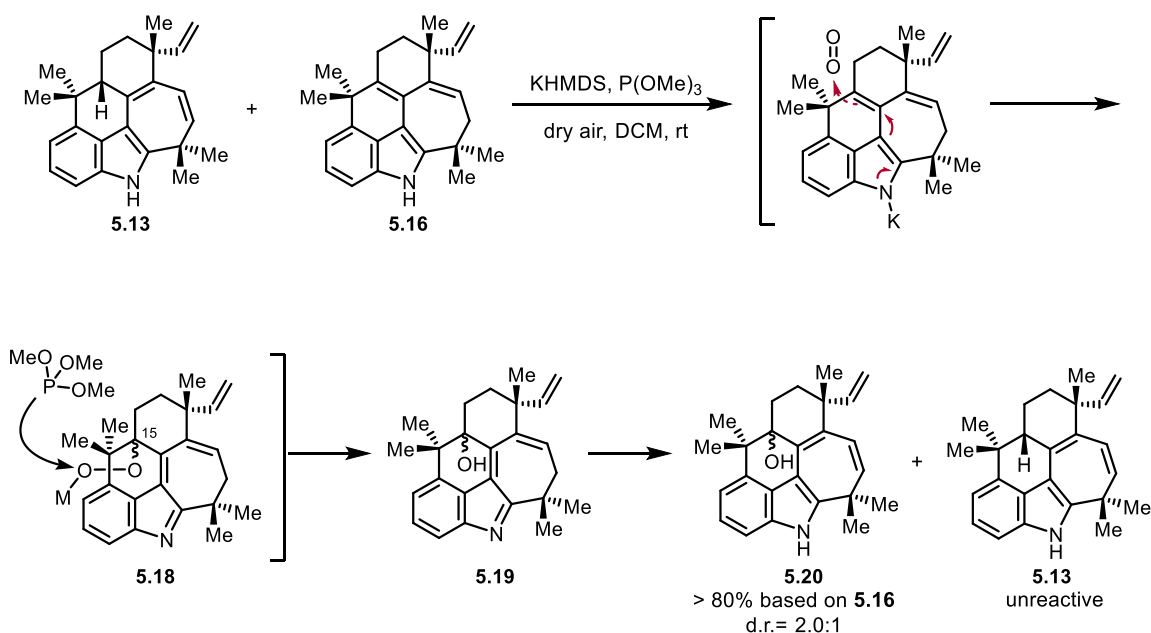


Scheme 5.2. Serendipitous findings of unexpected generation of ambiguine P.

In our second-generation synthesis of ambiguine P, a related reactivity was also observed. It was found serendipitously that the crude NMR of the mixture of diene **5.13** and cross-conjugated diene **5.16** after aqueous work often contained signals from ambiguine P in low intensity and the longer time the mixture was let exposed to air, the more obvious the peaks of ambiguine P. The cross-conjugated diene was later confirmed to be the substrate that is being oxidized to ambiguine P while diene **5.13** was inert to a short-period exposure to air. Combining this observation with the finding from the MsCl conditions, we hypothesized that the C10-C15 double bond was rendered highly electron rich and easily oxidizable by air due to a great overlap with the indole ring as a

³ Reactions performed by Dr. Jiasu Xu.

result of the ground state conformation of the pentacyclic ring system. Based on this hypothesis, different conditions were screened for the oxidation of cross-conjugated diene **5.16** and the combination of KHMDS and P(OMe)₃, a condition mostly applied for the hydroxylation of ketone enolate with oxygen gas, was found to provide the best results (Scheme 5.3). The KHMDS base probably facilitates the rate of air oxidation by deprotonating the N-H bond and thereby increasing the electron density of the of the C10-C15 double bond. The thus generated peroxide was then reduced by P(OMe)₃ to the alcohol product **5.19**, which was observed in crude NMR after aqueous workup. The imine formed **5.19** then tautomerized during aqueous workup as well as on silica gel, affording cleanly ambigine P and its C15 epimer.

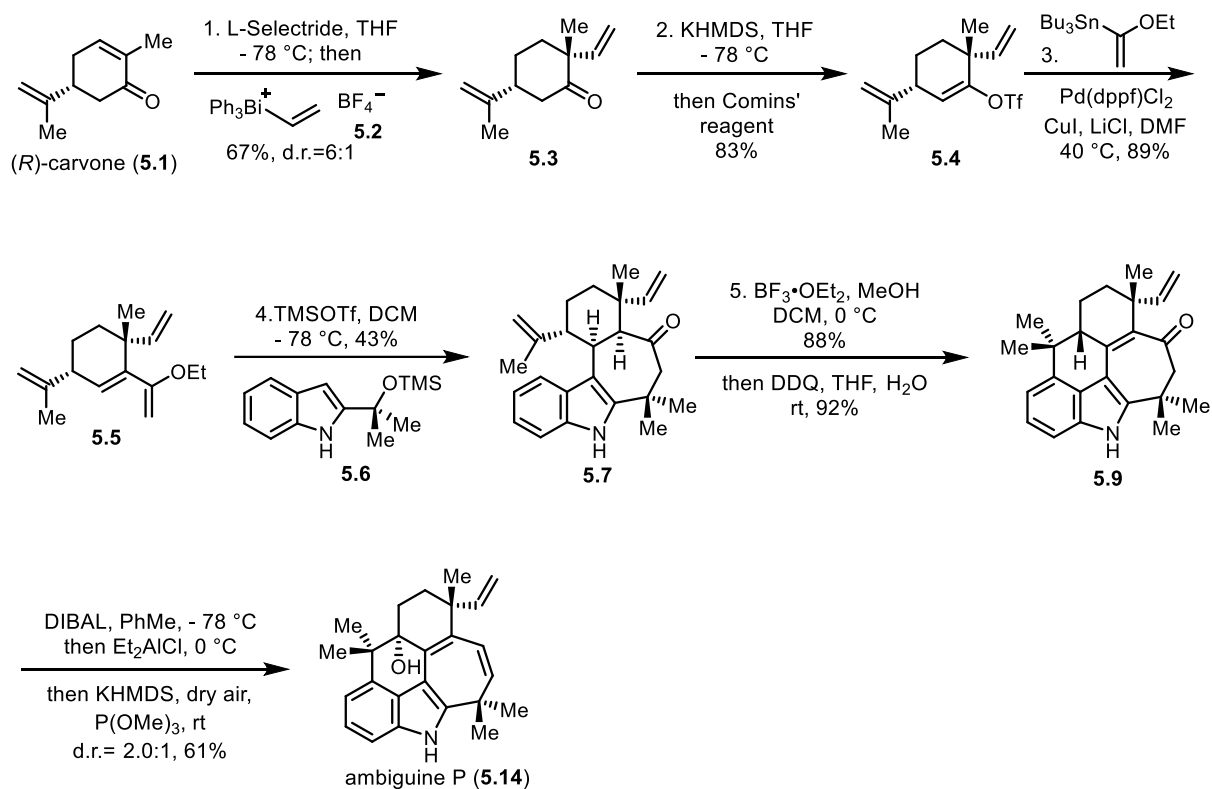


Scheme 5.3. Conversion of the mixture of dienes **5.13** and **5.16** into ambigine P through controlled air oxidation.

The enone reduction and dehydration steps were then combined with the oxidation step in one pot. It was found that DIBAL provided the cleanest reduction of the carbonyl group of **5.9**, and an addition of Et₂AlCl into the reaction mixture provided the highest ratio of cross-conjugated diene

5.16 to diene **5.13**. P(OMe)₃ was then added both as a reductant for the oxidation step as well as a quencher for the aluminum Lewis acids. Finally the addition of KHMDS while the reaction was stirring under a dry air atmosphere provided ambigine P and 15-*epi*-ambigine P in good yield and the same 2.0:1 d.r. as observed under the NBS oxidation conditions used in the previous-generation syntheses, a proof of our hypothesis that the diastereo-outcome at the C15 position is merely governed by the stereogenic C12 position.

With this one-pot reduction-dehydration-oxidation condition optimized, we further combined the Friedel-Crafts cyclization and the DDQ oxidation step (Scheme 5.4). The DDQ oxidation was first found to proceed smoothly in DCM, the solvent used in the cyclization step. However, a direct addition of DDQ to the Friedel-Crafts cyclization mixture after its completion led to the mixture of multiple unidentified products but not the desired product. Apparently BF₃·Et₂O was the cause of this unexpected result and it was therefore quenched by TBAF before the addition of DDQ. It was also found that the oxidation steps often provided low yields under strongly basic conditions and a small amount of water was thus added to the reaction mixture to attenuate the basicity of the naked fluoride ion.



Scheme 5.4. Third-generation synthesis of ambiguine P: 6 steps from (*R*)-carvone.

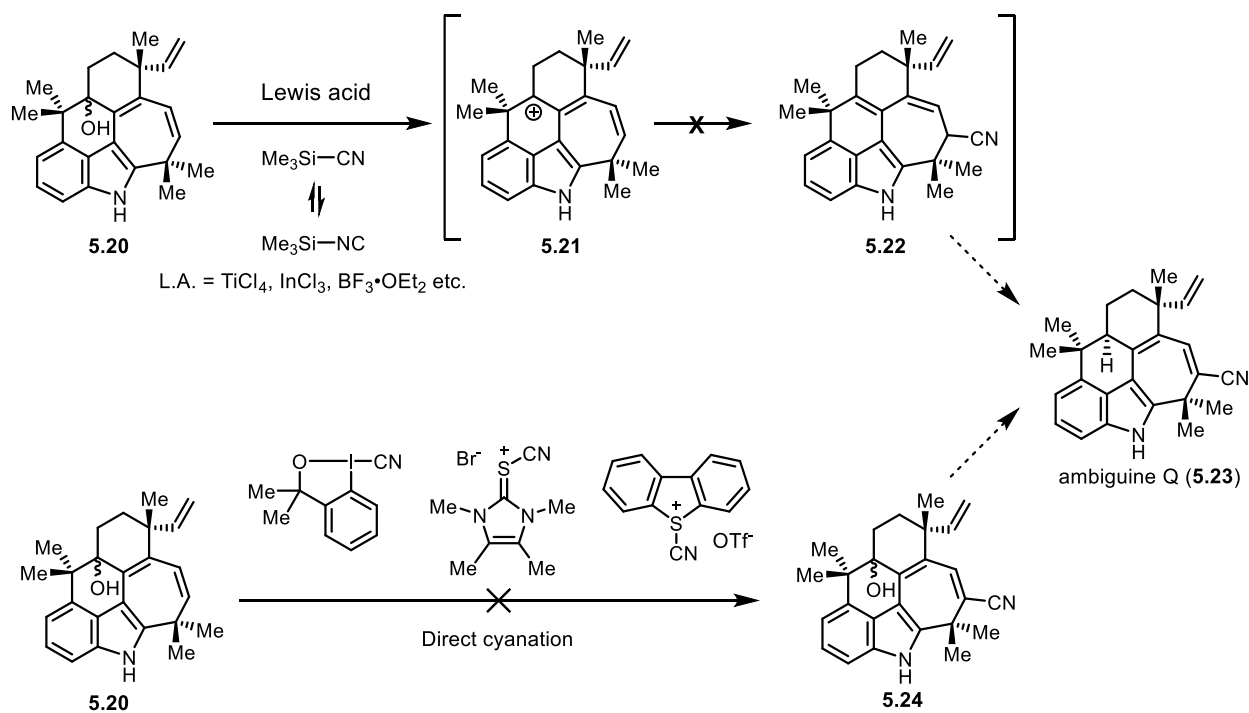
Ultimately, our key insight that the easily accessible ketone **5.3** was a valid replacement of ketone **4.1**, combined with the serendipitous finding that the cross-conjugated diene could be transformed into ambiguine P through air oxidation, helped us develop a highly efficient, 6-step synthesis of ambiguine P from (*R*)-carvone. The route provided ample supply of ambiguine P and 15-*epi*-ambiguine P, with which we further explore the chemistry towards ambiguine Q.

5.3 Synthesis of Ambiguine Q from Ambiguine P

Noticing that the C15 hydroxyl group of ambiguine P is at the allylic position of the diene extending from C10 to C23, we first wondered if a $\text{S}_{\text{N}}1$ -type reaction would provide a C23 functionalized product, which might be tautomerized into the desired ambiguine Q. Various

reaction conditions involving Lewis acids for the activation of the C15 hydroxyl group and TMS-CN as the nucleophile were explored, but to no avail. Decomposition of ambigine P was the only observed process.

Direct cyanation at the C23 position was then investigated. Highly electrophilic cyanating reagents were tried but the ambigine starting material remained intact. Based on the reported reactivities of these electrophilic cyanating reagents,^{4,5} the absence of reactivity in the ambigine system was probably due to the sterics at the C22 position that prevented the electrophile from approaching the C23 position.



Scheme 5.5. Unsuccessful attempts towards ambigine Q from ambigine P.

⁴ Talavera, G.; Peña, J.; Alcarazo, M. *J. Am. Chem. Soc.* **2015**, *137*, 8704.

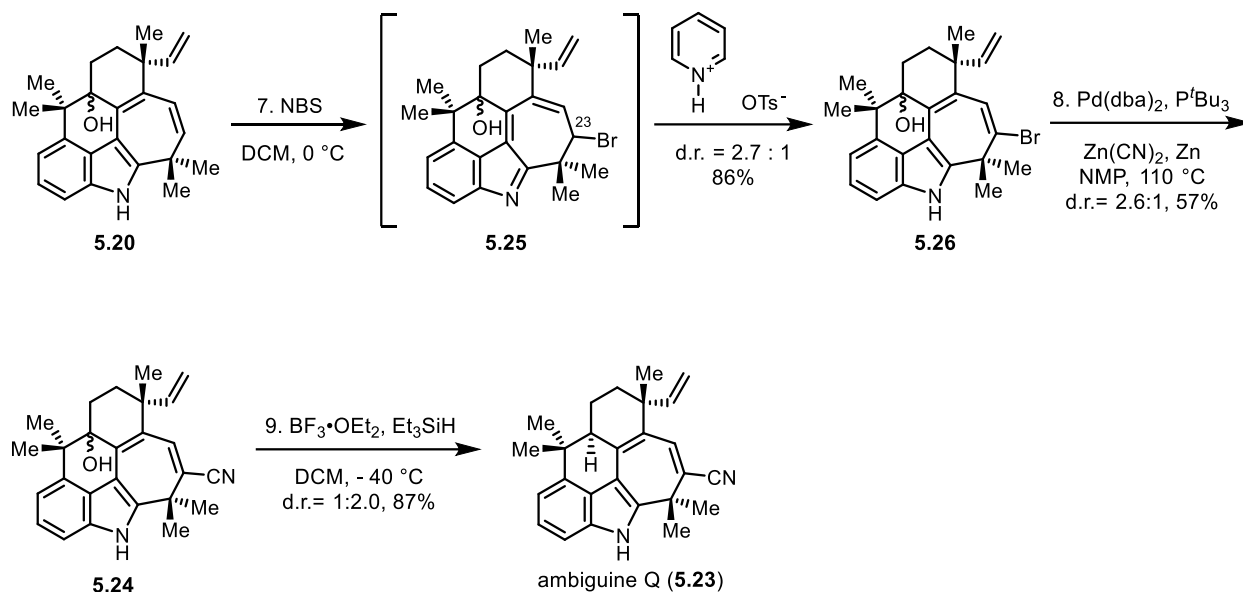
⁵ Li, X.; Golz, C.; Alcarazo, M. *Angew. Chem. Int. Ed.* **2019**, *58*, 9496.

Bromination of ambiguine P with NBS formed cleanly intermediate **5.25** (Scheme 5.6). The C23 position was selectively brominated in the presence of a terminal vinyl group, even at room temperature, probably due to the conjugation of the diene system with the indole ring. Intermediate **5.25**, with the C15 position blocked by the hydroxyl group, was semi-stable and only slowly tautomerized on silica gel. The tautomerization process was accelerated by the addition of pyridinium *p*-toluenesulfonate at room temperature, affording bromide **5.26**.

The transformation of the bromide into cyanide with palladium catalysis was then explored. The reaction condition was adapted from the work reported by Reuck-Braun and co-workers.⁶ The reaction first suffered from reproducibility issues; a known issue associated with palladium-catalyzed cyanation reactions. The yield could not be reproduced, and multiple by-products were obtained with different ratios in each run. After extensive experimentation, the ratio of zinc powder to palladium was found to be critical for the success of this transformation. A Zn:Pd ratio lower than 5 led to the initially observed irreproducible yields and multiple side reactions, but a simple increase of the Zn:Pd ratio to 10 provided a much cleaner reaction with consistent yields.

A reductive deoxygenation of cyanide **5.24** at – 40 °C in the presence of BF₃·Et₂O and excess Et₃SiH afforded a mixture ambiguine Q and 15-epi-ambiguine Q. After a final separation via chiral HPLC, ambiguine Q was ultimately obtained in 3 steps from ambiguine P and in a total of 9 steps from (*R*)-carvone, as a yellow solid.

⁶ Böttcher, C.; Zeyat, G.; Ahmed, S. A.; Irran, E.; Cordes, T.; Elsner, C.; Zinth, W.; Ruech-Braun, K. *Beilstein J. Org. Chem.* **2009**, *5*, No. 25.

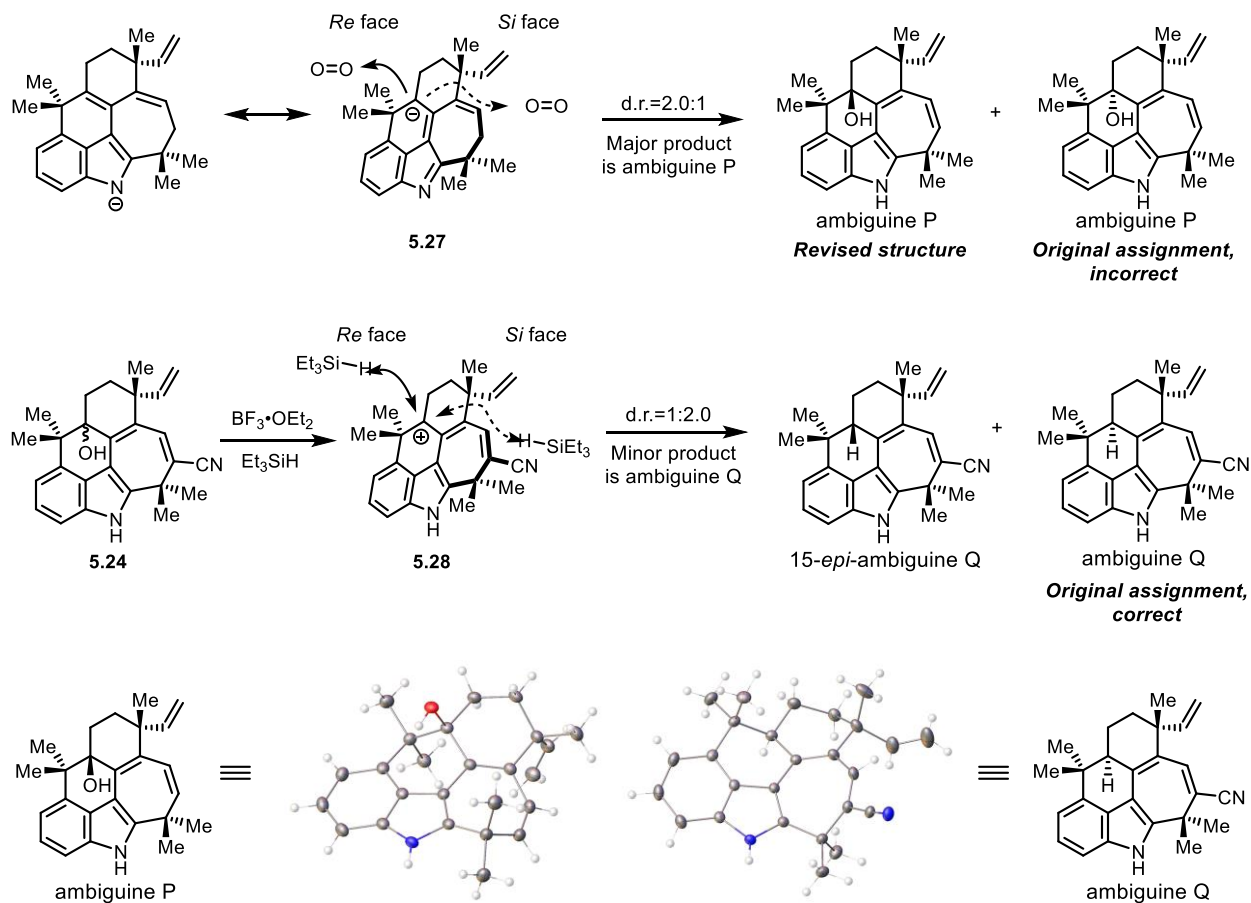


Scheme 5.6. Synthesis of ambiguiene Q from ambiguiene P.

5.4 Structural Revision of Ambiguiene P

Upon obtaining both ambiguienes P and Q, the diastereomer ratio observed in the two reactions leading to these natural products caught our attention. Ambiguiene P was the major diastereomer from the air oxidation reaction while ambiguiene Q was surprisingly the minor diastereomer from the reductive deoxygenation reaction. The d.r. values observed in both reactions were the same 2.0:1. However, as shown in Scheme 5.7, the chemical structures assigned to ambiguienes P and Q in the isolation paper suggested that the two natural products were the products of the electrophile (oxygen) or the nucleophile (Et₃SiH) approaching from the *Si* face of the proposed reaction intermediates **5.27** and **5.28**. Consequently, the two natural products should both be the major or the minor diastereomer obtained under the corresponding reaction conditions, which was inconsistent with the experimental result. This inconsistency led us to question the original assignment of ambiguiene P, since the C15 chirality of ambiguiene Q was consistent as the

corresponding carbon of ambiguines D and K whose structures had been confirmed by X-ray crystallography. Therefore, crystal structure data of both ambiguines P and Q were collected and the original assignment of ambigaine P was indeed incorrect at the C15 position.



Scheme 5.7. Structural revision of ambigaine P.

5.5 Conclusion

In conclusion, we achieved a 6-step total synthesis of ambigaine P and a 9-step total synthesis of ambigaine Q, starting from (*R*)-carvone. The high efficiency was made possible by a powerful one step ketone α -vinylation with the vinylbismuth reagent we developed, based on the insight

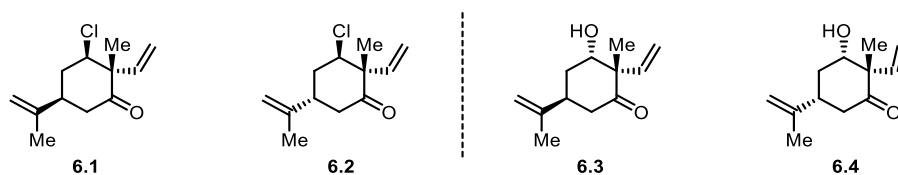
that ketone **5.3** would afford the ambigaine P with the same diastereoselectivity as ketone **4.1**, which was used in our first-generation synthesis but takes more steps to access. The synthetic route was made even more efficient by an unprecedented one pot reduction-elimination-oxidation sequence enabled by the unique reactivity embedded in the pentacyclic architecture of ambigaines. The inconsistency observed in the diastereoselectivity of the two reactions leading to ambigaines P and Q prompted us to investigate the structural assignment of the two natural products. The stereochemical assignment of the C15 hydroxyl group of ambigaine P was corrected based on single crystal X-ray analysis.

Chapter 6

Total Synthesis of Ambiguine G

Upon the successful synthesis of ambiguityine Q, we turned our attention to ambiguityine G, the 13-chloro analogue of ambiguityine Q.¹ In the ambiguityine family, all non-chlorinated ambiguityines had a 13-chlorinated congener, except ambiguityine P. We wished to use the synthesis of ambiguityine G to demonstrate that both non-chlorinated and 13-chloro ambiguityines could be accessed through the same, highly efficient [4+3] cycloaddition strategy.

6.1 Attempted Synthesis of Chloroketone **6.1** with the Vinylbismuth Reagent

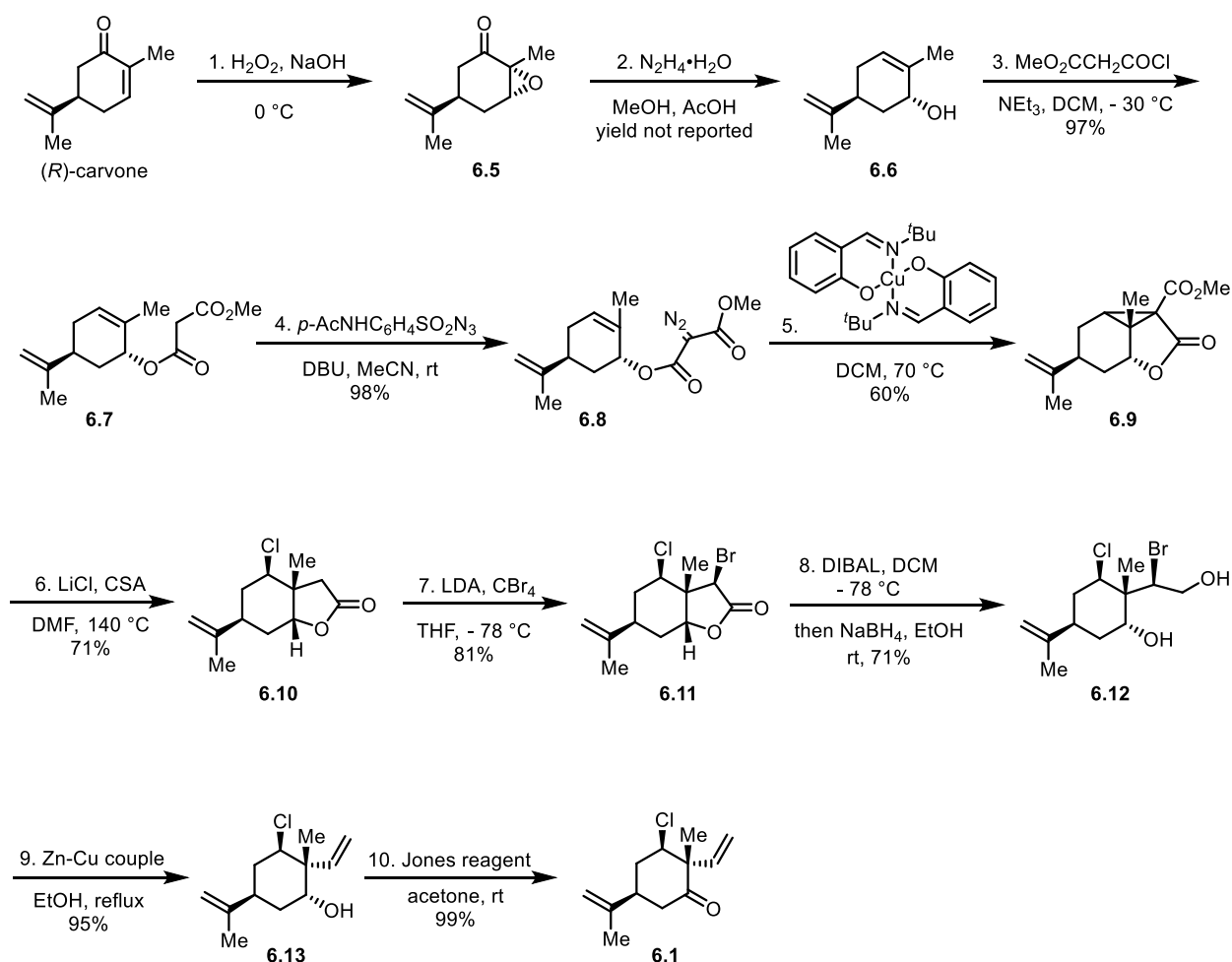


Scheme 6.1. Ketones suitable for the synthesis of ambiguityine G.

With the [4+3] cycloaddition strategy set, the key element for the synthesis of ambiguityine G was the synthesis of the ketones **6.1-6.4**. As discussed in Section 5.1, the chirality at the isopropenyl carbon was expected to have no impact in the synthesis. We decided to perform the early-stage chlorination and synthesize **6.1** or **6.2** to avoid a potential rearrangement involving the adjacent vinyl group in an advanced intermediate while performing a late-stage chlorination, as observed

¹ Huber, U.; Moore, R. E.; Patterson, G. M. L. *J. Nat. Prod.* **1998**, *61*, 1304.

in the synthesis of *N*-methylwelwitindolinone B.² Surprisingly, no synthesis of the seemingly simple chloroketone **6.2** was reported and only synthesis of **6.1** was achieved in 10-steps by Fukuyama and co-workers (Scheme 6.2) in their synthesis of hapalindole G, a structurally related natural product (*cf.* section 3.2).³ We therefore set out to devise a short synthesis of either ketone.

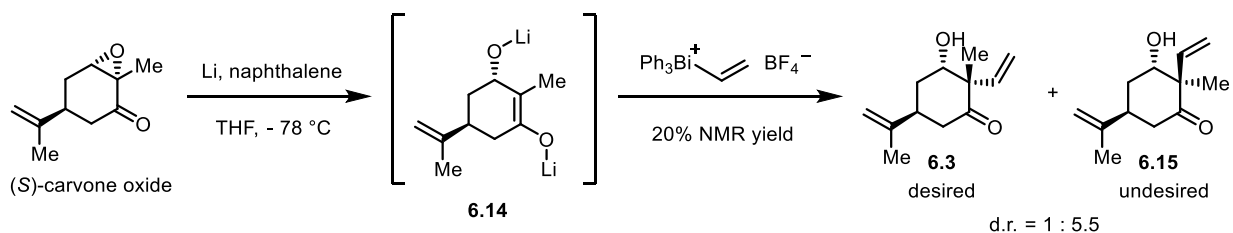


Scheme 6.2. Fukuyama's synthesis of chloroketone **6.1**.

² (a) Bhat, V.; MacKay, J. A.; Rawal, V. H. *Tetrahedron* **2011**, *67*, 10097. (b) Reyes, J. R.; Xu, J.; Kobayashi, K.; Bhat, V.; Rawal, V. H. *Angew. Chem. Int. Ed.* **2017**, *56*, 9962.

³ (a) Fukuyama, T.; Chen, X. *J. Am. Chem. Soc.* **1994**, *116*, 3125. (b) Chen, X. Total synthesis of (-)-hapalindole G: A novel tin-mediated indole synthesis. *Ph.D. Dissertation*, Rice University, Houston, TX, 1994.

We first attempted the synthesis of chloroketone **6.1** through ketone **6.3**. Potentially, **6.3** could be accessed through the bismuth(V) based vinylation of enolate **6.14**, which is easily generated from commercially available (*S*)-carvone oxide upon lithium naphthalene reduction. However, this route would only afford the desired product **6.3** if the hydroxyl group directed the cationic bismuth to approaching from the same face of the hydroxyl group. Otherwise, it is well documented that the electrophile would approach from the opposite face of the hydroxy group, due to both the ring conformation of the enolate as set by the isopropenyl group, as well as the steric repulsion between the incoming electrophile and the hydroxyl group. Experimentally, enolate **6.14** did react with the vinylbismuth reagent, but the undesired diastereomer was obtained as the major product. The observed 5.5:1 d.r. was comparable to the 6:1 d.r. in the synthesis of **5.3**, hinting that the lithium alkoxide had little to no directing effect. The reaction was thus not optimized for higher yield.

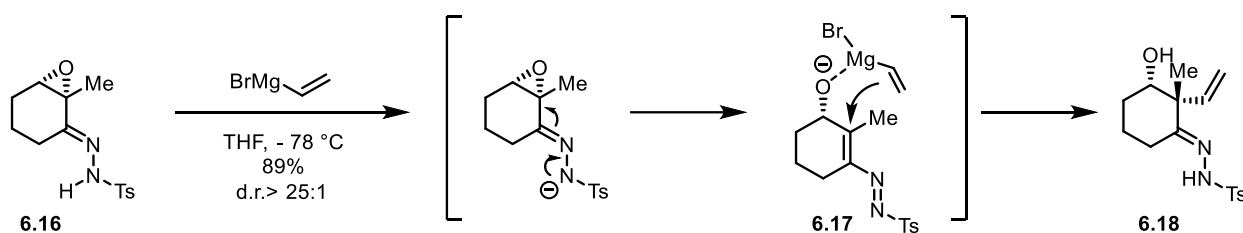


Scheme 6.3. Attempted synthesis of ketone **6.3** with the vinylbismuth reagent.

6.2 Synthesis of Chloroketone **6.1** Using Directed Vinyl Grignard Addition

In the search of a hydroxyl group directed ketone α -functionalization reaction, we were intrigued by an interesting reaction reported by Coltart and co-workers, who demonstrated that our desired hydroxyl group directed ketone α -functionalization could be achieved with α -epoxy *N*-

sulfonyl hydrazones using Grignard reagents, as shown in Scheme 6.4, with a high level of diastereoselectivity.⁴ It was proposed that one equivalent of Grignard generates an anionic nitrogen center through deprotonation, which then opens up the epoxide, forming an electrophilic α -carbon and an alkoxide that directs a second equivalent of Grignard to attack the α -carbon from the same face as the alkoxide. This transformation, despite never having been applied in natural product synthesis, seemed to be a promising solution to our problem.⁵ Thus, we decided to test this reaction on tosylhydrazone **6.19**.



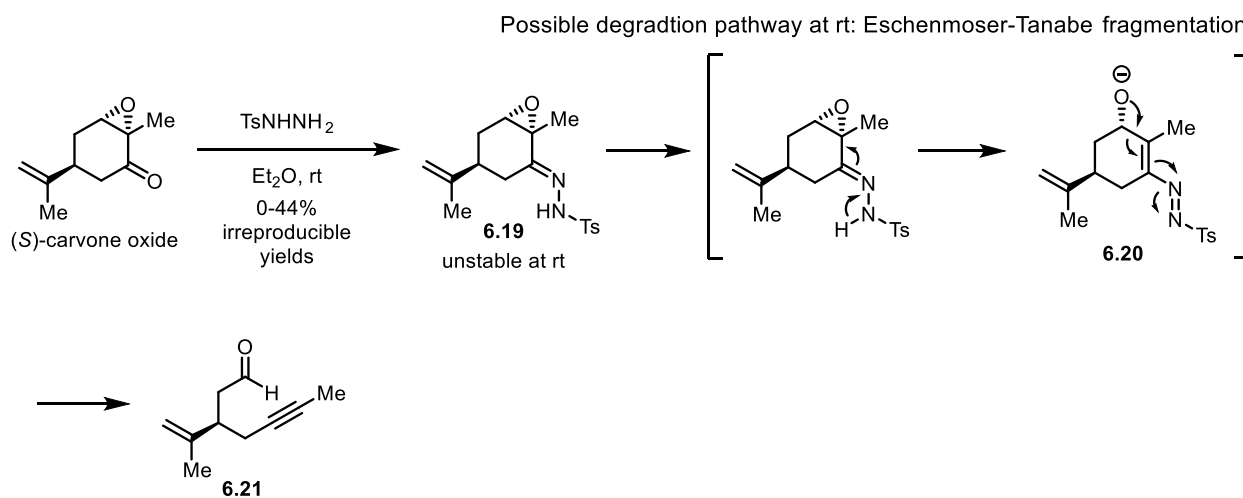
Scheme 6.4. Directed α -functionalization of α -epoxy *N*-sulfonyl hydrazones developed by Coltart and co-workers.

Initial attempts to synthesize **6.19** by condensing (*S*)-carvone oxide and tosyl hydrazide in Et₂O at room temperature resulted in low and irreproducible yields (0-44%). It was later found that tosylhydrazone **6.19** was not stable at room temperature and slowly degraded into various products, probably through the Eschenmoser-Tanabe fragmentation pathway. The reaction temperature was therefore maintained at 0 °C and the product was isolated via the removal of all volatiles *in vacuo*. Degradation of the product was still observed during the isolation step but to a much less extent.

⁴ (a) Uteuliyev, M. M.; Nguyen, T. T.; Coltart, D. M. *Nat. Chem.* **2015**, *7*, 1024. For similar transformations using organocuprates, see: (b) Corey, E. J.; Melvin, L. S. Jr.; Haslanger, M. F. *Tetrahedron Lett.* **1975**, *36*, 3117. (c) Fuchs, P. L. *J. Org. Chem.* **1976**, *41*, 2935. (d) Stork, G.; Ponaras, A. A. *J. Org. Chem.* **1976**, *41*, 2937.

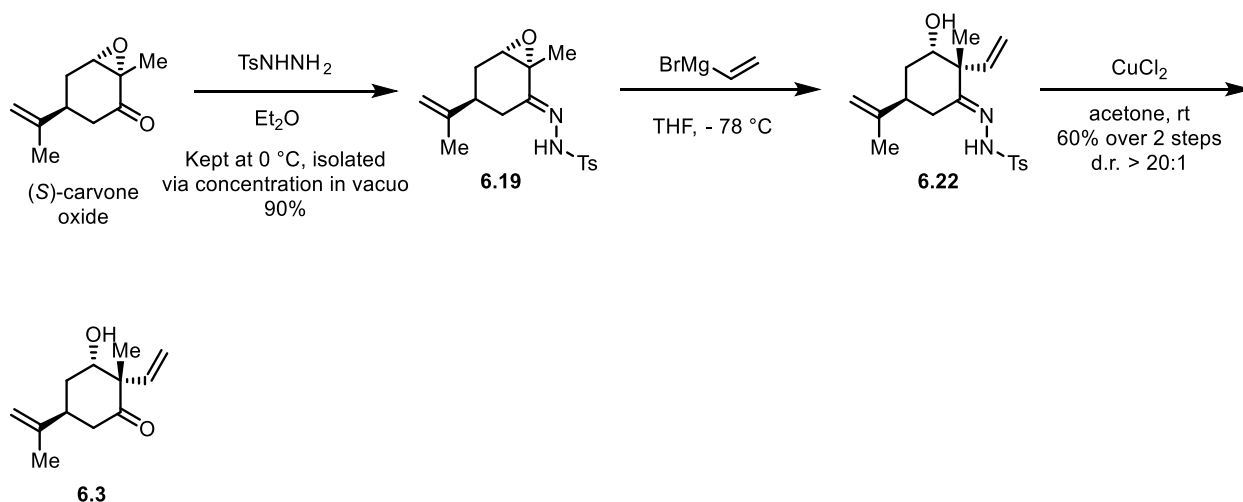
⁵ For related chemistry using oximes, see: Sawada, D.; Shibasaki, M. *Angew. Chem. Int. Ed.* **2000**, *39*, 209.

The directed Grignard addition provided the desired product with excellent diastereoselectivity, but the yield was moderate in large part due to the degradation of the deprotonated **6.19**, even at –78 °C. The addition product **6.22** was then isolated by column chromatography and subjected to hydrolysis in acetone with CuCl_2 as the catalyst.



Scheme 6.5. Problems with the synthesis of **6.19**.

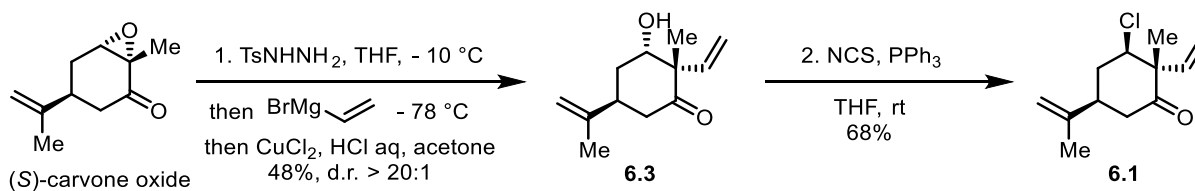
First-generation synthesis of ketone XXX:



Scheme 6.6. First-generation synthesis of **6.3**.

The three-step procedure succeeded in providing the desired hydroxyketone **6.3** but we wondered if they could be combined into one-step in order to minimize the degradation of **6.19** as well as to avoid a gram-scale chromatography step. The combination of the hydrazone condensation and the Grignard addition step was problematic since the Et₂O from the first transformation caused significant level of degradation of **6.19** upon Grignard addition, consistent with the results from Coltart and co-workers that Et₂O led to low yields. The problem was alleviated by switching the solvent of the hydrazone condensation to THF with the temperature kept below -10 °C. After the Grignard addition step, the basic solution was quenched by 1M HCl and the CuCl₂ catalyzed hydrolysis worked smoothly with the addition of acetone. With these optimizations, hydroxyl ketone was synthesized directly from (*S*)-carvone oxide in one pot with comparable yield to the overall yield of the three-step procedure.

Chloroketone **6.1** was then synthesized in one step from **6.3** through a stereoinvertive-deoxychlorination using *N*-chlorosuccinimide and PPh₃. Complete stereoinversion at the chlorine attaching carbon occurred and the stereoretentive chlorination product was not observed.



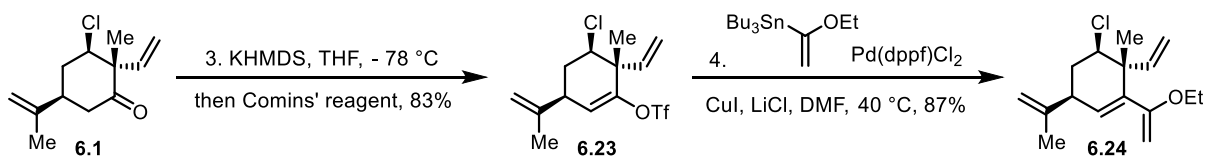
Scheme 6.7. Two-step synthesis of chloroketone **6.1**.

6.3 Synthesis of Ambiguine G

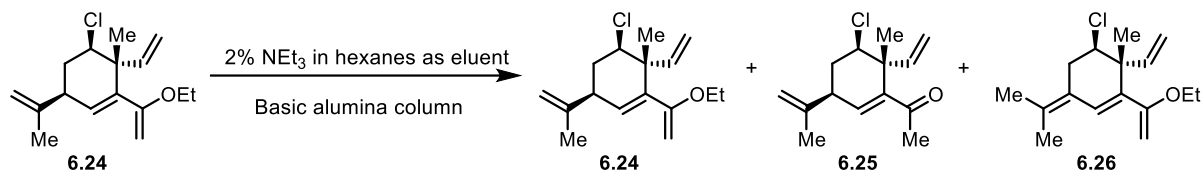
With chloroketone **6.1** in hand, we then started out to synthesize ambiguine G following the route developed for ambiguine Q. The ketone was first transformed into triflate **6.23** using

NaHMDS and Comins' reagent. A small amount of chlorine elimination product was observed in the first few trials and presumably arose from the elimination of the triflated product instead of the enolate of **6.1**. The elimination side pathway could be suppressed by a slow addition of a THF solution Comins' reagent to the enolate solution to maintain a low reaction temperature, as well as quenching the triflation step within 80 minutes.

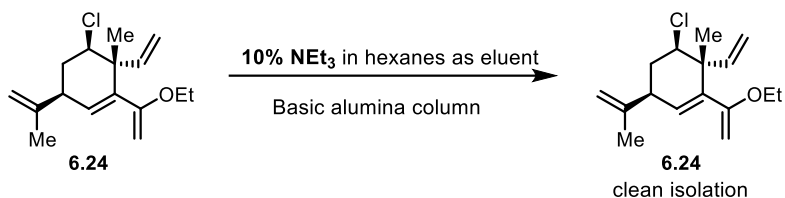
Siloxy diene **6.24** was then synthesized from **6.23** through Stille coupling. Although the reaction proceeded to afford **6.24** cleanly based on ^1H NMR of the reaction crude after aqueous workup, complications were encountered in the isolation process. The product underwent massive enol ether hydrolysis as well as alkene isomerization when rapidly flushed down a basic alumina column with 2% NEt_3 in hexane, the condition that worked flawlessly for the syntheses of ambiguines P and Q. Control experiments revealed that both side reaction pathways were induced not by NEt_3 but by basic alumina, probably due to a low level of acidic sites on the surface of the alumina particles. The eluent was therefore switched to 10% NEt_3 in hexane which, satisfyingly, suppressed the side reactions and gave **6.24** cleanly.



Sensitive ethoxy diene:



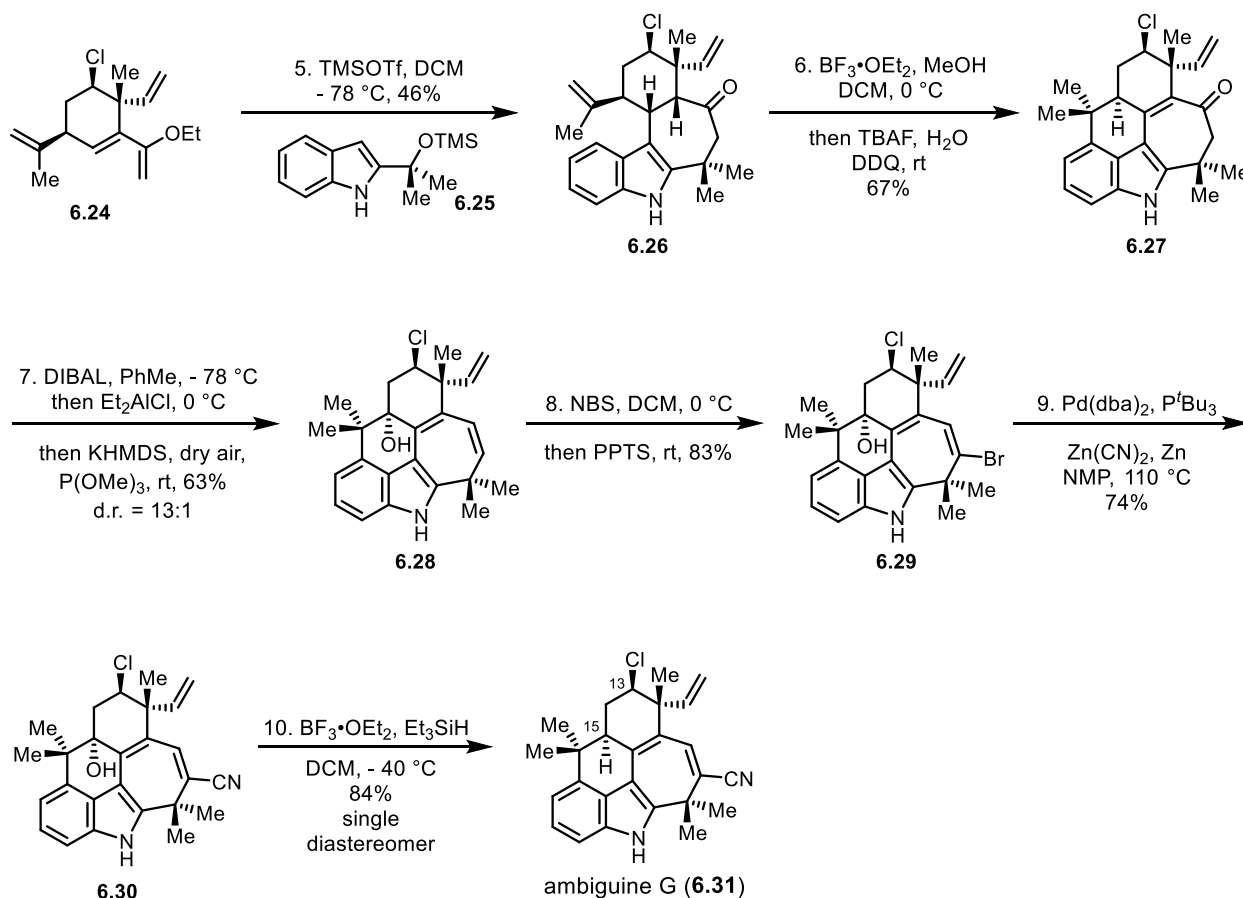
Unexpected solution to the isolation of ethoxy diene **6.24**: a simple increase of amount of NEt_3



Scheme 6.8. Synthesis and isolation of ethoxy diene **6.24**.

The [4+3] cycloaddition between **6.24** and **6.25** went smoothly, giving the cycloadduct **6.26** in 46% yield. The cyclization-oxidation sequence also worked well, but the reaction rate of the Friedel-Crafts type cyclization dropped significantly. Four days was required for the reaction to proceed to near completion instead of 20 hours as in the same step of the non-chlorinated version, presumably because of a slight change in the substrate's ground state conformation in the presence of the C13 chlorine. Quadrupling the loading of both $\text{BF}_3 \cdot \text{Et}_2\text{O}$ and MeOH led to no significant reduction in reaction time and lowered the yield. Higher reaction temperature was not pursued due to the elevated decomposition of the starting material and/or product under such conditions. The one pot reduction-elimination-oxidation was also applicable to the chlorinated enone **6.27** and **6.28** was obtained as the major diastereomer, with an unexpected high 13:1 d.r.

Bromination of **6.28**, followed by palladium-catalyzed cyanation provided **6.29** in good overall yield. A final reductive deoxygenation using $\text{BF}_3 \cdot \text{Et}_2\text{O}$ and Et_3SiH provided ambigaine G through total synthesis for the first time, again unexpectedly, as a single diastereomer.



Scheme 6.9. Total synthesis of ambigaine G.

6.4 Conclusion

Ambigaine G, a chlorinated congener in the ambigaine family of indole alkaloids, was synthesized in an enantiospecific manner from (*S*)-carvone oxide in 10 steps. The chlorine atom was installed at an early-stage to avoid a potential vinyl group participation in a polycyclic, rigid

scaffold during the chlorination at a late-stage. The pentacyclic scaffold of ambiguine G was constructed through the [4+3] cycloaddition strategy, which we envisioned could be applied to the synthesis of most pentacyclic ambiguines, if not all. The nitrile group was installed through the strategy applied in the synthesis of the non-chlorinated analogue ambiguine Q, which afforded ambiguine G as a single diastereomer. As far as we know, ambiguine G is the first C13-chlorinated ambiguine to yield to total synthesis.

Chapter 7

Synthetic Efforts Towards Ambiguine L

Having successfully synthesized ambiguines P, Q and G, ambiguity L was then chosen to be our next target.¹ Ambiguine L, as well as the rest of the pentacyclic ambiguines, contain a C11 isonitrile group, a functional group not commonly found in natural products, and a C10 hydroxyl group. Our synthetic strategy towards ambiguity L was to construct the pentacyclic scaffold with the [4+3] cycloaddition reaction, given the high efficiency of this design, followed by the installation of a nitrogen based functional group on C11 and then a hydroxyl group on C10, due to the probable acid- and heat-sensitive nature of the latter functional group. The formation of a carbon-nitrogen bond on the C11 position ended up being unexpectedly challenging and various mechanistically different strategies were explored.

7.1 C-N Bond Formation Through Sigmatropic Rearrangement

One of the first attempted strategies was the sigmatropic rearrangement reaction. It was inspired by the realization that the C15 substituent of ambiguity P sits at the allyl position of the C10-C11 π bond, which set the stage for a possible sigmatropic rearrangement.

Attempts to install nitrogen containing tethers on the C15 hydroxyl group of 15-*epi*-ambiguine P (Section 5.4) through the hydroxyl group were fruitless, leading only to decompositions. This

¹ Mo, S.; Kronic, A.; Chlipala, G.; Orjala, J. *J. Nat. Prod.* **2009**, 72, 894.

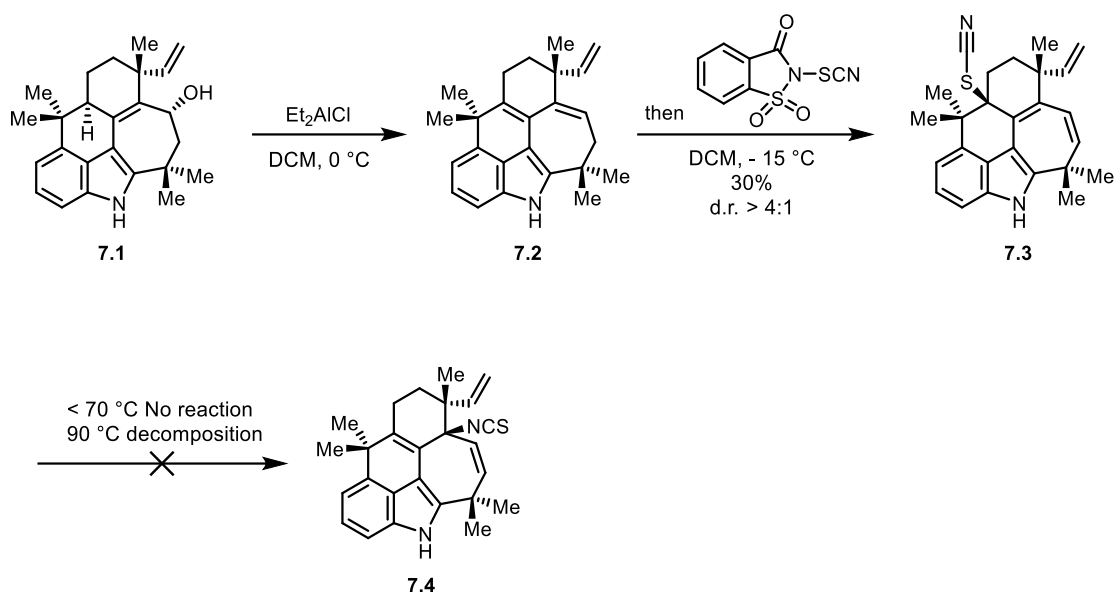
was probably due to the ease of generation of a carbon cation at the C15, which was stabilized by the C10-C23 conjugated system.

Since the rearrangement precursors with a C-O bond at C15 were inaccessible, we turned our attention to rearrangements involving an allylic C-S bond. The allylic thiocyanate rearrangement is known to favor the generation of allylic isothiocyanates through equilibration and has been applied in natural product synthesis.² This rearrangement, also known as Billeter-Gerlich rearrangement seemed like a feasible method to install the desired C-N bond and was worth exploring. Thus, the thiocyanate containing **7.3** was synthesized by oxidation of the cross-conjugated diene **7.2** with the electrophilic thiocyanating reagent as the oxidant,³ a similar process with the synthesis of ambiguine P from **7.2**. The products **7.2** were isolated as > 4:1 mixture of diastereomers (Scheme 7.1). The potential rearrangement of **7.2** was studied in xylenes, however no reaction was observed below 70 °C and decomposition of the starting material took place rapidly at 90 °C, leading to multiple unidentified products.⁴

² (a) Smith, P. A.; Emerson, D. W. *J. Am. Chem. Soc.* **1960**, *82*, 3076. (b) Huber, S.; Stamouli, P.; Jenny, T.; Neier, R. *Helv. Chim. Acta* **1986**, *69*, 1898. (c) Gonda, J.; Martinkova, M.; Imrich, J. *Tetrahedron* **2002**, *58*, 1611. (d) *Tetrahedron: Asymmetry* **2006**, *17*, 1875.

³ Wu, D.; Qiu, J.; Karmaker, G.; Yin, H.; Chem, F. *J. Org. Chem.* **2018**, *83*, 1576.

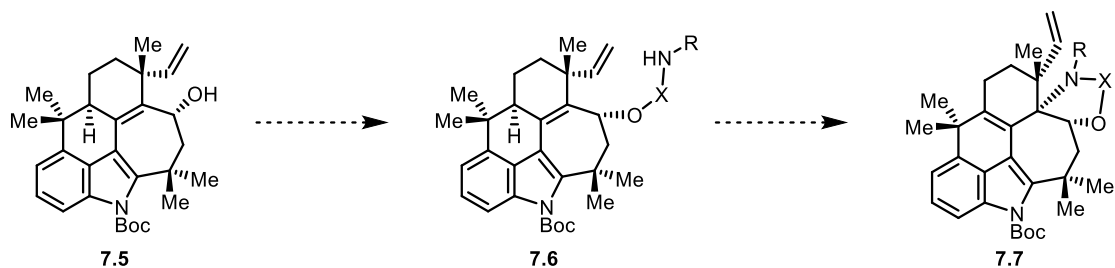
⁴ The undesired diastereomer was obtained as the major product, but because no rearrangement took place and optimizations trying to improve the diastereoselectivity was not pursued.



Scheme 7.1. Attempted thiocyanate rearrangement.

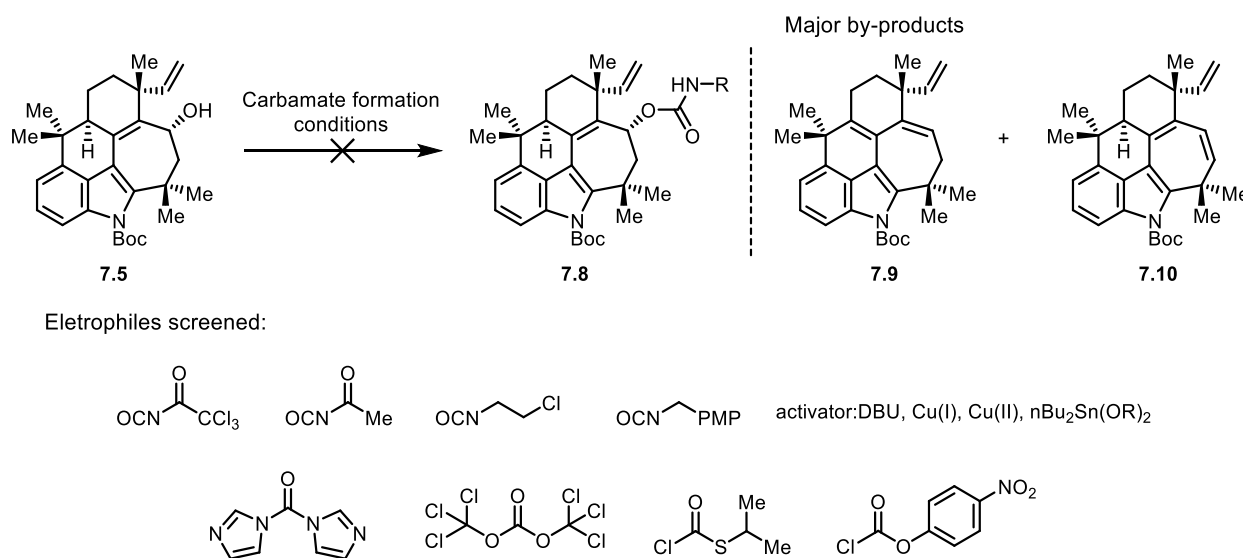
7.2 Functionalization of **7.5** for Intramolecular Cyclization Reactions

With the unsuccessful attempt of sigmatropic rearrangements, we then altered our strategy and decided to install a nitrogen containing tether onto the hydroxyl group of **7.5**, anticipating that a C-N bond would be formed on C11 with the desired stereochemistry through an intramolecular cyclization reaction, through nitrogen centered radical, nitrene intermediates or other types of reactive intermediates (Scheme 7.2).



Scheme 7.2. A possible intramolecular cyclization reaction to form the desired C-N bond.

The challenge with this route was the unforeseen difficulty with the installation of the nitrogen-containing tether. Isocyanates were first tried with the purpose of transforming the alcohol into carbamates (Scheme 7.3). No or extremely slow conversion of the addition of alcohol onto the isocyanate carbon was observed at room temperature of 40 °C in the presence of DBU, the base of choice for carbamate formation in general due to its proposed role of an activator of the carbamate.⁵ Further increase of the reaction temperature to 50 °C led to mainly the elimination of the alcohol. Activators that were reported to accelerate carbamate formation reactions for sterically hindered alcohol substrates, such as CuCl and dibutyltin dilaurate, failed to deliver the desired products and only resulted in a faster elimination reaction.^{6,7} Other types of electrophiles, such as triphosgene, carbonyldiimidazole and 4-nitrophenyl chloroformate, favored the elimination pathway as well.



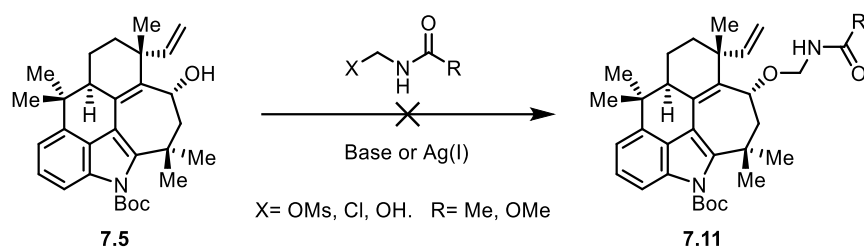
Scheme 7.3. Unsuccessful carbamate formation.

⁵ Tsuji, T.; Nishida, S.; Okuyama, M.; Osawa, E. *J. Am. Chem. Soc.* **1995**, *117*, 9804.

⁶ Duggan, M. I.; Imagire, J. S. *Synthesis* **1989**, 131.

⁷ Britain, J. W.; Gemeinhardt, P. G. *J. Appl. Polym. Sci.* **1960**, *4*, 207.

The use of the less electron-withdrawing tethers such as the amide or carbamate based hemiaminals were then studied. These types of hemiaminals had been reported to be stable compounds and models studies with simple alcohol substrates provided satisfying results.⁸ However, no desired product was ever obtained from the pentacyclic system (Scheme 7.4).

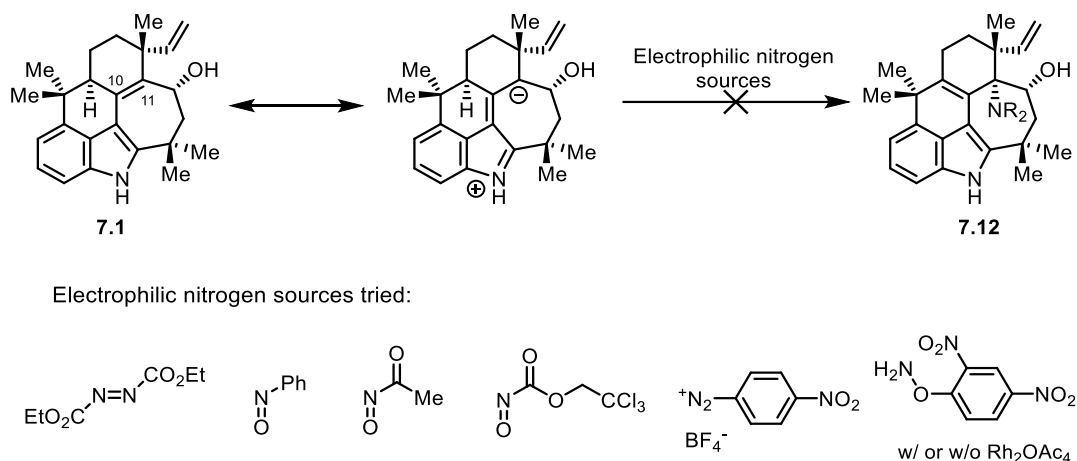


Scheme 7.4. Unsuccessful hemiaminal formation.

7.3 Electrophilic Amination

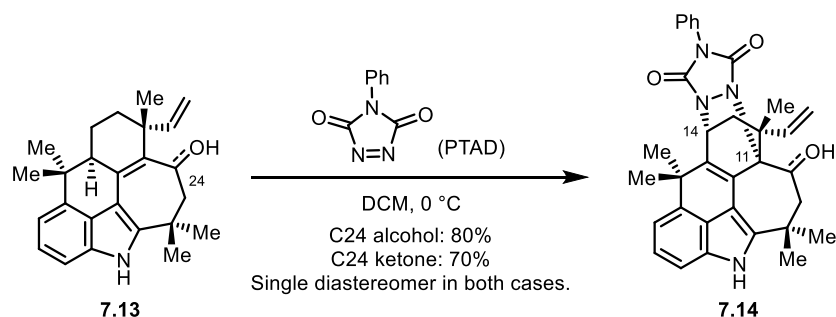
As inspired by the success of ambiguine P synthesis from the cross-conjugated diene, we wondered whether the conjugation of the indole ring and the C10-C11 π bond in **7.1** would also lead to a more electron rich π bond capable of reacting with electrophilic nitrogen species, most of which are inert towards inactivated alkene π bonds.

⁸ Shono, T.; Matsumura, Y.; Uchida, K.; Kobayashi, H. *J. Org. Chem.* **1985**, *50*, 3243.

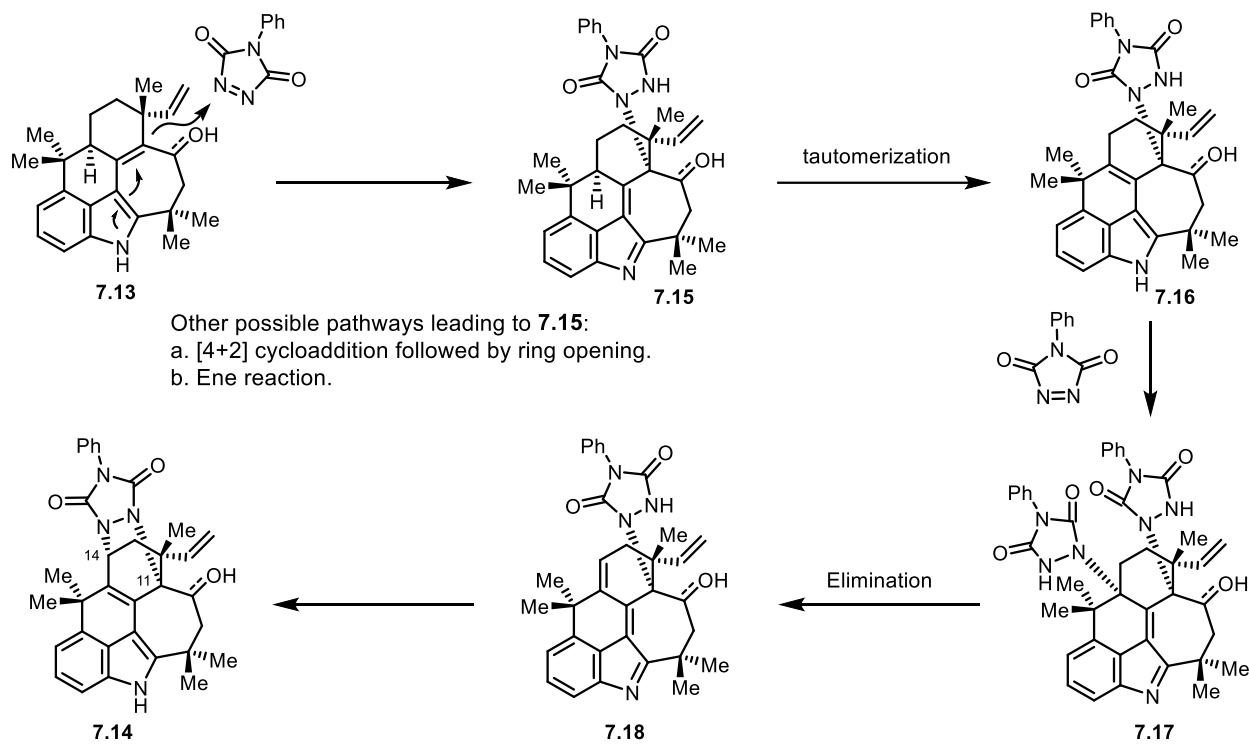


Scheme 7.5. Unsuccessful electrophilic aminations.

Most of the literature reported, reactive electrophilic nitrogen sources such as diethyl azodicarboxylate, nitroso compounds with various substitutions on nitrogen, aryl diazonium salt etc., were tested on the alcohol substrate **7.1** (Scheme 7.5). But in most cases, the substrate underwent either no reaction or decomposition. Curiously, when 4-phenyl-1,2,4-triazoline-3,5-dione (PTAD) was added to **7.13** (alcohol at C24) in DCM at 0 °C, a new product was quickly observed. The reaction required 2 equivalents of PTAD to completely consume all starting material and the product, obtained in 80% yield as a single diastereomer, was identified to the unexpected **7.14** (alcohol at C24), with two C-N bonds formed both on C11 and C14. More intriguingly, PTAD also reacted with the less nucleophilic enone **7.13** (carbonyl at C24) and provided the structurally similar product **7.14** (carbonyl at C24) in 70%, once again as a single diastereomer.



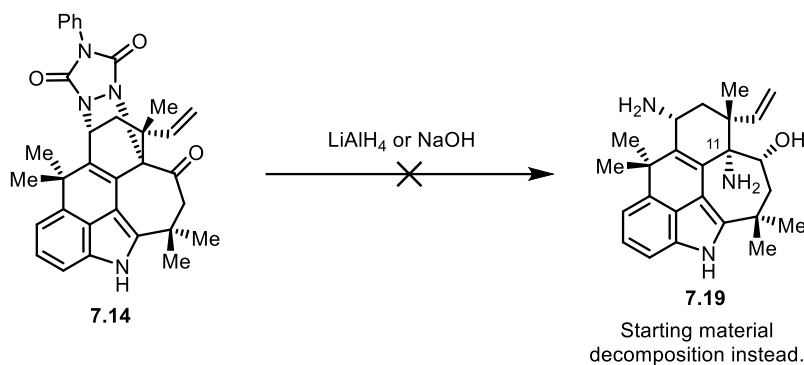
Possible mechanism:



Scheme 7.6. Unexpected reactivity with PTAD.

We proposed the mechanism shown in Scheme 7.6 to explain the formation of **7.14**. Enone **7.14** likely reacted 1 equivalent of PTAD to form intermediate **7.15** followed by tautomerization into **7.16**. Other pathways such as a [4+2] cycloaddition between **7.13** and PTAD or an ene reaction were also possible mechanisms leading to **7.16**. Another equivalent PTAD then reacted with **7.16** at the newly formed conjugated system, providing **7.17**. Elimination of the dihydro-PTAD from **7.17** afforded the imine product, which was trapped at the C14 position by the nitrogen from the

first equivalent of PTAD that has been staying on the pentacyclic scaffold during the whole process, providing the final product as a single diastereomer.



Scheme 7.7. Attempts of derivatizing **7.14** led to decomposition.

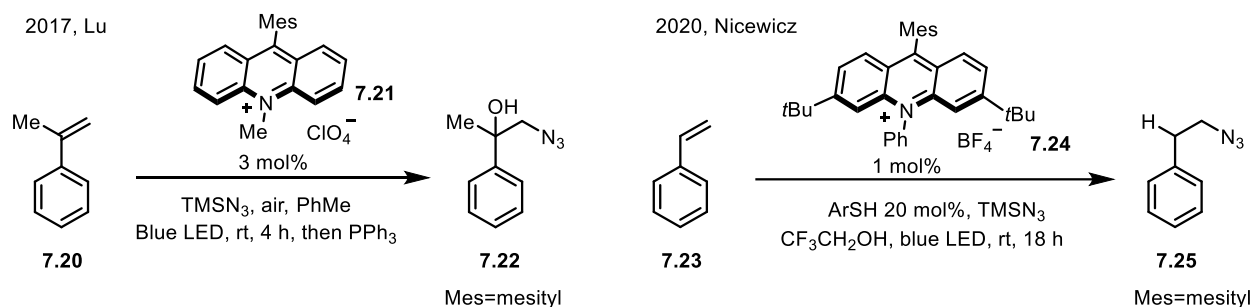
Even though all attempts derivatizing **7.14** into a C11 amino product failed, this interesting reactivity with PTAD clearly proved that the C11 position, despite being embedded in the pentacyclic scaffold and located next to a quaternary carbon center, is sterically accessible and a C-N bond at this C11 position could be formed in an intermolecular fashion.

7.4 Photocatalytic Azidation of the Pentacyclic Scaffold

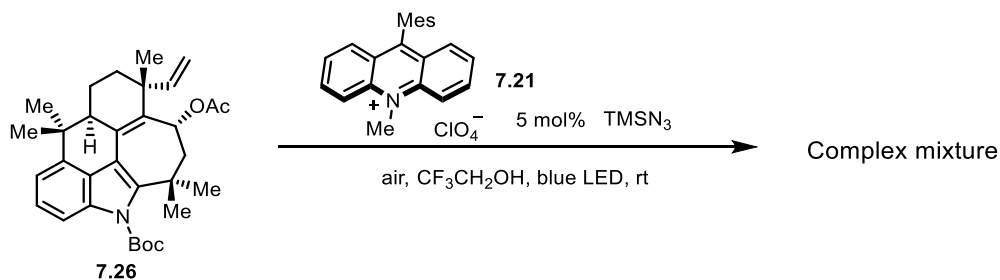
7.4.1 Unexpected Reactivity

With the realization that the steric environment around the C11 position of the pentacyclic compounds allowed a nitrogen-containing functional group to be installed intermolecularly, we then focused on strategies involving intermolecular C-N formation reactions. The pioneering works reported by both Lu and co-workers as well as Nicewicz and co-workers caught our

attention.^{9,10} Both groups demonstrated that in simple styrenyl systems, TMSN₃ was capable of azidating the β-carbon of styrene with an acridinium based photocatalyst (Scheme 7.8). A radical cation styrenyl species was proposed by both groups to be a probable intermediate responsible for the product formation.



Scheme 7.8. Seminal works reported by Lu and co-workers as well as Nicewicz and co-workers.



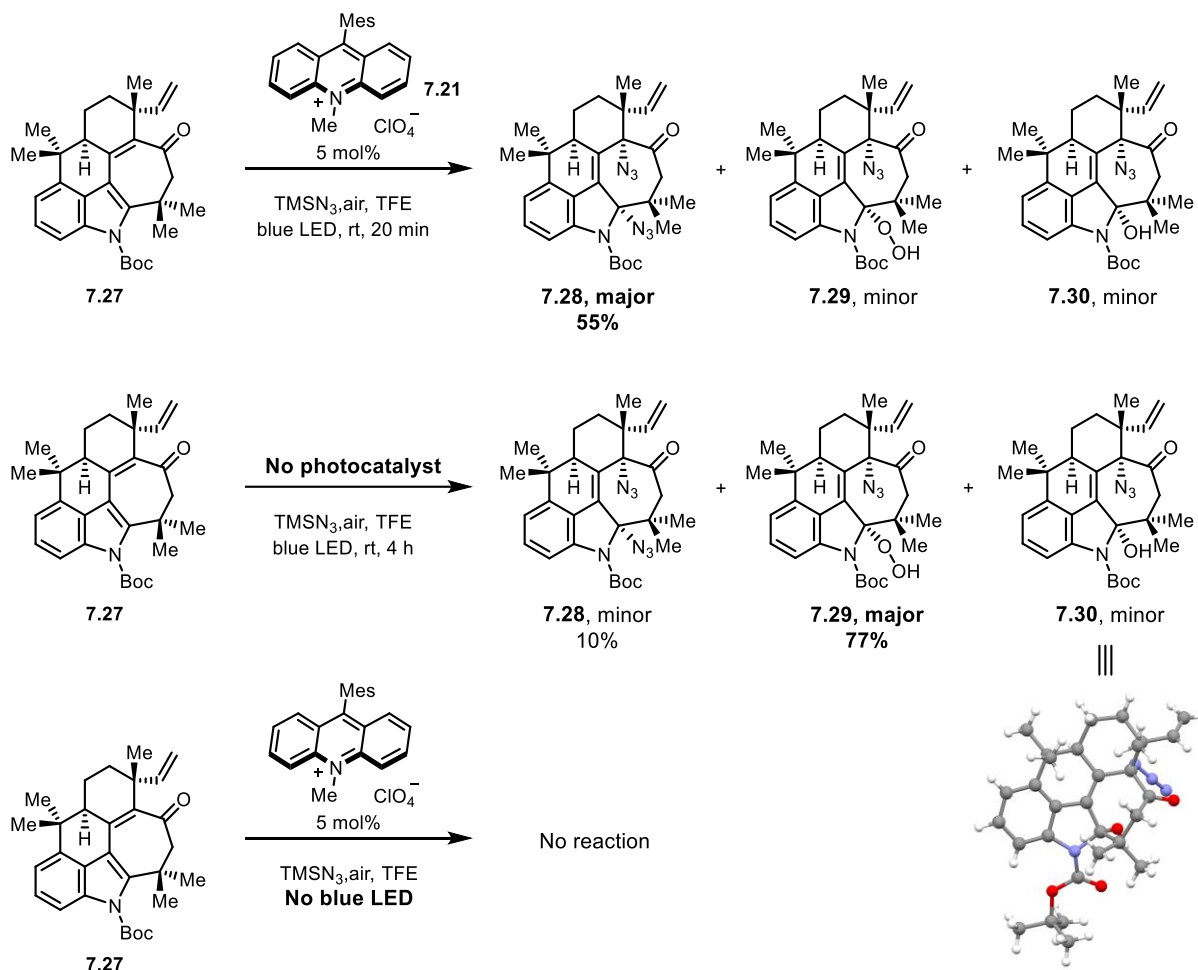
Scheme 7.9. Initial attempts of azidation of **7.26**.

Inspired by these seminal works, we decided to perform an azidation on the pentacyclic substrates utilizing photocatalysis conditions. Initial endeavors to apply the photocatalysis conditions on the acetate protected alcohol substrate **7.26** were fruitless. However, when enone **7.27** was subjected to the conditions shown in Scheme 7.10, reactivity was observed and enone **7.27** was mostly consumed within 20 minutes, affording quite cleanly three different products.

⁹ Yang, B.; Lu, Z. *ACS Catal.* **2017**, *7*, 8326.

¹⁰ Onuska, N. P. R.; Schutzbach-Horton, M. E.; Rosario Collazo, J. L.; Nicewicz, D. A. *Synlett* **2020**, *31*, 55.

Extensive NMR studies and reactivity studies indicated that the products were not the desired 1,2-addition products, but the 1,4-addition products: diazide **7.28**, azidoperoxide **7.29** and azidoalcohol **7.30**, the structure of which was confirmed by single crystal X-ray analysis. The diazide **7.28** was isolated as the major product with a 55% yield.



Scheme 7.10. Unexpected products observed in the photocatalysis conditions.

Control experiment without blue LED irradiation gave no reaction, proving that the products were generated from photo processes. However, a puzzling result was obtained when the reaction was performed in the absence of the acridinium photocatalyst: the reaction still proceeded cleanly, affording the same three products, but with the azidoperoxide **7.29** as the major product.

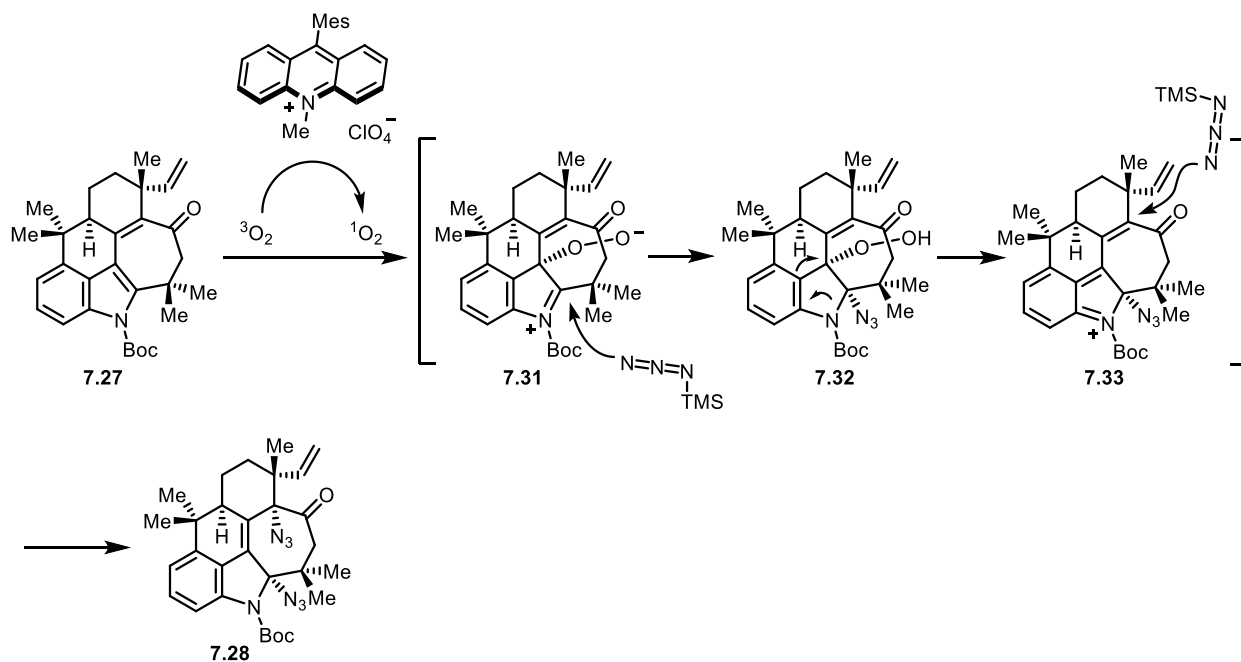
7.4.2 Proposed Mechanism for the Formation of Different Products

Shown in Scheme 7.11 are our proposed mechanisms to explain the formation of the three products under the reaction conditions both with or without photocatalyst, as well as their different ratios under different conditions. A radical cation intermediate was unlikely because the redox potential of **7.5** was +1.65 V (vs ferrocene in MeCN) as determined by cyclic voltammetry, which is essentially the same as that of the acridinium catalyst used (+1.66 V vs ferrocene in MeCN). The enone substrate **7.27** supposedly has a redox potential higher than 1.65 V that even if the photocatalyst is capable of oxidizing **7.27**, the process was expected to be slow, whereas the reaction in the presence of the acridinium photocatalyst completed within 20 minutes at room temperature.

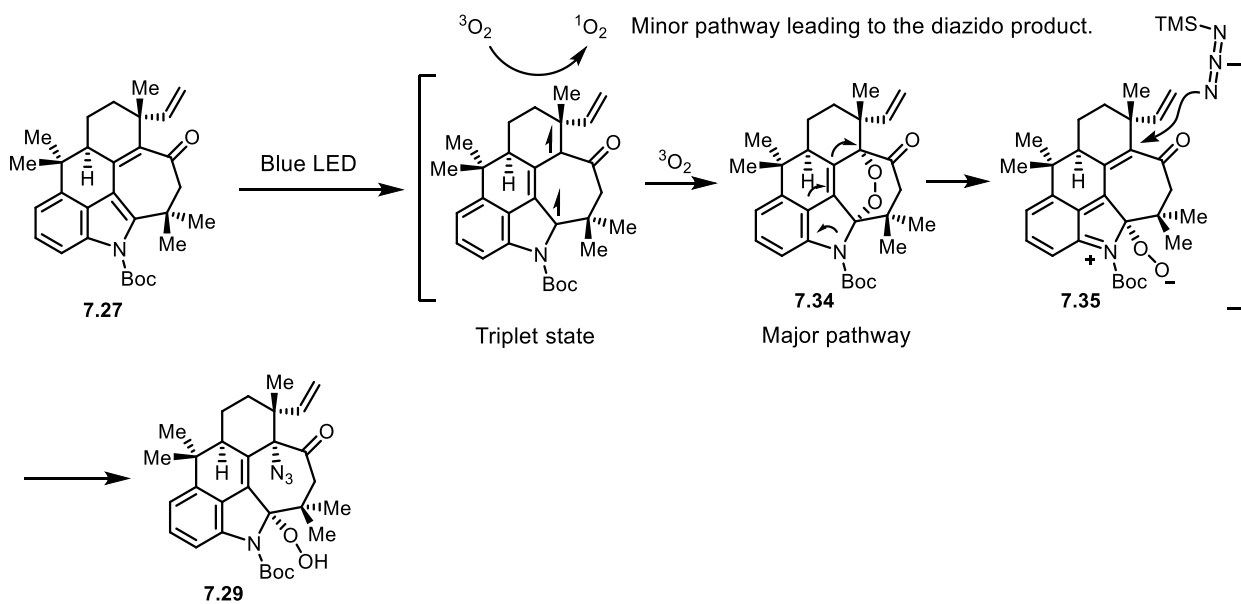
Two possible pathways might be accountable for the formation of the products observed. In the presence of the acridinium photocatalyst, upon blue LED irradiation, singlet oxygen was probably generated via the acridinium photocatalyst through energy transfer, which then reacted with the indole ring of **7.27** to form the zwitterionic intermediate **7.31**. This type of reactivity between singlet oxygen and indoles has been proposed by multiple research groups. The zwitterionic intermediate **7.31** was then trapped by one equivalent of TMSN₃ forming **7.32**. The peroxide moiety was expelled from **7.32** presumably as favored by the pentacyclic ring conformation, and the resulting **7.33** reacted with a second equivalent of TMSN₃ at the C11 position, forming the diazide product **7.28** that was observed as the major product under the acridinium catalyzed reaction condition.

Aside from the acridinium catalyst being photoexcitable, the enone substrate **7.27** is probably also photoexcitable. Enone **7.27** has a maximum absorption at 400 nm as measured by UV-vis and is likely excited upon irradiation with blue light (460 nm wavelength) to its triplet state. Some of the excited **7.27** generated singlet oxygen through energy transfer, which eventually provided a small amount of the diazide product as mentioned earlier, but the majority of the excited **7.27** reacted directly with triplet oxygen and formed the [4+2] cycloadduct **7.34**. The newly formed heterocycle underwent ring opening, affording **7.35** which is structurally related to **7.33**. TMSN_3 then reacted at the C11 position to form the product **7.29**. The azidoalcohol product probably arose from the reduction of the **7.29** and/or water trapping the iminium ion intermediate **7.31**.

Proposed mechanism of the generation of the diazido product:



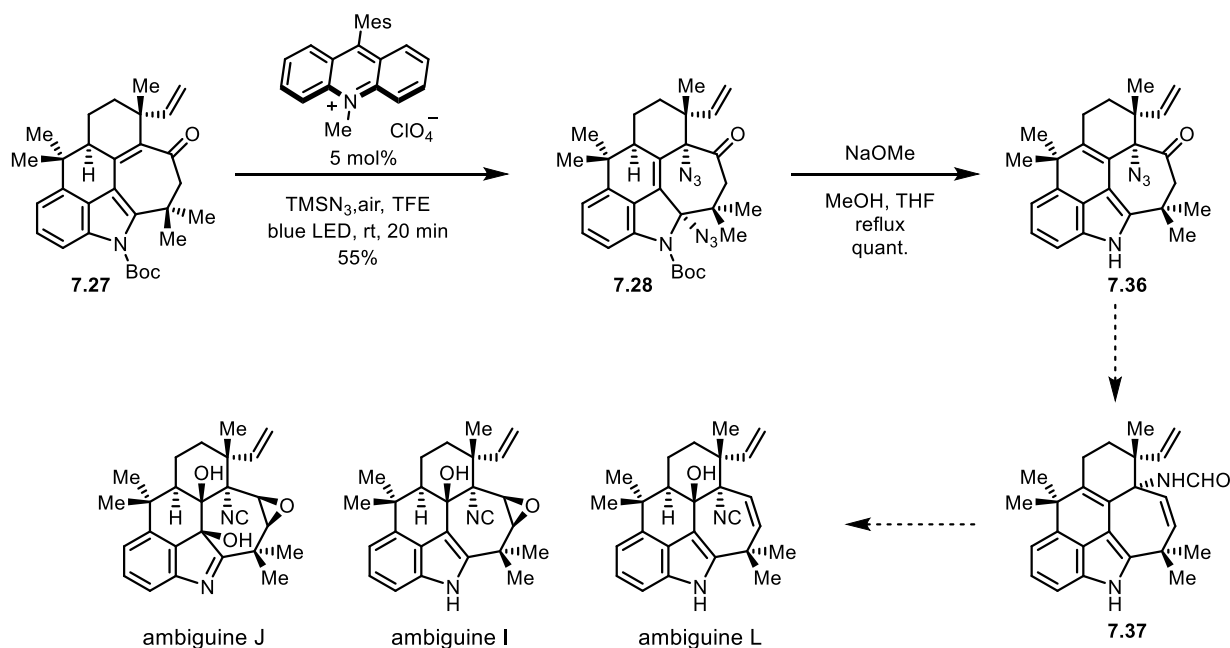
Proposed mechanism of the generation of the azidoperoxide product:



Scheme 7.11. Proposed mechanism of the generation of 7.28 and 7.29.

7.5 Synthesis Towards Ambiguine L Utilizing the Photocatalytic Reaction

The photocatalytic reaction provided three different products, but all three products contained the desired C11 azide group with the correct stereochemistry. Diazaide **7.28**, obtained as the major product under the acridinium photocatalysis condition, was then transformed into the alkene product **7.36** quantitatively, upon Boc deprotection in THF and MeOH with NaOMe as the base (Scheme 7.12). We envision that compound **7.37** could be easily accessed from **7.26**, and further chemical manipulations such as functionalization of the C10-C15 double bond would potentially lead to ambiguityne L and other pentacyclic ambiguitynes.



Scheme 7.12. Synthesis of **7.36**: a potential intermediate towards ambiguitynes L, I and J.

7.6 Conclusion

In summary, our strategy towards ambiguityne L was to construct the pentacyclic system with our [4+3] cycloaddition strategy, the efficiency of which had been proven in our syntheses of

ambiguines P, Q and G. The key steps from the pentacyclic intermediate were the installation of the C11 nitrogen-containing group and the C10 hydroxyl group. The formation of a carbon-nitrogen bond at the C11 position was unexpectedly challenging and various strategies were studied, including sigmatropic rearrangements, intramolecular cyclizations, intermolecular electrophilic amination, etc. Ultimately, unpredicted photocatalytic reactions afforded three different products containing the desired carbon-nitrogen bond at C11 with the correct stereochemistry. Two mechanisms were proposed to explain the formation of the observed products from the photocatalysis reactions: one involving singlet oxygen and the other involving a triplet state of **7.27** excited by blue LED. Azide **7.28** was eventually synthesized from the photoreaction followed by Boc deprotection. We anticipate ambigine L, and potentially ambiguines I, J and N, could be synthesized through the route discussed.

Chapter 8

Experimental Procedures and Characterization Data

8.1 General Information

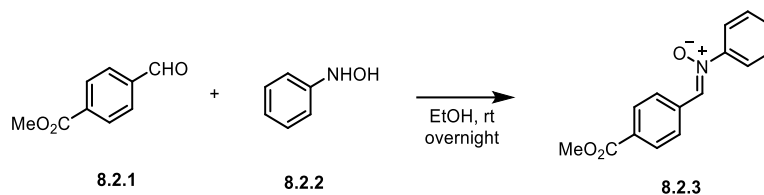
Unless stated otherwise, room temperature refers to 22-26 °C. Higher than room temperatures were maintained using pre-heated oil baths. Lower temperatures were maintained using acetone/CO₂(s) (−78 °C), MeCN/CO₂(s) (−40 °C) and water/ice (0 °C) baths. Dichloromethane (CH₂Cl₂ or DCM), tetrahydrofuran (THF), ether (Et₂O) and dimethylformamide (DMF) were dried by passage through an activated alumina column purification system (Innovative Technology Inc. Pure Solv™). All commercial reagents and solvents were used as received, except N-bromosuccinimide, (recrystallized from water) and N-chlorosuccinimide (recrystallized from acetic acid).

Thin-layer chromatography (TLC) was performed using EMD Millipore silica gel 60 Å F254 plates (250 μm) with F-254 fluorescent indicator and visualized by UV fluorescence quenching, ceric ammonium molybdate, or potassium permanganate staining. SiliCycle SiliaFlash P60 silica gel (particle size 40–63 μm) was used for flash chromatography. NMR spectra were measured on Bruker DRX and DMX spectrometers at 500 MHz for ¹H spectra and 125 MHz for ¹³C spectra, respectively, and calibrated to either TMS (δ = 0 for ¹H), residual CHCl₃ (δ = 7.26 for ¹H and δ = 77.23 for ¹³C), or residual benzene (δ = 7.16 for ¹H and δ = 128.06 for ¹³C). Splitting patterns are reported as apparent. Mass spectral data was measured on Agilent technologies 6224 TOF LC/MS. Optical rotations were measured on a Jasco DIP-1000 polarimeter using a 100 mm path-length cell,

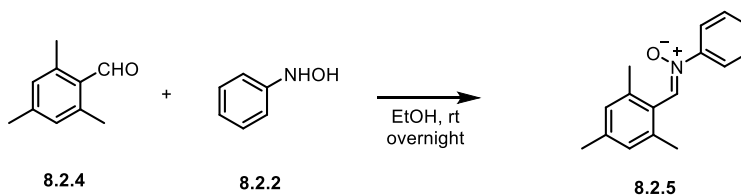
$c = \text{g}/100 \text{ mL}$. IR spectra were recorded on a Thermo Scientific Nicolet iS50 FT-IR spectrometer and are reported as frequency of absorption (cm^{-1}).

8.2 Experimental Procedures and Characterization Data for Chapter 2

8.2.1. Synthetic Procedures and Characterization Data for nitrones

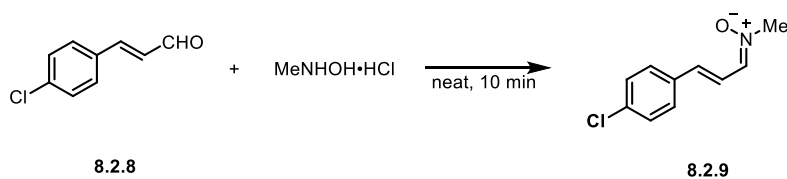


(Z)-1-(4-(Methoxycarbonyl)phenyl)-N-phenylmethanimine oxide (8.2.3) A 20 mL glass vial was charged with **8.2.1** (985 mg, 6.0 mmol, 1 equiv.) and **8.2.2** (720 mg, 6.6 mmol, 1.1 equiv.), which was then dissolved in EtOH (8 mL). The reaction mixture was then allowed to stir at room temperature overnight, during which time a pale-yellow precipitate formed. The precipitate was collected via vacuum filtration and azeotroped with toluene. The title compound was obtained as a white solid (1.40 g, 92%) and used without further purification. **¹H NMR** (500 MHz, CDCl₃) δ 8.45 (d, *J*=8.4 Hz, 1H), 8.14 (d, *J*= 8.4 Hz, 1H), 8.00 (s, 1H), 7.82-7.75 (m, 2H), 7.55-7.47 (m, 3H), 3.95 (s, 3H). **¹³C NMR** (125 MHz, CDCl₃) δ 166.5, 149.2, 134.6, 133.7, 131.6, 131.4, 130.0, 129.4, 128.7, 121.9, 52.4. **HRMS** Calculated for C₁₅H₁₃NO₃ [M+H]⁺: 256.0968. Found 256.0975.



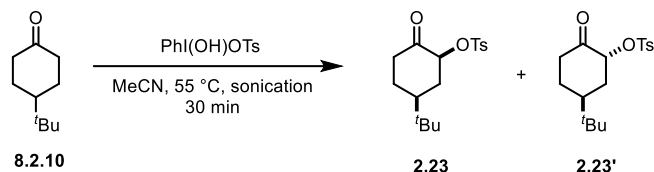
(Z)-1-Mesityl-N-phenylmethanimine oxide (8.2.5) A 20 mL glass vial was charged with **8.2.4** (885 μL, 6.0 mmol, 1 equiv.) and **8.2.2** (720 mg, 6.6 mmol, 1.1 equiv.), which was then dissolved in EtOH (6 mL). The reaction mixture was then allowed to stir at room temperature overnight,

during which time a pale-yellow precipitate formed. The precipitate was collected via vacuum filtration and azeotroped with toluene. The title compound was obtained as a white solid (985 mg, 68%) and used without further purification. $^1\text{H NMR}$ (500 MHz, CDCl_3) δ 8.07 (s, 1H), 7.83-7.74 (m, 2H), 7.54-7.44 (m, 3H), 6.94 (s, 2H), 2.35 (s, 6H), 2.32 (s, 3H). $^{13}\text{C NMR}$ (125 MHz, CDCl_3) δ 148.8, 139.8, 137.9, 135.3, 130.2, 129.3, 128.6, 125.8, 122.2, 21.3, 20.2. **HRMS** Calculated for $\text{C}_{16}\text{H}_{17}\text{NO}$ $[\text{M}+\text{H}]^+$: 240.1383. Found 240.1394.

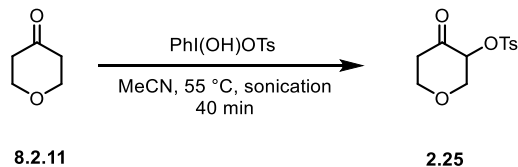


(1Z,2E)-3-(4-chlorophenyl)-N-methylprop-2-en-1-imine oxide (8.2.9) To a mortar was added 8.2.8 (716 mg, 4.3 mmol, 1 equiv.), N-methylhydroxyaminehydrochloride (718 mg, 8.6 mmol, 2 equiv.), Na_2CO_3 (1.00 g, 9.7 mmol, 2.2 equiv.) and Na_2SO_4 (3.05 g, 21.5 mmol, 5 equiv.). The mixture was grounded rapidly with a pestle at room temperature for 15 minutes. Methylene chloride (4.3 mL) was then added and the resulting mixture was filtered through a glass frit. The methylene chloride solution was collected and concentrated *in vacuo*. Silica gel column chromatography (5% methanol/methylene chloride \rightarrow 10% methanol/methylene chloride) afforded the title compound as a white solid (606 mg, 72%). R_f = 0.35 (10% methanol/methylene chloride). $^1\text{H NMR}$ (500 MHz, CDCl_3) δ 7.46-7.35 (m, 3H), 7.21 (d, J = 8.5 Hz, 2H), 7.24 (d, J = 9.0 Hz, 1H), 6.91 (d, J = 16.3 Hz, 1H), 3.76 (s, 3H). $^{13}\text{C NMR}$ (125 MHz, CDCl_3) δ 137.3, 136.5, 135.0, 134.6, 129.2, 128.5, 119.0, 52.6. **HRMS** Calculated for $\text{C}_{10}\text{H}_{10}\text{ClNO}$ $[\text{M}+\text{H}]^+$: 196.0524. Found 196.0503.

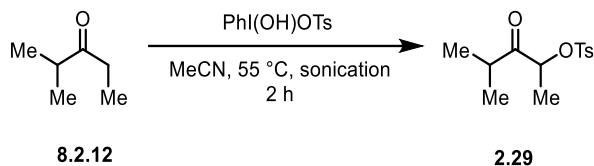
8.2.2. Synthetic Procedures and Characterization Data for α -tosyloxy ketones



5-(*tert*-Butyl)-2-oxocyclohexyl 4-methylbenzenesulfonate (2.23) A 25 mL round bottom flask was charged with **8.2.10** (1.18 g, 7.6 mmol, 1.5 equiv.) and PhI(OH)OTs (2.0 g, 5.1 mmol, 1.0 equiv.), which was then dissolved in acetonitrile (10 mL). The reaction mixture was then sonicated at 55 °C for 30 minutes. All solids should be dissolved upon completion of the reaction. The reaction mixture was concentrated *in vacuo* and the resulting oil was purified by silica gel column chromatography (5% ethyl acetate/hexane) to afford the title compound **2.23** (513 mg, 1.58 mmol, 31% yield) as a white solid, which is a mixture of two diastereomers (1e:1e' 5:1). $R_f = 0.35$ (20% ethyl acetate/hexane), visualized by UV. **$^1\text{H NMR}$** (500 MHz, CDCl_3) Major isomer **2.23** δ 7.86 (d, $J = 8.3$ Hz, 1H), 7.34 (d, $J = 8.3$ Hz, 1H), 5.09-5.01 (m, 1H), 2.53-2.36 (m, 5H), 2.34-2.23 (m, 1H), 2.10-2.03 (m, 1H), 1.70-1.57 (m, 2H), 1.45-1.34 (m, 1H), 0.90 (s, 9H). Observed minor isomer **2.23'** signals δ 7.78 (d, $J = 8.3$ Hz, 1H), 7.35 (d, $J = 8.3$ Hz, 1H), 4.51-4.48 (m, 1H), 2.74 (td, $J = 13.7, 6.1$ Hz, 1H), 1.90 (app. tt, $J = 12.5, 3.5$ Hz, 1H), 0.86 (s, 9H). **$^{13}\text{C NMR}$** (125 MHz, CDCl_3) δ 205.6, 202.3, 145.2, 144.6, 133.9, 132.8, 129.8, 129.5, 127.9, 127.7, 81.6, 81.5, 45.5, 40.1, 39.4, 37.4, 35.7, 34.2, 32.2, 31.9, 28.0, 27.5, 27.3, 27.2, 21.5, 21.4. **HRMS** Calculated for $\text{C}_{17}\text{H}_{24}\text{O}_4\text{S}$ $[\text{M}+\text{H}]^+$: 325.1468. Found 325.1482.



4-Oxotetrahydro-2H-pyran-3-yl 4-methylbenzenesulfonate (2.25) A 25 mL round bottom flask was charged with **8.2.11** (765 μL , 7.6 mmol, 1.5 equiv.) and PhI(OH)OTs (2 g, 5.1 mmol, 1.0 equiv.), which was then dissolved in acetonitrile (10 mL). The reaction mixture was then sonicated at 55 $^\circ\text{C}$ for 40 minutes. All solids should be dissolved upon completion of the reaction. The reaction mixture was concentrated *in vacuo* and the resulting oil was purified by silica gel column chromatography (20% ethyl acetate/hexane) to afford the title compound **1f** (692 mg, 2.56 mmol, 51%) as a white solid. $R_f=0.33$ (40% ethyl acetate/hexane), visualized by UV. $^1\text{H NMR}$ (500 MHz, CDCl_3) δ 7.84 (d, $J=8.3$ Hz, 1H), 7.36 (d, $J=8.3$ Hz, 1H), 4.92 (ddd, $J=9.7, 6.6, 1.1$ Hz, 1H), 4.28 (ddd, $J=11.1, 6.6, 1.6$ Hz, 1H), 4.16 (dddd, $J=11.2, 6.8, 2.7, 1.5$ Hz, 1H), 3.67 (td, $J=11.2, 3.2$ Hz, 1H), 3.61 (dd, $J=11.2, 9.7$ Hz, 1H), 2.66 (dddd, $J=14.4, 11.0, 6.7, 1.1$ Hz, 1H), 2.57 (td, $J=14.4, 3.0$ Hz, 1H), 2.45 (s, 3H). $^{13}\text{C NMR}$ (125 MHz, CDCl_3) δ 198.5, 145.4, 133.1, 129.9, 128.1, 78.0, 71.1, 68.3, 42.4, 21.7. **HRMS** Calculated for $\text{C}_{12}\text{H}_{14}\text{O}_5\text{S}$ $[\text{M}+\text{H}]^+$: 271.0635. Found 271.0641.

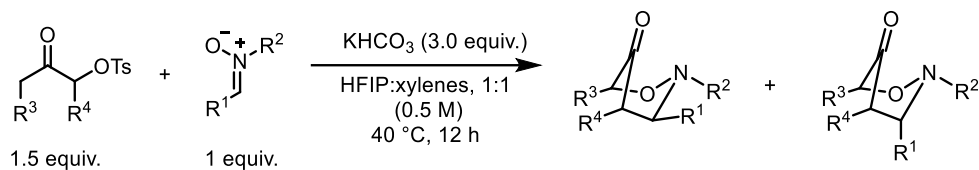


4-Methyl-3-oxopentan-2-yl 4-methylbenzenesulfonate (2.29) A 25 mL round bottom flask was charged with **8.2.12** (945 μL , 7.6 mmol, 1.5 equiv.) and PhI(OH)OTs (2 g, 5.1 mmol, 1.0

equiv.), which was then dissolved in acetonitrile (10 mL). The reaction mixture was then sonicated at 55 °C for 2 hours. All solids should be dissolved upon completion of the reaction. The reaction mixture was concentrated *in vacuo* and the resulting oil was purified by silica gel column chromatography (20% ethyl acetate/hexane) to afford the title compound **2.29** (692 mg, 2.56 mmol, 51%) as a white solid. $R_f = 0.24$ (20% diethyl ether), visualized by UV. $^1\text{H NMR}$ (500 MHz, CDCl_3) δ 7.81 (d, $J = 7.9$ Hz, 2H), 7.37 (d, $J = 7.9$ Hz, 2H), 4.99 (q, $J = 6.9$ Hz, 1H), 2.97 (hept, $J = 6.7$ Hz, 1H), 2.44 (s, 3H), 1.37 (d, $J = 7.0$ Hz, 1H), 1.05 (d, $J = 6.9$ Hz, 3H), 1.03 (d, $J = 6.9$ Hz, 3H). $^{13}\text{C NMR}$ (125 MHz, CDCl_3) δ 209.6, 145.1, 133.2, 129.8, 127.6, 79.2, 35.9, 21.3, 18.3, 17.6, 17.4. **HRMS** Calculated for $\text{C}_{13}\text{H}_{18}\text{O}_4\text{S}$ $[\text{M}+\text{H}]^+$: 271.0999. Found 271.1010.

8.2.3. General Procedure for the [3+3] Cycloaddition Reaction

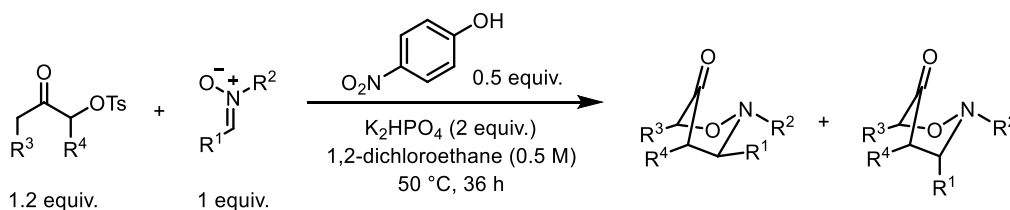
8.2.3.1 General Procedure A: [3+3] Cycloaddition Reaction in HFIP: xylenes Mixed Solvent



A 4 mL glass vial was charged with α -tosyloxy ketone (0.75 mmol, 1.5 equiv.), nitronium (0.5 mmol, 1.0 equiv.) and KHCO_3 (1.5 mmol, 3 equiv.). Xylene (500 μL) was added to the vial followed by HFIP (500 μL). The vial was then tightly capped and was put into a heating block on a stir plate pre-heated to 40 °C. The reaction was allowed to stir at this temperature for 12 h before cooling down to room temperature. The vial cap was then carefully unscrewed to release the CO_2 generated from the reaction. The reaction mixture was then diluted with 15 mL methylene chloride and washed with H_2O (2×8 mL). The aqueous phase was then back extracted with 3 mL

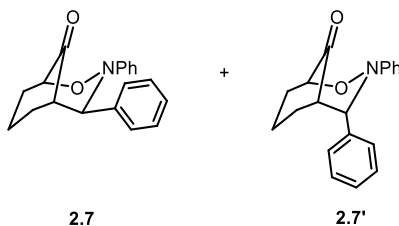
methylene chloride and the organic phase were combined, dried over anhydrous Na_2SO_4 and concentrated *in vacuo*. The residue was purified by silica gel column chromatography to afford the cycloaddition product.

8.2.3.2 General Procedure B: [3+3] Cycloaddition Reaction Catalyzed by 4-Nitrophenol

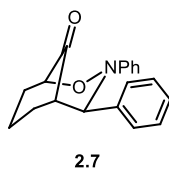


A 4 mL glass vial was charged with α -tosyloxy ketone (0.60 mmol, 1.2 equiv.), nitronium (0.5 mmol, 1.0 equiv.), 4-nitrophenol (0.25 mmol, 0.5 equiv.) and K_2HPO_4 (1 mmol, 2 equiv.), followed by the addition of 1,2-dichloroethane. The vial was then tightly capped and was put into a heating block on a stir plate pre-heated to 50 °C. The reaction was allowed to stir at this temperature for 36 hours before cooling down to room temperature. The reaction mixture was then diluted with 15 mL methylene chloride and washed with H_2O (2×8 mL). The aqueous phase was then back extracted with 3 mL methylene chloride and the organic phase were combined, dried over anhydrous Na_2SO_4 and concentrated *in vacuo*. The residue was purified by silica gel column chromatography to afford the cycloaddition product.

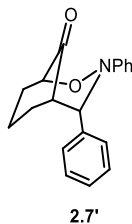
8.2.4. Characterization of [3+3] Cycloaddition Products



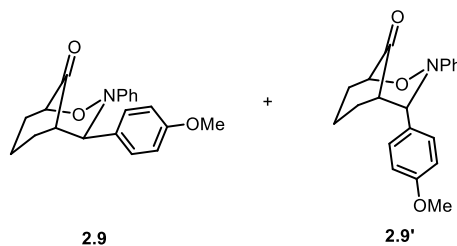
3,4-Diphenyl-2-oxa-3-azabicyclo[3.3.1]nonan-9-one (2.7). Following general procedure **A**, silica gel column chromatography (8% diethyl ether/hexane) afforded the title compounds (122 mg, 83%) as white solids. Following general procedure **B**, silica gel column chromatography (8% diethyl ether/hexane) afforded the title compounds (105 mg, 74%) as white solids.



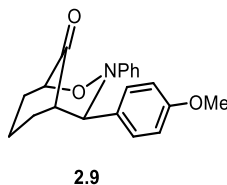
$R_f = 0.39$ (30% diethyl ether/hexane), visualized by Magic stain. $^1\text{H NMR}$ (500 MHz, CDCl_3) δ 7.23-7.11 (m, 7H), 7.10-7.01 (m, 3H), 4.87 (d, $J = 2.7$ Hz, 1H), 4.73 (ddd, $J = 5.0, 1.6, 1.6$ Hz, 1H), 3.03-2.98 (m, 1H), 2.73-2.61 (m, 1H), 2.42-2.35 (m, 1H), 2.35-2.28 (m, 1H), 2.03 (app. ddt, $J = 5.8, 4.6, 13.9$ Hz, 1H), 1.88 (dddd, $J = 14.2, 12.7, 5.2, 1.3$ Hz, 1H), 1.64-1.56 (m, 1H). $^{13}\text{C NMR}$ (125 MHz, CDCl_3) δ 212.5, 148.0, 140.6, 128.6, 128.3, 128.0, 128.0, 126.1, 123.1, 83.9, 76.5, 54.9, 34.7, 33.6, 16.2.



$R_f = 0.29$ (30% diethyl ether/hexane), visualized by Magic stain. $^1\text{H NMR}$ (500 MHz, CDCl_3) δ 7.33-7.23 (m, 4H), 7.22-7.12 (m, 3H), 6.95-6.90 (m, 2H), 6.84 (dd, $J = 8, 6.8$ Hz, 1H), 5.57 (d, $J = 9.5$ Hz, 1H), 4.81 (ddd, $J = 5.1, 1.6, 1.5$ Hz, 1H), 3.22-3.17 (m, 1H), 2.45-2.36 (m, 1H), 2.20-2.05 (m, 1H), 1.88 (dddd, $J = 14.3, 12.7, 5.6, 1.5$ Hz, 1H), 1.80-1.65 (m, 2H), 1.32-1.21 (m, 1H). $^{13}\text{C NMR}$ (125 MHz, CDCl_3) δ 211.5, 147.2, 136.7, 128.9, 128.4, 128.2, 127.2, 121.6, 115.6, 85.8, 67.5, 49.6, 33.9, 29.9, 17. 3. **HRMS** Calculated for $\text{C}_{19}\text{H}_{19}\text{NO}_2$ $[\text{M}+\text{H}]^+$: 294.1489. Found: 294.1479.

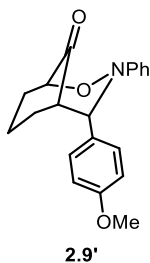


4-(4-Methoxyphenyl)-3-phenyl-2-oxa-3-azabicyclo[3.3.1]nonan-9-one (2.9) Following general procedure **A**, silica gel column chromatography (50% methylene chloride/hexane) afforded the title compounds (145 mg, 90%) as white solids. Following general procedure **B**, silica gel column chromatography (50% methylene chloride/hexane) afforded the title compounds (119 mg, 74%) as white solids.

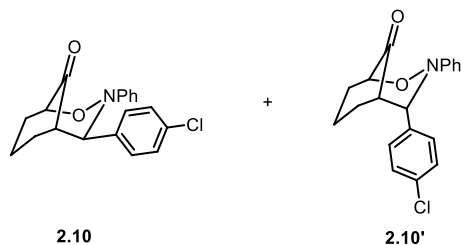


$R_f = 0.31$ (30% diethyl ether/hexane), visualized by Magic stain. $^1\text{H NMR}$ (500 MHz, CDCl_3) δ 7.18-7.11 (m, 2H), 7.09-6.99 (m, 5H), 6.71 (app. d, $J = 8.8$ Hz, 2H), 4.79 (d, $J = 2.7$ Hz, 1H), 4.70

(app. d, $J=5.1$ Hz, 1H), 3.72 (s, 3H), 3.03-2.97 (m, 1H), 2.72-2.60 (m, 1H), 2.42-2.33 (m, 1H), 2.33-2.25 (m, 1H), 2.06-1.96 (m, 1H), 1.92-1.83 (dddd, $J=14.3, 12.8, 5.1, 3.1$ Hz, 1H), 1.64-1.54 (m, 1H). ^{13}C NMR (125 MHz, CDCl_3) δ 212.9, 159.2, 148.2, 132.8, 129.3, 128.3, 126.11, 123.2, 113.9, 83.8, 76.1, 55.2, 55.1, 34.7, 33.5, 16.2.

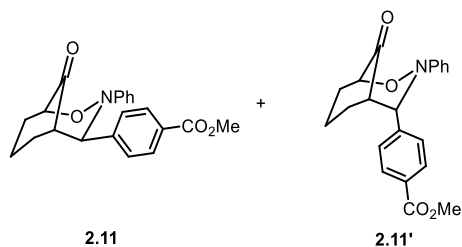


$R_f=0.22$ (30% diethyl ether/hexane), visualized by Magic stain. ^1H NMR (500 MHz, CDCl_3) δ 7.25-7.20 (m, 2H), 7.20-7.14 (m, 2H), 6.96-6.89 (m, 2H), 6.88-6.83 (m, 1H), 6.83-6.77 (m, 1H), 5.52 (d, $J=9.3$ Hz, 1H), 4.83-4.76 (m, 1H), 3.76 (s, 3H), 3.18-3.11 (m, 1H), 2.47-2.37 (m, 1H), 2.22-2.10 (m, 1H), 1.95-1.84 (m, 1H), 1.80-1.68 (m, 1H), 1.79-1.69 (m, 2H), 1.34-1.25 (m, 1H). ^{13}C NMR (125 MHz, CDCl_3) δ 211.6, 158.4, 147.1, 129.3, 128.7, 128.5, 121.5, 115.7, 113.7, 85.7, 67.2, 55.1, 49.8, 33.8, 29.8. HRMS Calculated for $\text{C}_{20}\text{H}_{21}\text{NO}_3$ $[\text{M}+\text{H}]^+$: 324.1594. Found 324.1592.



4-(4-Chlorophenyl)-3-phenyl-2-oxa-3-azabicyclo[3.3.1]nonan-9-one (2.10) Following general procedure **A**, silica gel column chromatography (50% methylene chloride/hexane) afforded the title compounds (129 mg, 79%) as a white solid. Following general procedure **B**, silica

gel column chromatography (50% methylene chloride/hexane) afforded the title compounds (109 mg, 67%) as a white solid. $R_f = 0.33, 0.20$ (30% diethyl ether/hexane), visualized by Magic stain. $^1\text{H NMR}$ (500 MHz, CDCl_3) δ 7.28-7.21 (m, 4H), 7.20-7.12 (m, 10H), 7.10-7.01 (m, 10H), 6.92-6.82 (m, 3H), 5.54 (d, $J=9.6$ Hz, 1H, **2.10'**), 4.86 (d, $J=2.6$ Hz, 1H, **2.10**), 4.74 (app. d, $J=4.9$ Hz, 1H, **2.10c'**), 4.71 (app. d, $J=5.0$ Hz, 1H, **2.10**), 3.22-3.12 (m, 1H, **2.10'**), 2.97-2.92 (m, 1H, **2.10**), 2.72-2.60 (m, 1H, **3cc**), 2.43-2.32 (m, 1H, **2.10**, m, 1H, **2.10'**), 2.33-2.23 (m, 1H, **2.10**), 2.09-1.96 (m, 1H, **2.10**, m, 1H, **2.10'**), 1.87 (app. ddd, $J=16.3, 12.6, 5.1$ Hz, 1H, **2.10**), 1.80-1.71 (m, 1H, **2.10'**), 1.71-1.63 (m, 1H, **2.10'**), 1.62-1.54 (m, 1H, **2.10**), 1.31-1.22 (m, 1H, **2.10'**). $^{13}\text{C NMR}$ (125 MHz, CDCl_3) δ 211.4, 211.0, 147.7, 139.1, 135.2, 133.8, 132.9, 129.6, 129.4, 128.9 (2C), 128.6, 128.5, 126.5, 123.2 (2C), 121.7, 115.3, 85.8, 83.9, 75.6, 66.8, 54.6, 49.2, 34.7, 33.8, 33.6, 29.7, 17.1, 16.2. **HRMS** Calculated for $\text{C}_{19}\text{H}_{18}\text{ClNO}_2$ $[\text{M}+\text{H}]^+$: 328.1099. Found 328.1108.

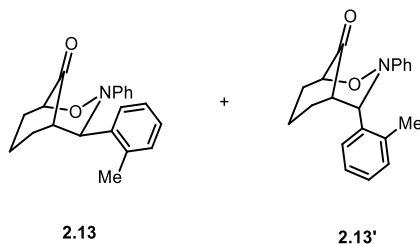


Methyl 4-(9-oxo-3-phenyl-2-oxa-3-azabicyclo[3.3.1]nonan-4-yl)benzoate (2.11) Following general procedure **A**, 3 equivalent of tosyloxy ketone **1c** was used. Silica gel column chromatography (80% methylene chloride/hexane) afforded the title compounds (141 mg, 80%) as white solids. $R_f = 0.43, 0.34$ (50% diethyl ether/hexane), visualized by Magic stain. $^1\text{H NMR}$ (500 MHz, CDCl_3) Major isomer **2.11** δ 7.90-7.84 (d, $J=8.0$ Hz, 2H), 7.24-7.20 (d, $J=8.0$ Hz, 2H), 7.18-7.12 (m, 2H), 7.10-7.01 (m, 3H), 4.96 (d, $J=2.5$ Hz, 1H), 4.74 (app. d, $J=4.9$ Hz, 1H), 3.87 (s, 3H), 2.98-2.91 (m, 1H), 2.73-2.60 (m, 1H), 2.44-2.30 (m, 1H), 2.10-2.00 (m, 1H), 1.95-

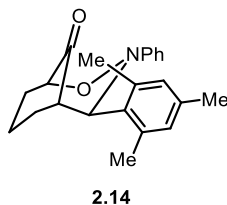
1.84 (m, 1H), 1.67-1.58 (m, 1H). Observed signals of the minor isomer **2.11'** δ 7.96 (d, $J= 8.2$ Hz, 2H), 7.41 (d, $J= 8.2$ Hz, 2H), 6.92-6.84 (m, 2H), 5.62 (d, $J= 9.6$ Hz, 1H), 4.84 (app. d, $J= 5.2$ Hz, 1H), 3.88 (s, 1H), 3.27-3.21 (m, 1H), 1.30-1.23 (m, 1H). ^{13}C NMR (125 MHz, CDCl_3) Major isomer **2.11** δ 212.2, 166.7, 147.6, 145.5, 130.1, 129.8, 128.6, 128.0, 126.6, 123.2, 84.0, 75.9, 54.6, 52.2, 34.7, 33.7, 16.2. **HRMS** Calculated for $\text{C}_{21}\text{H}_{21}\text{NO}_4$ $[\text{M}+\text{H}]^+$: 352.1543. Found 352.1555.



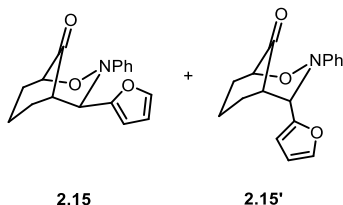
3-Phenyl-4-(m-tolyl)-2-oxa-3-azabicyclo[3.3.1]nonan-9-one (2.12) Following general procedure **A**, silica gel column chromatography (30% methylene chloride/hexane) afforded the title compounds (115 mg, 75%) as pale-yellow oils. Following general procedure **B**, silica gel column chromatography (30% methylene chloride/hexane) afforded the title compounds (106 mg, 69%) as pale-yellow oils. $R_f= 0.50, 0.39$ (30% diethyl ether/hexane), visualized by Magic stain. ^1H NMR (500 MHz, CDCl_3) Major isomer **2.12** δ 7.20-7.11 (m, 4H), 7.09-7.03 (m, 3H), 7.00-6.95 (m, 2H), 4.83 (d, $z= 2.7$ Hz, 1H), 4.72 (app. dt, $J= 5.1, 1.6$ Hz, 1H), 3.02-2.96 (m, 1H), 2.73-2.59 (m, 1H), 2.46-2.34 (m, 2H), 2.24 (s, 3H), 2.07-1.96 (m, 1H), 1.94-1.83 (m, 1H), 1.63-1.51 (m, 1H). Observed signals of minor isomer **2.12'** δ 5.52 (d, $J= 9.4$ Hz, 1H), 4.79 (app. dt, $J= 3.6, 1.5$ Hz, 1H), 3.20-3.14 (m, 1H), 2.30 (s, 3H), 2.21-2.10 (m, 1H), 1.89-1.84 (m, 1H), 1.77-1.68 (m, 2H), 1.62-1.58 (m, 1H), 1.31-1.26 (1H). ^{13}C NMR (125 MHz, CDCl_3) δ 212.8, 211.6, 148.1, 147.1, 140.6, 138.3, 137.9, 136.5, 128.8, 128.7, 128.5 (2C), 128.3, 128.2, 127.9, 126.1 (2C), 125.3, 125.1, 123.1, 121.4, 115.4, 85.7, 83.9, 76.4, 67.3, 54.9, 49.5, 34.8, 33.8, 33.6, 29.8, 21.6, 21.4, 17.3, 16.2. **HRMS** Calculated for $\text{C}_{20}\text{H}_{21}\text{NO}_2$ $[\text{M}+\text{H}]^+$: 308.1645. Found 308.1653.



3-Phenyl-4-(o-tolyl)-2-oxa-3-azabicyclo[3.3.1]nonan-9-one (2.13) Following general procedure **A**, silica gel column chromatography (30% methylene chloride/hexane) afforded the title compounds (112 mg, 73%) as colorless oils. Following general procedure **A**, silica gel column chromatography (30% methylene chloride/hexane) afforded the title compounds (104 mg, 68%) as colorless oils. $R_f = 0.40, 0.30$ (30% diethyl ether/hexane), visualized by Magic stain. **$^1\text{H NMR}$** (500 MHz, CDCl_3) Major isomer **2.13** δ 7.39-7.31 (m, 1H), 7.15-7.09 (m, 4), 7.05-7.01 (m, 3H), 6.84-6.81 (m, 1H), 5.18 (d, $J = 2.6$ Hz, 1H), 4.75 (app. d, $J = 5.2$ Hz, 1H), 3.01-2.94 (m, 1H), 2.77-2.62 (m, 1H), 2.43-2.35 (m, 1H), 2.31 (s, 3H), 2.10-1.98 (m, 2H), 1.93-1.82 (m, 1H), 1.64-1.56 (m, 1H). Observed signals of minor isomer **2.13** δ 5.65 (d, $J = 9.8$ Hz, 1H), 4.89 (app. d, $J = 5.3$ Hz, 1H), 3.36-3.29 (m, 1H), 2.30-2.26 (m, 1H), 2.10 (s, 3H), 1.80-1.72 (m, 1H), 1.56-1.50 (m, 2H), 1.25-1.20 (m, 1H). **$^{13}\text{C NMR}$** (125 MHz, CDCl_3) δ 213.1, 211.6, 148.3, 147.1, 139.2, 135.5, 135.1, 134.7, 130.5 (2C), 129.1, 129.0, 128.8, 128.3, 127.8, 127.3, 126.8, 126.2, 125.8, 122.9, 121.1, 114.7, 86.3, 84.0, 77.4, 64.7, 55.0, 47.7, 34.9, 34.0, 33.9, 29.8, 19.8, 19.5, 17.2, 16.3. **HRMS** Calculated for $\text{C}_{20}\text{H}_{21}\text{NO}_2$ $[\text{M}+\text{H}]^+$: 308.1645. Found 308.1656.

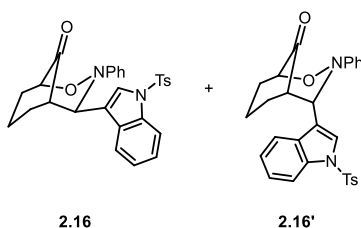


4-Mesityl-3-phenyl-2-oxa-3-azabicyclo[3.3.1]nonan-9-one (2.14) Following general procedure **A**, silica gel column chromatography (30% methylene chloride/hexane) afforded the title compounds (112 mg, 73%) as colorless oils. $R_f = 0.43$ (30% diethyl ether/hexane), visualized by Magic stain. $^1\text{H NMR}$ (500 MHz, CDCl_3) δ 7.15-7.07 (m, 4H), 7.04-6.99 (m, 1H), 6.78 (s, 1H), 6.59 (s, 1H), 5.45 (d, $J = 4.0$ Hz, 1H), 4.72 (app. d, $J = 3.6$ Hz, 1H), 3.07-3.01 (m, 1H), 2.81-2.68 (m, 1H), 2.51 (s, 3H), 2.41-2.35 (m, 1H), 2.24-2.19 (m, 1H), 2.14 (s, 3H), 2.10 (s, 3H), 2.03-1.94 (m, 1H), 1.91-1.82 (m, 1H), 1.65-1.57 (m, 1H). $^{13}\text{C NMR}$ (125 MHz, CDCl_3) δ 214.0, 148.7, 137.9, 137.3, 136.0, 133.5, 131.4, 129.0, 128.1, 126.4, 122.6, 84.0, 72.1, 54.5, 35.6, 34.4, 22.1, 21.5, 20.8, 15.8. **HRMS** Calculated for $\text{C}_{22}\text{H}_{25}\text{NO}_2$ $[\text{M}+\text{H}]^+$: 336.1958. Found 336.1972.



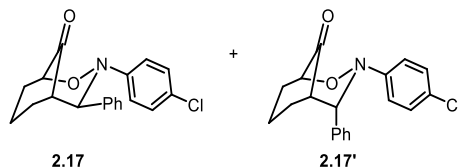
4-(Furan-2-yl)-3-phenyl-2-oxa-3-azabicyclo[3.3.1]nonan-9-one (2.15) Following general procedure **A**, silica gel column chromatography (30% methylene chloride/hexane) afforded the title compounds (123 mg, 87%) as a white solid. Following general procedure **B**, silica gel column chromatography (30% methylene chloride/hexane) afforded the title compounds (105 mg, 74%) as a white solid. $R_f = 0.30$ (30% diethyl ether/hexane), one spot, visualized by Magic stain. ^1H

NMR (500 MHz, CDCl₃) δ 7.36-7.34 (m, 1H), 7.29-7.28 (m, 1H), 7.24-7.18 (m, 4H), 7.09-7.04 (m, 1H), 7.04-7.00 (m, 2H), 6.97-6.89 (m, 3H), 6.25 (app. dd, J = 3.3 Hz, 1.8 Hz, 1H), 6.18 (app. dd, J = 3.3 Hz, 1.8 Hz, 1H), 6.16 (app. dd, J = 3.3 Hz, 0.7 Hz, 1H), 5.99 (app. d, J = 3.4 Hz, 1H), 5.53 (d, J = 9.5 Hz, 1H, **2.15'**), 4.99 (d, J = 3.2 Hz, 1H, **2.15**), 4.79 (app. ddd, J = 4.9, 1.6, 1.6 Hz, 1H, **2.15'**), 4.61-4.58 (m, 1H, **2.15**), 3.27-3.21 (m, 1H, **2.15'**), 3.14-3.07 (m, 1H, **2.15**), 2.69-2.56 (m, 1H, **2.15**), 2.49-2.28 (m, 2H, **2.15**, m, 2H, **2.15'**), 2.17-2.05 (m, 1H, **2.15'**), 2.02-1.93 (m, 1H, **2.15**), 1.93-1.81 (m, 3H, **2.15'**), 1.65-1.58 (m, 1H, **2.15**), 1.42-1.34 (m, 1H, **2.15'**). **¹³C NMR** (125 MHz, CDCl₃) δ 211.4, 210.8, 151.1, 150.2, 148.1, 147.1, 142.5, 141.8, 128.7, 128.4, 125.2, 122.2, 120.5, 115.7, 110.3 (2C), 109.9, 109.5, 85.9, 83.8, 69.2, 63.5, 51.3, 48.8, 34.7, 33.8, 33.6, 30.4, 17.2, 17.0. **HRMS** Calculated for C₁₇H₁₇NO₃ [M+H]⁺: 284.1281. Found 284.1289.

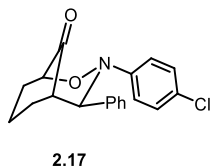


3-Phenyl-4-(1-tosyl-1H-indol-3-yl)-2-oxa-3-azabicyclo[3.3.1]nonan-9-one (2.16) Following general procedure **A**, 3 equivalent of **1c** was used. Silica gel column chromatography (20% diethyl ether/hexane) afforded the title compounds (177 mg, 73%) as a white solid. R_f = 0.35, 0.32 (50% diethyl ether/hexane), visualized by Magic stain. **¹H NMR** (500 MHz, CDCl₃) Major isomer **2.16** δ 7.84 (d, J = 7.8 Hz, 1H), 7.64 (d, J = 8.1 Hz, 1H), 7.41 (d, J = 8.1 Hz, 2H), 7.30-7.21 (m, 3H), 7.11 (d, J = 8.1 Hz, 2H), 7.04-6.94 (m, 5H), 5.08 (d, J = 3.1 Hz, 1H), 4.74 (app. d, J = 4.6 Hz, 1H), 3.11-3.00 (m, 1H), 2.77-2.63 (m, 1H), 2.47-2.33 (m, 2H), 2.34 (s, 3H), 2.10-1.99 (m, 1H), 1.98-1.87 (m, 1H), 1.68-1.61 (m, 1H). Observed signals of minor isomer **2.16'** δ 7.95 (d, J = 8.2 Hz, 1H), 7.49 (s,

1H), 5.74 (d, $J=9.8$ Hz, 1H), 4.88 (app. d, $J=5.1$ Hz, 1H), 3.39-3.31 (m, 1H), 2.30 (s, 3H), 2.27-2.15 (m, 1H), 1.92-1.85 (m, 1H), 1.79-1.70 (m, 1H), 1.66-1.55 (m, 2H), 1.25-1.19 (m, 1H). ^{13}C NMR (125 MHz, CD_2Cl_2) δ 213.4, 211.0, 148.6, 147.9, 145.7 (2C), 135.8, 135.4, 135.2, 135.1, 130.5, 130.4, 129.5, 129.2, 128.9, 127.1, 127.0, 126.8, 126.6, 125.8, 125.6 (2C), 124.3, 124.1, 122.8 (2C), 122.3, 122.0, 121.6, 119.4, 117.7, 116.0, 114.5, 114.2, 86.9, 84.7, 62.4, 53.9, 48.7, 35.4, 34.2, 34.1, 30.8, 30.3, 21.9 (2C), 18.0, 17.0. HRMS Calculated for $\text{C}_{28}\text{H}_{26}\text{N}_2\text{O}_4\text{S}$ $[\text{M}+\text{H}]^+$: 487.1686. Found 487.1685.

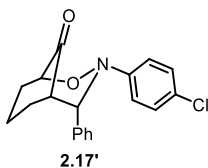


3-(4-Chlorophenyl)-4-phenyl-2-oxa-3-azabicyclo[3.3.1]nonan-9-one (2.17) Following general procedure **A**, silica gel column chromatography (20% methylene chloride/hexane) afforded the title compounds (138 mg, 84%) a white solid. Following general procedure **B**, silica gel column chromatography (20% methylene chloride/hexane) afforded the title compounds (116 mg, 71%) a white solid.

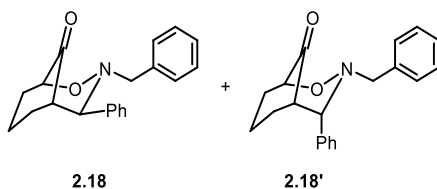


$R_f=0.41$ (30% diethyl ether/hexane), visualized by Magic stain. ^1H NMR (500 MHz, CDCl_3) δ 7.23-7.18 (m, 3H), 7.14-7.07 (m, 4H), 6.96 (app. d, $J=8.8$ Hz, 2H), 4.78 (d, $J=2.7$ Hz, 1H), 4.71 (ddd, $J=5.0, 1.6, 1.6$ Hz, 1H), 3.05-2.97 (m, 1H), 2.70-2.57 (m, 1H), 2.42-2.34 (m, 1H), 2.34-

2.26 (m, 1H), 2.07-1.98 (m, 1H), 1.89 (dddd, $J= 14.3, 12.6, 5.2, 1.4$ Hz, 1H), 1.64-1.57 (m, 1H). $^{13}\text{C NMR}$ (125 MHz, CDCl_3) δ 212.4, 146.8, 140.3, 131.6, 128.9, 128.5, 123.4, 128.2, 124.4, 84.1, 76.9, 54.9, 34.8, 33.7, 16.3.

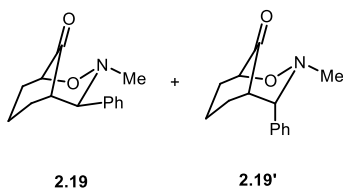


$R_f= 0.28$ (30% diethyl ether/hexane), visualized by Magic stain. $^1\text{H NMR}$ (500 MHz, CDCl_3) δ 7.31-7.27 (m, 4H), 7.25-7.20 (m, 1H), 7.12 (app. d, $J=8.9$ Hz, 2H), 6.84 (app. d, $J= 9.0$ Hz, 1H), 5.51 (d, $J= 9.5$ Hz, 1H), 4.80 (ddd, $J= 5.1, 1.4, 1.4$ Hz, 1H), 3.23-3.16 (m, 1H), 2.45-2.36 (m, 1H), 2.19-2.05 (m, 1H), 1.89 (dddd, $J= 14.3, 12.6, 5.6, 1.4$ Hz, 1H), 1.80-1.65 (m, 2H), 1.31-1.23 (m, 1H). $^{13}\text{C NMR}$ (125 MHz, CDCl_3) δ 211.3, 145.9, 136.3, 128.9, 128.6, 128.2, 127.4, 126.7, 116.9, 85.9, 67.8, 49.6, 33.9, 29.8, 17.3. **HRMS** Calculated for $\text{C}_{19}\text{H}_{18}\text{ClNO}_2$ $[\text{M}+\text{H}]^+$: 328.1099. Found 328.1097.



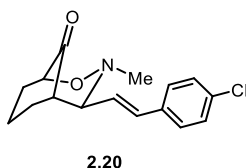
3-Benzyl-4-phenyl-2-oxa-3-azabicyclo[3.3.1]nonan-9-one (2.18) Following general procedure **A**, silica gel column chromatography (40% methylene chloride/hexane) afforded the title compounds (138 mg, 90%) an off-white solid. Following general procedure **B**, silica gel column chromatography (40% methylene chloride/hexane) afforded the title compounds (99 mg, 64%) an off-white solid. $R_f= 0.41$ (30% diethyl ether/hexane), one spot, visualized by Magic stain.

¹H NMR (500 MHz, CDCl₃) Major isomer **2.18** δ 7.42-7.35 (m, 2H), 7.35-7.30 (m, 4H), 7.30-7.24 (m, 4H), 4.48-4.44 (m, 1H), 4.39 (d, *J*= 2.8 Hz, 1H), 3.79 (d, *J*= 15.0 Hz, 1H), 3.53 (d, *J*= 15.0 Hz, 1H), 2.90-2.83 (m, 1H), 2.56-2.44 (m, 1H), 2.27-2.17 (m, 2H), 1.97-1.85 (m, 1H), 1.75-1.68 (app. td, *J*= 14.0, 5.0 Hz, 1H), 1.53-1.44 (m, 1H). Observed signals of minor isomer **2.18'** δ 4.45-4.43 (m, 1H), 4.12 (d, *J*= 14.9 Hz, 1H), 4.04-3.99 (m, 1H), 3.45 (d, *J*= 14.9 Hz, 1H), 3.16-3.04 (m, 1H), 2.16-2.02 (m, 2H), 1.84-1.75 (m, 2H), 1.29-1.24 (m, 1H). **¹³C NMR** (125 MHz, CDCl₃) δ 213.1, 212.1, 141.7, 138.4, 138.3, 137.9, 129.2 (2C), 129.0, 128.8, 128.4, 128.3, 128.2, 128.1, 127.6 (2C), 127.3, 127.0, 83.7, 81.7, 76.8, 76.2, 60.2, 58.7, 55.4, 52.0, 34.7, 34.2, 33.4, 29.7, 21.0, 15.8. **HRMS** Calculated for C₂₀H₂₁NO₂ [M+H]⁺: 308.1645. Found 308.1646.

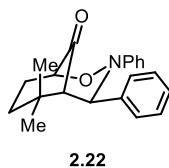


3-Methyl-4-phenyl-2-oxa-3-azabicyclo[3.3.1]nonan-9-one (2.19) Following general procedure **A**, silica gel column chromatography (40% methylene chloride/hexane) afforded the title compounds (96 mg, 83%) as a pale-yellow oil. Following general procedure **B**, silica gel column chromatography (40% methylene chloride/hexane) afforded the title compounds (97 mg, 84%) as a pale-yellow oil. *R_f*= 0.40 (30% diethyl ether/hexane), one spot, visualized by Magic stain. **¹H NMR** (500 MHz, CDCl₃) Major isomer **2.19** δ 7.41-7.35 (m, 2H), 7.35-7.27 (m, 3H), 4.13 (d, *J*= 3.1 Hz, 1H), 4.06-4.02 (m, 1H), 3.05-2.91 (m, 1H), 2.64-2.57 (m, 1H), 2.51 (s, 3H), 2.40-2.36 (m, 1H), 2.16-2.04 (m, 2H), 1.81-1.70 (m, 1H), 1.65-1.56 (m, 1H). Observed signals of minor isomer **2.19'** δ 4.60 (app. d, *J*= 5.2 Hz, 1H), 4.10 (d, *J*= 2.9 Hz, 1H), 2.84-2.79 (m, 1H),

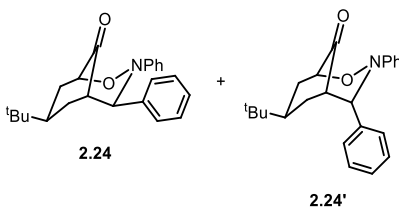
2.41 (s, 3H), 2.30-2.21 (m, 1H), 2.20-2.11 (m, 1H), 1.94-1.85 (m, 1H), 1.54-1.47 (m, 1H). ^{13}C NMR (125 MHz, CDCl_3) δ 212.6, 211.6, 138.6, 135.7, 129.1, 128.9, 128.4, 128.0, 127.7, 127.6, 83.4, 81.7, 78.8, 78.5, 54.9, 51.9, 44.7, 43.5, 34.9, 34.7, 33.4, 29.7, 21.0, 15.7. HRMS Calculated for $\text{C}_{14}\text{H}_{17}\text{NO}_2$ $[\text{M}+\text{H}]^+$: 232.1332. Found 232.1344.



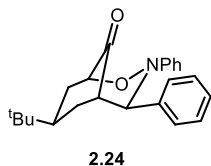
4-((E)-4-Chlorostyryl)-3-methyl-2-oxa-3-azabicyclo[3.3.1]nonan-9-one (2.20) Following general procedure **A**, 2 equivalent of **1c** was used. Silica gel column chromatography (40% methylene chloride/hexane) afforded the title compounds (118 mg, 81%) a pale-yellow oil. R_f = 0.40 (30% diethyl ether/hexane), one spot, visualized by Magic stain. ^1H NMR (500 MHz, CD_2Cl_2) δ 7.33 (app. d, J = 8.9 Hz, 2H), 7.30 (app. d, J = 8.9 Hz, 2H), 6.53 (d, J = 15.8 Hz, 1H), 6.03 (dd, J = 15.9, 9.4 Hz, 1H), 4.43 (app. dt, J = 5.1, 1.6 Hz, 1H), 3.80 (dd, J = 9.3 Hz, 1H), 2.58 (s, 3H), 2.57-2.54 (m, 1H), 2.47-2.35 (m, 1H), 2.24-2.10 (m, 2H), 1.95-1.82 (m, 1H), 1.69 (dddd, J = 14.3, 12.8, 5.0, 1.3 Hz, 1H), 1.52-1.44 (m, 1H). ^{13}C NMR (125 MHz, CD_2Cl_2) δ 212.5, 135.6, 134.2, 131.8, 129.6, 129.3, 128.4, 83.9, 77.5, 53.3, 43.9, 55.3, 33.4, 16.4. HRMS Calculated for $\text{C}_{16}\text{H}_{18}\text{ClNO}_2$ $[\text{M}+\text{H}]^+$: 292.1099. Found 292.1108.



6,6-Dimethyl-3,4-diphenyl-2-oxa-3-azabicyclo[3.3.1]nonan-9-one (3da) Following general procedure **A**, silica gel column chromatography (20% methylene chloride/hexane) afforded the title compounds (132 mg, 82%) a white solid. $R_f = 0.54, 0.43$ (30% diethyl ether/hexane), visualized by Magic stain. $^1\text{H NMR}$ (500 MHz, CDCl_3) δ 7.21-7.16 (m, 3H), 7.16-7.10 (m, 4H), 7.08-7.00 (m, 3H), 4.99 (d, $J = 3.0$ Hz, 1H), 4.66 (app. d, $J = 4.8$ Hz, 1H), 2.65-2.54 (m, 2H), 2.18 (dtd, $J = 14.8, 4.9, 1.7$ Hz, 1H), 1.91 (app. dt, $J = 14.7, 5.1$ Hz, 1H), 1.30 (app. dd, $J = 14.0, 4.9$ Hz, 1H), 1.19 (s, 3H), 0.96 (s, 3H). $^{13}\text{C NMR}$ (125 MHz, CDCl_3) δ 211.0, 148.1, 141.0, 128.7, 128.3, 128.1, 127.8, 126.3, 123.3, 82.9, 73.6, 65.8, 40.2, 29.8, 29.6, 28.5, 26.8. **HRMS** Calculated for $\text{C}_{21}\text{H}_{23}\text{NO}_2$ $[\text{M}+\text{H}]^+$: 322.1802. Found 322.1784.

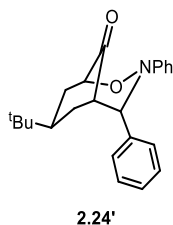


7-(tert-Butyl)-3,4-diphenyl-2-oxa-3-azabicyclo[3.3.1]nonan-9-one (2.24) Following general procedure **A**, silica gel column chromatography (5% diethyl ether/hexane) afforded the title compounds (134 mg, 77%) as a white solid.

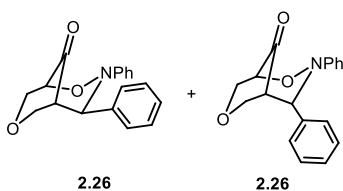


$R_f = 0.40$ (20% diethyl ether/hexane), visualized by Magic stain. $^1\text{H NMR}$ (500 MHz, CDCl_3) δ 7.20-7.10 (m, 7H), 7.09-7.00 (m, 3H), 4.87 (d, $J = 2.5$ Hz, 1H), 4.71 (app. dt, $J = 5.3, 1.6$ Hz, 1H), 3.00-2.94 (m, 1H), 2.76-2.67 (m, 1H), 2.48-2.39 (m, 1H), 2.36-2.28 (m, 1H), 1.83 (app. td, $J = 13.5,$

4.7 Hz, 1H), 1.66 (app. dd, $J= 14.0, 12.3$ Hz, 1H), 0.94 (s, 9H). ^{13}C NMR (125 MHz, CDCl_3) δ 2113.3, 147.9, 140.8, 128.7, 128.4, 128.1, 128.0, 126.2, 123.2, 83.6, 76.6, 54.1, 36.8, 35.9, 34.9, 32.3, 27.9.

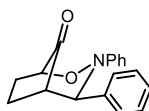


$R_f = 0.24$ (20% diethyl ether/hexane), visualized by Magic stain. ^1H NMR (500 MHz, CDCl_3) δ 7.34-7.27 (m, 4H), 7.23-7.14 (m, 3H), 6.94 (app. d, $J= 7.8$ Hz, 2H), 6.86 (app. t, $J= 7.3$ Hz, 1H), 5.57 (d, $J= 9.4$ Hz, 1H), 4.78 (app. d, $J= 5.3$ Hz, 1H), 3.23-3.14 (m, 1H), 2.44 (dtd, $J= 13.9, 5.0, 3.2$ Hz, 1H), 2.33-2.24 (m, 1H), 1.75-1.67 (m, 1H), 1.63 (app. dd, $J= 14.0, 12.4$ Hz, 1H), 1.51 (ddd, $J= 14.2, 13.0, 5.0$ Hz, 1H), 0.62 (s, 9H). ^{13}C NMR (125 MHz, CDCl_3) δ 211.9, 147.2, 136.6, 128.9, 128.4, 128.3, 127.2, 121.7, 115.8, 85.5, 67.3, 49.0, 37.6, 35.1, 32.0, 31.1, 27.4. HRMS Calculated for $\text{C}_{23}\text{H}_{27}\text{NO}_2$ $[\text{M}+\text{H}]^+$: 350.2115. Found 350.2124.



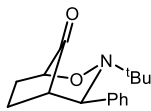
3,4-Diphenyl-2,7-dioxa-3-azabicyclo[3.3.1]nonan-9-one (2.24) Following general procedure A, silica gel column chromatography (50% methylene chloride/hexane) afforded the title compounds (52 mg, 35%) as a white solid. $R_f = 0.39, 0.26$ (40% diethyl ether/hexane), visualized by Magic stain. ^1H NMR (500 MHz, CDCl_3) Major isomer **2.26** δ 7.51 (app. d, $J= 7.7$ Hz, 2H),

7.33-7.26 (m, 2H), 7.26-7.10 (m, 3H), 6.96 (app. d, $J= 8.1$ Hz, 2H), 6.90-6.82 (m, 1H), 5.57 (d, $J= 9.5$ Hz, 1H), 4.85-4.77 (m, 1H), 4.50-4.44 (m, 1H), 3.82 (d, $J= 12.0$ Hz, 1H), 3.76 (d, $J= 12.3$ Hz, 1H), 3.66 (dd, $J= 11.9, 2.8$ Hz, 1H), 3.13 (dd, $J= 9.5, 2.3$ Hz, 1H). Observed signals of minor isomer **2.26'** δ 5.12 (d, $J= 3.0$ Hz, 1H), 4.73-4.67 (m, 1H), 4.44-4.35 (m, 2H), 3.88 (d, $J= 11.7$ Hz, 1H), 3.72 (d, $J= 12.2$ Hz, 1H), 3.09-3.05 (m, 1H). ^{13}C NMR (125 MHz, CDCl_3) δ 206.7, 205.8, 147.5, 147.0, 139.8, 135.9, 128.9, 128.8 (2C), 128.5 (2C), 128.4 (2C), 127.8, 127.1, 124.3, 122.2, 116.4, 86.4, 85.1, 76.2, 73.6, 73.2, 72.7, 70.4, 69.2, 58.5, 53.4. **HRMS** Calculated for $\text{C}_{18}\text{H}_{17}\text{NO}_3$ $[\text{M}+\text{H}]^+$: 296.1281. Found 296.1295.



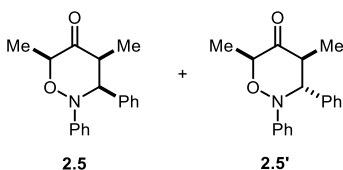
2.3

3,4-Diphenyl-2-oxa-3-azabicyclo[3.2.1]octan-8-one (2.3) Following general procedure A, reaction was run at room temperature for 12 hours. Silica gel column chromatography (50% methylene chloride/hexane) afforded the title compounds (78 mg, 56%) as a white solid. $R_f= 0.29$ (30% diethyl ether/hexane), visualized by Magic stain. ^1H NMR (500 MHz, CDCl_3) δ 7.36 (app. d, $J= 7.1$ Hz, 2H), 7.26-7.21 (m, 3H), 7.21-7.14 (m, 3H), 6.89 (app. d, $J= 6.8$ Hz, 2H), 6.82 (app. t, $J= 7.4$ Hz, 1H), 5.21 (d, $J= 4.0$ Hz, 1H), 4.21 (d, $J= 4.8$ Hz, 1H), 2.71 (app. ddd, $J= 5.7, 4.1, 1.3$ Hz, 1H), 2.46 (ddd, $J= 14.8, 10.9, 4.2$ Hz, 1H), 2.34-2.22 (m, 1H), 2.16-2.07 (m, 1H), 2.07-1.98 (m, 1H). ^{13}C NMR (125 MHz, CDCl_3) δ 209.8, 147.7, 137.06, 128.9, 128.7, 127.8, 127.7, 120.7, 114.7, 81.3, 73.9, 50.2, 23.7, 22.9. **HRMS** Calculated for $\text{C}_{18}\text{H}_{17}\text{NO}_2$ $[\text{M}+\text{H}]^+$: 280.1332. Found 280.1321.



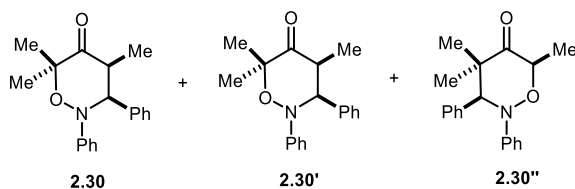
2.28

3-(tert-Butyl)-4-phenyl-2-oxa-3-azabicyclo[3.2.1]octan-8-one (2.28) Following general procedure **A**, reaction was run at room temperature. Silica gel column chromatography (20% diethyl ether/hexane) afforded the title compounds (83 mg, 64%) as a white solid. Structure of **2.28''** is tentatively assigned to be the *syn* product. $R_f = 0.31$ (30% diethyl ether/hexane), visualized by Magic stain. $^1\text{H NMR}$ (500 MHz, CDCl_3) δ 7.41-7.35 (m, 2H), 7.30-7.23 (m, 3H), 4.34 (d, $J = 3.6$ Hz, 1H), 4.06 (app. d, $J = 4.2$ Hz, 1H), 2.40-2.27 (m, 2H), 2.16 (ddd, $J = 11.7, 11.1, 4.6$ Hz, 1H), 2.01-1.91 (m, 1H), 1.83-1.74 (m, 1H), 0.97 (s, 9H). $^{13}\text{C NMR}$ (125 MHz, CDCl_3) δ 212.2, 141.1, 128.9, 128.2, 127.7, 81.2, 74.3, 58.1, 20.6, 27.5, 24.5, 23.1. **HRMS** Calculated for $\text{C}_{16}\text{H}_{21}\text{NO}_2$ $[\text{M}+\text{H}]^+$: 260.1645. Found 260.1650.



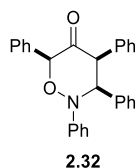
4,6-Dimethyl-2,3-diphenyl-1,2-oxazinan-5-one (2.5') Following general procedure **A**, silica gel column chromatography (3% diethyl ether/hexane) afforded the title compounds (111 mg, 79%) as a white solid. $R_f = 0.51, 0.43$ (30% diethyl ether/hexane), visualized by Magic stain. $^1\text{H NMR}$ (500 MHz, CDCl_3) Major isomer **2.5** δ 7.46-7.41 (m, 2H), 7.30-7.25 (m, 2H), 7.24-7.18 (m, 1H), 7.16-7.09 (m, 2H), 6.87-6.82 (m, 2H), 6.81-6.76 (m, 1H), 4.62 (q, $J = 7.1$ Hz, 1H), 4.50 (dm $J = 7.7$

Hz, 1H), 3.18 (dq, $J= 7.8, 6.7$ Hz, 1H), 1.48 (d, $J= 7.0$ Hz, 3H), 1.19 (d, $J= 6.7$ Hz, 3H). Observed signals of minor isomer **2.5'** δ 7.00-6.89 (m, 3H), 5.10 (d, $J= 7.8$ Hz, 1H), 4.62 (q, $J= 6.7$ Hz, 1H), 3.53 (app. p, $J= 7.0$ Hz, 1H), 1.62 (d, $J= 6.6$ Hz, 3H), 0.82 (d, $J= 6.9$ Hz, 3H). **^{13}C NMR** (125 MHz, CDCl_3) Major isomer **2.5** δ 213.0, 147.4, 139.9, 128.7, 128.6, 128.1, 127.9, 121.1, 114.9, 84.2, 71.9, 46.2, 15.2, 11.7. **HRMS** Calculated for $\text{C}_{18}\text{H}_{19}\text{NO}_2$ $[\text{M}+\text{H}]^+$: 282.1489. Found 282.1501.

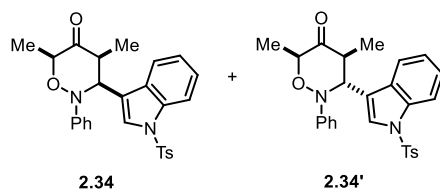


4,6,6-Trimethyl-2,3-diphenyl-1,2-oxazinan-5-one (2.30) Following general procedure A, 1.8 equivalent of NEt_3 was used as the base. Reaction was run at 40 °C for 60 hours. Silica gel column chromatography (3% diethyl ether/hexane) afforded the title compounds (134 mg, 79%) as a white solid. Structure of **2.30''** is tentatively assigned to be the *syn* product. $R_f= 0.35, 0.26$ (10% diethyl ether/hexane), two spots, visualized by Magic stain. **^1H NMR** (500 MHz, CDCl_3) Major isomer **2.30** δ 7.50-7.43 (m, 2H), 7.28-7.22 (m, 2H), 7.21-7.15 (m, 1H), 7.12-7.06 (m, 2H), 6.85-6.79 (m, 2H), 6.77-6.71 (m, 1H), 4.56 (d, $J= 7.3$ Hz, 1H), 3.22 (p, $J= 6.8$ Hz, 1H), 1.51 (s, 3H), 1.46 (s, 3H), 1.20 (d, $J= 6.8$ Hz, 3H). Observed signals of minor isomer **2.30'** δ 5.09 (d, $J= 8.9$ Hz, 1H), 3.73 (dq, $J= 8.9, 6.8$ Hz, 1H), 1.75 (s, 3H), 1.40 (s, 3H), 0.64 (d, $J= 6.8$ Hz, 3H). Observed signals of minor isomer **2.30''** δ 4.81 (q, $J= 6.8$ Hz, 1H), 4.62 (s, 1H), 1.60 (s, 3H), 1.54 (d, $J= 12.6$ Hz, 2H), 0.98 (s, 3H). **^{13}C NMR** (125 MHz, CDCl_3) Major isomer **2.30** δ 214.5, 147.9, 139.9, 128.6 (2C), 128.2, 127.9, 120.7, 115.0, 86.3, 72.6, 46.1, 22.7, 21.3, 11.9. Minor isomers **2.30'** and **2.30''** δ 215.7, 213.5, 149.3, 148.2, 138.3, 136.0, 129.6, 128.7 (2C), 128.5, 128.2 (2C), 128.0, 127.8, 122.9,

121.9, 117.8, 116.1, 89.3, 80.4, 77.0, 73.7, 47.1, 41.3, 27.5, 23.0, 22.5, 21.5, 14.5, 10.4. **HRMS**
Calculated for C₁₉H₂₁NO₂ [M+H]⁺: 296.1645. Found 296.1654.

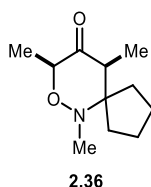


2,3,4,6-Tetraphenyl-1,2-oxazin-5-one (2.32) Following general procedure **A**, reaction was run at room temperature. Silica gel column chromatography (10% diethyl ether/hexane) afforded the title compounds (73 mg, 36%) as an off-white solid. *R*_f = 0.40 (20% diethyl ether/hexane), visualized by Magic stain. ¹H NMR (500 MHz, CDCl₃) δ 7.62 (app. d, *J* = 7.3 Hz, 2H), 7.45-7.36 (m, 3H), 7.34-7.27 (m, 3H), 7.22-7.10 (m, 9H), 6.95 (app. d, *J* = 8.0 Hz, 2H), 6.83 (app. t, 6.83, *J* = 7.3 Hz, 1H), 5.76 (s, 1H), 5.24 (d, *J* = 7.6 Hz, 1H), 4.39 (d, *J* = 7.6 Hz, 1H). ¹³C NMR (125 MHz, CDCl₃) δ 206.5, 147.1, 138.8, 134.7, 133.3, 130.2, 129.0 (2C), 128.9, 128.6 (2C), 127.9, 127.8 (2C), 126.4, 121.6, 115.2, 90.3, 73.1, 59.3. **HRMS** Calculated for C₂₈H₂₃NO₂ [M+H]⁺: 406.1802. Found 406.1814.



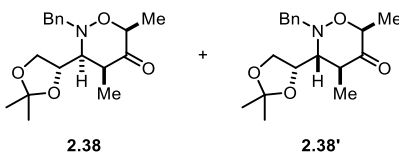
4,6-Dimethyl-2-phenyl-3-(1-tosyl-1H-indol-3-yl)-1,2-oxazin-5-one (2.34) Following general procedure **A**, 2 equivalent of ketone **1b** was used. Silica gel column chromatography (30% methylene chloride/hexane) afforded the title compounds (225 mg, 95%) as a white solid. Structure

of **2.34'** is tentatively assigned to be the *syn* product. $R_f = 0.27, 0.15$ (30% diethyl ether/hexane), visualized by Magic stain. $^1\text{H NMR}$ (500 MHz, CDCl_3) δ 7.88 (app.d, $J = 8.3$ Hz, 1H), 7.84 (app.d, $J = 8.1$ Hz, 1H), 7.78 (app.d, $J = 8.1$ Hz, 1H), 7.61 (s, 1H), 7.50 (d, $J = 8.2$ Hz, 2H), 7.47 (s, 1H), 7.39 (d, $J = 8.2$ Hz, 2H), 7.34-7.19 (m, 4H), 7.19-7.14 (m, 1H), 7.13-7.02 (m, 6H), 6.97-6.76 (m, 5H), 5.46 (d, $J = 7.2$ Hz, 1H, **2.34'**), 4.80 (d, $J = 7.0$ Hz, 1H, **2.34**), 4.74-4.66 (m, 1H **2.34'**, 1H **2.34**), 3.53 (p, $J = 6.9$ Hz, 1H, **2.34'**), 3.26 (p, $J = 6.8$ Hz, 1H, **2.34**), 2.31 (s, 3H, **2.34'**, 3H, **2.34**), 1.60 (d, $J = 6.9$ Hz, 3H, **2.34'**), 1.54 (d, $J = 6.8$ Hz, 3H, **2.34**), 1.23 (d, $J = 6.8$ Hz, 3H, **2.34**), 0.58 (d, $J = 6.9$ Hz, 3H, **2.34'**). $^{13}\text{C NMR}$ (125 MHz, CDCl_3) δ 212.3, 208.9, 148.1, 147.3, 144.8, 144.7, 135.2, 134.7, 134 (2C), 131.1, 129.8, 129.7, 129.2, 128.6, 128.5, 126.5, 126.4, 125.9, 125.7, 124.9, 124.8, 123.4 (2C), 1232.7, 121.6, 120.5 (2C), 119.2, 118.0, 116.8, 115.5, 113.9, 113.8, 84.3, 82.2, 65.1, 64.1, 45.9, 44.9, 21.5 (2C), 15.0, 13.5, 12.7, 10.8. **HRMS** Calculated for $\text{C}_{27}\text{H}_{26}\text{N}_2\text{O}_4\text{S}$ $[\text{M}+\text{H}]^+$: 475.1688. Found 475.1701.



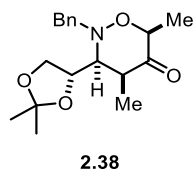
8,10-Dimethyl-6-phenyl-7-oxa-6-azaspiro[4.5]decan-9-one (2.36) Following general procedure **A**, silica gel column chromatography (30% diethyl ether/hexane) afforded the title compounds (69 mg, 70%) as a colorless oil. $R_f = 0.31$ (30% diethyl ether/hexane), visualized by Magic stain. $^1\text{H NMR}$ (500 MHz, CDCl_3) δ 4.33 (q, $J = 6.6$ Hz, 1H), 2.73 (q, $J = 6.8$ Hz, 1H), 2.61 (s, 1H), 1.89-1.80 (m, 1H), 1.80-1.73 (m, 2H), 1.71-1.62 (m, 2H), 1.55-1.43 (m, 2H), 1.42-1.34 (m, 1H), 1.21 (d, $J = 6.6$ Hz, 3H), 1.09 (d, $J = 6.9$ Hz, 3H). $^{13}\text{C NMR}$ (125 MHz, CDCl_3) δ 209.7,

80.7, 77.2, 52.3, 38.3, 35.3, 27.9, 26.3, 26.2, 13.4, 8.9. **HRMS** Calculated for C₁₁H₁₉NO₂ [M+H]⁺: 198.1489. Found 198.1498.

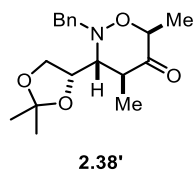


2-Benzyl-3-(2,2-dimethyl-1,3-dioxolan-4-yl)-4,6-dimethyl-1,2-oxazinan-5-one (2.38)

Following general procedure **A**, silica gel column chromatography (5% diethyl ether/hexane) afforded the title compounds (140 mg, 88%) as a colorless oil.

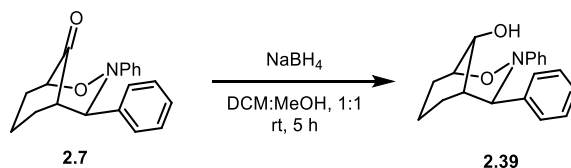


R_f = 0.33 (30% diethyl ether/hexane), visualized by Magic stain. ¹H NMR (500 MHz, CDCl₃) δ 7.38-7.29 (m, 4H), 7.29-7.24 (m, 1H), 4.63 (app. q, *J* = 6.8 Hz, 1H), 4.29 (q, *J* = 6.9 Hz, 1H), 4.24 (d, *J* = 14.0 Hz, 1H), 4.13 (dd, *J* = 8.4, 6.1 Hz, 1H), 3.92 (d, *J* = 14.2 Hz, 1H), 3.74 (t, *J* = 8.3 Hz, 1H), 3.26 (dd, *J* = 6.3, 2.8 Hz, 1H), 2.47 (qd, *J* = 7.2, 2.8 Hz, 1H), 1.43 (s, 3H), 1.40 (s, 3H), 1.34 (d, *J* = 7.2 Hz, 3H), 1.08 (d, *J* = 6.9 Hz, 3H). ¹³C NMR (125 MHz, CDCl₃) δ 213.5, 137.8, 128.9, 128.3, 127.4, 109.1, 81.8, 74.6, 70.6, 66.6, 59.6, 42.5, 26.7, 25.8, 17.9, 14.8.



$R_f = 0.27$ (30% diethyl ether/hexane), visualized by Magic stain. $^1\text{H NMR}$ (500 MHz, CDCl_3) δ 7.38-7.30 (m, 4H), 7.30-7.26 (m, 1H), 4.64 (td, $J = 7.0, 3.7$ Hz, 1H), 4.29 (q, $J = 7.0$ Hz, 1H), 4.21 (d, $J = 13.7$ Hz, 1H), 4.17 (dd, $J = 8.5, 6.5$ Hz, 1H), 3.80 (d, $J = 13.7$ Hz, 1H), 3.71 (dd, $J = 8.3, 7.2$ Hz, 1H), 3.03 (t, $J = 3.3$ Hz, 1H), 2.68 (qd, $J = 7.2, 2.9$ Hz, 1H), 1.41 (s, 3H), 1.38 (s, 3H), 1.35 (d, $J = 7.0$ Hz, 3H), 1.14 (d, $J = 6.8$ Hz, 3H). $^{13}\text{C NMR}$ (125 MHz, CDCl_3) δ 213.2, 137.3, 128.9, 128.4, 127.6, 109.6, 80.8, 74.0, 69.8, 67.7, 59.1, 42.6, 26.1, 25.1, 17.7, 14.9. **HRMS** Calculated for $\text{C}_{18}\text{H}_{25}\text{NO}_4$ $[\text{M}+\text{H}]^+$: 320.1856. Found 320.1873.

8.2.5 Derivatization of the [3+3] Cycloaddition Product



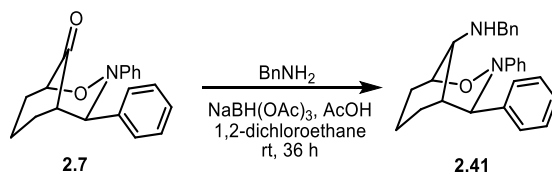
3,4-Diphenyl-2-oxa-3-azabicyclo[3.3.1]nonan-9-ol (2.39) A 4 mL glass vial was charged with **2.7** (37 mg, 0.13 mmol, 1 equiv.), which was then dissolved in a methanol:methylene chloride 1:1 solvent mixture (1.2 mL). NaBH_4 (29 mg, 0.78 mmol, 6 equiv.) was then added at room temperature to the above solution and the resulting mixture was allowed stir at room temperature for 5 h. The reaction was then diluted with methylene chloride (10 mL) and washed with saturated NH_4Cl aqueous solution (2×5 mL) and brine (5 mL). The organic phase was dried over anhydrous Na_2SO_4 , filtered and concentrated *in vacuo*. The resulting material was then purified by silica gel column chromatography (30% diethyl ether/hexane) to afford compound **2.39** as a white solid (35 mg, 93%, single diastereomer). $R_f = 0.26$ (30% diethyl ether/hexane), visualized by Magic stain. $^1\text{H NMR}$ (500 MHz, CDCl_3) δ 7.28-7.19 (m, 4H), 7.19-7.11 (m, 3H), 7.01-6.94 (m, 3H), 4.55 (d,

$J= 3.0$ Hz, 1H), 4.54-4.52 (m, 1H), 4.18 (d, $J= 11.4$ Hz, 1H), 3.70 (ddd, $J= 11.3, 3.2, 1.3$ Hz, 1H), 2.79-2.72 (m, 1H), 2.34-2.21 (m, 1H), 2.18-2.10 (m, 1H), 1.98-1.90 (m, 1H), 1.77-1.61 (m, 2H), 1.56-1.49 (m, 1H). ^{13}C NMR (125 MHz, CDCl_3) δ 148.1, 140.9, 128.9, 128.7, 128.6, 127.5, 124.2, 120.1, 78.9, 72.7, 71.0, 42.4, 30.5 (2C), 16.7. HRMS Calculated for $\text{C}_{19}\text{H}_{21}\text{NO}_2$ $[\text{M}+\text{H}]^+$: 296.1645. Found 296.1655.

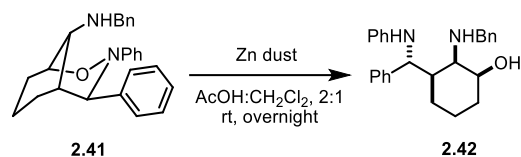


3-(Phenyl(phenylamino)methyl)cyclohexane-1,2-diol (2.40) A 10 mL round bottom flask was charged with **2.39** (81.4 mg, 0.28 mmol, 1 equiv.), which was then dissolved in an acetic acid:methylene chloride 2:1 solvent mixture (1.75 mL). Zinc dust (< 10 micron, 98%, 179 mg, 2.80 mmol, 10 equiv.) was added at room temperature in one portion. The reaction mixture was then allowed to stir overnight at room temperature before filtered through a Celite plug. The filtrate was then diluted with methylene chloride (10 mL), washed with saturated Na_2CO_3 aqueous solution (2×5 mL) and brine (5 mL), dried with anhydrous N_2SO_4 , filtered, and concentrated *in vacuo*. The resulting material was purified by silica gel column chromatography (60% diethyl ether/hexane) to afford compound **6** as a white solid (67 mg, 83%). $R_f= 0.15$ (60% diethyl ether/hexane), visualized by Magic stain. ^1H NMR (500 MHz, CDCl_3) δ 7.35-7.27 (m, 4H), 7.23-7.18 (m, 1H), 7.09-7.02 (m, 2H), 5.36 (s, 1H), 4.56 (d, $J= 5.6$ Hz, 1H), 3.88-3.83 (m, 1H), 3.49-3.42 (m, 1H), 2.33 (s, 1H), 1.83-1.72 (m, 2H), 1.72-1.61 (m, 4H), 1.38-1.31 (m, 1H), 1.29-1.25 (m, 1H). ^{13}C NMR (125 MHz, CDCl_3) δ 147.7, 142.8, 129.2, 128.5 (2C), 126.9, 116.6, 113.0, 70.7,

69.6, 60.6, 46.8, 28.3, 23.9, 23.5. **HRMS** Calculated for C₁₉H₂₃NO₂ [M+H]⁺: 298.1802. Found 298.1808.

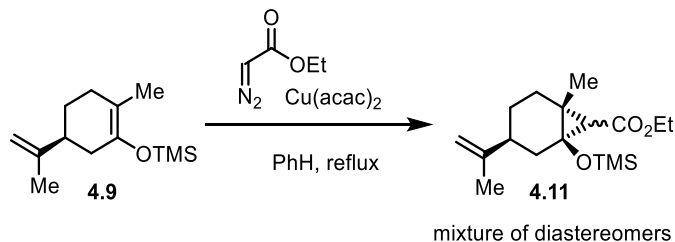


N-Benzyl-3,4-diphenyl-2-oxa-3-azabicyclo[3.3.1]nonan-9-amine (2.41) A 4 mL glass vial was charged with **2.7** (60 mg, 0.20 mmol, 1 equiv.) and NaBH(OAc)₃, which was then dissolved in 1,2-dichloroethane (0.6 mL). Benzyl amine (22 μ L, 0.20 mmol, 1 equiv.) and acetic acid (25 μ L, 0.40 mmol, 2 equiv.) were then added and the resulting reaction mixture was allowed to stir at room temperature for 36 h. The reaction mixture was then diluted with methylene chloride (10 mL), washed with H₂O (2 \times 5 mL) and brine (5 mL), dried with anhydrous N₂SO₄, filtered, and concentrated *in vacuo*. The resulting material was purified by silica gel column chromatography (5% diethyl ether/hexane) to afford compound **2.41** as a white solid (67 mg, 85%). R_f = 0.24 (5% diethyl ether/hexane), visualized by Magic stain. **¹H NMR** (500 MHz, CDCl₃) δ 7.39-7.34 (m, 2H), 7.27-7.21 (m, 2H), 7.19-7.10 (m, 6H), 6.88-6.81 (m, 4H), 6.76-6.70 (m, 1H), 4.99-4.95 (m, 1H), 4.36-4.31 (m, 1H), 3.40 (d, *J* = 12.7 Hz, 1H), 3.27 (d, *J* = 12.7 Hz, 1H), 2.83-2.77 (s, 1H), 2.64-2.59 (m, 1H), 2.34-2.22 (m, 2H), 2.21-2.14 (m, 1H), 1.89-1.75 (m, 3H), 1.64-1.54 (m, 1H). **¹³C NMR** (125 MHz, CDCl₃) δ 140.9, 140.3, 128.9, 128.6, 128.1, 127.9, 127.3, 126.6, 126.5, 118.7, 112.4, 77.8, 62.1, 57.8, 50.8, 36.1, 32.8, 30.6, 19.8. **HRMS** Calculated for C₂₆H₂₈N₂O [M+H]⁺: 385.2274. Found 385.2282.

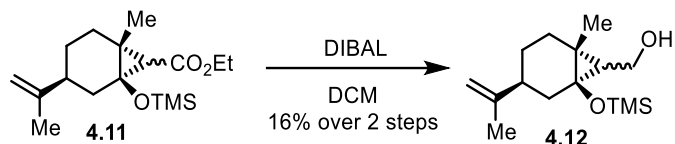


2-(Benzylamino)-3-(phenyl(phenylamino)methyl)cyclohexan-1-ol (2.42) A 10 mL round bottom flask was charged with **2.41** (67 mg, 0.17 mmol, 1 equiv.), which was then dissolved in an acetic acid:methylene chloride 2:1 solvent mixture (1.06 mL). Zinc dust (< 10 micron, 98%, 109 mg, 1.70 mmol, 10 equiv.) was added at room temperature in one portion. The reaction mixture was then allowed to stir overnight at room temperature before filtered through a Celite plug. The filtrate was then diluted with methylene chloride (10 mL), washed with saturated Na₂CO₃ aqueous solution (2 × 5 mL) and brine (5 mL), dried with anhydrous N₂SO₄, filtered, and concentrated *in vacuo*. The resulting material was purified by silica gel column chromatography (60% diethyl ether/hexane) to afford compound **2.42** as a white solid (54 mg, 83%). *R_f* = 0.15 (60% diethyl ether/hexane), visualized by Magic stain. **¹H NMR** (500 MHz, CDCl₃) δ 7.37-7.28 (m, 9H), 7.24-7.19 (m, 1H), 7.10-7.03 (m, 2H), 6.61-6.55 (m, 1H), 6.51-6.46 (m, 1H), 5.77 (d, *J* = 7.5 Hz, 1H), 4.43 (app. t, *J* = 7.2 Hz, 1H), 3.91 (d, *J* = 12.5 Hz, 1H), 3.86 (d, *J* = 12.5 Hz, 1H), 3.58-3.49 (m, 1H), 3.25-3.18 (m, 1H), 2.15 (d, *J* = 6.8 Hz, 1H), 1.77-1.62 (m, 3H), 1.36-1.23 (m, 3H), 1.23-1.13 (m, 1H). **¹³C NMR** (125 MHz, CDCl₃) δ 146.9, 142.6, 129.3, 129.0, 128.8, 128.7, 127.9 (2C), 127.2, 127.1, 117.8, 114.1, 74.4, 60.4, 59.3, 54.0, 45.8, 30.2, 24.9, 22.4. **HRMS** Calculated for C₂₆H₃₀N₂O [M+H]⁺: 387.2431. Found 387.2448.

8.3 Experimental Procedures and Characterization Data for Chapter 4

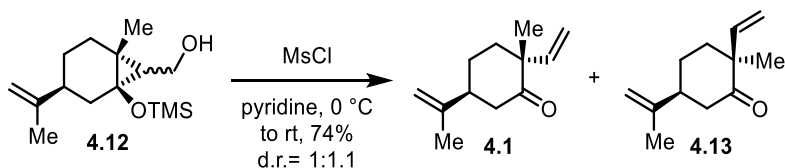


Cyclopropane 4.11. To a 25 mL round bottom flask was added **4.9** (430 mg, 1.92 mmol, 1 equiv), benzene (9.6 mL) and Cu(acac)₂ (50 mg, 0.192 mmol, 0.1 equiv). The reaction was heated to 80 °C. Ethyl diazoacetate (87% in DCM, 280 μL, 2.30 mmol, 1.2 equiv) in 1 mL DCM was added via syringe pump over 3 hours. The reaction was stirred at this temperature for another 3 hours. NaHCO₃ aq. (15 mL) was added and the reaction was extracted with EtOAc. The organic phase was combined, dried over Na₂SO₄, filtered and concentrated *in vacuo*. The crude material was purified by flash chromatography (15% Et₂O/hexanes) to afford the products as a mixture of diastereomers.

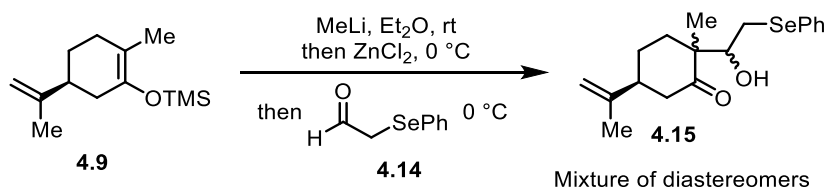


Alcohol 4.12. To a 25 mL round bottom flask was added **4.11** (290 mg, 0.934 mmol, 1 equiv) and DCM (9 mL). The reaction was cooled to -78 °C and DIBAL (25% wt in PhMe, 478 μL, 2.80 mmol, 3 equiv) was added dropwise. The reaction was stirred at this temperature for 1 hour before being quenched by Rochelle's salt aq. (saturated, 20 mL). The reaction was stirred at room

temperature for 3 hours. The aqueous phase was extracted with DCM (5 x 15 mL), which was then combined, dried over Na₂SO₄, filtered and concentrated *in vacuo*. The crude material was purified by flash chromatography (20% EtOAc/hexanes) to afford the products as a mixture of diastereomers.

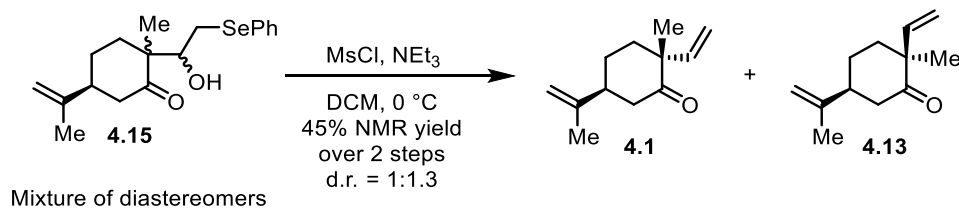


Vinyl ketone 4.1. To a 25 ml round bottom flask was added 4.12 (81 mg, 0.302 mmol, 1 equiv) and pyridine (3 mL). The reaction was cooled to 0 °C and MsCl (35 μ L, 0.453 mmol, 1.5 equiv) was added. The reaction was stirred at this temperature for 2 hours. 1 M HCl (15 mL) was then added and the mixture was extracted with Et₂O (5 x 10 mL). The organic phase was then combined, dried over MgSO₄, filtered and concentrated *in vacuo*. The crude material was purified by flash chromatography (4% Et₂O/hexanes) to afford the products as a mixture of diastereomers.

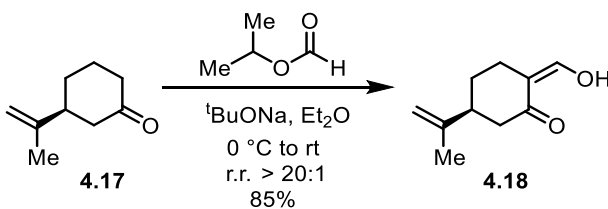


Hydroxyketone 4.15. To a 10 mL round bottom flask was added **4.9** (80 mg, 0.356 mmol, 1 equiv) and Et₂O (0.79 mL). The reaction was cooled to 0 °C and MeLi (1.6 M in Et₂O, 0.224 mL, 0.356 mmol, 1 equiv) was added. The reaction was allowed to stir at room temperature for 1.5 hours. The reaction was cooled to 0 °C, followed by the addition of ZnCl₂ (1 M in Et₂O, 0.178 mL,

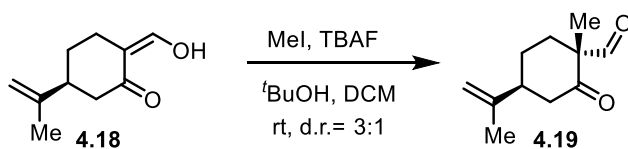
0.178 mmol, 0.5 equiv). After 10 minutes, (phenylseleno)acetaldehyde **4.14** (70 mg, 0.356 mmol, 1 equiv) in Et₂O (0.592 mL) was added in one portion. The reaction was stirred at the same temperature for 3 hours, before being quenched by NH₄Cl aq. (2 mL). The aqueous phase was extracted by Et₂O. The organic phase was combined and washed with brine, dried over Na₂SO₄, filtered and concentrated *in vacuo*. The resulting mixture was used in the next step without further purification.



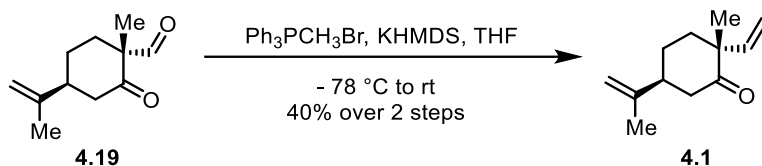
Vinyl ketone 4.1. To a 10 mL round bottom flask was added **4.15** from the previous step and DCM (2.95 mL). The mixture was cooled to 0 °C before the addition of NEt₃ (0.258 mL, 1.85 mmol, 5.2 equiv) and MsCl (0.087 mL, 1.12 mmol, 3.15 equiv). The reaction was then stirred at the same temperature for 1 hour before the addition of 1 M HCl (2 mL). The aqueous phase was then extracted with DCM (2 x 4 mL). The organic phase was combined, washed with brine (5 mL), dried over Na₂SO₄, filtered and concentrated *in vacuo*.



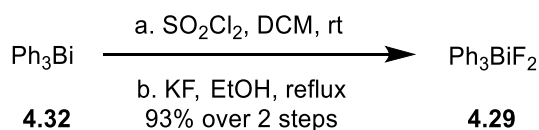
Formyl ketone 4.18. To a 25 mL round bottom flask was added **4.17** (100 mg, 0.724 mmol, 1 equiv), isopropyl formate (0.144 mL, 1.44 mmol, 2 equiv) and Et₂O (2.9 mL). The reaction was cooled to 0 °C before the addition of sodium *tert*-butoxide (104 mg, 1.09 mmol, 1.5 equiv) in one portion. The resulting orange slurry was stirred at this temperature for 1 hour, before being quenched by 1 M HCl (3 mL). The aqueous phase was extracted with Et₂O (5 x 5 mL), which was combined and dried over Na₂SO₄, filtered and concentrated *in vacuo*. The crude product was purified by flash chromatography (10% Et₂O/hexanes) to afford the product as an orange oil (102 mg, 85%) which slowly degraded in air and was used immediately in the next step. ¹H NMR (500 MHz, CDCl₃) δ 14.40 (d, *J* = 3.3 Hz, 1H), 8.66 (d, *J* = 3.2 Hz, 1H), 4.80 (t, *J* = 1.5 Hz, 1H), 4.73 (dt, *J* = 1.7, 0.9 Hz, 1H), 2.56 – 2.40 (m, 2H), 2.39 – 2.26 (m, 4H), 2.02 – 1.87 (m, 1H), 1.76 (t, *J* = 1.1 Hz, 3H), 1.54 – 1.44 (m, 1H). ¹³C NMR (125 MHz, CDCl₃) δ 187.4, 184.7, 147.4, 110.2, 108.4, 39.9, 36.5, 27.6, 22.8, 20.8.



Dicarbonyl 4.19. To a 10 mL round bottom flask was added **4.18** (100 mg, 0.602 mmol, 1 equiv), DCM (0.30 mL) and *t*BuOH (0.90 mL) and MeI (0.075 mL, 1.20 mmol, 2 equiv). TBAF (0.783 mL, 0.783 mmol, 1.3 equiv) was then added dropwise and the reaction was stirred at room temperature for 7 hours. NaHCO₃ aq. (2 mL) was then added and the aqueous phase was extracted by DCM (4 x 3 mL). The organic phase was combined, dried over Na₂SO₄, filtered and concentrated *in vacuo*. The crude product was purified by flash chromatography (15% Et₂O/hexanes) to afford a mixture of diastereomers that was used in the next step.



Vinyl ketone 1. To a 10 mL round bottom flask was added $\text{Ph}_3\text{PCH}_3\text{Br}$ (280 mg, 0.783 mmol, 2 equiv) and THF (3mL). The mixture was cooled to $0\text{ }^\circ\text{C}$ before the addition of KHMDS (1 M in THF, 0.391 mL, 1 equiv). The resulting yellow slurry was stirred at this temperature for 30 minutes. The reaction was then cooled to $-78\text{ }^\circ\text{C}$ and **4.19** (71 mg, 0.391 mmol, 1 equiv) was added as a THF solution (0.90 mL). The reaction was further stirred at this temperature for another 20 minutes and warmed to room temperature. After an extra 1 hour, NH_4Cl aq. (4 mL) was added and the reaction was extracted with Et_2O (3 x 4 mL). The organic phase was combined and dried over Na_2SO_4 , filtered and concentrated *in vacuo*. The crude product was purified by flash chromatography (1% Et_2O /hexanes) to afford the desired product as a colorless oil (43 mg, 40% over 2 steps). The NMRs matched literature reports.



Triphenylbismuth difluoride. To a 1 L round-bottom flask was added Ph_3Bi (20 g, 45.4 mmol, 1 equiv.) followed by DCM (268 mL, 0.17 M). Sulfuryl chloride (4.40 mL, 54.5 mmol, 1.2 equiv.) was then added slowly. The resulting solution was stirred at room temperature for 1 h. All volatiles were then removed *in vacuo* (Note 1). The resulting off white solid was dissolved in $\text{EtOH}:\text{H}_2\text{O}$ 20:1 (EtOH 228 mL, H_2O 11.4 mL, 0.19M) in the same flask. KF (26.4 g, 454 mmol, 10 equiv.)

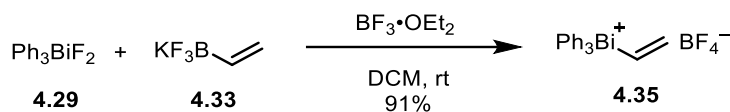
was added and the reaction was heated to reflux with rigorous stirring for another 1 h (*Note 2*). The reaction was checked by NMR before cooled down to room temperature. The solid was filtered off with a glass Buchner funnel and the filtrate was concentrated in vacuo until a thick slurry was obtained. The slurry was filtered once more with a glass Buchner funnel and the solid was washed with DCM (200 mL). The filtrate was transferred into a separatory funnel and diluted with more DCM (200 mL) (*Note 3*). The organic phase was washed with H₂O (3 x 200 mL) (*Note 4*), dried over MgSO₄, filtered and concentrated to provide the product as an off white solid (21.7g, 93% over 2 steps) (*Note 5*). *Note 1*: Excess sulfonyl chloride was also removed *in vacuo*. The reaction usually bumps at the end of the evaporation process and a large flask is recommended for the first step. *Note 2*: KF would gradually turn from free-flowing solids into hard chunks that often stuck to the side of the flask, which was normal. *Note 3*: KCl from the reaction should be filtered off as much as possible, otherwise Ph₃BiFCl may be generated during the aqueous workup process. *Note 4*: Brine should never be used, otherwise much Ph₃BiFCl would be generated. *Note 5*: Usually after this procedure, the crude product contained less than 5% Ph₃BiFCl and was used in the next step without further purification. However, the KF step could be repeated one more time to increase the purity.

Ph₃BiCl₂

¹H NMR (500 MHz, CDCl₃): δ 8.53 (d, *J* = 8.0 Hz, 6H), 7.67 (t, *J* = 7.7 Hz, 6H), 7.54 (t, *J* = 7.3 Hz, 3H). **¹³C NMR** (125 MHz, CDCl₃): δ 156.1, 134.6, 131.9, 131.6. **HRMS** (ESI) *m/z* calc'd for C₁₈H₁₅Bi³⁵Cl [M-Cl]⁺ 475.0666, found 475.0667.

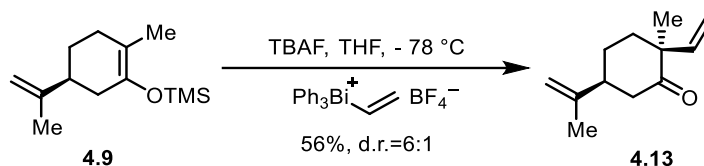
Ph₃BiF₂

¹H NMR (500 MHz, CDCl₃): δ 8.22 (dd, *J* = 8.2, 1.3 Hz, 6H), 7.65 (t, *J* = 7.6 Hz, 6H), 7.48 (ddt, *J* = 8.6, 6.0, 1.2 Hz, 3H). **¹³C NMR** (125 MHz, CDCl₃): δ 153.70 (t, *J*_{19F-13C} = 9.3 Hz), 134.45 (t, *J*_{19F-13C} = 3.6 Hz), 132.0, 131.6. **¹⁹F NMR** (470 MHz, PhCF₃) : d -162.0.

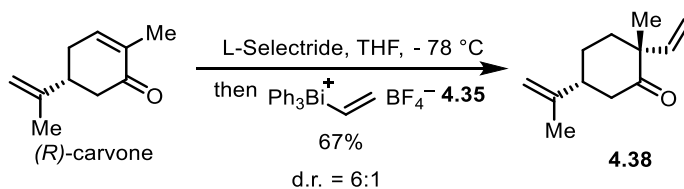


Triphenylvinylbismuthonium tetrafluoroborate 4.35. To a 1 L round-bottom flask was added Ph₃BiF₂ (18 g, 37.6 mmol, 1 equiv.), potassium vinyltrifluoroborate (5.54 g, 41.4 mmol, 1.1 equiv.) and DCM (502 mL, 0.075M). BF₃·Et₂O (5.57 mL, 45.1 mmol, 1.2 equiv.) was then added slowly and the resulting white suspension was stirred at room temperature for 3 h, during which time the reaction turned less turbid (*Note 1*). Upon completion of the reaction (checked by NMR), the reaction was washed with saturated NaBF₄ aq. (2 x 150 mL, *Note 2*) and dried over MgSO₄. The organic phase was then filtered and concentrated *in vacuo*. The resulting beige solid was gently scrapped off the side of the flask. The residue solid in the flask was transferred into a 100 mL round-bottom flask using DCM, concentrated and scrapped off the side of the flask gently (*Note 3*). The beige solid was combined (20.9 g, 91%) and used without further purification (*Note 4*). *Note 1*: The excess potassium vinyltrifluoroborate remained insoluble upon completion of the reaction. *Note 2*: When H₂O was used in this step, the anion may not be exclusively BF₄⁻. However, it did not seem to affect the reactivity of the reagent, although the molecular weight would be inaccurate. Brine should never be used. *Note 3*: The product seemed to react with glass as it was concentrated and therefore the product that stuck on the side of the flask was not scrapped off the flask with

force but rather transferred into a smaller flask and collected. A small amount of product was discarded eventually. *Note 4:* The product contained a small portion of impurities (< 5%) that was not easily removed by crystallization or flash chromatography with SiO₂. However, the impurities did not seem to affect the reactivity of the reagent. **¹H NMR** (400 MHz, DMSO-*d*₆): δ 8.1 (app. s, 1H), 7.83 (app. d, *J* = 6.8 Hz, 6H), 7.69 (app. t, *J* = 7.0 Hz, 6H), 7.62 (app. tt, *J* = 7.2, 1.3 Hz, 3H), 7.27 (app. s, 1H), 6.30 (d, *J* = 17.5 Hz, 1H). **¹³C NMR** (125 MHz, CDCl₃): δ 143.5, 141.6, 135.6, 135.2, 131.5, 131.3. **HRMS** (ESI) *m/z* calc'd for C₂₀H₁₈Bi [M-BF₄]⁺ 467.1212, found 467.1229.



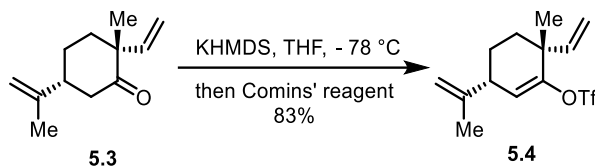
Vinyl ketone 4.13. To a 10 mL round bottom flask was added **4.9** (44 mg, 0.20 mmol, 1 equiv), bismuth reagent (122 mg, 0.22 mmol, 1.1 equiv) and THF (2 mL). The reaction was cooled to -78 °C before the addition of TBAF (1 M in THF, 0.20 mL, 0.20 mmol, 1 equiv). The reaction was stirred at this temperature for 1 hour before the addition of NH₄Cl aq. (2 mL). The aqueous phase was extracted with EtOAc (3 x 3 mL). The organic phase was combined and dried over Na₂SO₄, filtered and concentrated *in vacuo*. The crude product was purified by flash chromatography (1% Et₂O/hexanes) to afford a mixture of diastereomers.



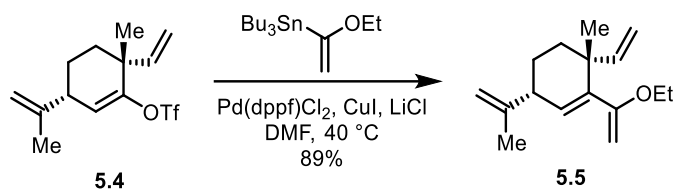
Vinyl ketone 4.38. To an oven-dried 100 mL round-bottom flask was added (*R*)-carvone (450 mg, 3 mmol, 1 equiv.) and THF (16.7 mL, 0.18 M). The reaction was cooled to $-78\text{ }^{\circ}\text{C}$. L-Selectride (1 M in THF, 3.3 mL, 3.3 mmol, 1.1 equiv.) was added dropwise and the reaction was stirred at $-78\text{ }^{\circ}\text{C}$ for 75 min. The bismuth reagent (1.91 g, 3.45 mmol, 1.15 equiv.) was then added as a solid in one portion (*Note 1*). The resulting suspension was stirred rigorously at $-78\text{ }^{\circ}\text{C}$ for 30 min, at which point the reaction turned into a clear, orange solution. Hexanes (40 mL) was added to the reaction and the cooling bath was removed. NaOH aq. (1 M, 15 mL) and H₂O₂ (30% aq., 1.13 mL) was added sequentially and the resulting biphasic solution was stirred rigorously at room temperature for 4 h (*Note 2*), before being poured into a separatory funnel. The two phases were separated and the aqueous phase was extracted with hexanes (20 mL). The organic phase was then combined and washed with saturated NH₄Cl aq. (20 mL), H₂O (20 mL), brine (20 mL), dried over MgSO₄, filtered and concentrated *in vacuo*. The crude product was purified by flash chromatography (20% DCM/hexanes) to afford Ph₃Bi (*Note 3*) and a mixture of **4.38** and its diastereomer (358 mg, 67%, d.r. = 6:1). The diastereomers were then subjected to flash chromatography (1% → 3%, Et₂O/hexanes) to afford the desired product **15** (292 mg) as a colorless oil. *Note 1*: The bismuth reagent needs to be added into the reaction mixture. The reverse addition, where the reduction product was cannulated into a bismuth THF suspension at $-78\text{ }^{\circ}\text{C}$, led to a much lower yield. *Note 2*: The H₂O₂ step seemed to help with the aqueous workup. Without the addition of NaOH and H₂O₂, much unidentified insoluble solid was observed during aqueous workup, which led to a slight decrease in yield. *Note 3*: Partly due to the excess L-Selectride used, a small amount of diphenylvinylbismuth were generated which co-eluted with Ph₃Bi in the first few fractions. The later fractions containing Ph₃Bi were clean and Ph₃Bi could be recovered with 60-80% yield. However, due to the low cost of Ph₃Bi, the recovery of Ph₃Bi was not done routinely.

$R_f = 0.41$ (10% Et₂O/hexanes). **¹H NMR** (500 MHz, CDCl₃): δ 5.91 (dd, $J = 17.7, 10.7$ Hz, 1H), 5.16 (d, $J = 5.8$ Hz, 1H), 5.00 (dd, $J = 17.6, 0.7$ Hz, 1H), 4.77-4.73 (m, 1H), 4.73-4.69 (m, 1H), 2.56 (t, $J = 13.9$ Hz, 1H), 2.38-2.34 (m, 1H), 2.34-2.29 (m, 1H), 2.06 (dt, $J = 13.7, 3.4$ Hz, 1H), 1.80-1.73 (m, 2H), 1.72 (s, 3H), 1.64-1.55 (m, 1H) 1.14 (s, 3H). **¹³C NMR** (125 MHz, CDCl₃): δ 212.5, 147.6, 142.4, 115.6, 109.8, 51.7, 46.8, 44.2, 38.9, 27.1, 24.1, 20.5. **HRMS** (ESI) m/z calc'd for C₁₂H₁₉O [M+H]⁺ 179.1436, found 179.1431. $[\alpha]_D^{22} = +155.5^\circ$ (c=1.05, CHCl₃).

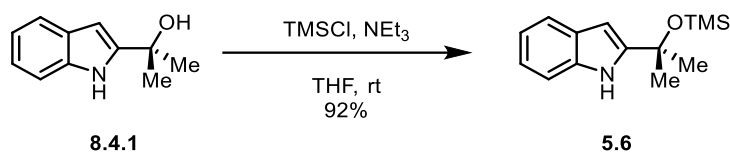
8.4 Experimental Procedures and Characterization Data for Chapter 5



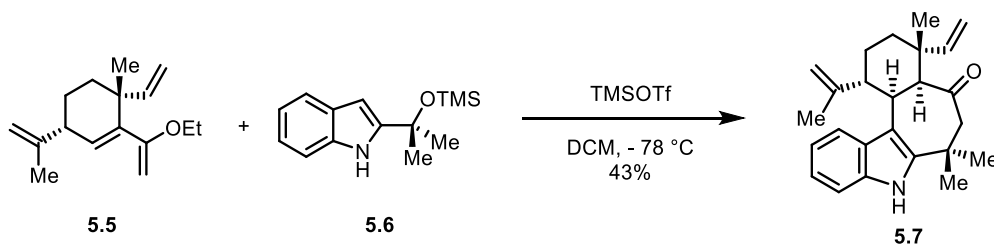
Enol triflate 5.4. To a flame-dried 250 mL round-bottom flask was added ketone **5.3** (1.16 g, 6.51 mmol, 1 equiv.) and THF (24.1 mL, 0.27 M). The colorless solution was cooled to $-78\text{ }^{\circ}\text{C}$ followed by the slow addition of KHMDS (1 M in THF, 8.46 mL, 8.46 mmol, 1.3 equiv.). The yellow solution was stirred at $-78\text{ }^{\circ}\text{C}$ for 1.5 h. Comins' reagent (4.09 g, 10.4 mmol, 1.6 equiv.) in THF (9.5 mL) was added dropwise and the reaction mixture was stirred at $-78\text{ }^{\circ}\text{C}$ for another 1.5 h (*Note 1*), before being quenched with saturated NH_4Cl aq. (20 mL). The reaction was warmed to room temperature, transferred into a separatory funnel containing 10 mL of H_2O and extracted with EtOAc (1 x 30 mL, 2 x 15 mL), washed with saturated NH_4Cl aq. (20 mL), brine (20 mL), dried over MgSO_4 , filtered and concentrated *in vacuo*. The crude product was purified by flash chromatography (0% \rightarrow 1% EtOAc/hexanes) to afford enol triflate **5.4** (1.68 g, 83%) as a colorless oil. *Note 1*: the reaction should be kept at $-78\text{ }^{\circ}\text{C}$ during the triflation step, otherwise large amounts of by product that were inseparable from the desired product would be generated. $R_f = 0.25$ (hexanes). **$^1\text{H NMR}$** (500 MHz, CDCl_3): δ 5.77-5.68 (m, 2H), 5.18 (dd, $J = 10.6, 0.8$ Hz, 1H), 5.13 (dd, $J = 17.4, 0.8$ Hz, 1H), 4.85-4.81 (m, 1H), 4.81-4.76 (m, 1H), 2.98 (ddd, $J = 8.6, 5.8, 3.1$ Hz, 1H), 1.79 (ddd, $J = 12.5, 6.2, 2.5$ Hz, 1H), 1.76-1.69 (m, 4H), 1.67-1.59 (m, 1H), 1.58-1.50 (m, 1H), 1.26 (s, 3H). **$^{13}\text{C NMR}$** (125 MHz, CDCl_3): δ 152.9, 146.8, 141.7, 121.1, 118.5 (q, $J_{19\text{F}-13\text{C}} = 319.5$ Hz), 115.3, 111.9, 43.7, 41.7, 36.36, 23.9, 23.7, 20.8. **HRMS** (ESI) m/z calc'd for $\text{C}_{13}\text{H}_{18}\text{F}_3\text{O}_3\text{S}$ $[\text{M}+\text{H}]^+$ 311.0929, found 311.0930. $[\alpha]_D^{22} = -23.2^{\circ}$ ($c = 1.50$, CHCl_3).



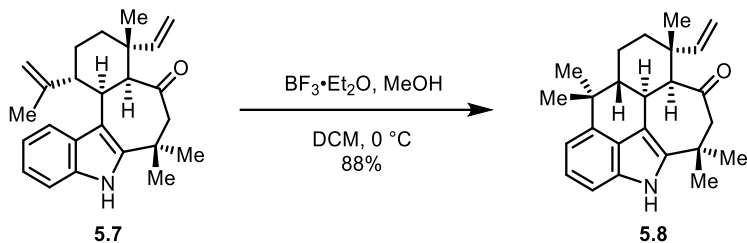
Ethoxy diene 5.5. To a flame-dried 50 mL round-bottom flask was added enol triflate **5.4** (574 mg, 1.85 mmol, 1 equiv.) and DMF (bubbled with N₂ for 45 min before use, 12.5 mL). CuI (35 mg, 0.19 mmol, 0.1 equiv.), Pd(dppf)Cl₂·DCM (151 mg, 0.19 mmol, 0.1 equiv.), LiCl (416 mg, 9.81 mmol, 5.3 equiv.) was added sequentially. Another 6 mL of DMF (bubbled with N₂ for 45 min before use) was added to make a 0.1 M solution. The dark red reaction mixture was bubbled with Ar for 15 min before the addition of tributyl(1-ethoxyvinyl)tin (712 mL, 2.13 mmol, 1.15 equiv.). The reaction was bubbled with Ar for another 20 min before being heated to 40 °C. After 2.5 d at 40 °C, the dark red solution was transferred into a separatory funnel containing NH₃·H₂O:H₂O 1:2 (60 mL), which was extracted with hexanes (1 x 30 mL, 1 x 20 mL, 2 x 15 mL). The organic phase was combined and washed with NH₃·H₂O: H₂O 1:2 (3 x 30 mL), brine (30 mL), dried over Na₂SO₄, filtered and concentrated *in vacuo*. The crude material was purified by flash chromatography (basic alumina, 2% NEt₃/hexanes) to afford the ethoxy diene **5.5** as a colorless oil (421 mg, 89%). *R*_f = 0.66 (alumina, hexanes). ¹H NMR (500 MHz, C₆D₆): δ 6.25 (dd, *J* = 3.0, 0.8 Hz, 1H), 5.99 (dd, *J* = 17.4, 10.6 Hz, 1H), 5.20-5.08 (m, 2H), 4.90-4.85 (m, 1H), 4.82-4.77 (m, 1H), 4.32 (d, *J* = 1.6 Hz, 1H), 3.98 (d, *J* = 1.6 Hz, 1H), 3.45 (qd, *J* = 7.0, 2.6 Hz, 2H), 2.73 (ddd, *J* = 9.3, 6.1, 2.9 Hz, 1H), 1.71-1.53 (m, 6H), 1.49-1.39 (m, 1H), 1.35 (s, 3H), 1.07 (t, *J* = 7.0 Hz, 4H). ¹³C NMR (125 MHz, C₆D₆): δ 163.3, 148.9, 147.0, 141.4, 131.6, 112.9, 111.0, 84.2, 62.8, 44.6, 40.2, 37.9, 26.5, 24.3, 20.8, 14.6. HRMS (ESI) *m/z* calc'd for C₁₆H₂₅O [M+H]⁺ 233.1905, found 233.1905. [α]_D²² = +13.3 ° (c=0.40, CHCl₃).



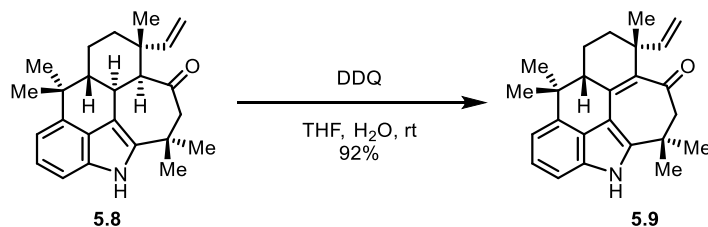
TMS alcohol 5.6. To an oven-dried 100 mL round-bottom flask was added alcohol **8.4.1** (2.856 g, 16.3 mmol, 1 equiv.), NEt_3 (6.82 mL, 48.9 mmol, 3 equiv.) and THF (16.3 mL, 1 M). TMSCl (4.14 mL, 32.6 mmol, 2 equiv.) was added slowly at room temperature. The resulting solution was stirred at room temperature for 2 d before being quenched with saturated NaHCO_3 aq. (15 mL). The mixture was then transferred into a separatory funnel containing saturated NaHCO_3 aq. (75 mL) and H_2O (75 mL) and extracted with EtOAc (2 x 60 mL 1 x 20 mL). The organic phase was combined and washed with brine (50 mL), dried over Na_2SO_4 , filtered and concentrated *in vacuo*. The crude product was purified by flash chromatography (3% \rightarrow 5% EtOAc/hexanes) to afford the desired TMS alcohol **5.6** as an off white solid (3.71 g, 92%). $R_f = 0.21$ (5% EtOAc/hexanes). $^1\text{H NMR}$ (500 MHz, CDCl_3): δ 8.29 (s, 1H), 7.55 (dd, $J = 7.8, 1.1$ Hz, 1H), 7.36 (dd, $J = 8.1, 0.9$ Hz, 1H), 7.15 (ddd, $J = 8.2, 7.1, 1.2$ Hz, 1H), 7.07 (ddd, $J = 8.0, 7.0, 1.0$ Hz, 1H), 6.23 (dd, $J = 2.1, 0.9$ Hz, 1H), 1.67 (s, 6H), 0.10 (s, 9H). $^{13}\text{C NMR}$ (125 MHz, CDCl_3): δ 146.8, 135.3, 128.6, 121.5, 120.5, 119.7, 110.9, 96.5, 72.3, 31.7, 2.3. **HRMS** (ESI) m/z calc'd for $\text{C}_{14}\text{H}_{22}\text{NOSi}$ $[\text{M}+\text{H}]^+$ 248.1471, found 248.1467.



Tetracycle 5.7. To a flame-dried 50 mL round-bottom flask was added ethoxy diene **5.5** (383 mg, 1.65 mmol, 2 equiv.), TMS alcohol **5.6** (204 mg, 0.82 mmol, 1 equiv.) and DCM (16 mL, 0.1 M). The mixture was cooled to -78 °C, followed by the dropwise addition of TMSOTf (redistilled, 313 μ L, 0.87 mmol, 1.05 equiv.). The resulting black solution was stirred at -78 °C for 35 min. The cooling bath was then removed and H₂O (1.6 mL) was added in one portion. The biphasic solution was stirred rigorously at room temperature for 20 min before being quenched by saturated NaHCO₃ aq. (8 mL). The two phases were separated and the aqueous phase was washed with DCM (2 x 15 mL). The organic phase was combined, washed with brine (25 mL), dried over Na₂SO₄, filtered and concentrated *in vacuo*. The crude material was purified by flash chromatography twice (1st column, 5% \rightarrow 15% EtOAc/hexanes, 2nd column, 2% acetone, 30% DCM, 58% hexanes) to afford the desired product tetracycle **5.7** as a white solid (128 mg, 43%). R_f = 0.37 (20% EtOAc/hexanes). **¹H NMR** (500 MHz, CDCl₃): δ 7.91 (s, 1H), 7.46 (d, J = 8.0 Hz, 1H), 7.26 (d, J = 8.2 Hz, 1H), 7.11 (ddd, J = 8.1, 7.0, 1.1 Hz, 1H), 7.01 (ddd, J = 8.1, 7.0, 1.0 Hz, 1H), 5.83 (dd, J = 17.7, 11.0 Hz, 1H), 5.17 (d, J = 11.0 Hz, 1H), 5.13 (d, J = 17.7 Hz, 1H), 4.66 (app. s, 1H), 4.46-4.41 (m, 1H), 3.58 (dd, J = 11.7, 4.6 Hz, 1H), 3.01 (d, J = 4.6 Hz, 1H), 2.78 (d, J = 10.4 Hz, 1H), 2.68 (d, J = 10.4 Hz, 1H), 2.46 (td, J = 13.7, 4.3 Hz, 1H), 2.29 (td, J = 12.0, 3.4 Hz, 1H), 1.90 (qd, J = 13.0, 4.0 Hz, 1H), 1.71-1.65 (m, 1H), 1.65-1.59 (m, 1H), 1.54 (s, 3H), 1.40 (m, 1H), 1.18 (m, 1H), 1.06 (m, 1H). **¹³C NMR** (125 MHz, CDCl₃): δ 212.0, 148.4, 147.5, 140.1, 133.9, 129.7, 121.6, 120.0, 118.8, 113.8, 112.6, 111.3, 110.1, 61.4, 58.8, 45.3, 40.3, 36.7, 34.7, 32.2, 29.9, 29.8, 28.9, 28.3, 23.1. **IR** (thin film): 3408, 2962, 2926, 1685, 1459, 1308, 1266, 742 cm⁻¹. **HRMS** (ESI) m/z calc'd for C₂₅H₃₂NO [M+H]⁺ 362.2484, found 362.2489. $[\alpha]_D^{21}$ = -1.5 ° (c=0.50, CHCl₃).

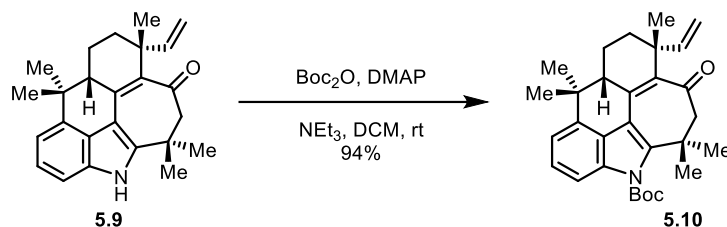


Pentacycle 5.8. To a 10 mL round bottom flask was added **5.7** (88 mg, 0.243 mmol, 1 equiv) and DCM (4.06 mL). The reaction was then cooled to 0°C . $\text{BF}_3 \cdot \text{OEt}_2$ (120 μL , 0.972 mmol, 4 equiv) was added dropwise and the reaction turned orange. MeOH (9.9 μL , 0.243 mmol, 1 equiv) was added and the reaction was stirred at 0°C for 23 hours, before being quenched by NaHCO_3 aq. (15 mL). The aqueous phase was extracted with DCM (3 x 15 mL). The organic phase was dried over Na_2SO_4 , filtered and concentrated *in vacuo*. The crude product was purified by flash chromatography (30% EtOAc/hexanes) to afford the product as a white solid (78 mg, 88%). $R_f = 0.29$ (20% EtOAc/hexanes). $^1\text{H NMR}$ (500 MHz, CDCl_3): δ 7.76 (s, 1H), 7.11-7.04 (m, 2H), 6.97 (dd, $J = 6.6, 1.5$ Hz, 1H), 5.90 (dd, $J = 17.7, 11.0$ Hz, 1H), 5.20-5.12 (m, 2H), 4.11 (dt, $J = 7.5, 1.6$ Hz, 1H), 3.31 (dd, $J = 11.2, 7.5$ Hz, 1H), 2.90 (d, $J = 14.7$ Hz, 1H), 2.62 (dd, $J = 14.7, 1.5$ Hz, 1H), 2.29 (td, $J = 13.3, 3.5$ Hz, 1H), 1.87 (s, 3H), 1.78 (dq, $J = 12.7, 3.6, 3.2$ Hz, 1H), 1.65-1.46 (m, 6H), 1.38 (s, 3H), 1.17 (s, 3H), 1.06 (s, 3H). $[\alpha]_D^{22} = +135.7^\circ$ ($c = 0.29$, CHCl_3).



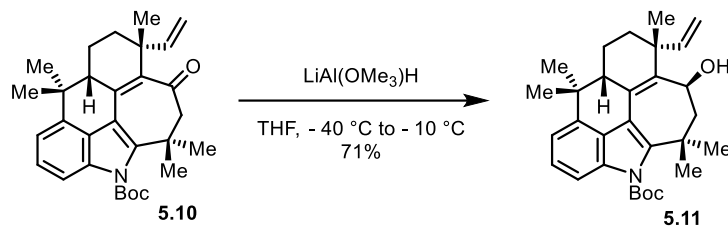
Enone 5.9. To a 10 mL round bottom flask was added **5.8** (21 mg, 0.058 mmol, 1 equiv), THF (1.05 mL) and H_2O (0.117 mL). DDQ (92 mg, 0.406 mmol, 7 equiv) was then added in one portion.

The reaction was stirred at room temperature for 6 hours and quenched with 2 M NaOH aq. (1 mL). The mixture was then stirred for 15 minutes. Another 5 mL of 2 M NaOH aq. was added and the aqueous phase was extracted by EtOAc (4 x 5 mL). The organic phase was combined and washed with 2 M NaOH (2 x 5 mL), H₂O (5 mL), brine (5 mL), dried over Na₂SO₄, filtered and concentrated *in vacuo*. The crude product was purified by flash chromatography (20% EtOAc/hexanes) to afford the product as a yellow solid (19 mg, 92%). For characterization data, see the third-generation procedure.



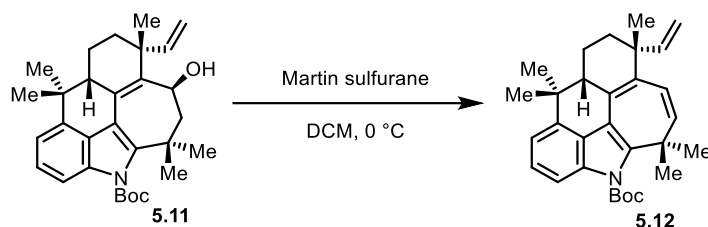
Boc-pentacycle 5.10. To a 25 mL round bottom flask was added **5.9** (80 mg, 0.223 mmol, 1 equiv), DMAP (2.7 mg, 0.022 mmol, 0.1 equiv) and DCM (5.57 mL). NEt₃ (155 μL, 1.12 mmol, 5 equiv) and Boc₂O (194 mg, 0.892 mmol, 4 equiv) was then added and the reaction was stirred at room temperature for 20 hours, before being quenched by NaHCO₃ aq. (5 mL). The aqueous phase was extracted with DCM (3 x 5 mL), dried with Na₂SO₄, filtered and concentrated *in vacuo*. The crude product was purified by flash chromatography (6% EtOAc/hexanes) to afford the product as a yellow solid (96 mg, 94%). *R*_f = 0.32 (5% EtOAc/hexanes). ¹H NMR (500 MHz, CDCl₃): δ 7.54 (d, *J* = 8.3 Hz, 1H), 7.25 (t, *J* = 7.9 Hz, 1H), 7.13 (d, *J* = 7.4 Hz, 1H), 5.95 (dd, *J* = 17.3, 10.4 Hz, 1H), 5.08 (dd, *J* = 10.5, 1.5 Hz, 1H), 4.88 (dd, *J* = 17.3, 1.5 Hz, 1H), 2.93 (d, *J* = 12.9 Hz, 1H), 2.87 (d, *J* = 13.0 Hz, 1H), 2.61 (dd, *J* = 11.2, 6.2 Hz, 1H), 1.93 – 1.79 (m, 1H), 1.79-1.66 (m, 11 H), 1.59 (s, 3H), 1.56-1.51 (m, 4H), 1.49 (s, 3H), 1.39 (s, 3H), 1.03 (s, 3H). ¹³C NMR (125 MHz,

CDCl₃): δ 200.3, 151.4, 146.4, 146.0, 142.9, 141.3, 140.3, 134.4, 125.3, 124.8, 116.4, 116.0, 113.0, 111.0, 84.8, 61.1, 49.6, 41.5, 38.7, 37.8, 35.1, 28.6, 28.2, 27.8, 25.0, 23.8, 22.7, 19.6. $[\alpha]_D^{22} = -54.8^\circ$ (c=0.53, CHCl₃).

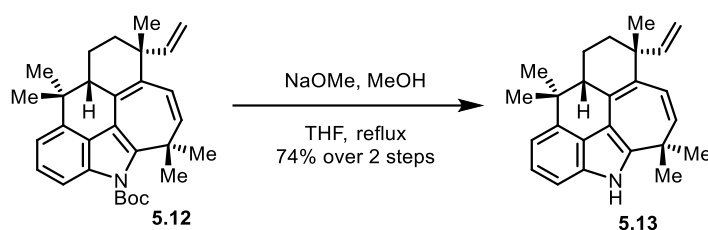


Alcohol 5.11. To a 10 mL round bottom flask was added LiAlH₄ (1 M in THF, 1.72 mL, 1.72 mmol, 10 equiv). The solution was cooled to 0 °C before the addition of MeOH (70 μ L, 1.72 mmol, 10 equiv). To another 25 mL round bottom flask was added **5.10** (96 mg, 0.172 mmol, 1 equiv) and THF (4.9 mL). The mixture was cooled to -40 °C before the addition of the freshly prepared LiAl(OMe)₃H solution (1.25 mL, 7 equiv). The reaction was allowed to slowly warm to -10 °C over 2.5 hours. The reaction was then quenched sequentially with H₂O (50 μ L), 2 M NaOH (120 μ L) and H₂O (50 μ L), dried over MgSO₄, filtered and concentrated *in vacuo*. The crude product was purified by flash chromatography (8% EtOAc/hexanes) to afford the product as a yellow solid (96 mg, 94%). $R_f = 0.33$ (10% EtOAc/hexanes). ¹H NMR (500 MHz, CDCl₃): δ 7.51 (d, $J = 8.4$ Hz, 1H), 7.23 (dd, $J = 8.4, 7.3$ Hz, 1H), 7.10 (d, $J = 7.4$ Hz, 1H), 6.07 (dd, $J = 17.4, 10.3$ Hz, 1H), 5.22 (dd, $J = 10.3, 1.8$ Hz, 1H), 5.11 (dd, $J = 17.4, 1.8$ Hz, 1H), 4.83 (dt, $J = 8.0, 1.6$ Hz, 1H), 2.43 (ddd, $J = 10.2, 5.9, 2.2$ Hz, 1H), 2.35 (s, 1H), 2.12 (dd, $J = 13.3, 7.8$ Hz, 1H), 1.96 (d, $J = 13.3$ Hz, 1H), 1.80 (s, 3H), 1.79 – 1.74 (m, 5H), 1.72 (s, 9H), 1.69 – 1.60 (m, 2H), 1.57 (s, 3H), 1.48 (s, 3H), 1.45 (s, 3H), 0.98 (s, 3H). ¹³C NMR (125 MHz, CDCl₃): δ 151.8, 149.9, 144.9, 143.1, 142.1, 134.9,

125.3, 125.3, 124.3, 115.5, 114.9, 114.7, 111.5, 84.0, 72.0, 55.1, 46.6, 42.7, 38.3, 38.2, 38.0, 29.7, 28.3, 28.2, 28.0, 28.0, 27.7, 25.3, 23.9, 19.6. $[\alpha]_D^{22} = -153.6^\circ$ ($c=0.19$, CHCl_3).

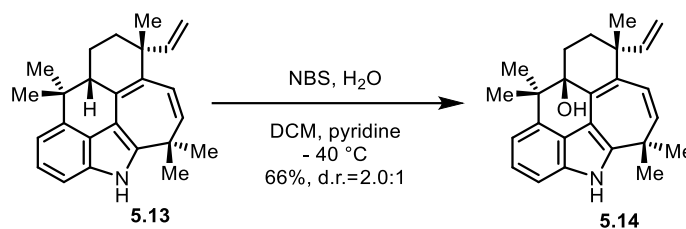


Boc-diene 5.12. To a 10 mL flask was added **5.11** (26 mg, 0.056 mmol, 1 equiv) and DCM (2.2 mL). The reaction was cooled to 0 °C. Martin sulfurane (113 mg, 0.168 mmol, 3 equiv) was added in one portion. The reaction was stirred at 0 °C for 1 hour and was quenched by NaHCO_3 aq. (2 mL). The aqueous phase was extracted with DCM (3 x 3 mL) and the organic phase was dried over Na_2SO_4 , filtered and concentrated *in vacuo*. The crude product was purified by flash chromatography (3% EtOAc/hexanes) to afford the product and an inseparable impurity. The mixture was used directly in the next step.

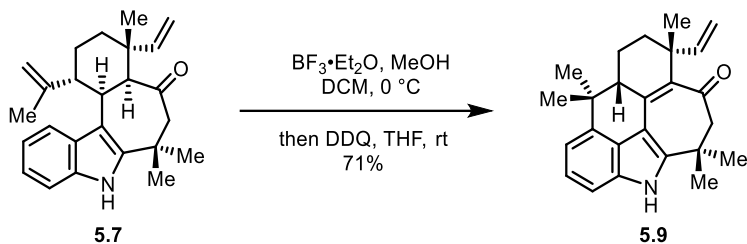


Diene 5.13. To a 25 mL round bottom flask was added **5.12** (70 mg, 0.158 mmol, 1 equiv), THF (3.2 mL) and NaOMe (as a 25 wt% MeOH solution, 361 μL , 1.58 mmol, 10 equiv). The reaction was heated to reflux and stirred at this temperature of 16 hours. The reaction was then cooled to

room temperature. NaHCO₃ aq. (20 mL) was added and the aqueous phase was extracted with DCM (4 x 20 mL). The organic phase was combined, dried over Na₂SO₄, filtered and concentrated *in vacuo*. The crude product was purified by flash chromatography (10% Et₂O/hexanes) to afford the product (74% over 2 steps) as a white solid which slowly turned orange upon expose to air. ¹H NMR (500 MHz, C₆D₆): δ 7.59 – 7.29 (m, 1H), 7.18-7.13 (m, 1H), 7.03 (d, *J* = 8.0 Hz, 1H), 6.97 (s, 1H), 6.17 (dd, *J* = 11.4, 1.1 Hz, 1H), 5.88 (dd, *J* = 17.3, 10.5 Hz, 1H), 5.30 (dd, *J* = 11.4, 0.9 Hz, 1H), 5.19-5.08 (m, 2H), 2.78 (dd, *J* = 11.6, 6.1 Hz, 1H), 1.86 – 1.70 (m, 1H), 1.64 (dq, *J* = 12.7, 6.6, 3.2 Hz, 3H), 1.55 – 1.49 (m, 1H), 1.46 (s, 4H), 1.31 (s, 4H), 1.17 (s, 4H), 1.08 (s, 4H), 1.04 (s, 4H). ¹³C NMR (125 MHz, C₆D₆): δ 146.9, 141.1, 138.3, 133.3, 133.1, 131.8, 130.5, 128.5, 126.1, 123.1, 114.7, 113.7, 110.8, 108.5, 47.4, 41.5, 39.9, 37.3, 35.4, 29.0, 26.6, 25.8, 25.6, 23.7, 19.8. [α]_D²² = -82.0 ° (c=0.19, CHCl₃).

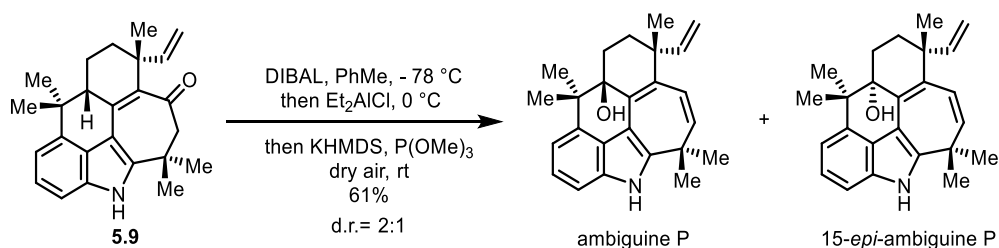


Ambiguine P. To a 4 mL vial was added **5.13** (6.3 mg, 0.0183 mmol, 1 equiv), DCM (0.75 mL), pyridine (0.75 mL) and H₂O (0.040 mL, 120 equiv). The reaction was cooled to -40 °C and NBS (3.3 mg, 0.0183 mmol, 1 equiv) was added. The reaction was stirred at the same temperature for 30 minutes and quenched with Na₂S₂O₃ aq. (2 mL), and extracted with DCM. The organic phase was combined, dried over Na₂SO₄, filtered and concentrated *in vacuo*. The crude material was purified by prep-TLC (30% EtOAc/hexanes) to afford the desired product as a mixture of diastereomers as a white solid.



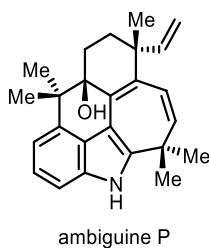
Enone 5.9. To an oven-dried 25 mL round-bottom flask was added tetracycline **5.7** (105 mg, 0.290 mmol, 1 equiv.) and DCM (4.83 mL, 0.06 M). The mixture was cooled to 0 °C followed by the addition of $\text{BF}_3 \cdot \text{Et}_2\text{O}$ (143 μL , 1.16 mmol, 4 equiv.), which changed the colorless solution into a dark red solution. MeOH (anhydrous, 12 mL, 0.290 mmol, 1 equiv.) was added and the flask was placed into a Cryocool cooler pre-set at 0 °C. After being stirred at 0 °C for 21 h, TBAF (1 M in THF, 1.45 mL, 1.45 mmol, 5 equiv.) was added and the dark red color became less intense. The reaction mixture was stirred at 0 °C for 15 min before H_2O (100 mL, 5.80 mmol, 20 equiv.) was added. The reaction mixture was stirred at the same temperature for another 15 min. DDQ (264 mg, 1.16 mmol, 4 equiv.) was added as a solid and the resulting black solution was removed from the 0 °C cooling bath and stirred at room temperature for 2.5 h, before it was quenched with 1 M NaOH aq. (10 mL). The aqueous phase was separated and extracted with DCM (4 x 5 mL). The organic phase was combined, washed with 1 M NaOH (2 x 10 mL), brine (10 mL), dried over MgSO_4 , filtered and concentrated *in vacuo*. The crude product was purified by flash chromatography (5% \rightarrow 15% EtOAc/hexanes) to afford enone **5.9** as a yellow solid (74 mg, 71%). $R_f = 0.26$ (20% EtOAc/hexanes). $^1\text{H NMR}$ (500 MHz, CDCl_3): δ 8.01 (s, 1H), 7.19-7.12 (m, 2H), 7.03 (dd, $J = 6.4, 1.5$ Hz, 1H), 5.96 (dd, $J = 17.3, 10.5$ Hz, 1H), 5.12 (dd, $J = 10.5, 1.6$ Hz, 1H), 5.01 (dd, $J = 17.3, 1.6$ Hz, 1H), 3.27 (d, $J = 11.4$ Hz, 1H), 2.68 (dd, $J = 11.2, 6.6$ Hz, 1H), 2.58 (d, $J = 11.4$ Hz, 1H), 1.89-1.77 (m, 2H), 1.77-1.69 (m, 1H), 1.60 (td, $J = 13.1, 3.5$ Hz, 1H), 1.50 (s,

3H), 1.48 (s, 3H), 1.35 (s, 3H), 1.20 (s, 3H), 1.00 (s, 3H). ^{13}C NMR (125 MHz, CDCl_3): δ 203.9, 146.6, 141.9, 141.2, 138.4, 137.5, 132.8, 125.5, 123.1, 113.7, 113.6, 108.4, 107.9, 56.3, 48.1, 41.1, 39.2, 37.9, 35.1, 29.0, 28.2, 27.2, 25.6, 23.6, 19.8. HRMS (ESI) m/z calc'd for $\text{C}_{25}\text{H}_{30}\text{NO}$ $[\text{M}+\text{H}]^+$ 360.2327, found 360.2318. IR (thin film): 3355, 2964, 2868, 1663, 1541, 1448, 1466, 1325, 1173, 758, 738 cm^{-1} . $[\alpha]_D^{21} = -69.3^\circ$ ($c=0.35$, CHCl_3).

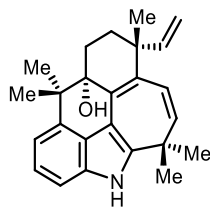


Ambiguine P and 15-*epi*-ambiguine P. To a flame-dried 25 mL round-bottom flask was added enone **5.9** (10 mg, 0.0278 mmol, 1 equiv.) and PhMe (2.78 mL, 0.01 M). The pale yellow solution was cooled to -78°C before the dropwise addition of DIBAL (1 M in PhMe, 111 mL, 0.111 mmol, 4 equiv.). The resulting orange solution was stirred at -78°C for 2.5 h before the dropwise addition of Et_2AlCl (1 M in hexanes, 222 mL, 0.222 mmol, 8 equiv.). After 15 min at -78°C , the dry-ice acetone bath was changed to ice water bath and the reaction was stirred at 0°C for 10 min, during which time the reaction turned red. P(OMe)_3 (119 mL, 1.00 mmol, 36 equiv.) was added that cause the red color to fade into yellow. The reaction mixture was then cooled to -78°C . KHMDS (1 M in THF, 417 mL, 0.417 mmol, 15 equiv.) was added and the cooling bath was removed. Dry air was bubbled through the reaction mixture as it warmed to room temperature. The bubbling continued for a total of 20 min while the reaction was at room temperature before 1 M NaOH (50 mL) was added. The reaction mixture was stirred at room temperature for another 15 min before the addition of MgSO_4 . The resulting suspension was stirred for an additional 15 min before

filtration. The filtrate was concentrated *in vacuo* and purified by flash chromatography (2% → 8% EtOAc/hexanes) to afford a mixture of ambiguine P and 15-*epi*-ambiguine P as a white solid (6.1 mg, d.r.=2:1, 61%). The mixture of the two diastereomers was usually used in the next step without further purification since both compounds provided ambiguine Q. However, ambiguine P and C15-*epi*-ambiguine P could be separated through HPLC (OD-H column, 250 x 4.6 mm, 5% *i*PrOH in hexanes, 1 mL/min, 254 nm). Ambiguine P (retention time: 23.4 min) and 15-*epi*-ambiguine P (retention time: 11.9 min) were isolated as white solids.

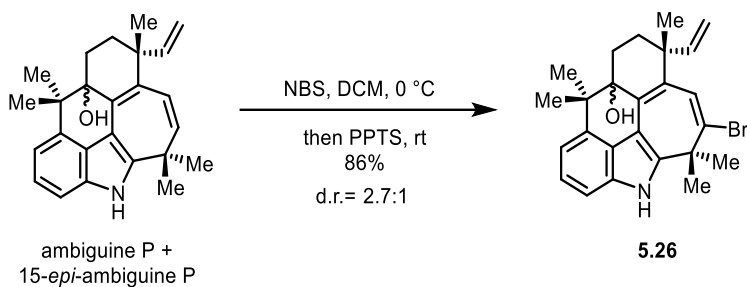


Ambiguine P: R_f = 0.36 (20% EtOAc/hexanes). $^1\text{H NMR}$ (500 MHz, CD_3OD): δ 7.16 (dd, J = 7.9, 0.7 Hz, 1H), 7.07 (dd, J = 8.0, 7.2 Hz, 1H), 6.95 (dd, J = 7.2, 0.7 Hz, 1H), 5.93 (d, J = 11.6 Hz, 1H), 5.89 (dd, J = 17.4, 10.5 Hz, 1H), 5.40 (d, J = 11.5 Hz, 1H), 5.11 (dd, J = 10.5, 1.8 Hz, 1H), 4.93 (dd, J = 17.4, 1.8 Hz, 1H), 2.15 (td, J = 14.0, 3.0 Hz, 1H), 1.96 (ddd, J = 14.2, 13.0, 2.7 Hz, 1H), 1.79 (ddd, J = 13.6, 3.9, 2.6 Hz, 1H), 1.68 (s, 3H), 1.61 (ddd, J = 13.1, 3.9, 3.0 Hz, 1H), 1.53 (s, 3H), 1.23 (s, 3H), 1.02 (s, 3H), 1.00 (s, 3H). $^{13}\text{C NMR}$ (125 MHz, CD_3OD): δ 146.9, 142.1, 139.2, 135.0, 133.9, 133.5, 133.3, 128.7, 125.6, 123.5, 114.9, 114.6, 109.6, 108.8, 77.2, 45.9, 42.5, 36.7, 34.0, 29.2, 28.9, 27.5, 27.1, 26.4, 18.6. **HRMS** (ESI) m/z calc'd for $\text{C}_{25}\text{H}_{30}\text{NO}$ $[\text{M}+\text{H}]^+$ 360.2327, found 360.2311. **IR** (thin film): 3552, 3306, 2960, 2922, 1559, 1458, 1360, 1320, 1265, 1156, 1086, 1029, 751, 699 cm^{-1} . $[\alpha]_D^{22}$ = -192.2° (c =0.10, MeOH).



15-*epi*-ambiguine P

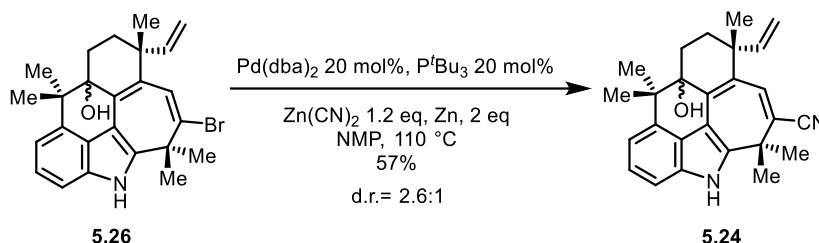
15-*epi*-ambiguine P: $R_f = 0.36$ (20% EtOAc/hexanes). $^1\text{H NMR}$ (500 MHz, CD_3OD): δ 7.16 (d, $J = 8.0$ Hz, 1H), 7.07 (t, $J = 7.6$ Hz, 1H), 6.96 (d, $J = 7.1$ Hz, 1H), 5.89 (d, $J = 11.6$ Hz, 1H), 5.88 (dd, $J = 17.5, 10.7$ Hz), 5.34 (d, $J = 11.5$ Hz, 1H), 5.11 (dd, $J = 17.5, 1.4$ Hz, 1H), 5.00 (dd, $J = 10.7, 1.4$ Hz, 1H), 2.31 (td, $J = 14.2, 3.3$ Hz, 1H), 2.04 (dt, $J = 13.8, 3.2$ Hz, 1H), 1.91 (dt, $J = 13.8, 3.4$ Hz, 1H), 1.66 (s, 3H), 1.56 (s, 3H), 1.49 (dt, $J = 13.2, 3.4$ Hz, 1H), 1.39 (s, 3H), 1.04 (s, 3H), 1.02 (s, 3H). $^{13}\text{C NMR}$ (125 MHz, CD_3OD): δ 150.0, 141.9, 139.0, 135.3, 135.0, 133.0, 131.9, 128.6, 125.6, 123.5, 114.9, 111.4, 109.6, 108.7, 77.0, 45.7, 41.5, 36.7, 34.1, 29.0, 27.6, 27.4, 26.5, 23.0, 18.5. **HRMS** (ESI) m/z calc'd for $\text{C}_{25}\text{H}_{30}\text{NO}$ $[\text{M}+\text{H}]^+$ 360.2327, found 360.2305. **IR** (thin film): 3343, 2966, 2360, 2342, 1559, 1457, 1380, 1317, 1059, 912, 748, 668 cm^{-1} . $[\alpha]_D^{22} = +62.2^\circ$ ($c=0.09$, MeOH).



Bromide 5.26. To an oven dried 4 mL vial was added a mixture of Ambiguine P and C15-*epi*-ambiguine P (4.5 mg, 0.0125 mmol, 1 equiv.) and DCM (500 mL). The colorless solution was cooled to 0 °C. *N*-bromosuccinimide (2.23 mg, 0.0125 mmol, 1 equiv.) was added as a DCM

solution (300 mL from a stock solution made by dissolving 9 mg of *N*-bromosuccinimide in 1.20 mL DCM). The resulting orange solution was stirred at 0 °C for 10 min before the addition of pyridinium *p*-toluenesulfonate (6.3 mg, 0.0250 mmol, 2equiv.) as a DCM solution (230 mL from a stock solution made by dissolving 19 mg pyridinium *p*-toluenesulfonate in 690 mL DCM). The red solution was stirred at 0 °C and then at room temperature. The reaction was monitored with TLC every 10 min after the first 80 min, and was quenched immediately with saturated NaHCO₃ aq. (2 mL) once a spot with a *R_f* = 0.61 (20% EtOAc/hexanes) showed up (*Note 1*). The two phases were separated, and the aqueous phase was extracted with DCM (3 x 1 mL). The organic phase was combined, dried over Na₂SO₄, filtered and concentrated *in vacuo*. The crude product was purified by preparative TLC (40% EtOAc/hexanes) to afford bromide **5.26** as a mixture of diastereomers as an off white solid (4.7 mg, d.r.=2.7:1, 86%). *Note 1*: the tautomerization step needed to be closely monitored after 80 min. If the reaction was not quenched soon after the *R_f* = 0.61 spot showed up, the product would degrade very quickly into various products. Usually the reaction was quenched at 110-140 min. *R_f* = 0.32 (20% EtOAc/hexanes). **¹H NMR** (500 MHz, CDCl₃, identifiable peaks): δ 8.00 (s, 1H), 7.97 (minor, s), 7.25-7.19 (m, 2H, minor 2H), 7.14-7.04 (m, 1H, minor, 1H), 6.68 (s, 1H), 6.62 (minor, s, 1H), 5.84 (dd, *J* = 17.4, 10.5 Hz, 1H), 5.84 (minor, 1H), 5.17 – 5.12 (m, 1H), 5.15-5.07 (minor, 2H), 4.96 (dd, *J* = 17.4, 1.5 Hz, 1H), 2.35 – 2.20 (minor, m, 1H), 2.10 (td, *J* = 14.2, 3.3 Hz, 1H), 2.06-1.80 (m, 5H, minor, 5H), 1.64 (dt, *J* = 13.1, 3.4 Hz, 1H), 1.60 (minor, s, 3H), 1.57 (s, 3H), 1.39 (minor, s, 3H), 1.25 (s, 3H, minor, s, 3H), 1.10 (s, 3H), 1.09 (minor, s, 3H), 1.05 (s, 3H). **¹³C NMR** (125 MHz, CDCl₃, identifiable peaks): δ 147.5, 144.8, 138.3, 138.1, 137.1, 136.7, 135.4, 133.9, 132.8, 132.4, 131.8, 130.4, 124.2, 124.2, 123.5, 123.5, 122.6, 122.5, 115.8, 114.9, 112.0, 108.9, 108.8, 76.2, 76.0, 45.5, 45.3, 41.6, 41.4, 41.3, 40.6, 33.2, 33.0, 29.9, 28.7, 28.7, 28.6, 28.5, 28.3, 25.6, 25.3, 24.9, 24.8, 22.5, 18.3, 18.2. **HRMS** (ESI)

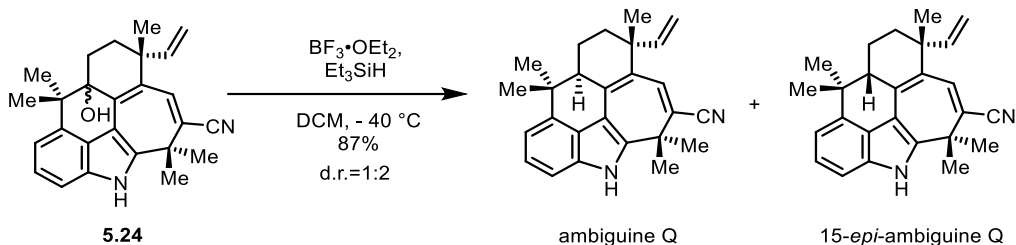
m/z calc'd for $C_{25}H_{27}^{79}BrN$ $[M+H-H_2O]^+$ 420.1321, found 420.1327. **IR** (thin film, mixture of diastereomers): 3323, 2968, 1559, 1472, 1457, 1361, 1264, 1033, 920, 759, 734 cm^{-1} .



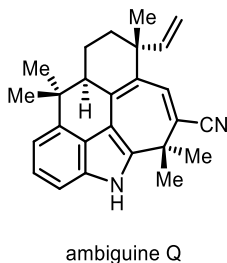
Nitrile 5.24. Tri-*tert*-butyl phosphine (9.1 mg) was weighed into an oven-dried 4 mL vial in a glove box. The vial was then capped and taken out of the glove box. *N*-Methylpyrrolidinone (NMP, bubbled with N_2 for 1 h before use, 1.41 ml) was added into the vial to make a colorless solution. To different oven-dried 4 mL vial was added $Pd(dba)_2$ (9.4 mg) and NMP (bubbled with N_2 for 1 h before use, 500 mL). The dark red solution was purged with Ar for 3 min, before 500 mL of the Tri-*tert*-butyl phosphine NMP solution was added. The mixture was stirred at room temperature for 1 h.

To an oven-dried 4 mL vial was added bromide **5.26** (2.9 mg, 0.0066 mmol, 1 equiv.), $Zn(CN)_2$ (0.9 mg, 0.0079 mmol, 1.2 equiv. *Note 1*), Zn dust (0.9 mg, 0.0132 mmol, 2 equiv. *Note 2*) and NMP (bubbled with N_2 for 1 h before use, 250 mL). The vial was purged with Ar for 5 min. The pre-prepared $Pd(dba)_2$ - P^tBu_3 NMP solution (80 mL, containing $Pd(dba)_2$ 0.76 mg, 0.0013 mmol, 0.2 equiv.; P^tBu_3 0.27 mg, 0.0013 mmol, 0.2 equiv.) was added into the vial containing **5.26** with rigorous stirring. The reaction mixture was immediately put in a 110 °C oil bath and stirred for 2.5 h. The reaction mixture was then filter through a pad of celite and flashed with EtOAc. The organic phase was washed with H_2O (3 x 1 mL), brine (1 mL), dried over Na_2SO_4 , filtered and concentrated

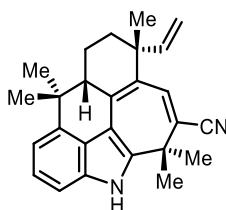
in vacuo. The crude material was purified by prep-TLC (40% EtOAc/hexanes) to afford the desired product as a mixture of diastereomers as a yellow solid (1.4 mg, d.r.=2.6:1, 57%). *Note 1*: When more than 2 equivalent of Zn(CN)₂ was used, the reaction proceeded with a low conversion of bromide **5.26**. *Note 2*: The ratio of Zn dust to Pd(dba)₂ was 10 to 1. When the reaction was run at a lower Zn/Pd ratio, such as 5:1, an unidentified by-product was produced in high yield. *R_f* = 0.14 (20% EtOAc/hexanes). **¹H NMR** (500 MHz, CD₃OD, enriched major isomer): δ 7.23 (dd, *J* = 8.1, 0.7 Hz, 1H), 7.22 (minor d, *J* = 8.1 Hz, 1H), 7.16 (dd, *J* = 8.1, 7.1 Hz, 1H, minor 1H), 7.03 (dd, *J* = 7.2, 0.7 Hz, 1H, minor, 1H), 6.82 (s, 1H), 6.79 (s, 1H), 5.95 (dd, *J* = 17.4, 10.6 Hz, 1H), 5.86 (minor, dd, *J* = 17.5, 10.7 Hz, 1H), 5.21 (dd, *J* = 10.5, 1.5 Hz, 1H), 5.21-5.17 (minor, 1H), 5.11 (minor, dd, *J* = 10.7, 1.1 Hz, 1H), 4.94 (dd, *J* = 17.4, 1.5 Hz, 1H), 2.42 – 2.32 (minor, m, 1H), 2.19 (td, *J* = 14.1, 3.1 Hz, 1H), 2.10-2.02 (minor, m, 1H), 1.97 (td, *J* = 13.8, 2.7 Hz, 1H), 1.91 (s, 3H), 1.89 (minor, s, 3H), 1.83 (dd, *J* = 3.9, 2.7 Hz, 1H), 1.66 (dt, *J* = 13.2, 3.5 Hz, 1H), 1.59 (minor, s, 3H), 1.56 (s, 3H), 1.45 (minor, s, 3H), 1.27 (s, 3H), 1.081 (s, 3H), 1.06 (minor, s, 3H), 1.06 (minor, s, 3H), 1.02 (s, 3H). **¹³C NMR** (125 MHz, CDCl₃, enriched major isomer): δ 144.5, 142.8, 139.3, 138.1, 137.9, 133.1, 133.0, 124.7, 123.5, 116.4, 115.3, 110.7, 109.2, 108.4, 76.0, 45.5, 41.6, 35.7, 32.7, 29.9, 28.5, 28.4, 25.2, 25.0, 24.9, 18.2. **HRMS** (ESI) *m/z* calc'd for C₂₆H₂₇N₂ [M+H-H₂O]⁺ 367.2174, found 367.2175. **IR** (thin film, mixture of diastereomers): 3329, 2968, 2925, 2205, 1558, 1533, 1458, 1364, 1309, 1267, 1034, 917, 762, 738 cm⁻¹.



Ambigaine Q and 15-*epi*-ambigaine Q. To a flame-dried 10 mL round-bottom flask containing nitrile **5.24** (3.9 mg, 0.0101 mmol, 1 equiv.) was added DCM (595 mL, 0.017 M), followed by Et_3SiH (32 mL, 0.203 mmol, 20 equiv.). The resulting yellow solution was cooled to $-40\text{ }^\circ\text{C}$. $\text{BF}_3\cdot\text{OEt}_2$ (6.3 mL, 0.0507 mmol, 5 equiv.) was added to the reaction mixture slowly as a DCM solution (195 mL, made by dissolving 38 mL $\text{BF}_3\cdot\text{OEt}_2$ in 1.13 mL DCM), which caused the reaction to turn into a light brown, opaque solution. The reaction was stirred at $-40\text{ }^\circ\text{C}$ for 30 min and quenched with saturated NaHCO_3 aq. (2 mL) at the same temperature. The resulting mixture was then allowed to warm to rt and extracted with DCM (2 x 2 mL). The organic phase was washed with saturated NaHCO_3 aq. (1 x 2 mL), dried with Na_2SO_4 , filtered and concentrated *in vacuo*. The crude product was purified by prep-TLC (40% EtOAc/hexanes) to afford a mixture of ambigaine Q and 15-*epi*-ambigaine Q as a yellow solid (3.3 mg, d.r.=1:2, 87%). Ambigaine Q and 15-*epi*-ambigaine Q were separated by HPLC (OD-H column, 250 x 4.6 mm, 3% *i*PrOH in hexanes, 1 mL/min, 254 nm.). Ambigaine Q (1 mg from 3.3 mg mixture, retention time: 15.2 min) and 15-*epi*-ambigaine (2 mg from 3.3 mg mixture, retention time: 11.1 min) were isolated as yellow solids.



Ambiguine Q: $R_f = 0.37$ (20% EtOAc/hexanes). $^1\text{H NMR}$ (500 MHz, CD_3OD): δ 7.19 (d, $J = 8.0$ Hz, 1H), 7.13 (app. t, $J = 7.2$ Hz, 1H), 7.00 (d, $J = 7.2$ Hz, 1H), 6.78 (s, 1H), 5.84 (dd, $J = 17.8, 10.9$ Hz, 1H), 5.17 (dd, $J = 17.4, 1.2$ Hz, 1H), 5.09 (dd, $J = 10.6, 1.2$ Hz, 1H), 2.92 (dd, $J = 10.2, 8.2$ Hz, 1H), 2.07-1.95 (m, 2H), 1.87 (s, 3H), 1.75-1.68 (m, 2H), 1.55 (s, 3H), 1.46 (s, 3H), 1.02 (s, 3H), 1.00 (s, 3H). $^{13}\text{C NMR}$ (125 MHz, CD_3OD): δ 149.4, 143.9, 141.1, 139.3, 139.0, 135.0, 134.2, 125.9, 124.4, 121.1, 114.5, 112.3, 111.5, 109.9, 109.1, 41.3, 40.8, 37.4, 36.6, 25.9, 25.2, 24.9, 24.1, 23.8, 20.1. A 48.4 signal was buried under CD_3OD solvent peak. **HRMS** (ESI) m/z calc'd for $\text{C}_{26}\text{H}_{29}\text{N}_2$ $[\text{M}+\text{H}]^+$ 369.2331, found 369.2330. **IR** (thin film): 3335, 2963, 2202, 1653, 1559, 1540, 1472, 1457, 759 cm^{-1} . $[\alpha]_D^{19} = +47.9^\circ$ ($c=0.08$, MeOH).

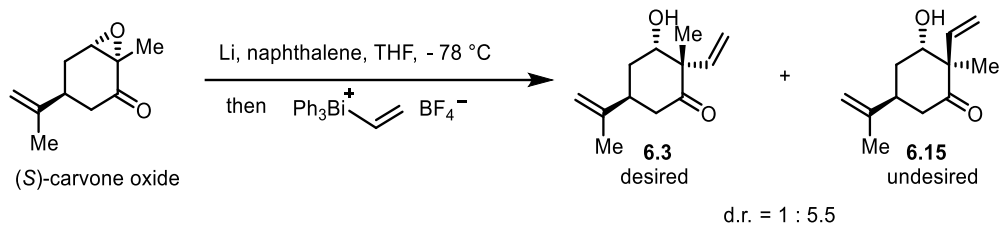


15-*epi*-ambiguine Q

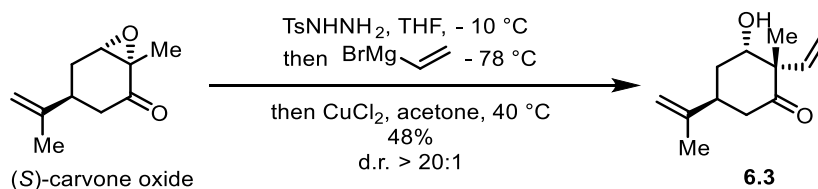
15-*epi*-Ambiguine Q: $R_f = 0.37$ (20% EtOAc/hexanes). $^1\text{H NMR}$ (500 MHz, CD_3OD): δ 7.20 (d, $J = 8.1$ Hz, 1H), 7.13 (ddd, $J = 8.0, 7.2, 0.6$ Hz, 1H), 6.99 (d, $J = 7.2$ Hz, 1H), 6.81 (s, 1H), 5.97 (ddd, $J = 17.4, 10.5, 1.2$ Hz, 1H), 5.23 (dt, $J = 10.5, 1.2$ Hz, 1H), 4.96 (dt, $J = 17.4, 1.2$ Hz, 1H), 2.84 (dd, $J = 11.2, 6.7$ Hz, 1H), 1.92-1.86 (m, 4H), 1.86-1.77 (m, 2H), 1.65-1.58 (m, 1H), 1.52 (s, 3H), 1.25 (s, 3H), 1.03 (s, 3H), 0.96 (s, 3H). $^{13}\text{C NMR}$ (125 MHz, CD_3OD): δ 147.2, 143.9, 141.2, 140.3, 139.6, 135.2, 132.6, 126.0, 124.4, 120.9, 115.5, 114.5, 111.4, 109.9, 109.6, 42.3, 41.0, 37.5, 36.6, 29.4, 25.8, 25.7, 24.8, 23.9, 20.2. A 48 signal was buried under CD_3OD solvent peak. **HRMS** (ESI) m/z calc'd for $\text{C}_{26}\text{H}_{29}\text{N}_2$ $[\text{M}+\text{H}]^+$ 369.2331, found 369.2326. **IR** (thin film):

3335, 2962, 2925, 2855, 2203, 1558, 1532, 1457, 1438, 1364, 1317, 1199, 1168, 999, 921, 759,
738 cm^{-1} . $[\alpha]_D^{21} = -205.7^\circ$ (c=0.09, MeOH).

8.5 Experimental Procedures and Characterization Data for Chapter 6

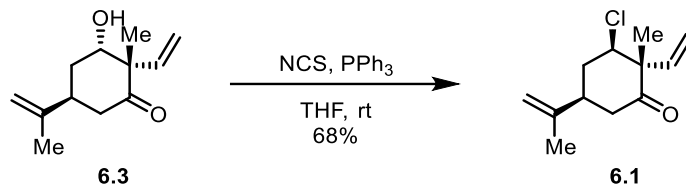


Ketone 6.3. To a 10 mL round bottom flask was added naphthalene (341 mg, 1.33 mmol) and THF (5mL). Lithium wire (washed with hexanes, 13.9 mg, 2.0 mmol) was added at room temperature. The flask was sonicated for 30 minutes. The resulting dark blue solution was then stirred at room temperature for 3 hours. To another 10 mL round bottom flask was added (S)-carvone oxide(33 mg, 0.20 mmol, 1 equiv) and THF (1.25 mL). The mixture was cooled to $-78\text{ }^\circ\text{C}$. The pre-mixed Lithium naphthalenide solution (1.06 mL, 2.12 equiv) was added at this temperature and the reaction was allowed to stir at the same temperature for 30 minutes. Vinylbismuth reagent (133 mg, 0.24 mmol, 1.2 equiv) was then added and the reaction stirred at $-78\text{ }^\circ\text{C}$ for another 2 hours, before being quenched by brine (2 mL). Trimethoxybenzene (11.1 mg) was then added and the aqueous phase was extracted with EtOAc (3 x 3 mL). The organic phase was dried over MgSO_4 , filtered and concentrated *in vacuo*. The yield was determined by ^1H NMR (20%, d.r.=1:5.5).

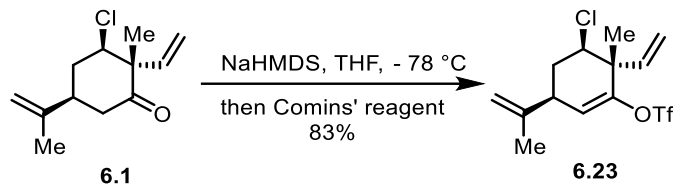


Ketone 6.3. To a 500 mL round bottom flask was added (*S*)-carvone oxide (0.814 g, 4.90 mmol, 1 equiv.) and THF (8.2 ml, 0.6 M). The reaction mixture was then placed in a Cryocooler pre-set at - 10 °C. TsNHNH₂ (0.912 g, 4.90 mmol, 1 equiv.) was added in one portion and the resulting colorless solution was stirred at - 10 °C for 1.5 days, at which time the reaction turned slightly yellow. The flask was then cooled to - 78 °C and another 100 ml of THF was added. The reaction was stirred at this temperature for 5 minutes. Vinylmagnesium bromide (1 M in THF, 22 mL, 22 mmol, 4.5 equiv.) was added slowly into the reaction mixture over 20 minutes. The resulting deep brown solution was stirred at - 78 °C for another 1.5 hours, before the addition of 1 M HCl aq. (22 mL) The cooling bath was removed and acetone (100 ml) was added, followed addition of CuCl₂ (0.658 g, 4.90 mmol, 1 equiv.) in one portion. The copper salt soon dissolved upon heating to 40 °C, giving a dark brown solution, which gradually faded into a light brown solution over 1.5 hours. After a total of 2.5 hours at 40 °C (*Note 1*), the reaction was cooled down to room temperature. Most volatiles were removed *in vacuo* and the resulting black aqueous phase was extracted with EtOAc (1 x 50 mL, 3 x 20 mL). The organic layers were combined and washed with 1 M HCl (2 x 40 mL), brine (40 mL), dried over MgSO₄, filtered and concentrated *in vacuo*. The crude product was purified by flash chromatography (15% → 20% EtOAc/hexanes) to afford a mixture of the desired product and other inseparable by products. The mixture was then dissolved in hexane and ran through a short celite plug to afford the desired product **6.3** (0.456 g, 48%) as a colorless oil. *Note 1*: Long reaction time led to significant amounts of byproducts. *R_f* = 0.27 (20% Et₂O/hexanes), visualized using KMnO₄. ¹H NMR (500 MHz, CDCl₃): δ 6.48 (dd, *J* = 18.1, 11.1 Hz, 1H), 5.37 (dd, *J* = 11.2, 0.9 Hz, 1H), 5.23 (dd, *J* = 18.1, 0.9 Hz, 1H), 4.85-4.81 (m, 1H), 4.77-4.73 (m, 1H), 4.03 (app. t, *J* = 5.4 Hz, 1H), 2.87 (dq, *J* = 10.2, 5.4, 4.9 Hz, 1H), 2.59 (dd, *J* = 14.6, 10.3 Hz, 1H), 2.50 (ddd, *J* = 14.6, 5.3, 1.1 Hz, 1H), 2.10-2.03 (m, 2H), 1.97 (s, 1H), 1.78 (app. s,

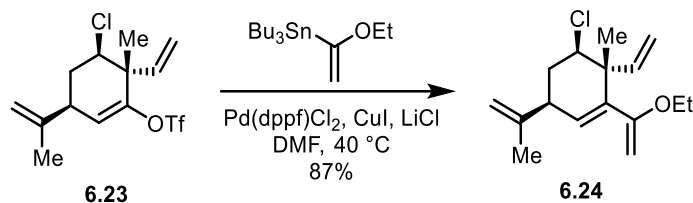
3H), 1.30 (s, 3H). ^{13}C NMR (126 MHz, CDCl_3): δ 211.8, 147.1, 138.5, 116.4, 110.7, 75.8, 56.0, 42.3, 38.6, 32.4, 22.0, 21.2. HRMS (ESI) m/z calc'd for $\text{C}_{12}\text{H}_{19}\text{O}_2$ $[\text{M}+\text{H}]^+$ 195.1385, found 195.1380. $[\alpha]_D^{20} = -11.7^\circ$ ($c=0.72$, CHCl_3).



Chloroketone 6.1. To a flame-dried 25 mL round bottom flask was added N-chlorosuccinimide (116 mg, 0.87 mmol, 1.05 equiv.), THF (3.2 mL, 0.26 M) and PPh₃ (228 mg, 0.87 mmol, 1.05 equiv.) sequentially. The resulting pink slurry was stirred for 30 minutes at room temperature in the dark. Hydroxy ketone **6.3** (161 mg, 0.83 mmol, 1 equiv.) in 1.5 mL THF was then added to the reaction mixture, followed by another 1.7 mL of THF. The resulting slurry was stirred at room temperature for 17 hours, at which point the reaction turned into a burgundy solution. The reaction mixture was concentrated *in vacuo*. The resulting black oil was purified by flash chromatography (2% → 4% Et₂O/hexanes) to afford chloroketone **6.1** (120 mg, 68%) as a white solid. $R_f = 0.35$ (10% Et₂O/hexanes), visualized using KMnO₄. ^1H NMR (500 MHz, CDCl_3): δ 5.88 (dd, $J = 17.5$, 10.9 Hz, 1H), 5.36 (dd, $J = 10.8$, 0.7 Hz, 1H), 5.20 (dd, $J = 17.5$, 0.7 Hz, 1H), 4.86-4.81 (m, 1H), 4.78 (app. q, $J = 1.0$ Hz, 1H), 4.11 (dd, $J = 12.1$, 4.2 Hz, 1H), 2.62 (app. t, $J = 13.9$ Hz, 1H), 2.43-2.29 (m, 3H), 2.16 (app. q, $J = 12.2$ Hz, 1H), 1.76 (app. s, 3H), 1.39 (s, 3H). ^{13}C NMR (126 MHz, CDCl_3): δ 209.7, 145.6, 138.9, 116.8, 111.0, 64.2, 57.2, 42.2, 41.6, 36.8, 20.4, 16.1. HRMS (ESI) m/z calc'd for $\text{C}_{12}\text{H}_{18}^{35}\text{ClO}$ $[\text{M}+\text{H}]^+$ 213.1046, found 213.1040. $[\alpha]_D^{20} = +4.5^\circ$ ($c=0.13$, CHCl_3).

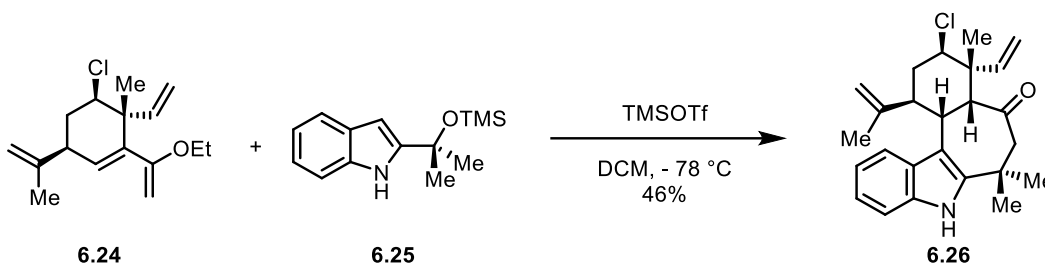


Enol triflate 6.23. To a flame-dried 100 mL round-bottom flask was added chloroketone **6.1** (1.18 g, 5.55 mmol, 1 equiv.) and THF (18.5 mL, 0.30 M). The colorless solution was cooled to –78 °C followed by the slow addition of NaHMDS (1 M in THF, 6.38 mL, 6.38 mmol, 1.15 equiv.). The yellow solution was stirred at –78 °C for 1.5 hour. Comins' reagent (3.27 g, 8.33 mmol, 1.5 equiv.) in THF (7.9 mL) was added dropwise (*Note 1*) and the reaction mixture was stirred at –78 °C for another 1 hour (*Note 2*), before being quenched with saturated NH₄Cl aq. (20 mL). The reaction was warmed to room temperature, transferred into a separatory funnel containing 10 mL of H₂O and extracted with EtOAc (1 x 30 mL, 2 x 15 mL), washed with saturated NH₄Cl aq. (20 mL), brine (20 mL), dried over MgSO₄, filtered and concentrated *in vacuo*. The crude product was purified by flash chromatography (0% → 2% DCM/hexanes) to afford enol triflate **6.23** (1.59 g, 83%) as a colorless oil. *Note 1*: The addition of Comins' reagent needs to be slow to keep the temperature in the flask low to suppress chlorine elimination. *Note 2*: Extended reaction time led to chlorine elimination. *R*_f = 0.19 (1% Et₂O/hexanes), visualized using KMnO₄. **¹H NMR** (500 MHz, CDCl₃): δ 5.74-5.66 (m, 2H), 5.41 (d, *J* = 10.7 Hz, 1H), 5.31 (d, *J* = 17.3 Hz, 1H), 4.91-4.85 (m, 1H), 4.83 (dt, *J* = 1.4, 0.8 Hz, 1H), 4.10 (dd, *J* = 12.9, 3.3 Hz, 1H), 3.13 (ddd, *J* = 11.0, 6.0, 2.5 Hz, 1H), 2.28 (dddd, *J* = 13.3, 6.1, 3.3, 1.0 Hz, 1H), 1.95 (td, *J* = 13.1, 10.9 Hz, 1H), 1.75 (dd, *J* = 1.5, 0.8 Hz, 3H), 1.39 (s, 3H). **¹³C NMR** (126 MHz, CDCl₃): δ 150.9, 145.3, 138.7, 120.3, 118.9, 118.3 (q, *J*_{19F-13C} = 319.8 Hz), 112.6, 63.4, 47.3, 42.4, 34.3, 20.2, 17.0. **HRMS** (ESI) *m/z* calc'd for C₁₃H₁₇³⁵ClF₃O₃S [M+H]⁺ 345.0539, found 345.0530. [α]_D²¹ = -51.5 ° (c=0.25, CHCl₃).



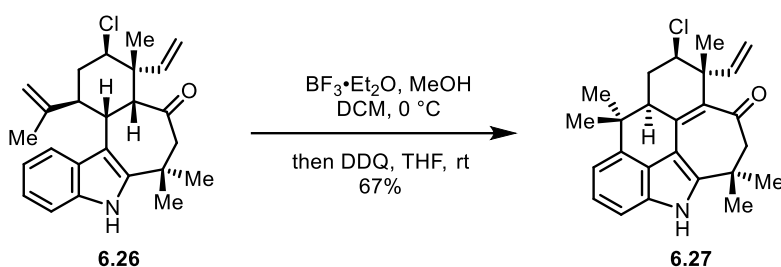
Ethoxy diene 6.24. To a flame-dried 100 mL round-bottom flask was added enol triflate **6.23** (1.587 g, 4.60 mmol, 1 equiv.) and DMF (bubbled with N₂ for 45 min before use, 35 mL). CuI (88 mg, 0.46 mmol, 0.1 equiv.), Pd(dppf)Cl₂·DCM (376 mg, 0.46 mmol, 0.1 equiv.), LiCl (1.034 g, 24.40 mmol, 5.3 equiv.) was added sequentially. Another 11 mL of DMF (bubbled with N₂ for 45 min before use) was added to make a 0.1 M solution. The reaction flask was purged with Ar for 10 min before the addition of tributyl(1-ethoxyvinyl)tin (1.79 mL, 5.29 mmol, 1.15 equiv.). The dark red solution was then heated to 40 °C. After 2.5 days at 40 °C, the brown solution was transferred into a separatory funnel containing NH₃·H₂O:H₂O 1:2 (90 mL), which was extracted with hexanes (1 x 90 mL, 3 x 40 mL). The organic phase was combined and washed with NH₃·H₂O:H₂O 1:2 (3 x 60 mL), brine (60 mL), dried over Na₂SO₄, filtered and concentrated *in vacuo*. The crude material was purified by flash chromatography (basic alumina, pre-saturated with 10% NEt₃/hexanes for 30 minutes, flushed with 10% NEt₃/hexanes) to afford the ethoxy diene **6.24** as a colorless oil (1.068 g, 87%). *R*_f = 0.31 (alumina, hexanes), visualized using KMnO₄. ¹H NMR (500 MHz, C₆D₆): δ 5.87 (dd, *J* = 2.7, 1.1 Hz, 1H), 5.82 (dd, *J* = 17.4, 10.7 Hz, 1H), 5.24-5.15 (m, 2H), 4.73 (dt, *J* = 1.8, 0.9 Hz, 1H), 4.69-4.66 (m, 1H), 4.12 (d, *J* = 1.7 Hz, 1H), 3.93 (dd, *J* = 12.5, 3.7 Hz, 1H), 3.85 (d, *J* = 1.6 Hz, 1H), 3.35 (ddq, *J* = 34.1, 9.4, 7.0 Hz, 2H), 2.63 (ddd, *J* = 11.0, 6.9, 2.6 Hz, 1H), 2.08 (dddd, *J* = 13.1, 6.9, 3.7, 1.1 Hz, 1H), 2.01 (td, *J* = 12.8, 10.9 Hz, 1H), 1.63 (s, 3H), 1.49 (dt, *J* = 1.8, 0.9 Hz, 3H), 1.03 (t, *J* = 7.0 Hz, 3H). ¹³C NMR (126 MHz, C₆D₆): δ 163.7, 147.1, 143.6, 142.8, 129.7, 114.5, 111.4, 84.6, 66.4, 63.1, 45.5, 44.9, 34.8, 20.0,

19.1, 14.5. **HRMS** (ESI) m/z calc'd for $C_{16}H_{24}^{35}ClO$ $[M+H]^+$ 267.1516, found 267.1509. $[\alpha]_D^{20} = -96.5^\circ$ ($c=0.25$, $CHCl_3$).



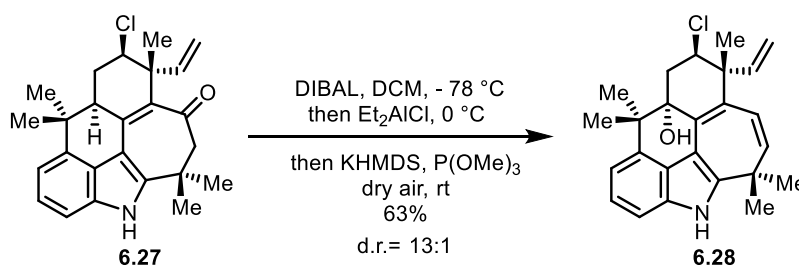
Tetracycle 6.26. To a flame-dried 50 mL round-bottom flask was added ethoxy diene **6.24** (534 mg, 2.00 mmol, 2 equiv.), TMS alcohol **6.25** (248 mg, 1.00 mmol, 1 equiv.) and DCM (10 mL, 0.1 M). The mixture was cooled to $-78^\circ C$, followed by the dropwise addition of TMSOTf (redistilled, 190 μ L, 2.10 mmol, 1.05 equiv.). The resulting black solution was stirred at $-78^\circ C$ for 30 min. The cooling bath was then removed and H_2O (10 mL) was added in one portion. The biphasic solution was stirred rigorously at room temperature for 15 min before the addition of 1 M HCl aq. (1.5 mL). The resulting biphasic solution was stirred for another 15 min at the same temperature. The two phases were separated, and the aqueous phase was washed with DCM (3 x 15 mL). The organic phase was combined, washed with $NaHCO_3$ aq (25 mL) and brine (25 mL), dried over Na_2SO_4 , filtered and concentrated *in vacuo*. The crude material was purified by flash chromatography twice (1st column, 5% \rightarrow 15% EtOAc/hexanes, 2nd column, 2% acetone, 30% DCM, 58% hexanes) to afford the desired product tetracycle **6.26** as a white solid (182 mg, 46%). $R_f = 0.35$ (20% EtOAc/hexanes). **1H NMR** (500 MHz, $CDCl_3$): δ 7.96 (s, 1H), 7.53 (d, $J = 8.0$ Hz, 1H), 7.29 (d, $J = 8.1$ Hz, 1H), 7.15 (ddd, $J = 8.0, 7.0, 1.1$ Hz, 1H), 7.05 (ddd, $J = 8.1, 7.0, 1.0$ Hz, 1H), 6.23 (dd, $J = 17.7, 11.0$ Hz, 1H), 5.44 (dd, $J = 11.9, 4.9$ Hz, 1H), 5.102-5.01 (m, 2H), 4.77

(app. s, 1H), 4.57-4.52 (m, 1H), 3.76-3.66 (m, 1H), 3.23 (d, $J = 4.5$ Hz, 1H), 2.80 (d, $J = 10.2$ Hz, 1H), 2.38 (d, $J = 10.2$ Hz, 1H), 2.32-2.24 (m, 2H), 2.20-2.14 (m, 1H), 1.55 (s, 3H), 1.42 (s, 3H), 1.35 (s, 3H), 1.13 (s, 3H). ^{13}C NMR (126 MHz, CDCl_3): δ 211.4, 146.6, 145.7, 140.5, 133.7, 129.7, 121.9, 119.9, 119.1, 113.5, 112.2, 111.7, 110.3, 65.4, 63.6, 59.1, 45.2, 44.9, 38.7, 36.4, 34.4, 29.9, 29.3, 23.4, 19.6. **IR** (thin film): 3439, 3079, 2964, 2926, 1696, 1490, 1344 cm^{-1} . **HRMS** (ESI) m/z calc'd for $\text{C}_{25}\text{H}_{31}^{35}\text{ClNO}$ $[\text{M}+\text{H}]^+$ 369.2094, found 369.2094. $[\alpha]_D^{19} = -1.8^\circ$ ($c=0.12$, CHCl_3).



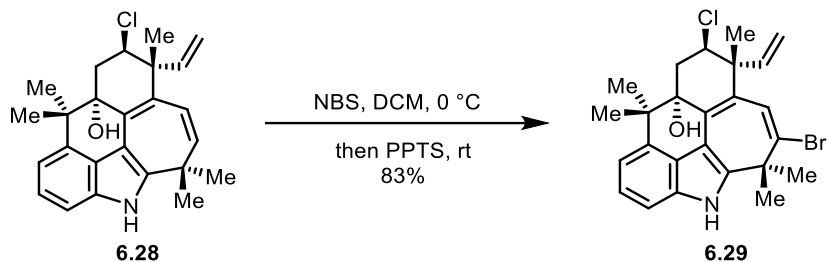
Enone 6.27. To an oven-dried 25 mL round-bottom flask was added tetracycline **6.26** (58 mg, 0.146 mmol, 1 equiv.) and DCM (2.43 mL, 0.06 M). The mixture was cooled to 0°C followed by the addition of $\text{BF}_3 \cdot \text{Et}_2\text{O}$ (72 μL , 0.58 mmol, 4 equiv.), which changed the colorless solution into a dark red solution. MeOH (anhydrous, 6 mL, 0.146 mmol, 1 equiv.) was added and the flask was placed into a Cryocooler pre-set at 0°C . After being stirred at 0°C for 4 days, TBAF (1 M in THF, 0.659 mL, 0.659 mmol, 4.5 equiv.) was added and the dark red color became less intense. The reaction mixture was stirred at 0°C for 15 min before H_2O (52 mL, 2.92 mmol, 20 equiv.) was added. The reaction mixture was stirred at the same temperature for another 15 min. DDQ (133 mg, 0.58 mmol, 4 equiv.) was added as a solid and the resulting black solution was removed from the 0°C cooling bath and stirred at room temperature for 2 hours, before it was quenched with 1 M NaOH aq. (5 mL). The aqueous phase was separated and extracted with DCM (4 x 5 mL). The

organic phase was combined, washed with 1 M NaOH (2 x 10 mL), brine (10 mL), dried over MgSO₄, filtered and concentrated *in vacuo*. The crude product was purified by flash chromatography (5% → 15% EtOAc/hexanes) to afford enone **6.27** as a yellow solid (39 mg, 67%). *R_f* = 0.31 (20% EtOAc/hexanes). **¹H NMR** (500 MHz, CDCl₃): δ 8.02(s, 1H), 7.20-7.12 (m, 2H), 7.03 (dd, *J* = 6.9, 1.2 Hz, 1H), 5.74 (dd, *J* = 17.5, 10.7 Hz, 1H), 5.21 (dd, *J* = 10.7, 0.8 Hz, 1H), 5.15 (dd, *J* = 17.4, 0.8 Hz, 1H), 4.24 (dd, *J* = 12.9, 3.6 Hz, 1H), 3.21 (d, *J* = 11.0 Hz, 1H), 2.93 (dd, *J* = 11.5, 6.7 Hz, 1H), 2.46 (d, *J* = 11.0 Hz, 1H), 2.40 (ddd, *J* = 13.1, 6.6, 3.6 Hz, 1H), 2.27 (app. q, *J* = 12.6 Hz, 1H), 1.65 (s, 3H), 1.54 (s, 3H), 1.49 (s, 3H), 1.33 (s, 3H), 1.04 (s, 3H). **¹³C NMR** (126 MHz, CDCl₃): δ 203.9, 144.0, 141.6, 140.1, 138.6, 133.4, 133.0, 125.1, 123.3, 115.6, 113.7, 108.2, 107.1, 67.0, 55.6, 48.3, 45.8, 39.0, 35.9, 30.7, 29.2, 29.0, 25.1, 23.5, 20.1. **HRMS** (ESI) *m/z* calc'd for C₂₅H₃₉³⁵ClNO [M+H]⁺ 376.1832, found 376.1825. **IR** (thin film): 3364, 2966, 1670, 1448, 1466, 1367, 1320, 1176, 756 cm⁻¹. [α]_D¹⁹ = +51.3 ° (c=0.11, CHCl₃).



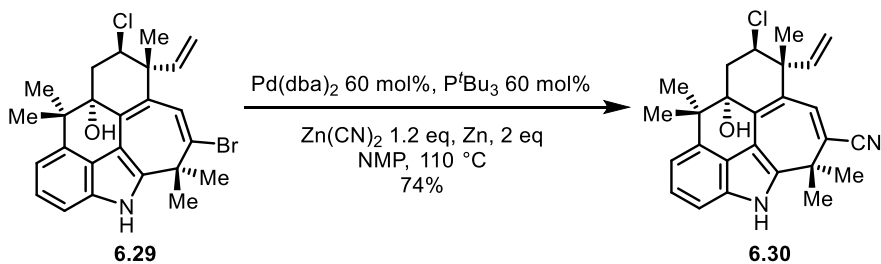
Pentacyclic alcohol 6.28. To a flame-dried 25 mL round-bottom flask was added enone **6.27** (8 mg, 0.0203 mmol, 1 equiv.) and DCM (2.03 mL, 0.01 M). The pale-yellow solution was cooled to -78 °C before the dropwise addition of DIBAL (1 M in PhMe, 81 mL, 0.0812 mmol, 4 equiv.). The resulting orange solution was stirred at -78 °C for 1.5 h before the dropwise addition of HCl (4M in dioxane, 18 mL, 0.0711 mmol, 3.5 equiv.), followed by Et₂AlCl (1 M in hexanes, 20 mL,

0.0203 mmol, 1 equiv.). After 15 min at -78 °C, the dry-ice acetone bath was changed to ice water bath and the reaction was stirred at 0 °C for 10 min, during which time the reaction turned red. P(OMe)₃ (17 mL, 0.143 mmol, 7 equiv.) was added and the red color faded into yellow. The reaction mixture was then cooled to -78 °C. KHMDS (1 M in THF, 102 mL, 0.102 mmol, 5 equiv.) was added and the cooling bath was removed. Dry air was bubbled through the reaction mixture as it warmed to room temperature. The bubbling continued for a total of 20 min while the reaction was at room temperature before 1 M NaOH (50 mL) was added. The reaction mixture was stirred at room temperature for another 15 min before the addition of MgSO₄. The resulting suspension was stirred for an additional 15 min before filtration. The filtrate was concentrated *in vacuo* and purified by flash chromatography (2% → 8% EtOAc/hexanes) to afford a mixture of **23** and its diastereomer as a white solid (5 mg, 63%). The resulting solid was further purified by preparative TLC (4% acetone, 30% DCM, 56% hexanes) to afford **6.28** (3.7 mg) as a white solid. *R*_f = 0.33 (20% EtOAc/hexanes). ¹H NMR (500 MHz, CDCl₃): δ 7.96 (s, 1H), 7.23-7.19 (m, 2H), 7.09 (dd, *J* = 4.9, 3.0 Hz, 1H), 5.92 (d, *J* = 11.5 Hz, 1H), 5.76 (dd, *J* = 17.4, 10.7 Hz, 1H), 5.41 (d, *J* = 11.5 Hz, 1H), 5.29 (dd, *J* = 10.7, 1.0 Hz, 1H), 5.23 (dd, *J* = 17.4, 1.0 Hz, 1H), 4.51 (dd, *J* = 12.9, 3.8 Hz, 1H), 2.59 (td, *J* = 13.3, 2.1 Hz, 1H), 2.46 (dd, *J* = 13.6, 3.8 Hz, 1H), 2.04 (app. d, *J* = 2.3 Hz, 1H), 1.67 (s, 3H), 1.60 (s, 3H), 1.46 (s, 3H), 1.11 (s, 3H), 1.02 (s, 3H). ¹³C NMR (126 MHz, CDCl₃): δ 144.4, 140.9, 137.0, 133.9, 133.0, 132.4, 130.2, 127.7, 123.8, 123.7, 115.7, 115.4, 108.9, 106.8, 78.0, 63.8, 46.8, 45.3, 36.4, 35.6, 28.2, 26.6, 26.2, 18.2, 17.5. HRMS (ESI) *m/z* calc'd for C₂₅H₂₇³⁵ClNO [M+H-H₂O]⁺ 376.1832, found 376.1825. IR (thin film): 3536, 3344, 2969, 1570, 1473, 1458, 1458, 1361, 1308, 1266, 911, 744, 707 cm⁻¹. [α]_D¹⁹ = +8.7 ° (c=0.17, CHCl₃).



Bromide 6.29. To an oven dried 4 mL vial was added **6.28** (2.0 mg, 0.0051 mmol, 1 equiv.) and DCM (250 mL). The colorless solution was cooled to 0 °C. *N*-bromosuccinimide (0.9 mg, 0.0051 mmol, 1 equiv.) was added as a DCM solution (50 mL of a stock solution made by dissolving 9 mg of *N*-bromosuccinimide in 500 mL DCM). The resulting orange solution was stirred at 0 °C for 10 min before the addition of pyridinium *p*-toluenesulfonate (2.6 mg, 0.010 mmol, 2 equiv.) as a DCM solution (100 mL of a stock solution made by dissolving 13 mg pyridinium *p*-toluenesulfonate in 500 mL DCM). The red solution was stirred at 0 °C and then at room temperature. The reaction was stirred at this temperature for 90 minutes before being quenched by NaHCO₃ aq. (500 mL). The two phases were separated, and the aqueous phase was extracted with DCM (3 x 1 mL). The organic phase was combined, dried over Na₂SO₄, filtered and concentrated *in vacuo*. The crude product was purified by preparative TLC (40% EtOAc/hexanes) to afford bromide **6.29** as a yellow solid (1.8 mg, 83%). *R*_f = 0.30 (20% EtOAc/hexanes). **¹H NMR** (500 MHz, CDCl₃): δ 8.03 (s, 1H), 7.26-7.22 (m, 2H), 7.11 (dd, *J* = 5.6, 2.2 Hz, 1H), 6.61 (s, 3H), 5.73 (dd, *J* = 17.4, 10.6 Hz, 1H), 5.33 (d, *J* = 10.6 Hz, 1H), 5.26 (d, *J* = 17.4 Hz, 1H), 4.47 (dd, *J* = 12.9, 3.7 Hz, 1H), 2.58 (app. t, *J* = 13.4 Hz, 1H), 2.45 (dd, *J* = 13.7, 3.8 Hz, 1H), 2.01 (s, 1H), 1.90 (s, 3H), 1.60 (s, 3H), 1.47 (s, 3H), 1.11 (s, 3H), 1.09 (s, 3H). **¹³C NMR** (126 MHz, CDCl₃): δ 143.6, 137.3, 137.1, 133.5, 132.9, 131.5, 130.5, 124.5, 123.5, 123.2, 116.1, 115.9, 109.2, 108.0, 77.9, 63.3, 46.8, 45.5, 41.4, 36.3, 28.7, 28.3, 25.0, 18.1, 17.4. **HRMS** (ESI) *m/z* calc'd for

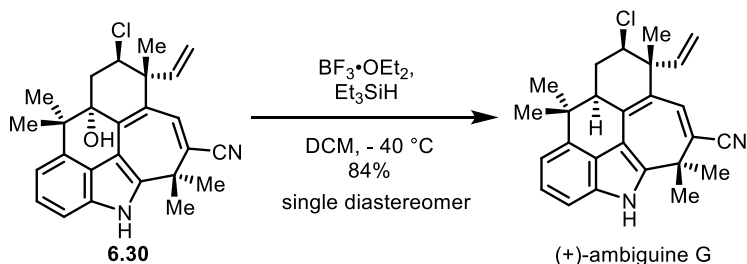
C₂₅H₂₆⁷⁹Br³⁵CIN [M+H-H₂O]⁺ 4543.0937, found 454.0929. **IR** (thin film): 3522, 3334, 2966, 1559, 1472, 1457, 1362, 1308, 923, 760 cm⁻¹. [α]_D²⁶ = +23.0 ° (c=0.15, CHCl₃).



Nitrile 6.30. Tri-*tert*-butyl phosphine (12.3 mg) was weighed into an oven-dried 4 mL vial in a glove box. The vial was then capped and taken out of the glove box. *N*-Methylpyrrolidinone (NMP, bubbled with N₂ for 40 minutes before use, 958 ml) was added into the vial to make a colorless solution. To different oven-dried 4 mL vial was added Pd(dba)₂ (11.0 mg) and NMP (bubbled with N₂ for 40 minutes before use, 300 mL). The dark red solution was purged with N₂ for 3 min, before 300 mL of the tri-*tert*-butyl phosphine NMP solution was added. Another 150 mL of NMP was added and the mixture was stirred at room temperature for 1 hour.

To an oven-dried 4 mL vial was added bromide **6.29** (3.0 mg, 0.0063 mmol, 1 equiv.), Zn(CN)₂ (0.9 mg, 0.0076 mmol, 1.2 equiv.), Zn dust (3.3 mg, 0.0508 mmol, 8 equiv. *Note 1*) and NMP (bubbled with N₂ for 40 minutes before use, 270 mL). The vial was purged with N₂ for 3 min. The mixture was heated to 110 °C and the pre-prepared Pd(dba)₂-P'^tBu₃ NMP solution (50 mL, contained Pd(dba)₂ 0.73 mg, 0.0013 mmol, 0.2 equiv.; P'^tBu₃ 0.26 mg, 0.0013 mmol, 0.2 equiv.) was added into the vial containing **6.29** with rigorous stirring. The resulting clear brown solution was stirred at this temperature for 40 minutes. Another 100 mL of the Pd(dba)₂-P'^tBu₃ NMP solution (contained Pd(dba)₂ 1.46 mg, 0.0026 mmol, 0.4 equiv.; P'^tBu₃ 0.51 mg, 0.0026 mmol, 0.4

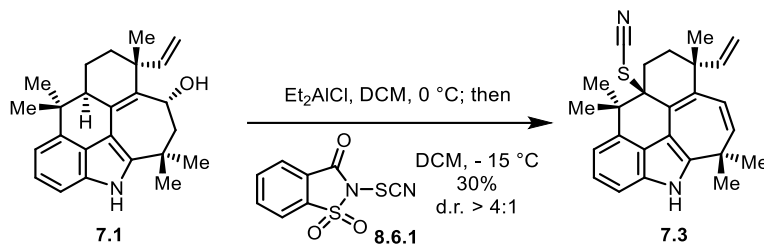
equiv.) was added and the brown solution was stirred at the same temperature for an extra 40 minute. The reaction mixture was then filter through a pad of celite and flashed with EtOAc. The organic phase was washed with H₂O (3 x 1 mL), brine (1 mL), dried over Na₂SO₄, filtered and concentrated *in vacuo*. The crude material was purified by prep-TLC (50% EtOAc/hexanes) to afford the desired product nitrile **6.30** as a yellow solid (2.0 mg, 74%). *Note 1*: The ratio of Zn dust to Pd(dba)₂ needs to be at least 10 to 1 to ensure reproducible results. *R_f*= 0.14 (20% EtOAc/hexanes). **¹H NMR** (500 MHz, CDCl₃): δ 8.17 (s, 3H), 7.30-7.25 (m, 2H), 7.14 (dd, *J* = 5.4, 2.5 Hz, 1H), 6.78 (s, 3H), 5.72 (dd, *J* = 17.4, 10.6 Hz, 1H), 5.35 (d, *J* = 10.6 Hz, 1H), 5.28 (d, *J* = 17.4 Hz, 1H), 4.46 (dd, *J* = 12.9, 3.7 Hz, 1H), 2.60 (t, *J* = 13.3 Hz, 1H), 2.47 (dd, *J* = 13.7, 3.8 Hz, 1H), 2.07 (s, 3H), 1.93 (s, 3H), 1.61 (s, 3H), 1.50 (s, 3H), 1.11 (s, 3H), 1.08 (s, 3H). **¹³C NMR** (125 MHz, CDCl₃): δ 143.3, 142.2, 139.7, 136.7, 136.3, 133.1, 132.7, 125.0, 123.1, 119.5, 116.7, 116.6, 111.0, 109.5, 107.6, 78.0, 62.7, 46.7, 45.5, 36.2, 35.7, 28.0, 25.1, 25.0, 18.0, 17.7. **HRMS** (ESI) *m/z* calc'd for C₂₆H₂₆³⁵CIN₂ [M+H-H₂O]⁺ 401.1785, found 401.1777. **IR** (thin film): 3333, 2972, 2927, 2206, 1559, 1535, 1471, 1363, 1309, 1265, 1078, 1054, 914, 761, 736 cm⁻¹. [α]_D¹⁹ = +82.2 ° (c=0.13, CHCl₃).



(+)-Ambiguine G. To a flame-dried 10 mL round-bottom flask containing nitrile **6.30** (2.6 mg, 0.0062 mmol, 1 equiv.) was added DCM (478 mL, 0.013 M), followed by Et₃SiH (20 mL, 0.124

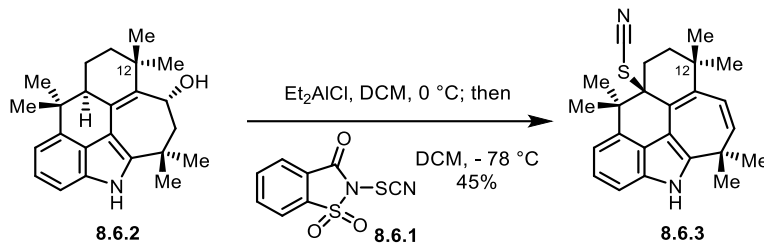
mmol, 20 equiv.). The resulting yellow solution was cooled to - 40 °C. BF₃·OEt₂ (3.8 mL, 0.0310 mmol, 5 equiv.) was added to the reaction mixture slowly as a DCM solution (50 mL, made by dissolving 38 mL BF₃·OEt₂ in 462 mL DCM), which caused the reaction to turn into a light brown, opaque solution. The reaction was stirred at - 40 °C for 30 min and quenched with saturated NaHCO₃ aq. (2 mL) at the same temperature. The resulting mixture was then allowed to warm to rt and extracted with DCM (2 x 2 mL). The organic phase was washed with saturated NaHCO₃ aq. (1 x 2 mL), dried with Na₂SO₄, filtered and concentrated *in vacuo*. The crude product was purified by prep-TLC (25% EtOAc/hexanes) to afford (+)-ambiguine G as a yellow solid (2.1 mg, single diastereomer, 84%). *R*_f = 0.29 (20% EtOAc/hexanes). **¹H NMR** (500 MHz, CD₃OD): δ 8.04 (s, 1H), 7.25-7.20 (m, 2H), 7.08 (dd, *J* = 5.5, 2.3 Hz, 1H), 6.76 (s, 3H), 5.70 (dd, *J* = 17.4, 10.6 Hz, 1H), 5.32 (d, *J* = 10.6 Hz, 1H), 5.26 (d, *J* = 17.3 Hz, 1H), 4.19 (dd, *J* = 12.9, 3.8 Hz, 1H), 3.18 (dd, *J* = 11.4, 7.4 Hz, 1H), 2.44 (ddd, *J* = 13.4, 7.4, 3.8 Hz, 1H), 2.34 (app. q, *J* = 12.6 Hz, 1H), 1.91 (s, 3H), 1.56 (s, 3H), 1.52 (s, 3H), 1.06 (s, 3H), 1.04 (s, 3H). **¹³C NMR** (125 MHz, CD₃OD): δ 143.9, 142.3, 139.7, 137.5, 135.9, 133.0, 132.5, 124.7, 124.2, 119.9, 116.3, 114.6, 110.3, 109.5, 109.0, 65.5, 48.1, 46.3, 40.3, 35.5, 30.3, 25.1, 24.8, 24.8, 23.4, 18.8. **HRMS** (ESI) *m/z* calc'd for C₂₆H₂₈³⁵ClN₂ [M+H]⁺ 403.1941, found 403.1930. **IR** (thin film): 3343, 2974, 2202, 1653, 1539, 1472, 1457, 1362, 1315 cm⁻¹. [α]_D²⁰ = +143.2 ° (c=0.05, CHCl₃).

8.6 Experimental Procedures and Characterization Data for Chapter 7

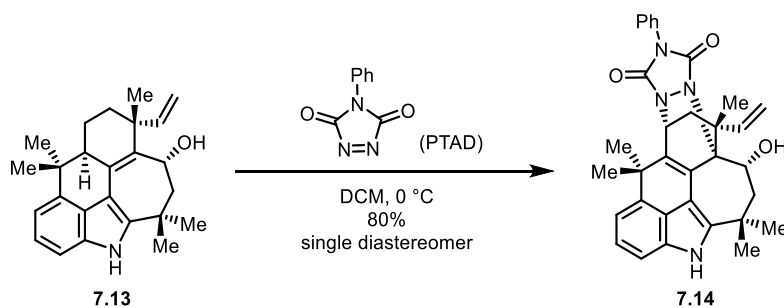


Thiocyanate 7.3. To a 4 mL vial was added **7.1** (3 mg, 0.0083 mmol, 1 equiv) and DCM (0.750 mL). The reaction was cooled to $0\text{ }^\circ\text{C}$ before the addition of Et_2AlCl (1M in hexanes, $8.3\text{ }\mu\text{L}$, 0.0083 mmol, 1 equiv). The reaction was stirred at this temperature and then cooled to $-15\text{ }^\circ\text{C}$. Thiocyanation reagent **8.6.1** (3 mg, 0.0124 mmol, 1.5 equiv) was added. The reaction was stirred at this temperature for 20 minutes. Before being quenched by NaHCO_3 aq. (1 mL). The aqueous phase was extracted with DCM. The organic phase was combined, dried over MgSO_4 , filtered and concentrated *in vacuo*. The crude product was purified by prep-TLC (30% EtOAc/hexanes) to afford the desired product as a white solid which gradually turned orange. $^1\text{H NMR}$ (400 MHz, CDCl_3 , major isomer) δ 7.95 (s, 1H), 7.24 – 7.14 (m, 2H), 7.03 (dd, $J = 7.0, 0.9\text{ Hz}$, 1H), 5.95 (d, $J = 11.4\text{ Hz}$, 1H), 5.83 (dd, $J = 17.4, 10.5\text{ Hz}$, 1H), 5.49 (d, $J = 11.4\text{ Hz}$, 1H), 5.14 (dd, $J = 10.5, 1.5\text{ Hz}$, 1H), 2.25 – 2.15 (m, 1H), 2.07 – 1.88 (m, 3H), 1.69 (s, 3H), 1.61 (s, 3H), 1.29 (s, 3H), 1.10 (s, 3H), 1.07 (s, 3H).

A slightly modified procedure was applied to the C12-dimethyl analogue, which provided a cleaner conversion to the desired product.

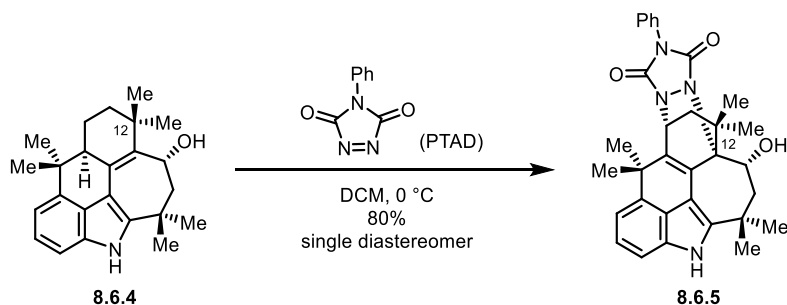


Thiocyanate 8.6.3. To a 4 mL vial was added **8.6.2** (4 mg, 0.0114 mmol, 1 equiv) and DCM (0.750 mL). The reaction was cooled to 0 °C before the addition of Et₂AlCl (1M in hexanes, 11.4 μL, 0.0114 mmol, 1 equiv). The reaction was stirred at this temperature and then cooled to –78 °C. Thiocyanation reagent **8.6.1** (3 mg, 0.0114 mmol, 1.1 equiv) was added. The reaction was stirred at this temperature for 20 minutes. Before being quenched by NaHCO₃ aq. (1 mL). The aqueous phase was extracted with DCM. The organic phase was combined, dried over MgSO₄, filtered and concentrated *in vacuo*. The crude product was purified by prep-TLC (30% EtOAc/hexanes) to afford the desired product as a white solid which gradually turned orange. ¹H NMR (500 MHz, CDCl₃) δ 7.91 (s, 1H), 7.23 – 7.11 (m, 2H), 7.03 (dd, *J* = 7.1, 0.8 Hz, 1H), 6.08 (d, *J* = 11.4 Hz, 1H), 5.52 (d, *J* = 11.4 Hz, 1H), 2.27 (td, *J* = 14.1, 3.0 Hz, 1H), 2.09 (dt, *J* = 14.0, 3.5 Hz, 1H), 1.92 (td, *J* = 13.9, 3.0 Hz, 1H), 1.71-1.65 (m, 4H), 1.63 (s, 3H), 1.27 (s, 3H), 1.20 (s, 3H), 1.08 (s, 3H), 1.07 (s, 3H). IR (thin film): 3402, 2964, 2923, 2065, 1576, 1559, 1471, 1457, 1362, 1328, 1037 cm⁻¹.



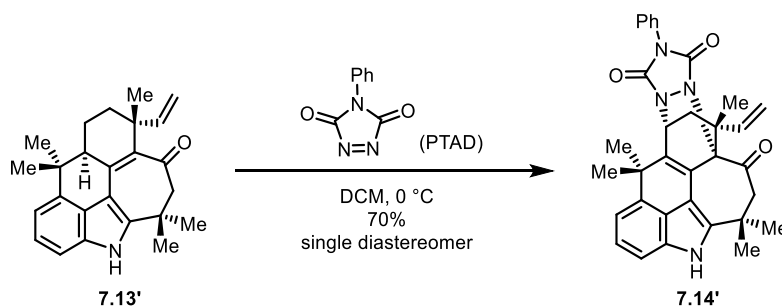
Aminated product 7.14. To a 4 mL vial was added **7.13** (3 mg, 0.0083 mmol, 1 equiv) and DCM (420 μ L). The reaction was cooled to 0 $^{\circ}$ C before the addition of PTAD (4 mg, 0.0233 mmol, 2.8 equiv). The resulting red solution was stirred at 0 $^{\circ}$ C for 30 min, at which point the reaction was pink. All volatiles were removed *in vacuo* and the crude product was purified by prep-TLC (50% EtOAc/hexanes) to afford the desired product as a white solid (3.6 mg, 80%). R_f = 0.42 (40% EtOAc/hexanes). $^1\text{H NMR}$ (400 MHz, CDCl_3) δ 7.68 (s, 1H), 7.51 – 7.41 (m, 4H), 7.41 – 7.32 (m, 1H), 7.23 – 7.17 (m, 1H), 7.12 – 7.05 (m, 1H), 7.00 (dd, J = 7.4, 0.7 Hz, 1H), 6.50 (dd, J = 17.5, 10.8 Hz, 1H), 5.27 (dd, J = 3.4, 2.4 Hz, 1H), 5.16 (d, J = 12.2 Hz, 1H), 5.12 (dd, J = 10.9, 0.8 Hz, 1H), 5.08 – 5.00 (m, 1H), 4.66 (dd, J = 12.2, 9.0 Hz, 1H), 2.81 (dd, J = 14.6, 9.1 Hz, 1H), 2.48 (dd, J = 13.6, 3.5 Hz, 1H), 1.94 (d, J = 14.6 Hz, 1H), 1.61-1.57 (m, 1H), 1.54 (s, 5H), 1.50 (s, 3H), 1.33 (s, 3H), 1.25 (s, 3H), 1.19 (s, 3H).

A similar reaction was performed on the C12-dimethyl analogue, whose structure was confirmed by HMBC and HSQC.

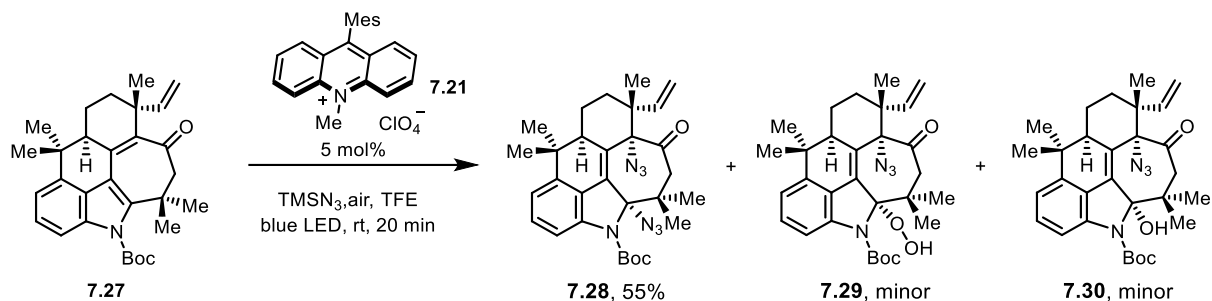


Aminated product 8.6.5. To a 4 mL vial was added **8.6.4** (7 mg, 0.0083 mmol, 1 equiv) and DCM (1 mL). The reaction was cooled to 0 $^{\circ}$ C before the addition of PTAD (10.5 mg, 0.0249 mmol, 3 equiv). The resulting red solution was stirred at 0 $^{\circ}$ C for 30 min, at which point the reaction was pink. All volatiles were removed *in vacuo* and the crude product was purified by prep-TLC (50% EtOAc/hexanes) to afford the desired product as a white solid (8.0 mg, 76%). R_f =

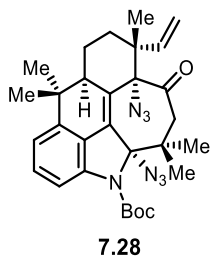
0.46 (40% EtOAc/hexanes). **¹H NMR** (500 MHz, CD₂Cl₂, -40 °C) δ 8.05 (s, 1H), 7.50 – 7.39 (m, 4H), 7.36 (t, *J* = 7.3 Hz, 1H), 7.13 (t, *J* = 7.7 Hz, 1H), 7.03 (d, *J* = 7.9 Hz, 1H), 6.94 (d, *J* = 7.4 Hz, 1H), 5.35 (s, 1H), 5.16 (s, 1H), 4.68 (dd, *J* = 12.1, 9.4 Hz, 1H), 2.78 (dd, *J* = 14.6, 9.5 Hz, 1H), 2.09 (dd, *J* = 13.2, 3.2 Hz, 1H), 1.86 (d, *J* = 14.6 Hz, 1H), 1.62 (dd, *J* = 13.1, 2.7 Hz, 1H), 1.48 (s, 3H), 1.46 (s, 3H), 1.43 (s, 3H), 1.39 (s, 3H), 1.27 (s, 3H), 0.99 (s, 3H). **¹³C NMR** (125 MHz, CD₂Cl₂) δ 151.1, 148.8, 140.1, 137.3, 133.5, 129.0, 128.2, 127.3, 125.8, 124.3, 123.9, 114.6, 107.4, 104.7, 76.2, 66.0, 49.9, 48.2, 43.0, 40.5, 38.2, 34.6, 30.9, 30.7, 28.6, 28.1, 27.6, 26.0, 13.9.



Aminated product 7.14'. To a 4 mL vial was added **7.13'** (3 mg, 0.0083 mmol, 1 equiv) and DCM (420 μL). The reaction was cooled to 0 °C before the addition of PTAD (4 mg, 0.0233 mmol, 2.8 equiv). The resulting red solution was stirred at 0 °C for 30 min, at which point the reaction was pink. All volatiles were removed *in vacuo* and the crude product was purified by prep-TLC (50% EtOAc/hexanes) to afford the desired product as a white solid (3.2 mg, 70%). *R_f* = 0.52 (40% EtOAc/hexanes). **¹H NMR** (500 MHz, CDCl₃) δ 7.77 (s, 1H), 7.35 (m, *J* = 4.8 Hz, 3H), 7.29-7.26 (m, 2H), 7.23 (d, *J* = 7.7 Hz, 1H), 7.11 (d, *J* = 7.9 Hz, 1H), 7.03 (d, *J* = 7.4 Hz, 1H), 6.51 (dd, *J* = 17.5, 10.9 Hz, 1H), 5.23 (d, *J* = 10.9 Hz, 1H), 5.20 (dd, *J* = 4.1, 2.0 Hz, 1H), 5.11 (d, *J* = 17.5 Hz, 1H), 3.20 (d, *J* = 11.8 Hz, 1H), 3.01 (d, *J* = 11.8 Hz, 1H), 2.65 (dd, *J* = 13.0, 4.0 Hz, 1H), 1.54 (s, 6H), 1.52 (s, 3H), 1.48 (s, 3H), 1.26 (s, 3H).

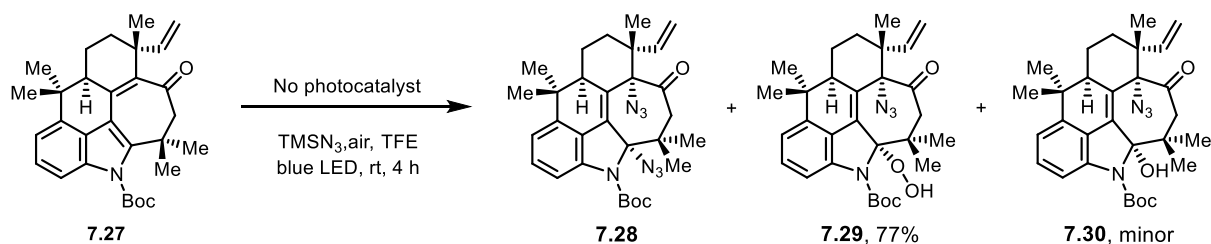


Azidation with photocatalyst 7.21. To an 8 mL vial was added **7.27** (8 mg, 0.0174 mmol, 1 equiv), TFE (670 μL), acridinium photocatalyst **7.21** (0.4 mg, 0.00087 mmol, 0.05 equiv, in 200 μL TFE) and TMSN_3 (23 μL , 0.174 mmol, 10 equiv). The vial was then purged with air and irradiated with blue LED. After 20 minutes, all volatiles were removed *in vacuo* and the crude product was purified by prep-TLC (50% EtOAc/hexanes) to afford the products.

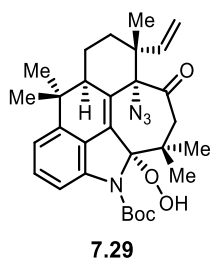


$^1\text{H NMR}$ (500 MHz, C_6D_6) δ 7.96 (d, $J = 8.1$ Hz, 1H), 7.12 (t, $J = 7.9$ Hz, 1H), 6.73 (d, $J = 7.6$ Hz, 1H), 6.38 (dd, $J = 17.4, 11.0$ Hz, 1H), 5.21 (dd, $J = 10.9, 1.1$ Hz, 1H), 5.10 (dd, $J = 17.5, 1.2$ Hz, 1H), 2.72 (d, $J = 10.8$ Hz, 1H), 2.58 (dd, $J = 12.2, 7.5$ Hz, 1H), 2.19 (td, $J = 13.8, 4.5$ Hz, 1H), 1.85 (d, $J = 10.7$ Hz, 1H), 1.72 (s, 3H), 1.40 (s, 9H), 1.37 – 1.30 (m, 1H), 1.20 – 1.14 (m, 1H), 1.10 (s, 3H), 0.82 (s, 3H), 0.76 (s, 3H), 0.72 (s, 4H). $^{13}\text{C NMR}$ (101 MHz, C_6D_6) δ 202.0, 151.4, 142.4, 142.3, 141.5, 136.4, 131.8, 130.6, 123.3, 117.5, 115.0, 113.8, 92.4, 82.9, 74.7, 53.3, 45.0,

43.8, 42.4, 37.7, 30.5, 28.0, 26.4, 25.7, 23.9, 23.0, 21.3, 19.5, 14.2. **IR** (thin film): 3559, 2925, 2111, 1717, 1456, 1323, 1157 cm^{-1} .

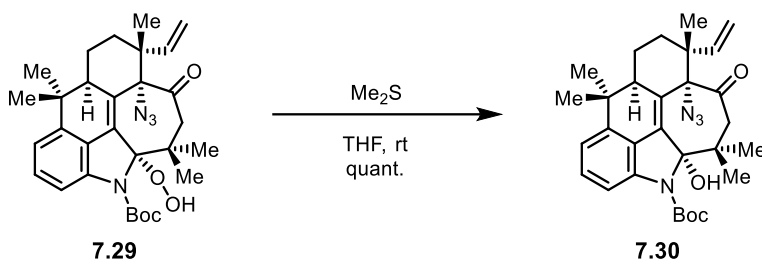


Azidation without photocatalyst. To a 20 mL vial was added **7.27** (9 mg, 0.0196 mmol, 1 equiv), TFE (980 μL) and TMSN_3 (26 μL , 0.196 mmol, 10 equiv). The vial was then purged with air and irradiated with blue LED. After 4 hours, NaHCO_3 aq. (3 mL) was added and the mixture was extracted with EtOAc. The organic phase was combined, dried over Na_2SO_4 , filtered and concentrated *in vacuo*. The crude product was purified by prep-TLC (15% EtOAc/hexanes) to afford the products.

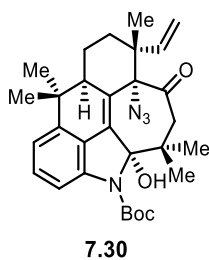


$^1\text{H NMR}$ (500 MHz, CDCl_3) δ 9.63 (s, 1H), 7.48 (d, $J = 8.1$ Hz, 1H), 7.24 (t, $J = 8$ Hz, 1H), 6.92 (d, $J = 7.7$ Hz, 1H), 6.18 (dd, $J = 17.6, 10.9$ Hz, 1H), 5.37 – 5.21 (m, 2H), 3.05 (d, $J = 10.6$ Hz, 1H), 2.66 (dd, $J = 12.3, 7.3$ Hz, 1H), 2.32 (td, $J = 13.7, 4.2$ Hz, 1H), 2.12 (d, $J = 10.6$ Hz, 1H), 1.99 (td, $J = 8.7, 7.2, 3.7$ Hz, 1H), 1.81 (qd, $J = 13.7, 4.4$ Hz, 1H), 1.66-1.58 (m, 10H), 1.57 (s, 3H), 1.45 (s, 3H), 1.07 (s, 3H), 1.05 (s, 3H), 0.96 (s, 3H). **$^{13}\text{C NMR}$** (101 MHz, CDCl_3) δ 205.0, 151.6,

142.6, 141.2, 141.1, 136.4, 131.3, 128.4, 123.0, 116.8, 116.7, 114.2, 107.3, 82.5, 73.1, 55.2, 44.9, 43.8, 42.7, 37.8, 29.9, 28.5, 27.5, 23.8, 23.7, 23.4, 22.3, 19.5. **IR** (thin film): 3303, 2971, 2929, 2100, 1736, 1455, 1358, 1327, 1164, 1005, 966 cm^{-1} .

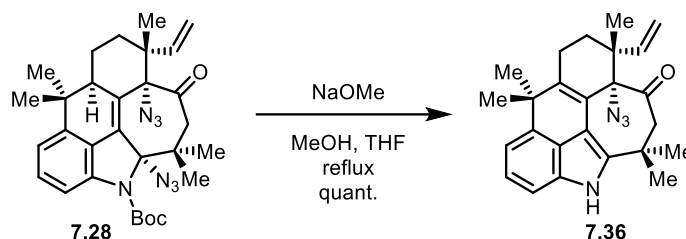


Azidoalcohol 7.30. To a 10 mL round bottom flask was added **7.29** (4.4 mg, 0.00823 mmol, 1 equiv), THF (823 μL) and Me_2S (6 μL , 0.0823 mmol, 10 equiv). The reaction was stirred at room temperature for 10 min and all volatiles were removed *in vacuo*. The product was obtained as a white solid and used without further purification.



$^1\text{H NMR}$ (500 MHz, CDCl_3) δ 7.27-7.24 (m, 1H), 7.22 (t, $J = 7.7$ Hz, 1H), 6.97 (d, $J = 7.4$ Hz, 1H), 6.19 (dd, $J = 17.6, 11.0$ Hz, 1H), 6.04 – 5.97 (m, 1H), 5.12 (d, $J = 11.0$ Hz, 1H), 4.99 (d, $J = 17.5$ Hz, 1H), 2.94 (d, $J = 10.8$ Hz, 1H), 2.66 (dd, $J = 12.3, 7.3$ Hz, 1H), 2.19 (td, $J = 13.9, 4.3$ Hz, 1H), 2.05 (d, $J = 10.4$ Hz, 1H), 1.93 (ddt, $J = 14.2, 7.2, 3.6$ Hz, 1H), 1.81 (qd, $J = 13.6, 4.4$ Hz, 1H), 1.58 (s, 9H), 1.48 (s, 3H), 1.46 (s, 3H), 1.42 (dt, $J = 13.8, 3.8$ Hz, 1H), 1.10 (s, 3H), 1.07 (s, 3H), 0.92 (s, 3H). **$^{13}\text{C NMR}$** (126 MHz, CDCl_3) δ 203.2, 153.7, 142.5, 141.9, 140.9, 137.9, 131.1,

127.3, 123.4, 117.6, 113.5, 113.5, 99.0, 83.4, 54.9, 47.0, 43.1, 42.7, 38.1, 31.6, 29.9, 28.5, 27.0, 24.3, 24.1, 23.5, 20.8, 19.5.



Azide 7.36. To a 4 mL vial was added **7.28** (1 mg, 0.0018 mmol, 1 equiv), THF (180 μ L) and NaOMe (25% wt in MeOH, 8 μ L). The reaction was heated to reflux and stirred at this temperature for 1 hour. The reaction was then cooled to room temperature. NH_4Cl aq. (1 mL) was added at the mixture was extracted with EtOAc (3 x 1 mL). The organic phase was combined, dried over Na_2SO_4 , filtered and concentrated *in vacuo*. The crude product was purified by prep-TLC (20% EtOAc/hexanes) to afford the desired product as a white solid. $^1\text{H NMR}$ (500 MHz, CDCl_3) δ 8.03 (s, 1H), 7.21 – 7.12 (m, 2H), 7.01 (dd, $J = 6.6, 1.5$ Hz, 1H), 5.87 (dd, $J = 17.5, 10.7$ Hz, 1H), 5.16 (dd, $J = 17.5, 0.9$ Hz, 1H), 5.09 (dd, $J = 10.6, 0.9$ Hz, 1H), 3.35 (d, $J = 10.8$ Hz, 1H), 2.45 (d, $J = 10.8$ Hz, 1H), 2.39 – 2.31 (m, 1H), 2.17 (dt, $J = 14.2, 3.6$ Hz, 1H), 2.08 – 2.00 (m, 1H), 1.62 (dt, $J = 14.1, 3.7$ Hz, 1H), 1.57 (s, 4H), 1.52 (s, 3H), 1.51 (s, 3H), 1.36 (s, 3H), 1.11 (s, 3H).

Appendix

Selected ^1H and ^{13}C NMR spectra

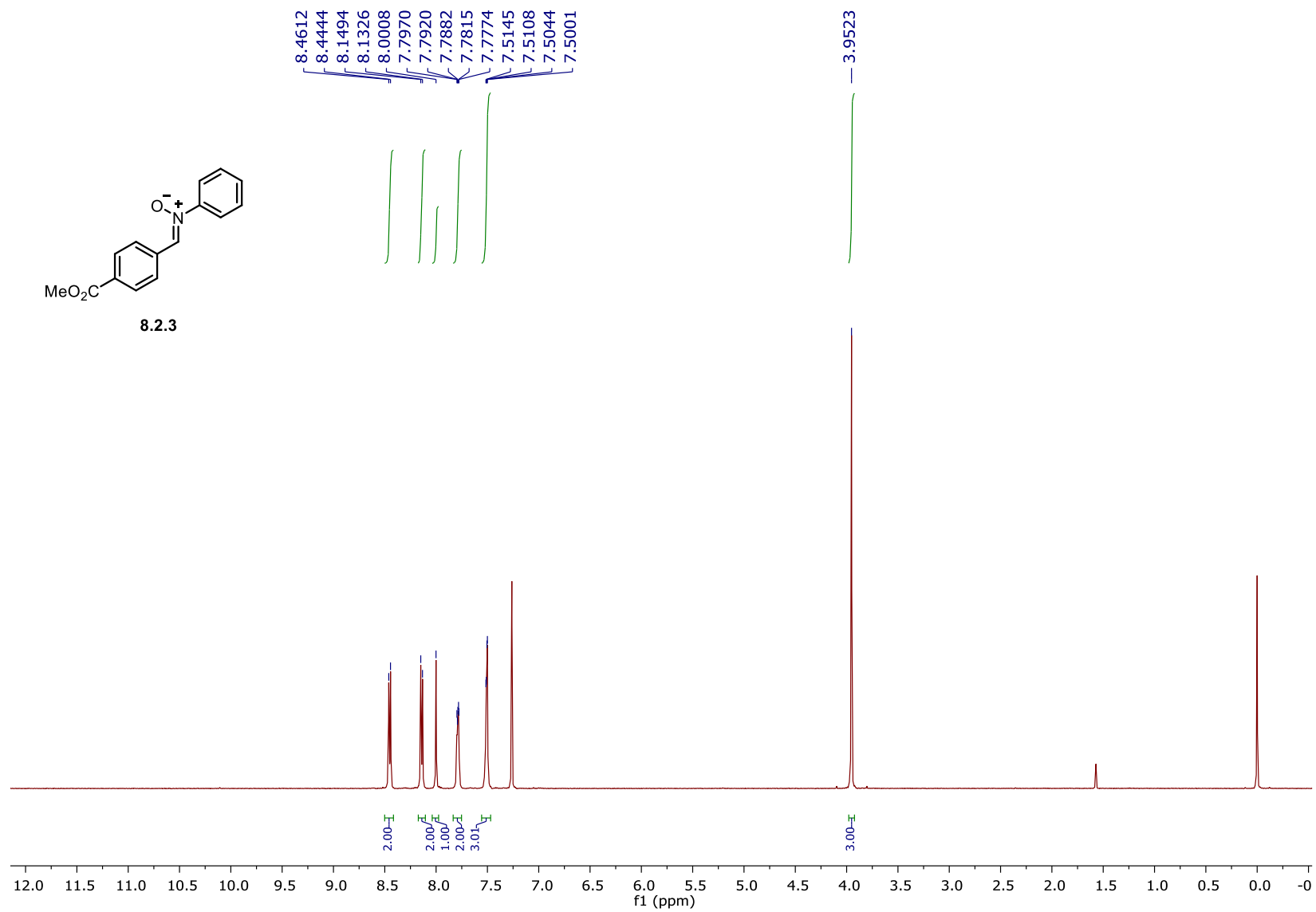


Figure 1. ^1H NMR spectrum of **8.2.3** (500 MHz, CDCl_3).

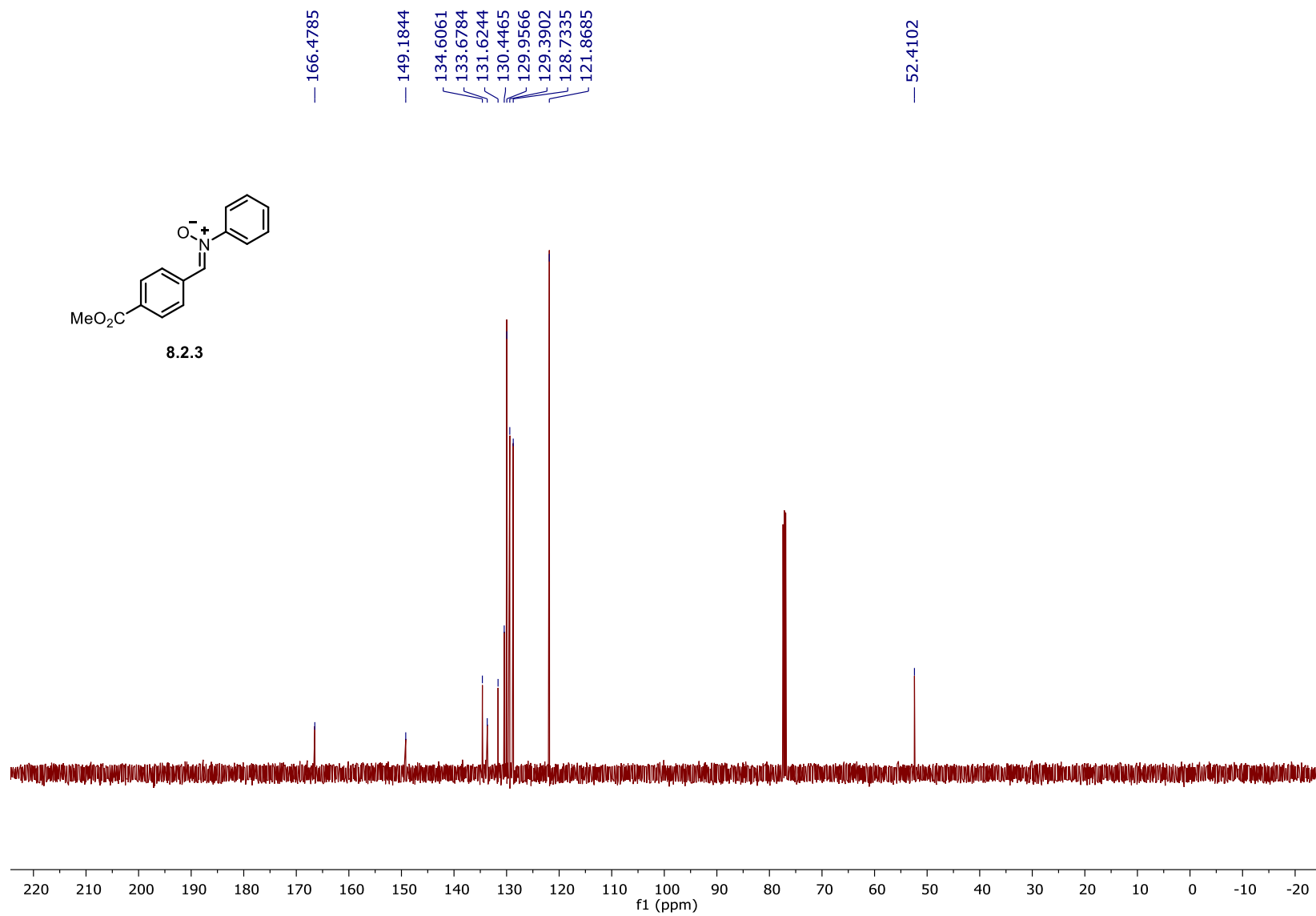


Figure 2. ^{13}C NMR spectrum of **8.2.3** (125 MHz, CDCl_3).

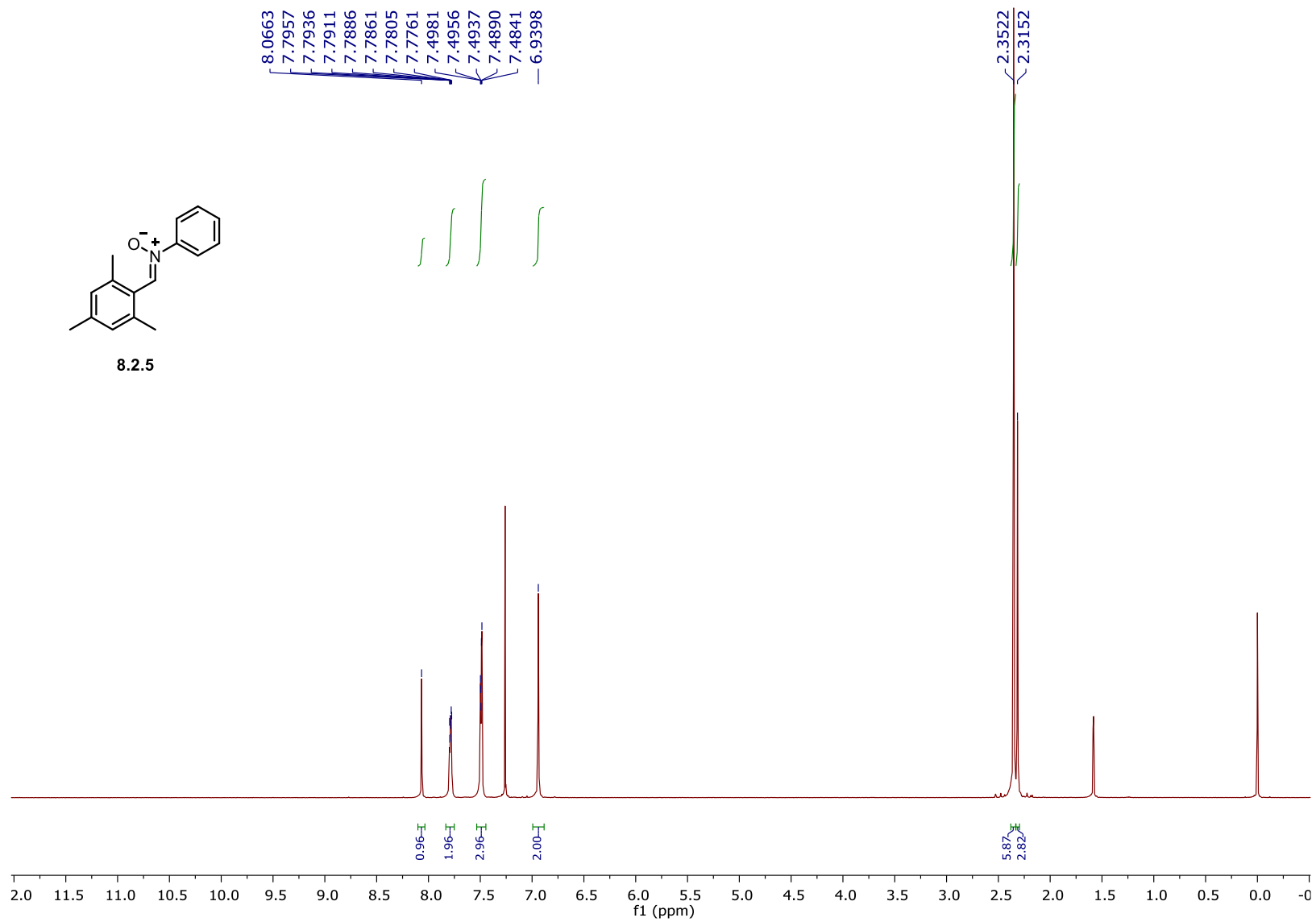


Figure 3. ¹H NMR spectrum of **8.2.5** (500 MHz, CDCl₃).

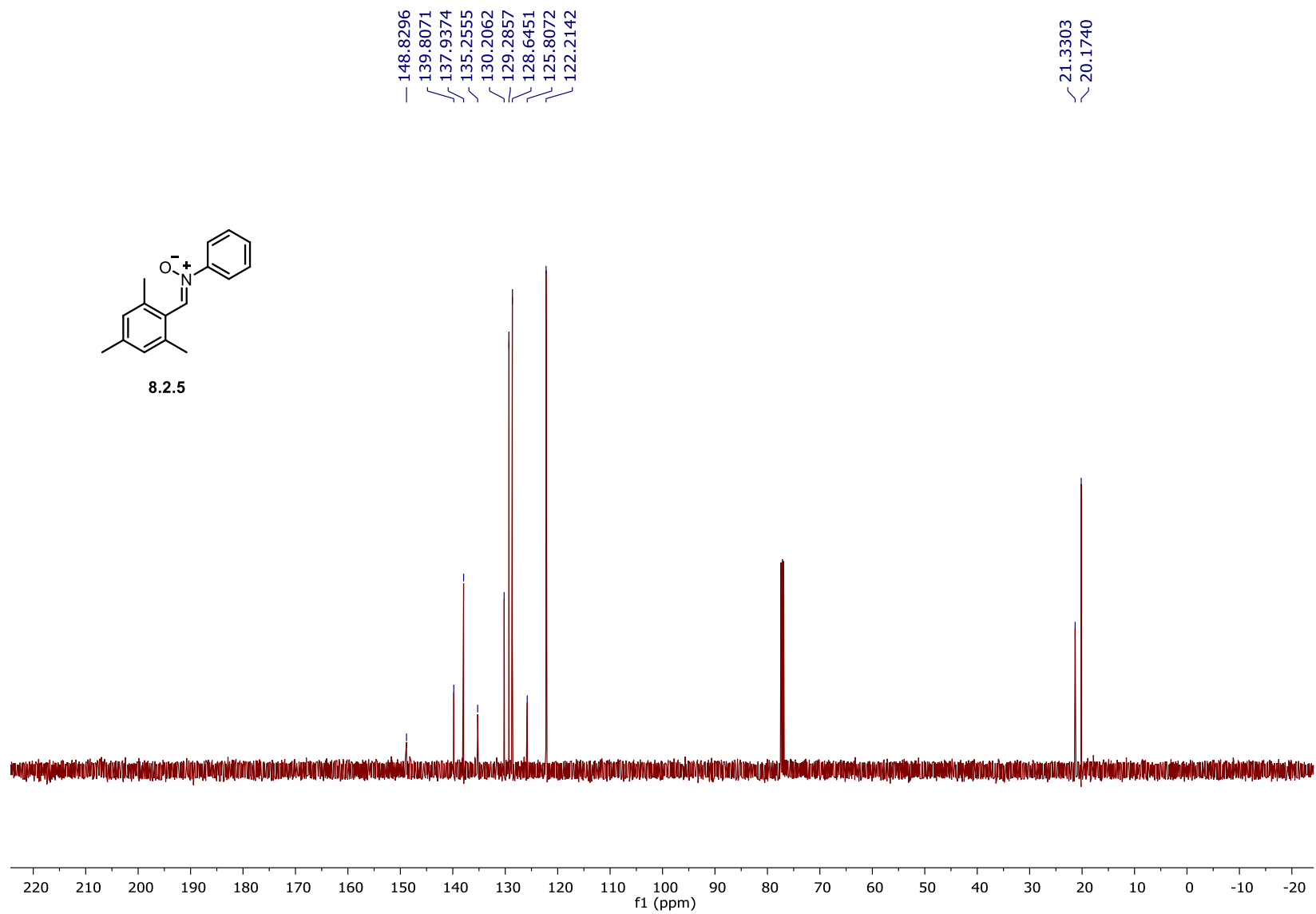


Figure 4. ^{13}C NMR spectrum of **8.2.5** (125 MHz, CDCl_3).

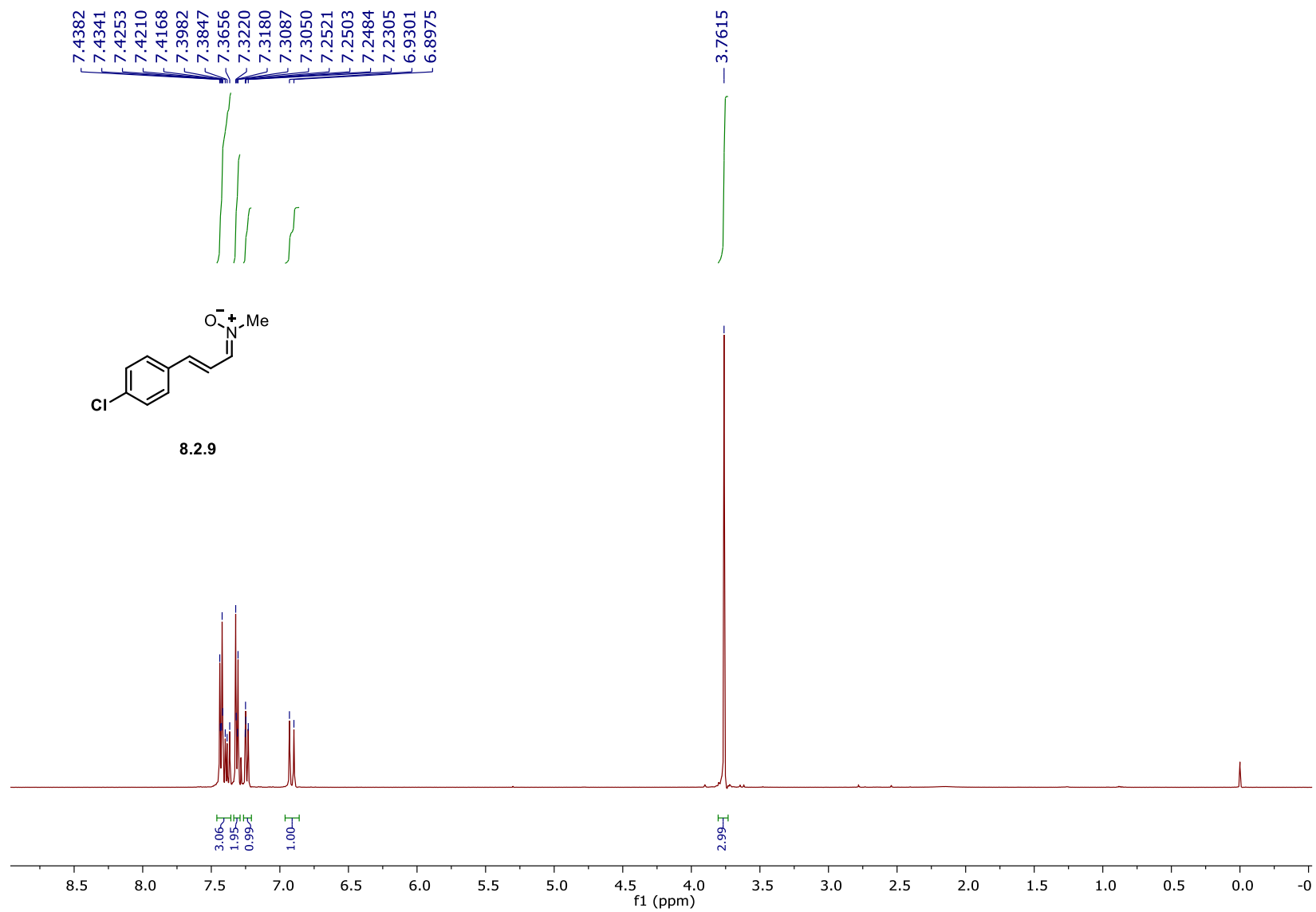


Figure 5. ^1H NMR spectrum of **8.2.9** (500 MHz, CDCl_3).

178

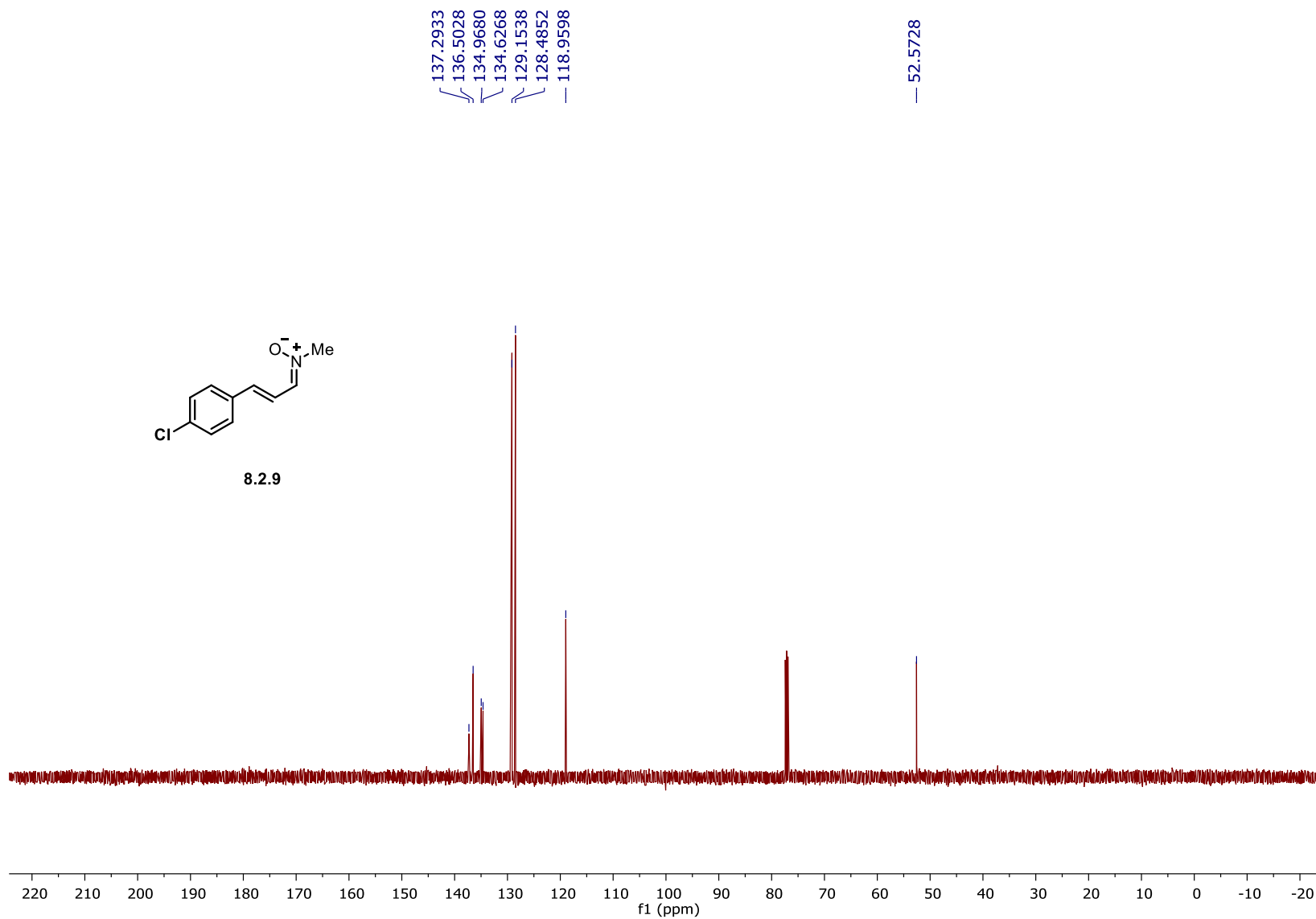


Figure 6. ^{13}C NMR spectrum of **8.2.9** (125 MHz, CDCl_3).

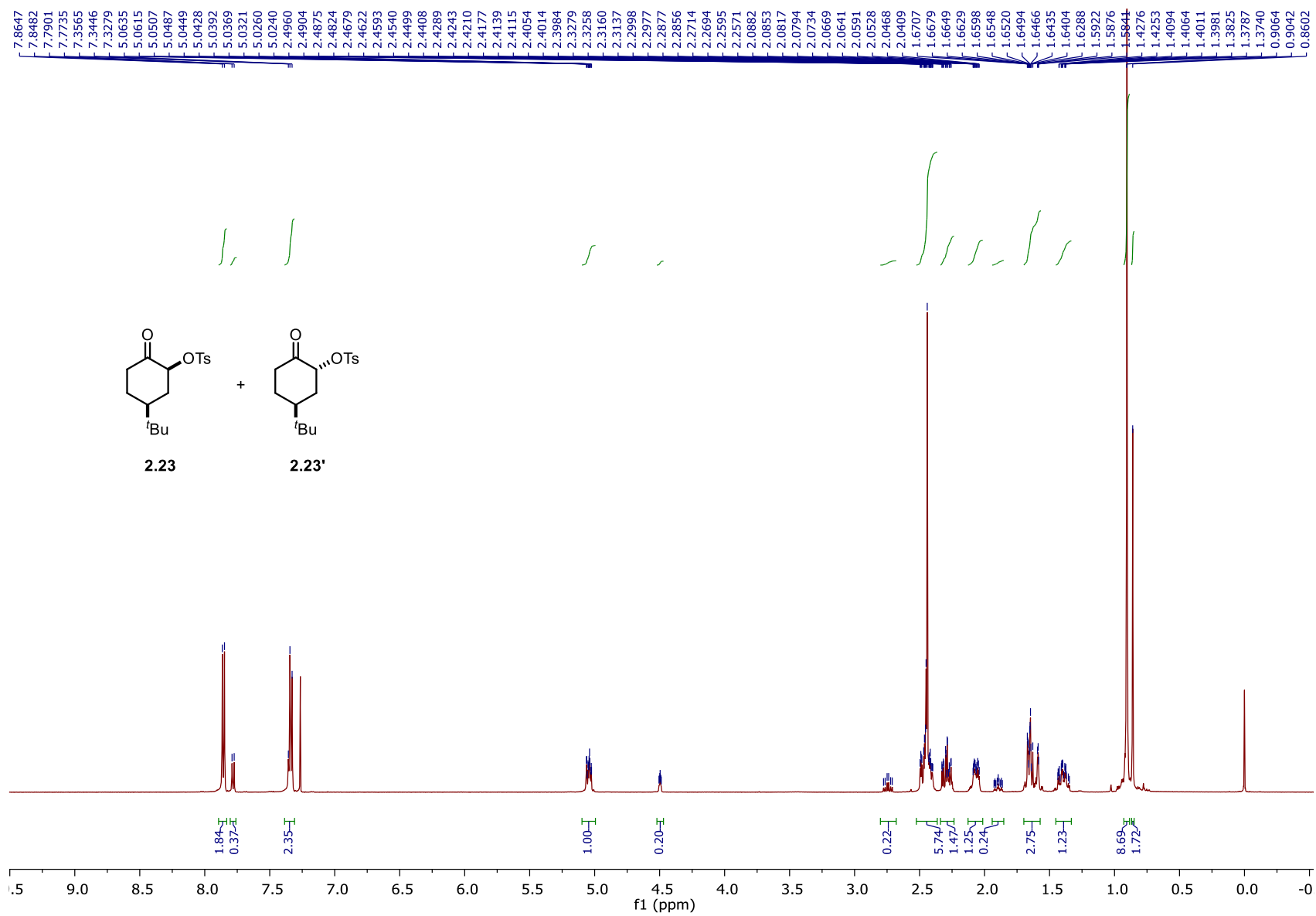


Figure 7. ^1H NMR spectrum of 2.23 (500 MHz, CDCl_3).

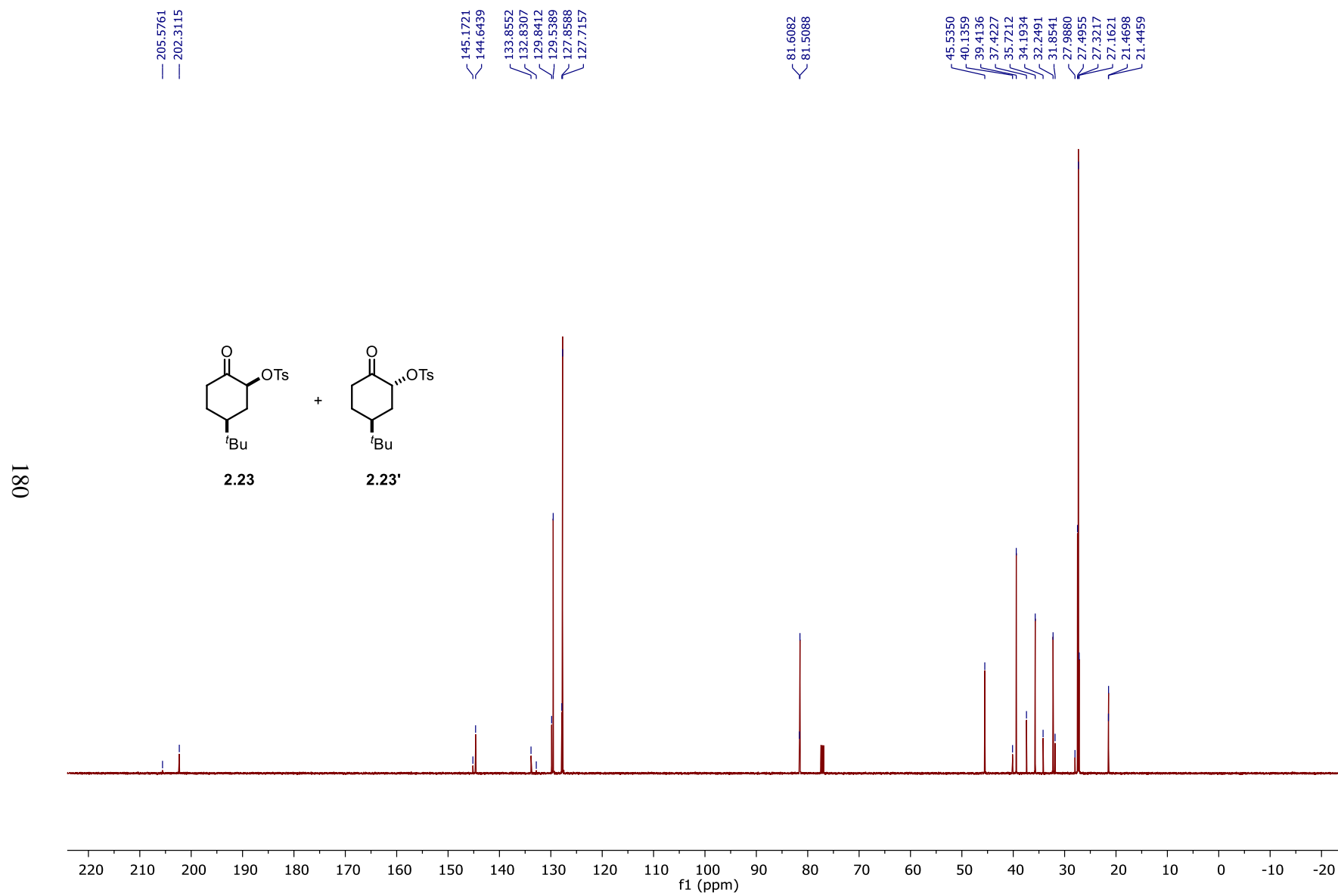


Figure 8. ^{13}C NMR spectrum of **2.23** (125 MHz, CDCl_3).

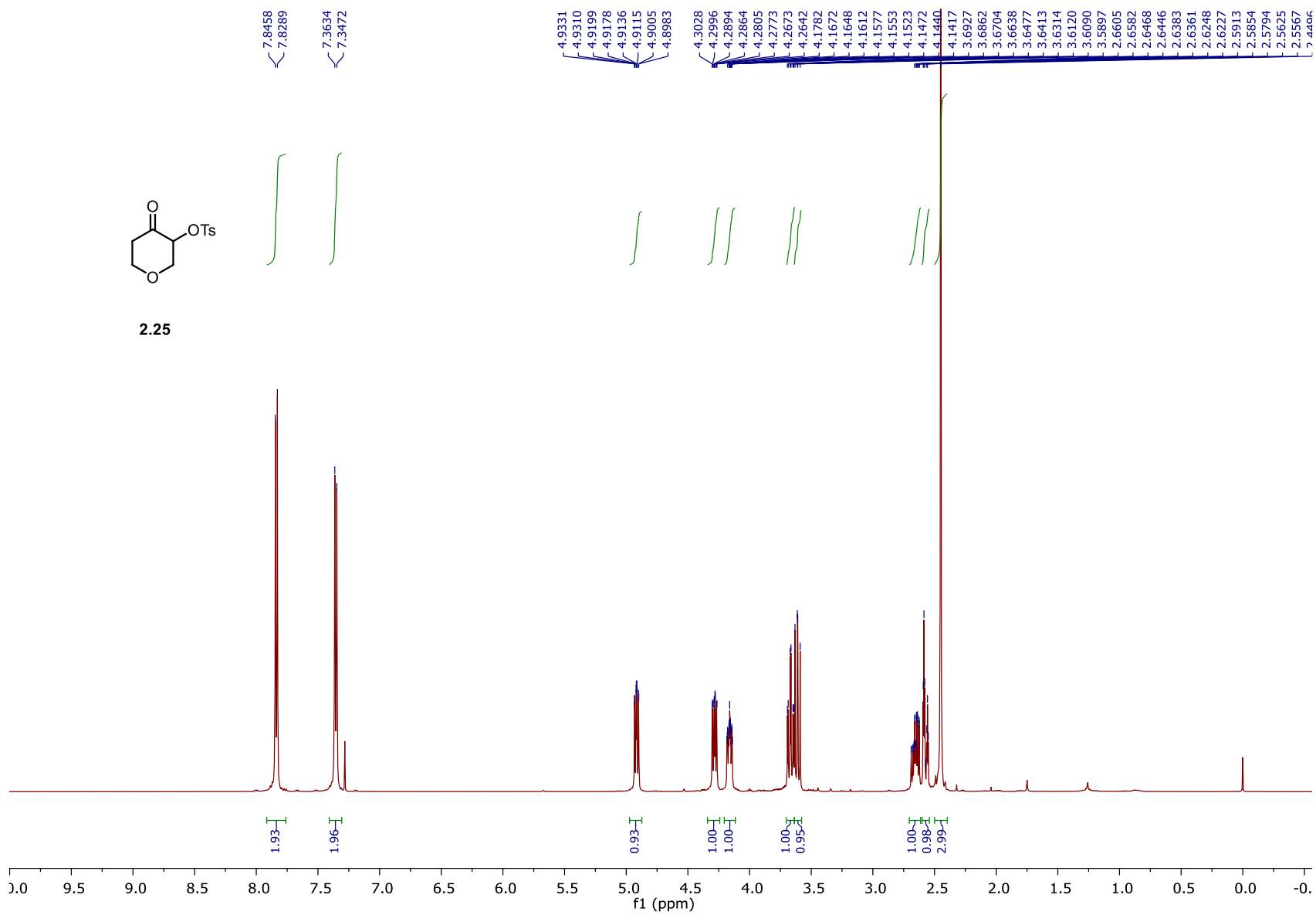


Figure 9. ^1H NMR spectrum of **2.25** (500 MHz, CDCl_3).

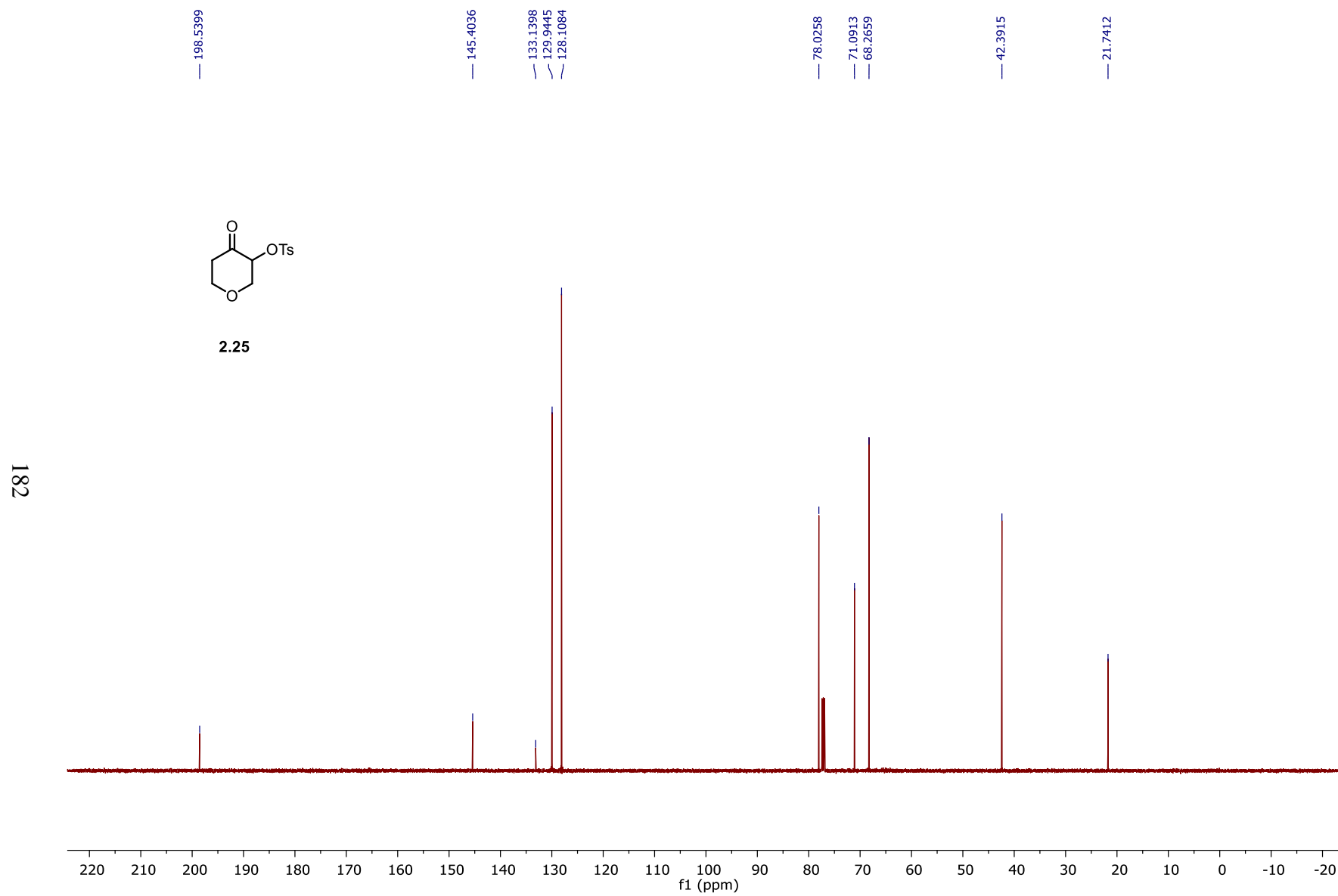


Figure 10. ^{13}C NMR spectrum of **2.25** (125 MHz, CDCl_3).

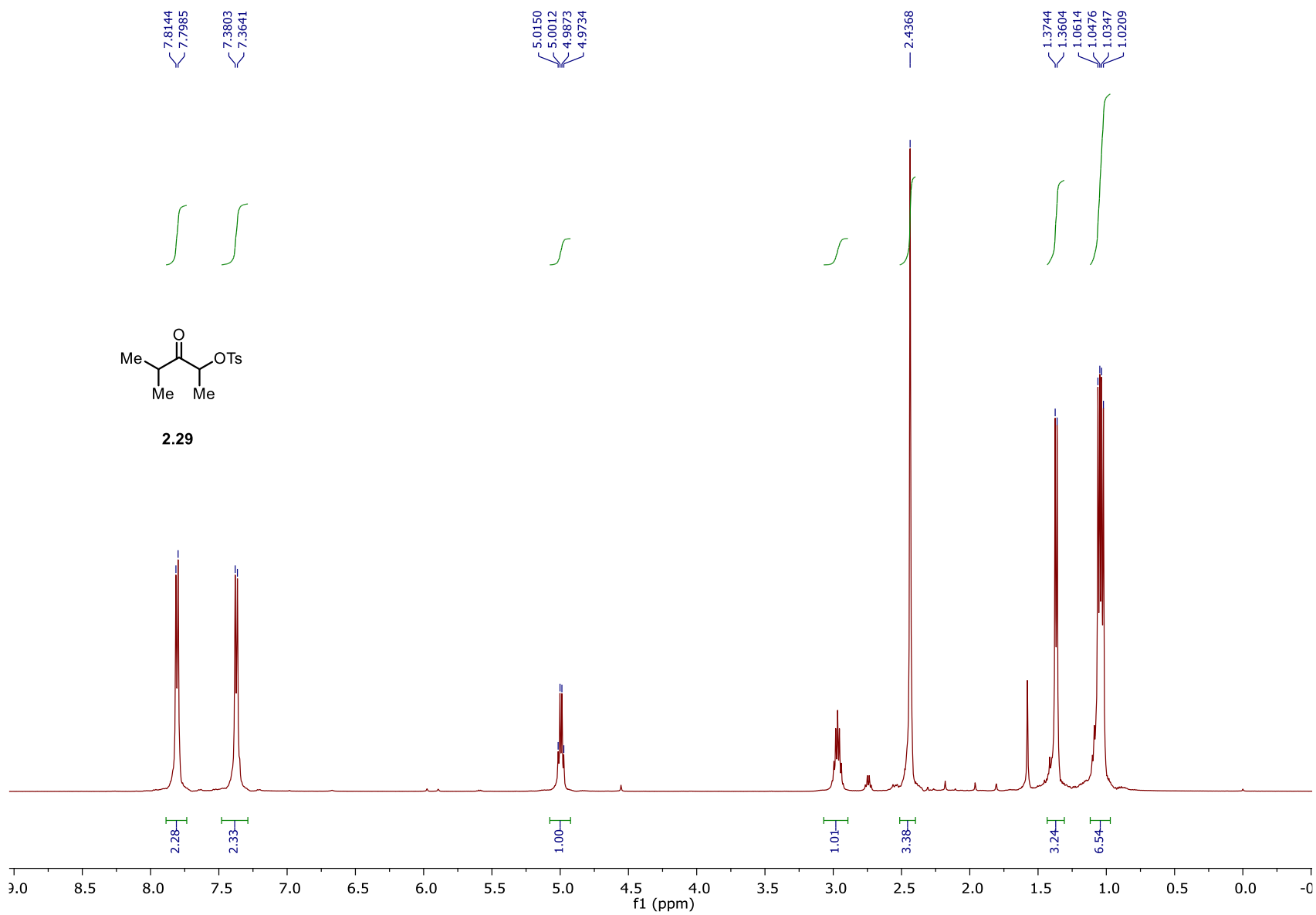


Figure 11. ^1H NMR spectrum of **2.29** (500 MHz, CDCl_3).

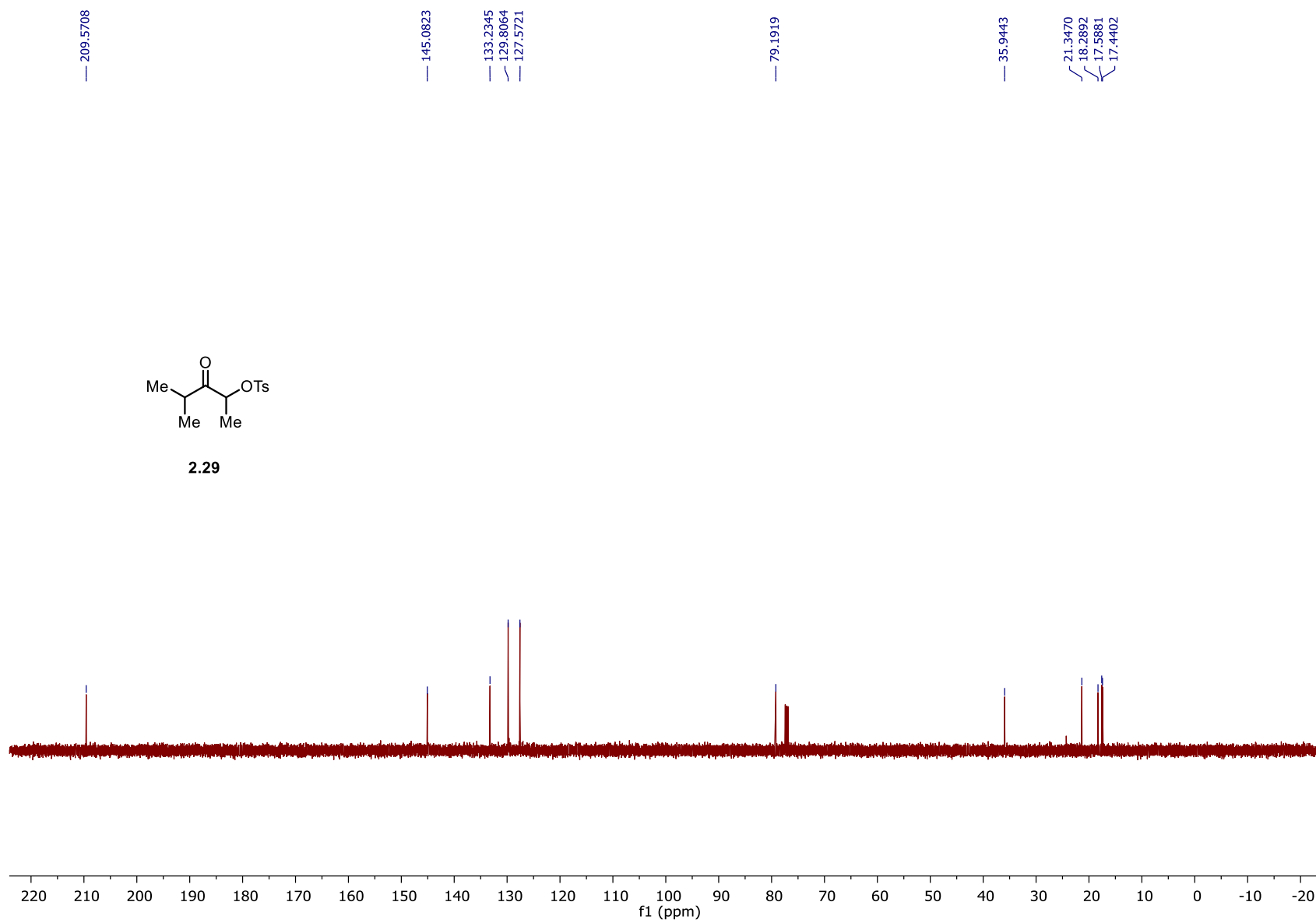


Figure 12. ^{13}C NMR spectrum of **2.29** (125 MHz, CDCl_3).

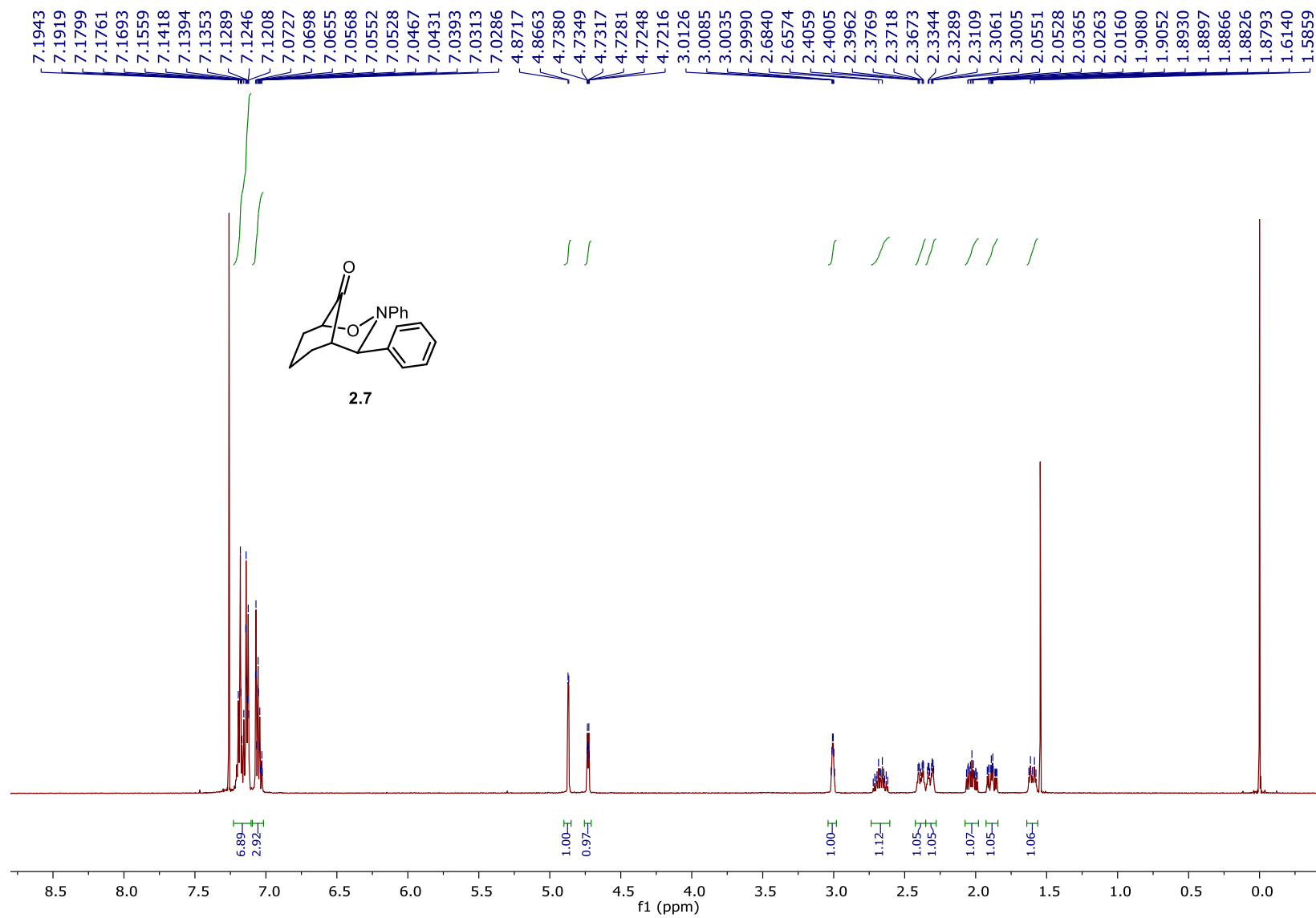


Figure 13. ¹H NMR spectrum of **2.7** (500 MHz, CDCl₃).

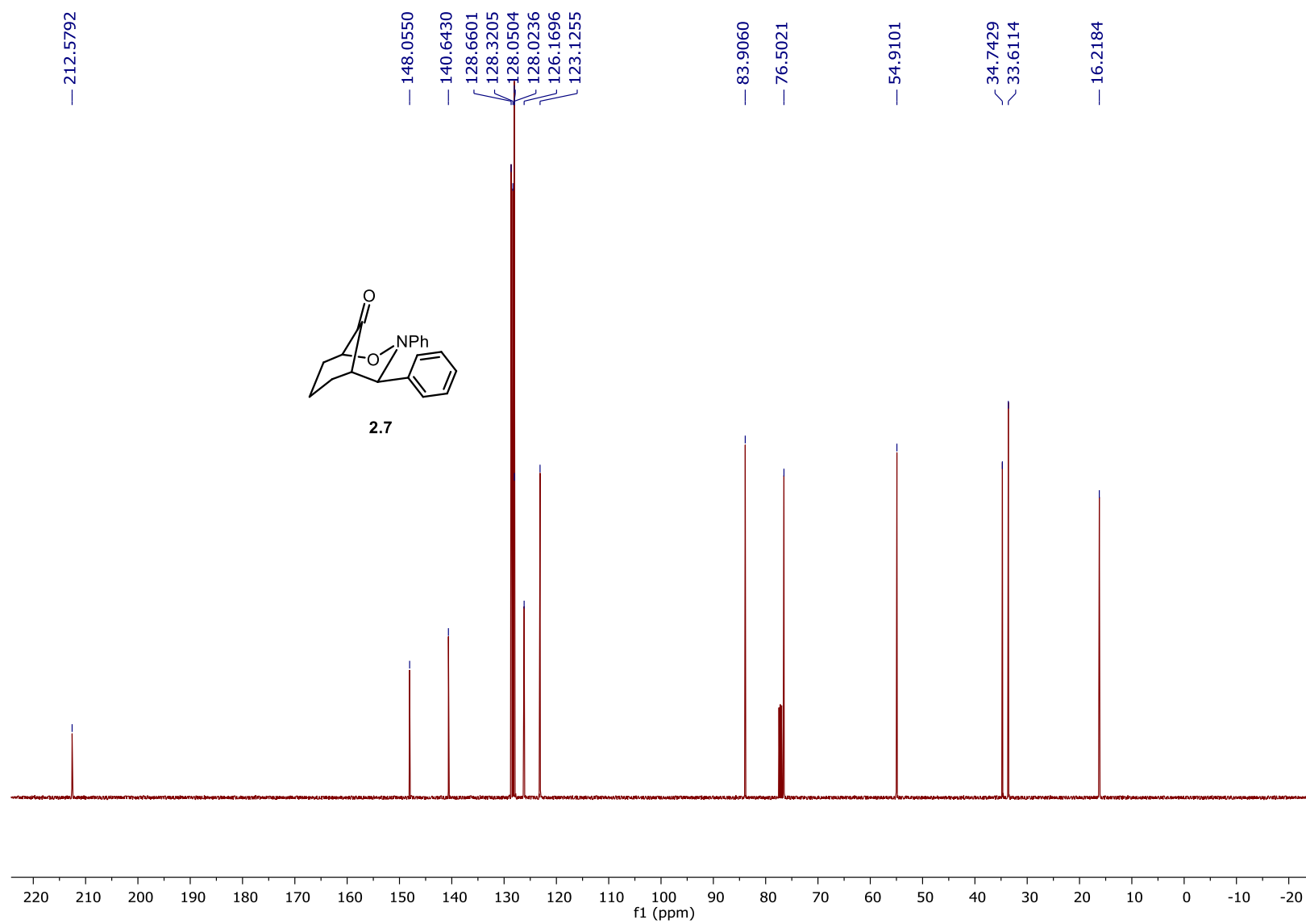


Figure 14. ^{13}C NMR spectrum of **2.7** (125 MHz, CDCl_3).

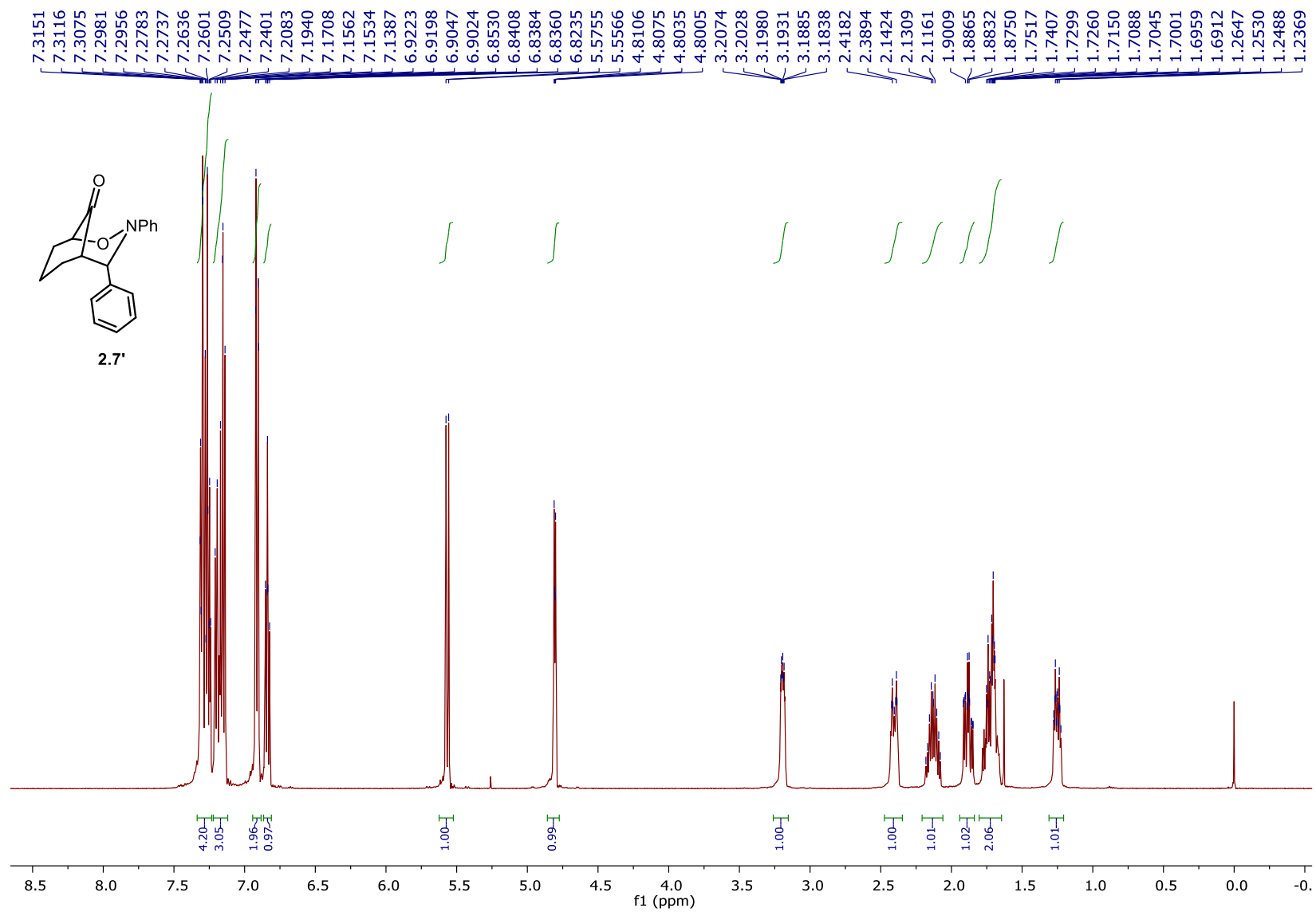


Figure 15. ^1H NMR spectrum of **2.7'** (500 MHz, CDCl_3).

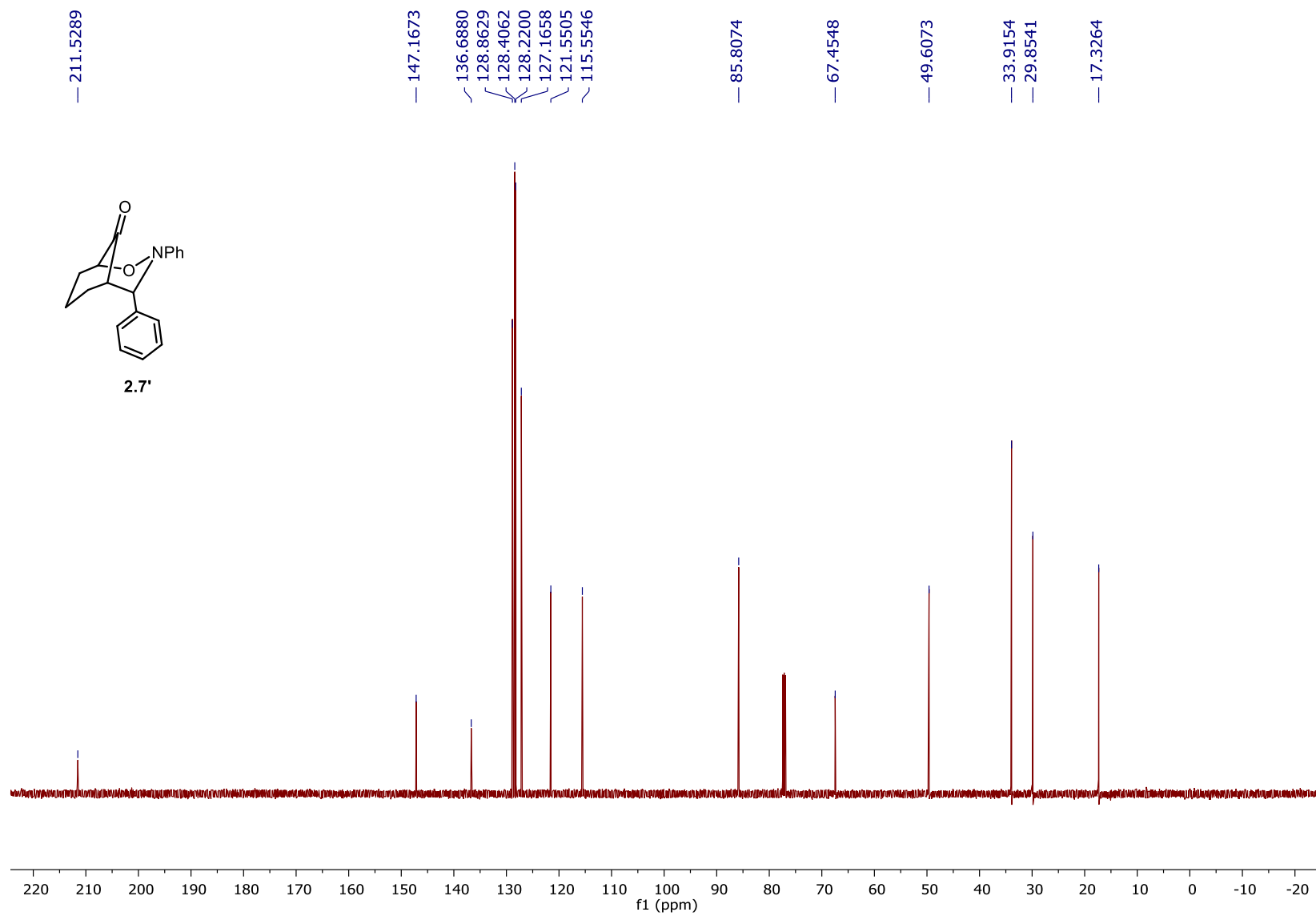


Figure 16. ^{13}C NMR spectrum of **2.7'** (125 MHz, CDCl_3).

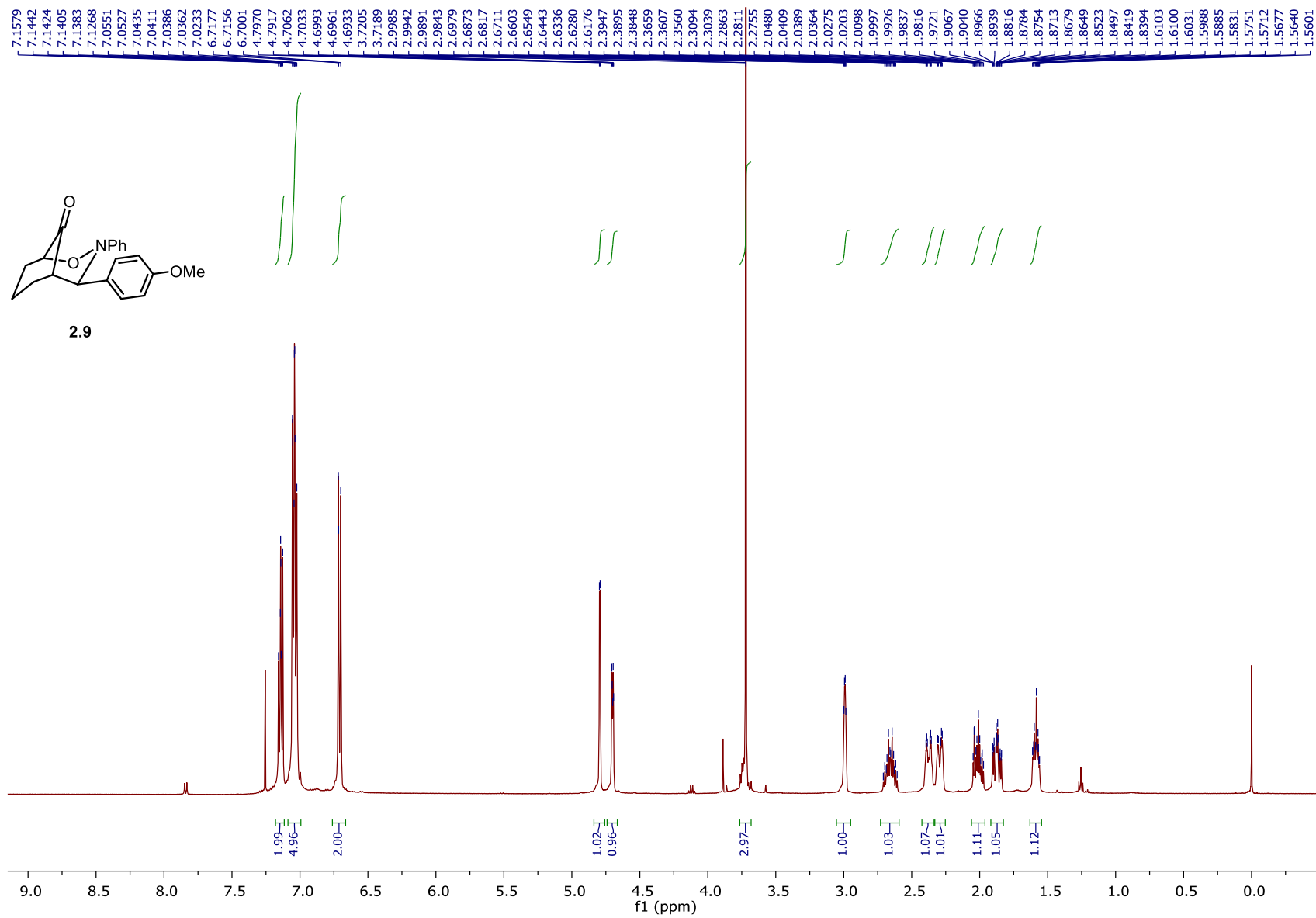


Figure 17. ^1H NMR spectrum of **2.9** (500 MHz, CDCl_3).

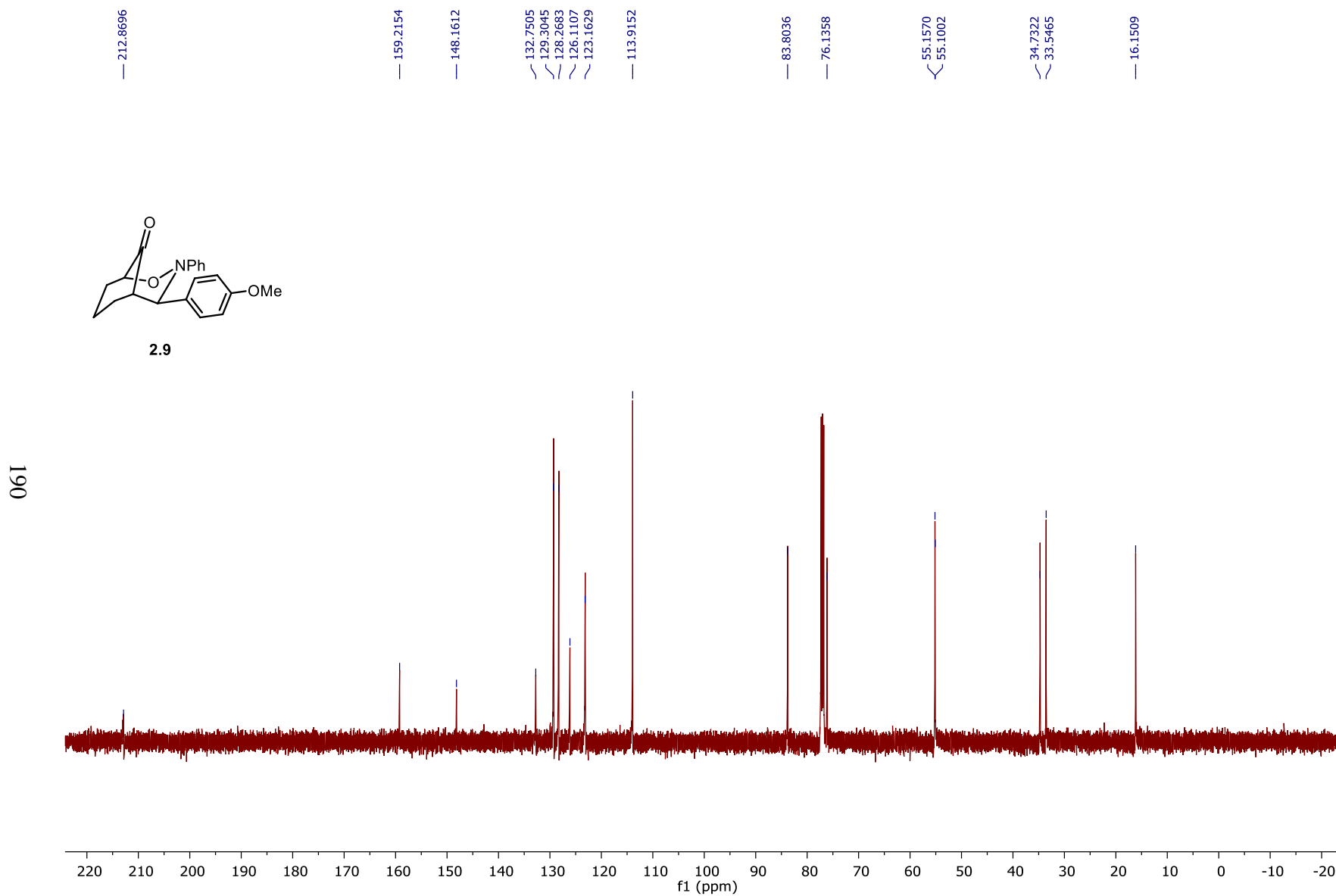


Figure 18. ^{13}C NMR spectrum of **2.9** (125 MHz, CDCl_3).

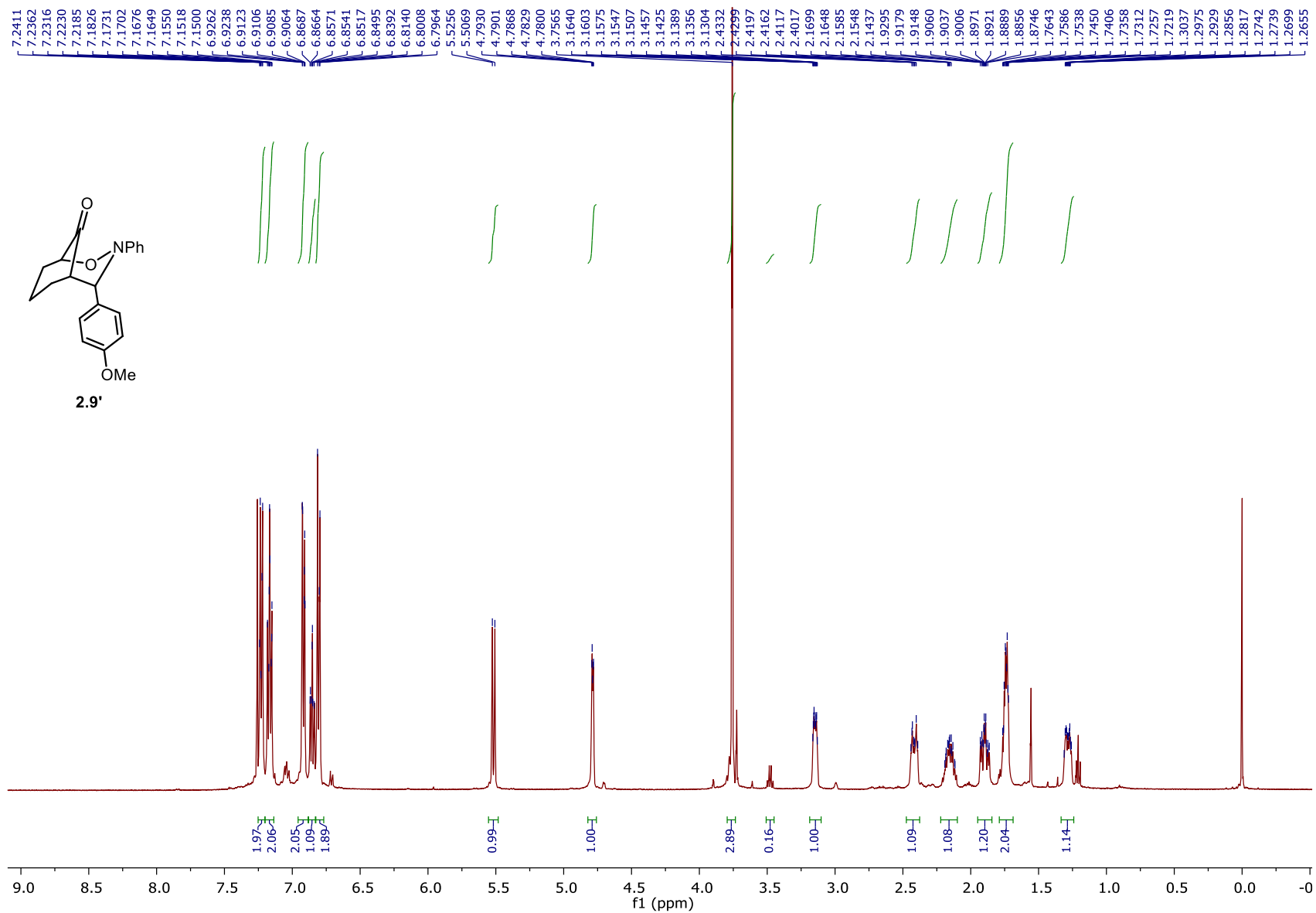


Figure 19. ¹H NMR spectrum of **2.9'** (500 MHz, CDCl₃).

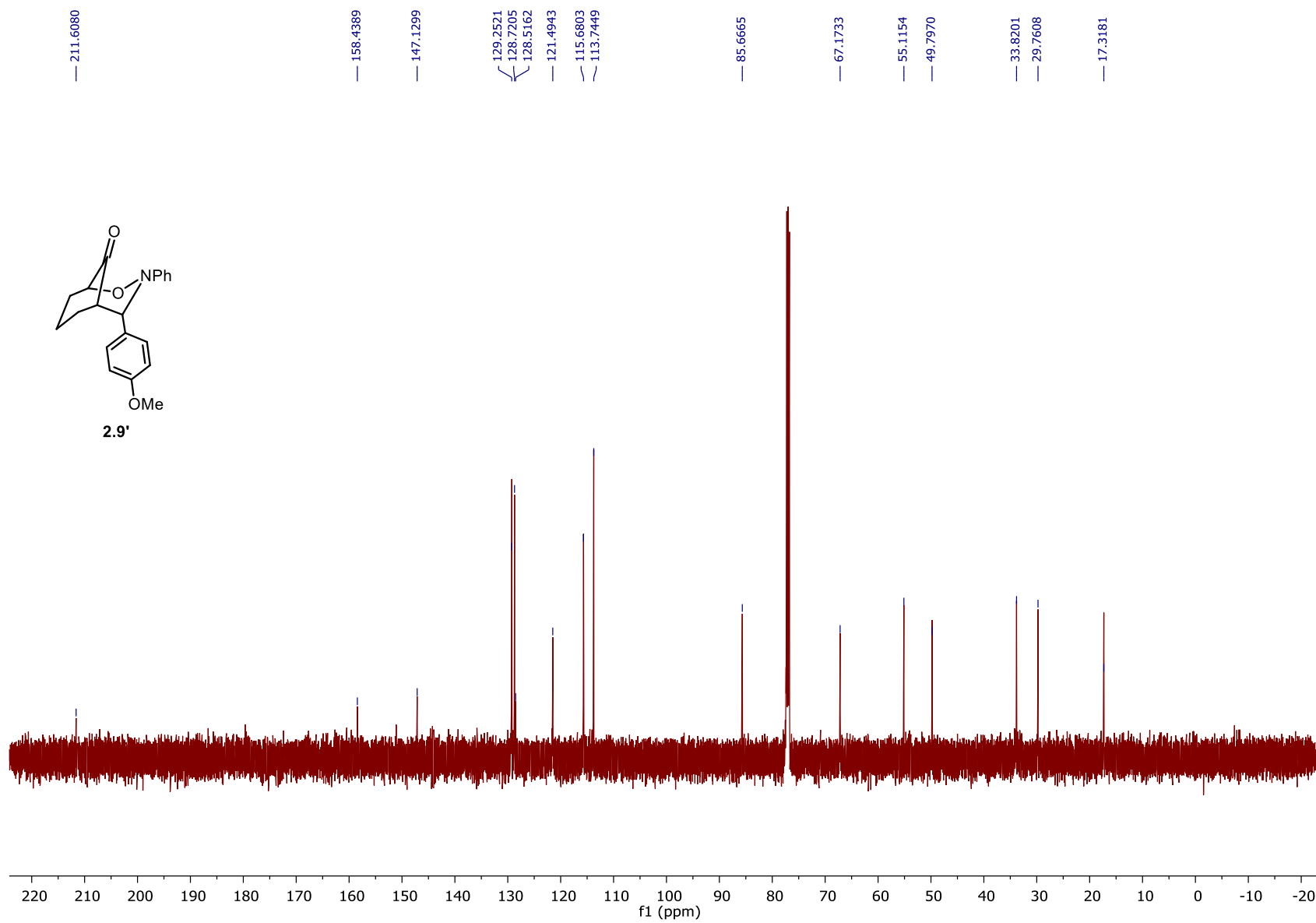


Figure 20. ^{13}C NMR spectrum of **2.9'** (125 MHz, CDCl_3).

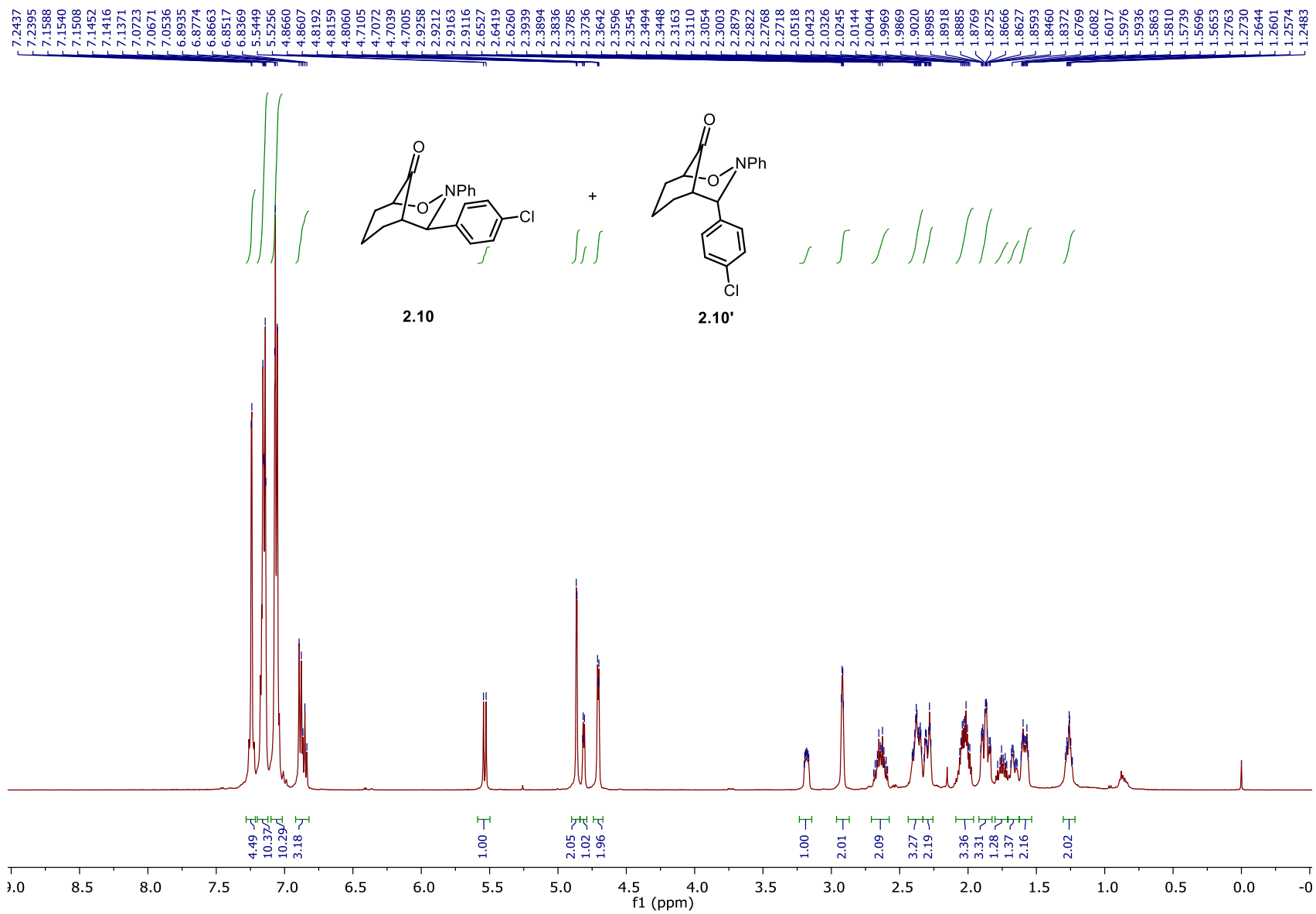


Figure 21. ^1H NMR spectrum of **2.10** (500 MHz, CDCl_3).

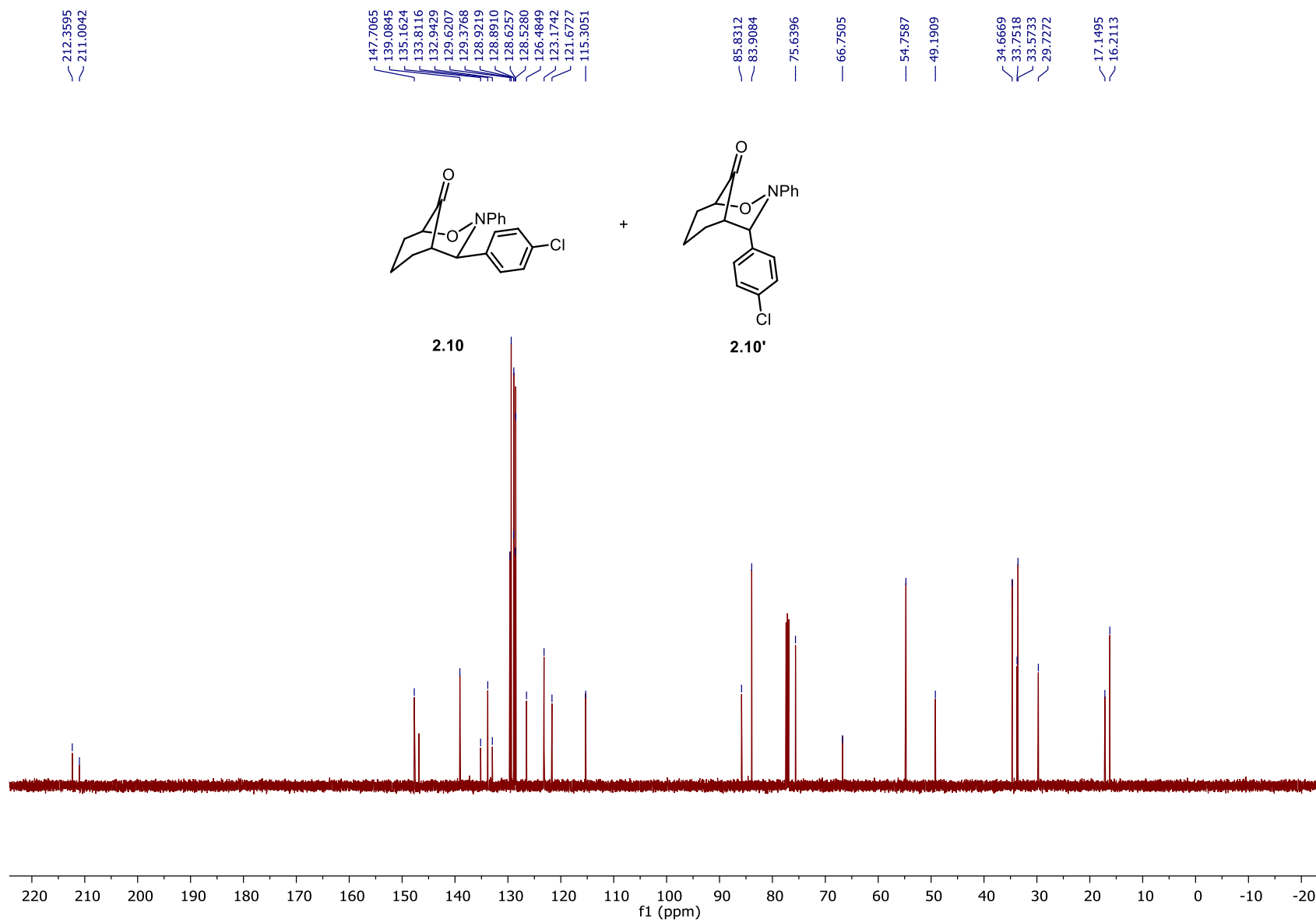


Figure 22. ^{13}C NMR spectrum of **2.10** (125 MHz, CDCl_3).

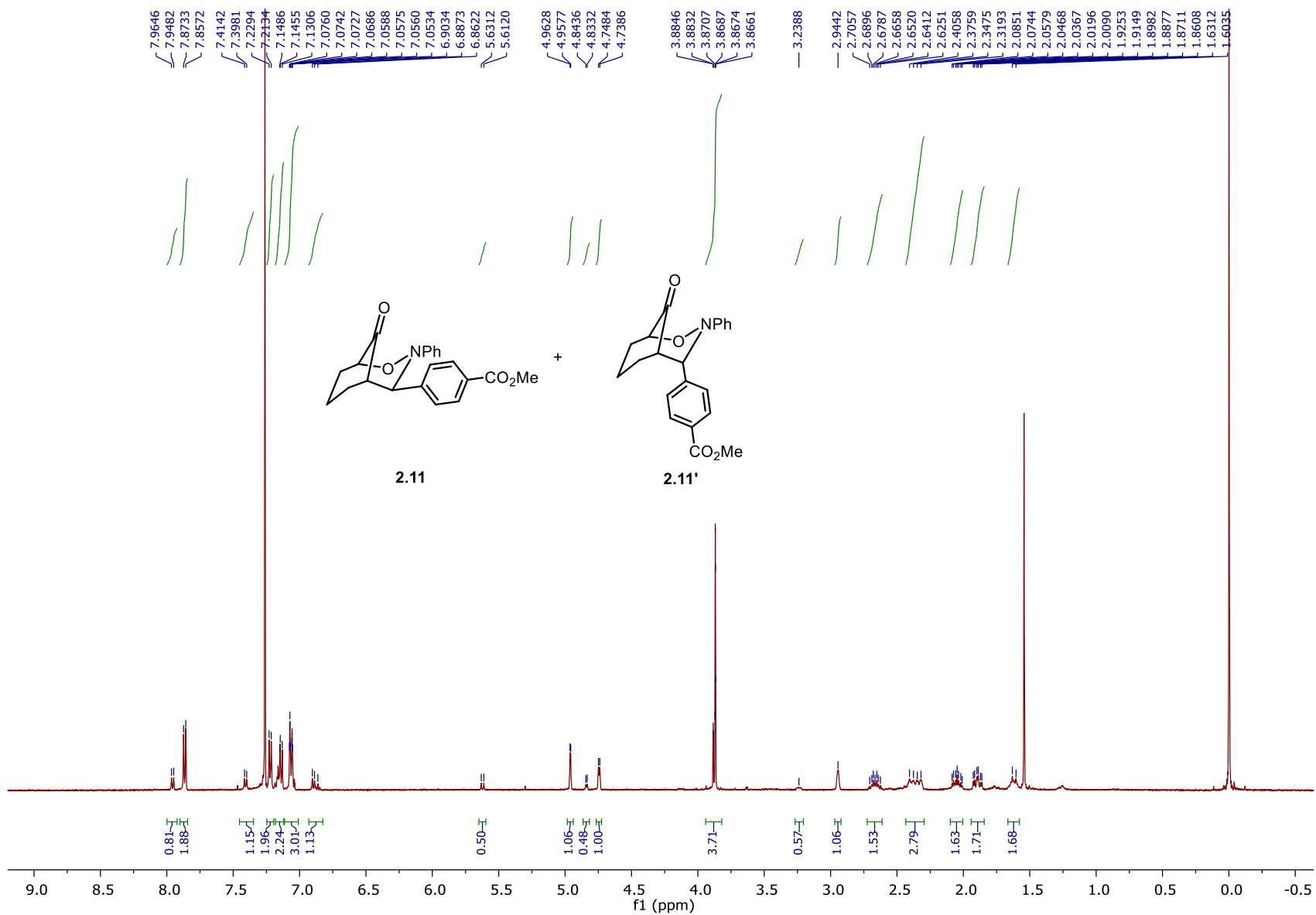


Figure 23. ^1H NMR spectrum of **2.11** (500 MHz, CDCl_3).

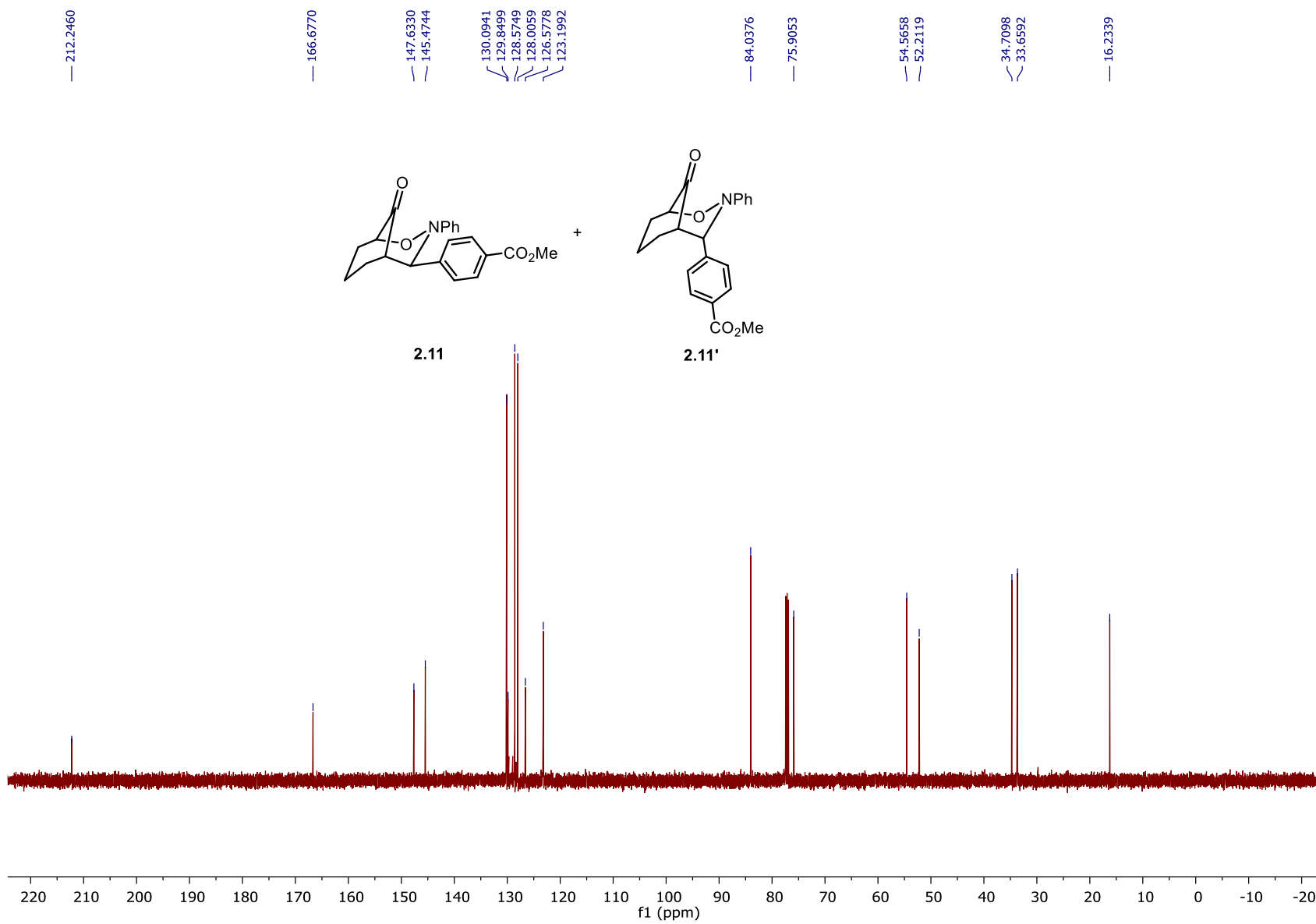


Figure 24. ^{13}C NMR spectrum of **2.11** (125 MHz, CDCl_3).

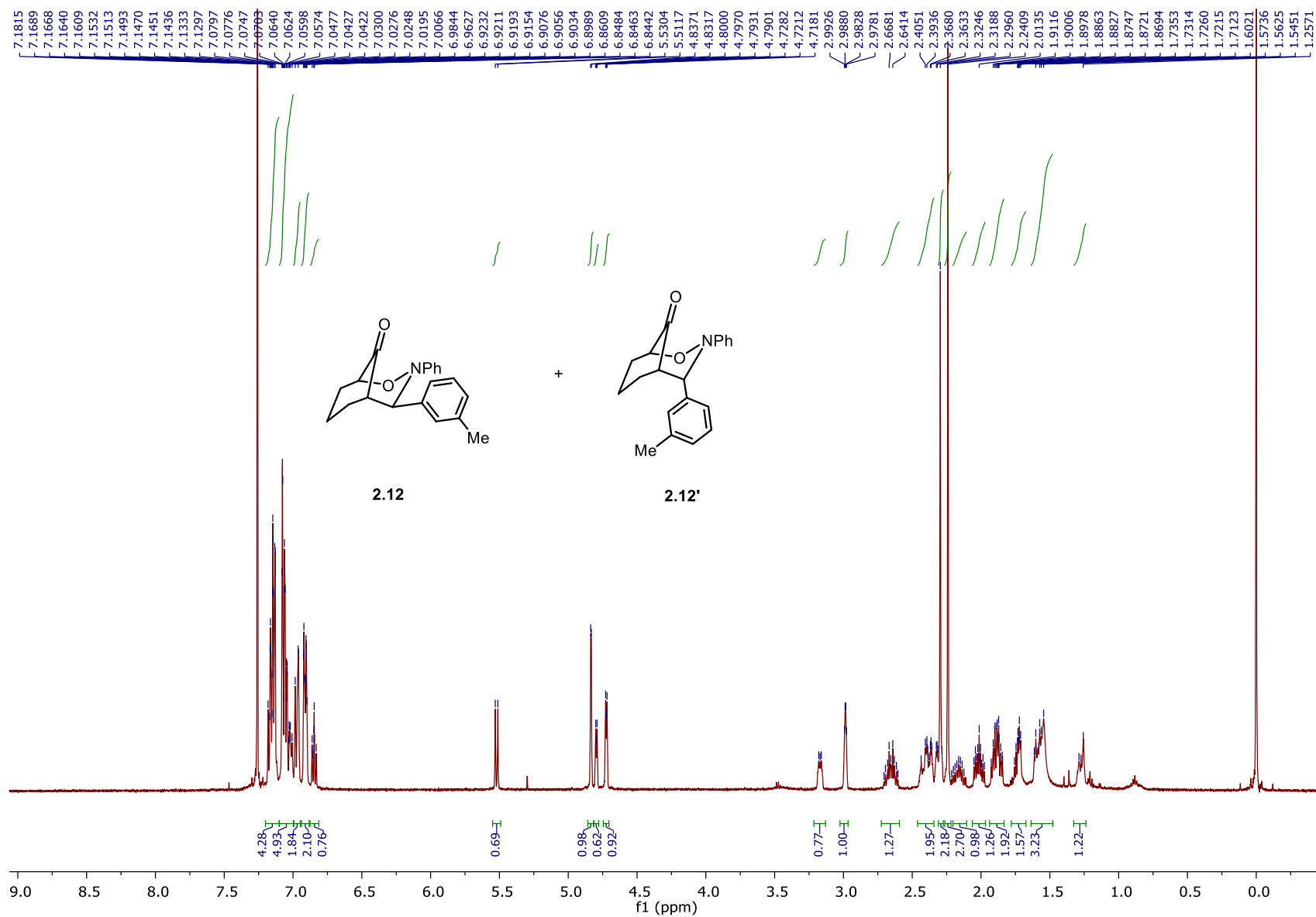


Figure 25. ^1H NMR spectrum of **2.12** (500 MHz, CDCl_3).

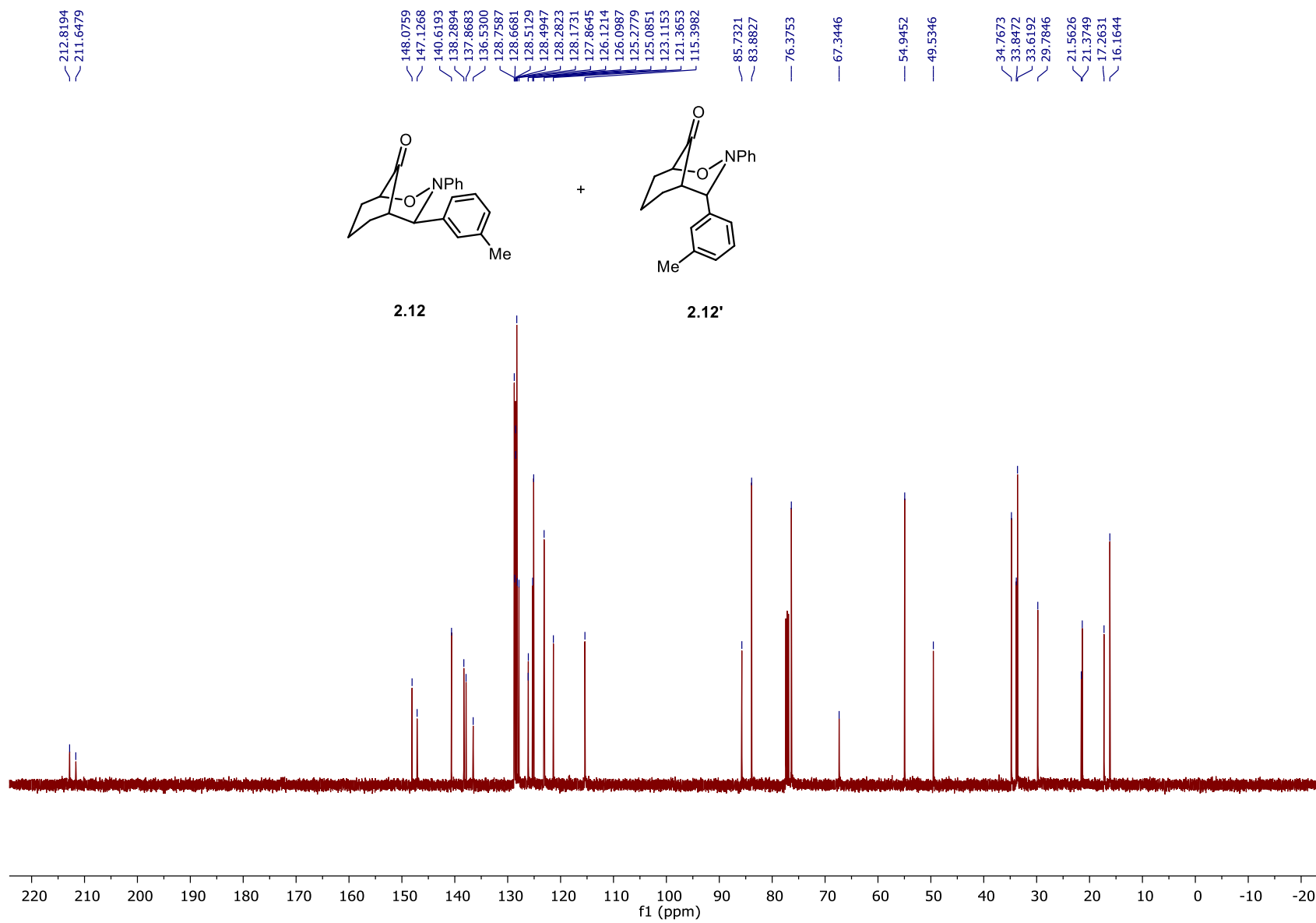


Figure 26. ^{13}C NMR spectrum of **2.12** (125 MHz, CDCl_3).

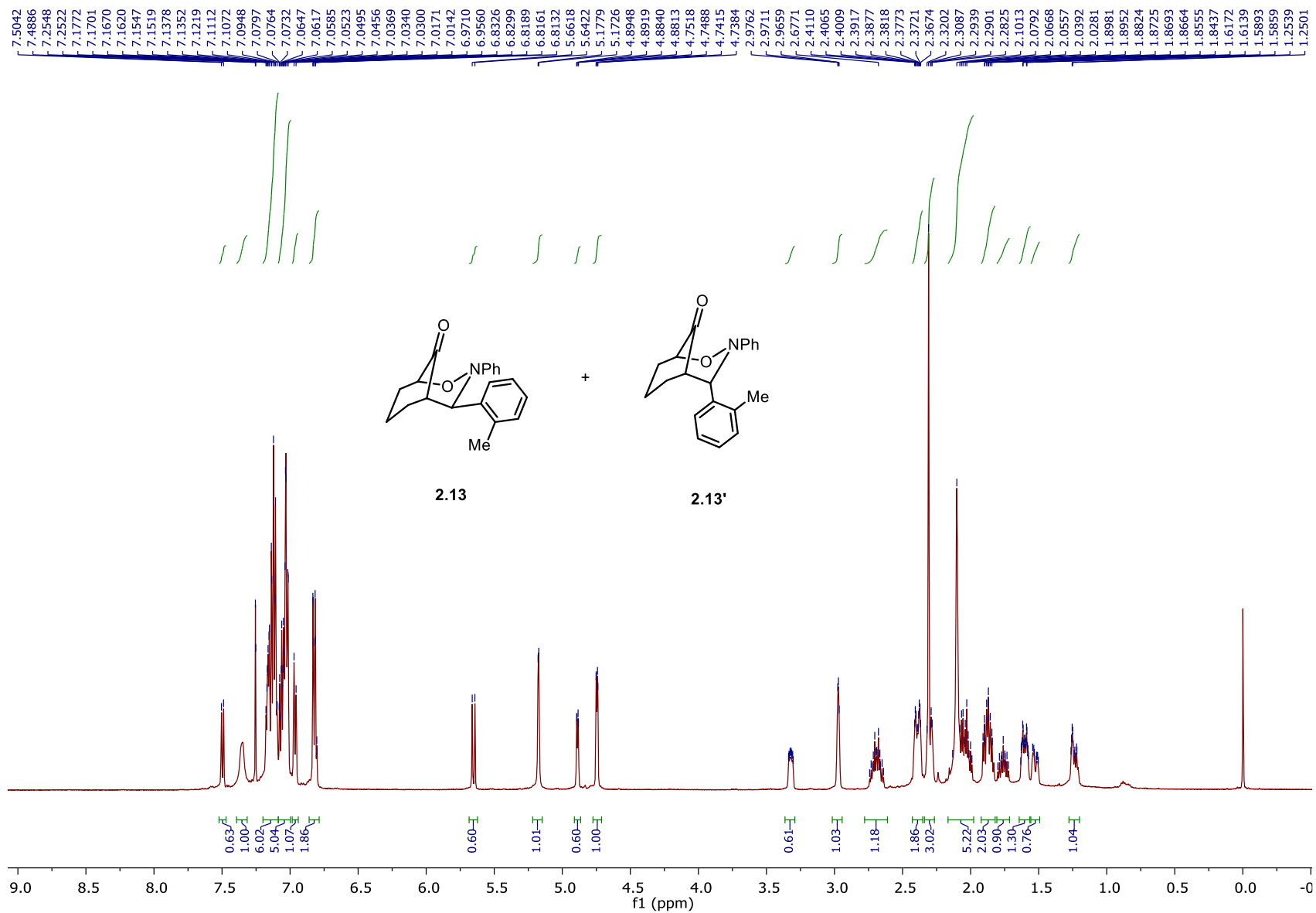


Figure 27. ¹H NMR spectrum of **2.13** (500 MHz, CDCl₃).

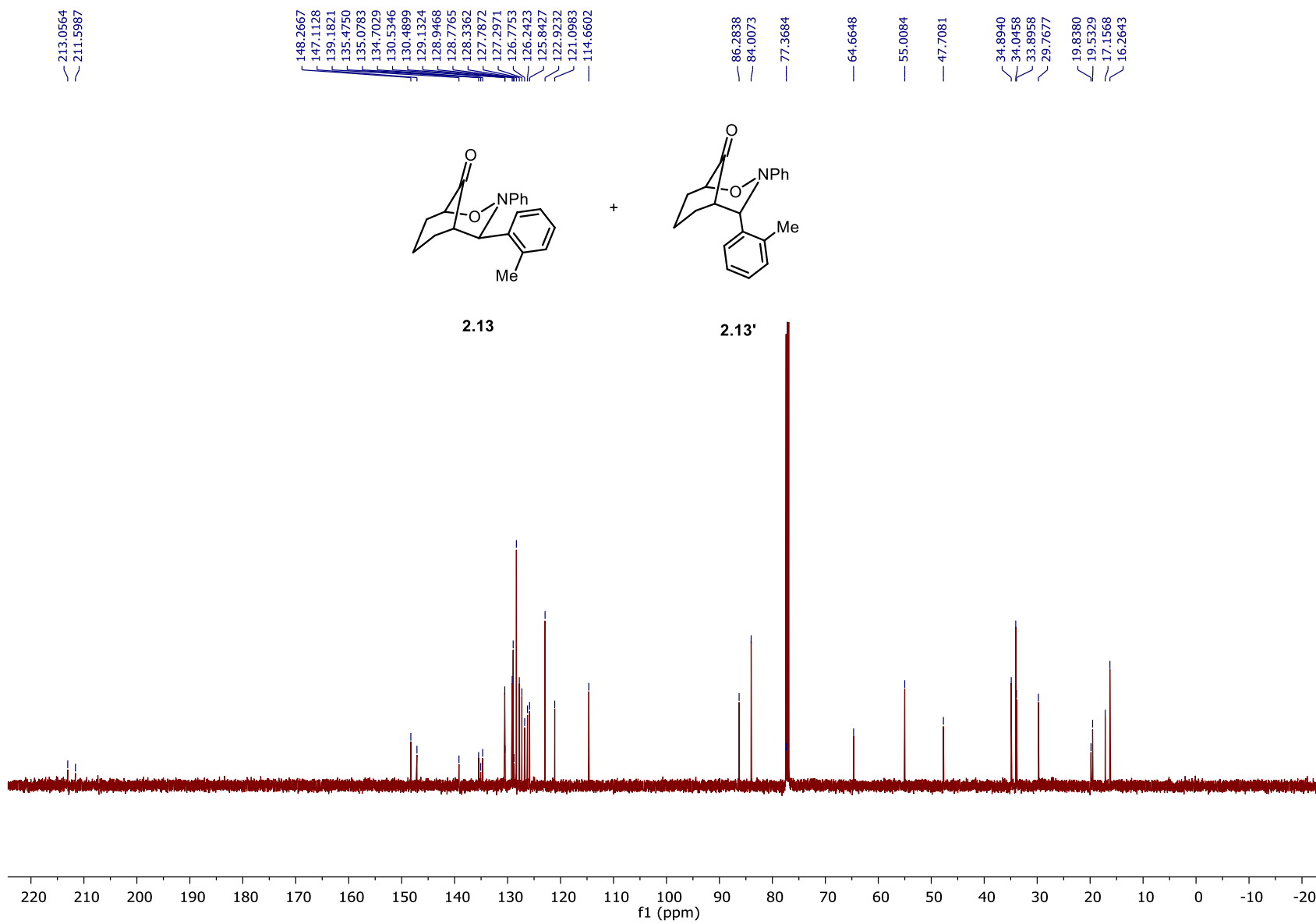


Figure 28. ^{13}C NMR spectrum of **2.13** (125 MHz, CDCl_3).

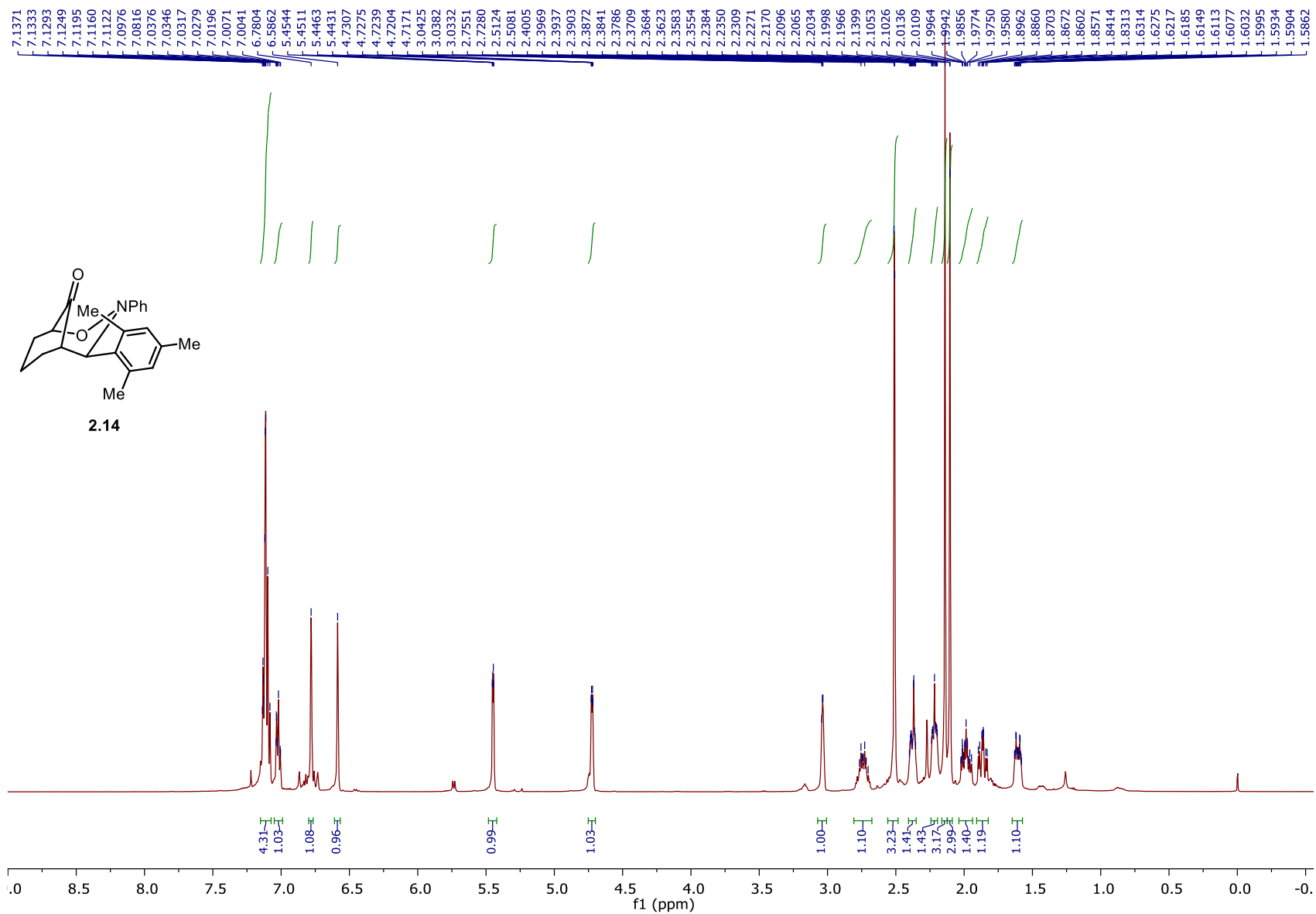


Figure 29. ¹H NMR spectrum of **2.14** (500 MHz, CDCl₃).

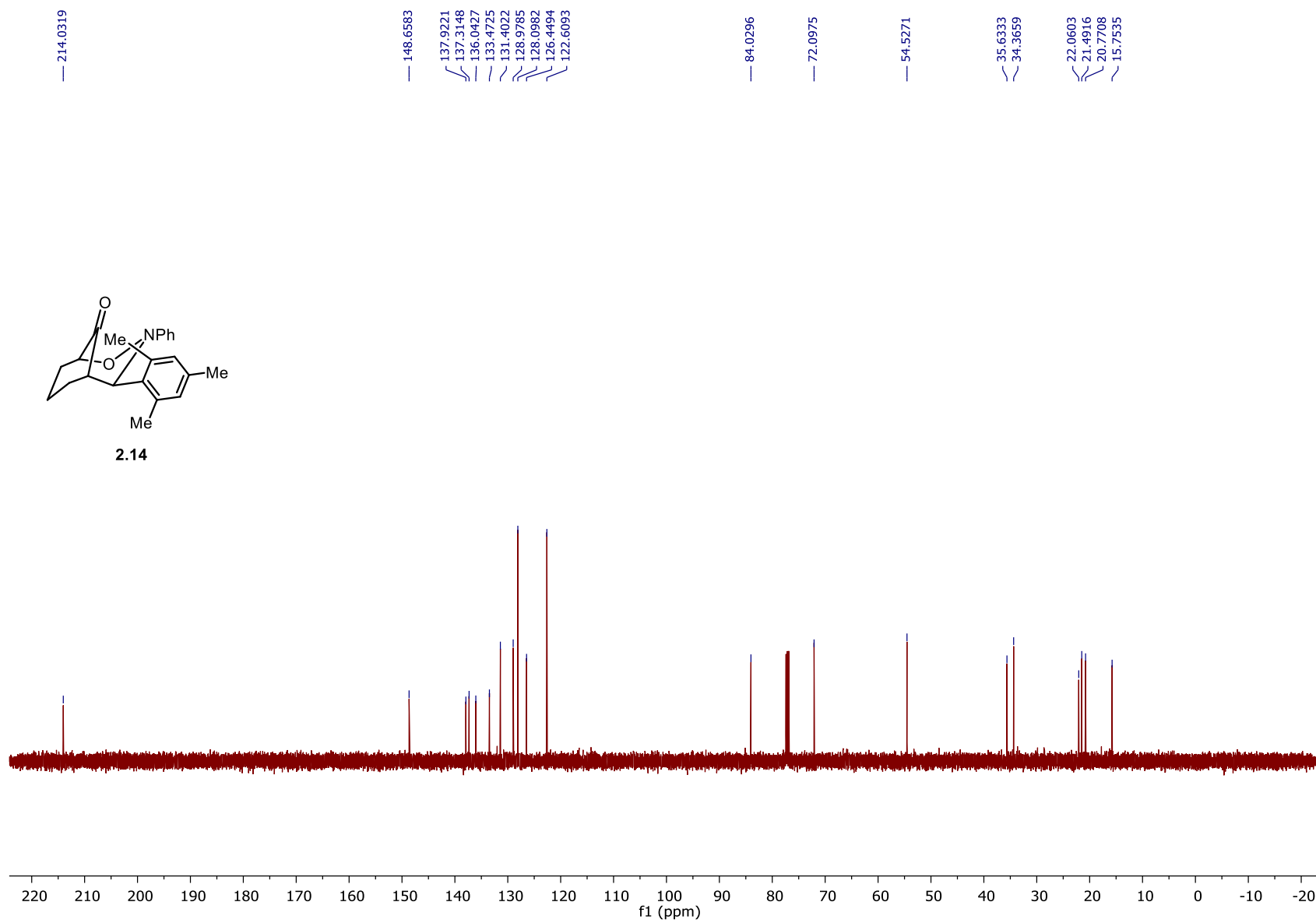


Figure 30. ^{13}C NMR spectrum of **2.14** (125 MHz, CDCl_3).

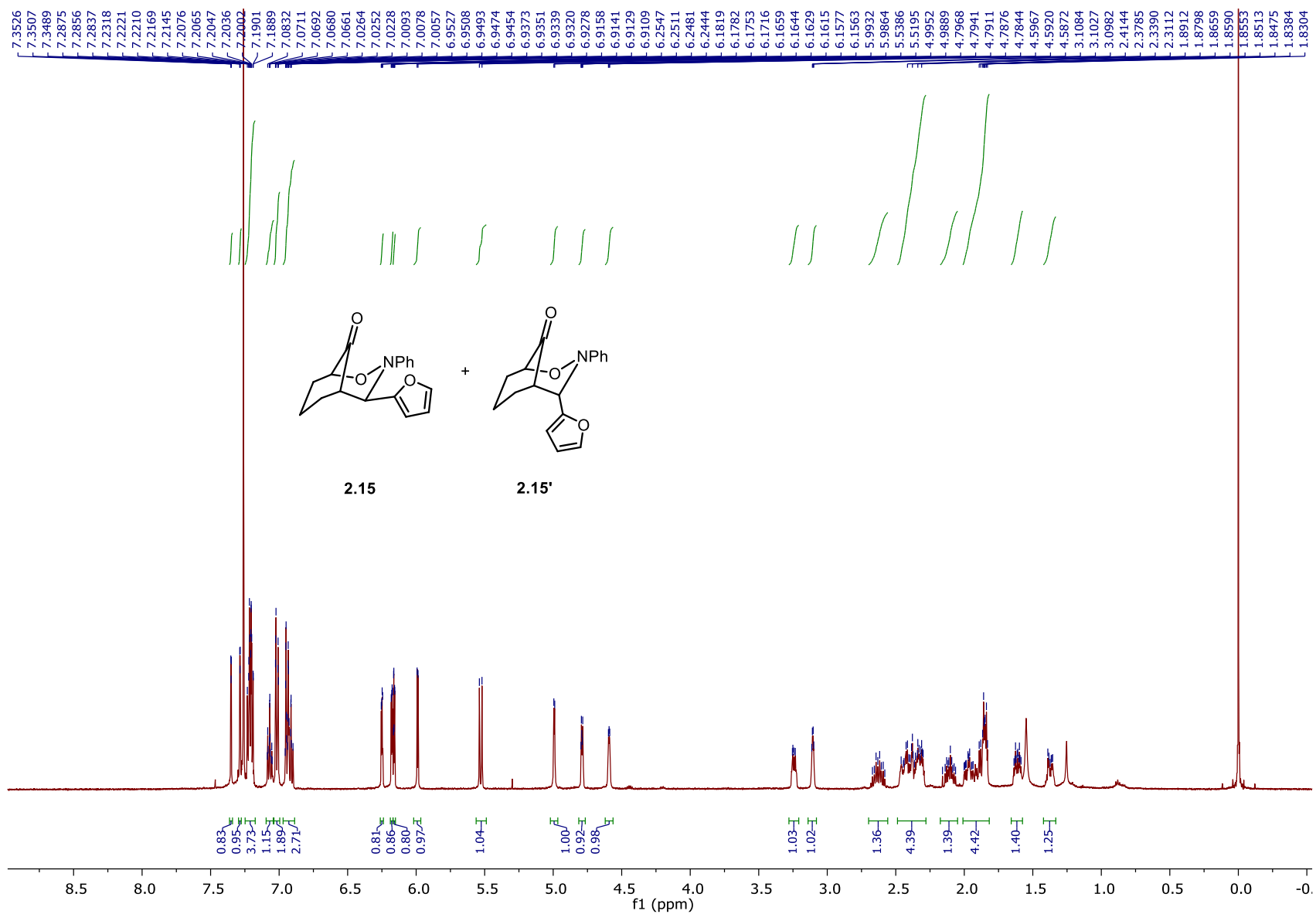


Figure 31. ¹H NMR spectrum of 2.15 (500 MHz, CDCl₃).

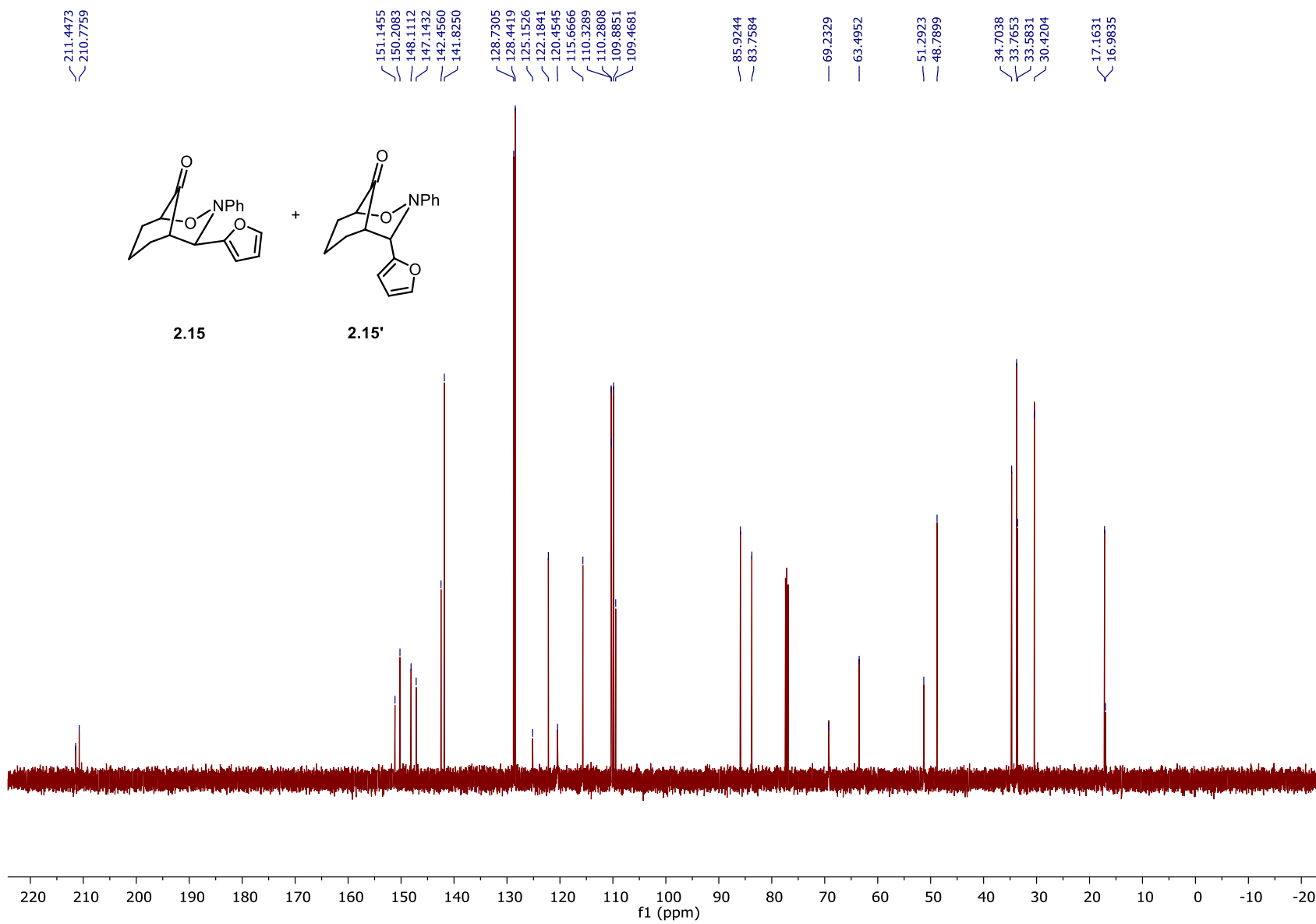


Figure 32. ^{13}C NMR spectrum of **2.15** (125 MHz, CDCl_3).

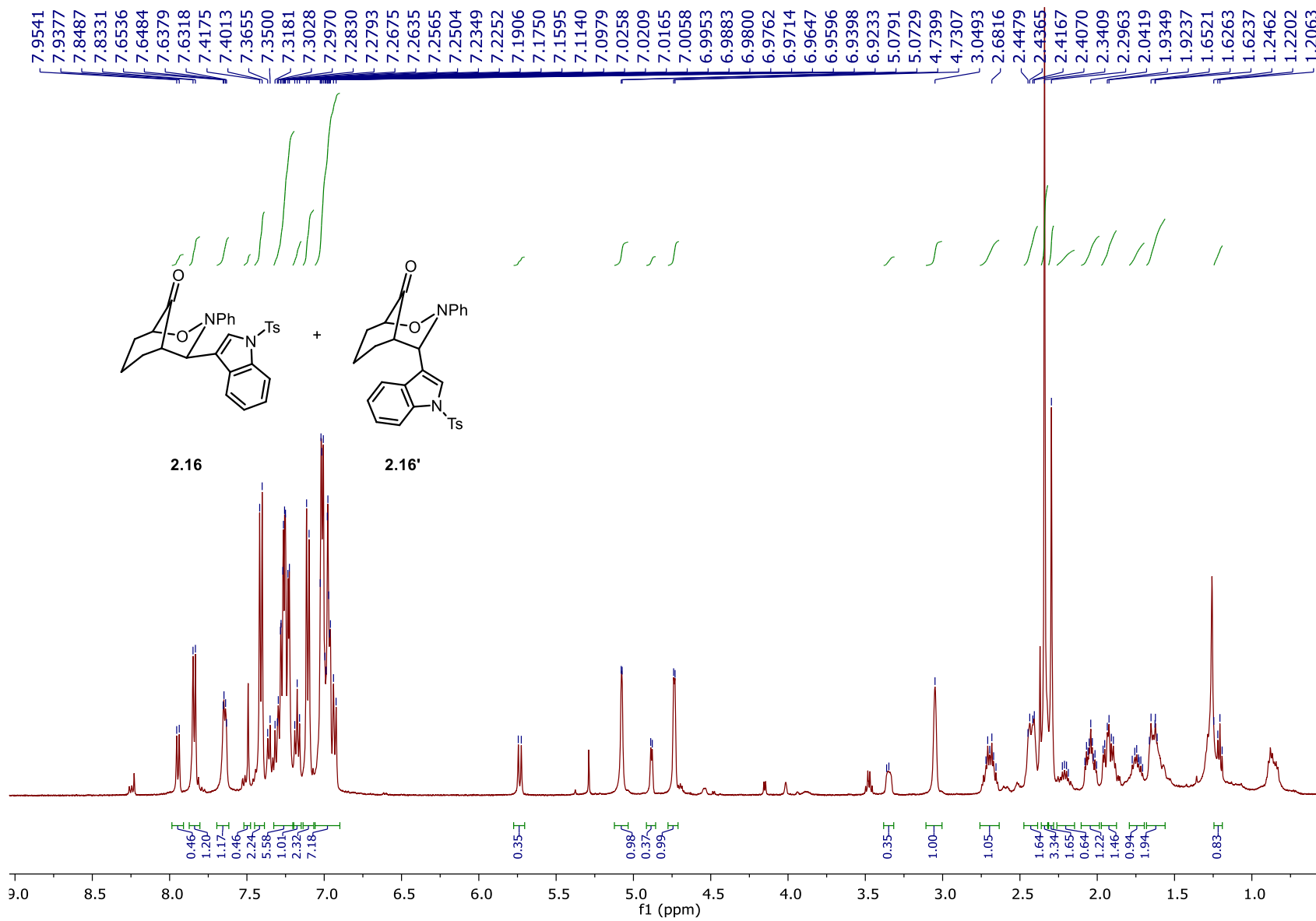


Figure 33. ^1H NMR spectrum of **2.16** (500 MHz, CDCl_3).

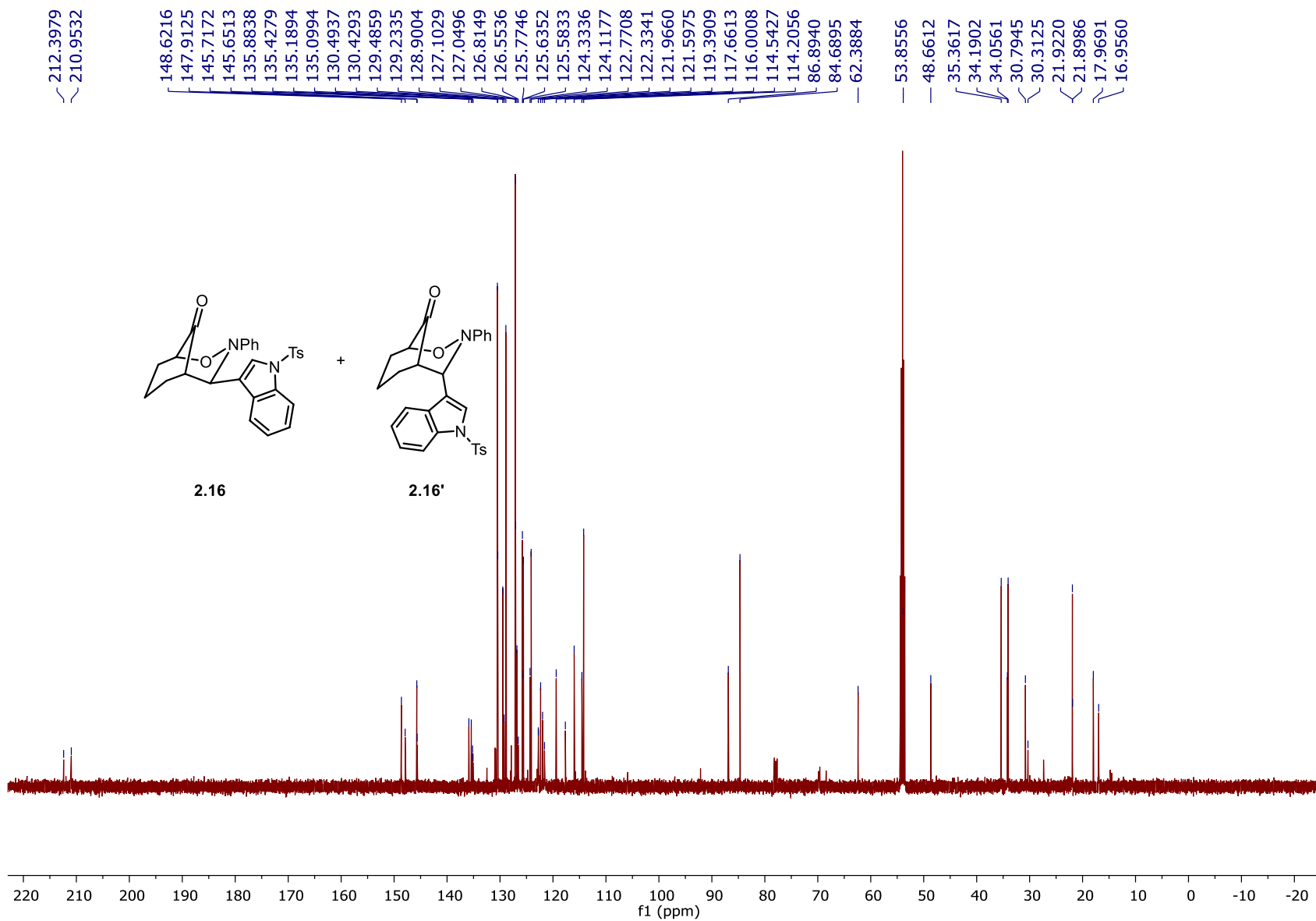


Figure 34. ^{13}C NMR spectrum of **2.16** (125 MHz, CDCl_3).

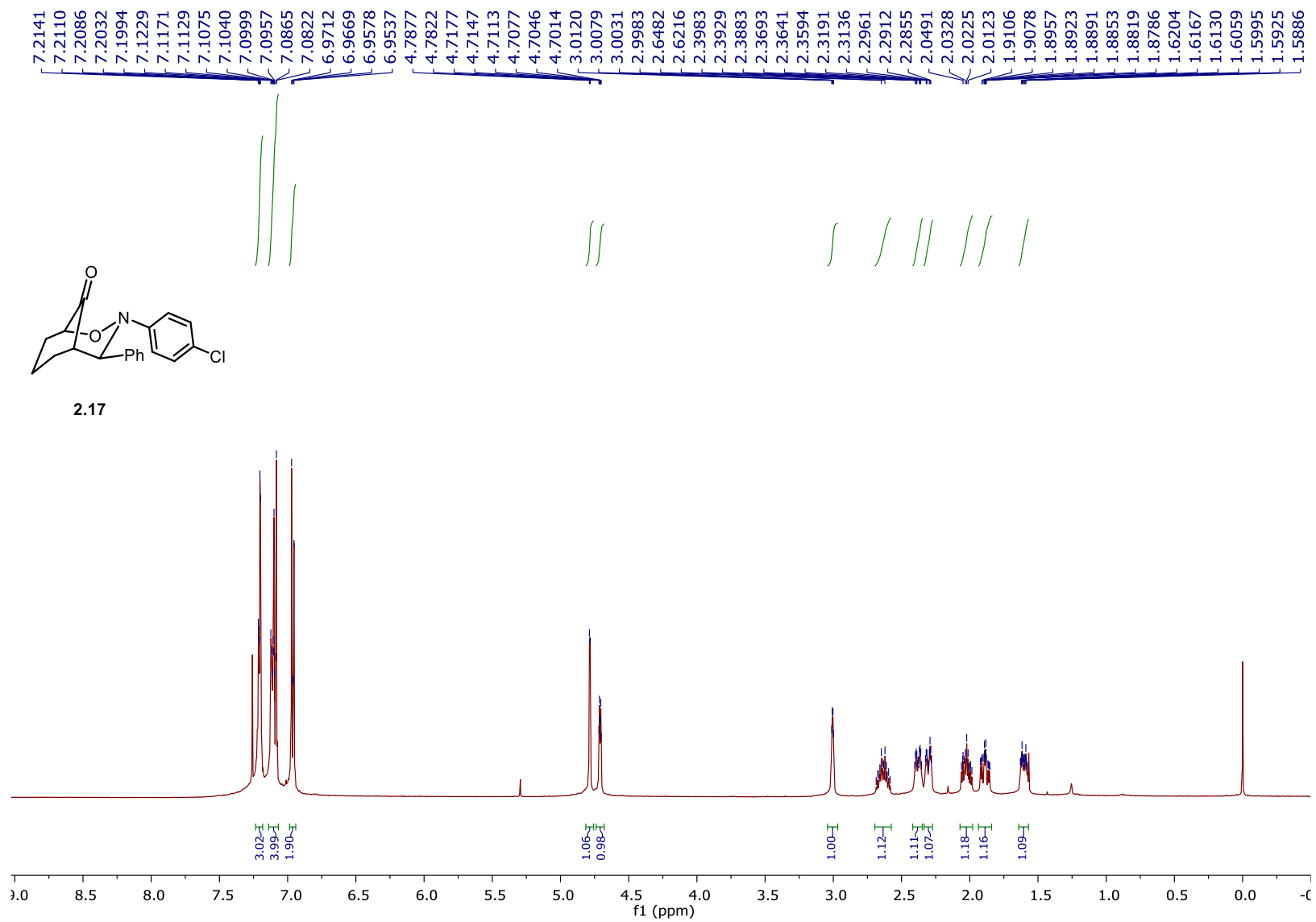


Figure 35. ¹H NMR spectrum of **2.17** (500 MHz, CDCl₃).

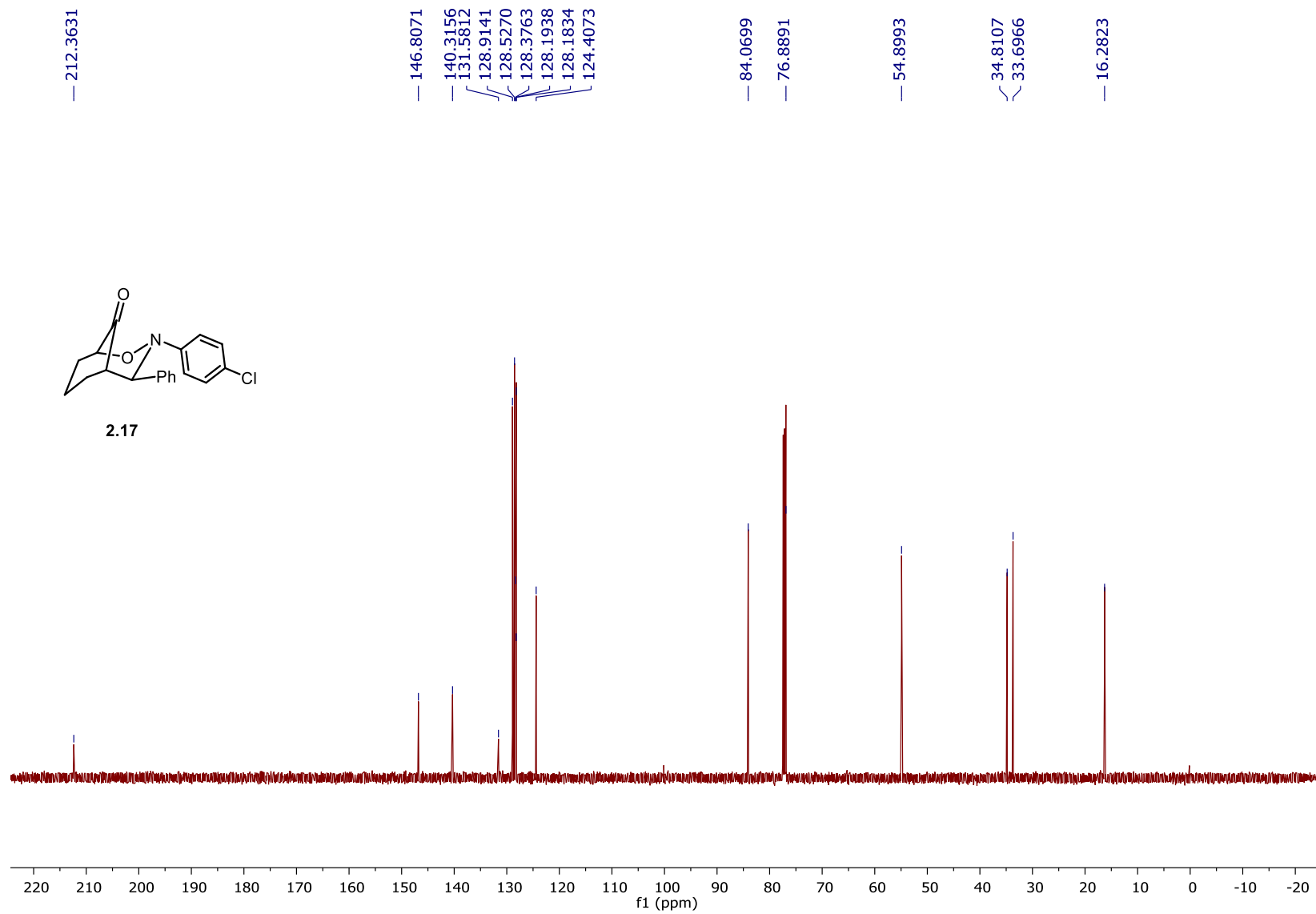


Figure 36. ^{13}C NMR spectrum of **2.17** (125 MHz, CDCl_3).

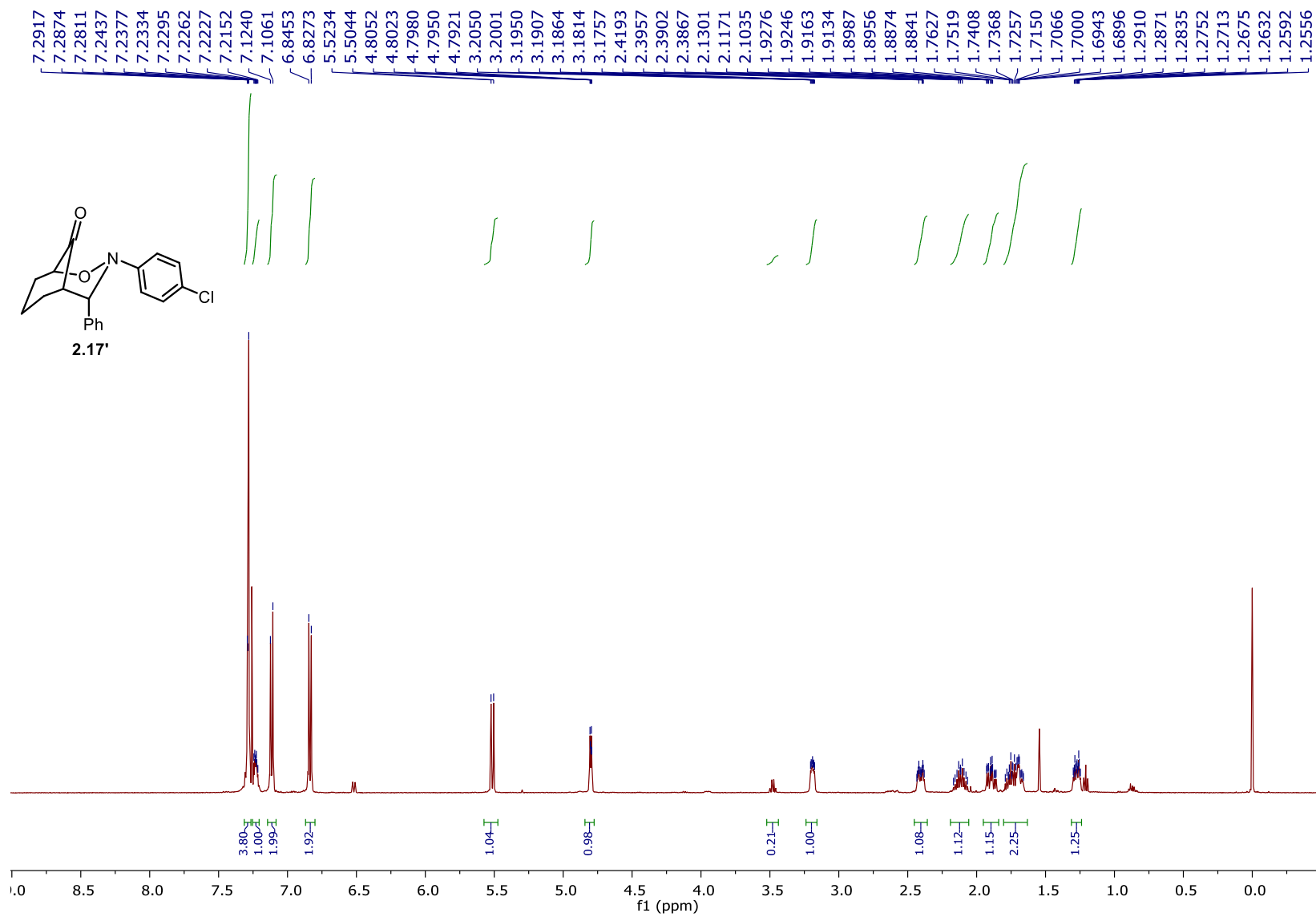


Figure 37. ¹H NMR spectrum of **2.17'** (500 MHz, CDCl₃).

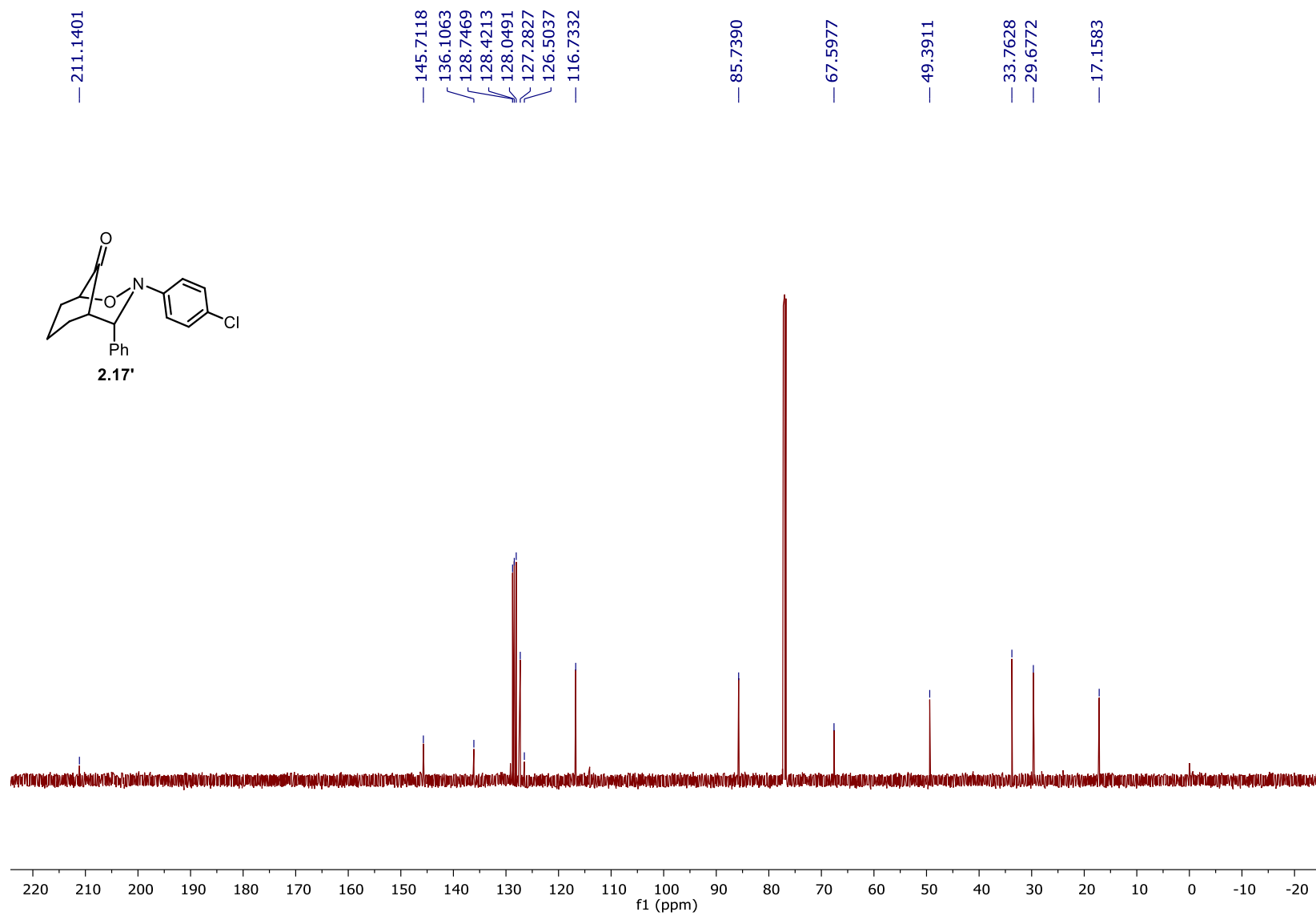


Figure 38. ^{13}C NMR spectrum of **2.17'** (125 MHz, CDCl_3).

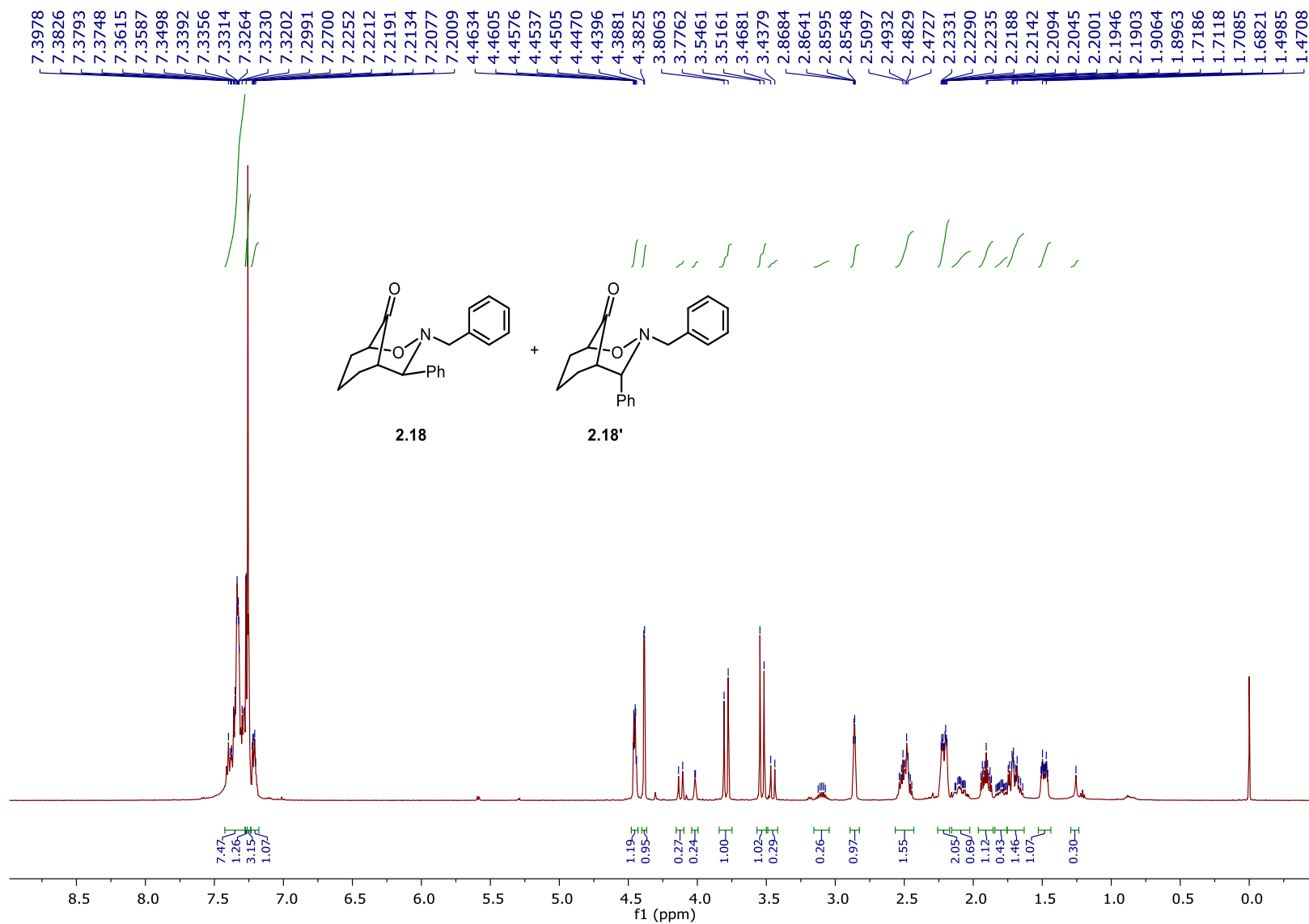


Figure 39. ^1H NMR spectrum of **2.18** (500 MHz, CDCl_3).

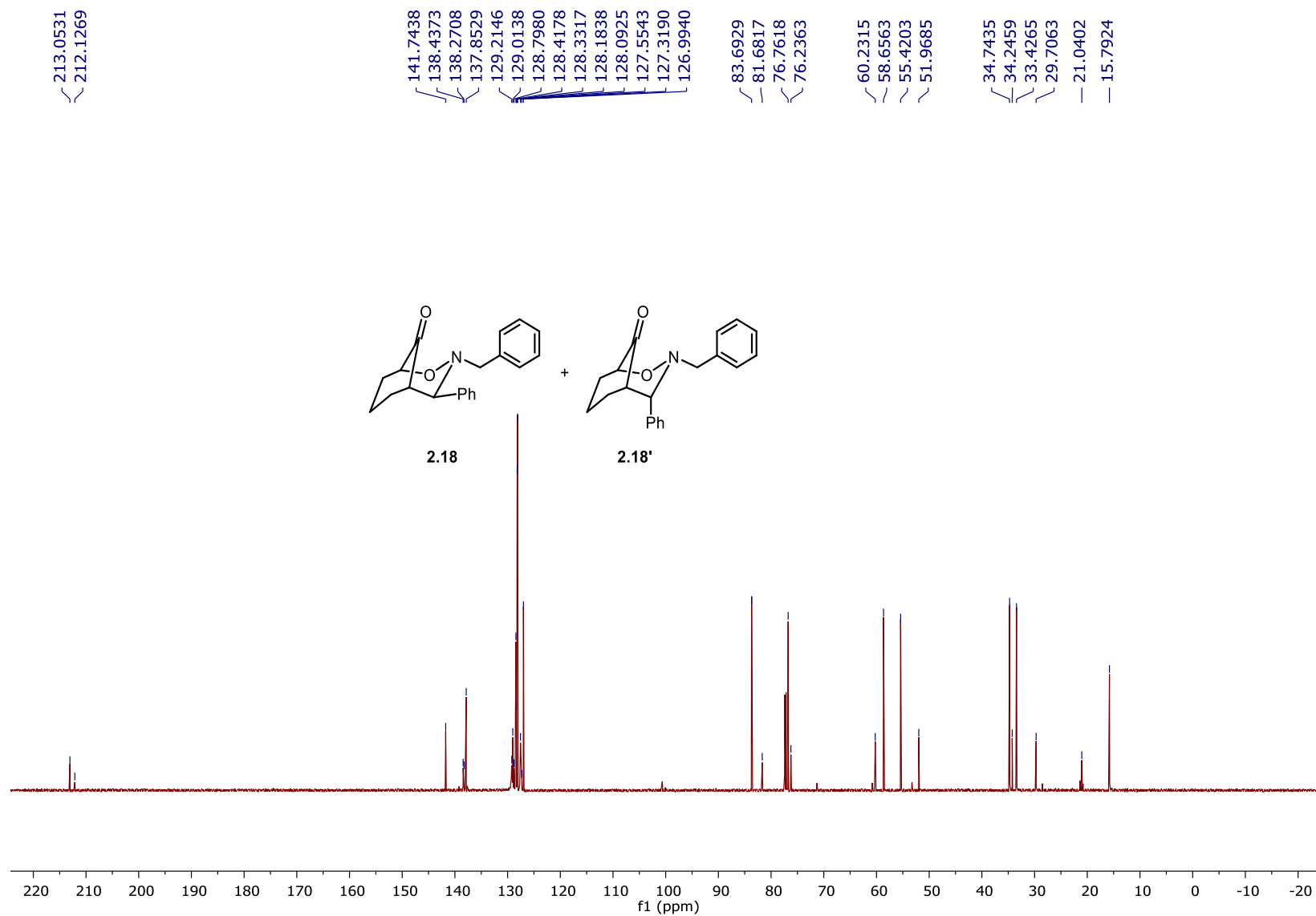


Figure 40. ^{13}C NMR spectrum of **2.18** (125 MHz, CDCl_3).

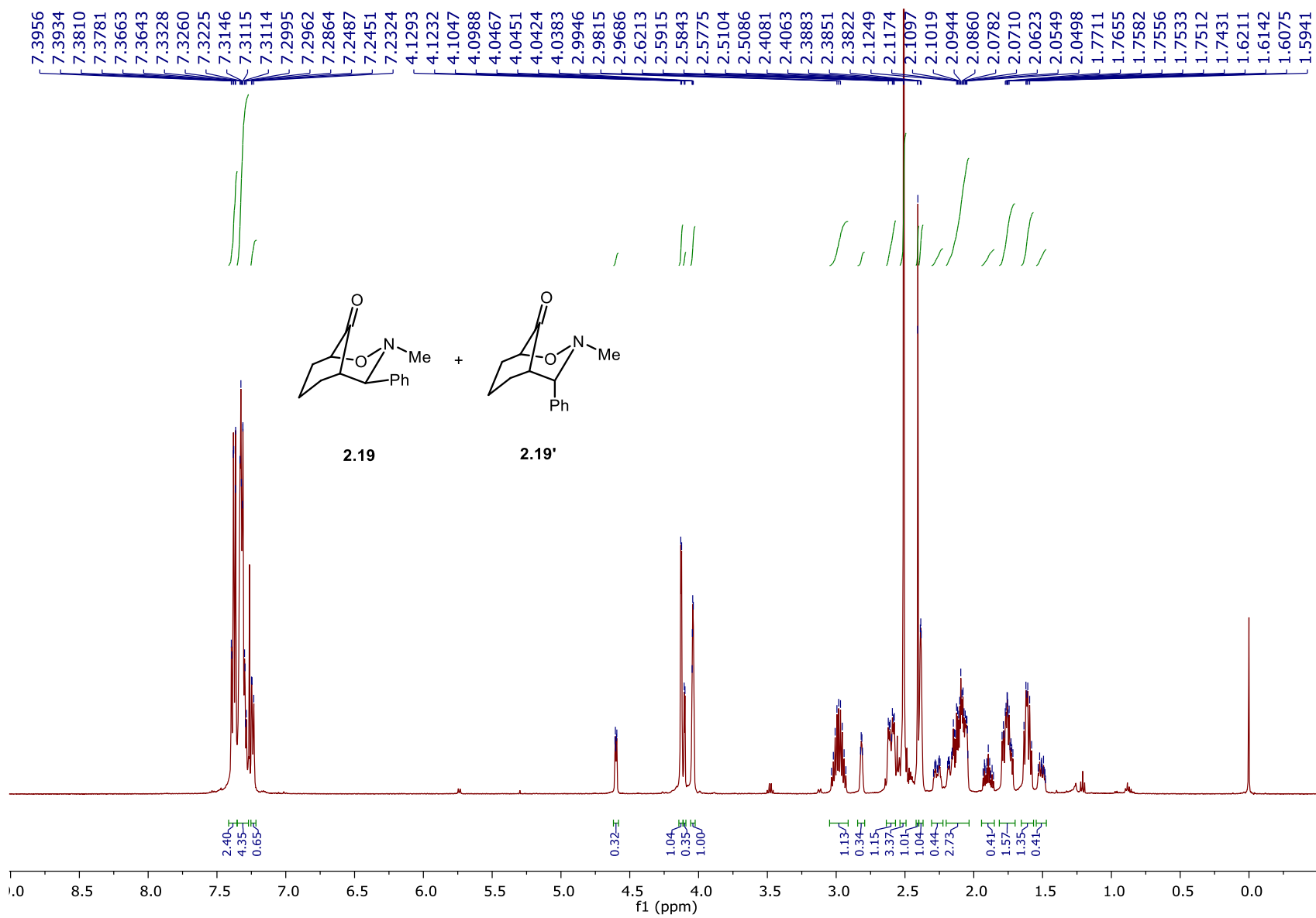


Figure 41. ¹H NMR spectrum of 2.19 (500 MHz, CDCl₃).

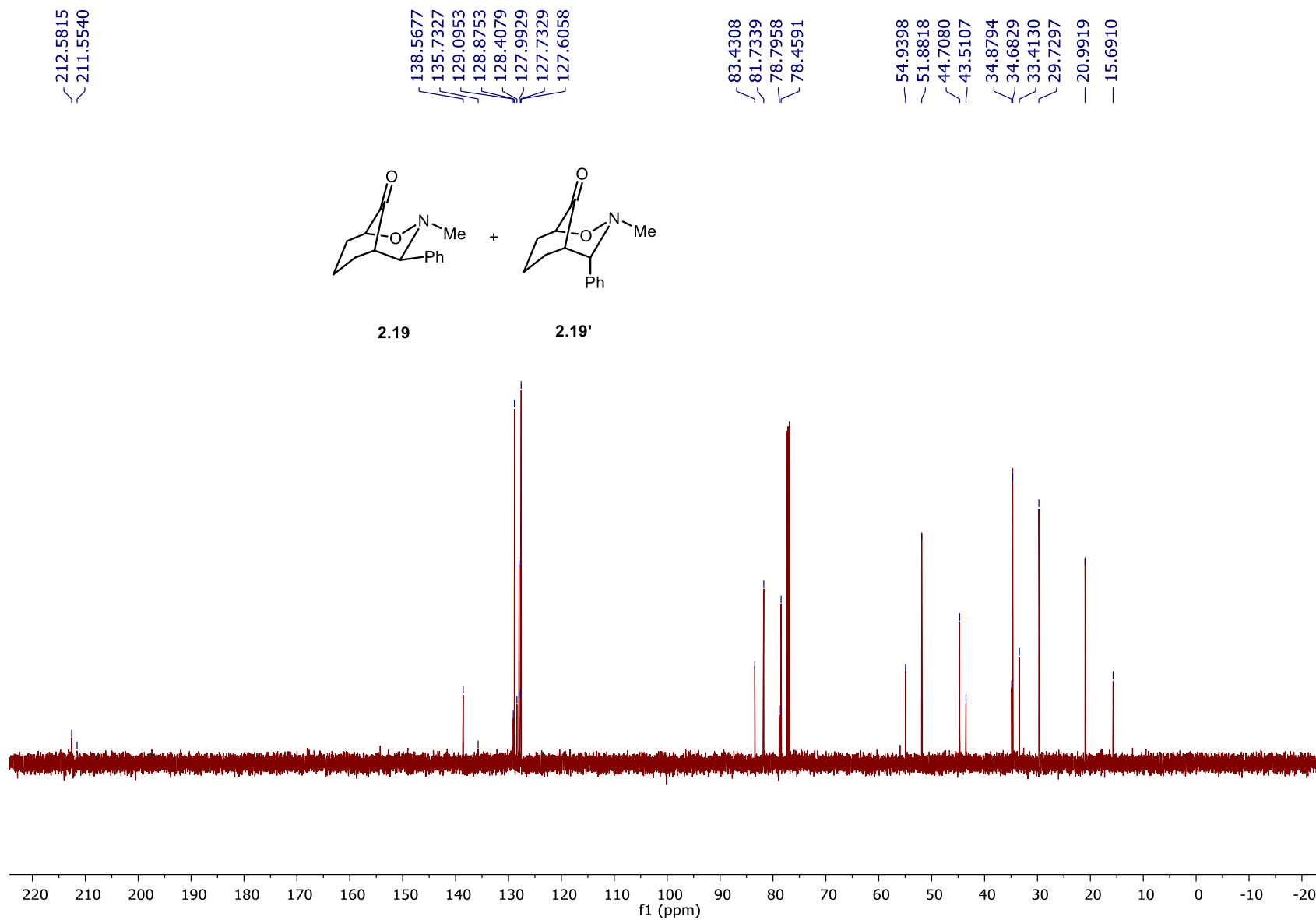


Figure 42. ^{13}C NMR spectrum of **2.19** (125 MHz, CDCl_3).

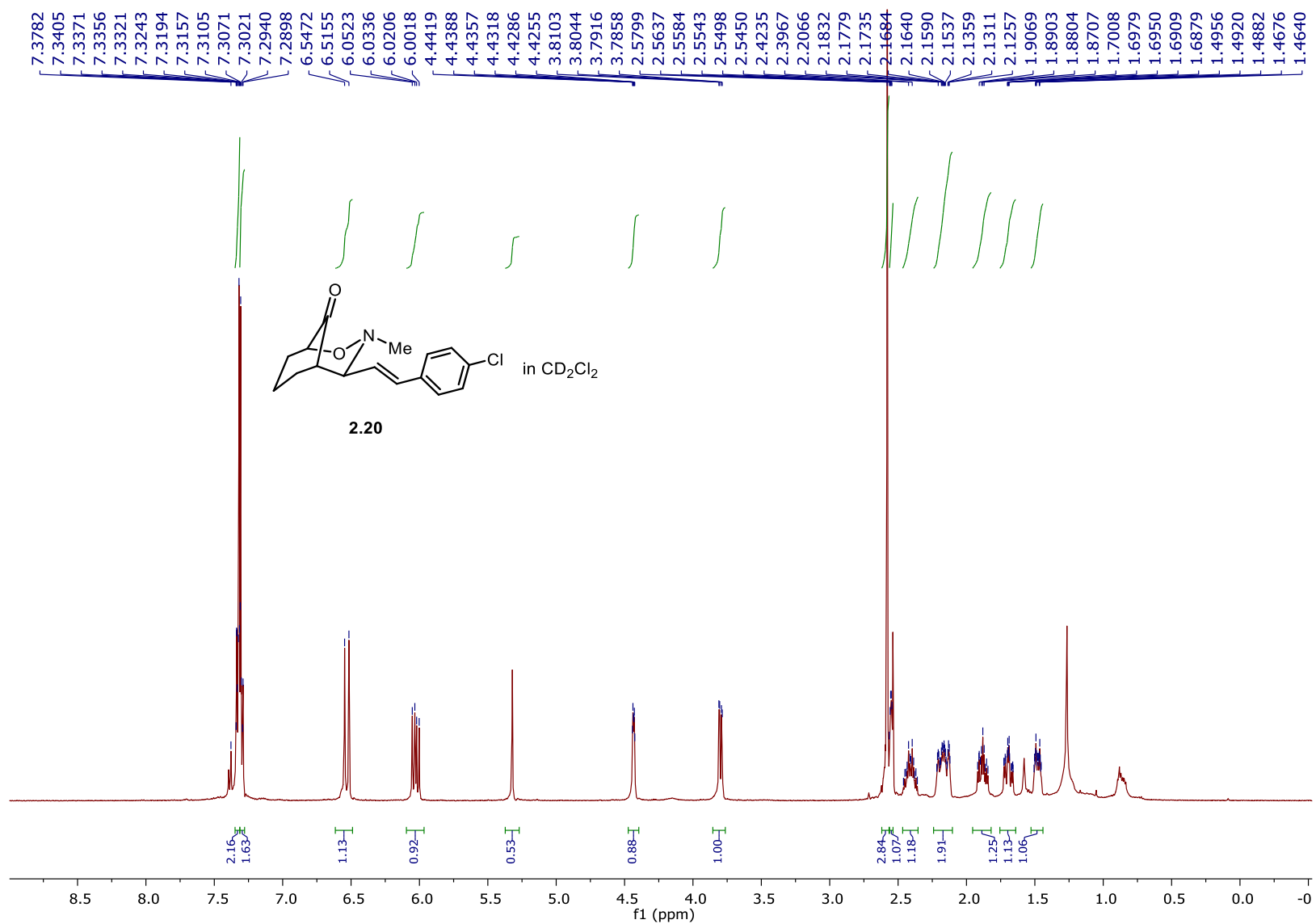


Figure 43. ^1H NMR spectrum of **2.20** (500 MHz, CD_2Cl_2).

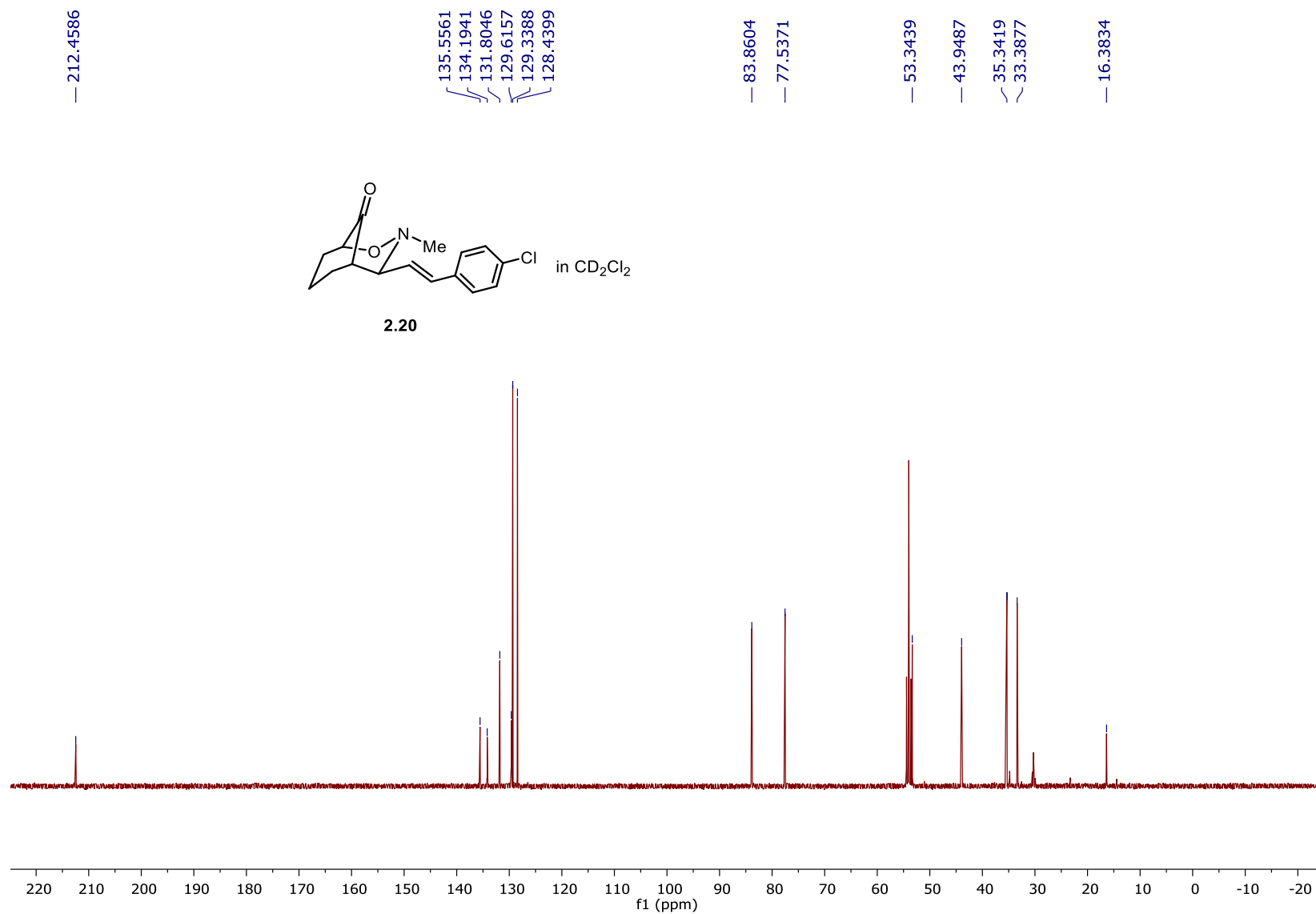


Figure 44. ^{13}C NMR spectrum of **2.20** (125 MHz, CD_2Cl_2).

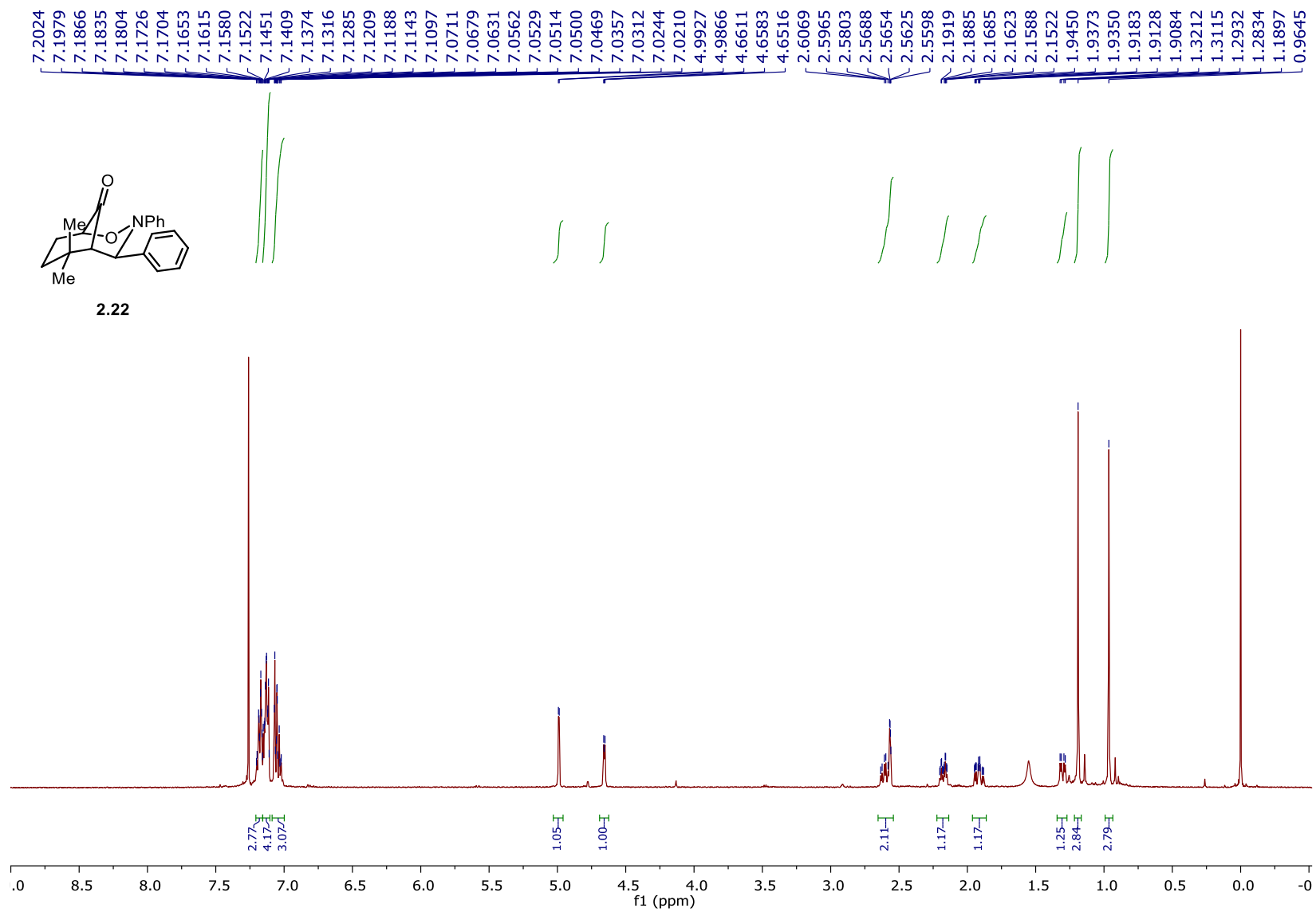


Figure 45. ¹H NMR spectrum of **2.22** (500 MHz, CDCl₃).

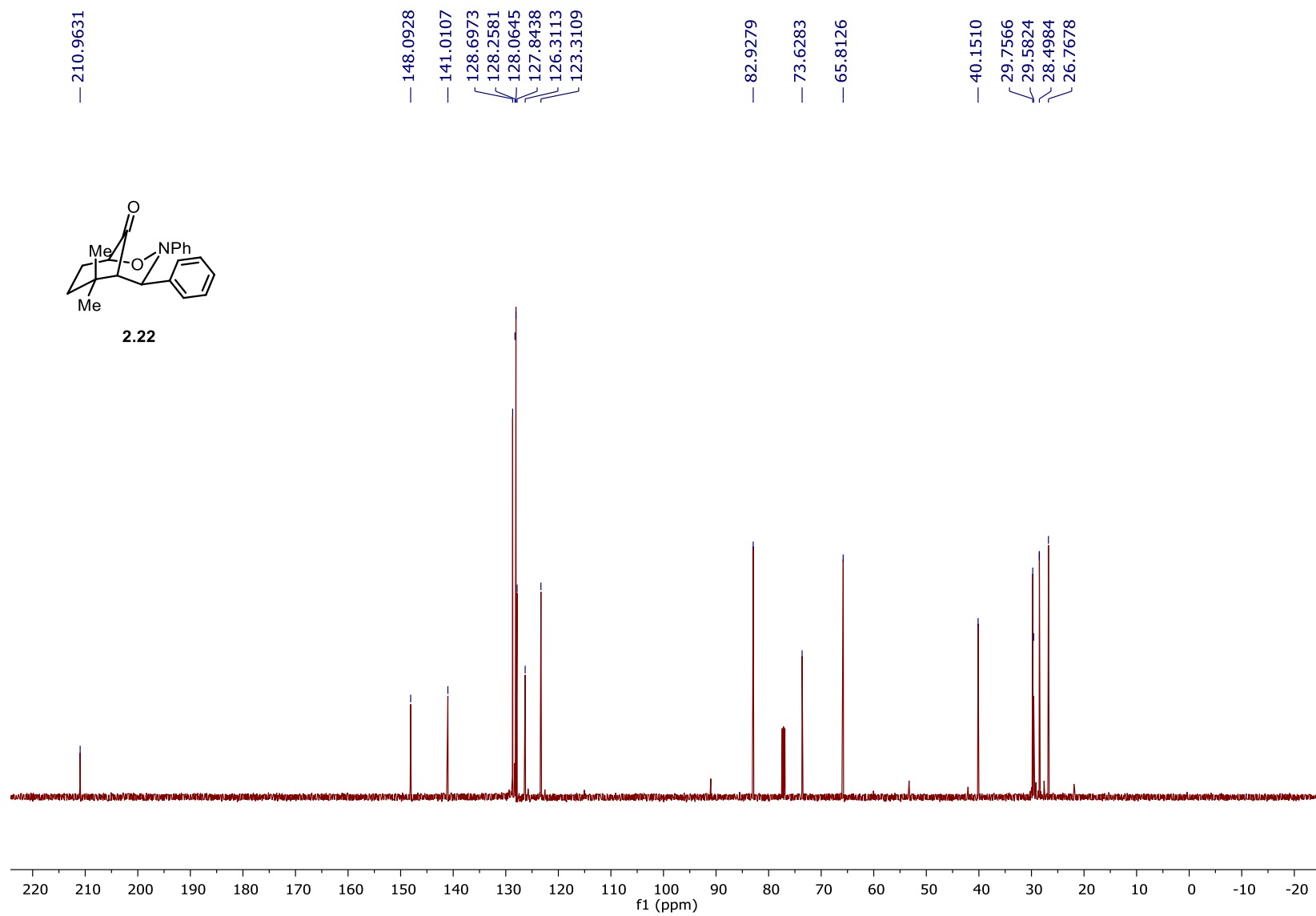


Figure 46. ^{13}C NMR spectrum of **2.22** (125 MHz, CDCl_3).

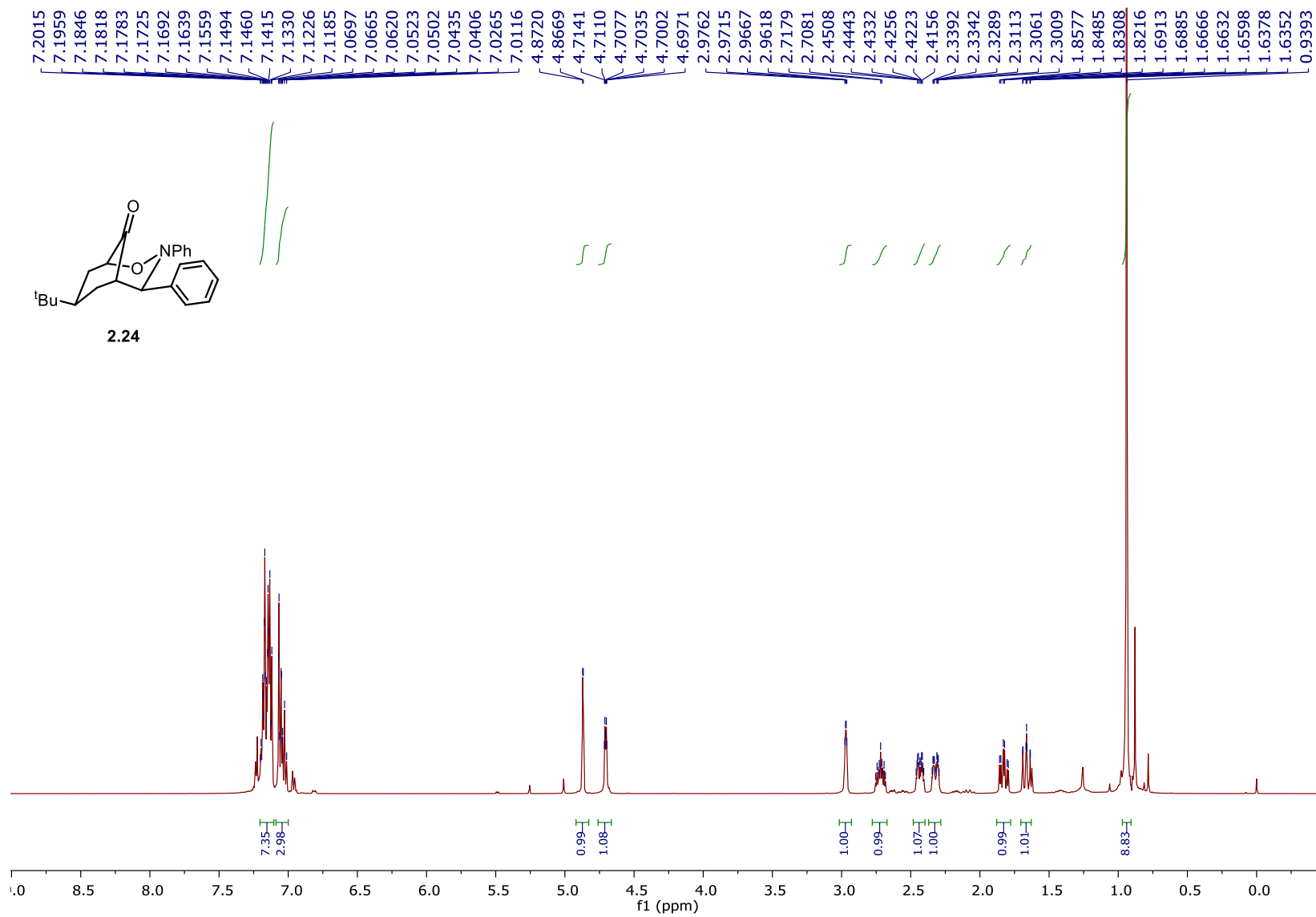


Figure 47. ¹H NMR spectrum of **2.24** (500 MHz, CDCl₃).

220

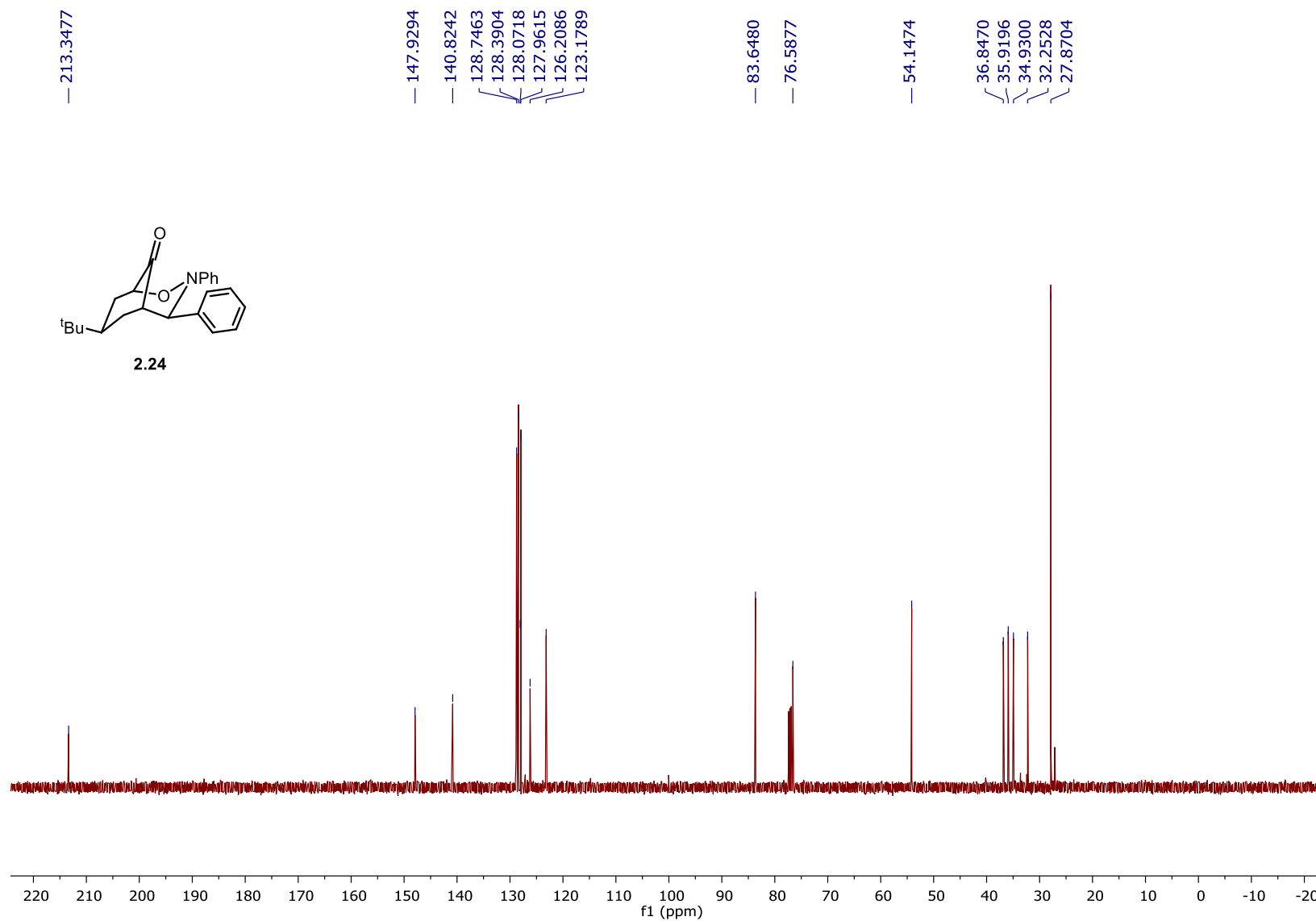


Figure 48. ^{13}C NMR spectrum of **2.24** (125 MHz, CDCl_3).

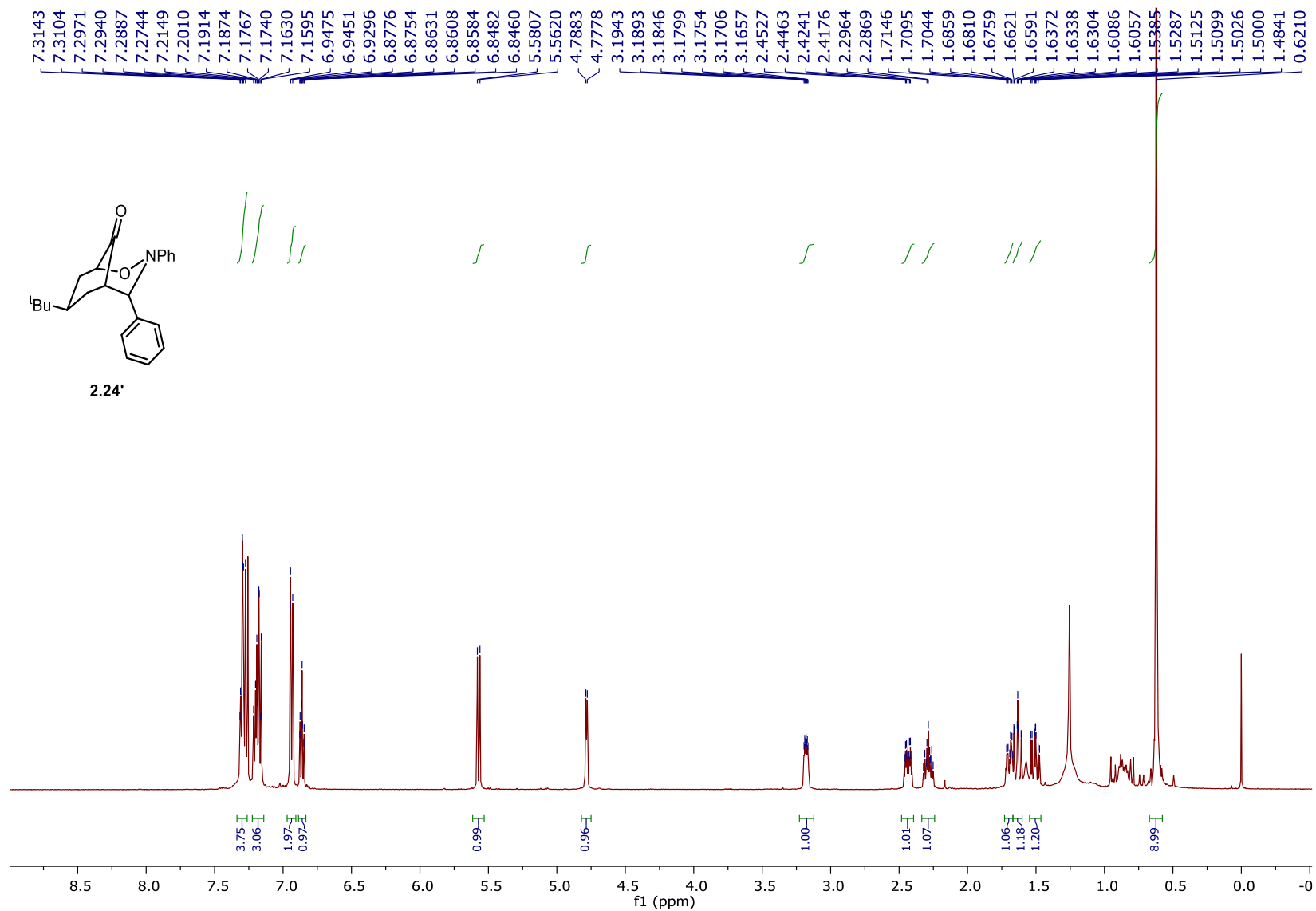


Figure 49. ^1H NMR spectrum of **2.24'** (500 MHz, CDCl_3).

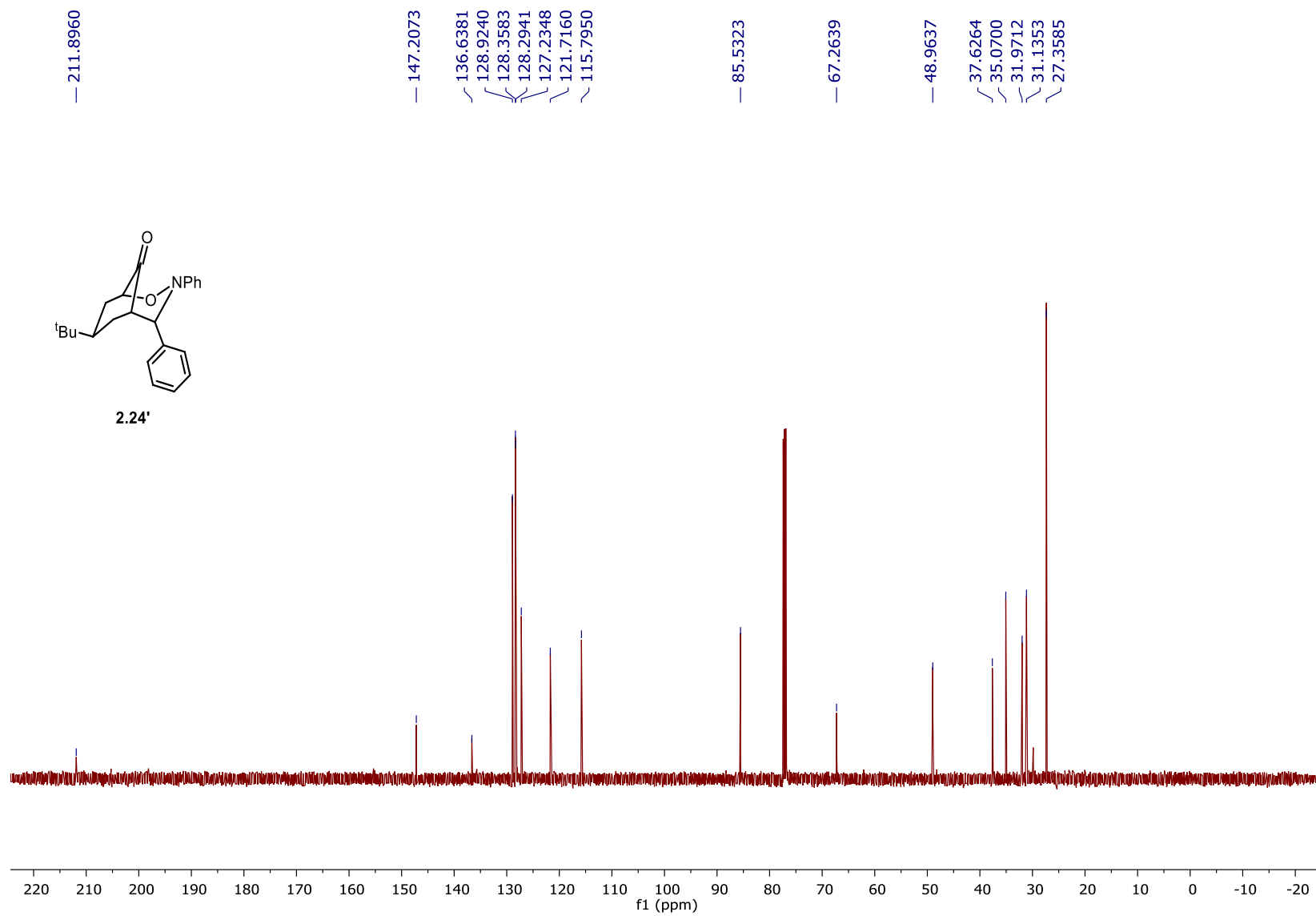


Figure 50. ¹³C NMR spectrum of 2.24' (125 MHz, CDCl₃).

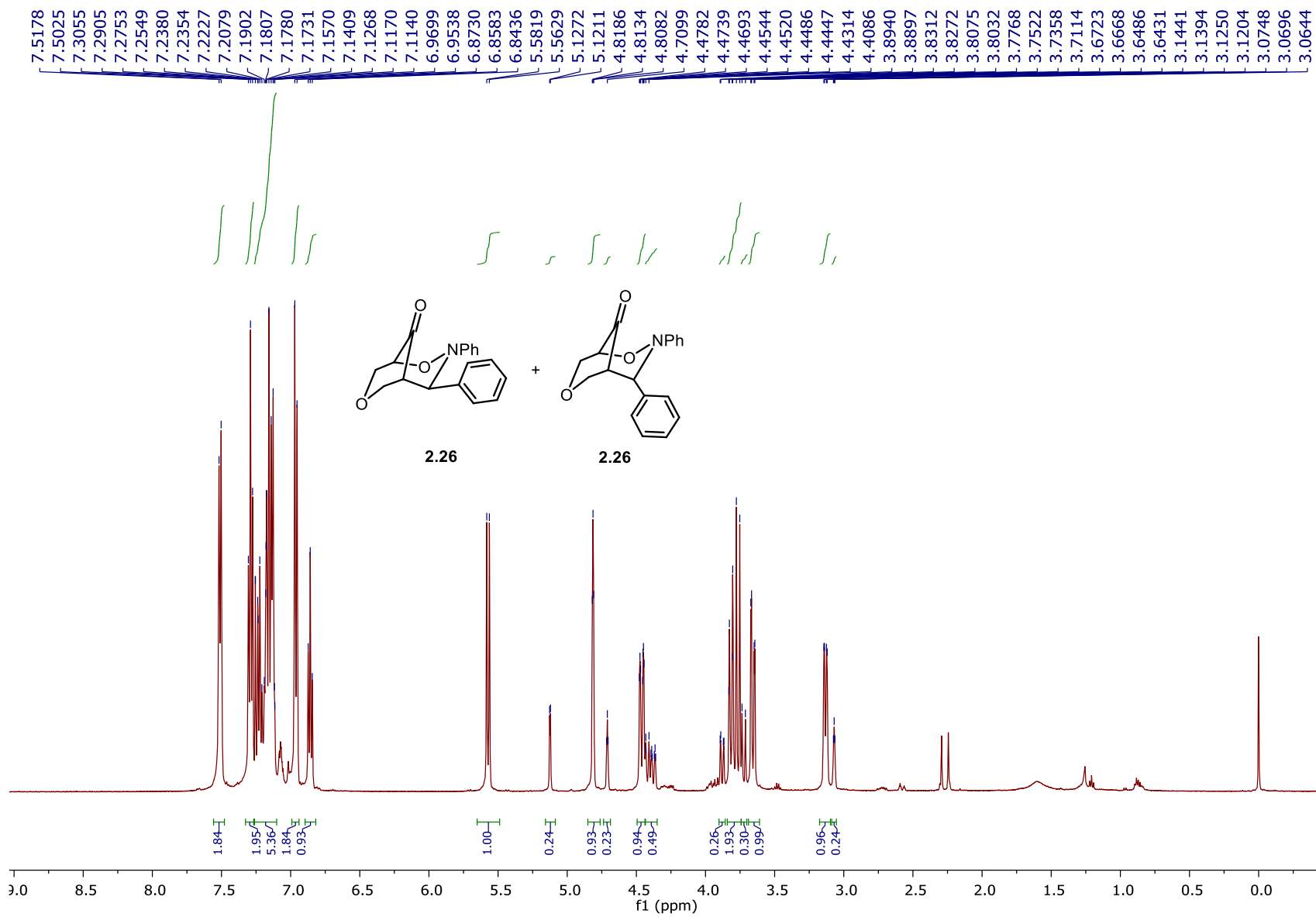


Figure 51. ^1H NMR spectrum of **2.26** (500 MHz, CDCl_3).

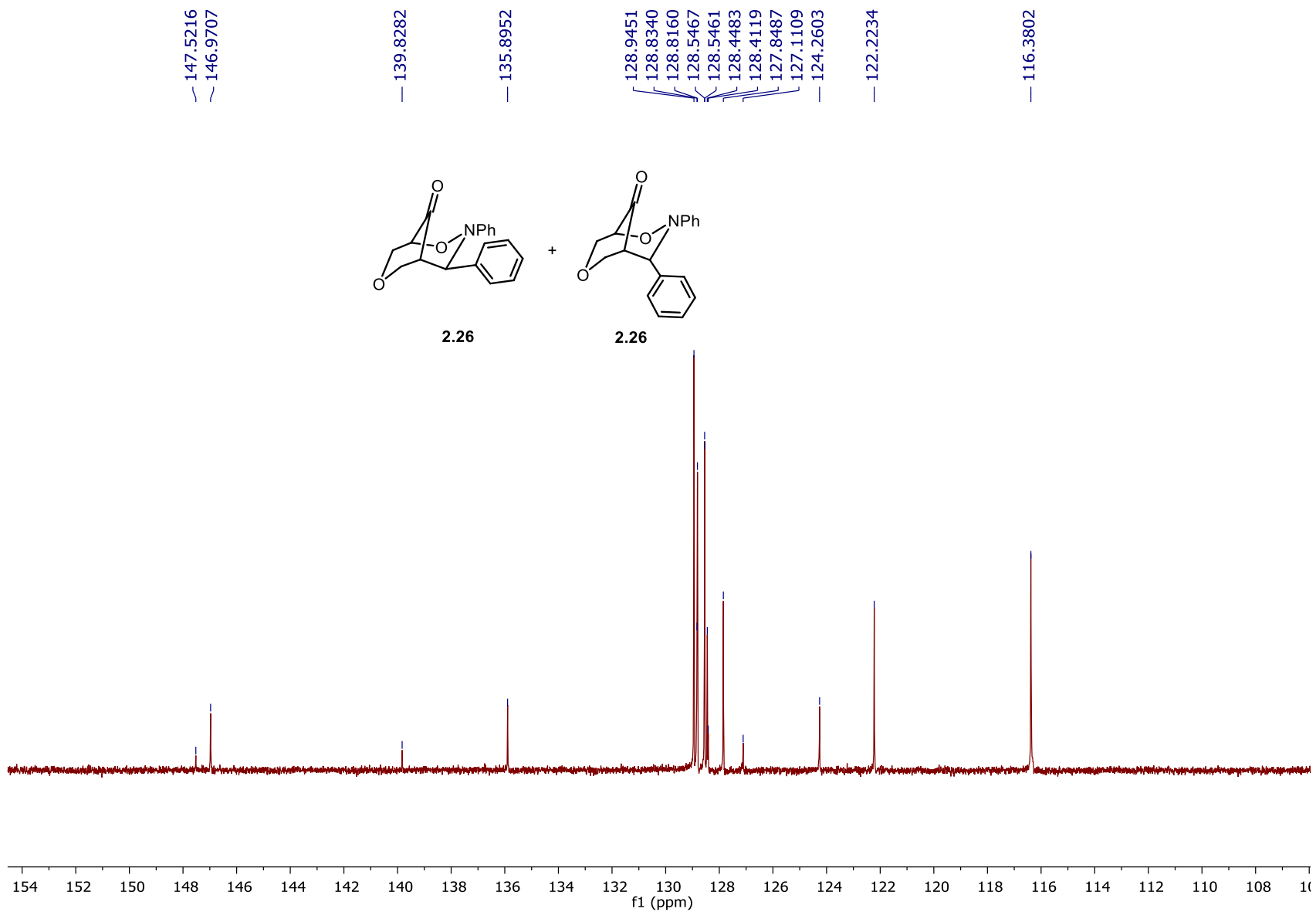


Figure 52. ^{13}C NMR spectrum of **2.26** (125 MHz, CDCl_3).

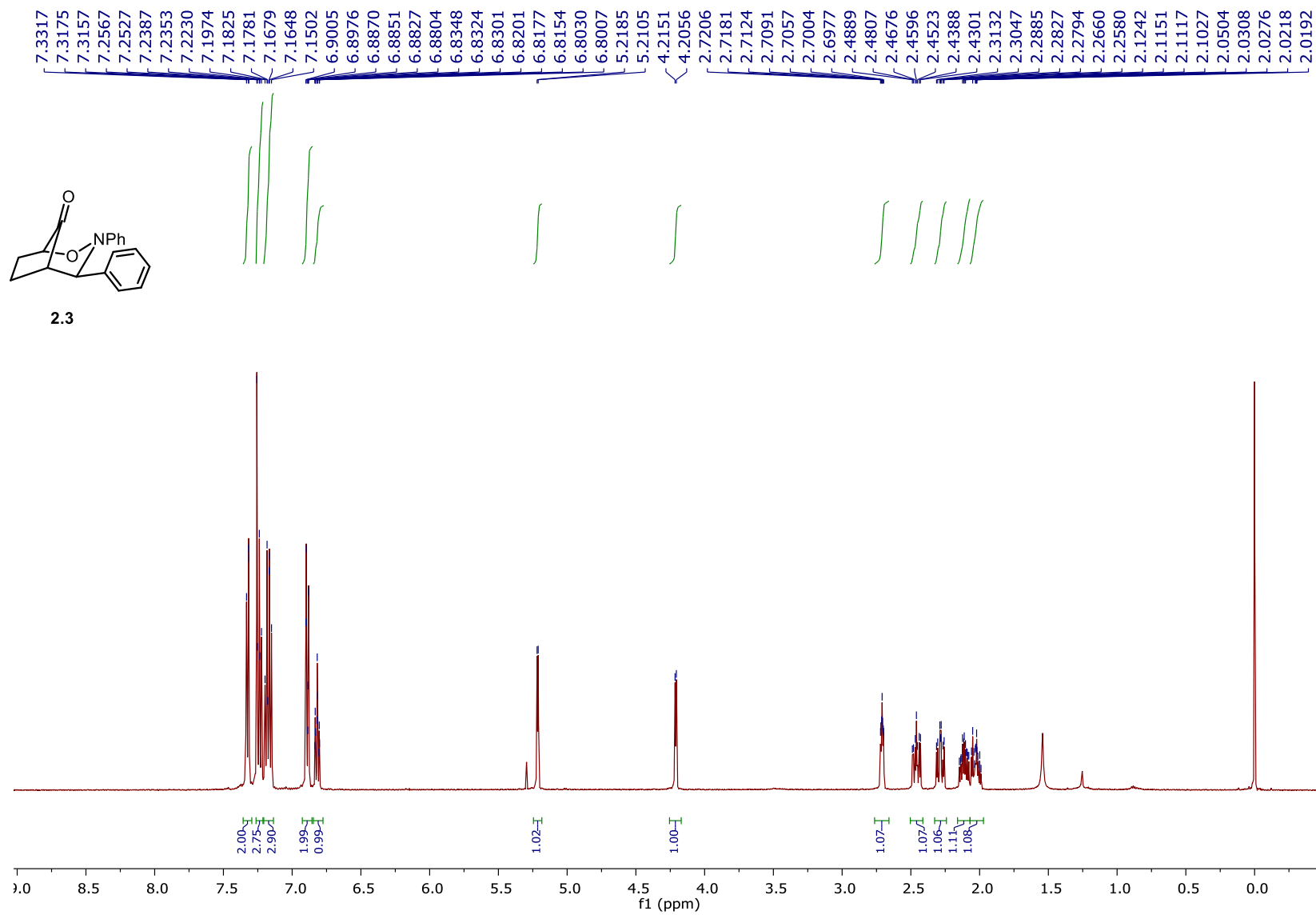


Figure 53. ^1H NMR spectrum of **2.3** (500 MHz, CDCl_3).

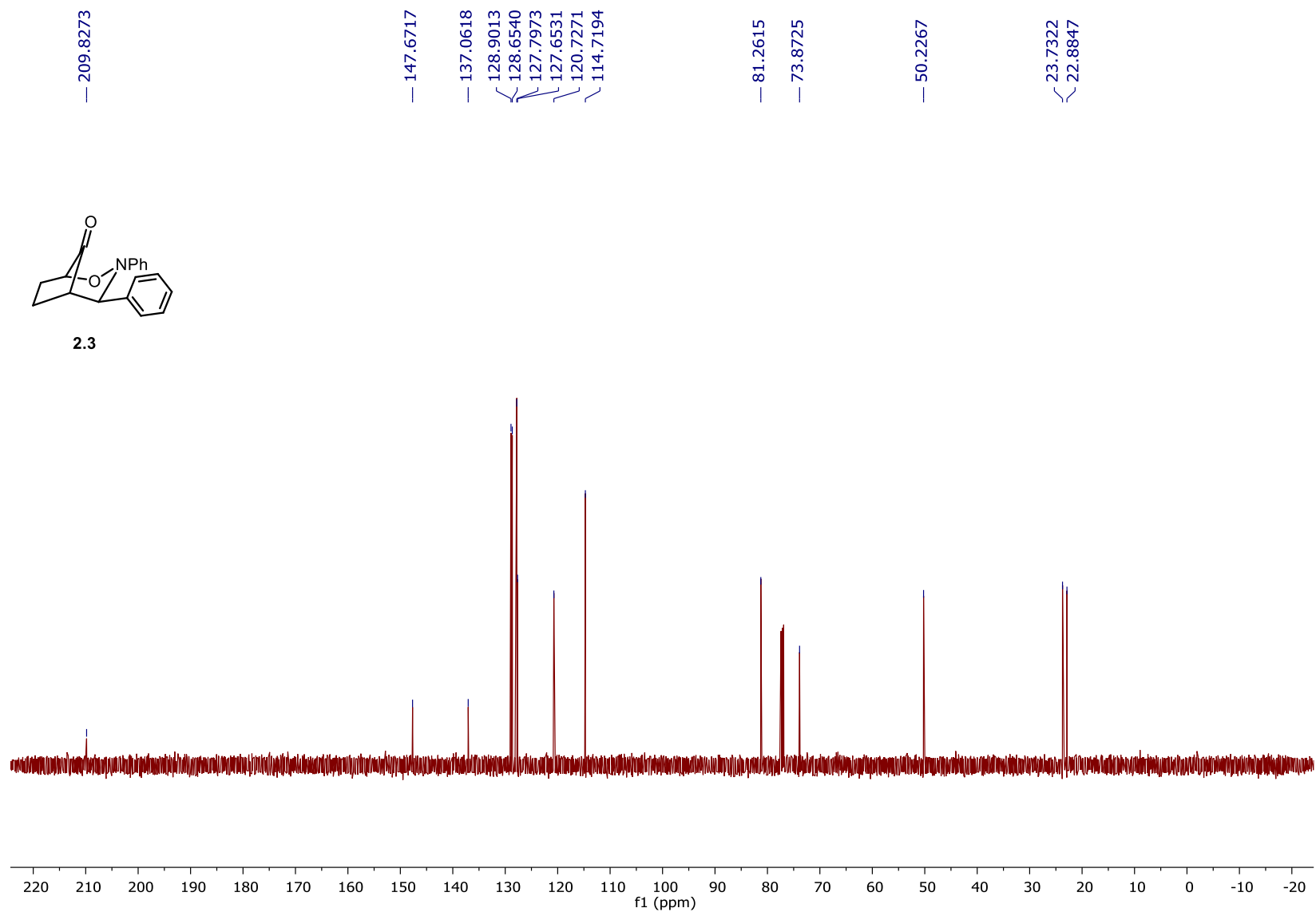


Figure 54. ^{13}C NMR spectrum of **2.3** (125 MHz, CDCl_3).

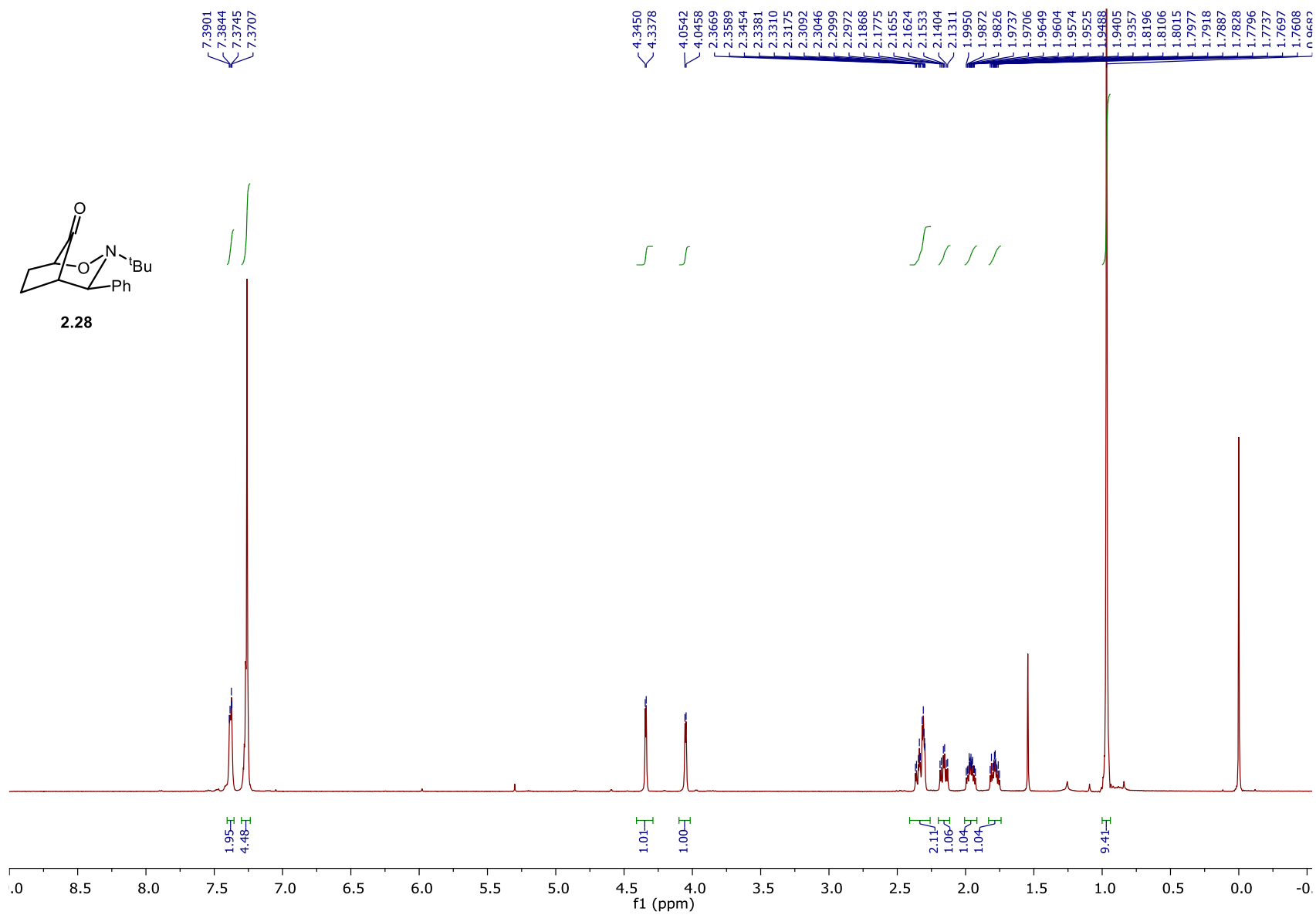


Figure 55. ^1H NMR spectrum of **2.28** (500 MHz, CDCl_3).

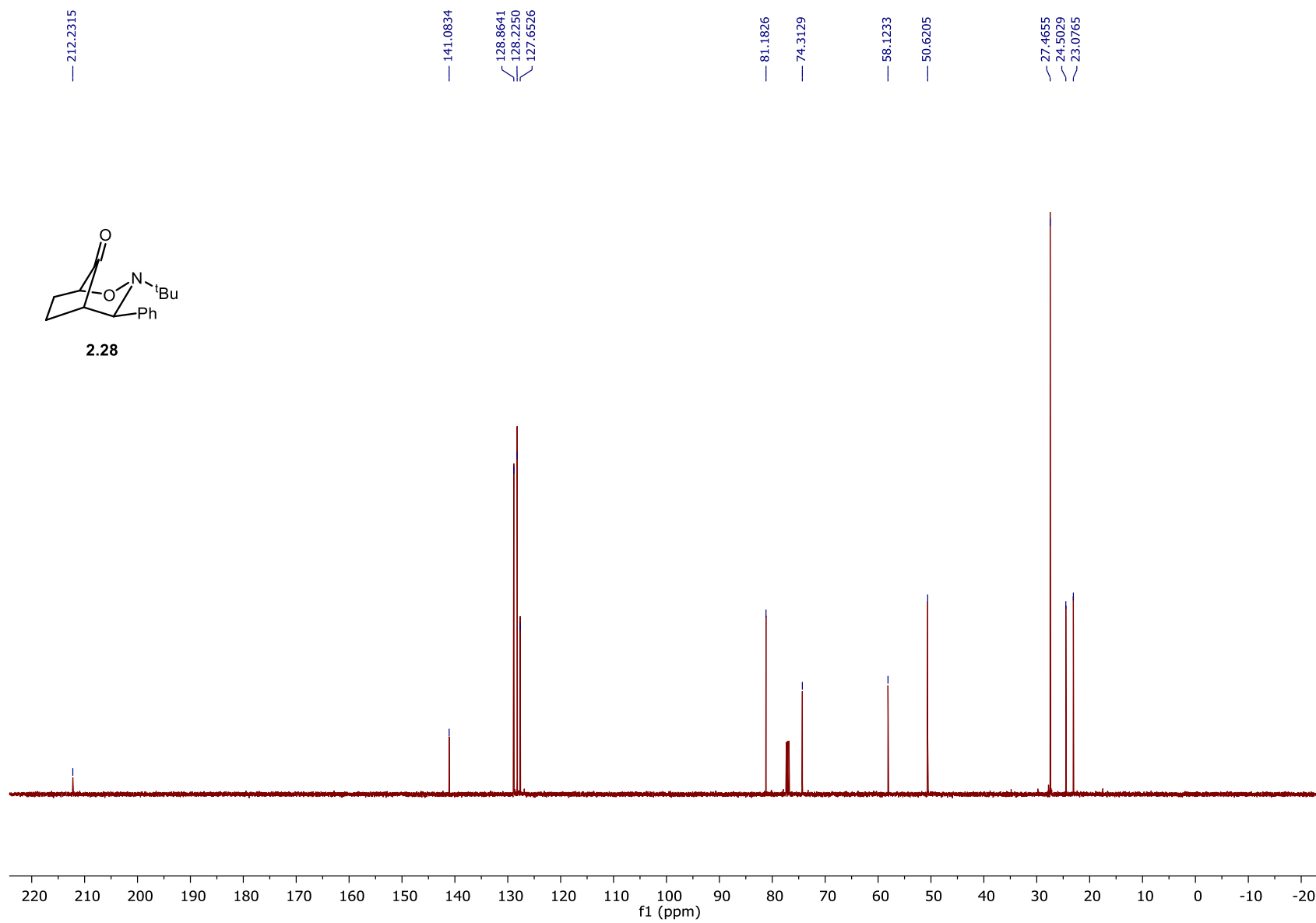


Figure 56. ^{13}C NMR spectrum of **2.28** (125 MHz, CDCl_3).

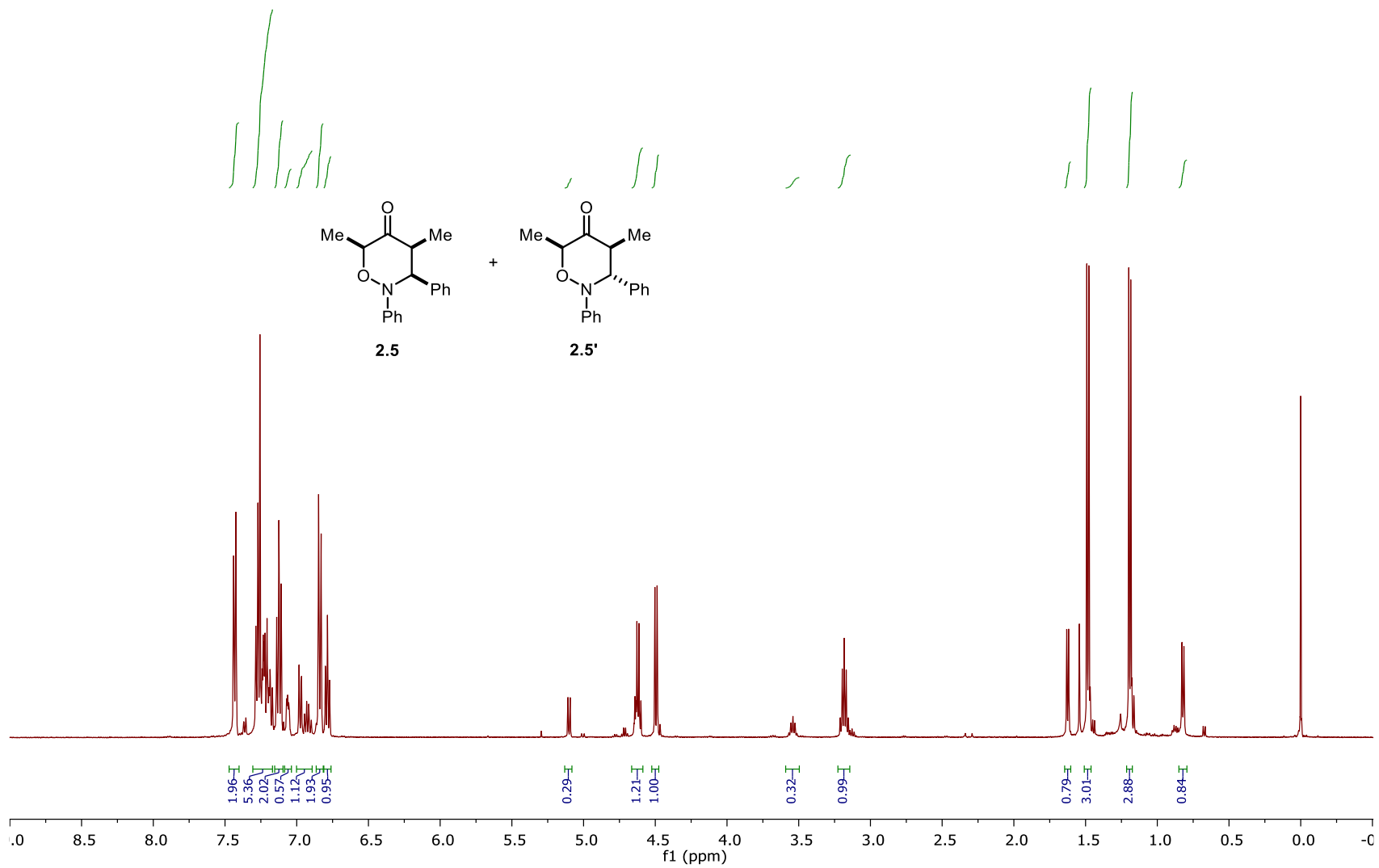


Figure 57. ^1H NMR spectrum of **2.5** (500 MHz, CDCl_3).

230

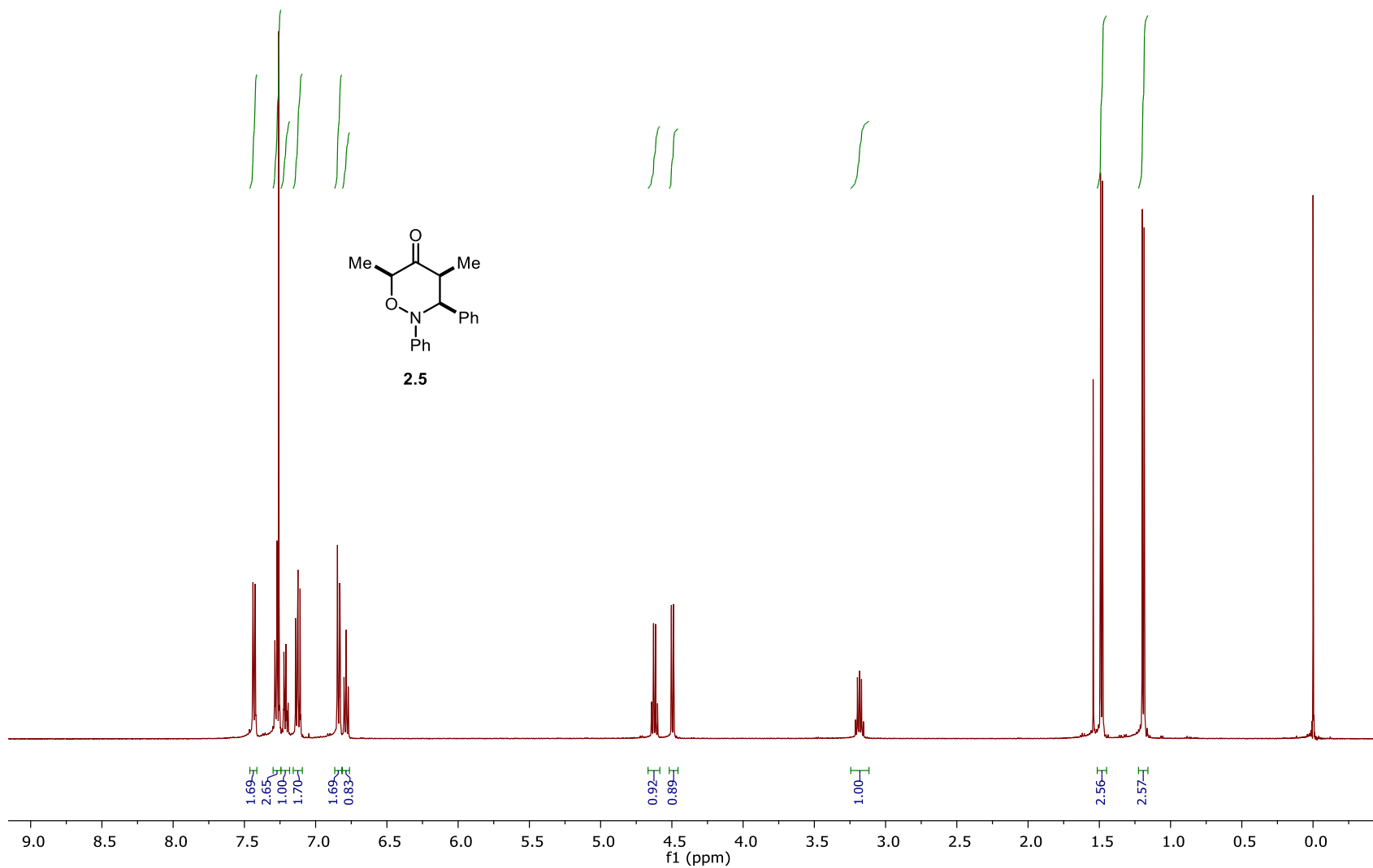


Figure 58. ^1H NMR spectrum of **2.5** (500 MHz, CDCl_3).

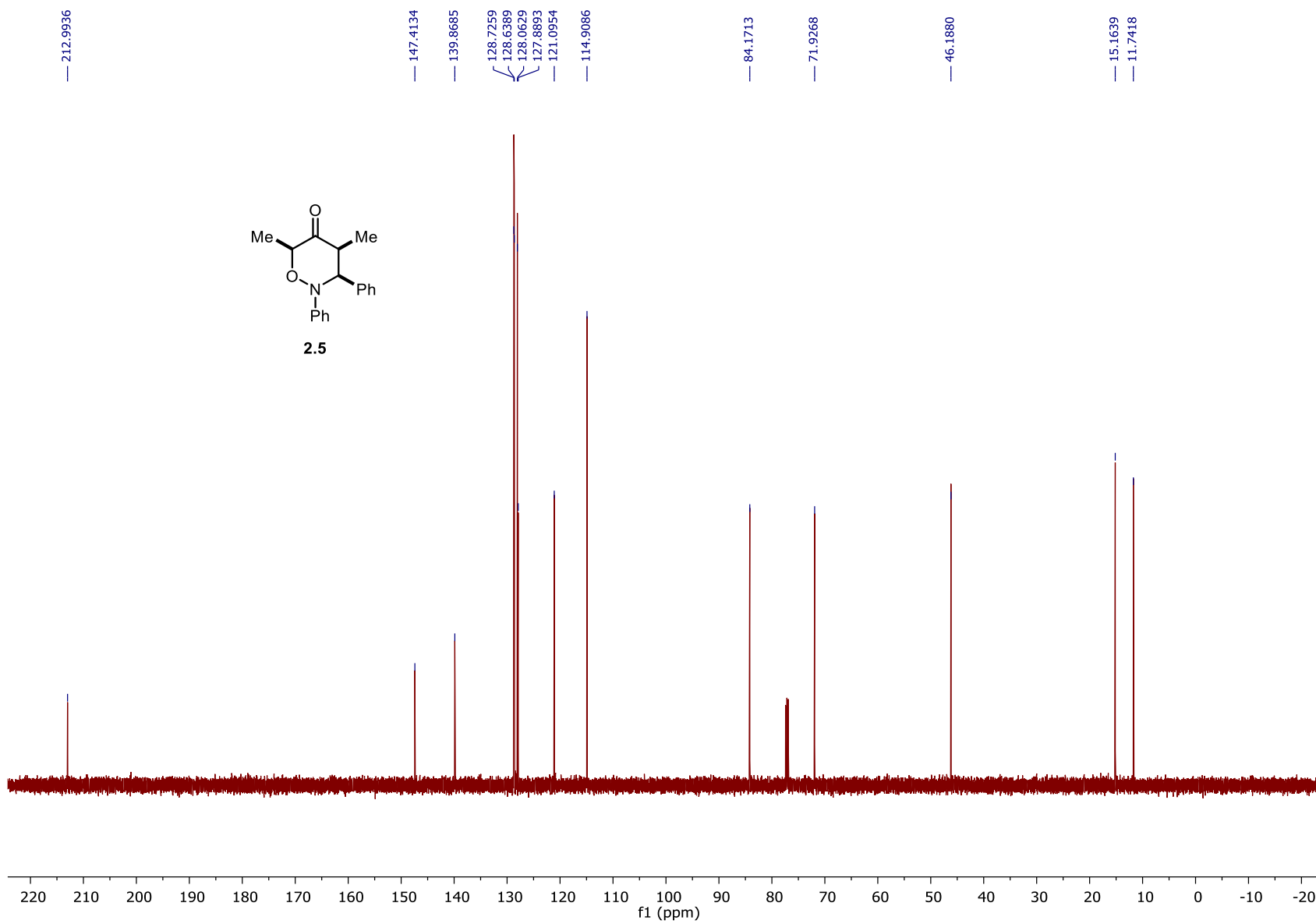


Figure 59. ^{13}C NMR spectrum of **2.5** (125 MHz, CDCl_3).

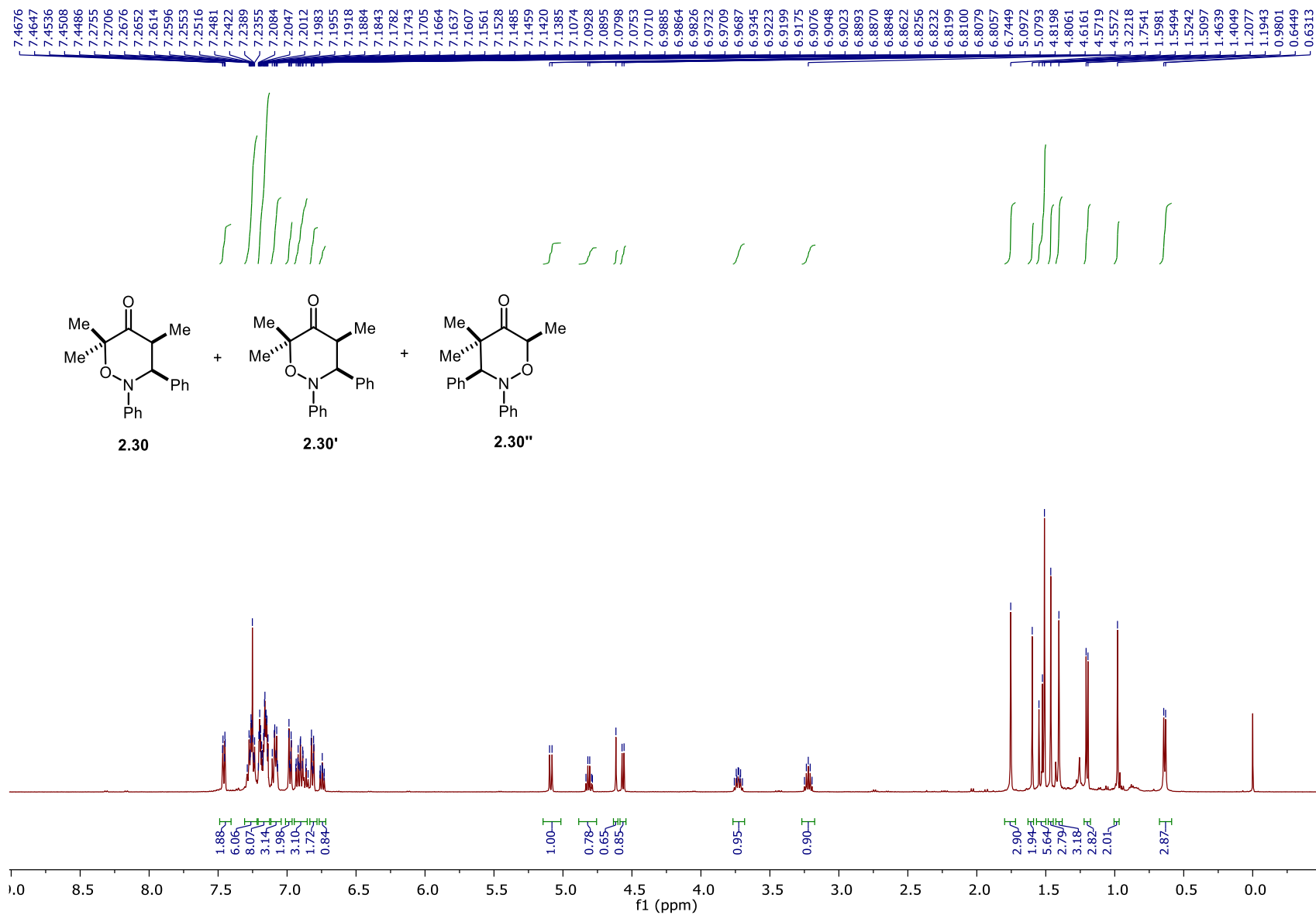


Figure 60. ¹H NMR spectrum of **2.30** (500 MHz, CDCl₃).

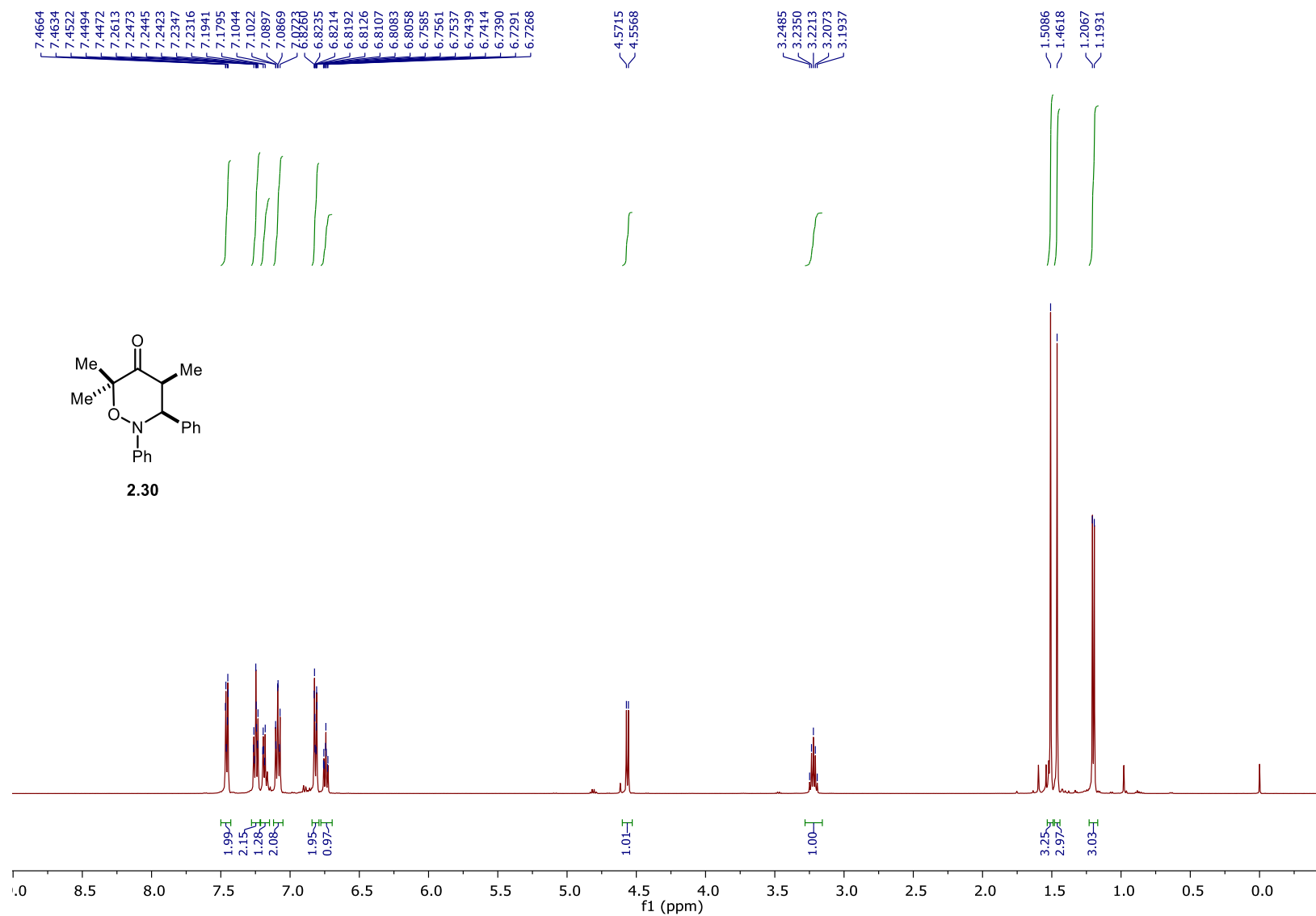


Figure 61. ^1H NMR spectrum of **2.30** (500 MHz, CDCl_3).

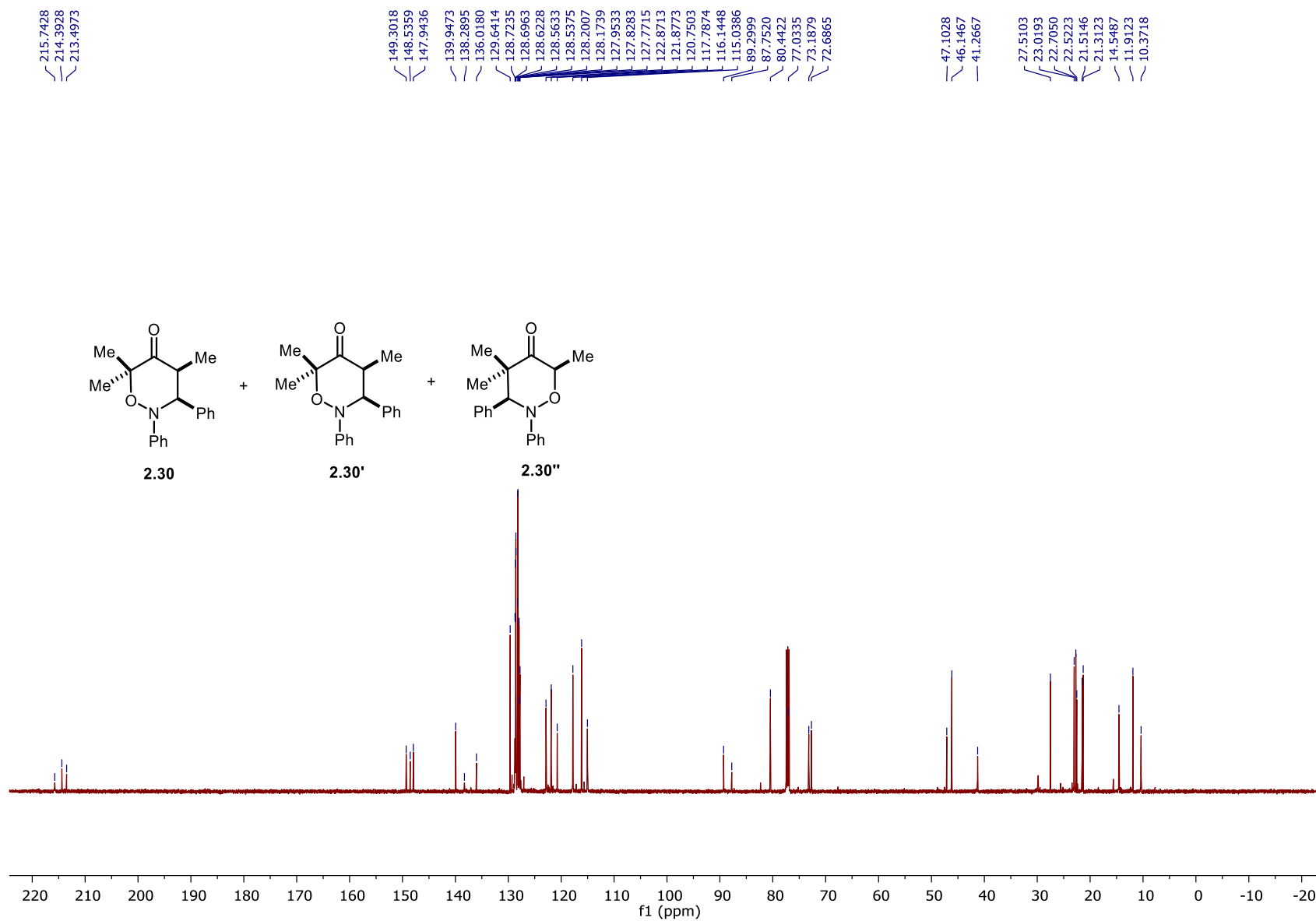


Figure 62. ^{13}C NMR spectrum of **2.30** (125 MHz, CDCl_3).

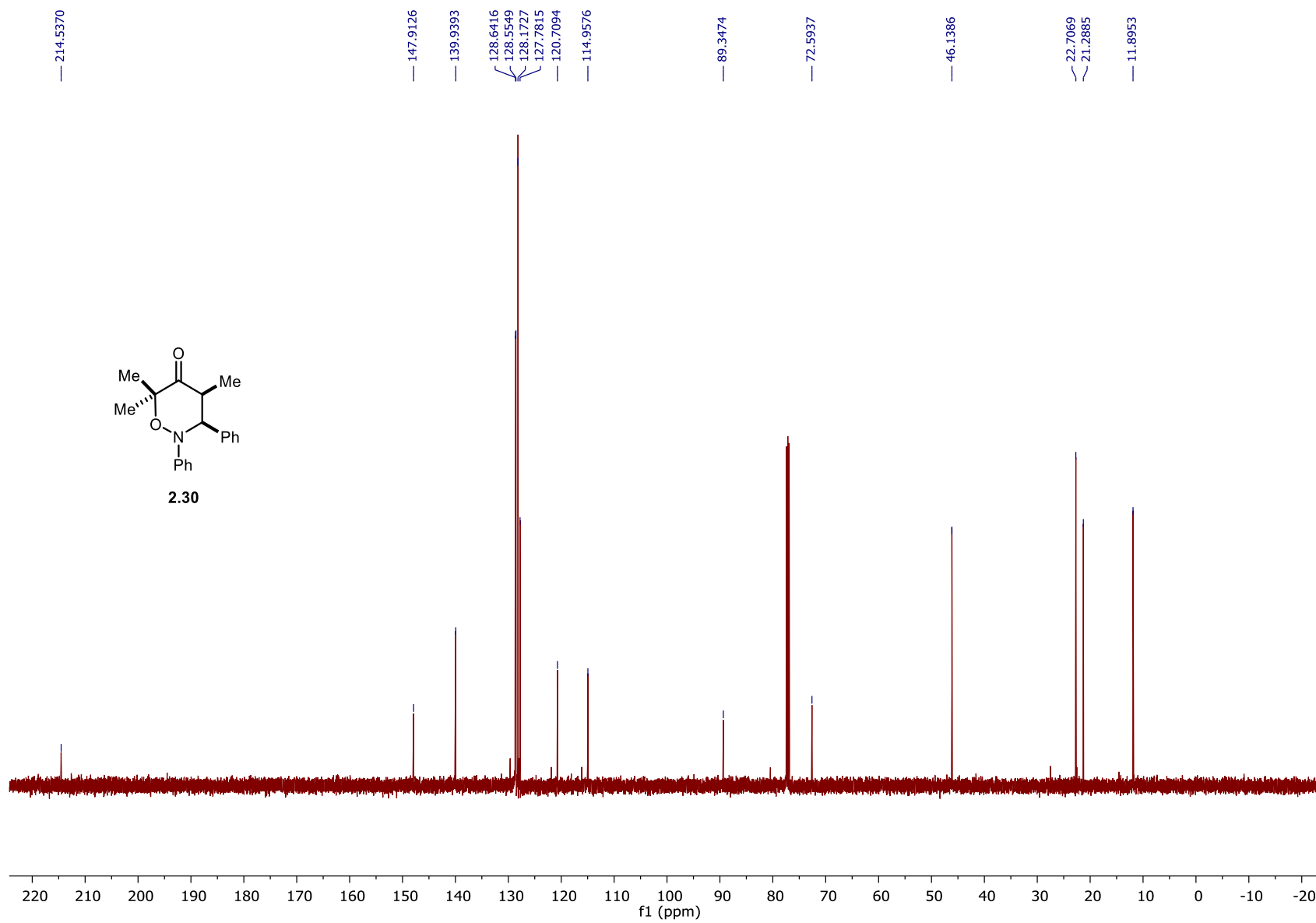


Figure 63. ^{13}C NMR spectrum of **2.30** (125 MHz, CDCl_3).

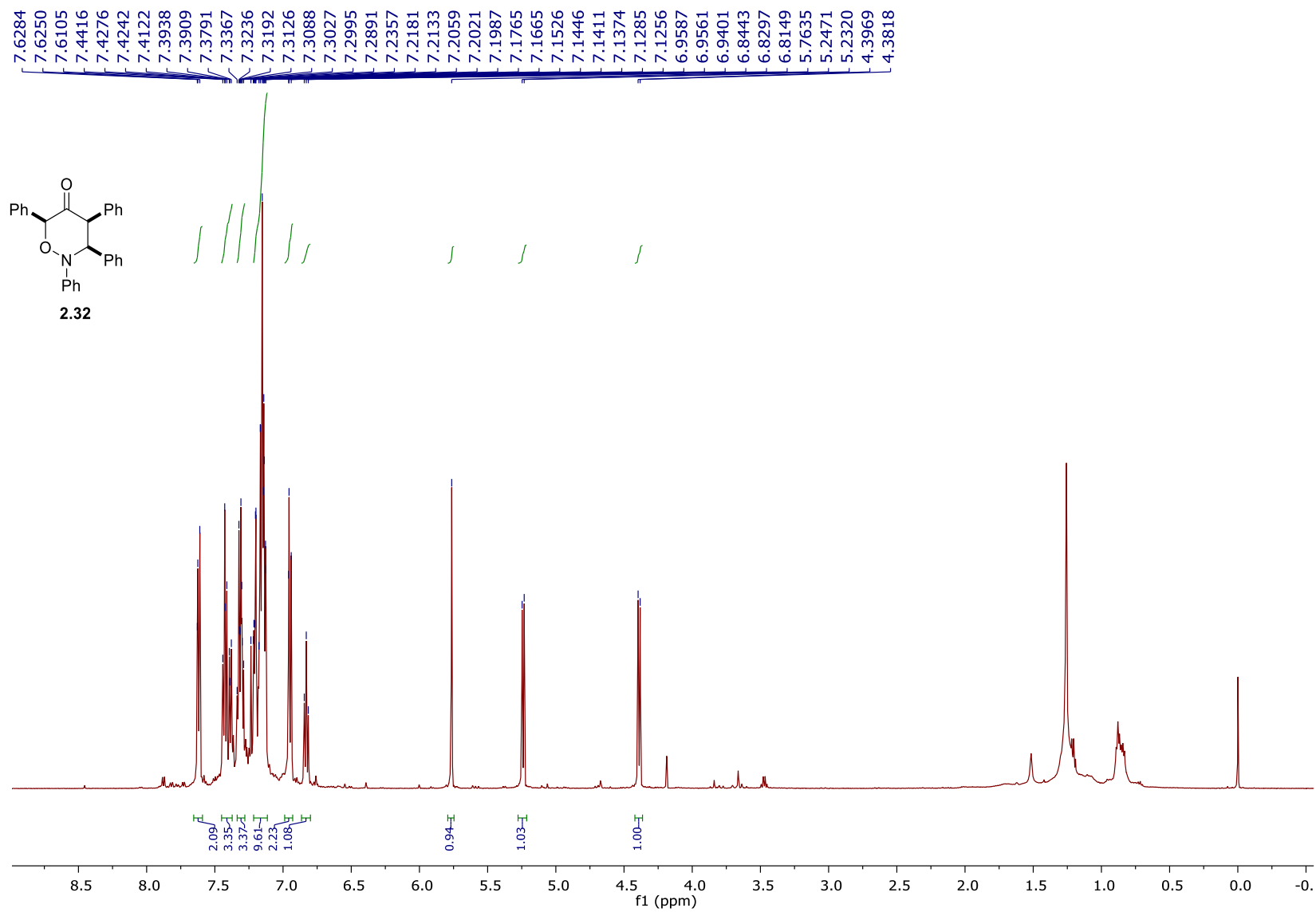


Figure 64. ¹H NMR spectrum of **2.32** (500 MHz, CDCl₃).

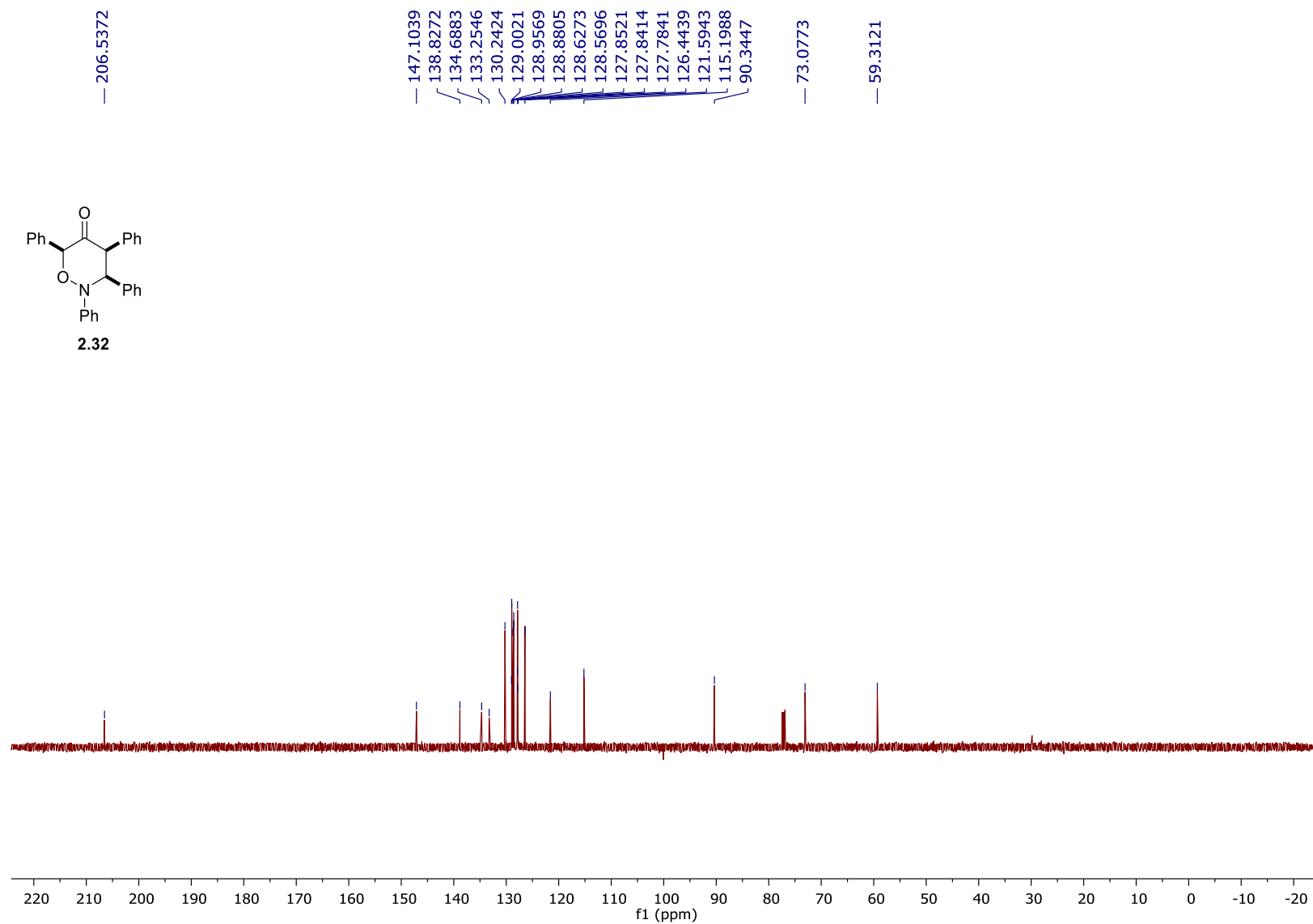


Figure 65. ^{13}C NMR spectrum of **2.32** (125 MHz, CDCl_3).

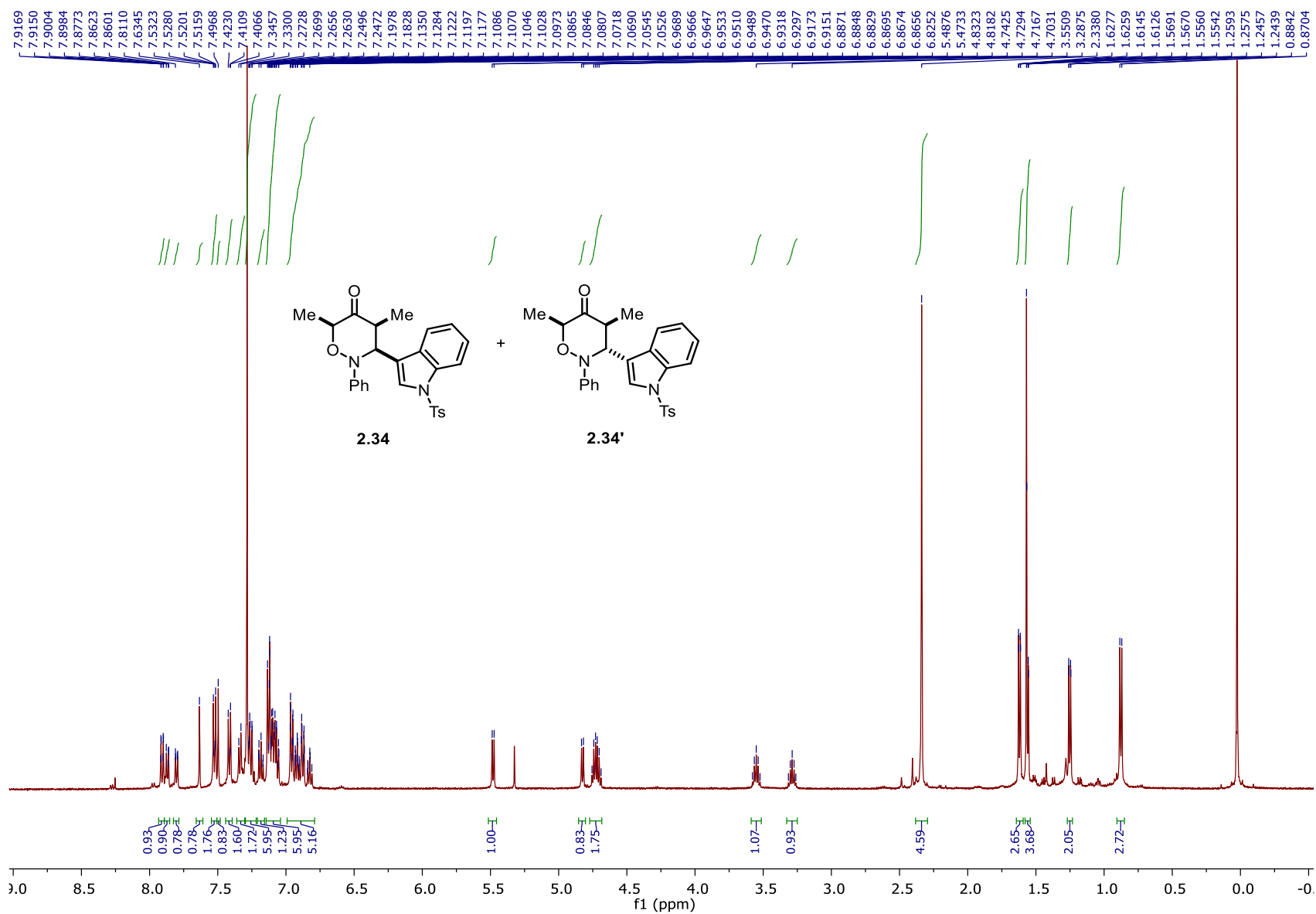


Figure 66. ¹H NMR spectrum of **2.34** (500 MHz, CDCl₃).

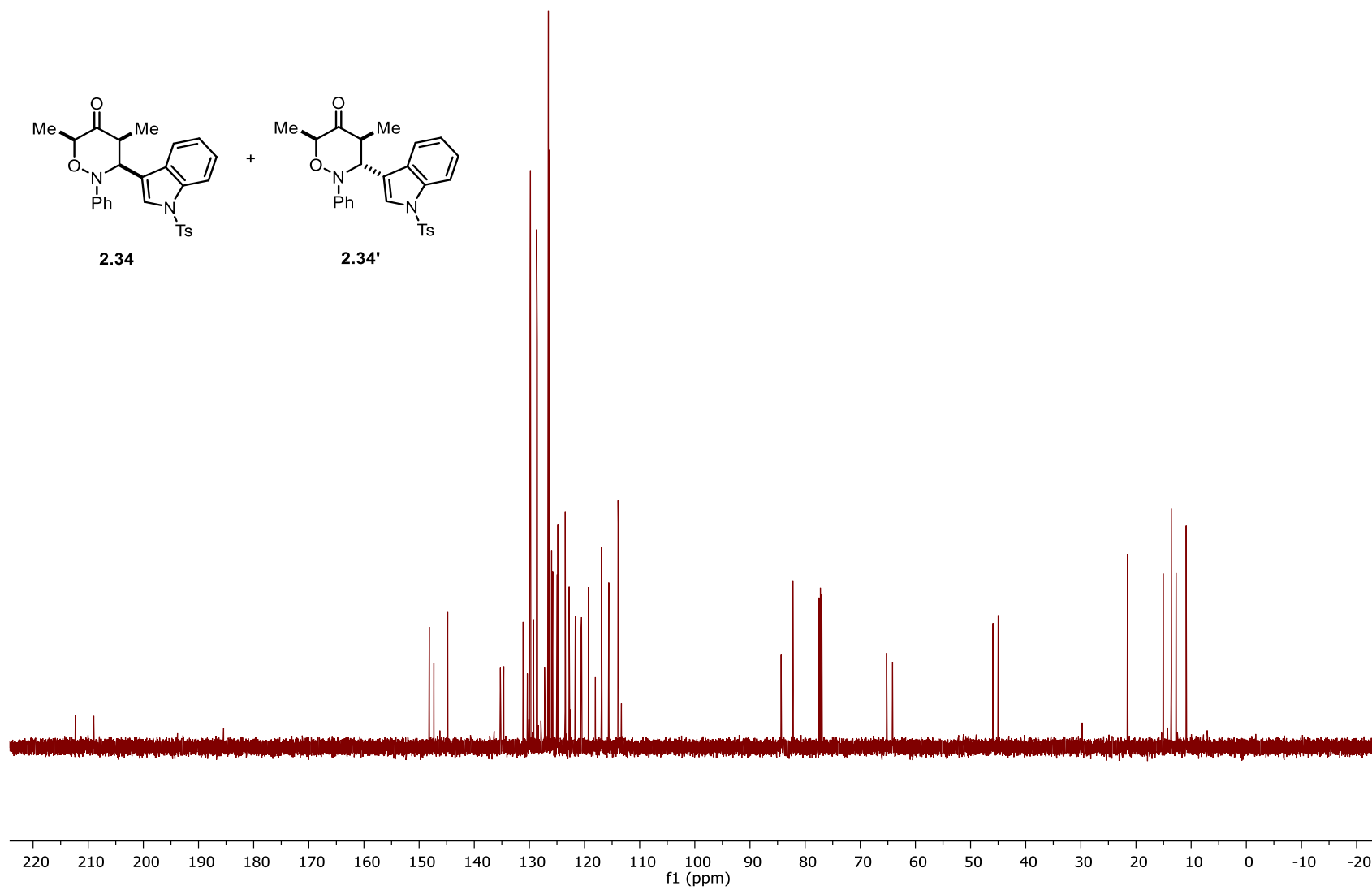


Figure 67. ^{13}C NMR spectrum of **2.34** (125 MHz, CDCl₃).

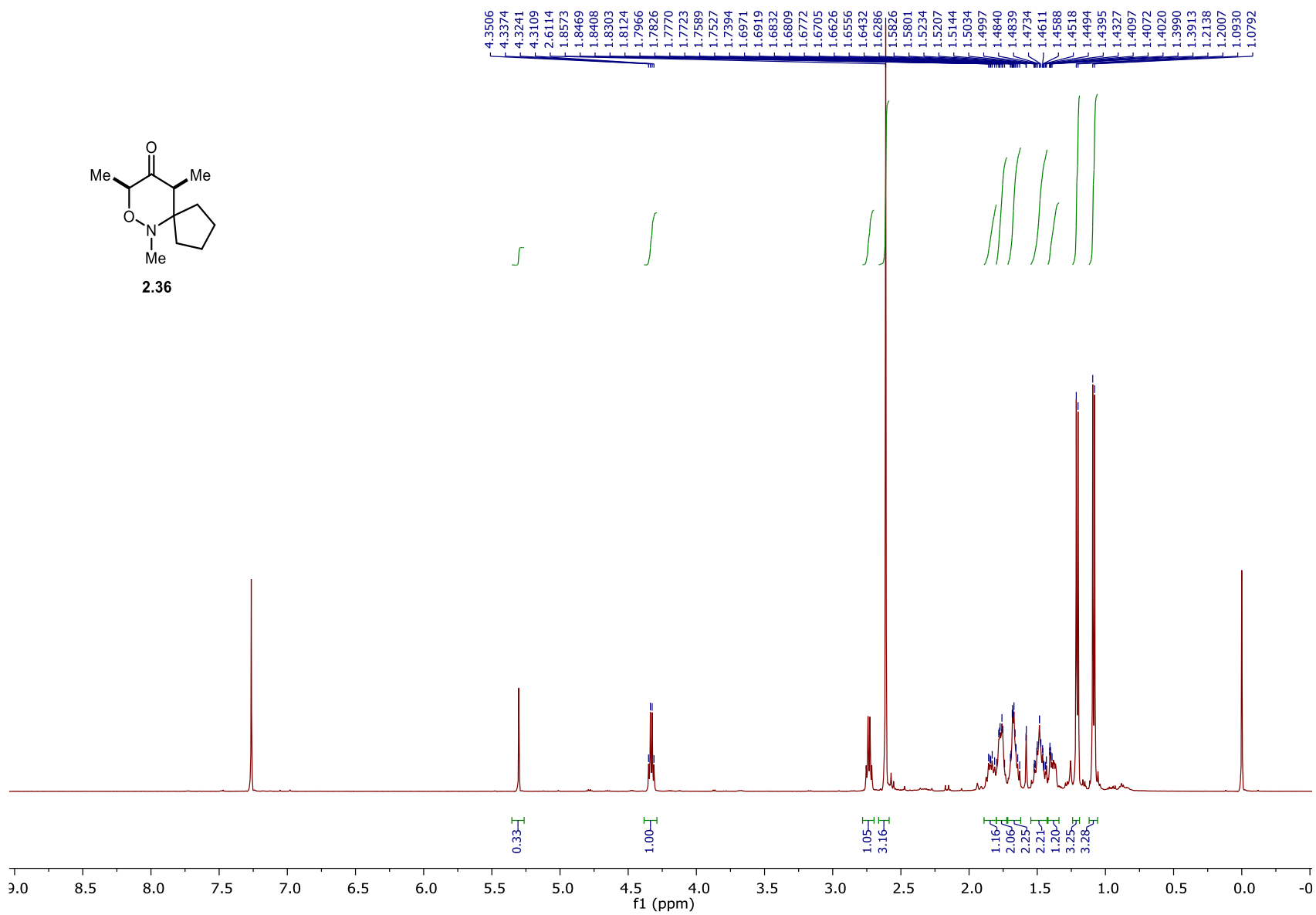


Figure 68. ¹H NMR spectrum of **2.36** (500 MHz, CDCl₃).

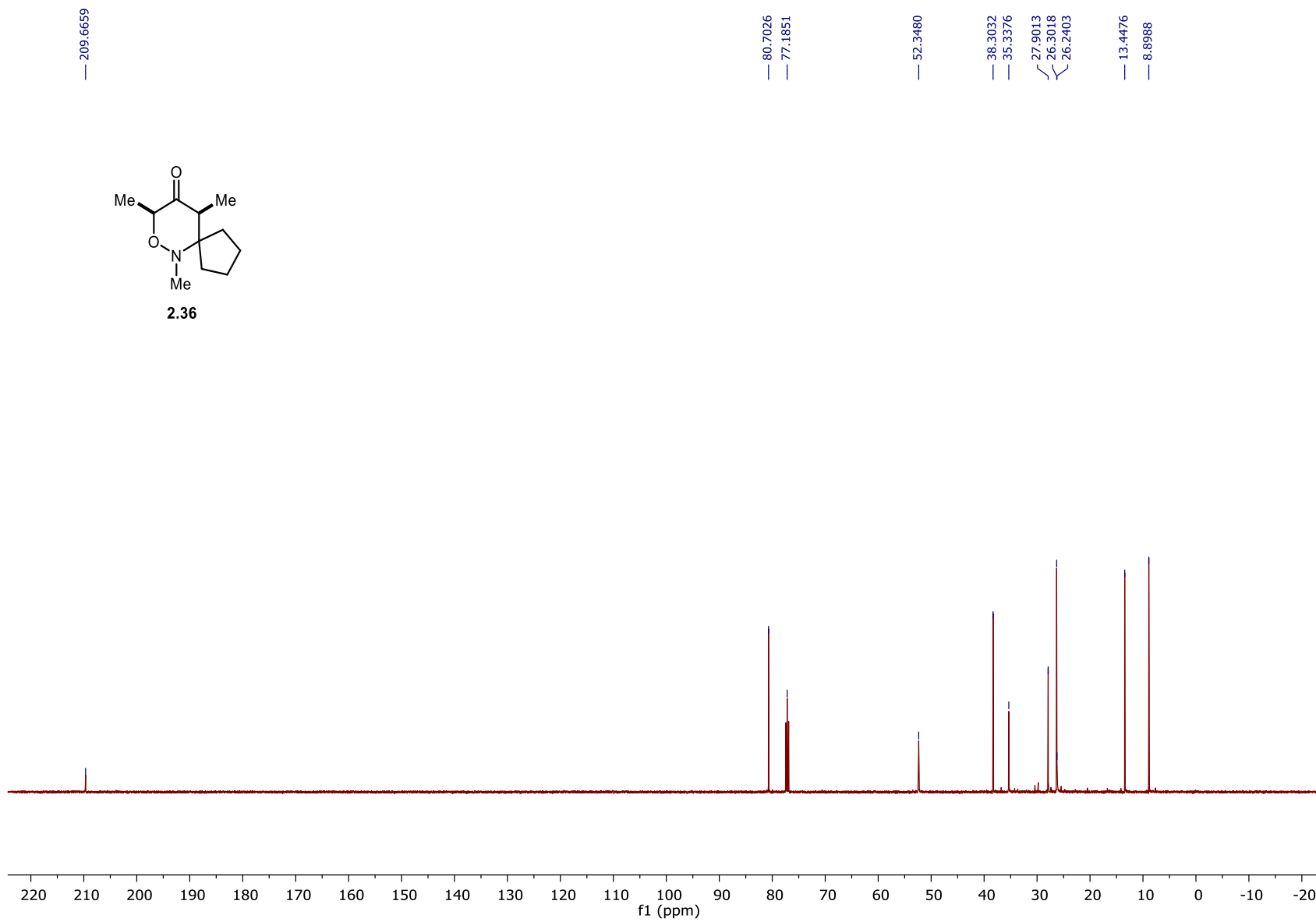


Figure 69. ¹³C NMR spectrum of **2.36** (125 MHz, CDCl₃).

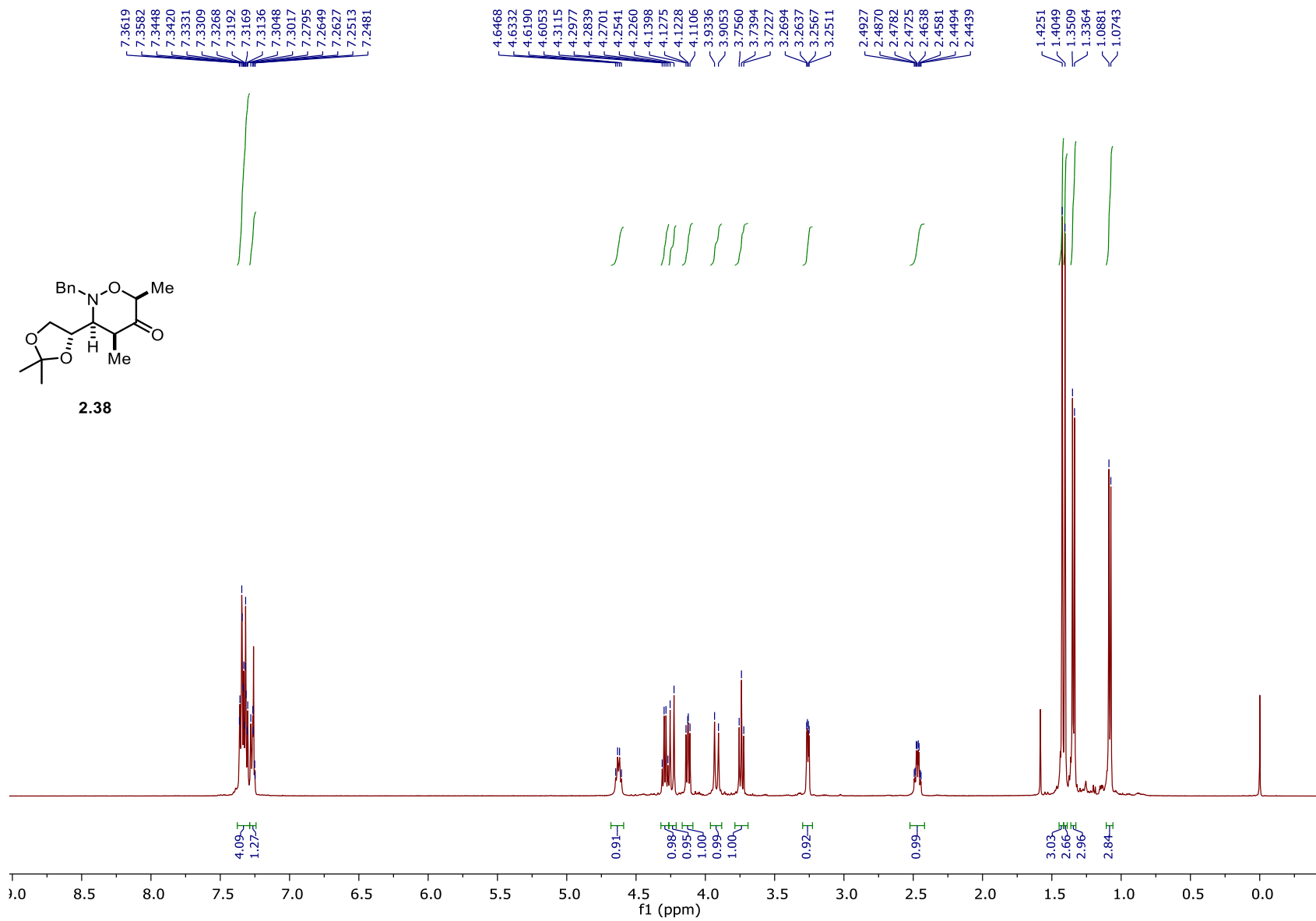


Figure 70. ^1H NMR spectrum of **2.38** (500 MHz, CDCl_3).

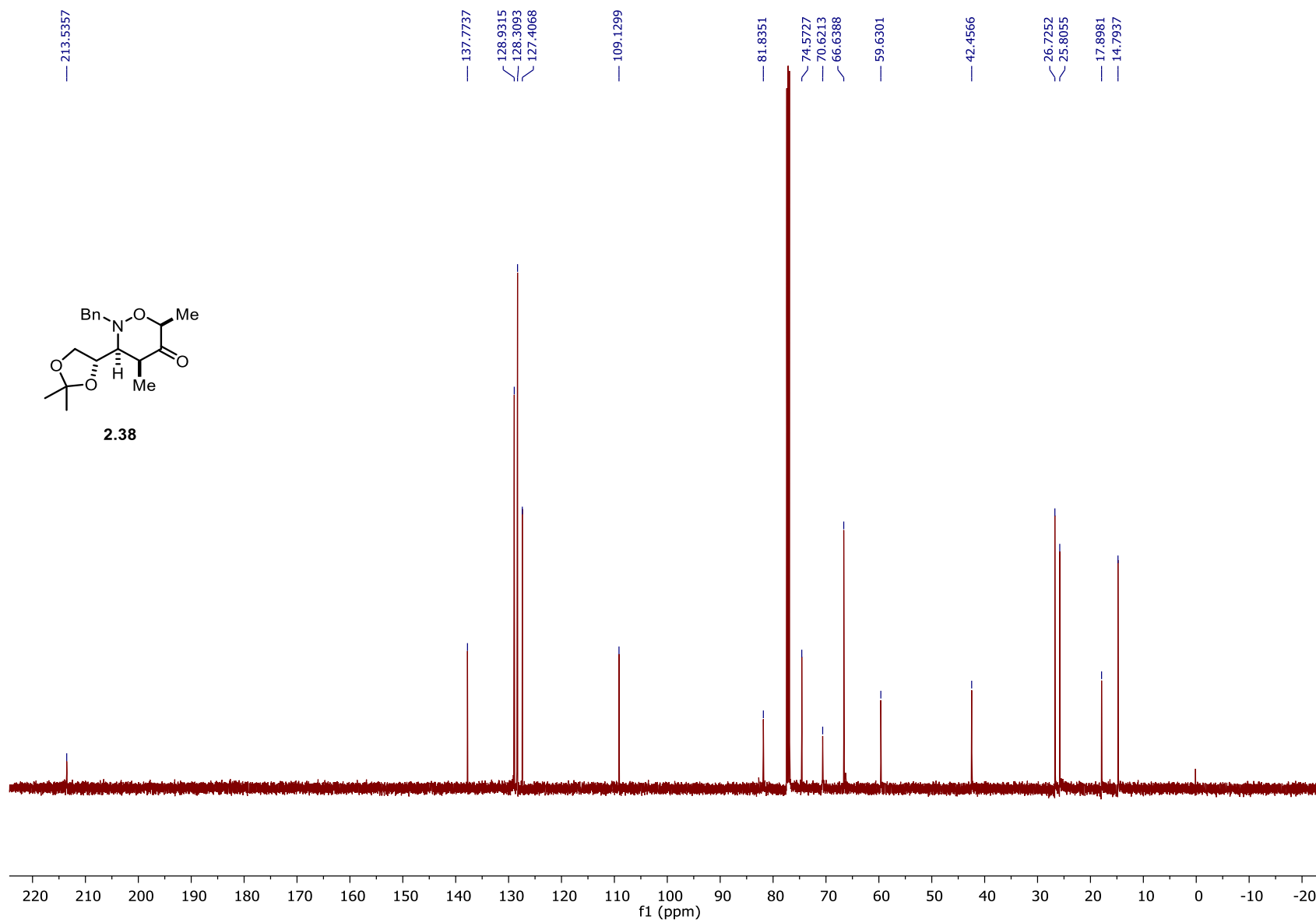


Figure 71. ^{13}C NMR spectrum of **2.38** (125 MHz, CDCl_3).

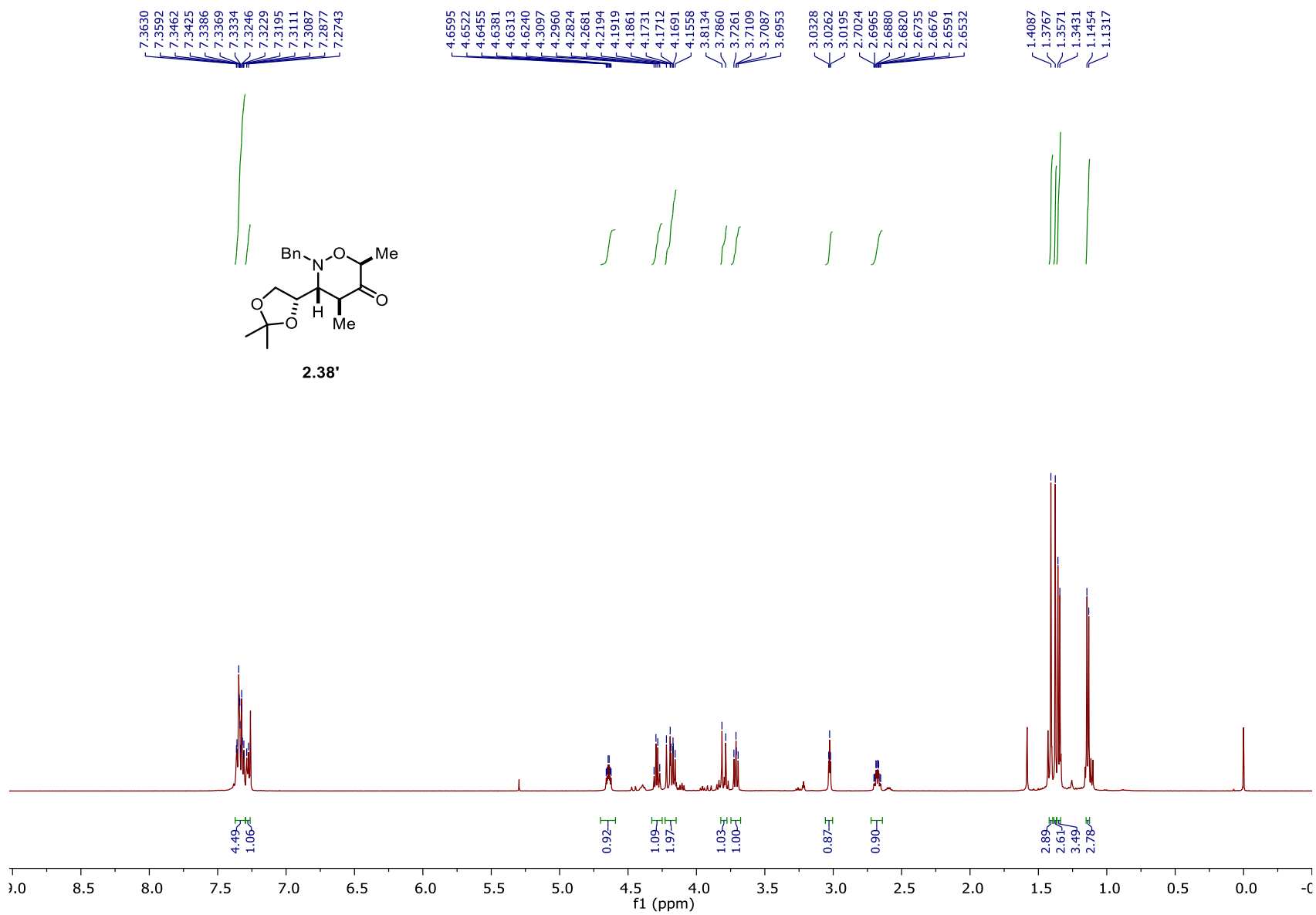


Figure 72. ^1H NMR spectrum of **2.38'** (500 MHz, CDCl_3).

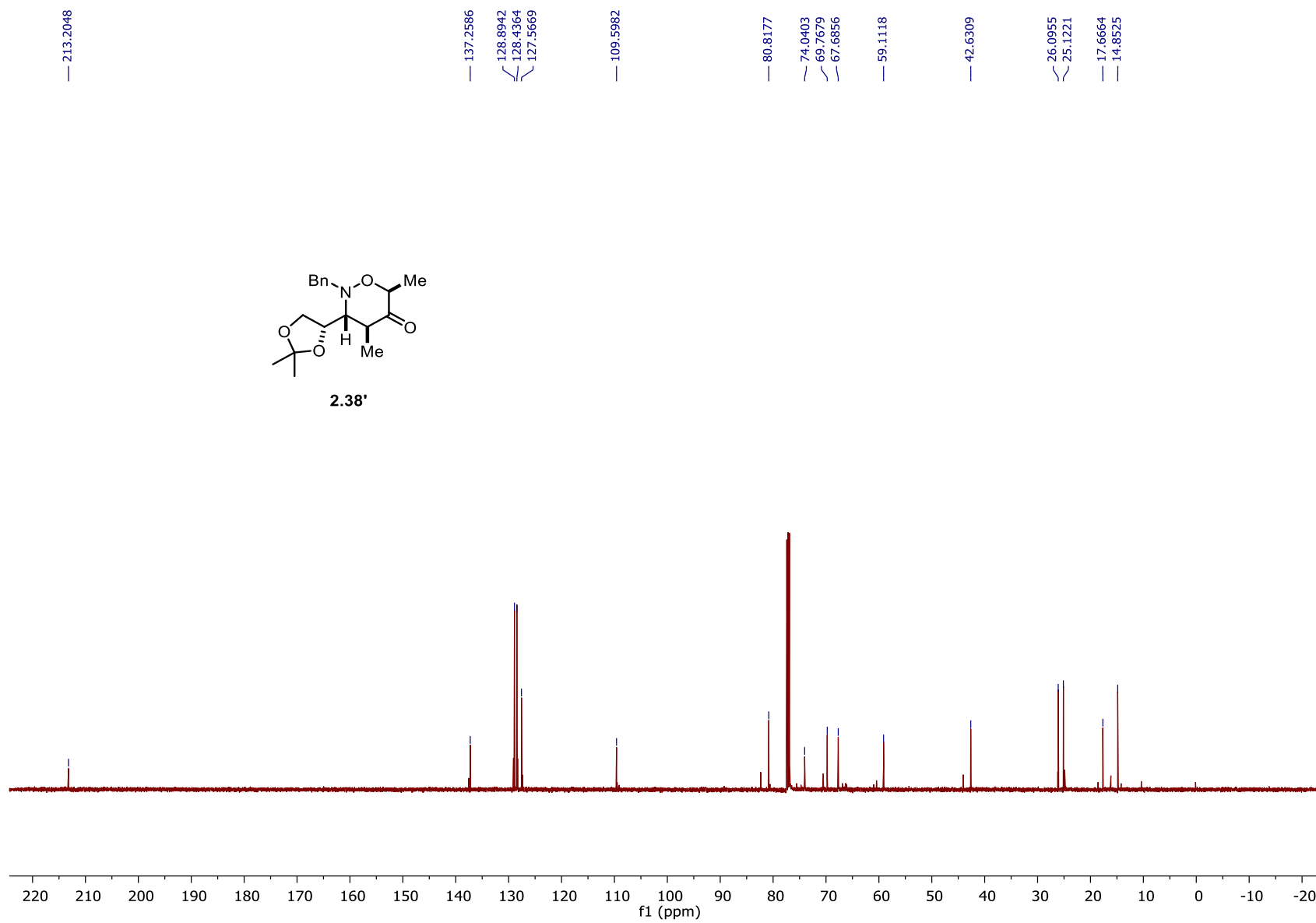


Figure 73. ^{13}C NMR spectrum of **2.38'** (125 MHz, CDCl_3).

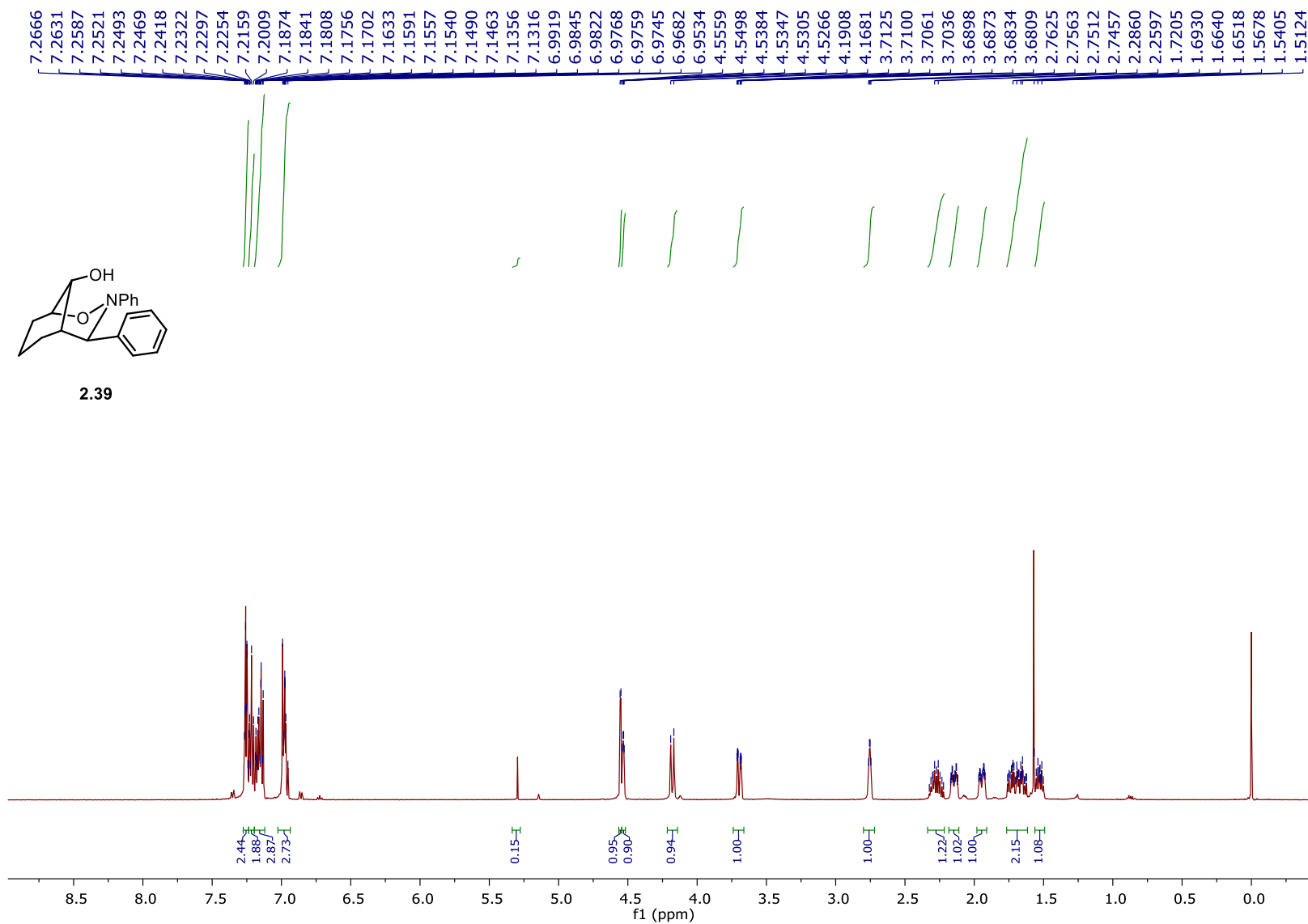


Figure 74. ^1H NMR spectrum of **2.39** (500 MHz, CDCl_3).

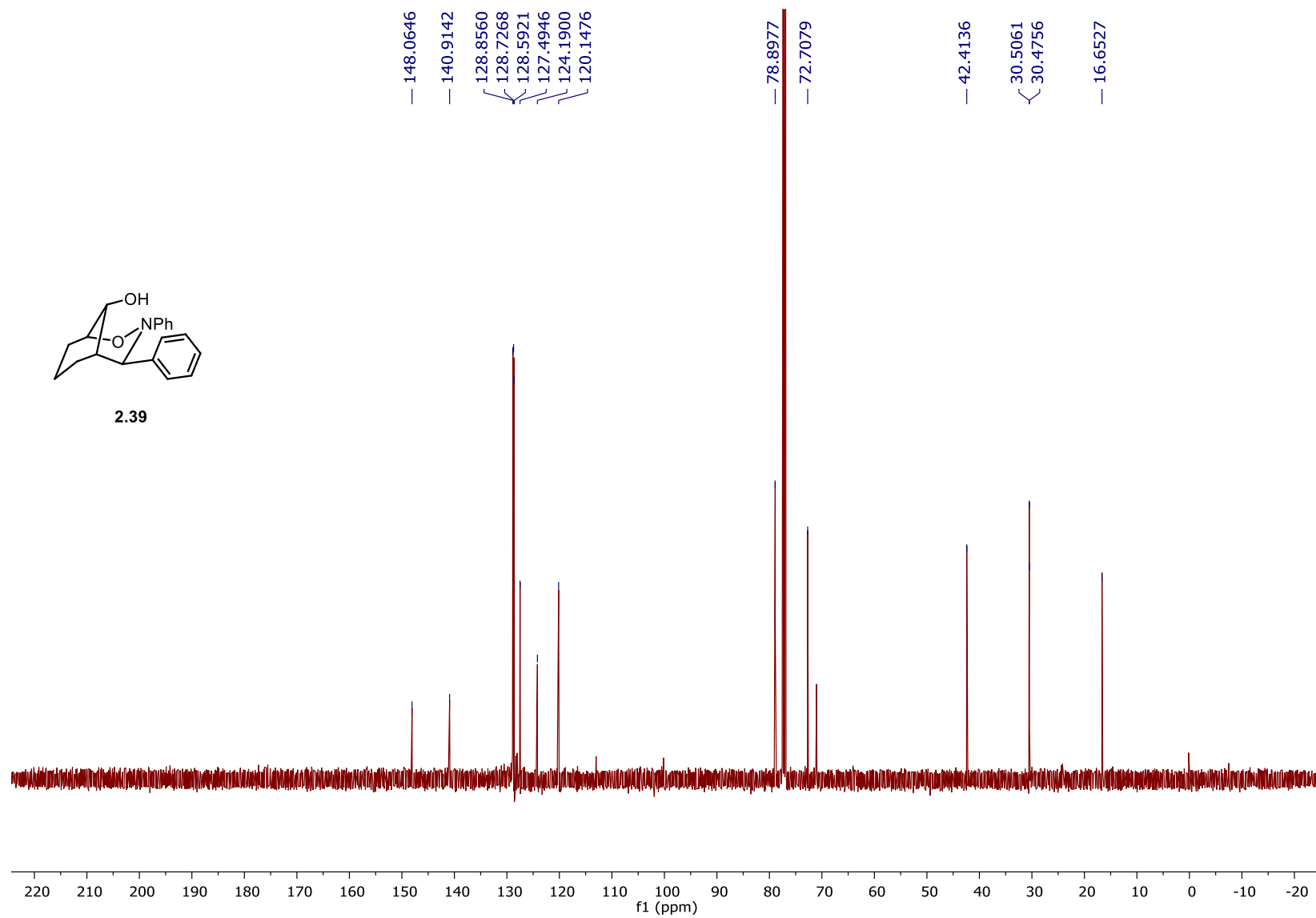


Figure 75. ^{13}C NMR spectrum of **2.39** (125 MHz, CDCl_3).

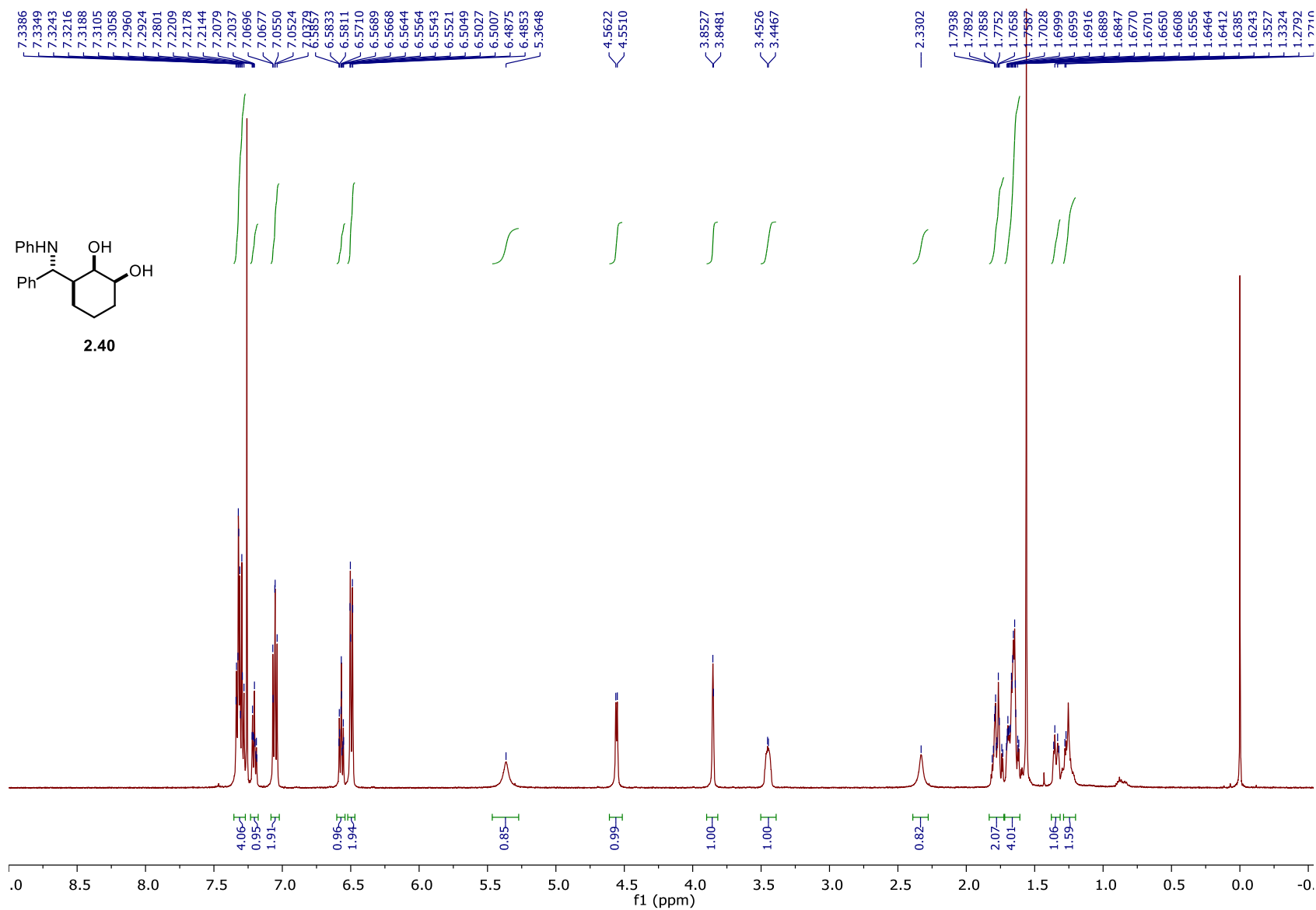


Figure 76. ^1H NMR spectrum of **2.40** (500 MHz, CDCl_3).

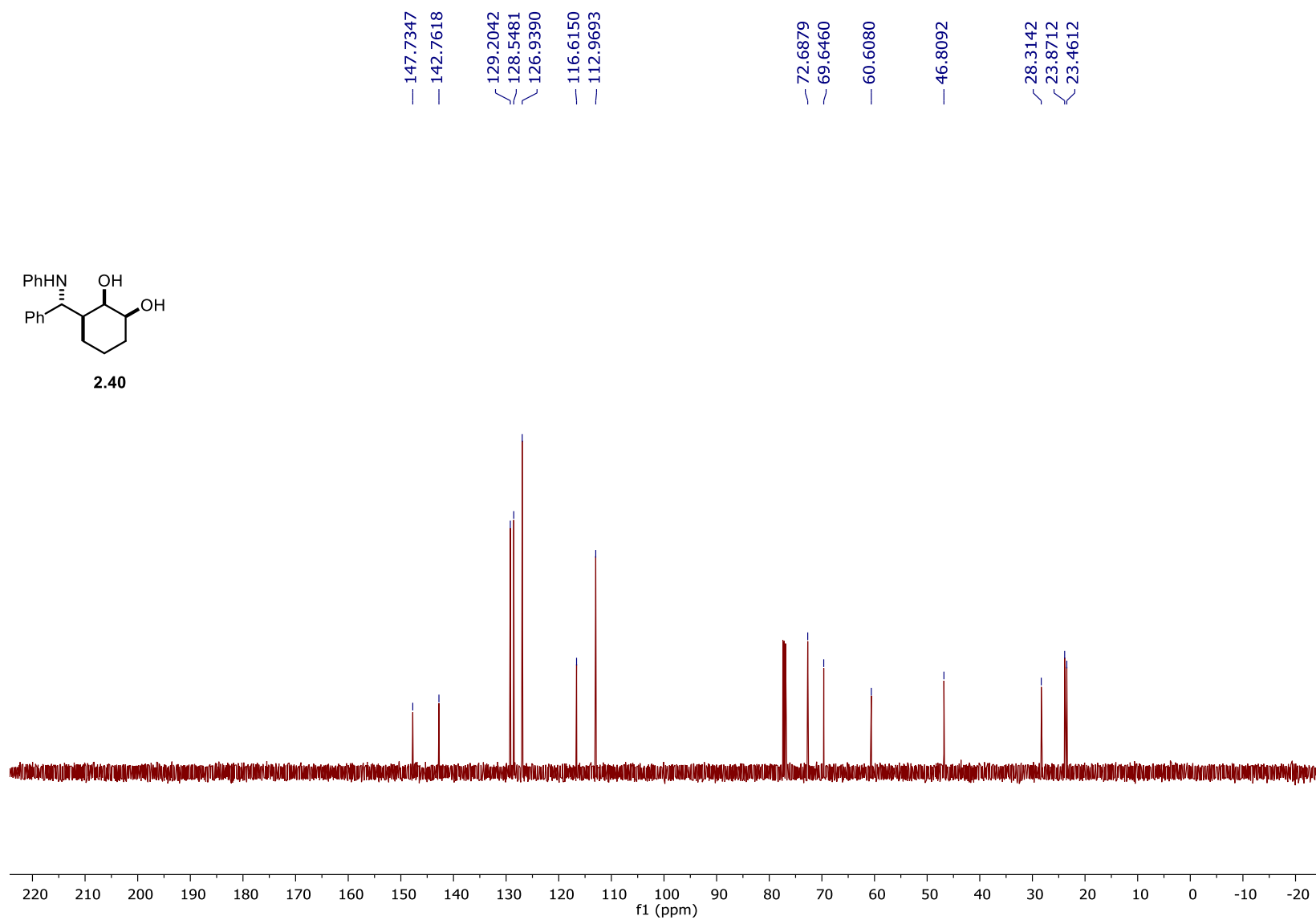
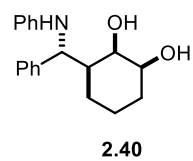


Figure 77. ^{13}C NMR spectrum of **2.40** (125 MHz, CDCl_3).

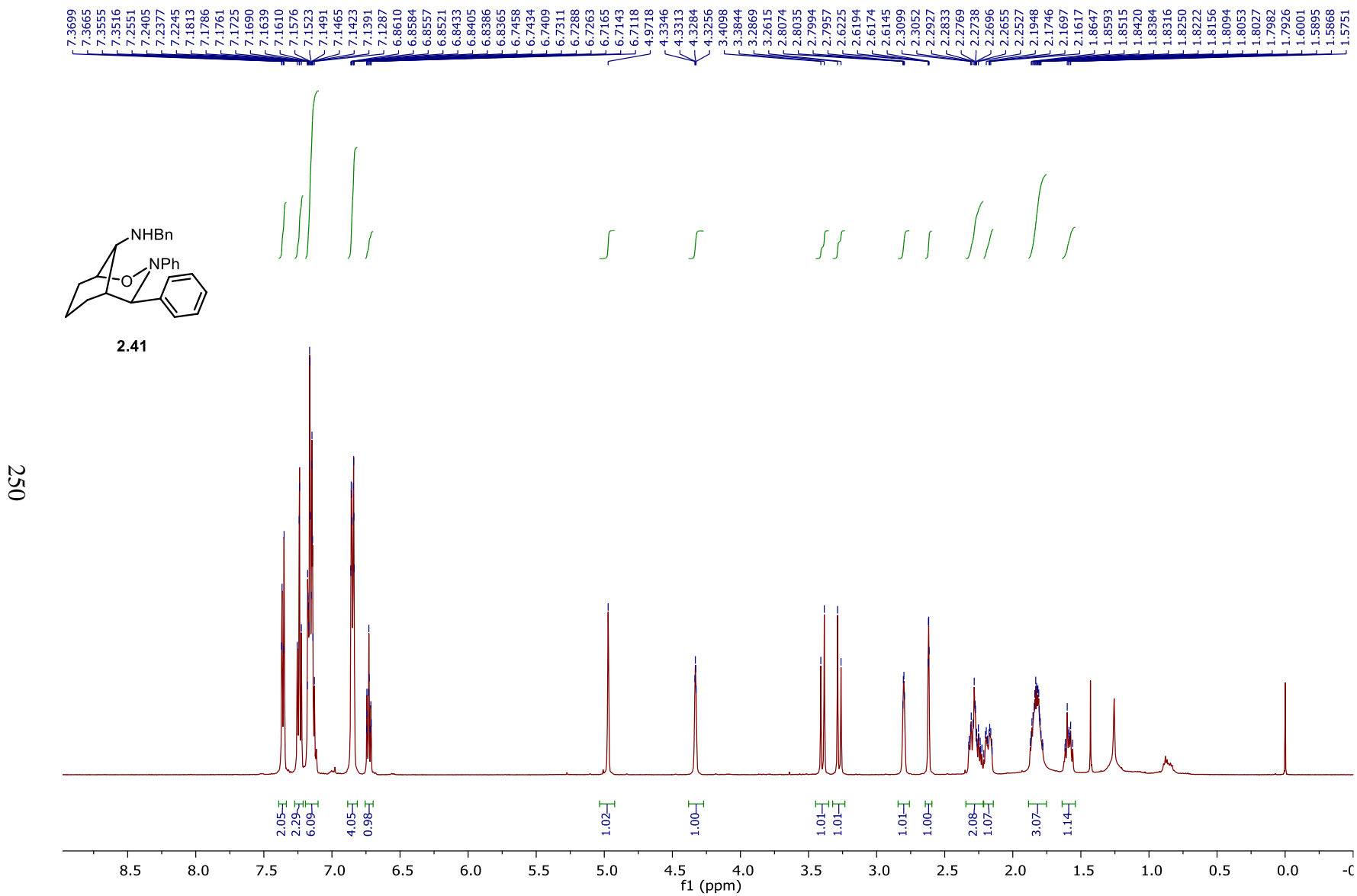
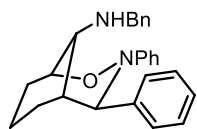
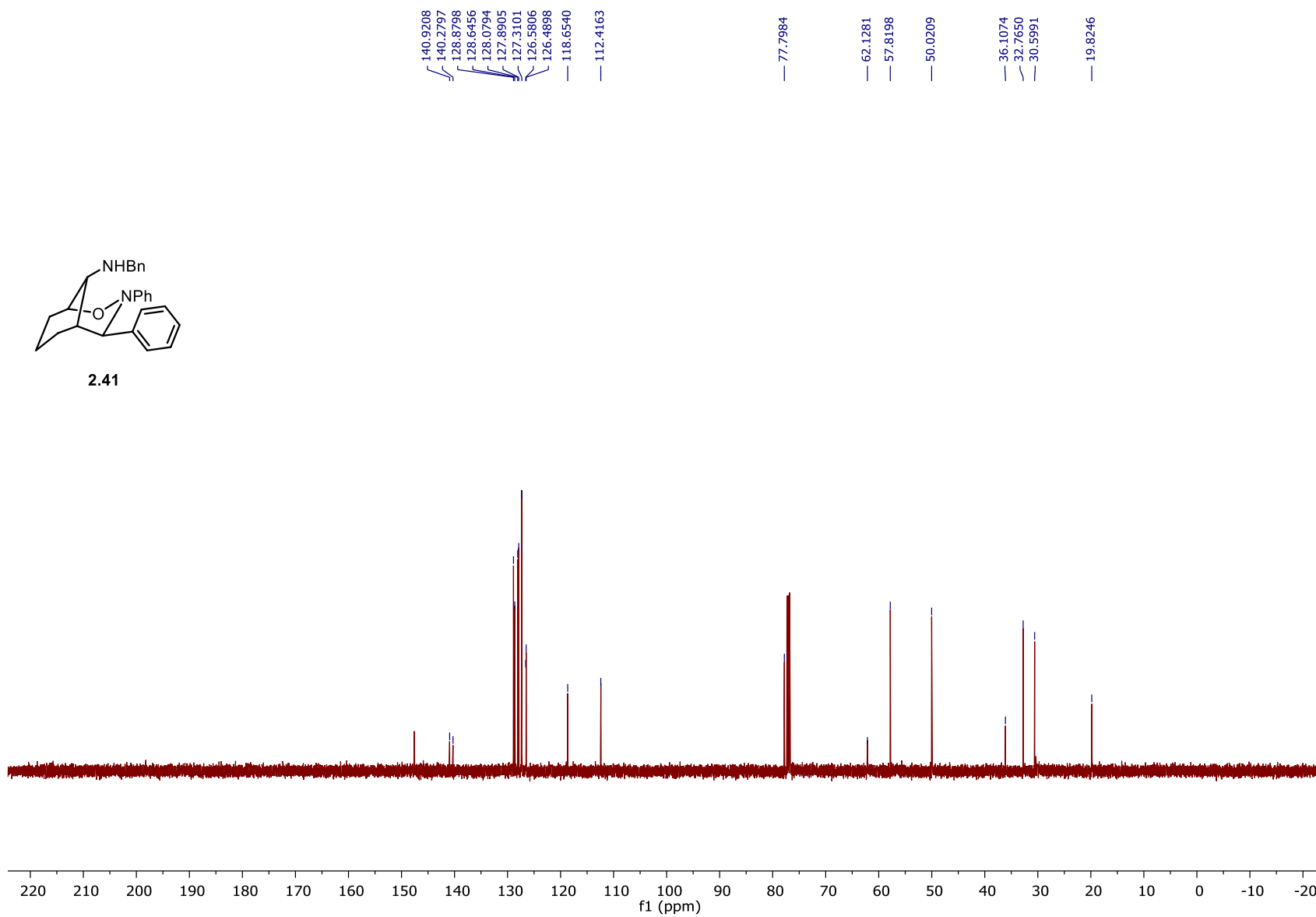


Figure 78. ^1H NMR spectrum of **2.41** (500 MHz, CDCl_3).

**2.41****Figure 79.** ^{13}C NMR spectrum of **2.41** (125 MHz, CDCl_3).

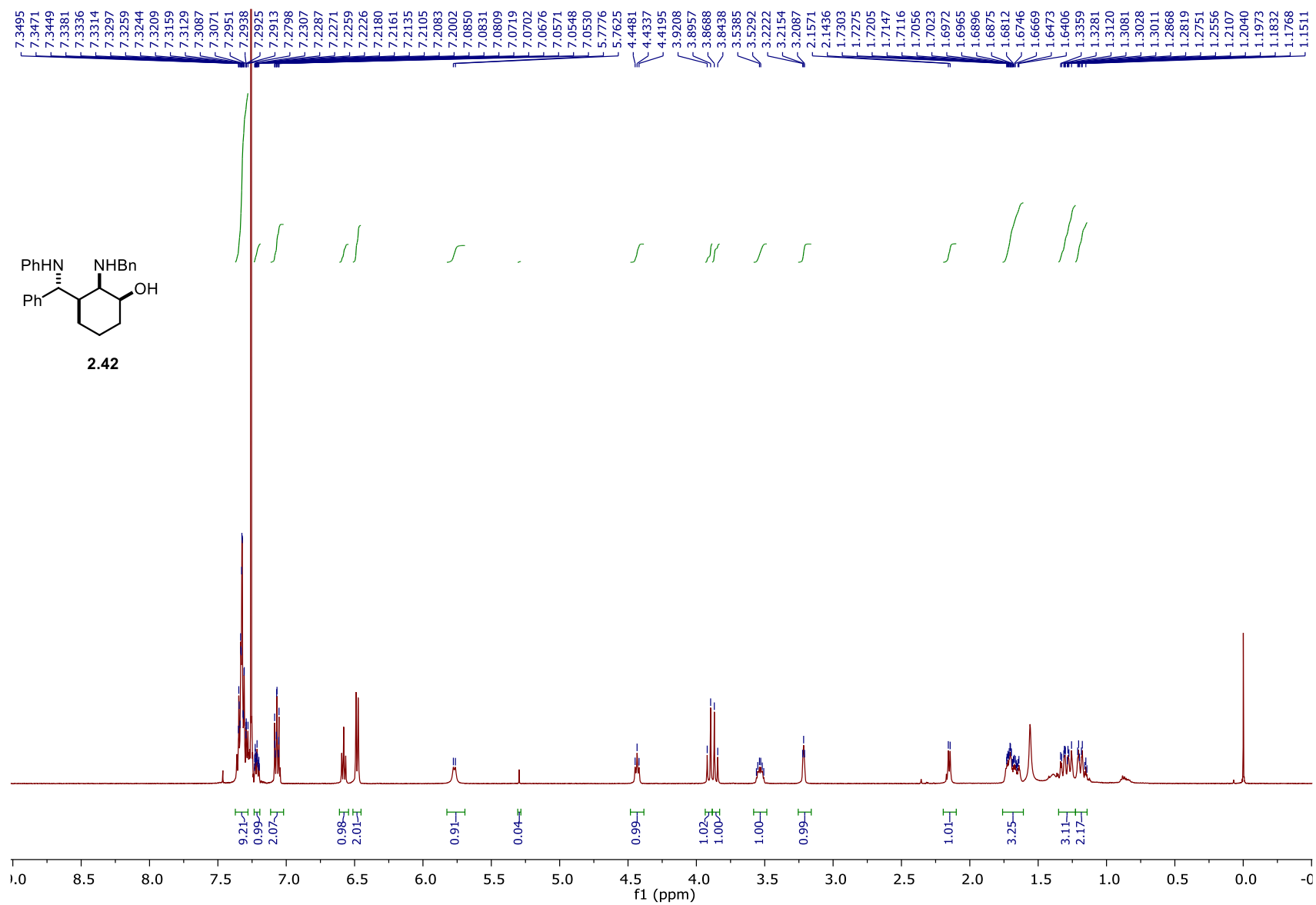


Figure 80. ^1H NMR spectrum of **2.42** (500 MHz, CDCl_3).

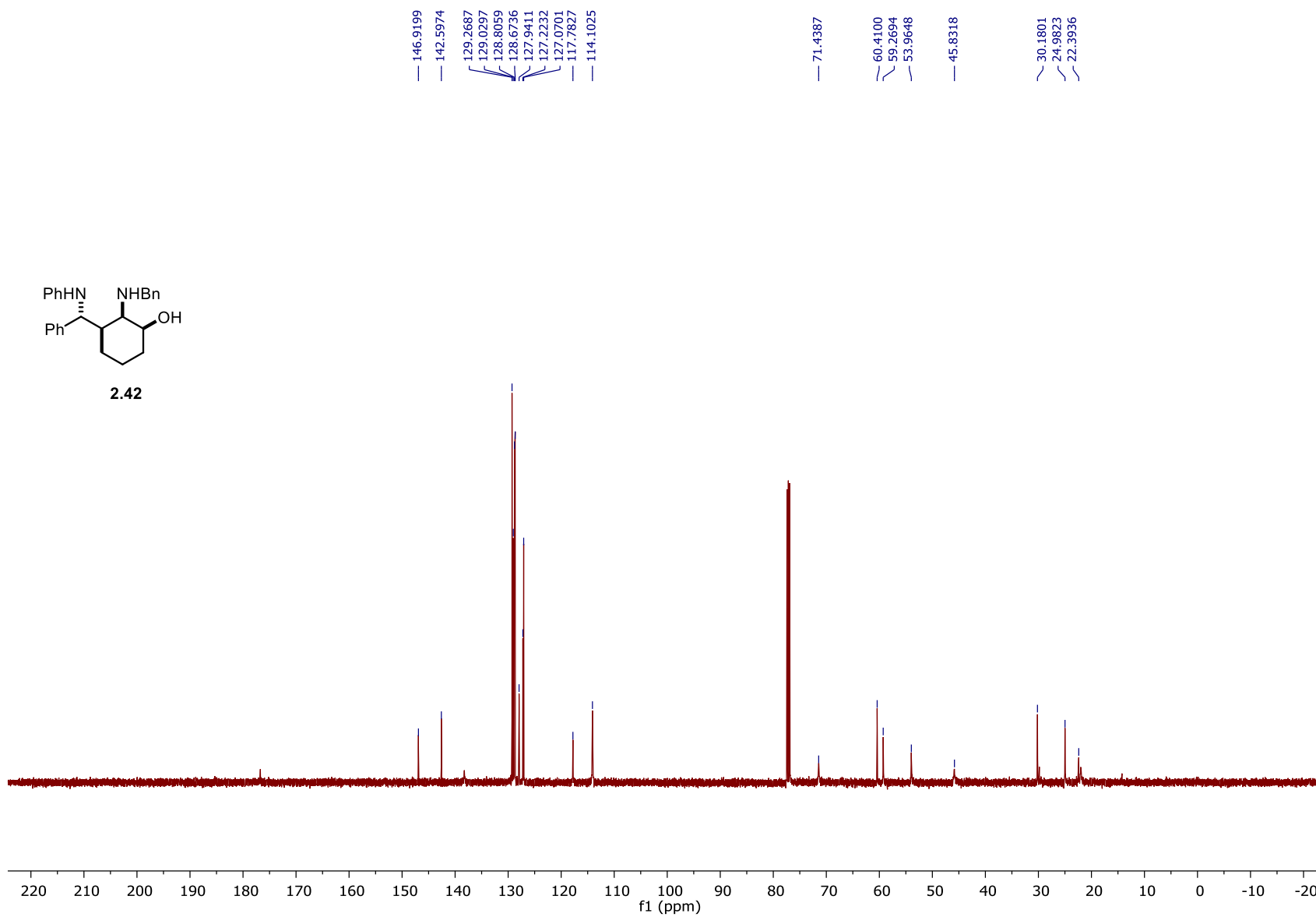


Figure 81. ^{13}C NMR spectrum of **2.42** (125 MHz, CDCl_3).

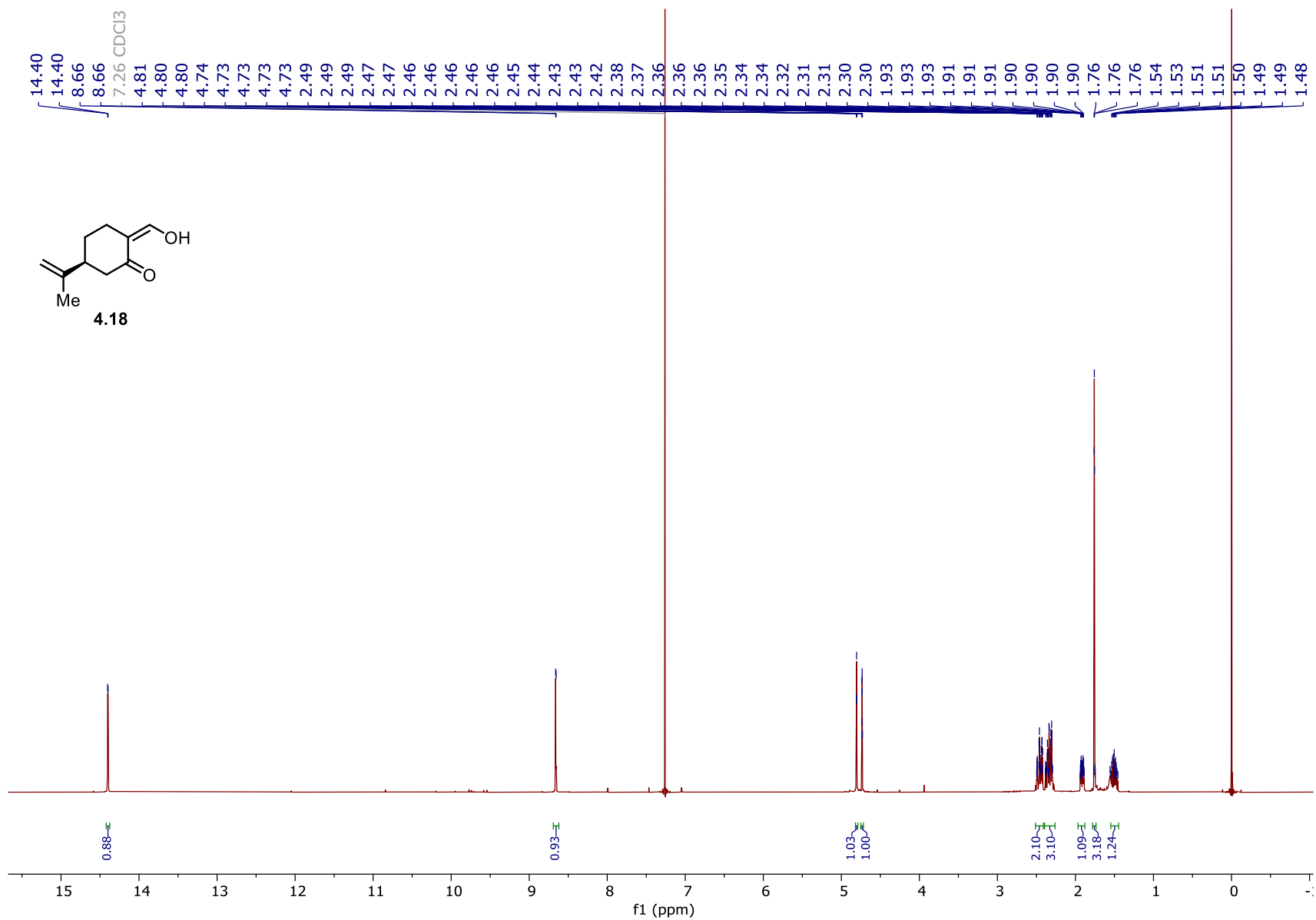


Figure 82. ¹H NMR spectrum of **4.18** (500 MHz, CDCl₃).

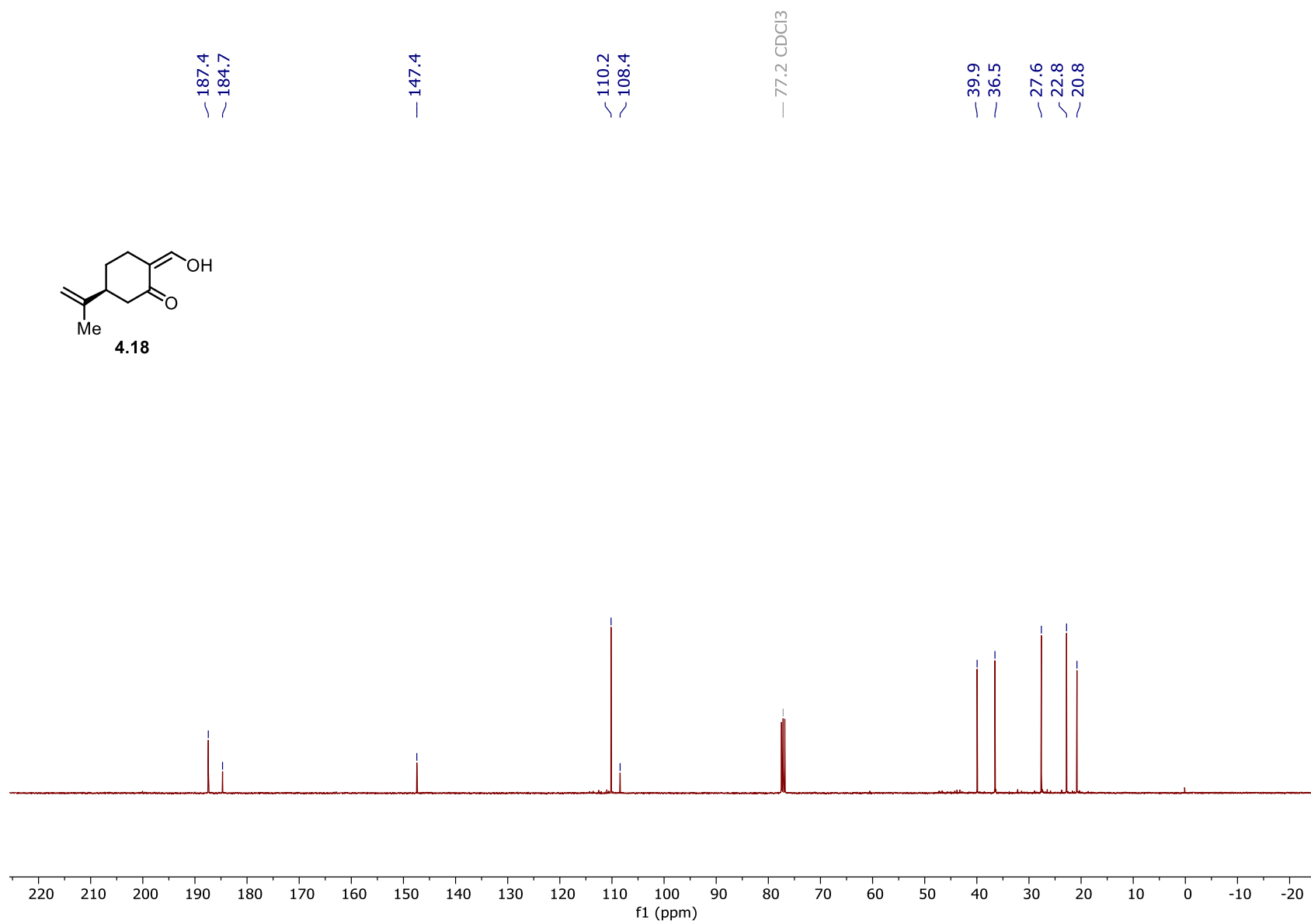


Figure 83. ^{13}C NMR spectrum of **4.18** (125 MHz, CDCl₃).

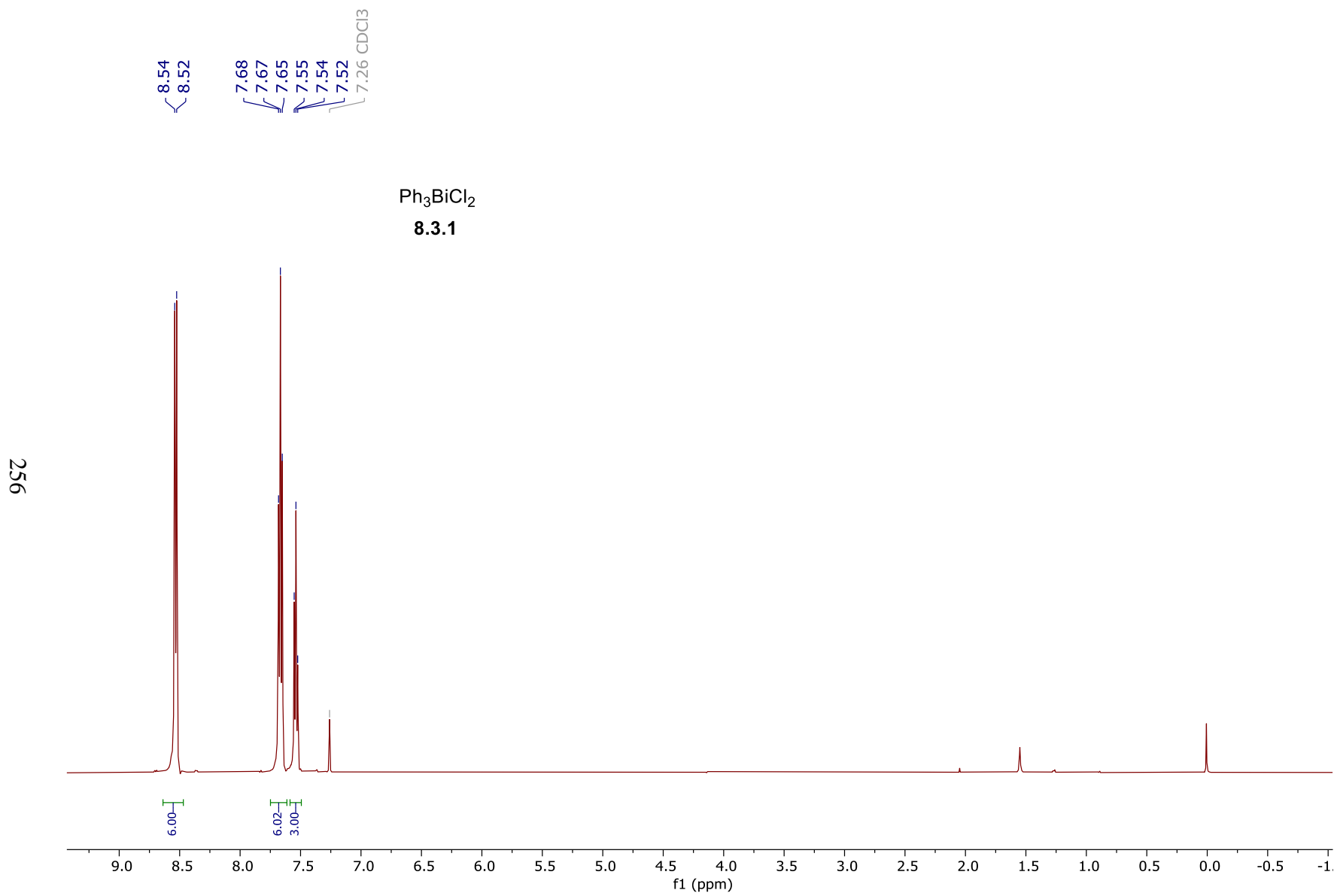


Figure 84. ^1H NMR spectrum of **8.3.1** (500 MHz, CDCl_3).

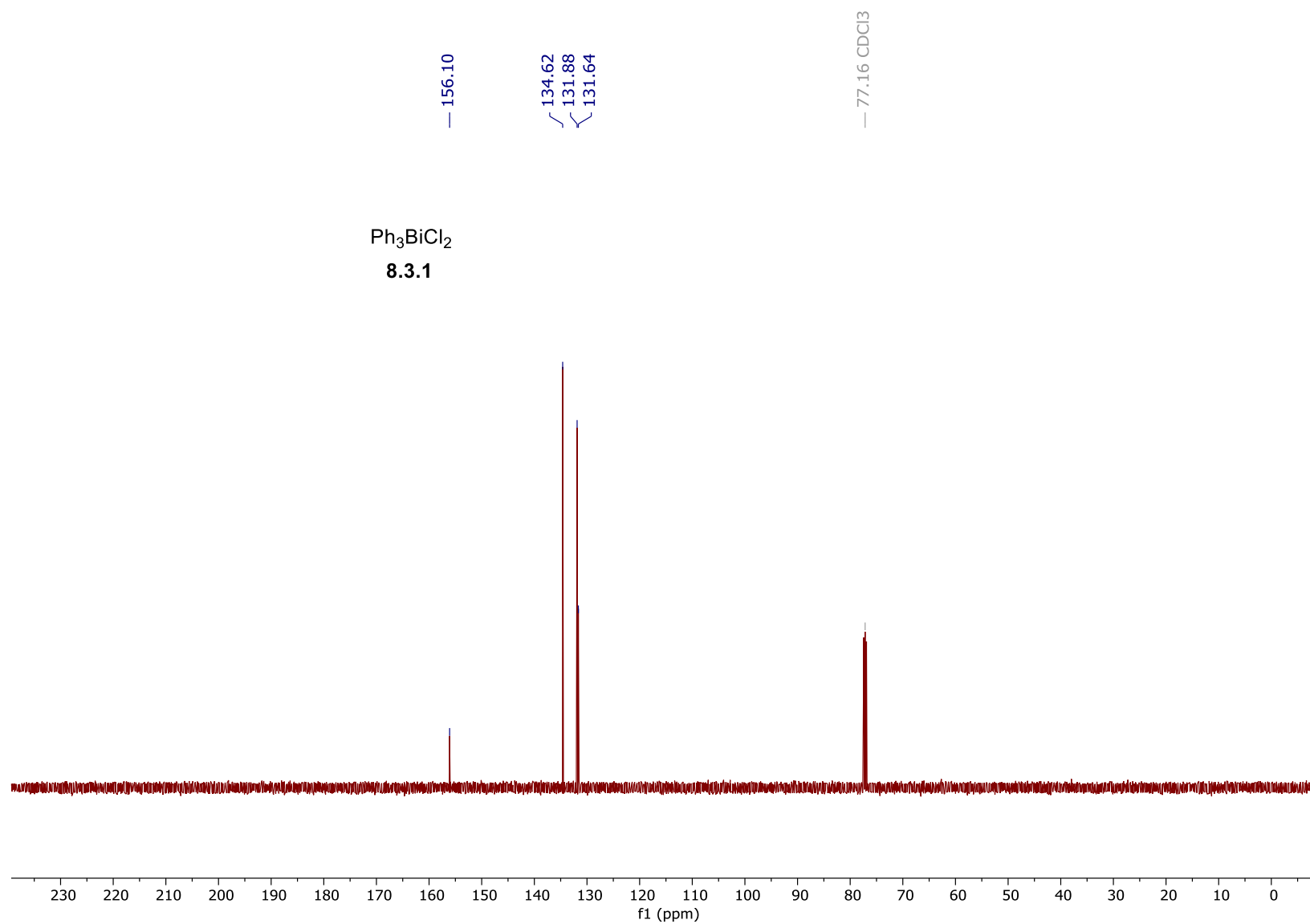


Figure 85. ^{13}C NMR spectrum of **8.3.1** (125 MHz, CDCl_3).

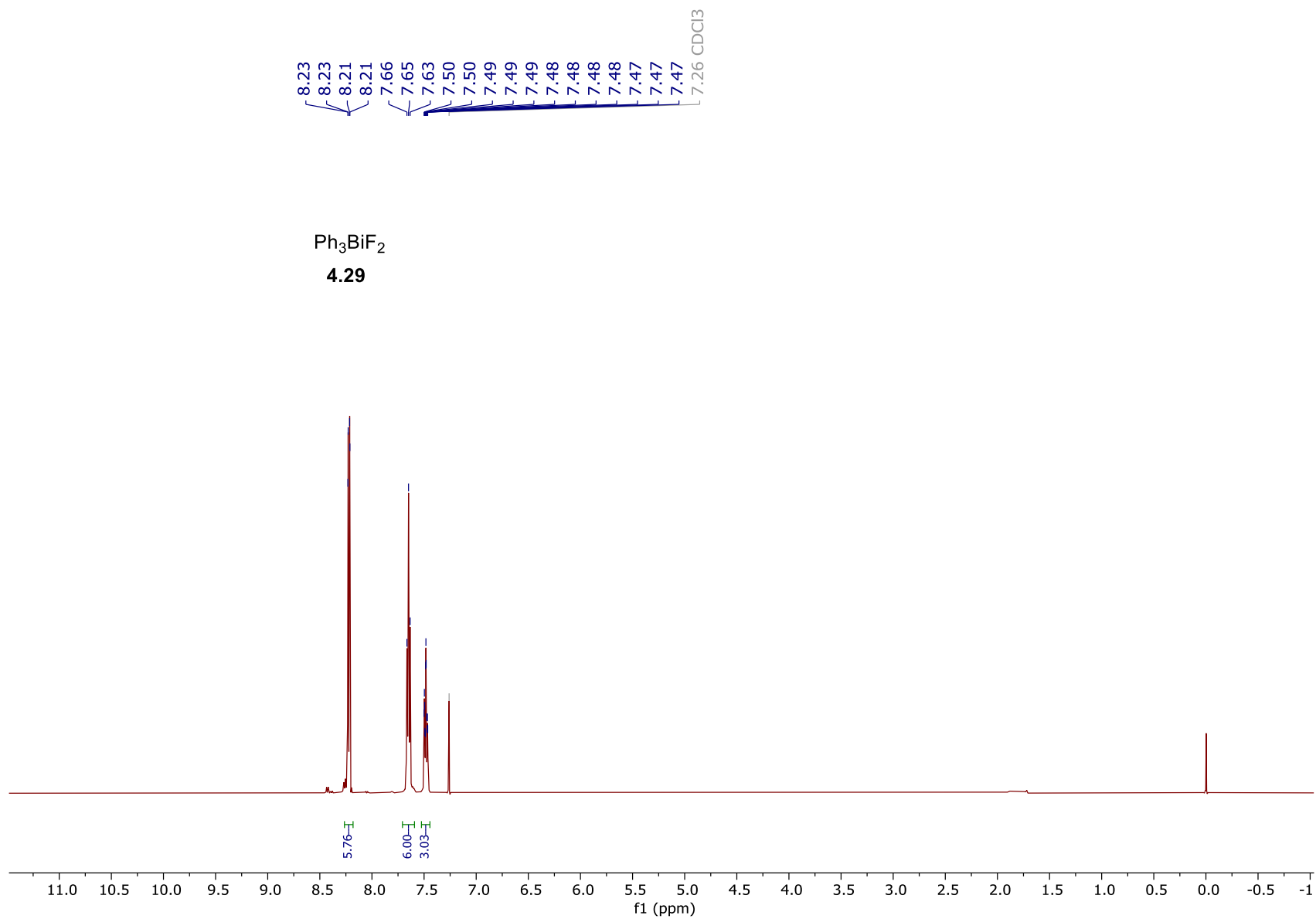


Figure 86. ¹H NMR spectrum of **4.29** (500 MHz, CDCl₃).



Figure 87. ¹³C NMR spectrum of **2.42** (125 MHz, CDCl₃).

260

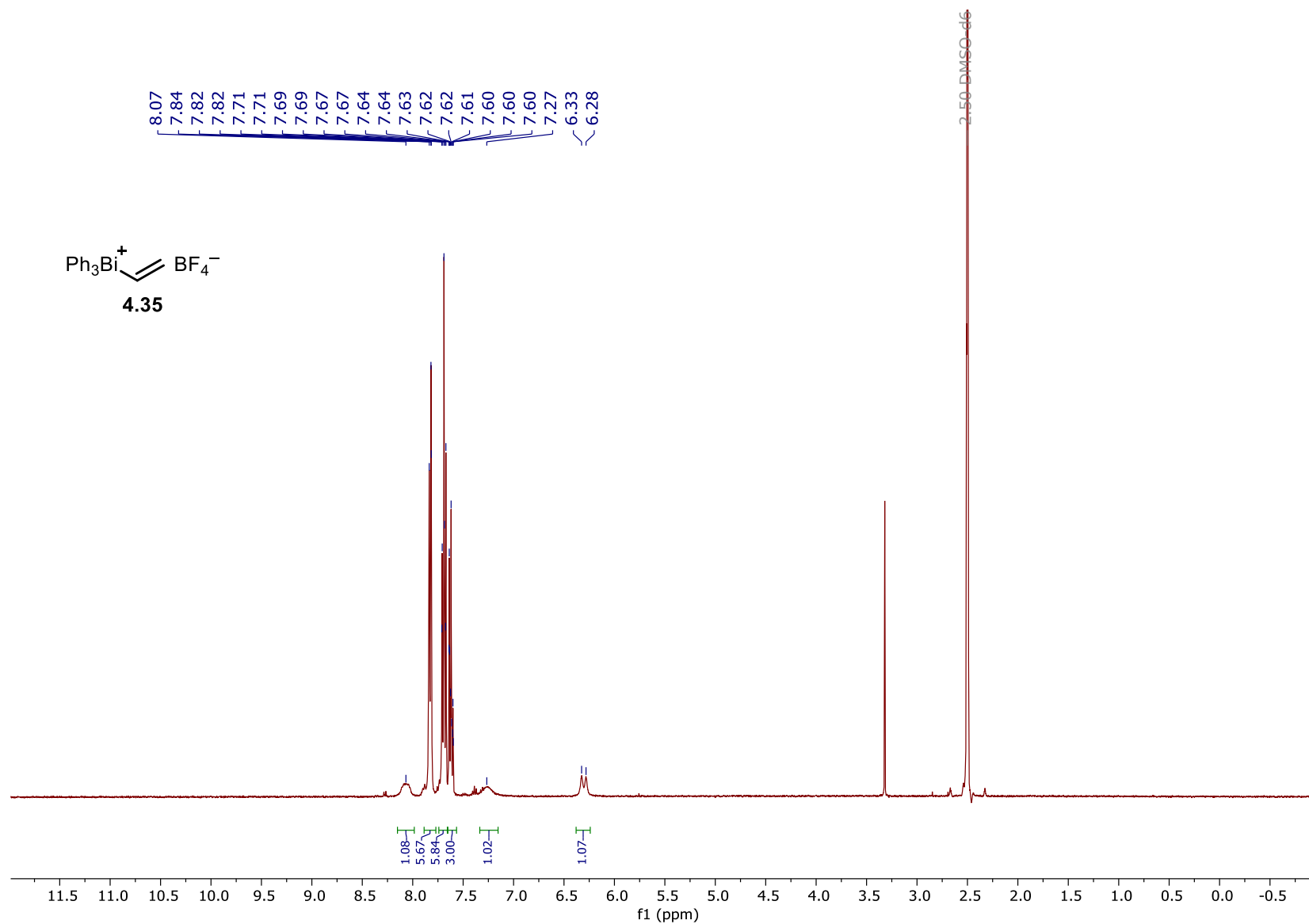


Figure 88. ^1H NMR spectrum of **4.35** (400 MHz, $\text{DMSO}-d_6$).

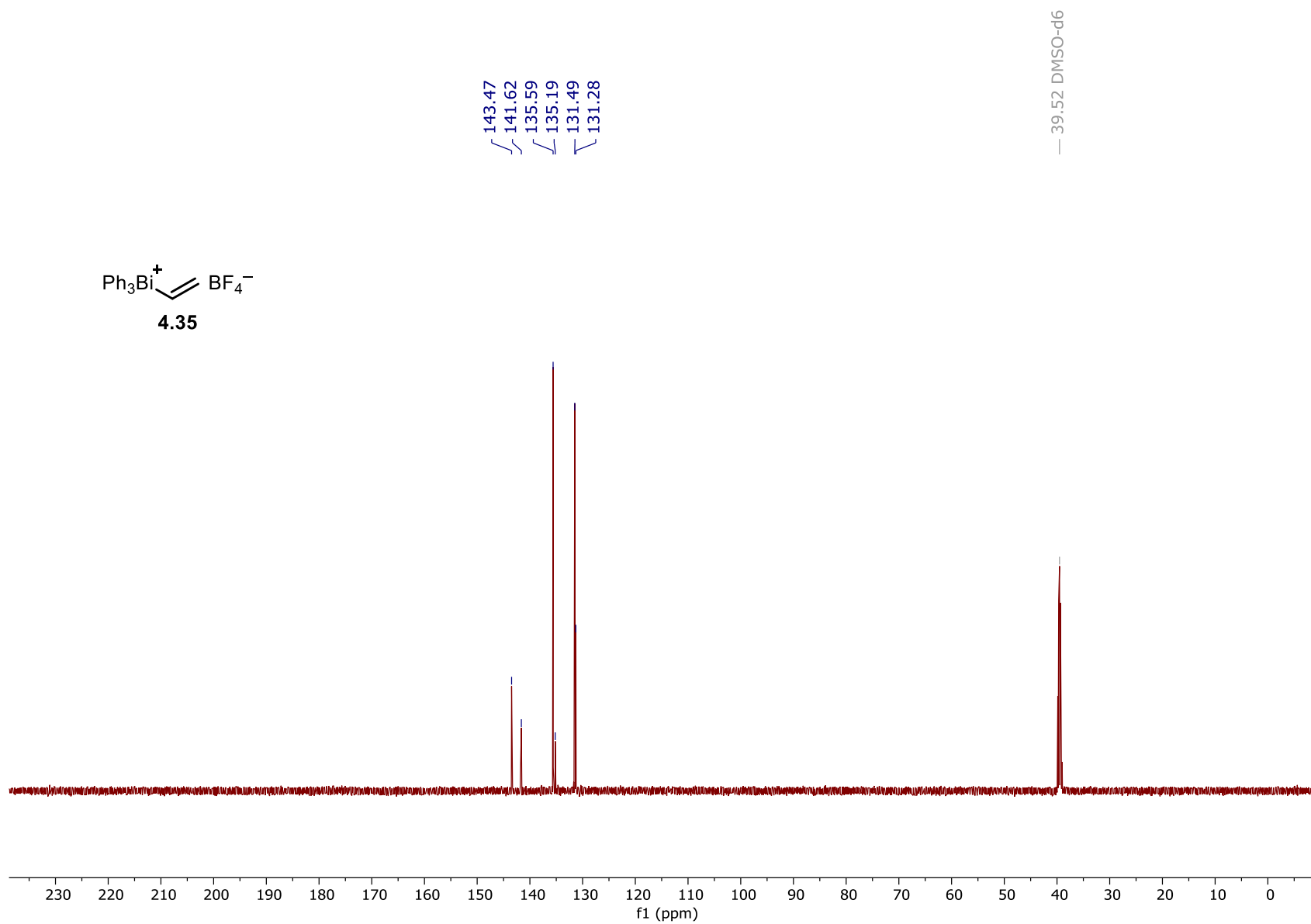


Figure 89. ^{13}C NMR spectrum of **4.35** (125 MHz, $\text{DMSO-}d_6$).

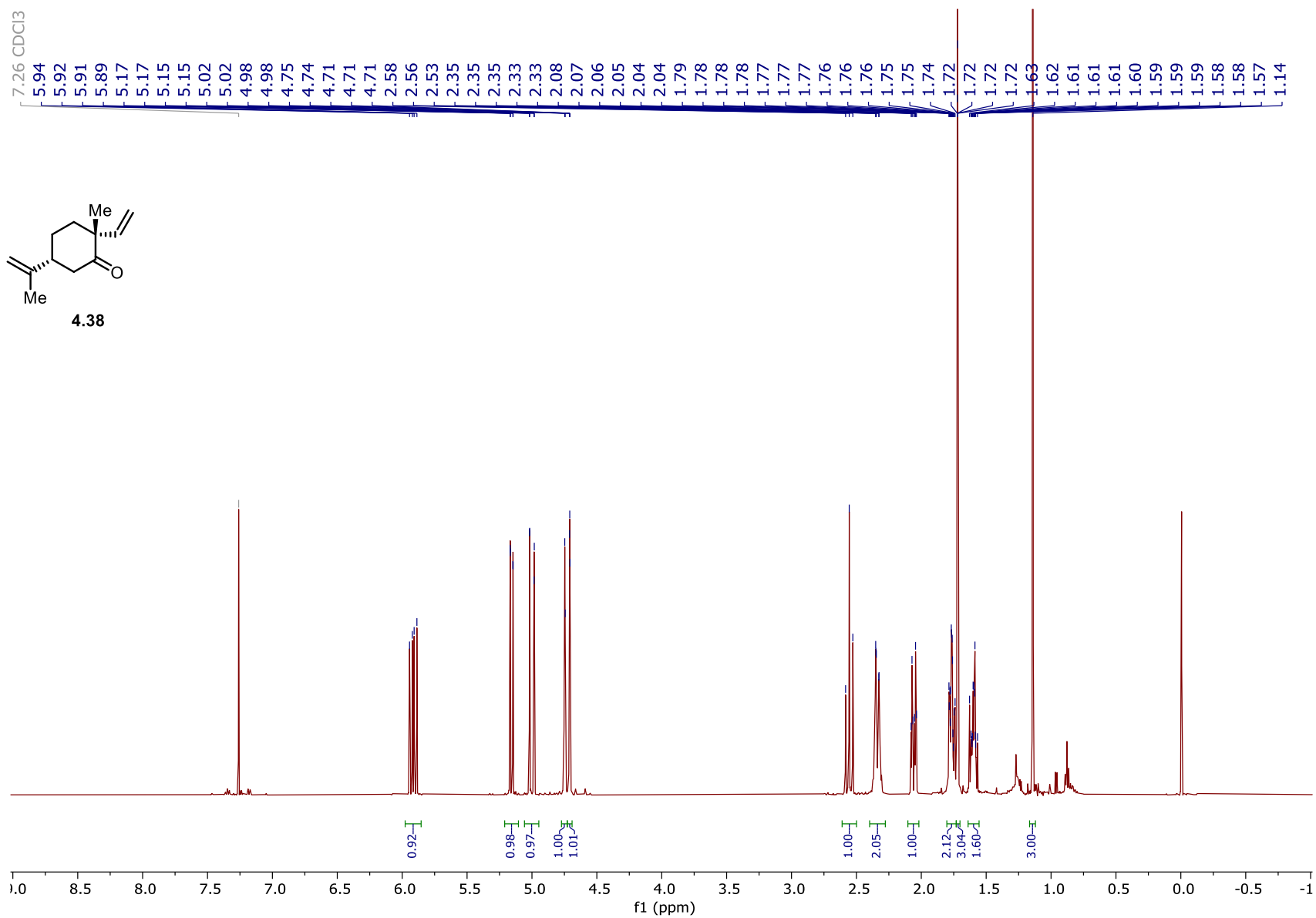


Figure 90. ¹H NMR spectrum of **4.38** (500 MHz, CDCl₃).

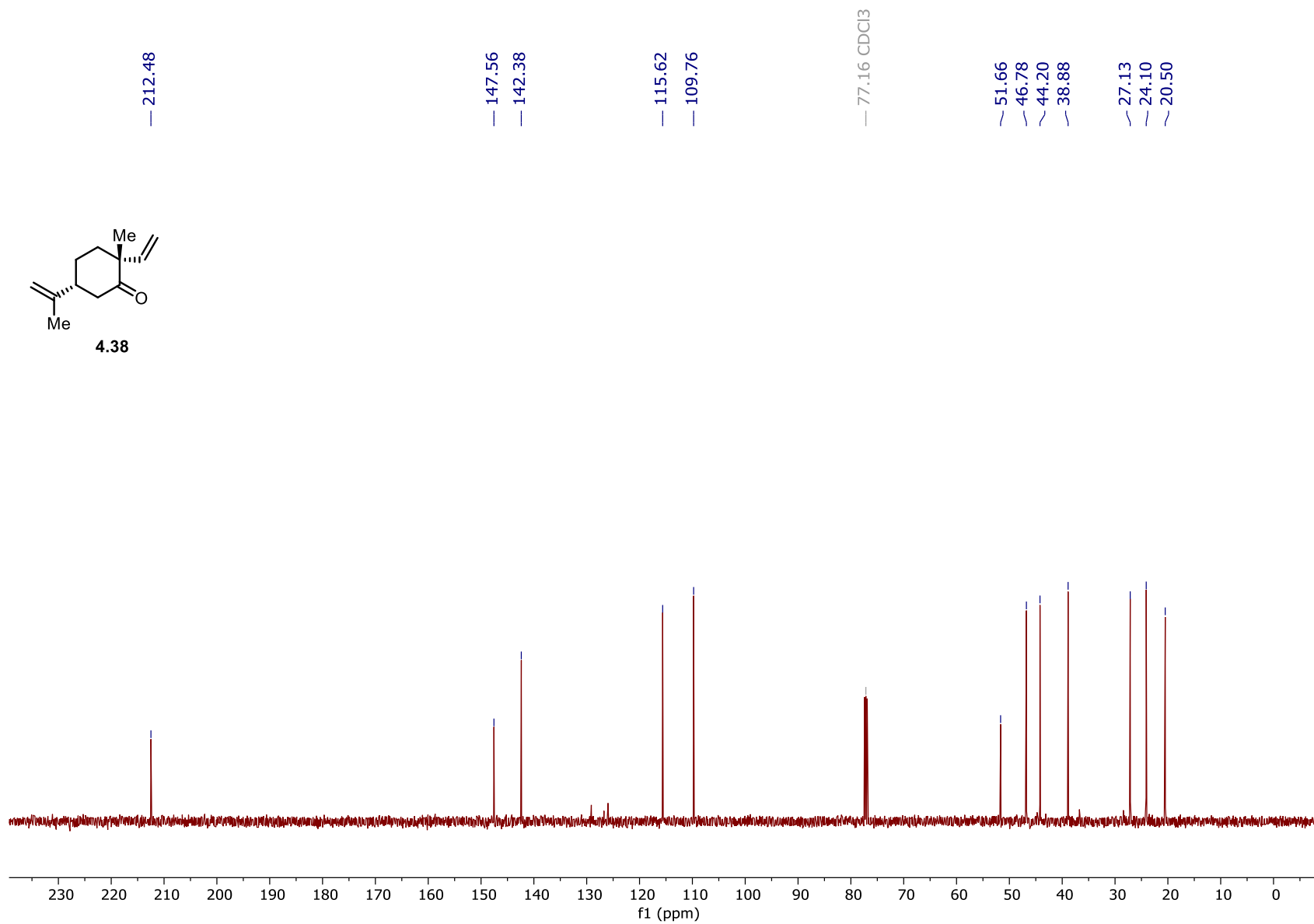


Figure 91. ^{13}C NMR spectrum of **4.38** (125 MHz, CDCl_3).

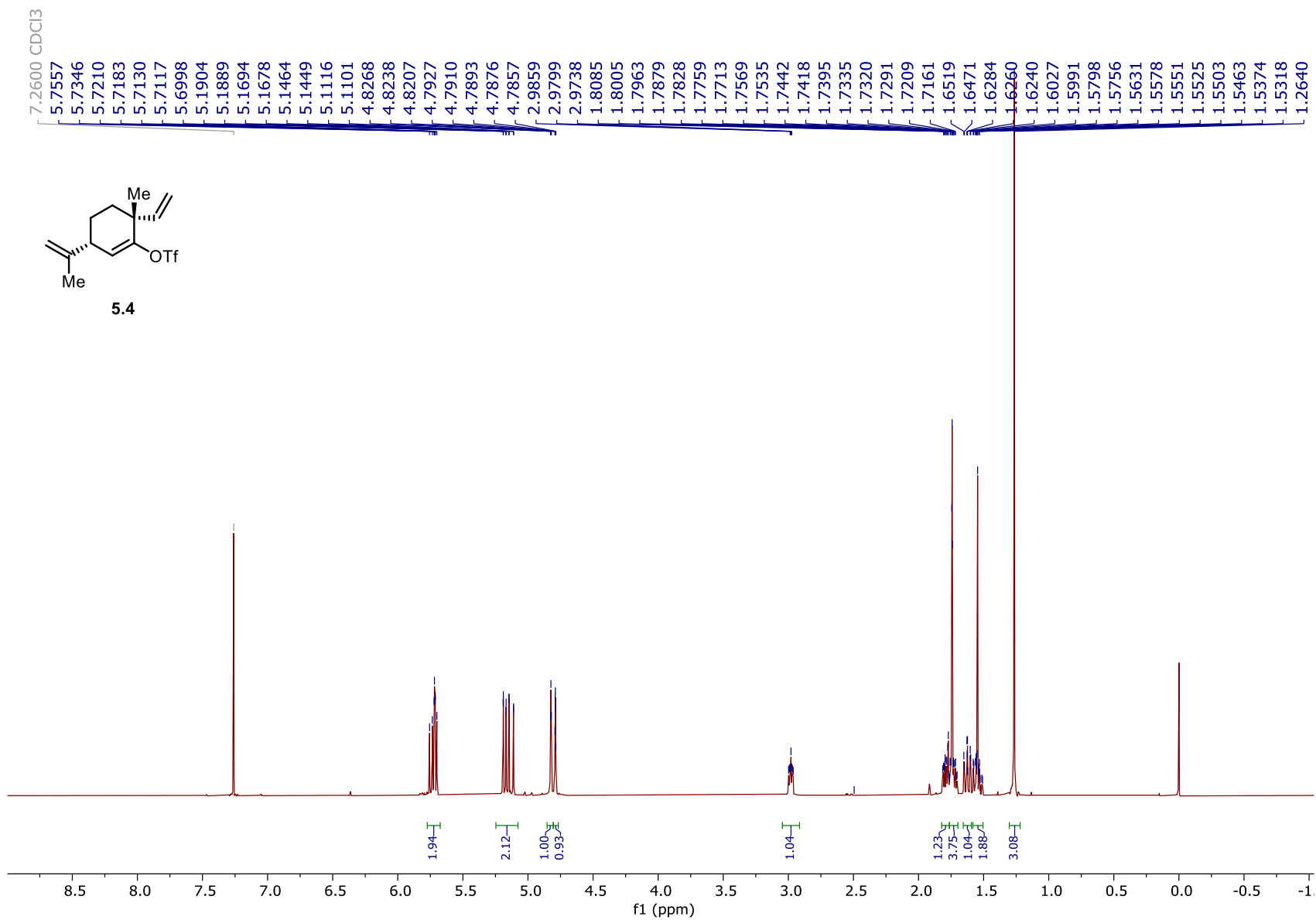


Figure 92. ¹H NMR spectrum of **5.4** (500 MHz, CDCl₃).

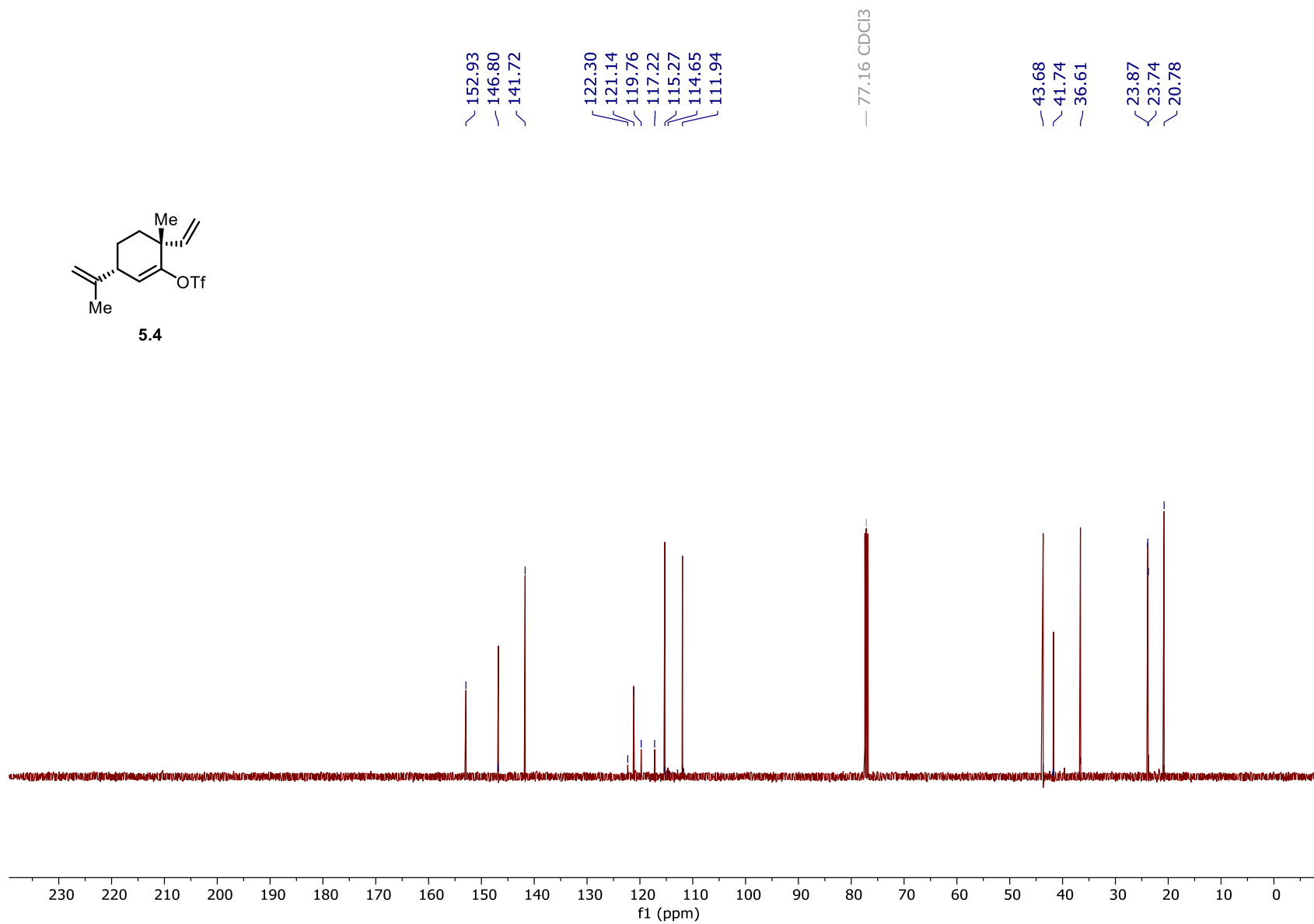


Figure 93. ^{13}C NMR spectrum of **5.4** (125 MHz, CDCl_3).

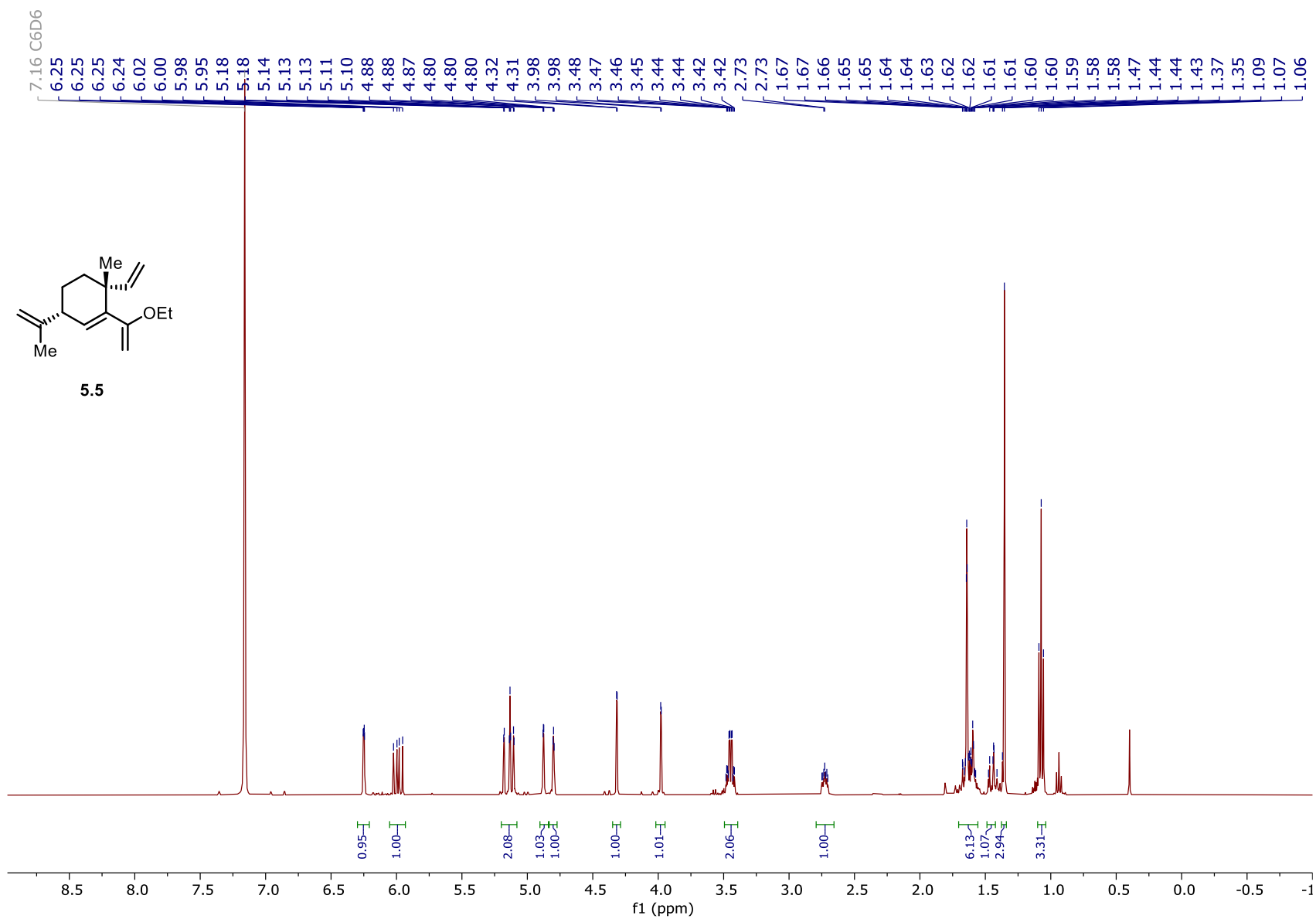
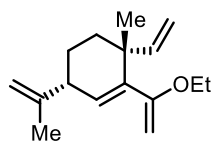
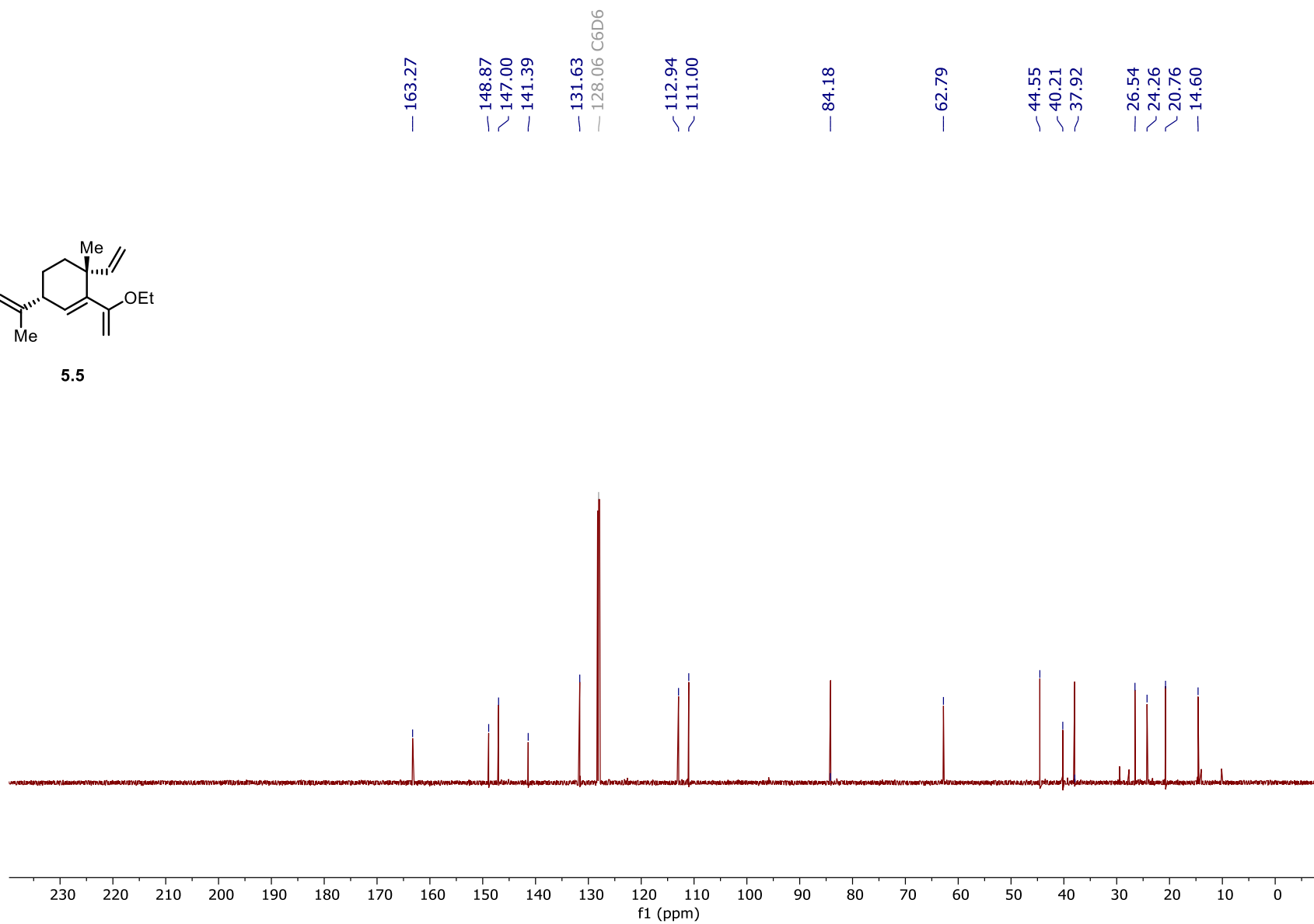


Figure 94. ¹H NMR spectrum of **5.5** (500 MHz, C₆D₆).

**5.5****Figure 95.** ¹³C NMR spectrum of **5.5** (125 MHz, C₆D₆).

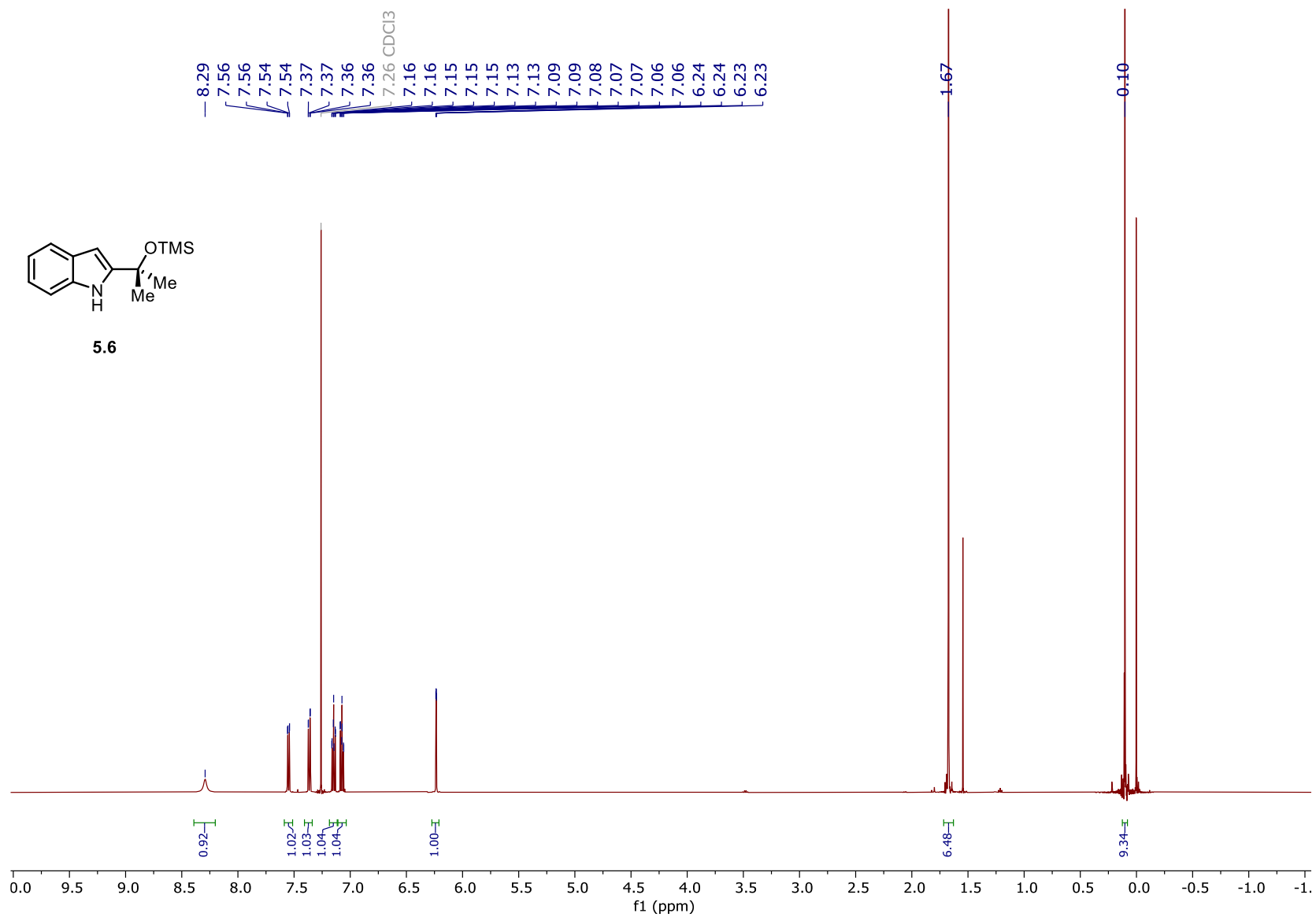


Figure 96. ¹H NMR spectrum of **5.6** (500 MHz, CDCl₃).

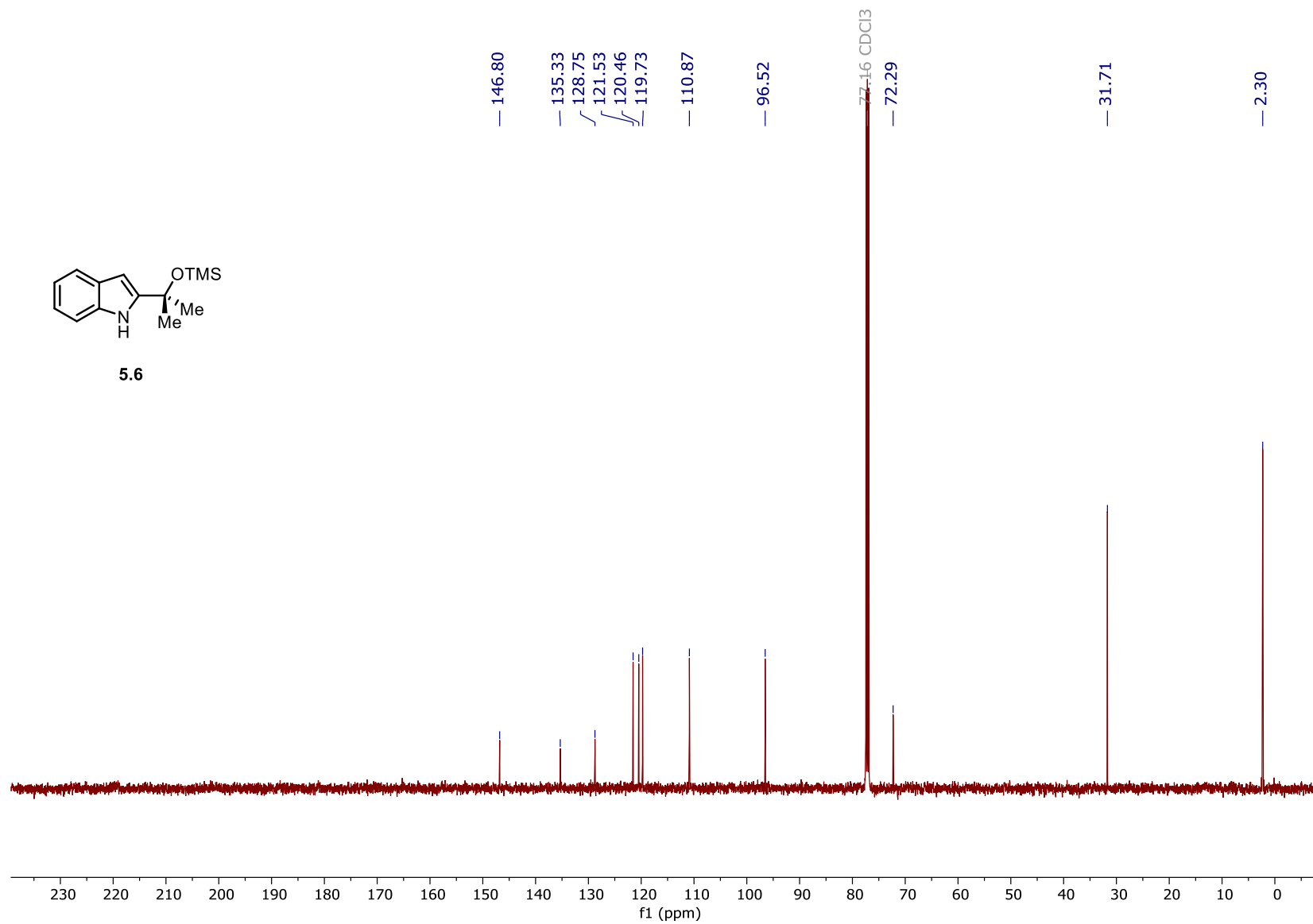


Figure 97. ¹³C NMR spectrum of **5.6** (125 MHz, CDCl₃).

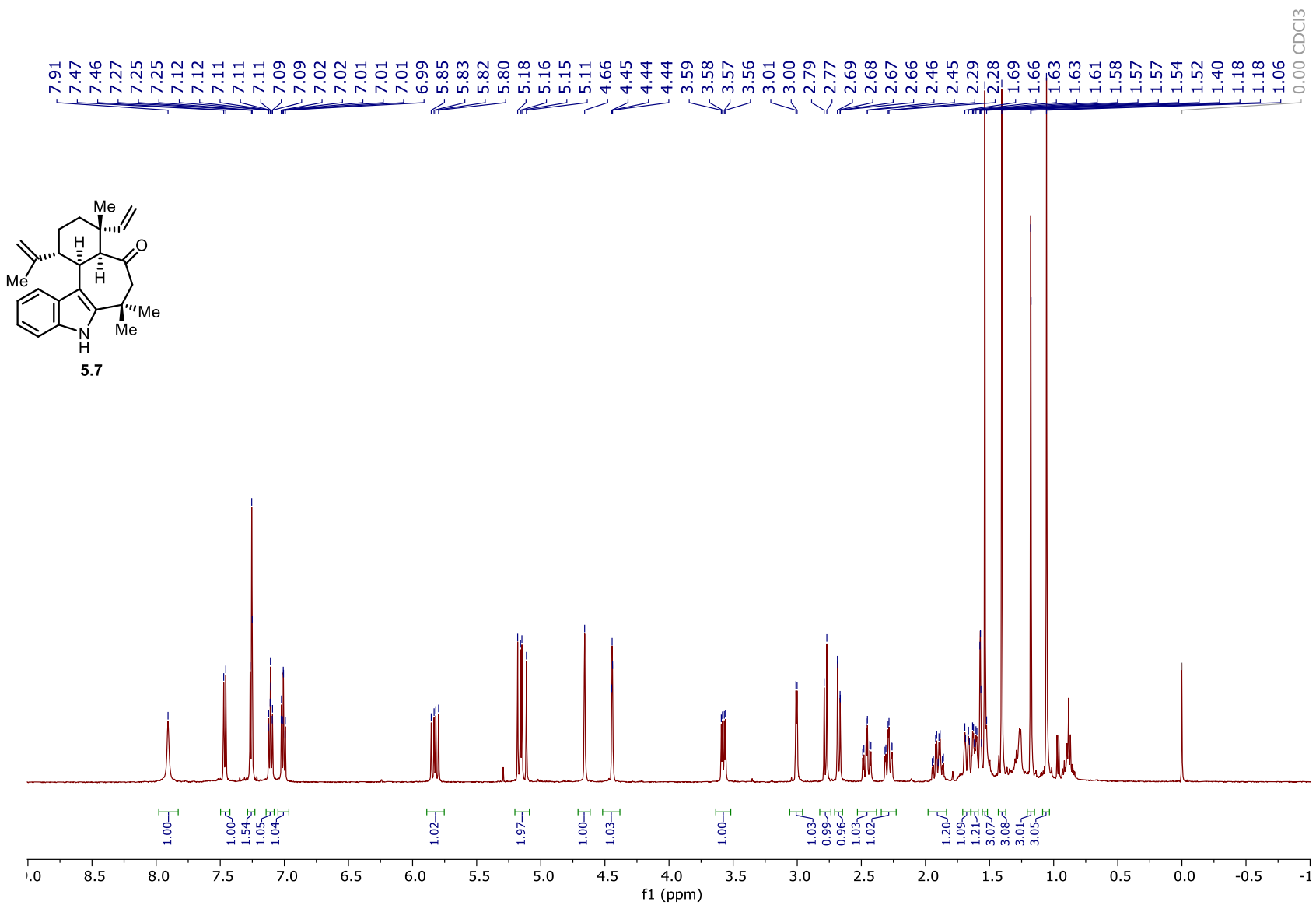


Figure 98. ¹H NMR spectrum of **5.7** (500 MHz, CDCl₃).

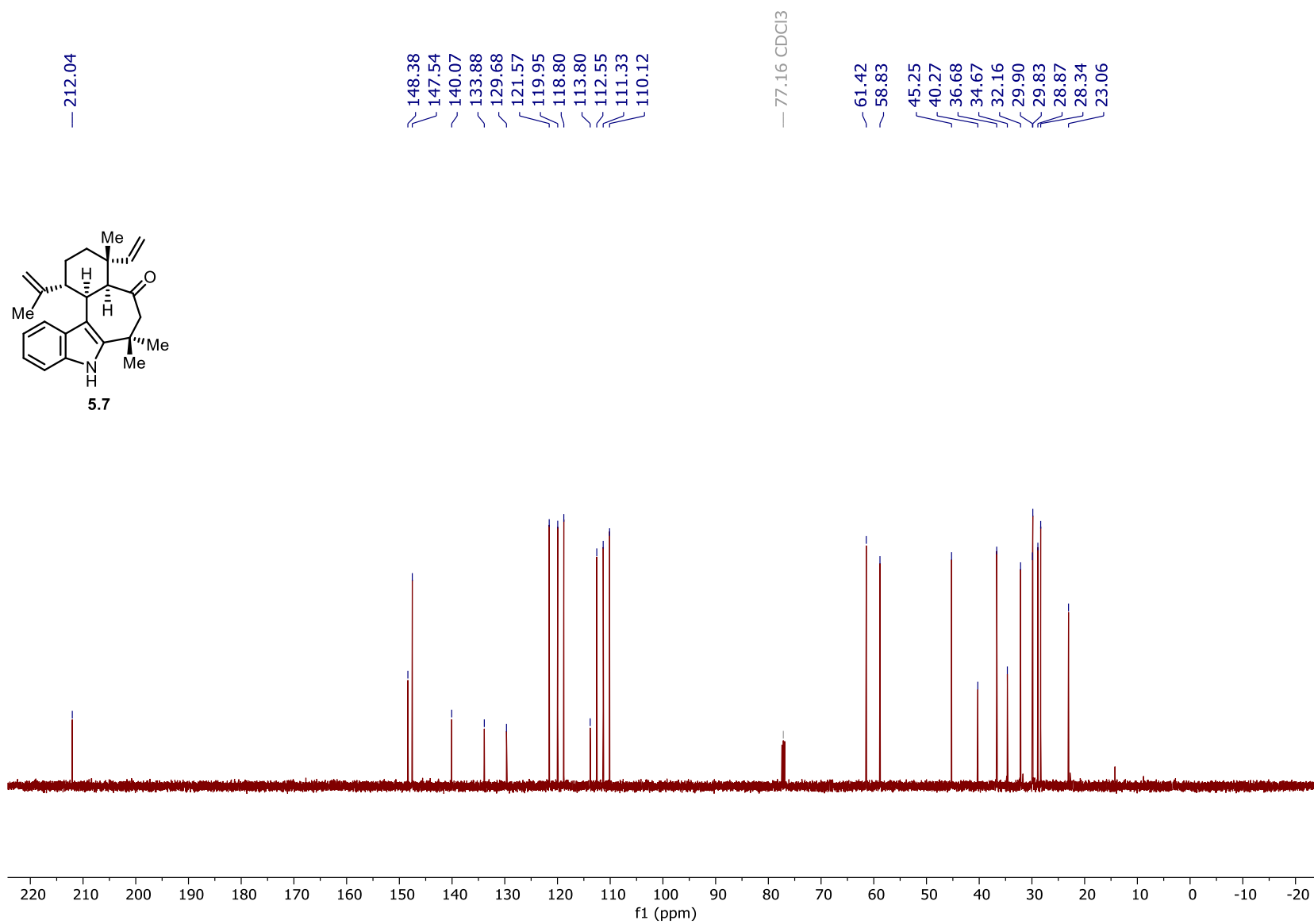


Figure 99. ^{13}C NMR spectrum of **5.7** (125 MHz, CDCl_3).

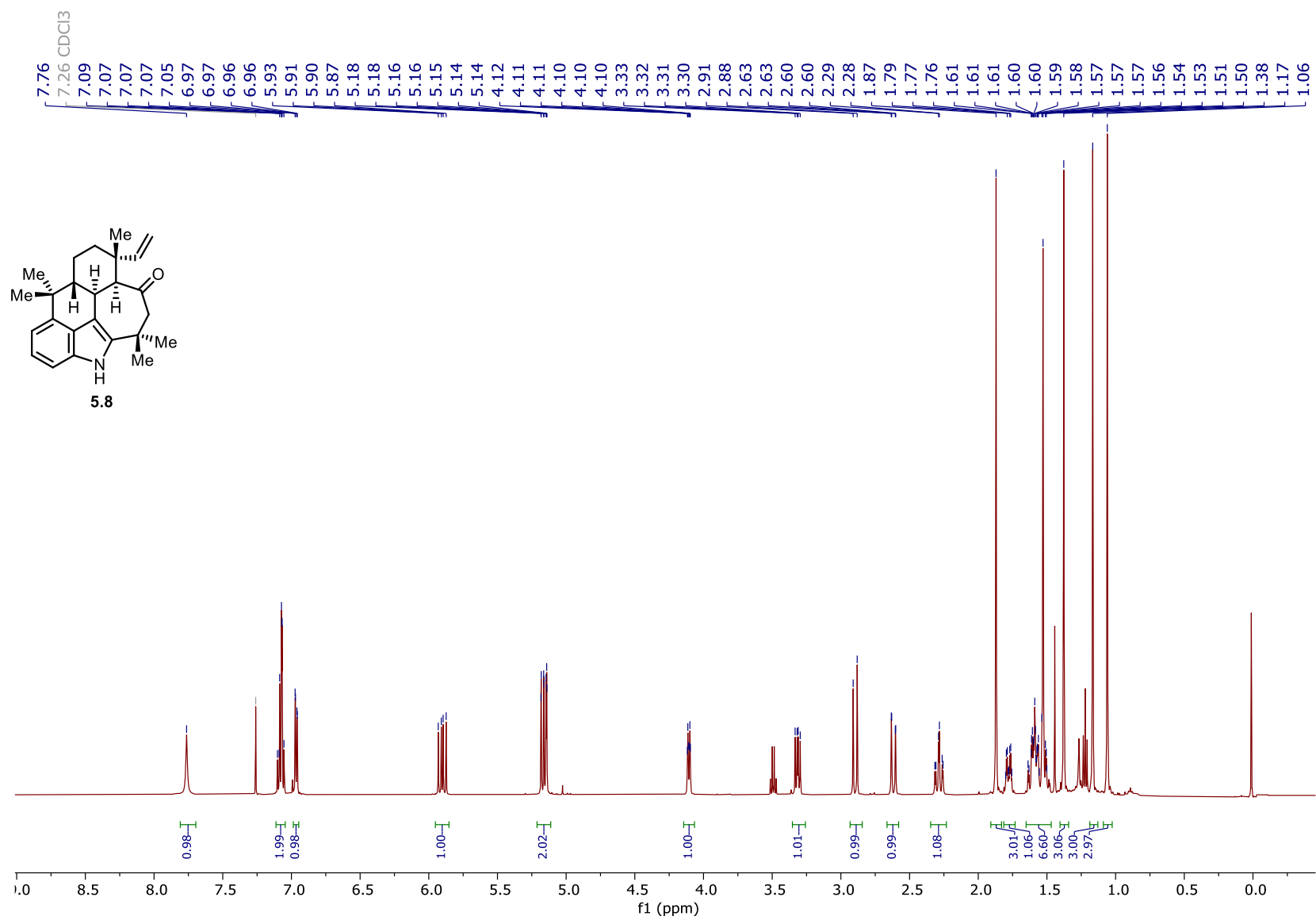


Figure 100. ¹H NMR spectrum of **5.8** (500 MHz, CDCl₃).

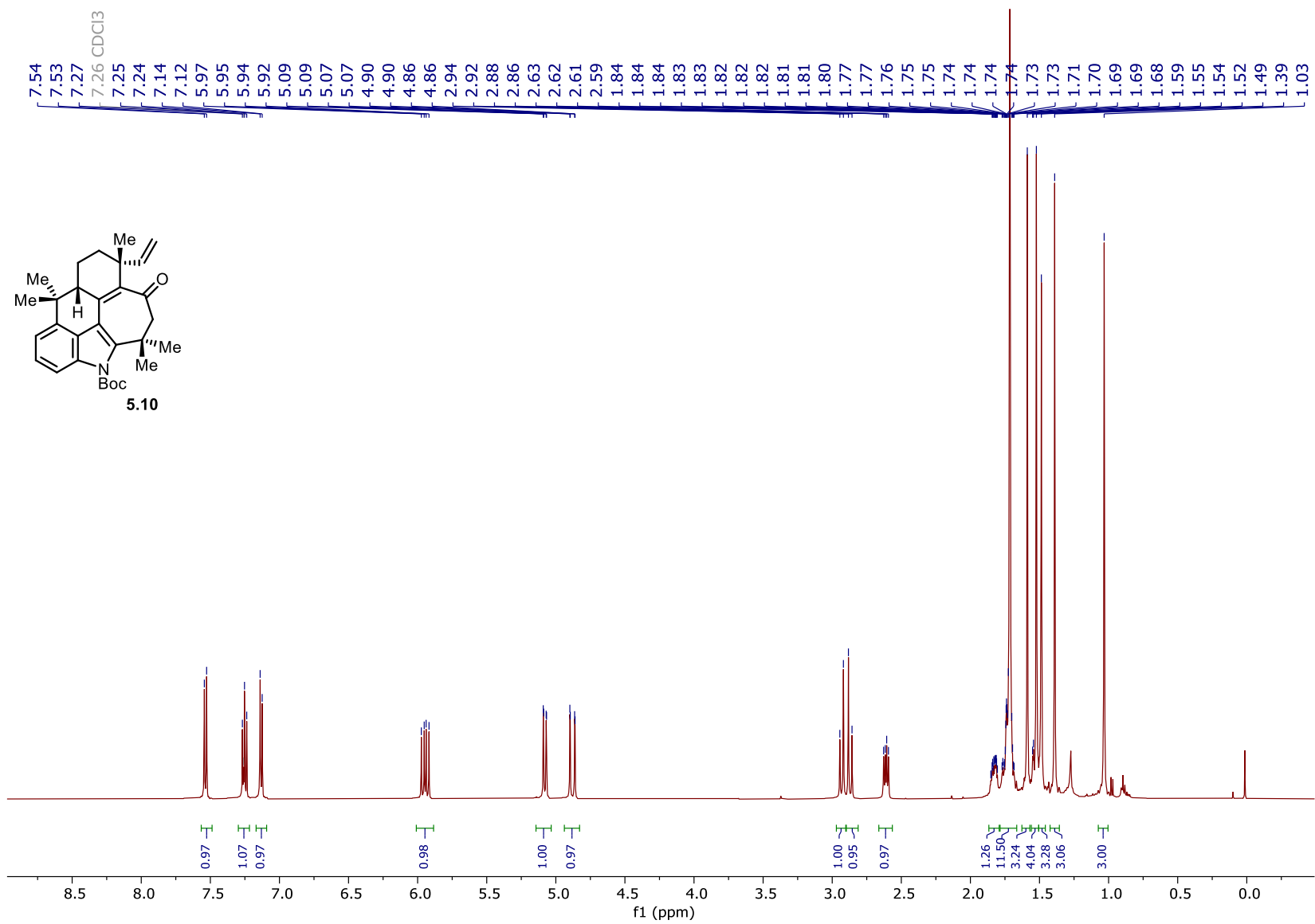


Figure 101. ^1H NMR spectrum of **5.10** (500 MHz, CDCl_3).

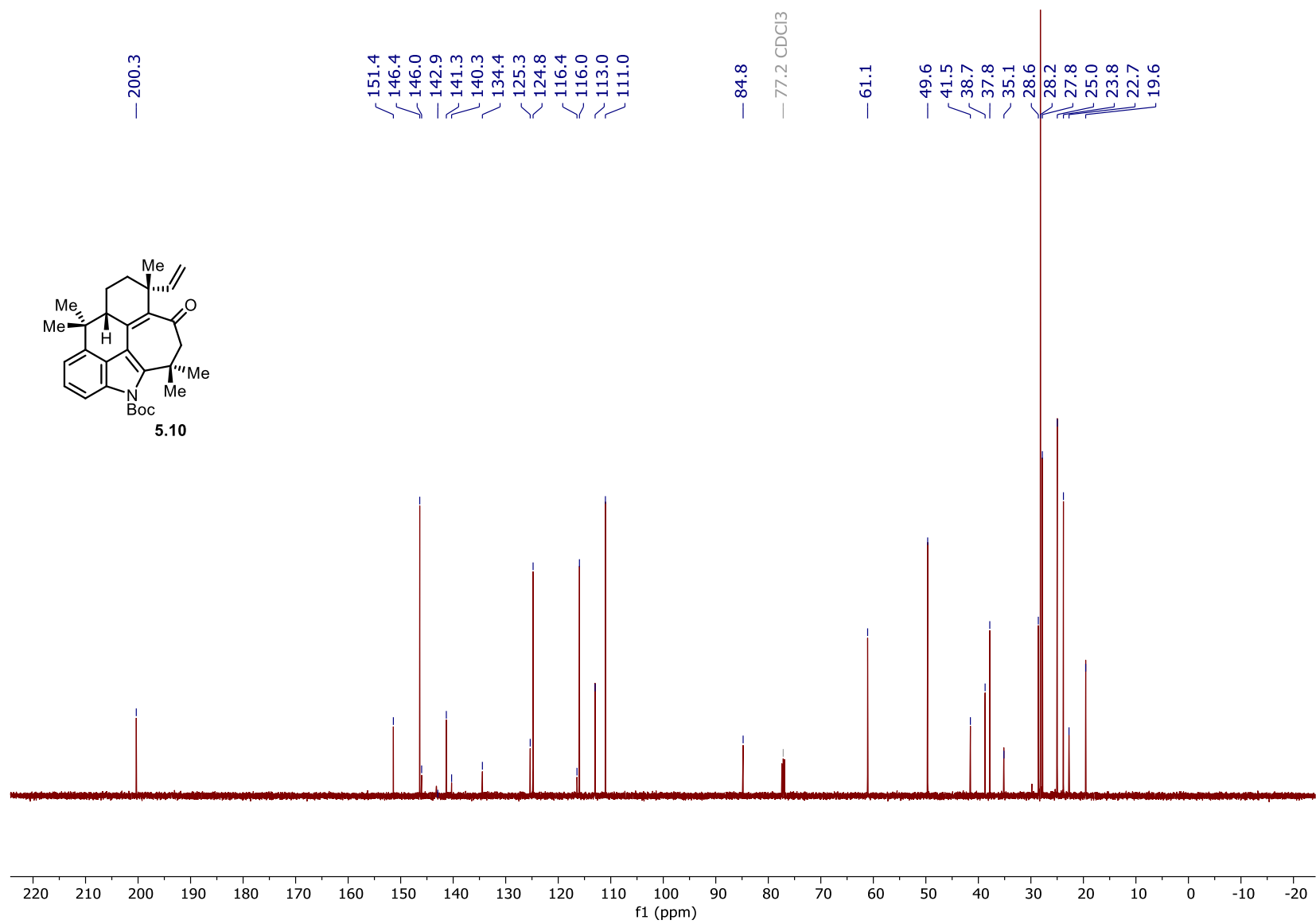


Figure 102. ¹³C NMR spectrum of **5.10** (125 MHz, CDCl₃).

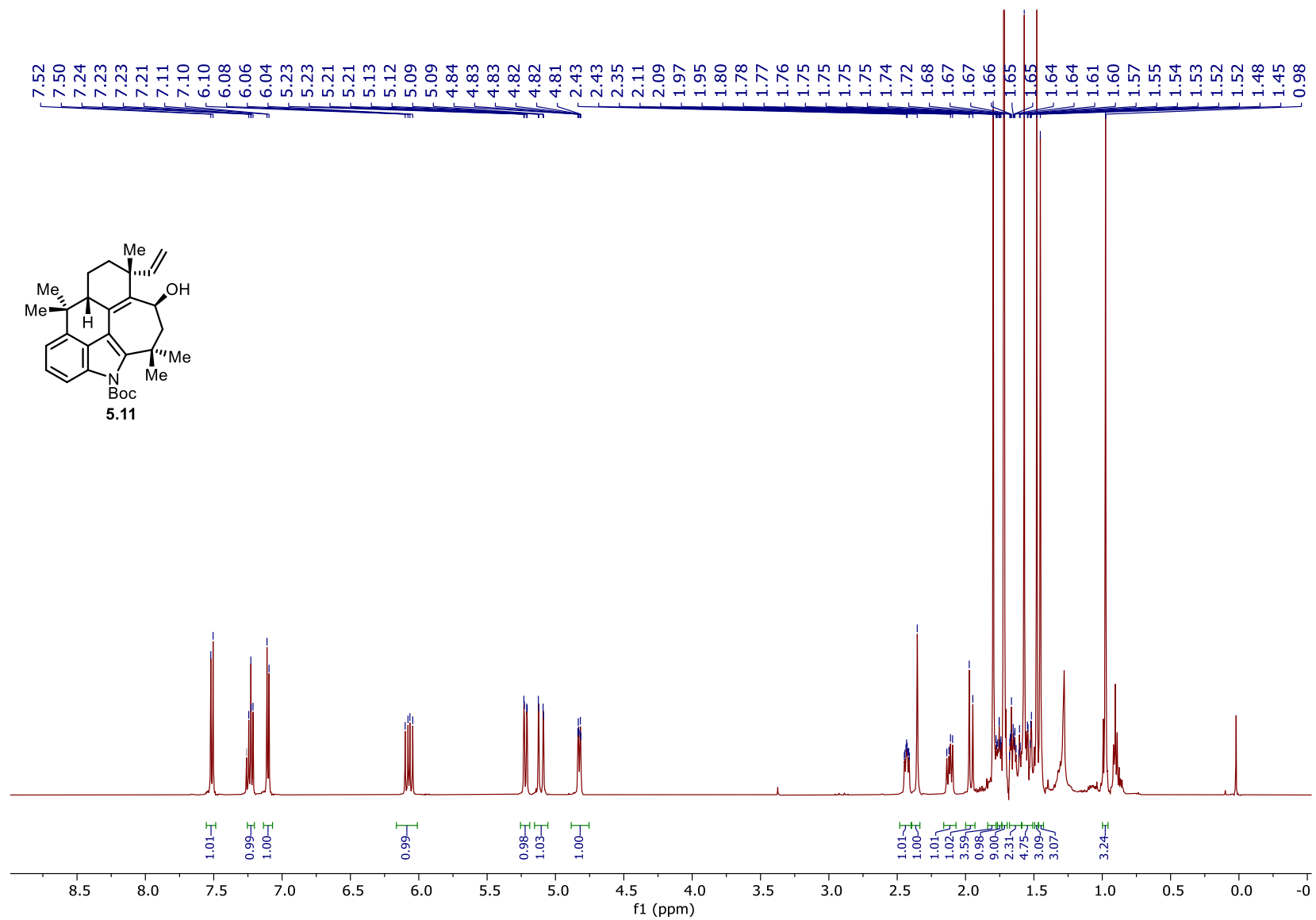


Figure 103. ¹H NMR spectrum of **5.11** (500 MHz, CDCl₃).

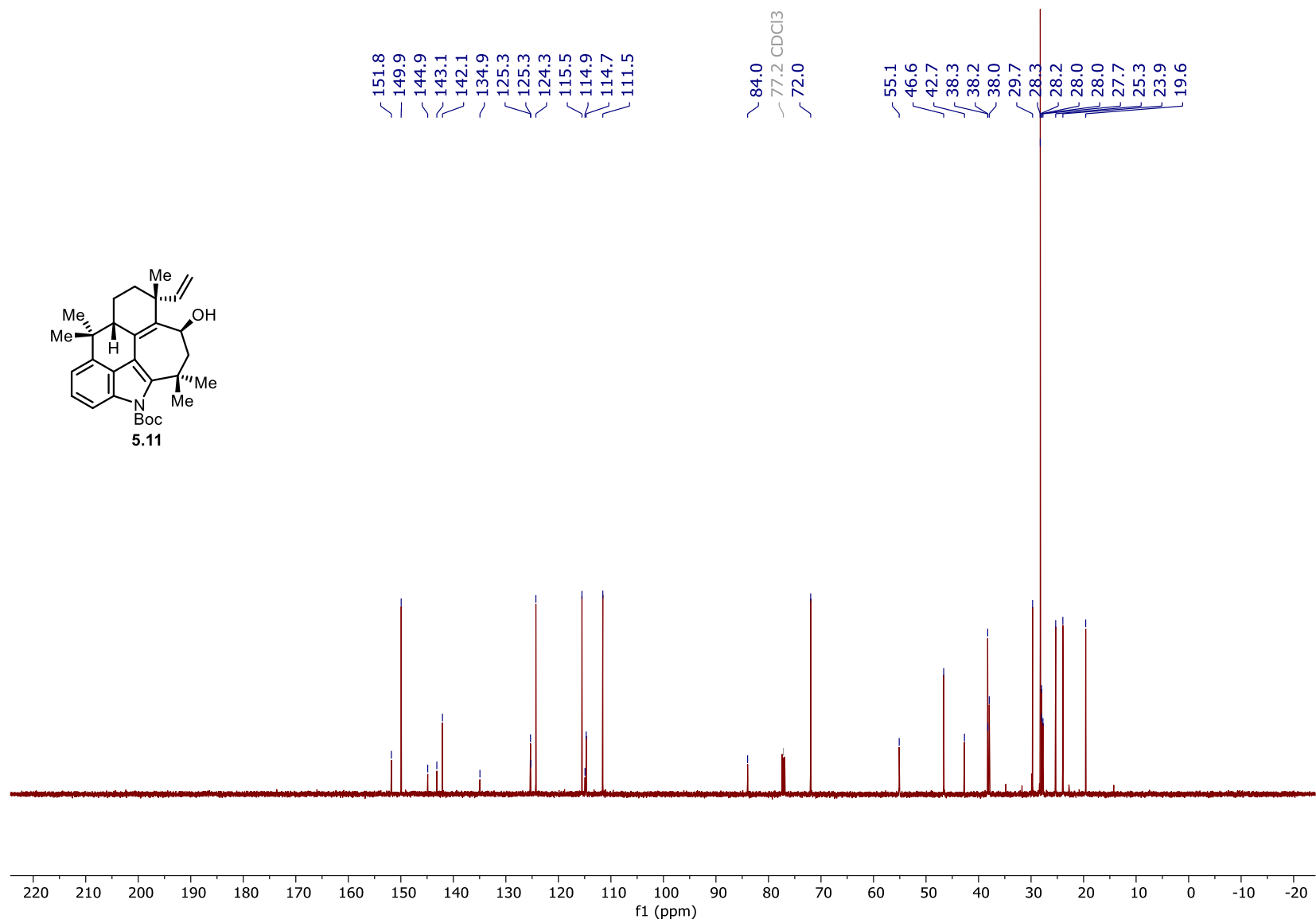


Figure 104. ^{13}C NMR spectrum of **5.11** (125 MHz, CDCl_3).

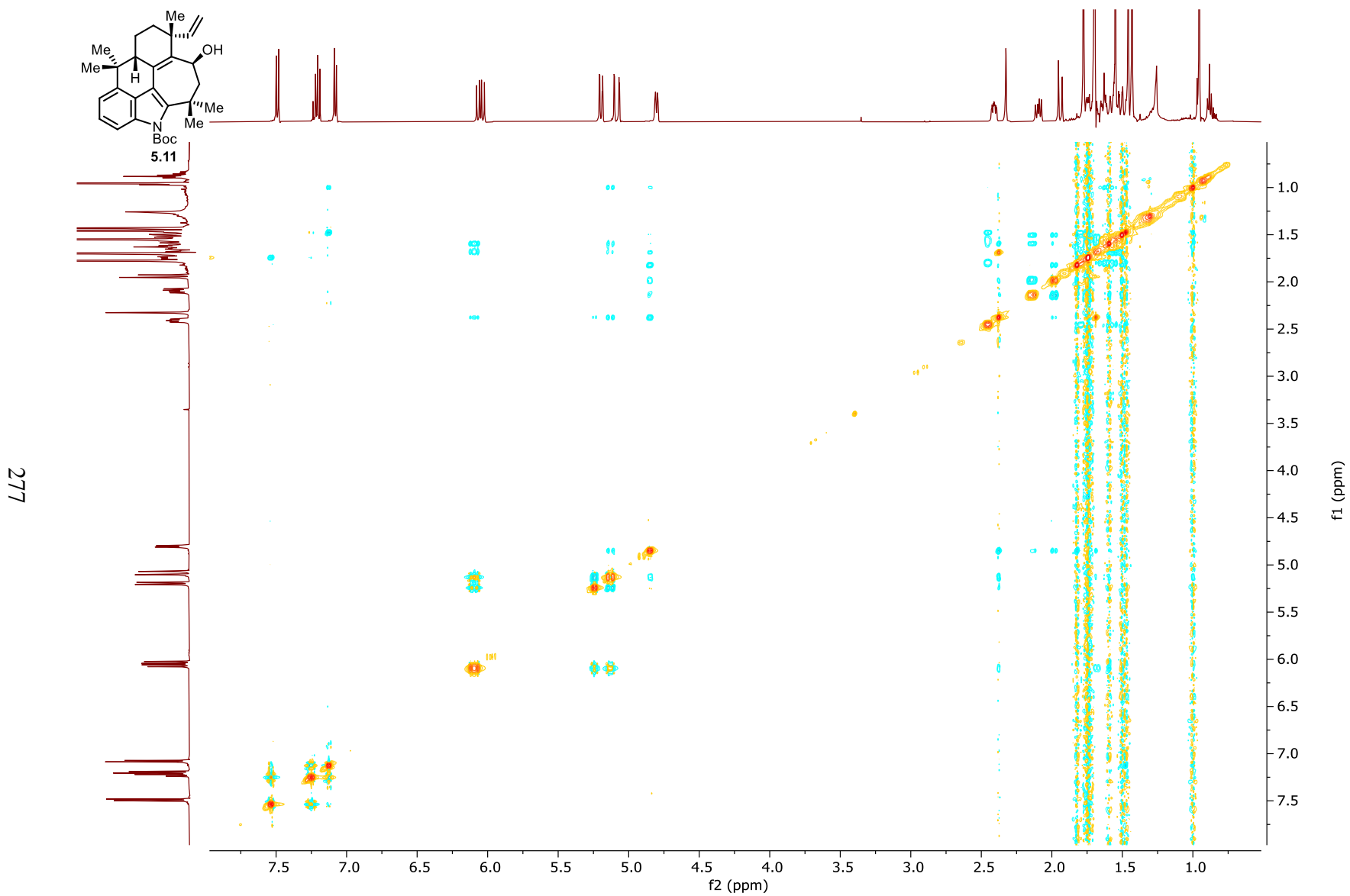


Figure 105. NOESY spectrum of **5.11** (CDCl₃).

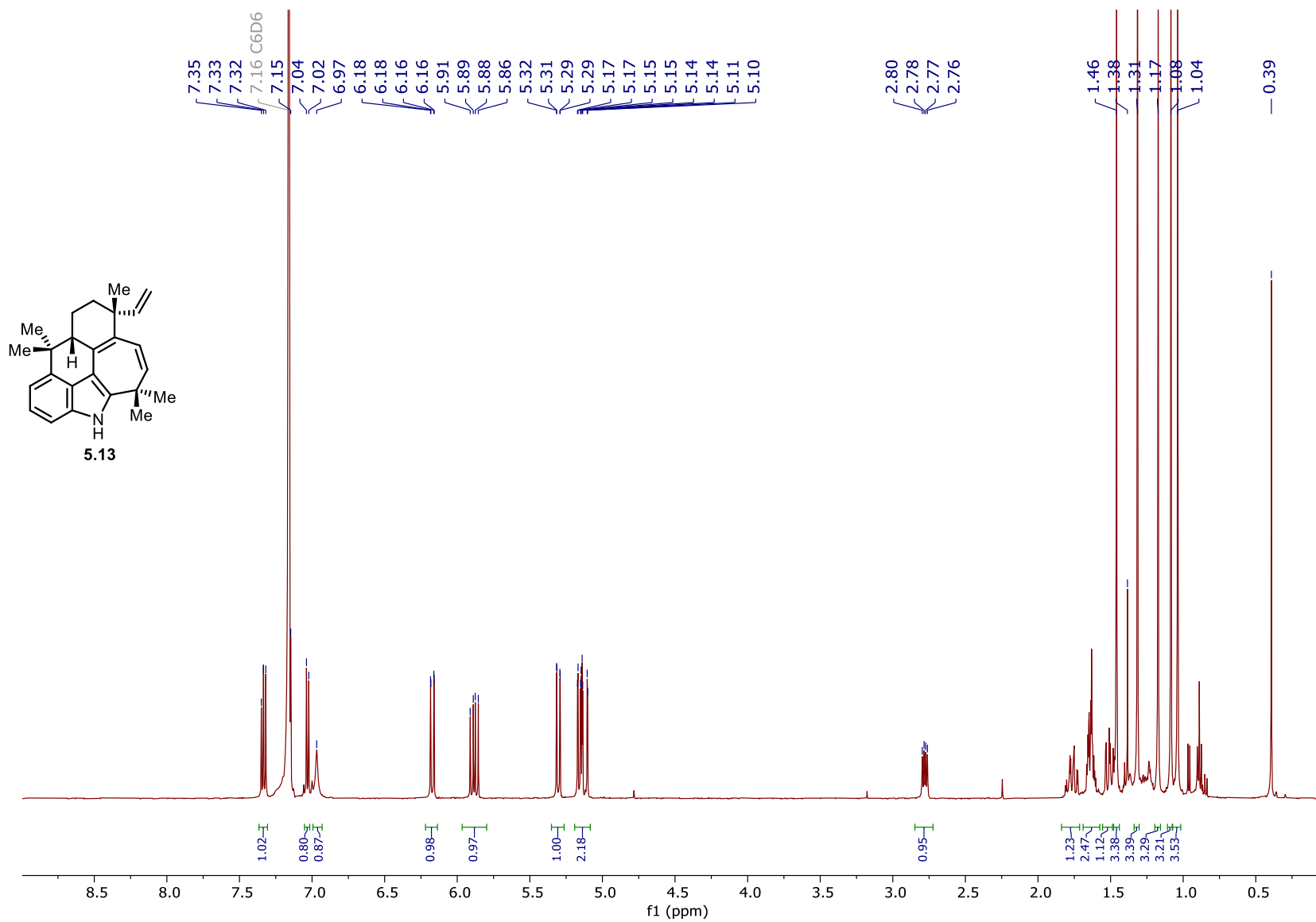


Figure 106. ¹H NMR spectrum of **5.13** (500 MHz, C₆D₆).

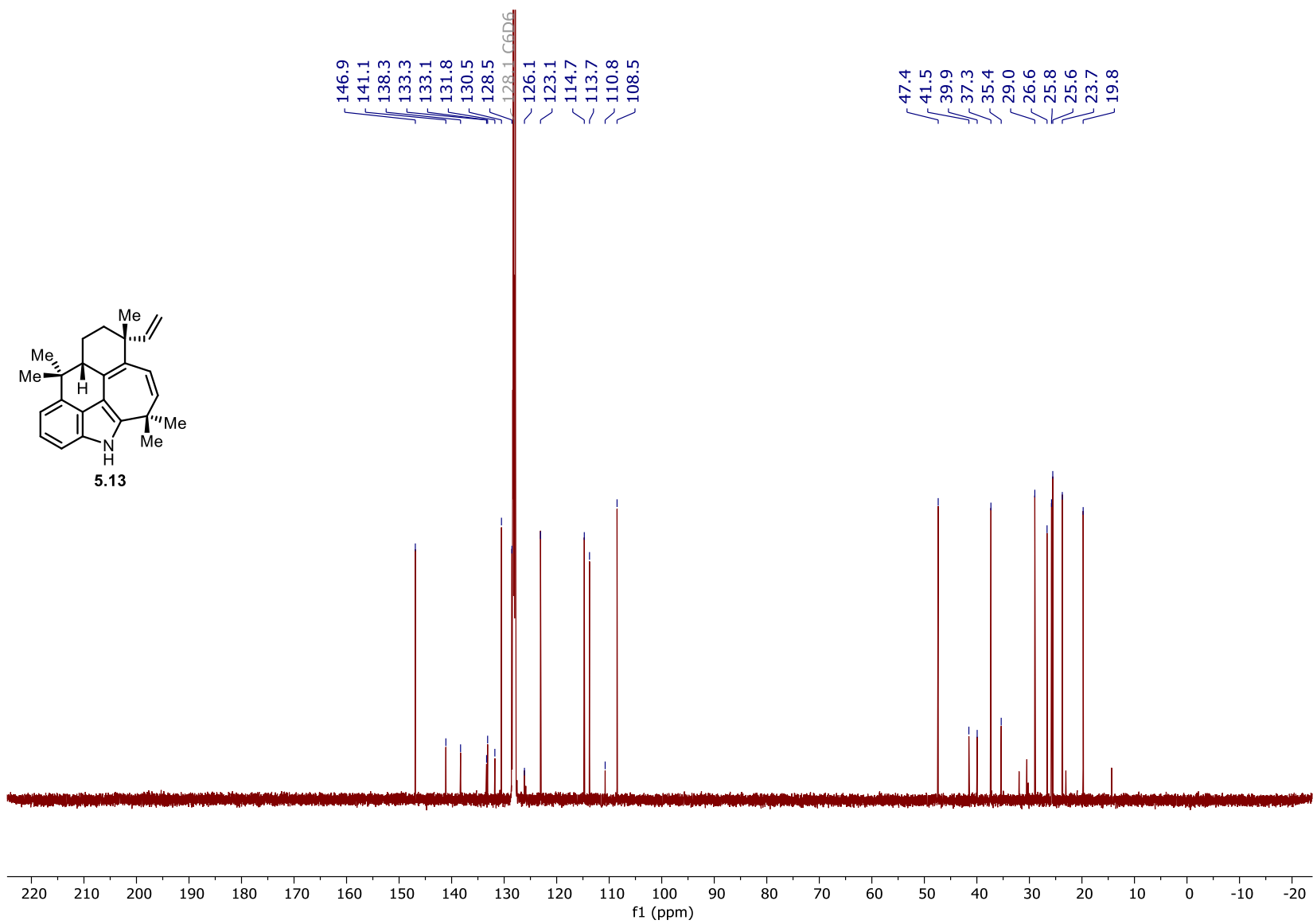


Figure 107. ¹³C NMR spectrum of 5.13 (125 MHz, C₆D₆).

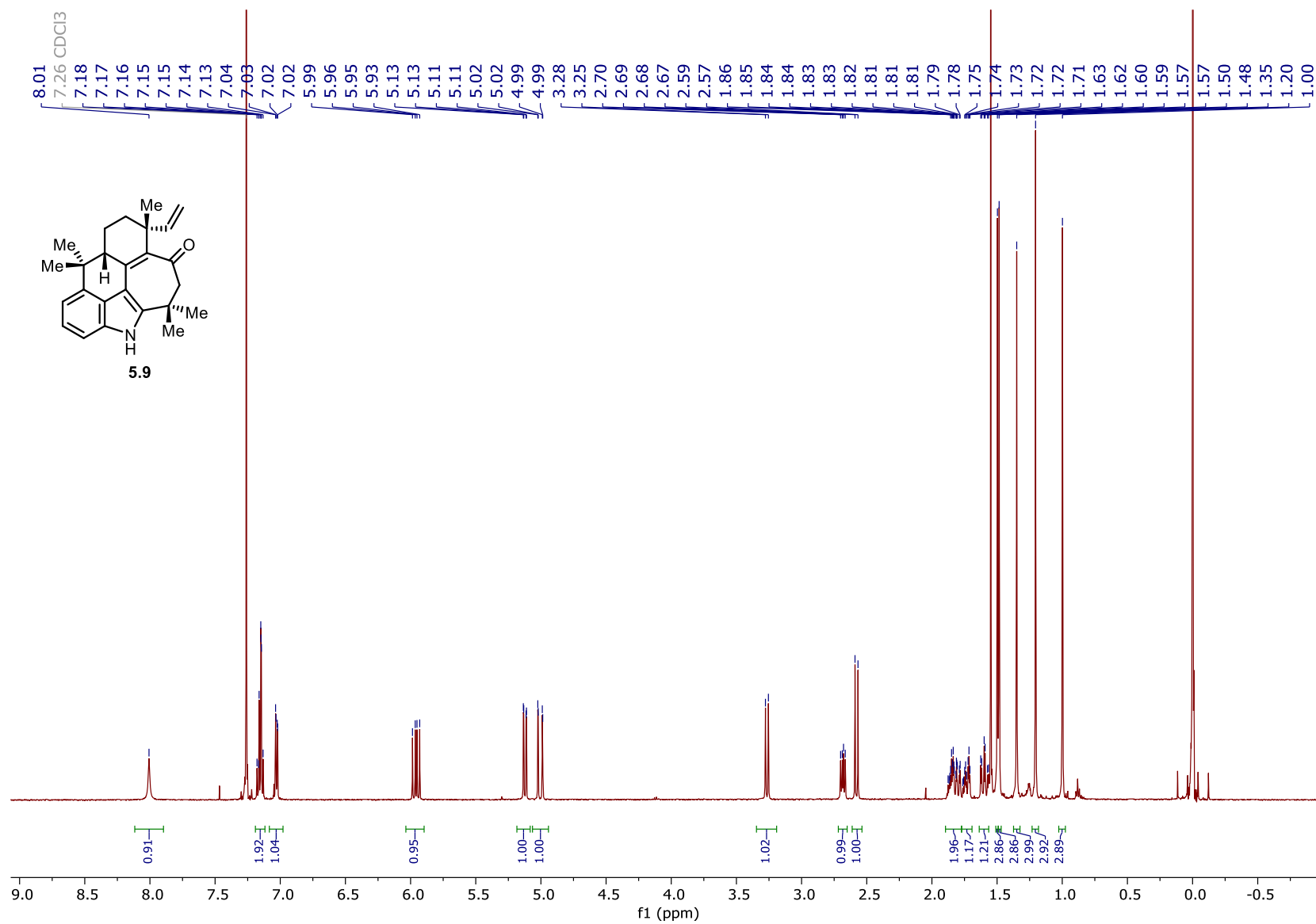


Figure 108. ^1H NMR spectrum of **5.9** (500 MHz, CDCl_3).

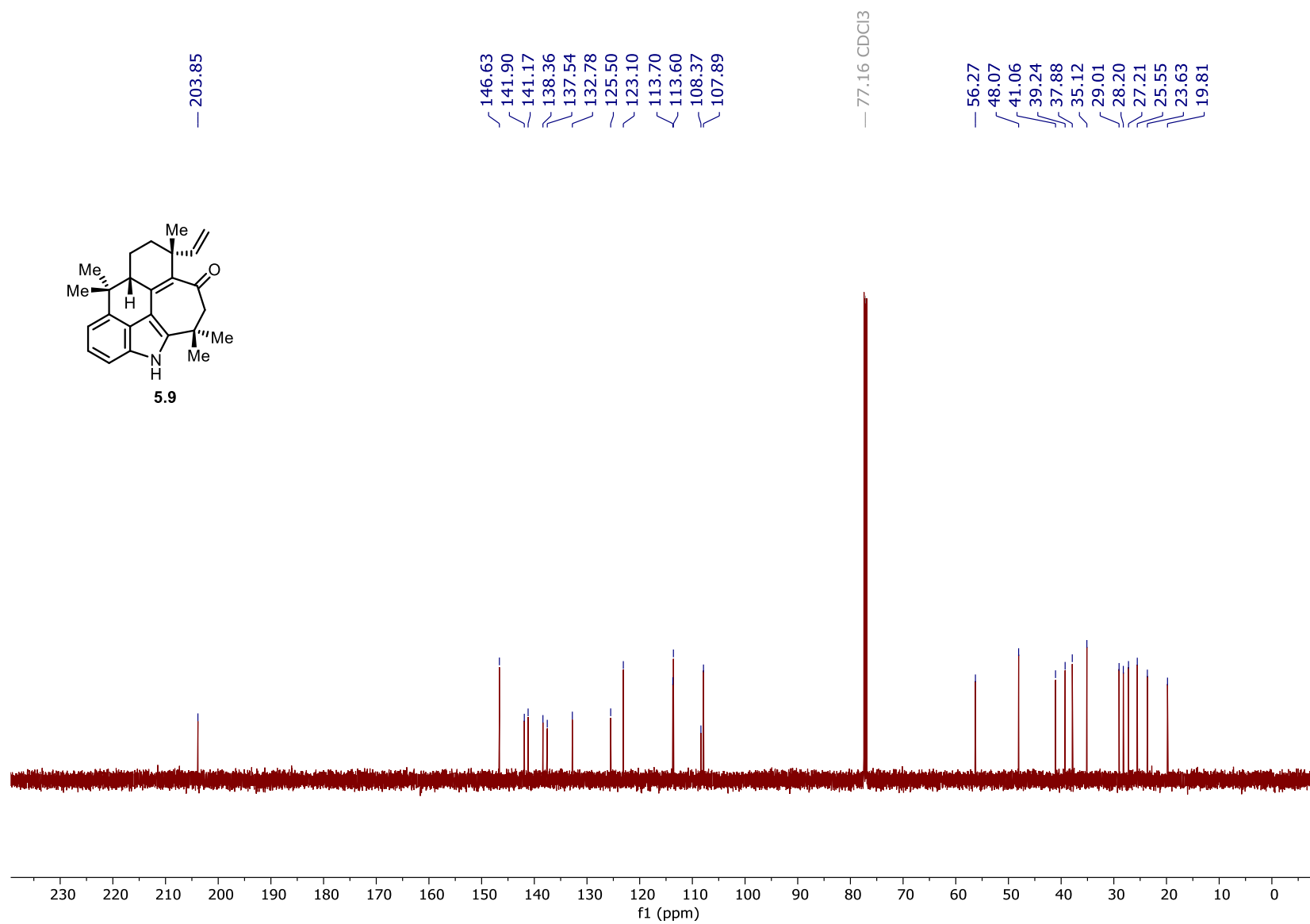


Figure 109. ^{13}C NMR spectrum of **5.9** (125 MHz, CDCl_3).

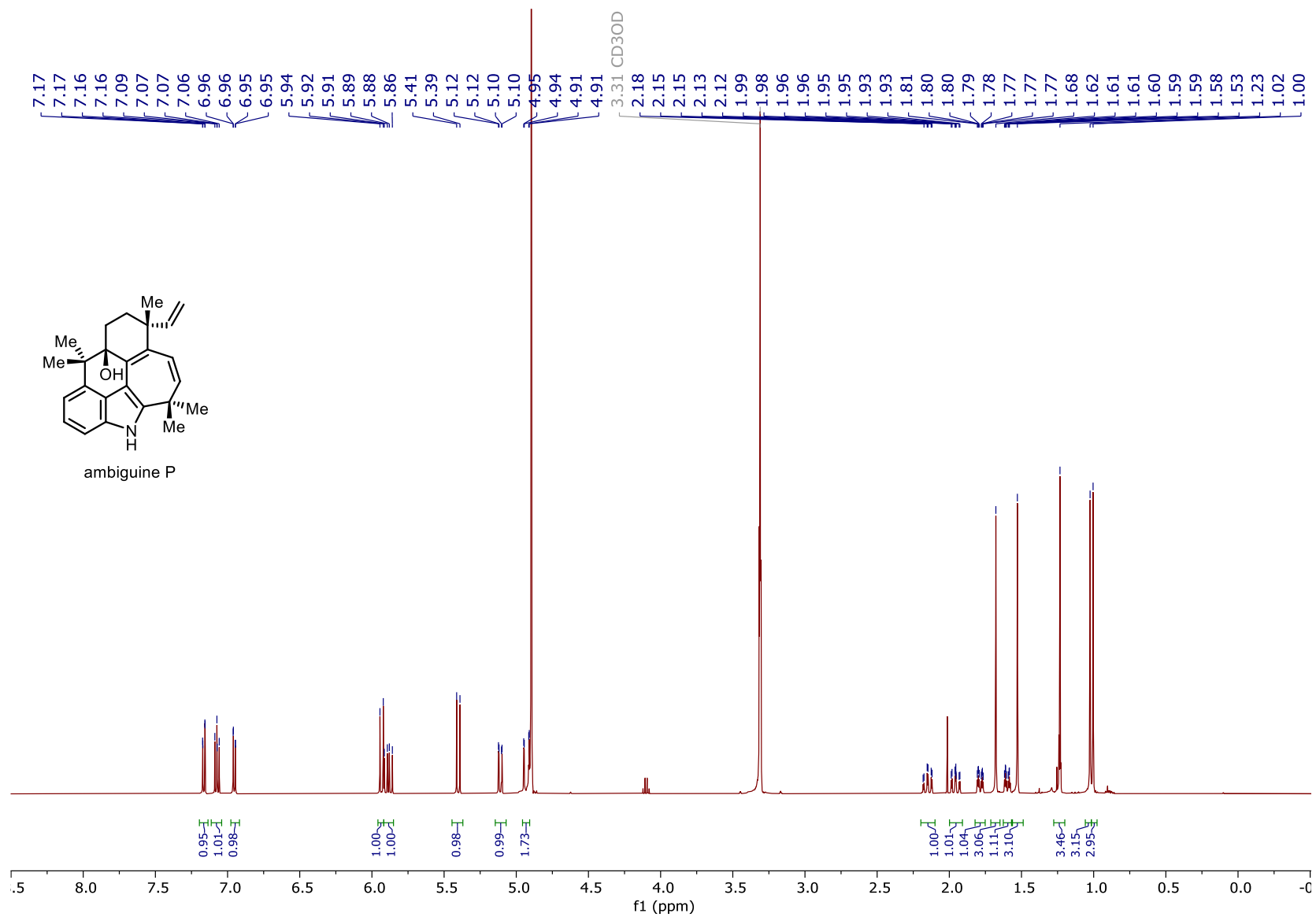


Figure 110. ¹H NMR spectrum of ambiguline P (500 MHz, CD₃OD).

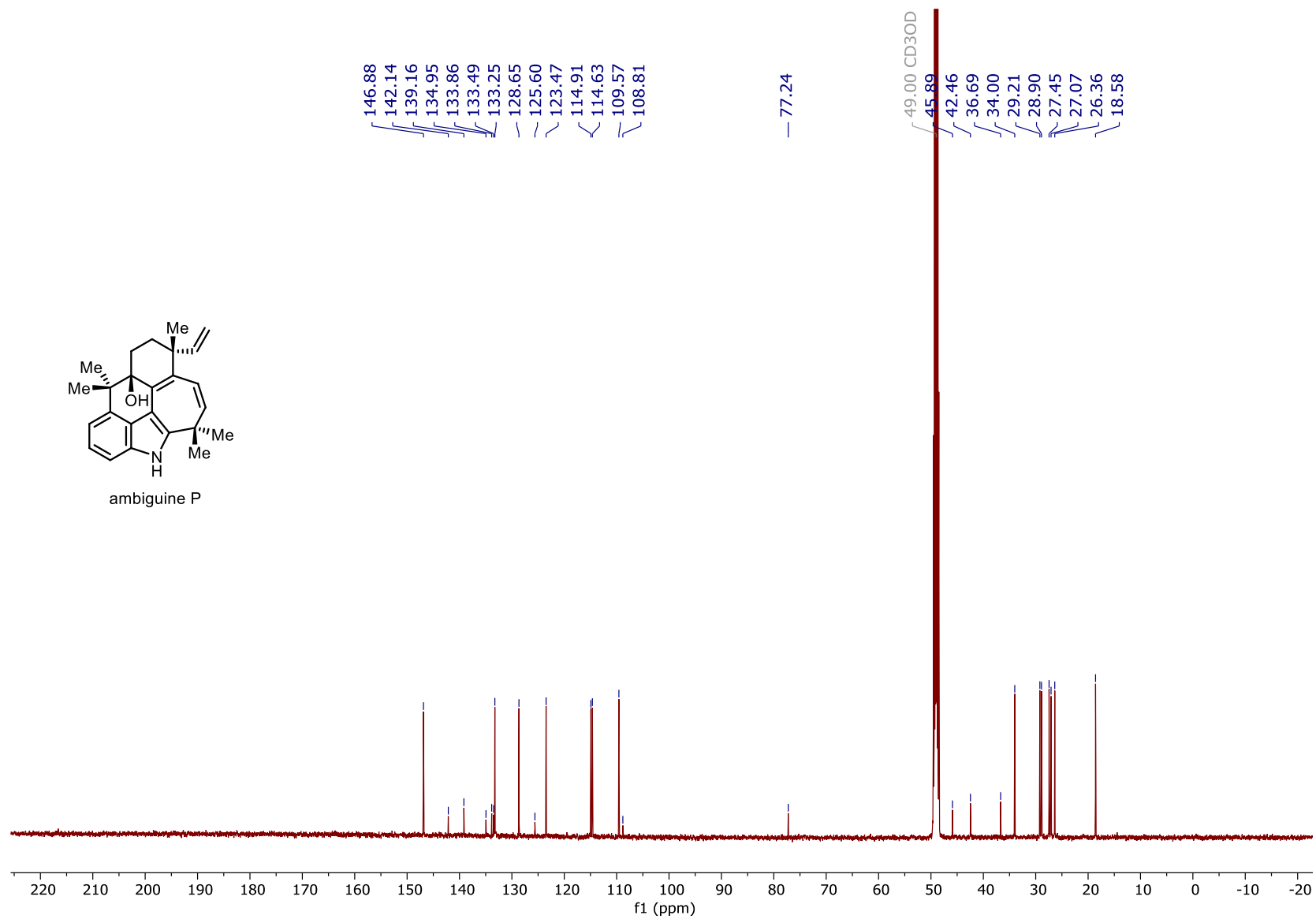


Figure 111. ^{13}C NMR spectrum of ambiguine P (125 MHz, CD_3OD).

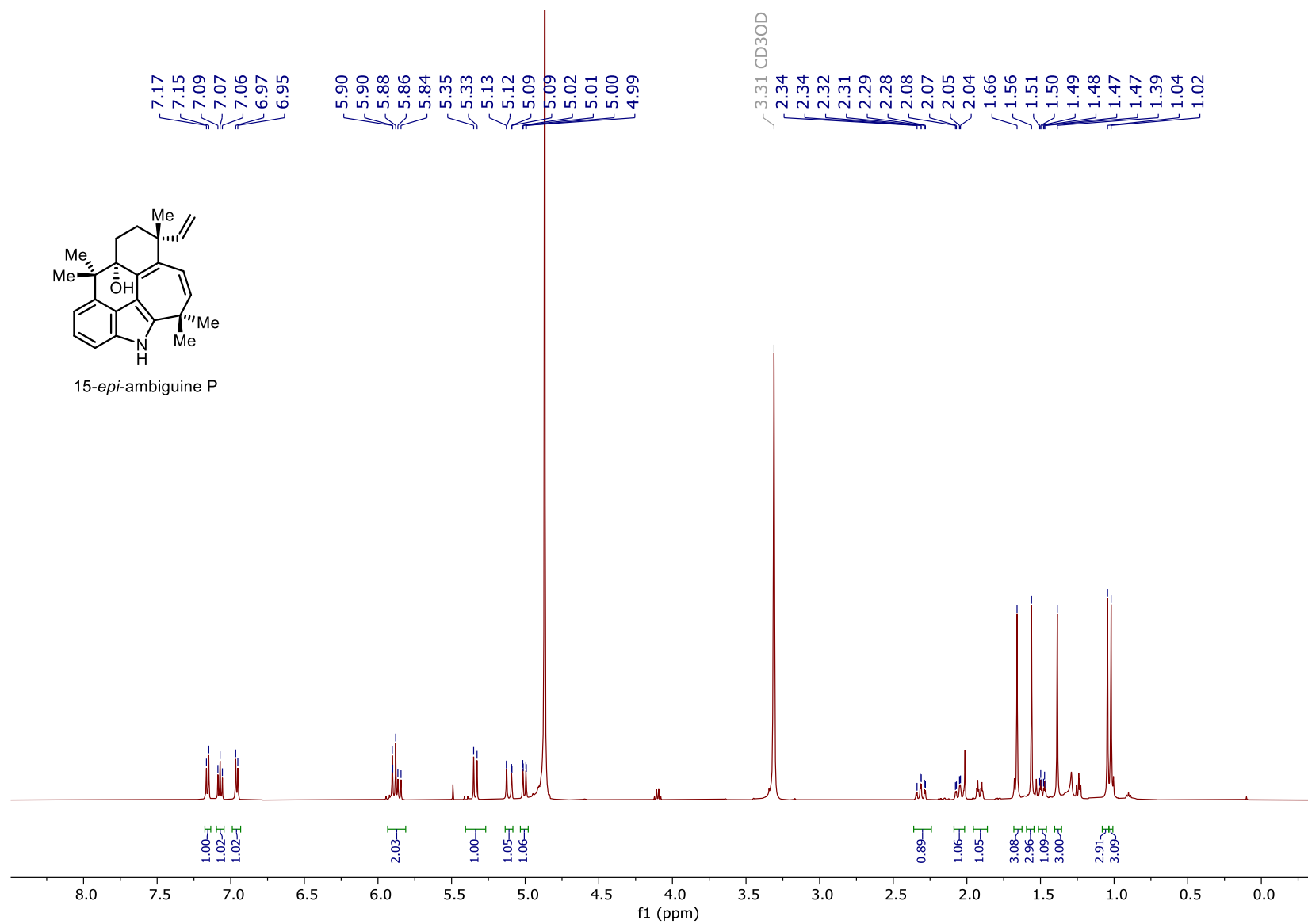


Figure 112. ^1H NMR spectrum of 15-*epi*-ambiguine P (500 MHz, CD_3OD).

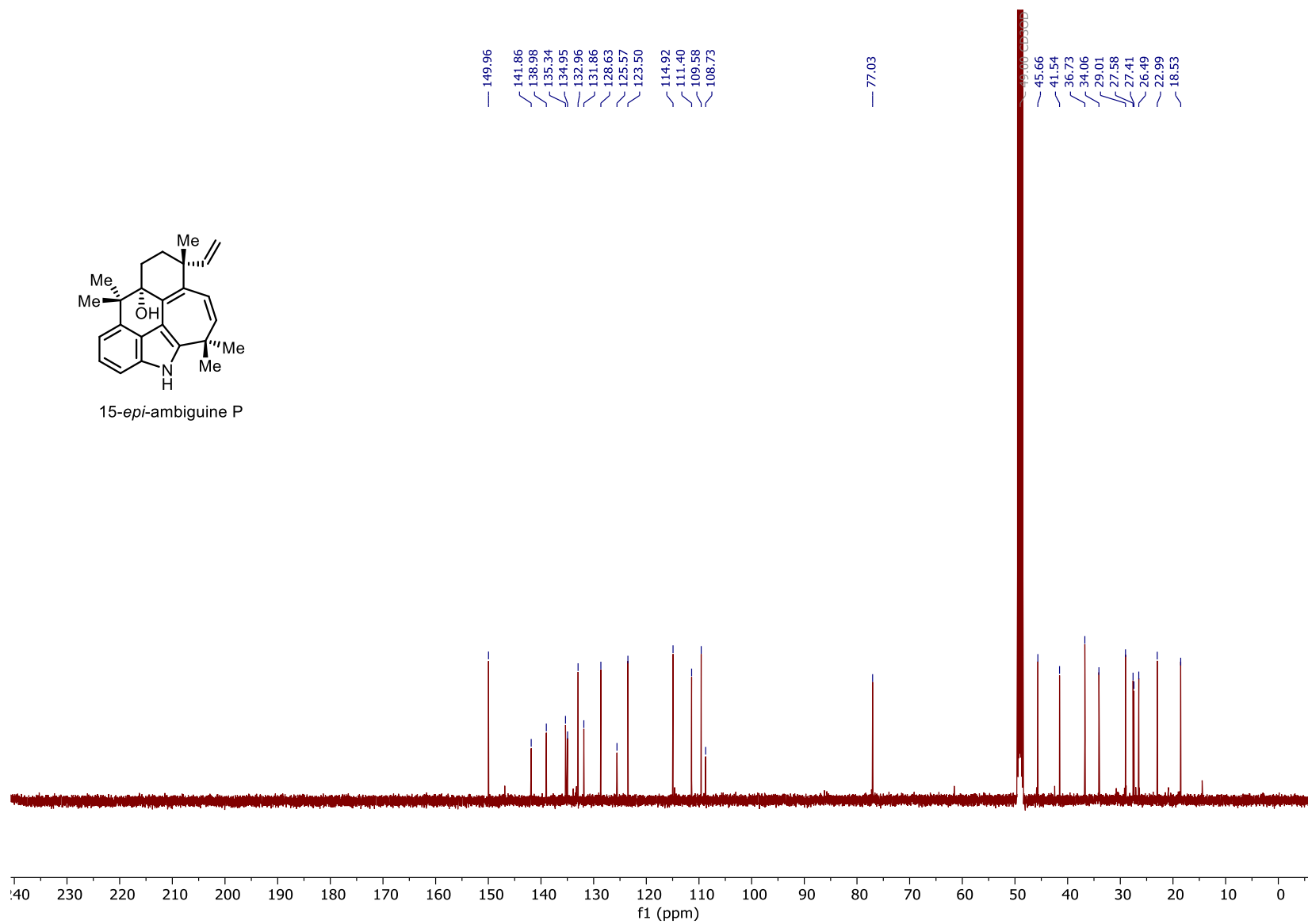


Figure 113. ^{13}C NMR spectrum of 15-*epi*-ambiguine P (125 MHz, CD_3OD).

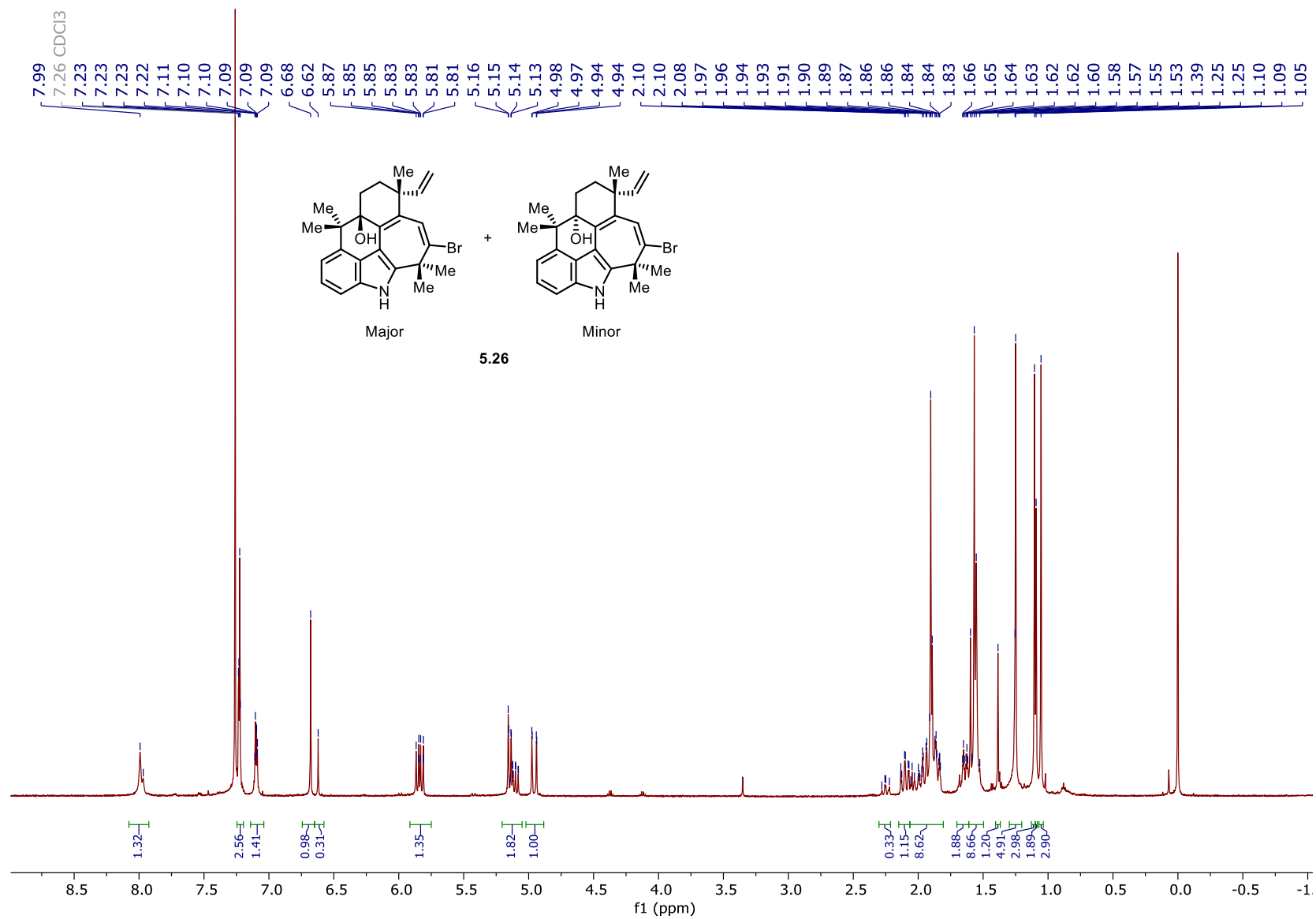


Figure 114. ^1H NMR spectrum of **5.26** (500 MHz, CDCl_3).

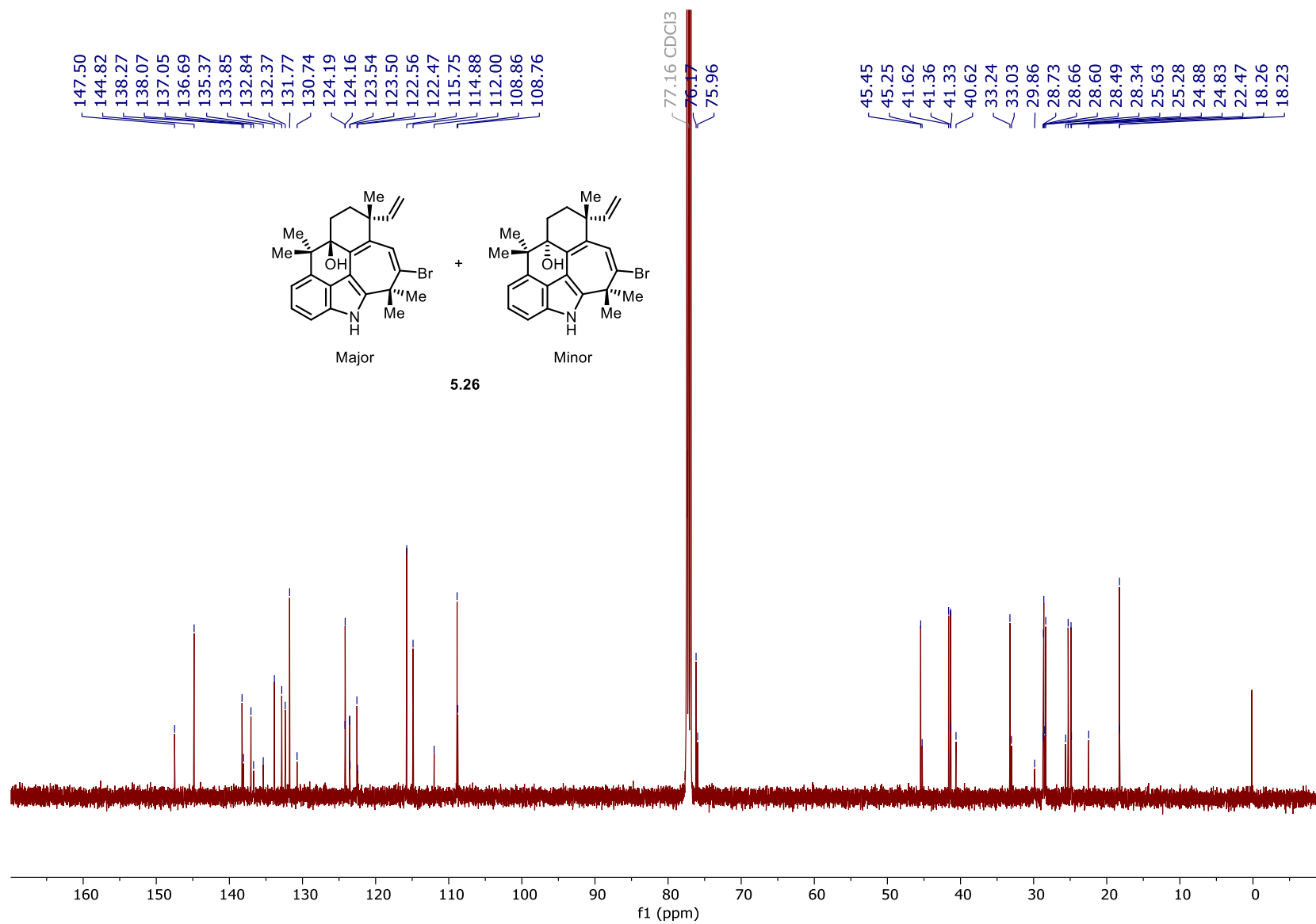


Figure 115. ^{13}C NMR spectrum of **5.26** (125 MHz, CDCl₃).

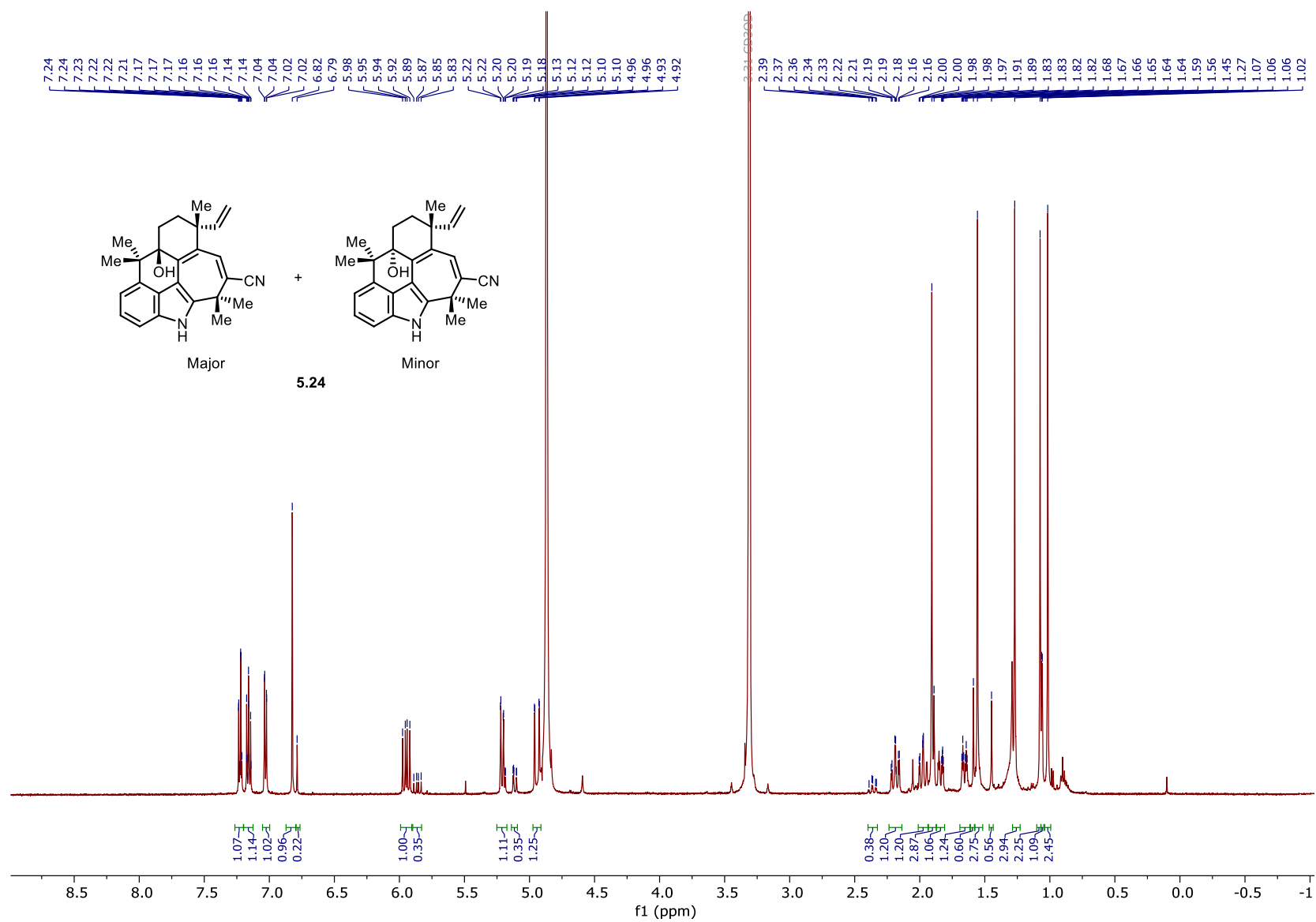


Figure 116. ^1H NMR spectrum of **5.24** (500 MHz, CDCl_3).

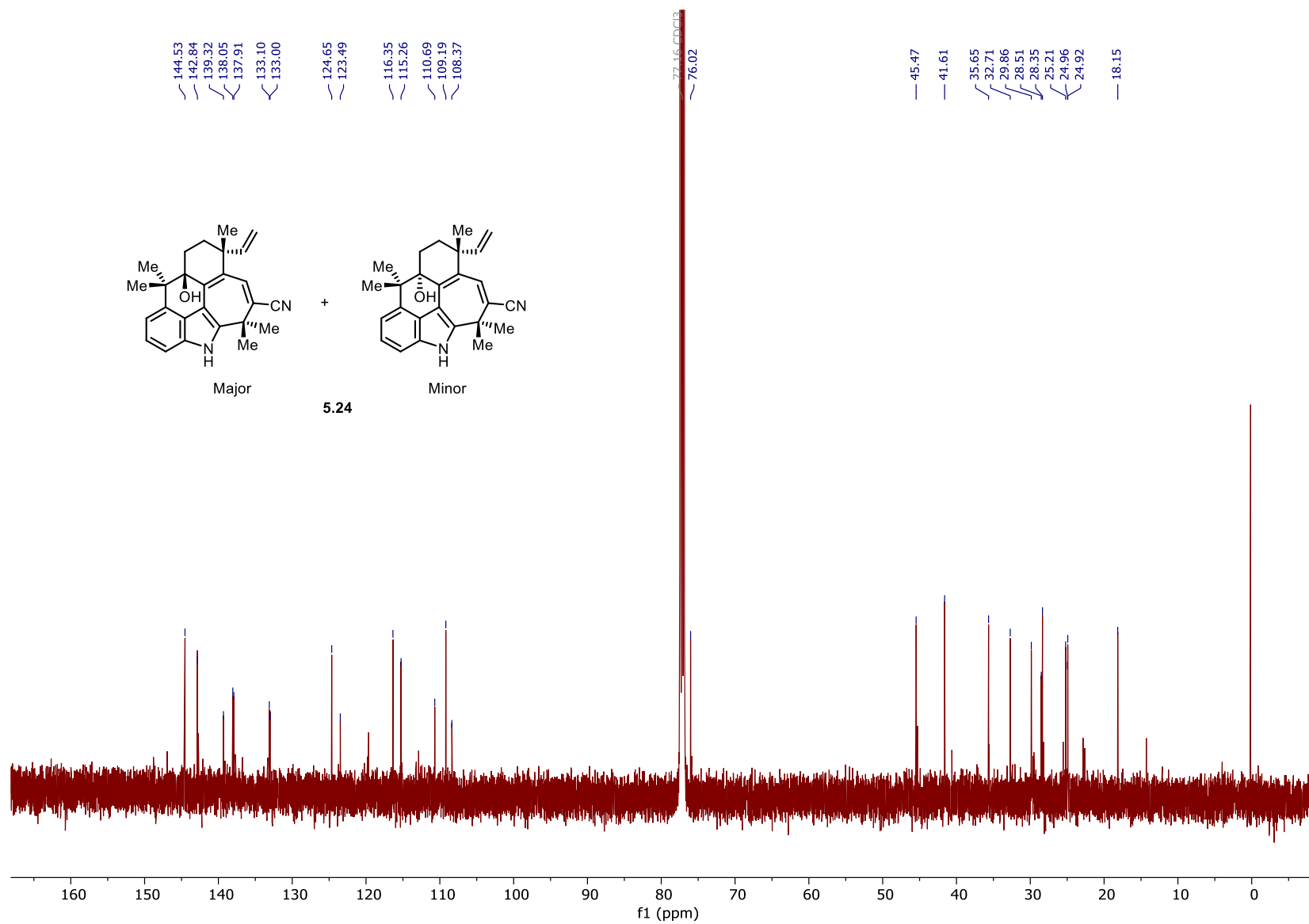


Figure 117. ¹³C NMR spectrum of **5.24** (125 MHz, CDCl₃).

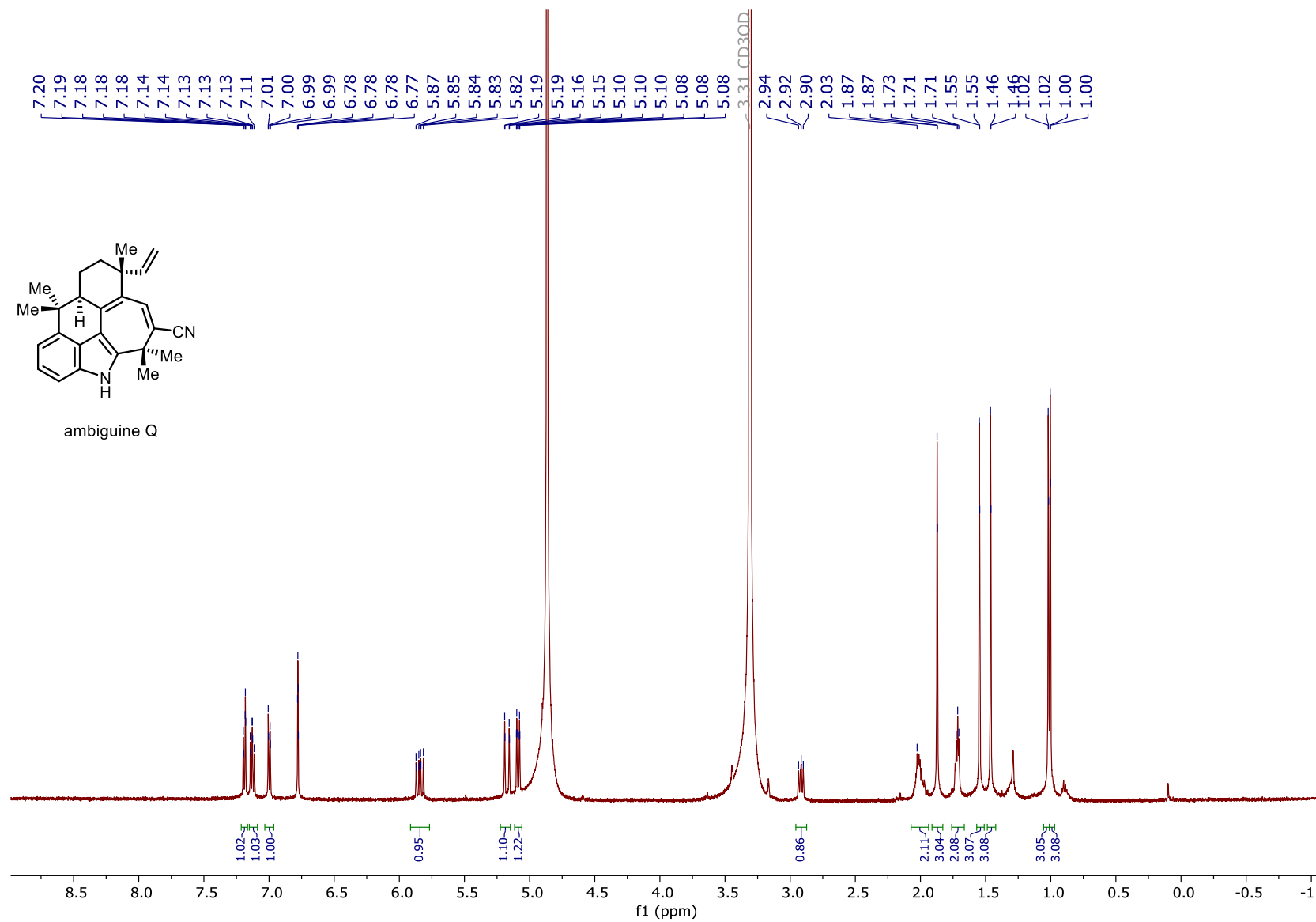


Figure 118. ¹H NMR spectrum of ambiguine Q (500 MHz, CD₃OD).

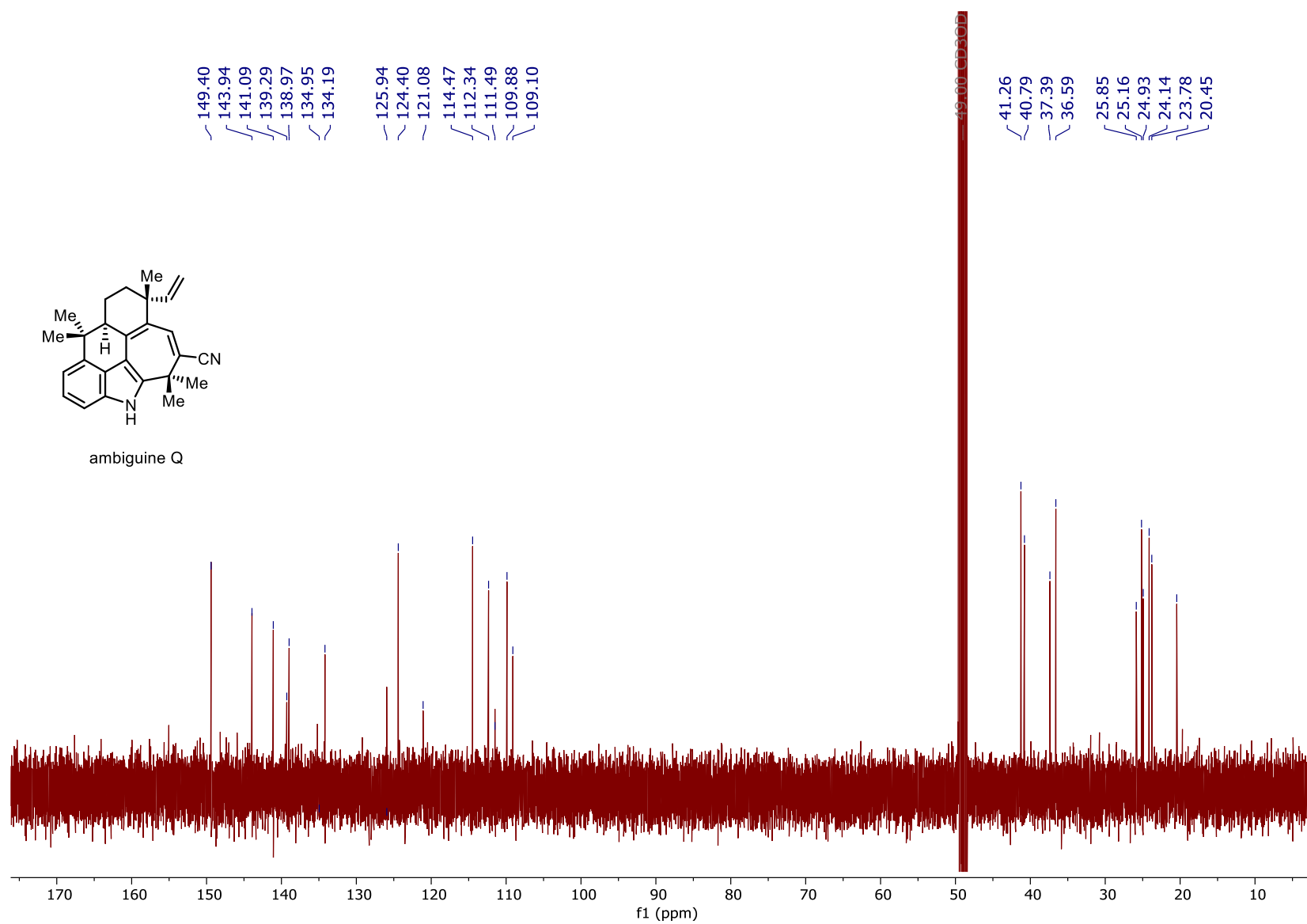


Figure 119. ^{13}C NMR spectrum of ambiguine Q (125 MHz, CD_3OD).

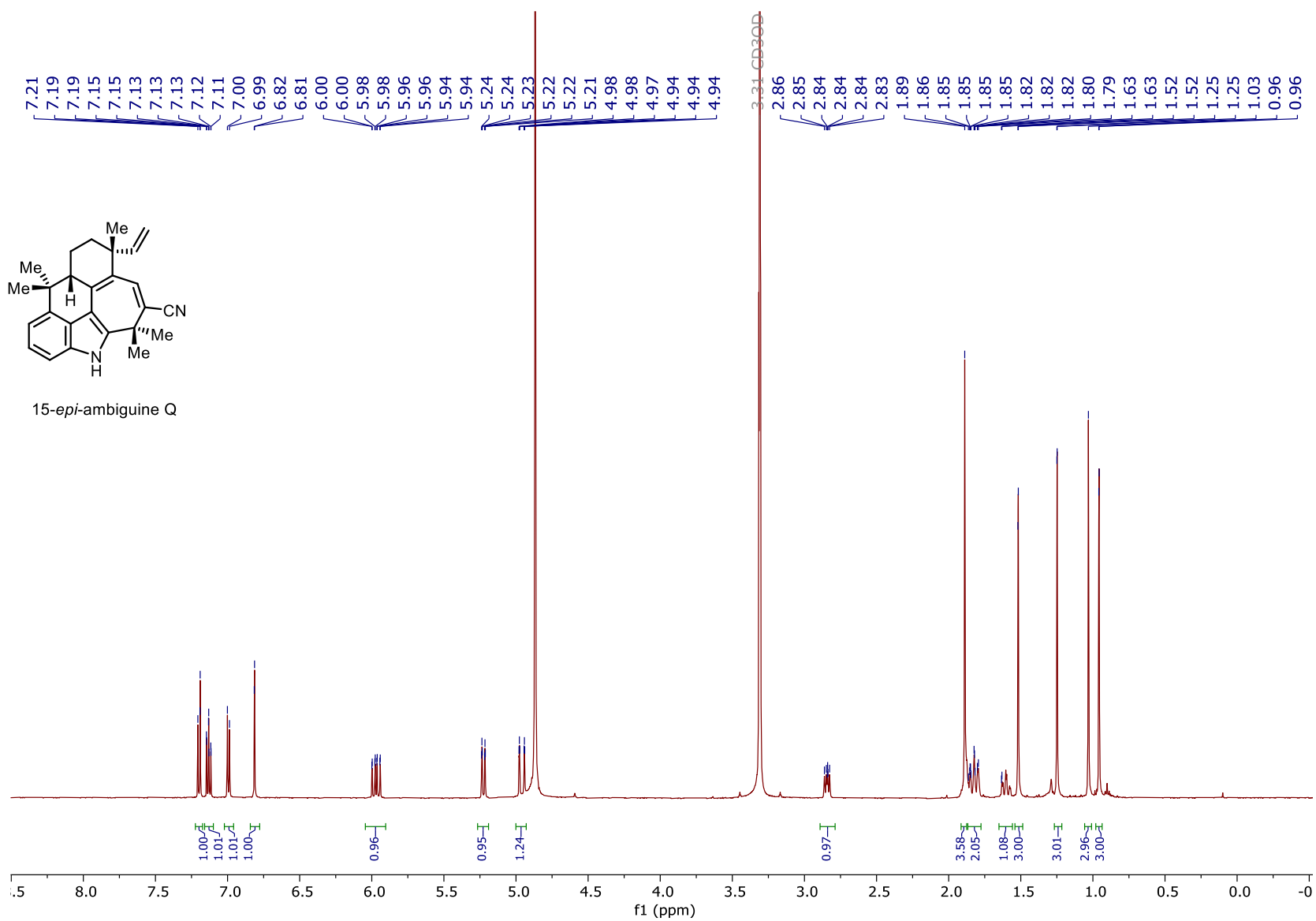


Figure 120. ¹H NMR spectrum of 15-*epi*-ambiguine Q (500 MHz, CD₃OD).

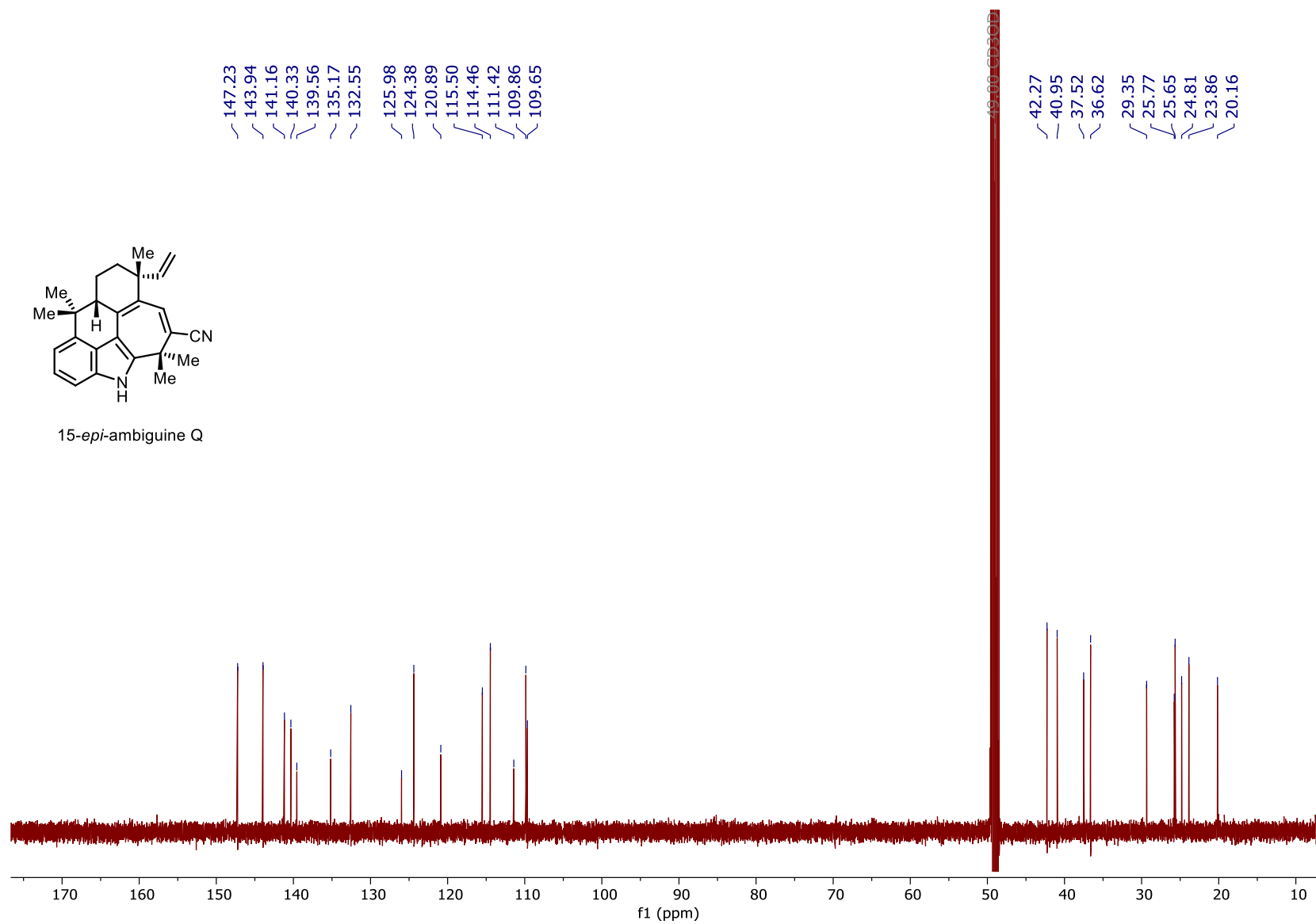


Figure 121. ¹³C NMR spectrum of 15-*epi*-ambiguine Q (125 MHz, CD₃OD).

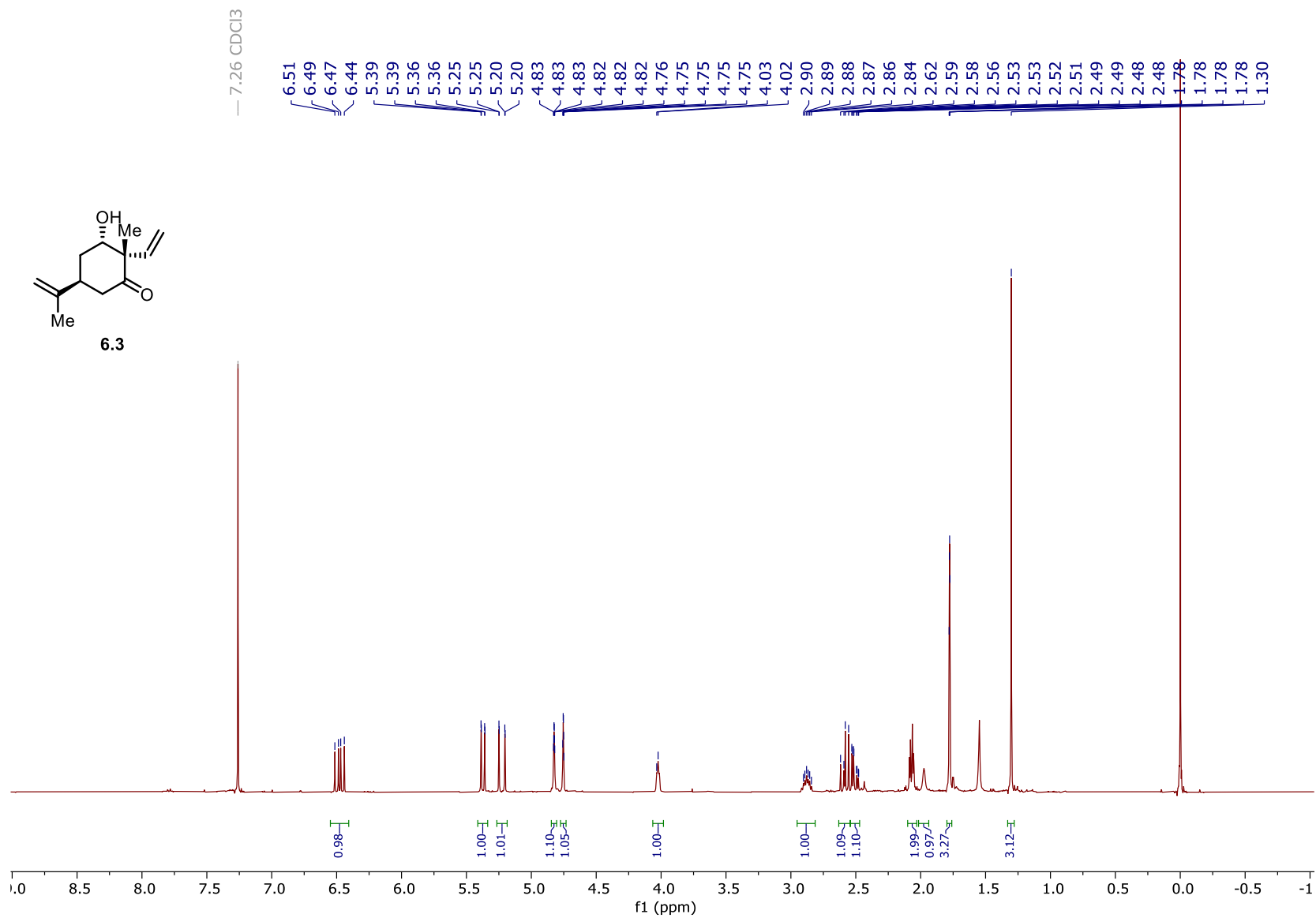


Figure 122. ¹H NMR spectrum of **6.3** (500 MHz, CDCl₃).

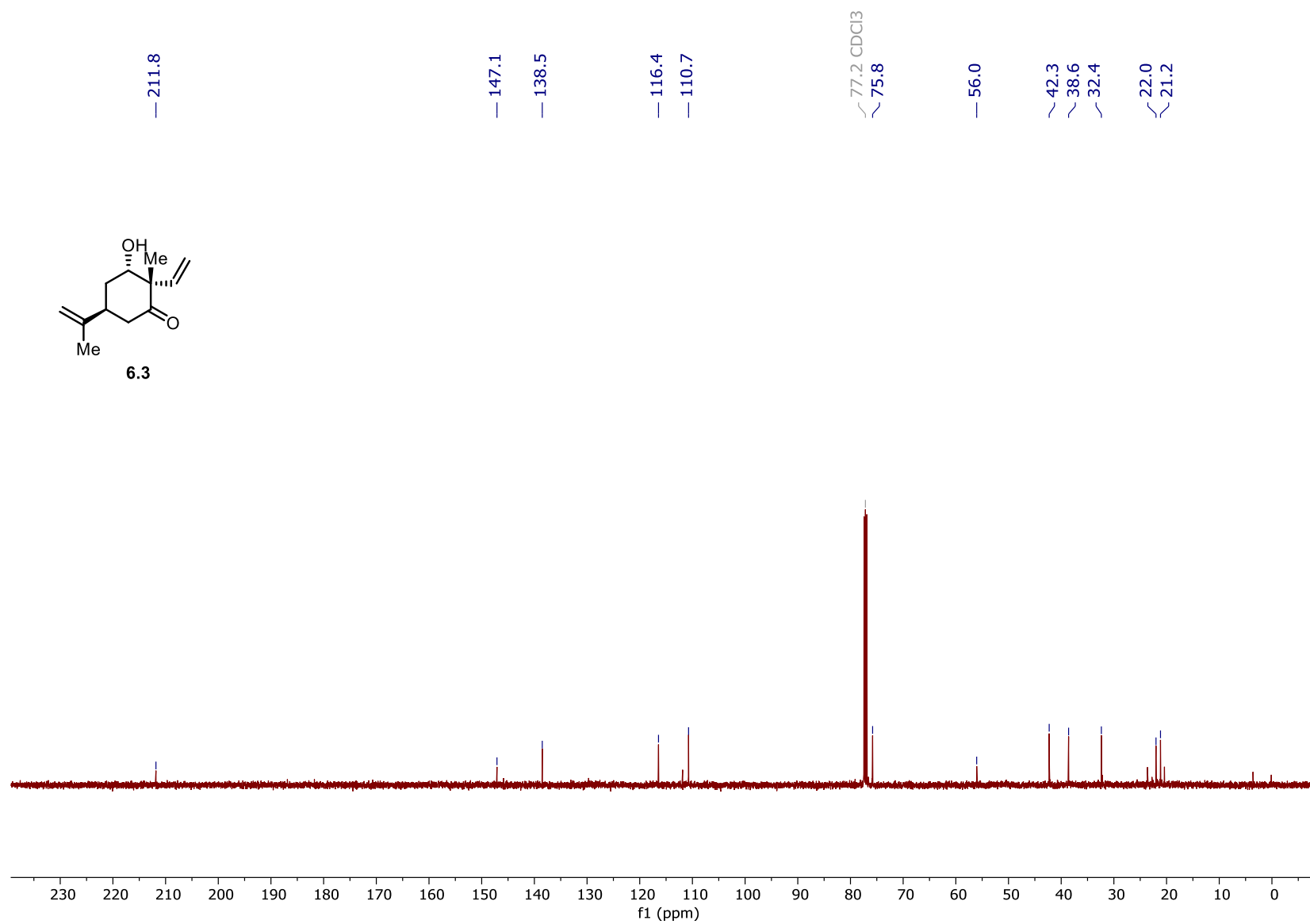


Figure 123. ^{13}C NMR spectrum of **6.3** (125 MHz, CDCl_3).

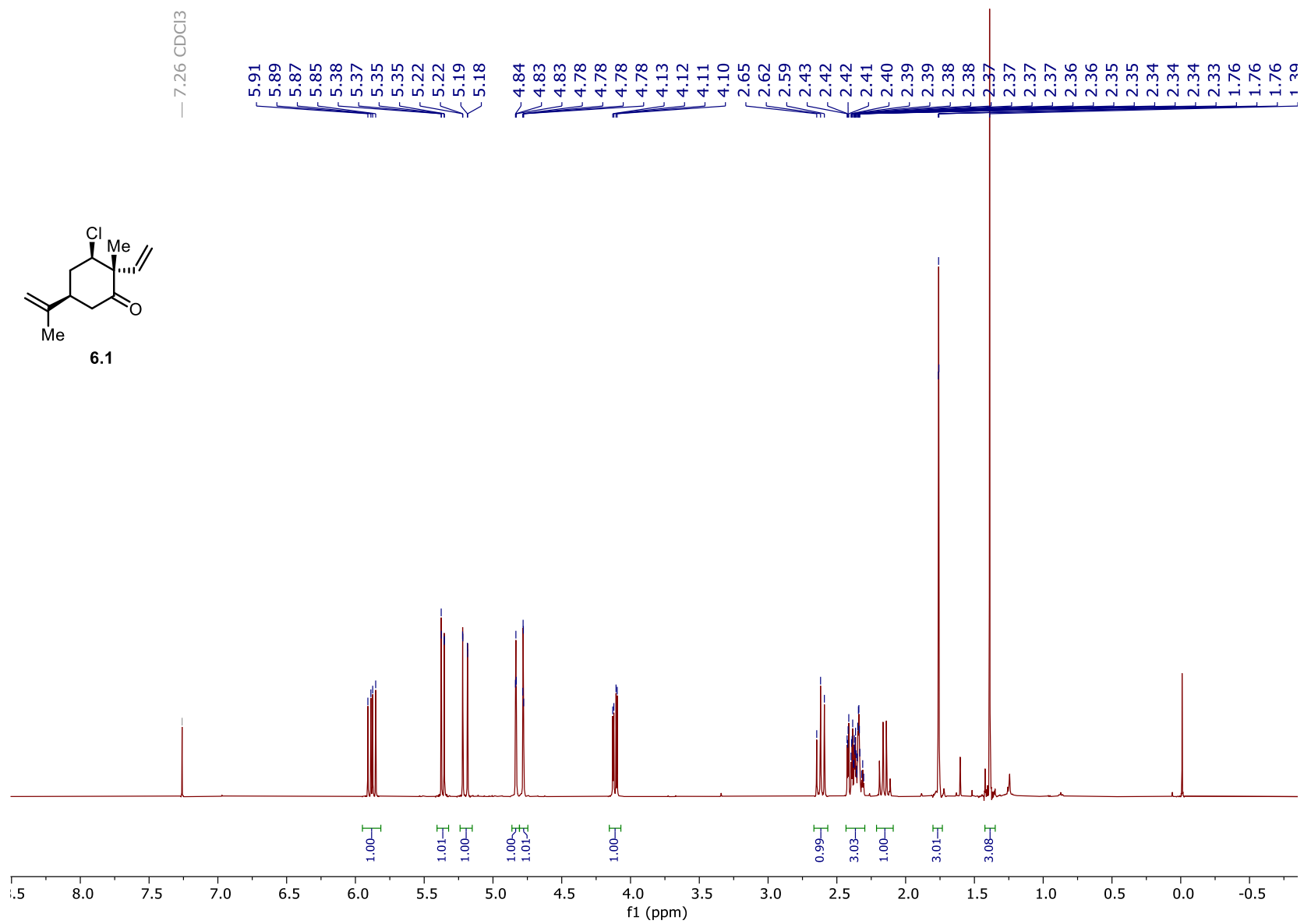


Figure 124. ¹H NMR spectrum of **6.1** (500 MHz, CDCl₃).

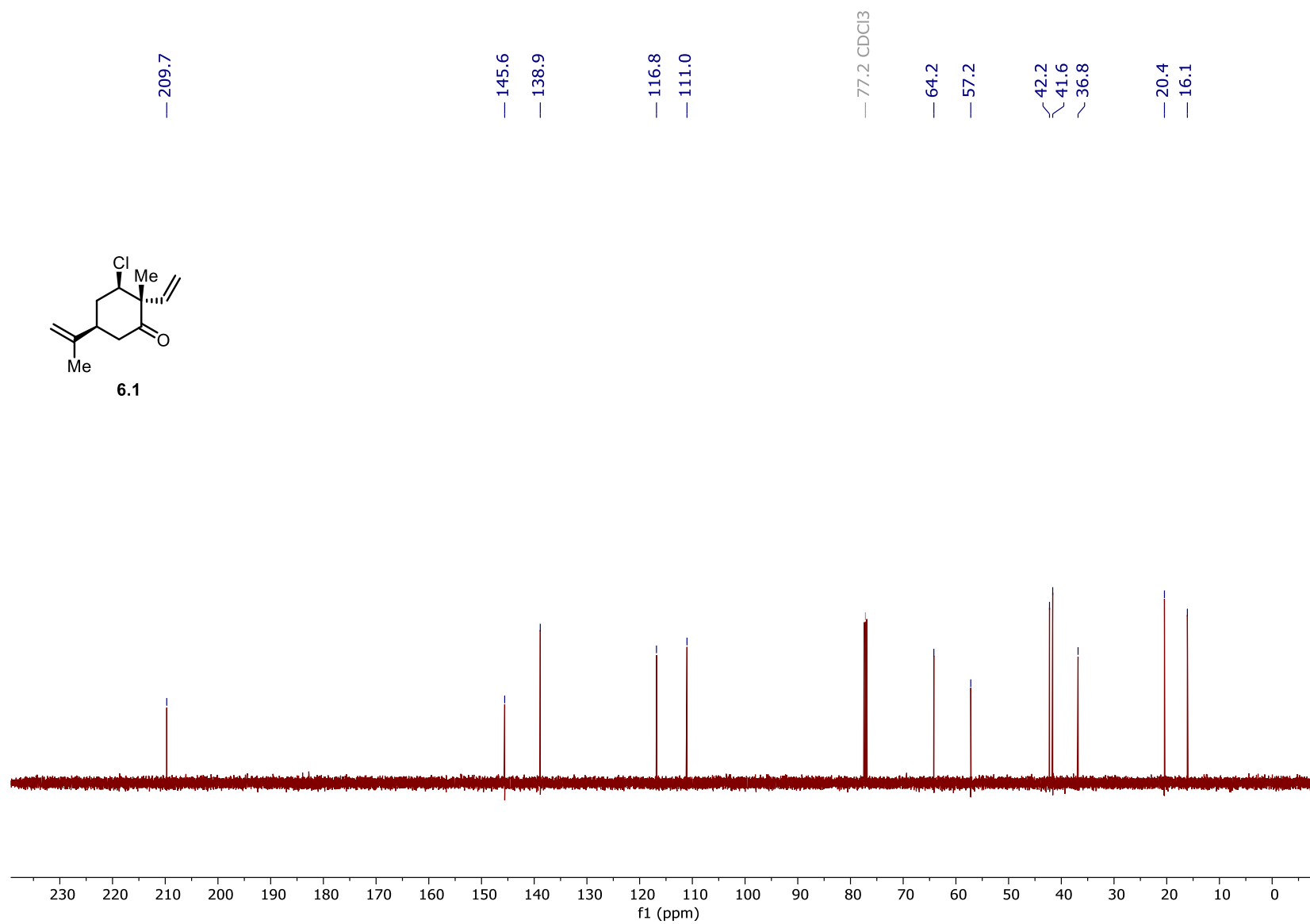


Figure 125. ^{13}C NMR spectrum of **6.1** (125 MHz, CDCl_3).

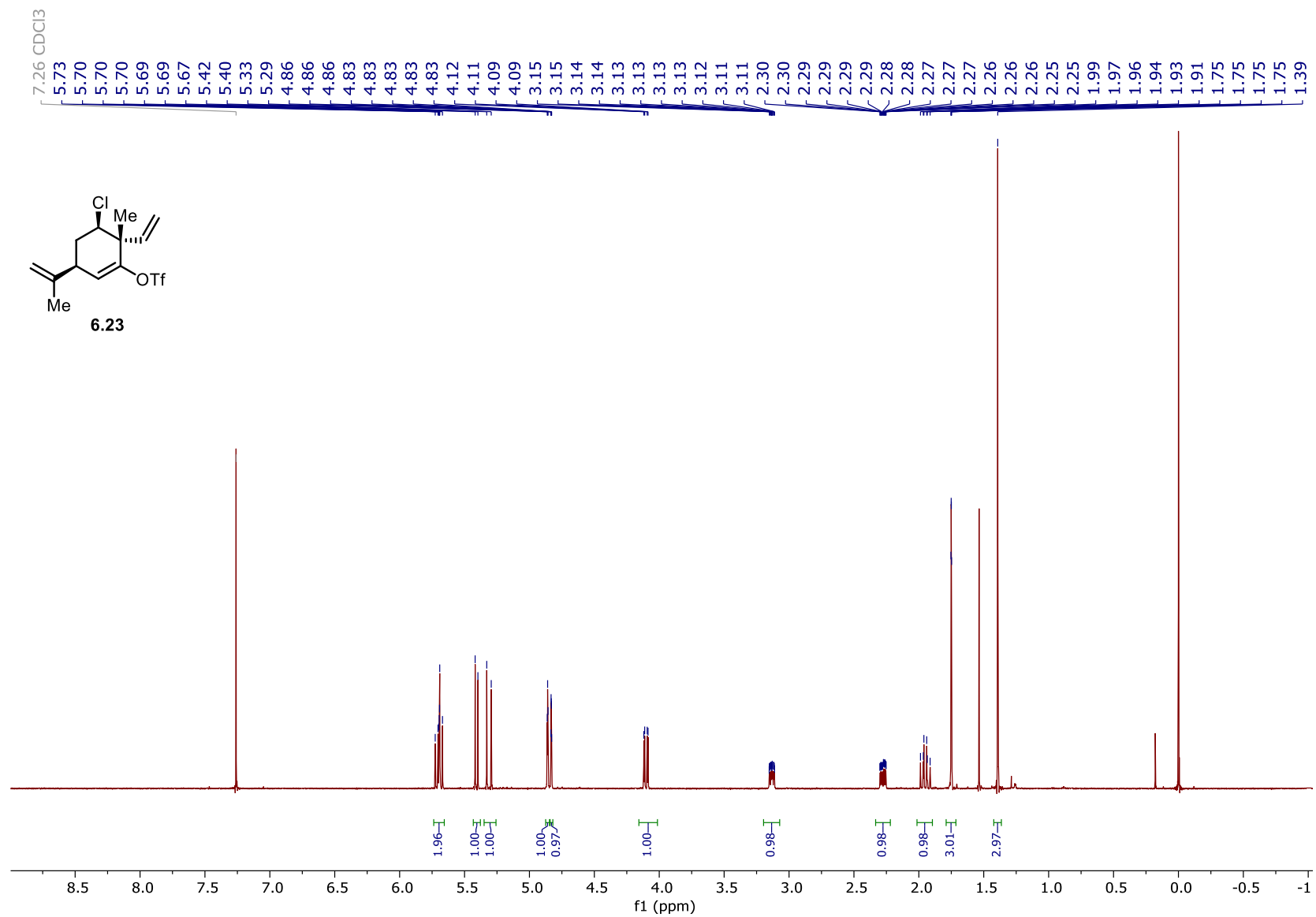


Figure 126. ^1H NMR spectrum of **6.23** (500 MHz, CDCl_3).

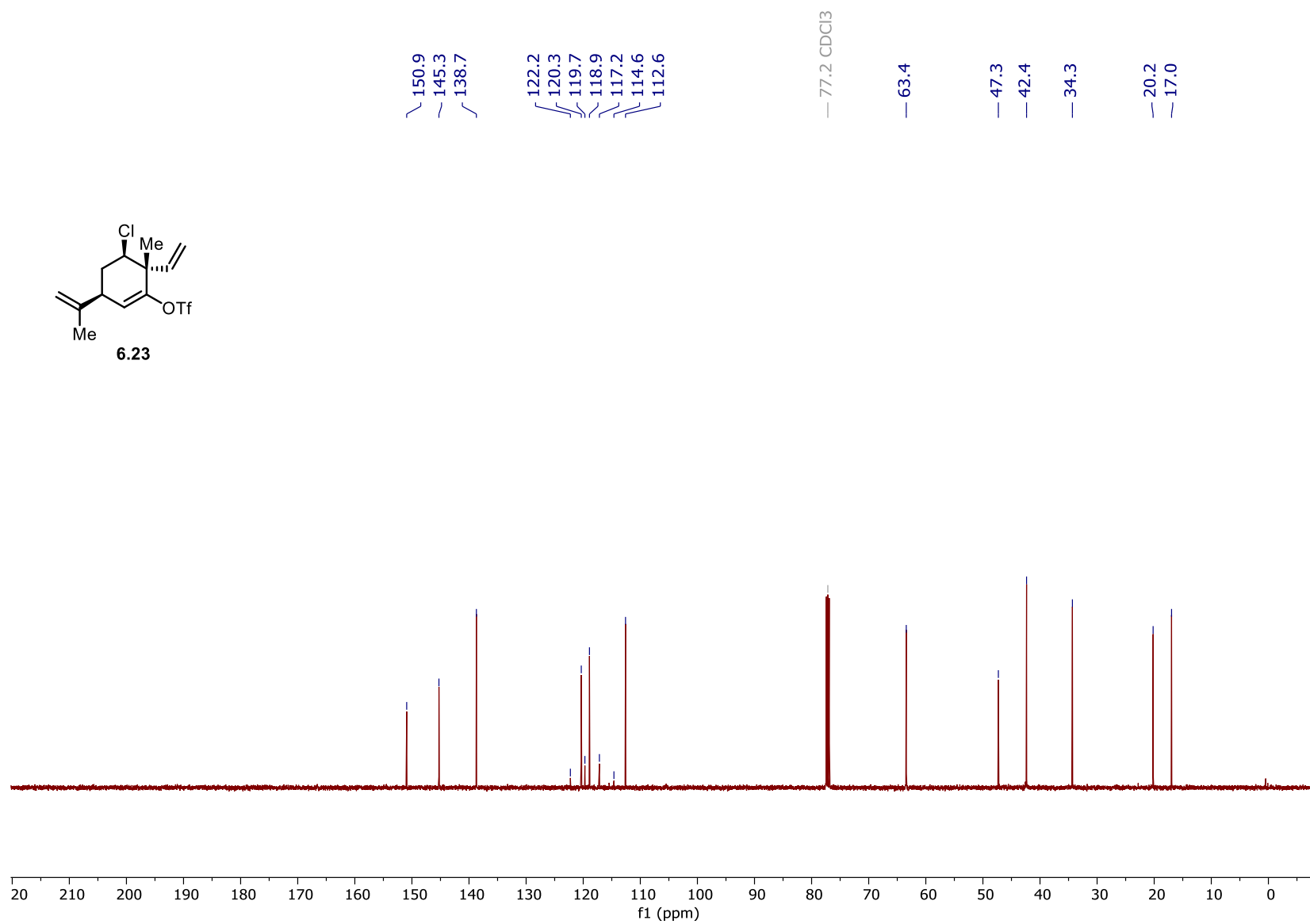


Figure 127. ¹³C NMR spectrum of **6.23** (125 MHz, CDCl₃).

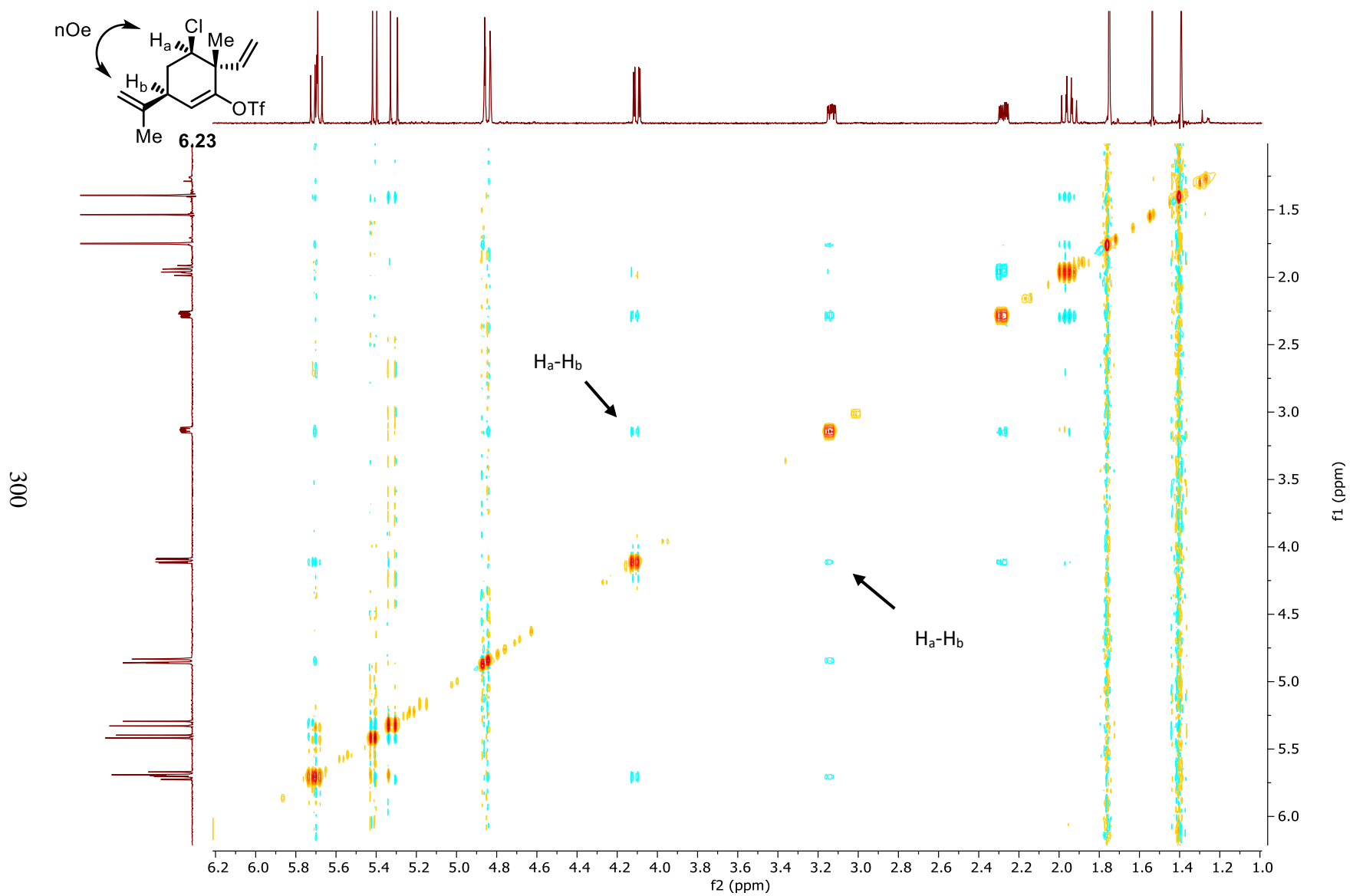


Figure 128. NOESY spectrum of **6.23** (CDCl₃).

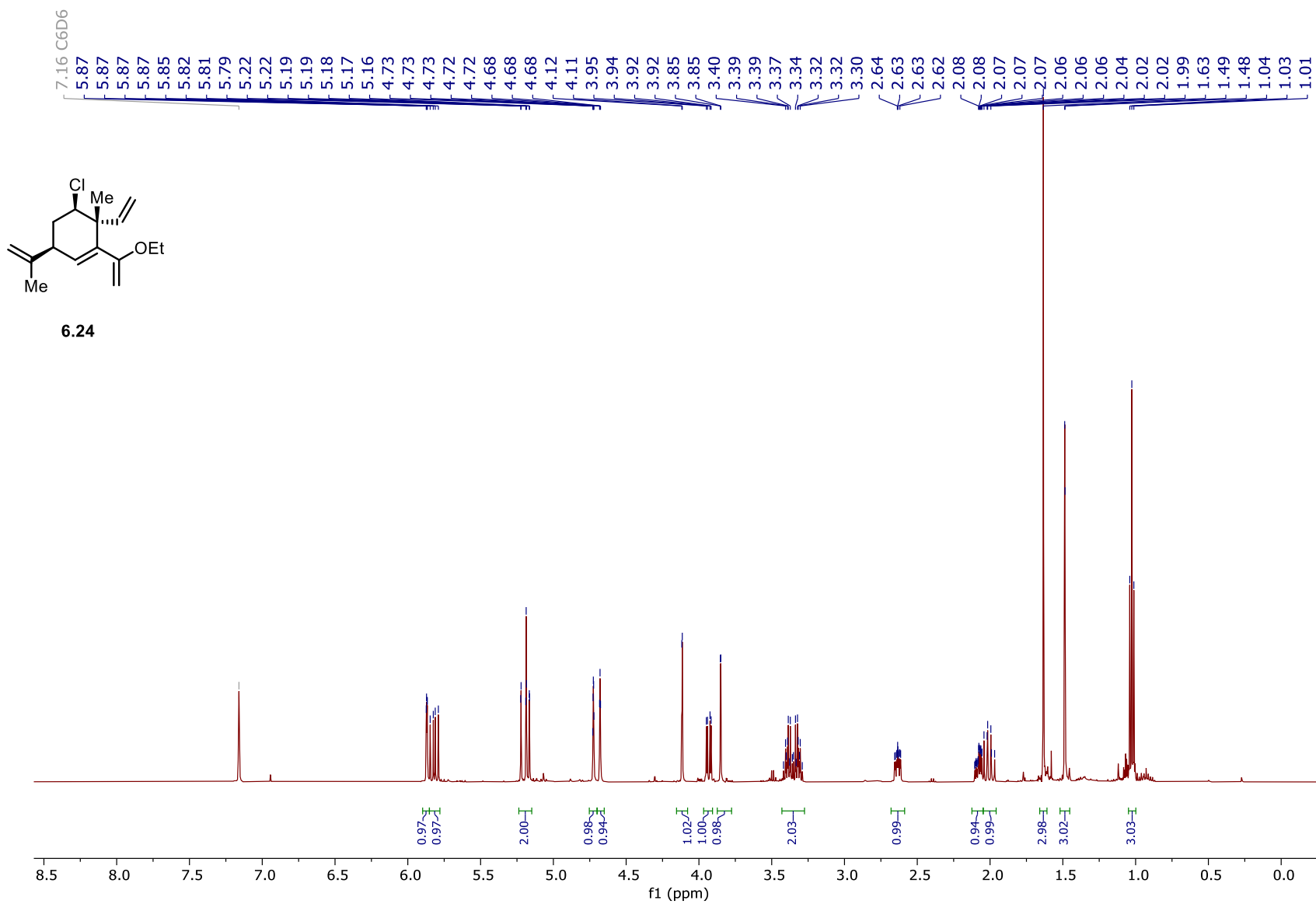


Figure 129. ^1H NMR spectrum of **6.24** (500 MHz, CDCl_3).

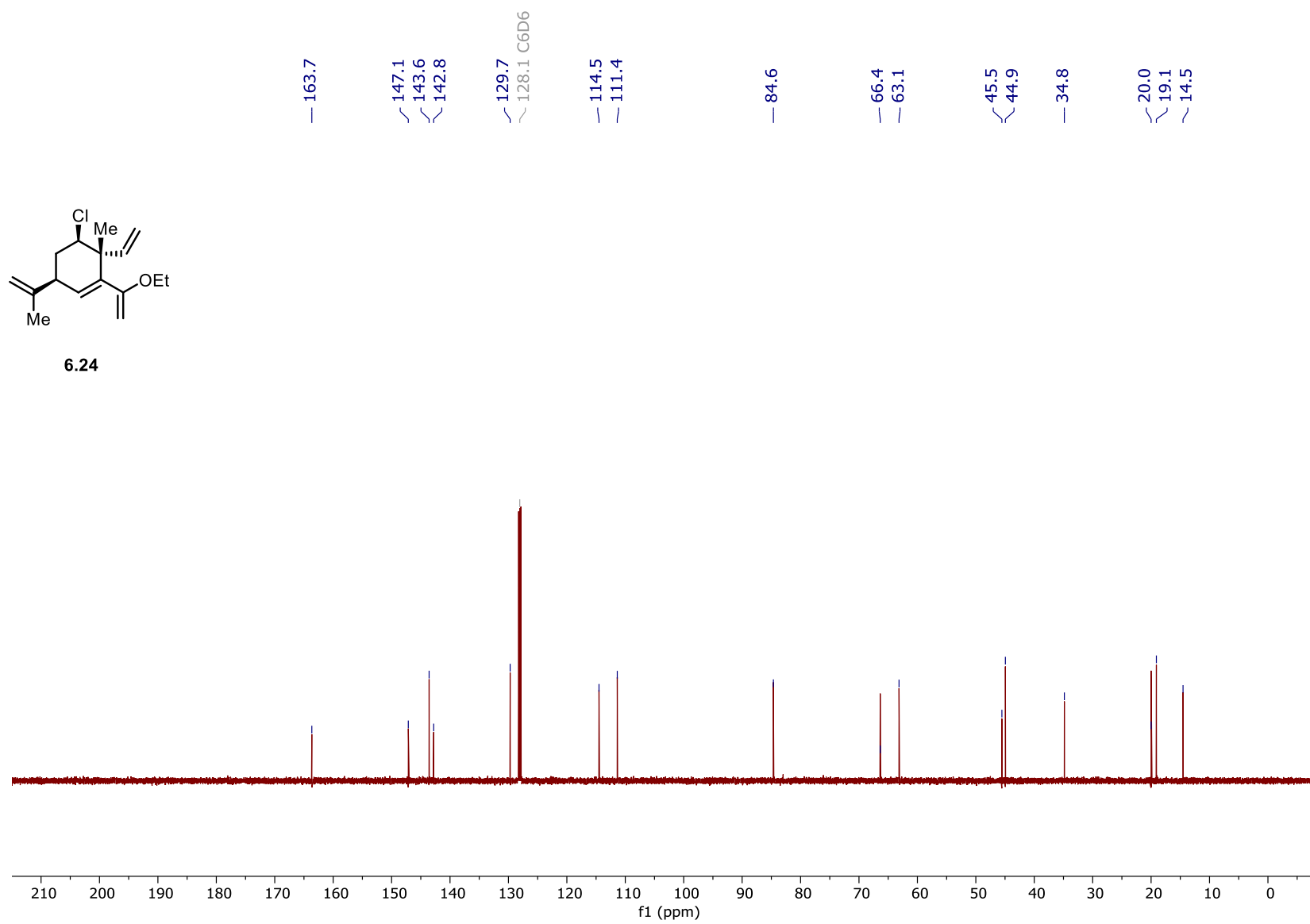


Figure 130. ^{13}C NMR spectrum of **6.24** (125 MHz, C_6D_6).

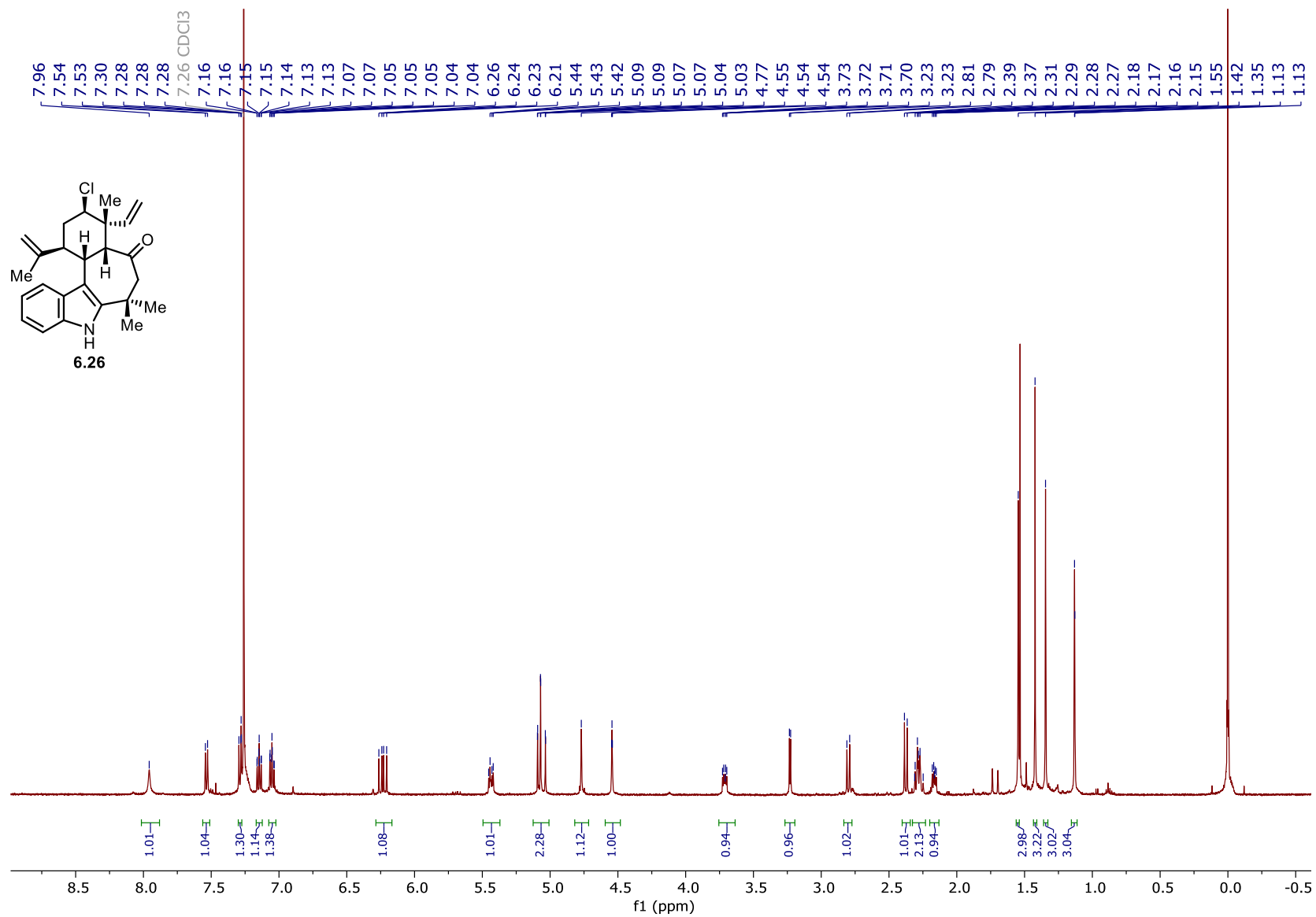


Figure 131. ¹H NMR spectrum of **6.26** (500 MHz, CDCl₃).

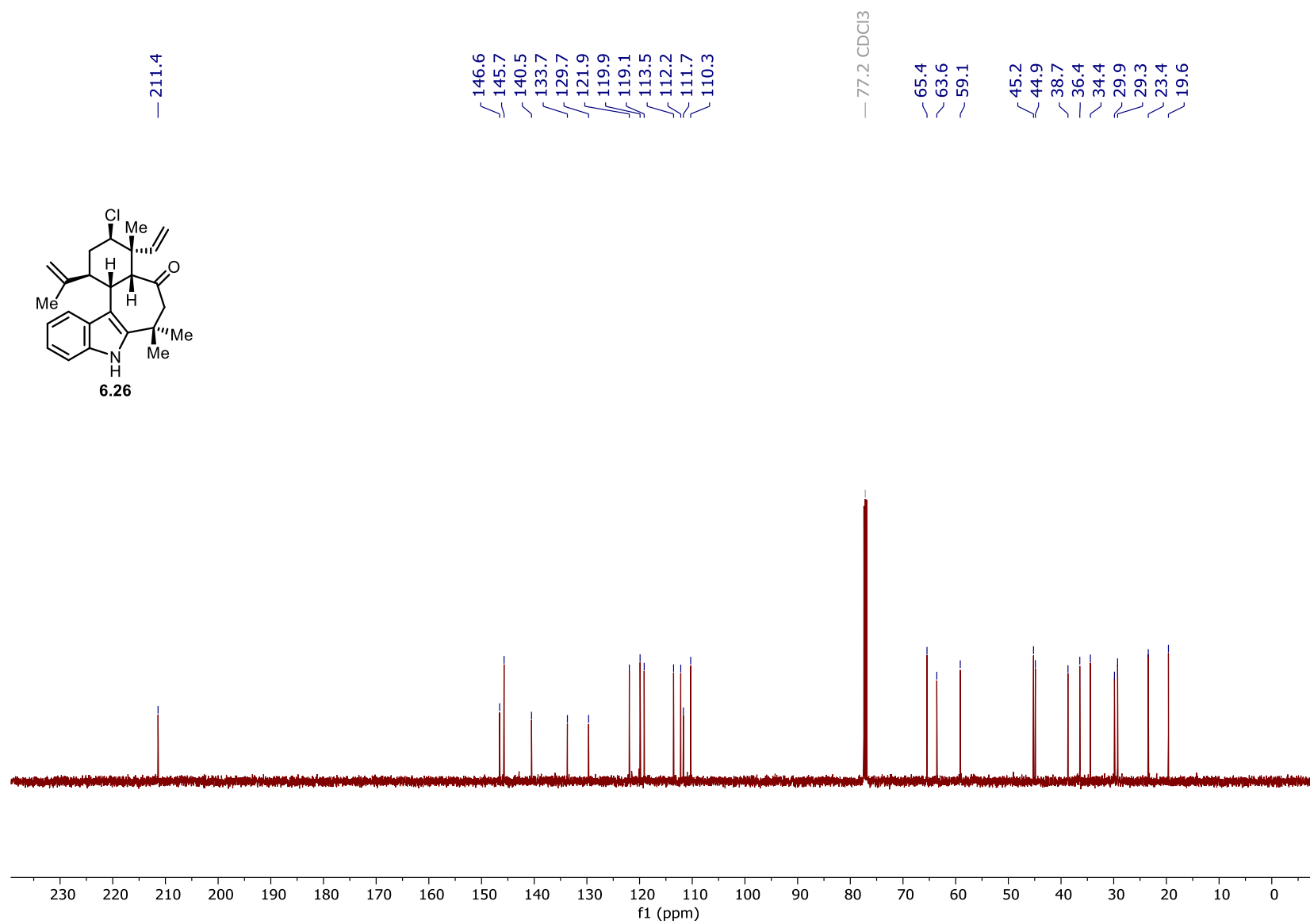


Figure 132. ¹³C NMR spectrum of **6.26** (125 MHz, CDCl₃).

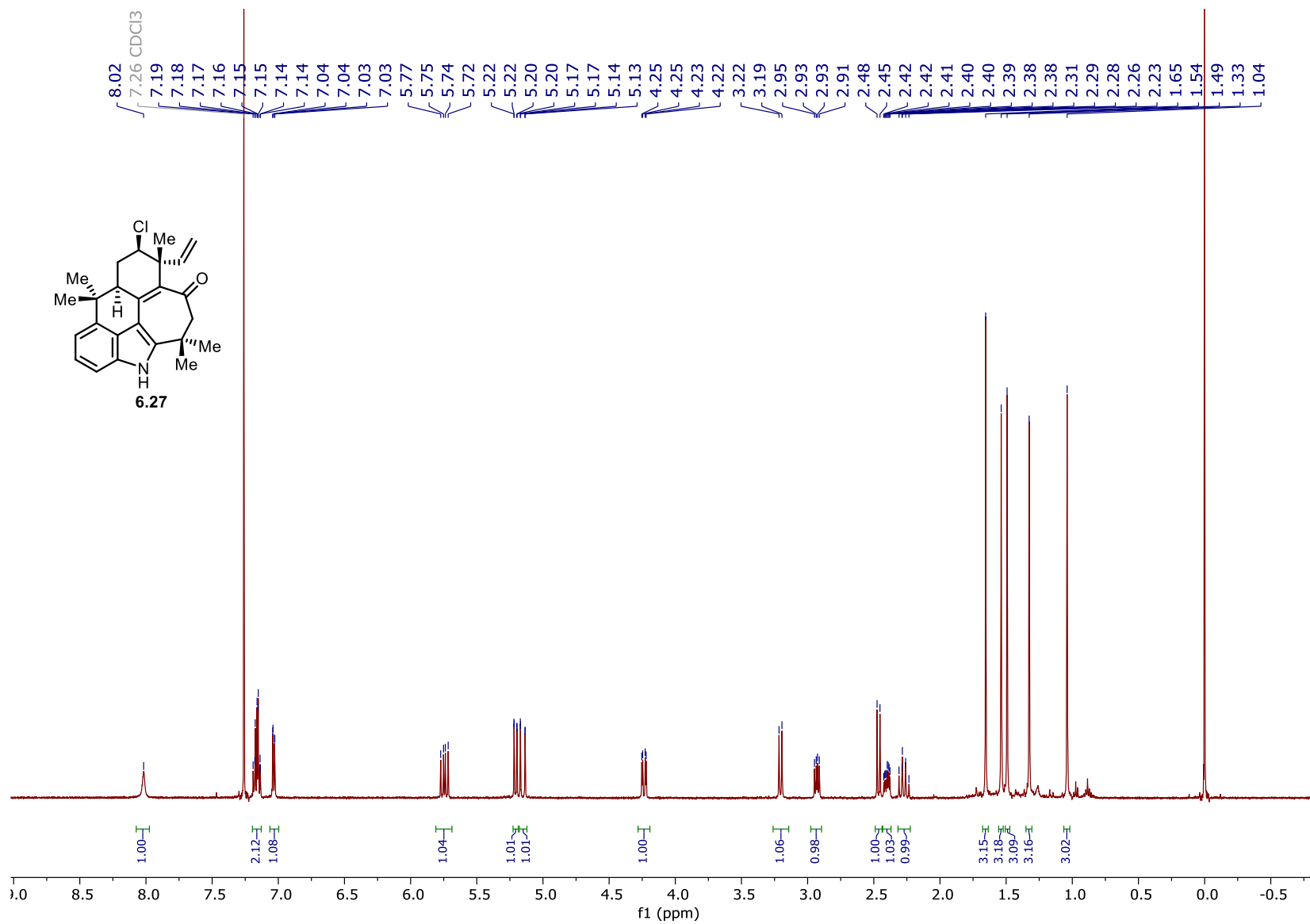


Figure 133. ^1H NMR spectrum of **6.27** (500 MHz, CDCl_3).

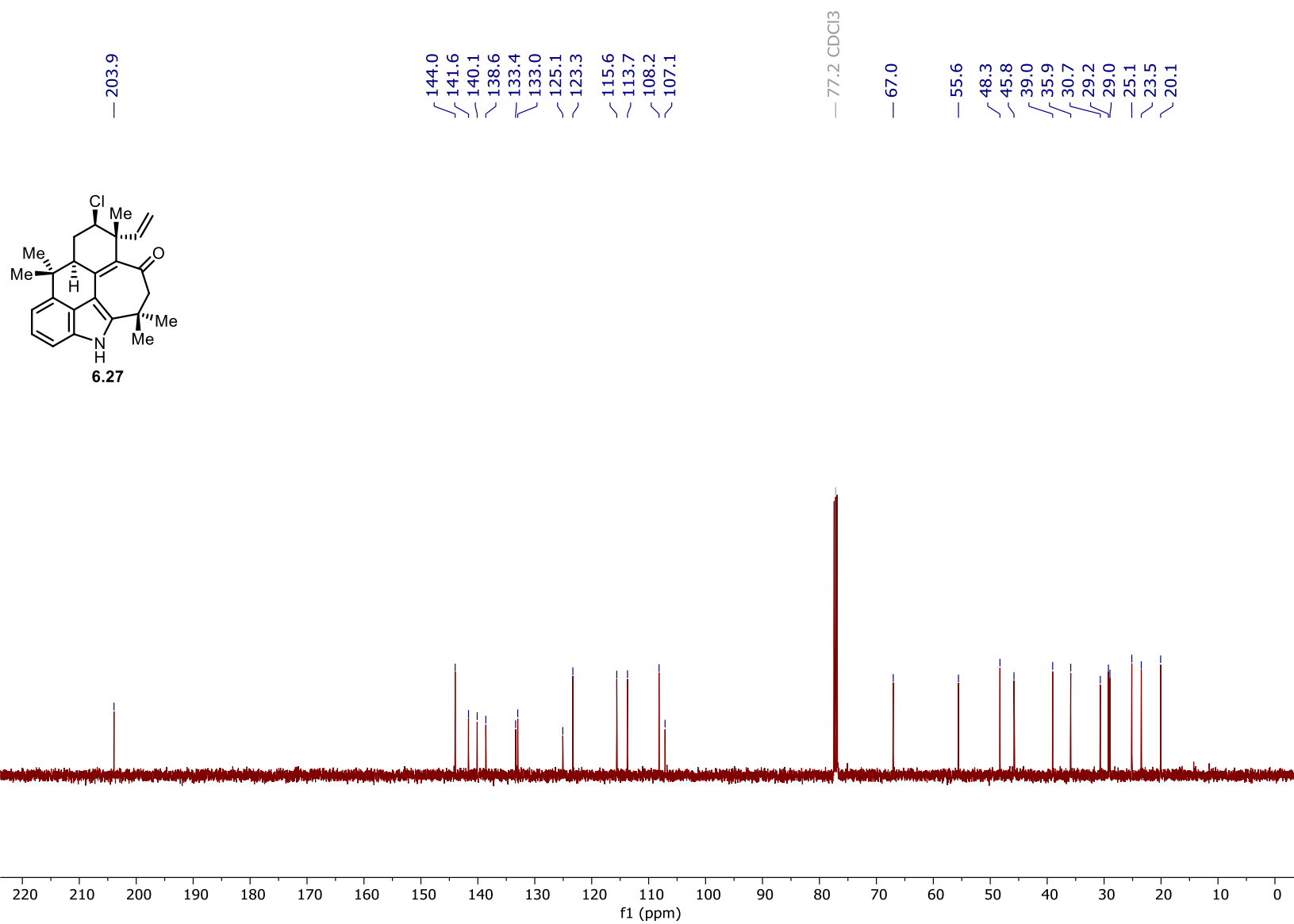


Figure 134. ^{13}C NMR spectrum of **6.27** (125 MHz, CDCl_3).

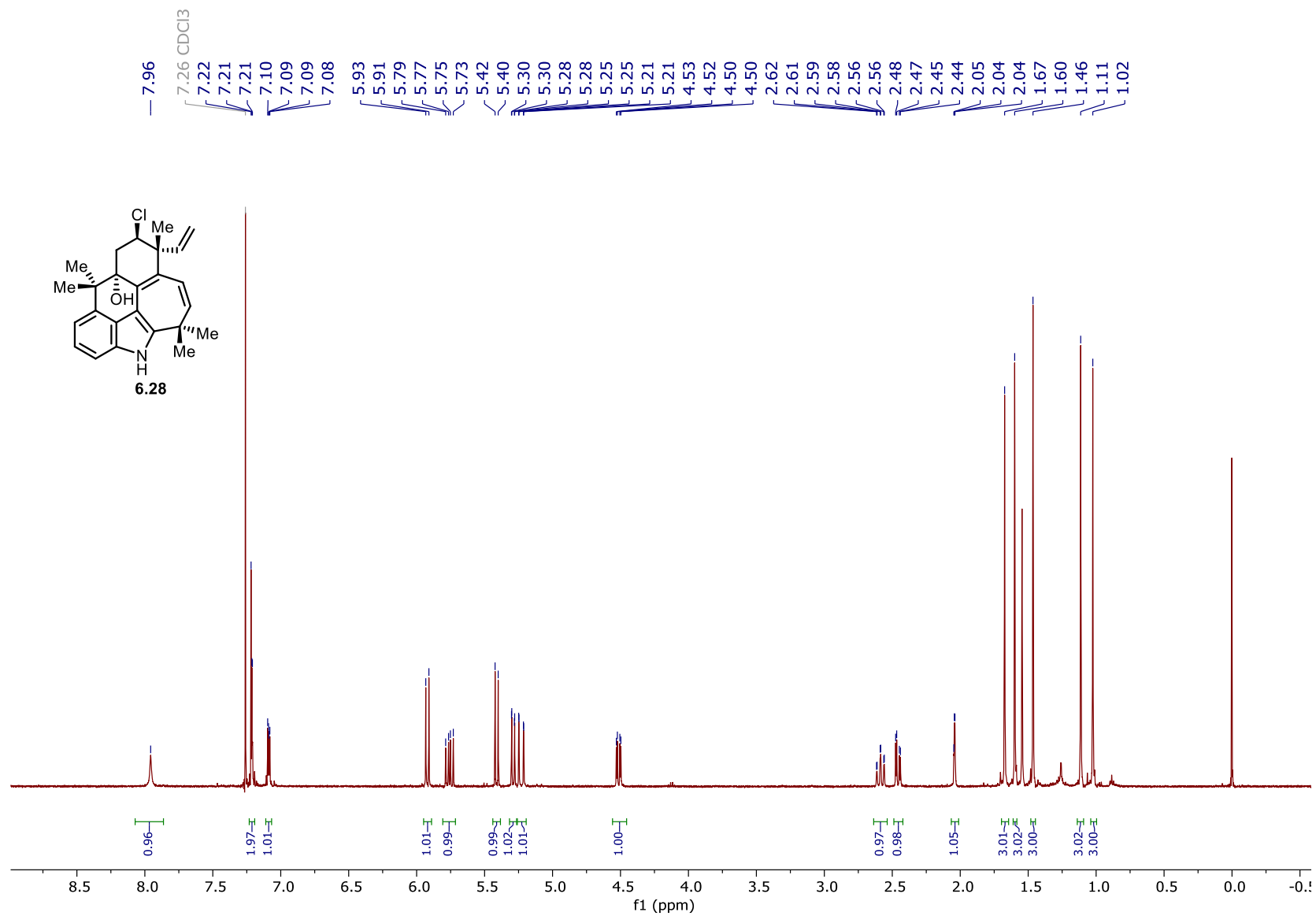


Figure 135. ^1H NMR spectrum of **6.28** (500 MHz, CDCl_3).

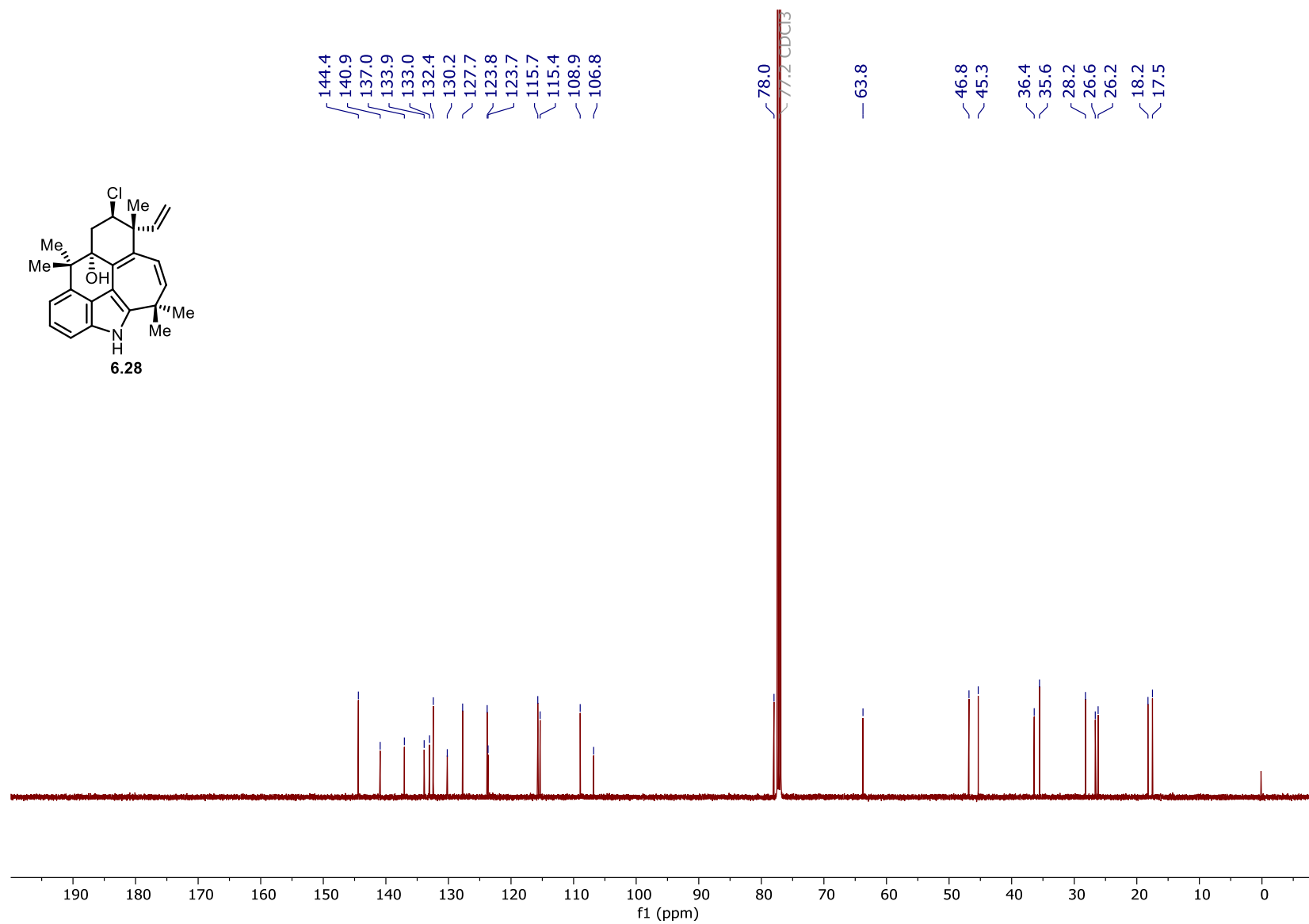


Figure 136. ^{13}C NMR spectrum of **6.28** (125 MHz, CDCl_3).

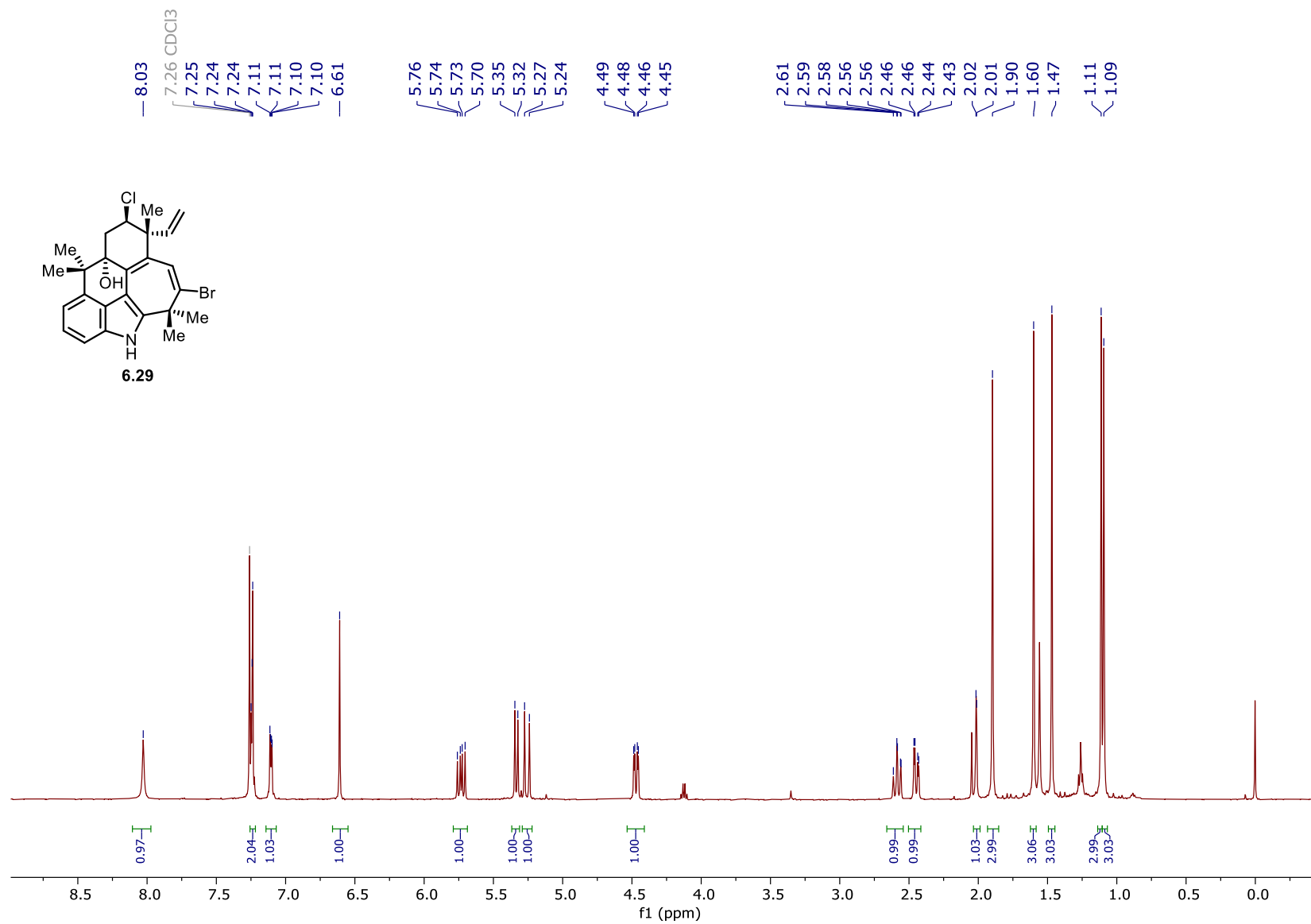


Figure 137. ^1H NMR spectrum of **6.29** (500 MHz, CDCl_3).

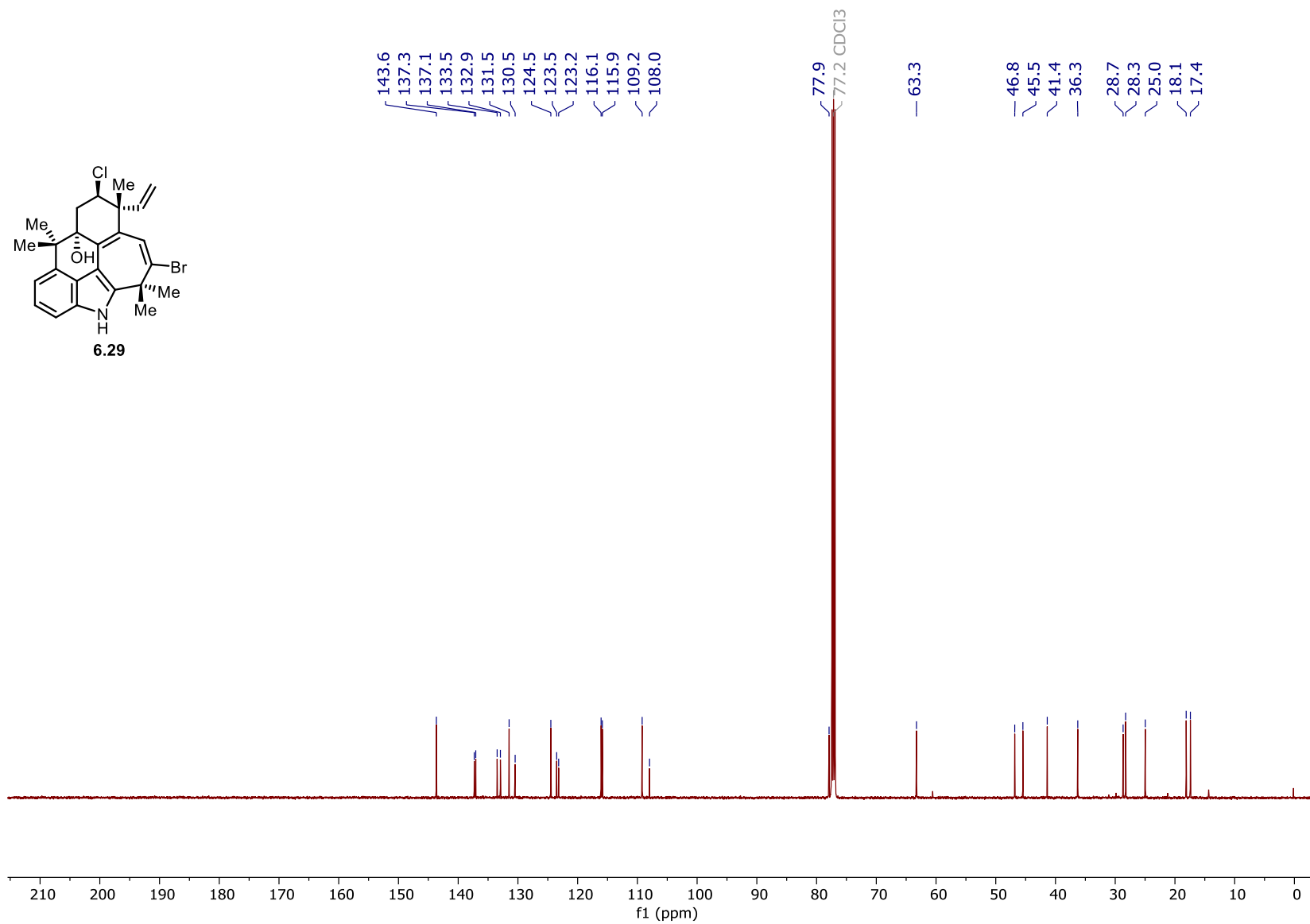


Figure 138. ^{13}C NMR spectrum of **6.29** (125 MHz, CDCl_3).

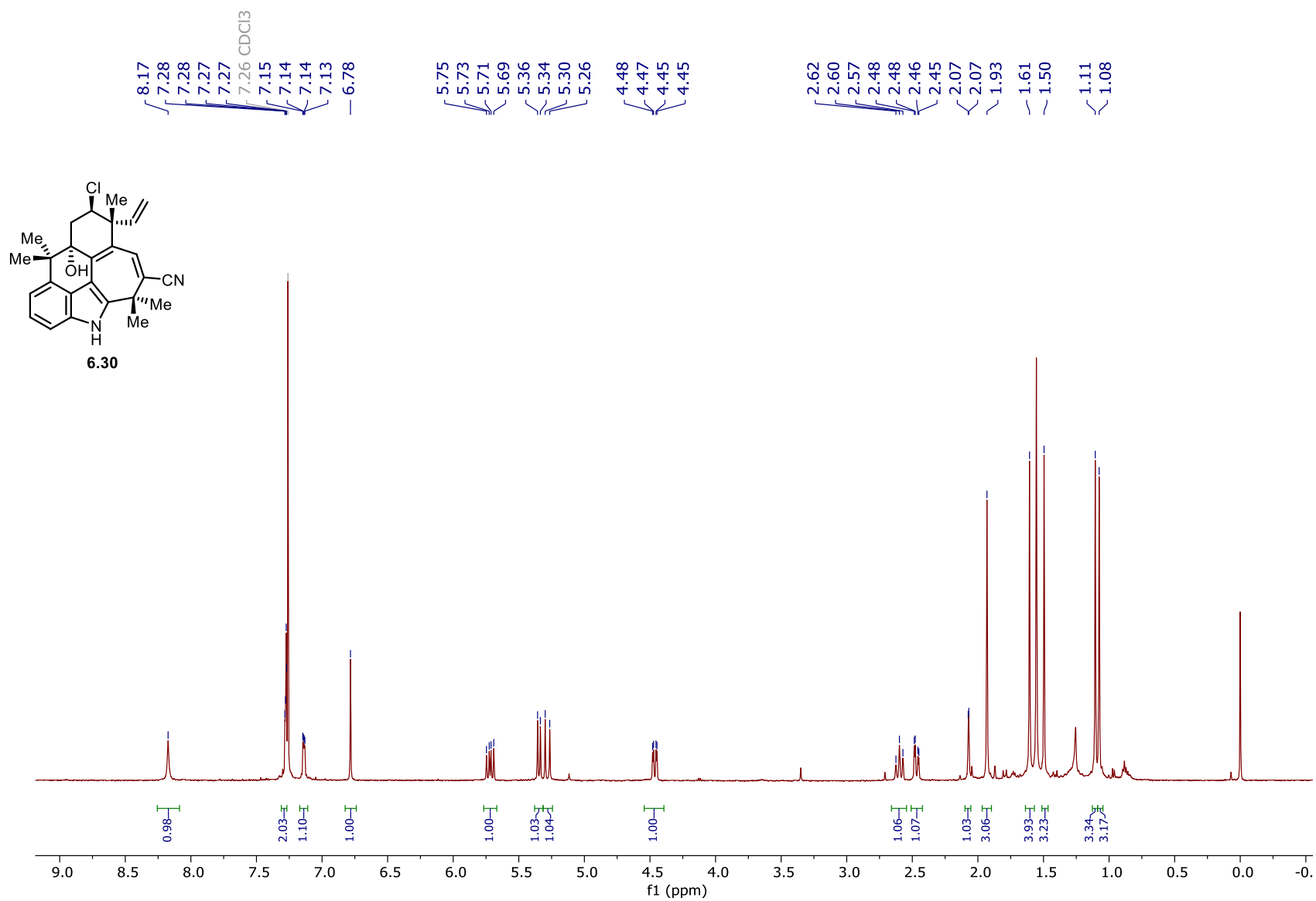


Figure 139. ^1H NMR spectrum of **6.30** (500 MHz, CDCl_3).

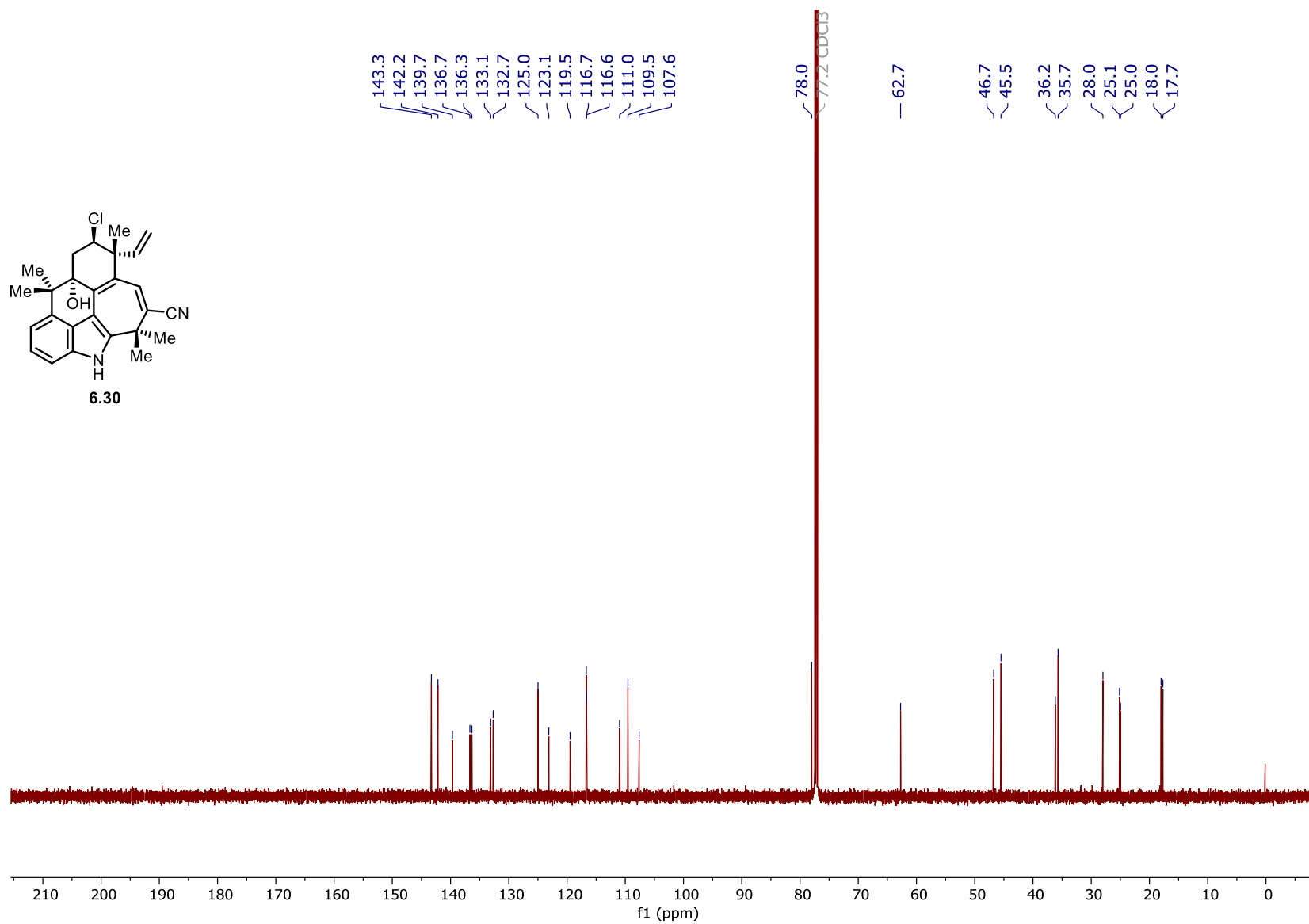


Figure 140. ^{13}C NMR spectrum of **6.30** (125 MHz, CDCl_3).

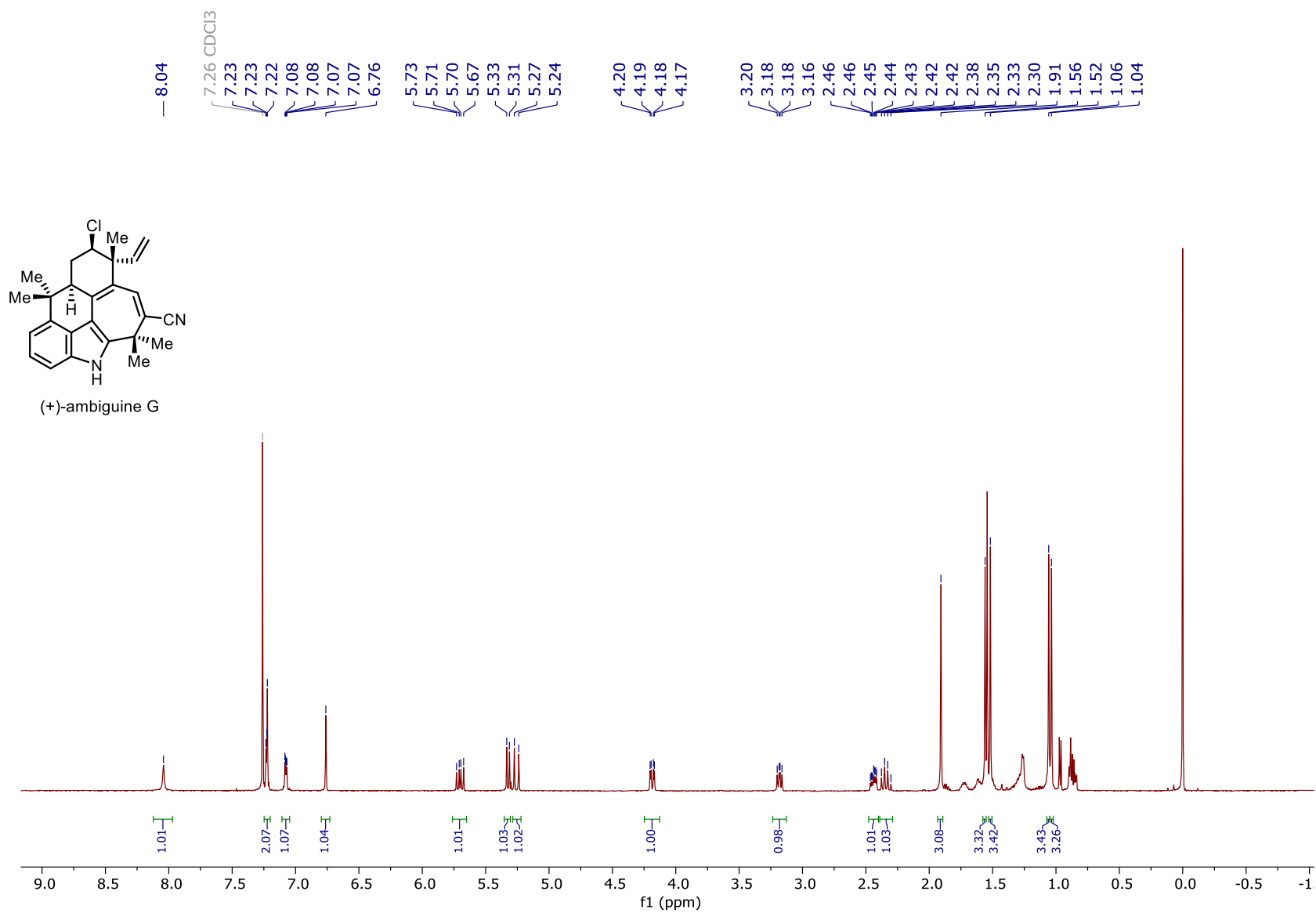


Figure 141. ^1H NMR spectrum of ambiguity G (500 MHz, CDCl_3).

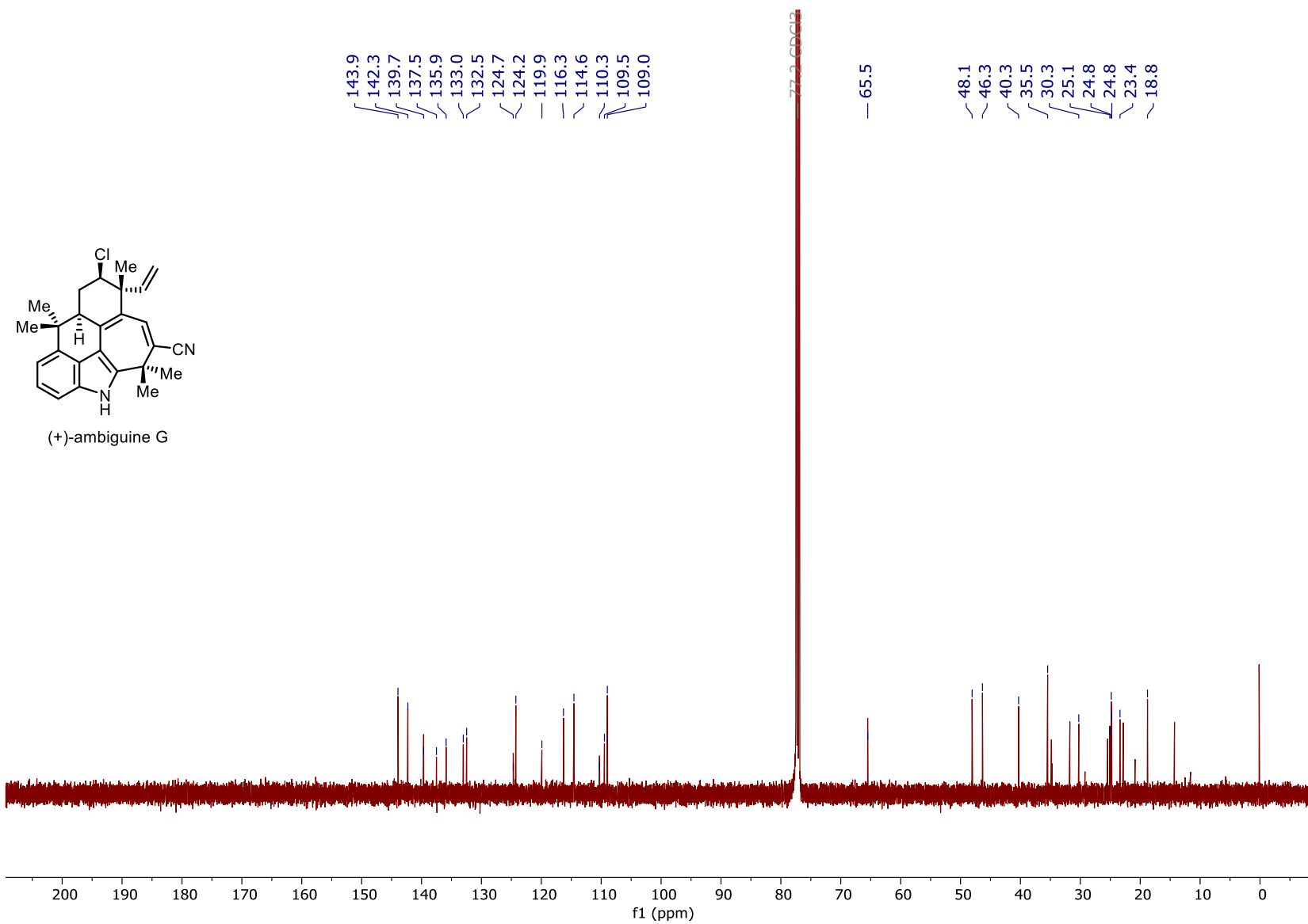


Figure 142. ^{13}C NMR spectrum of ambiguity G (125 MHz, CDCl_3).

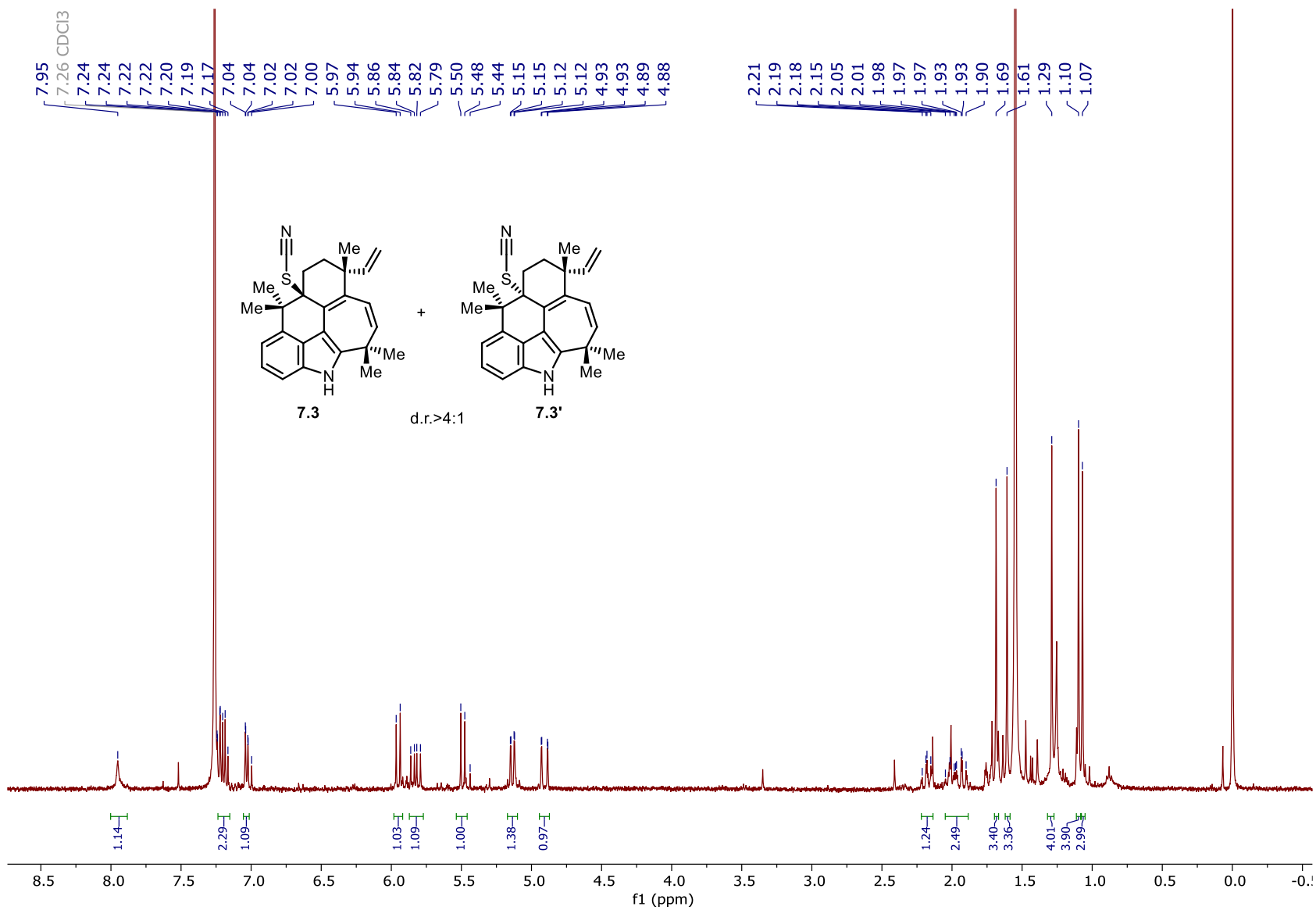


Figure 143. ^1H NMR spectrum of **7.3** (400 MHz, CDCl_3).

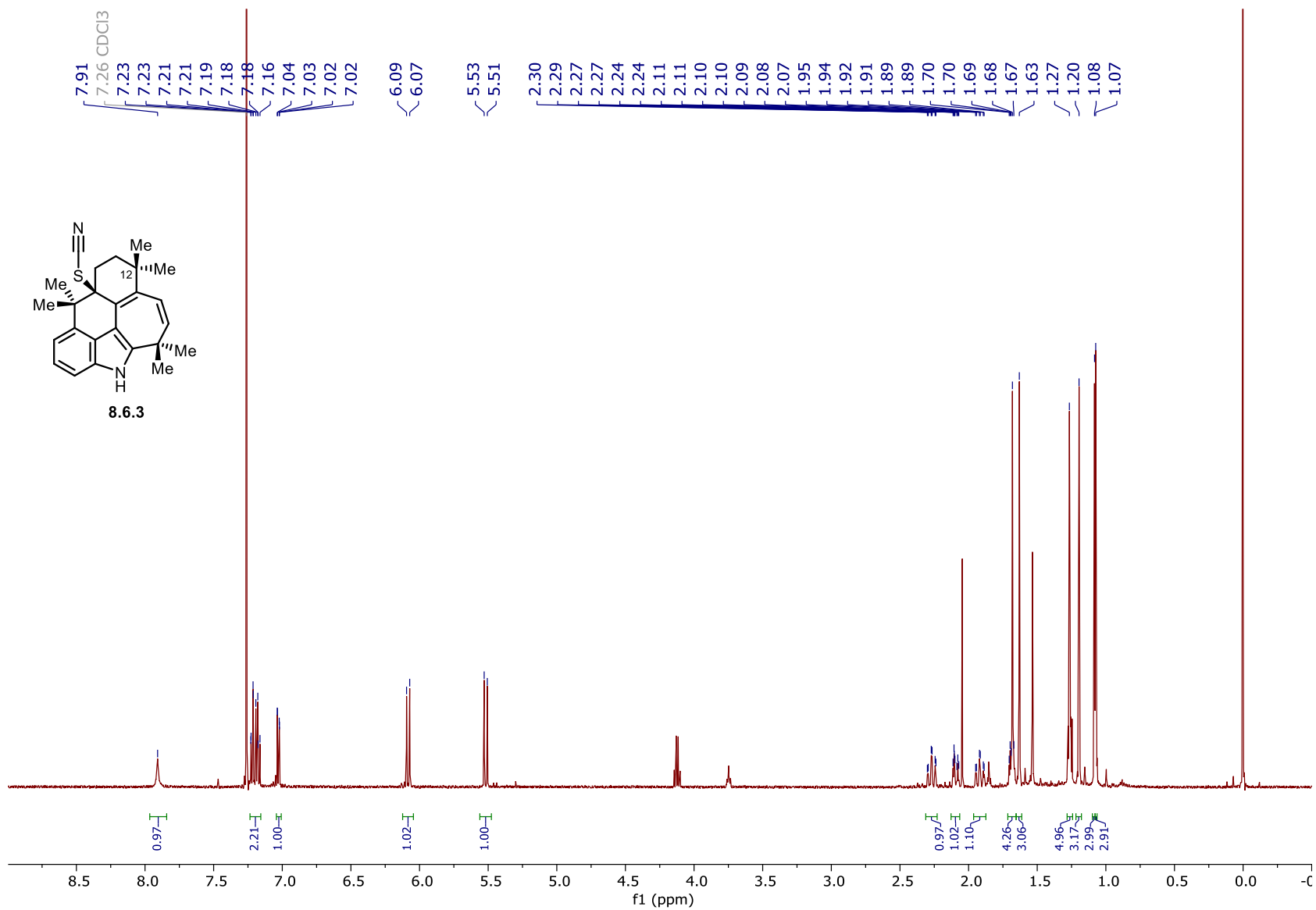


Figure 144. ^1H NMR spectrum of **8.6.3** (500 MHz, CDCl_3).

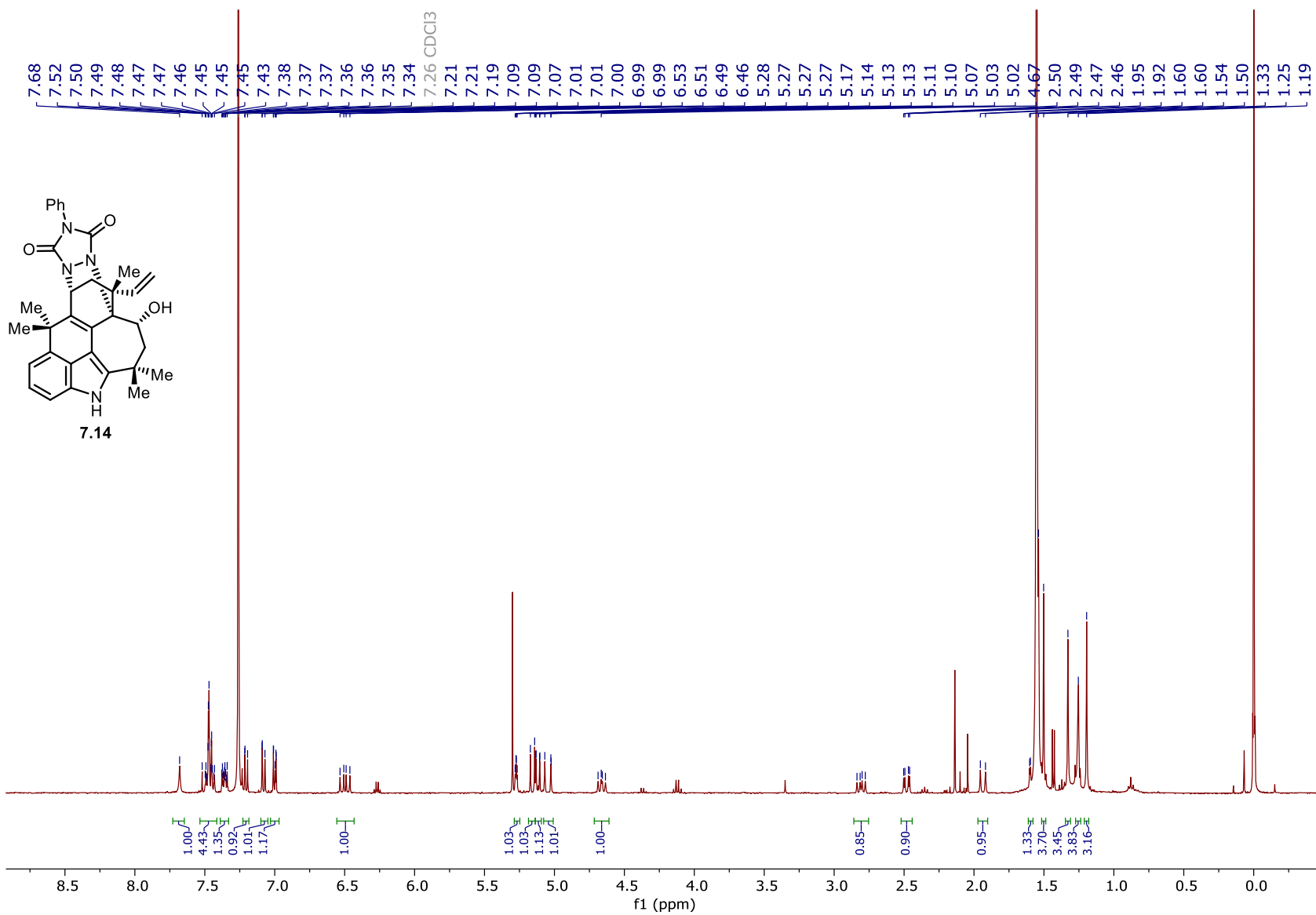


Figure 145. ^1H NMR spectrum of **7.14** (400 MHz, CDCl_3).

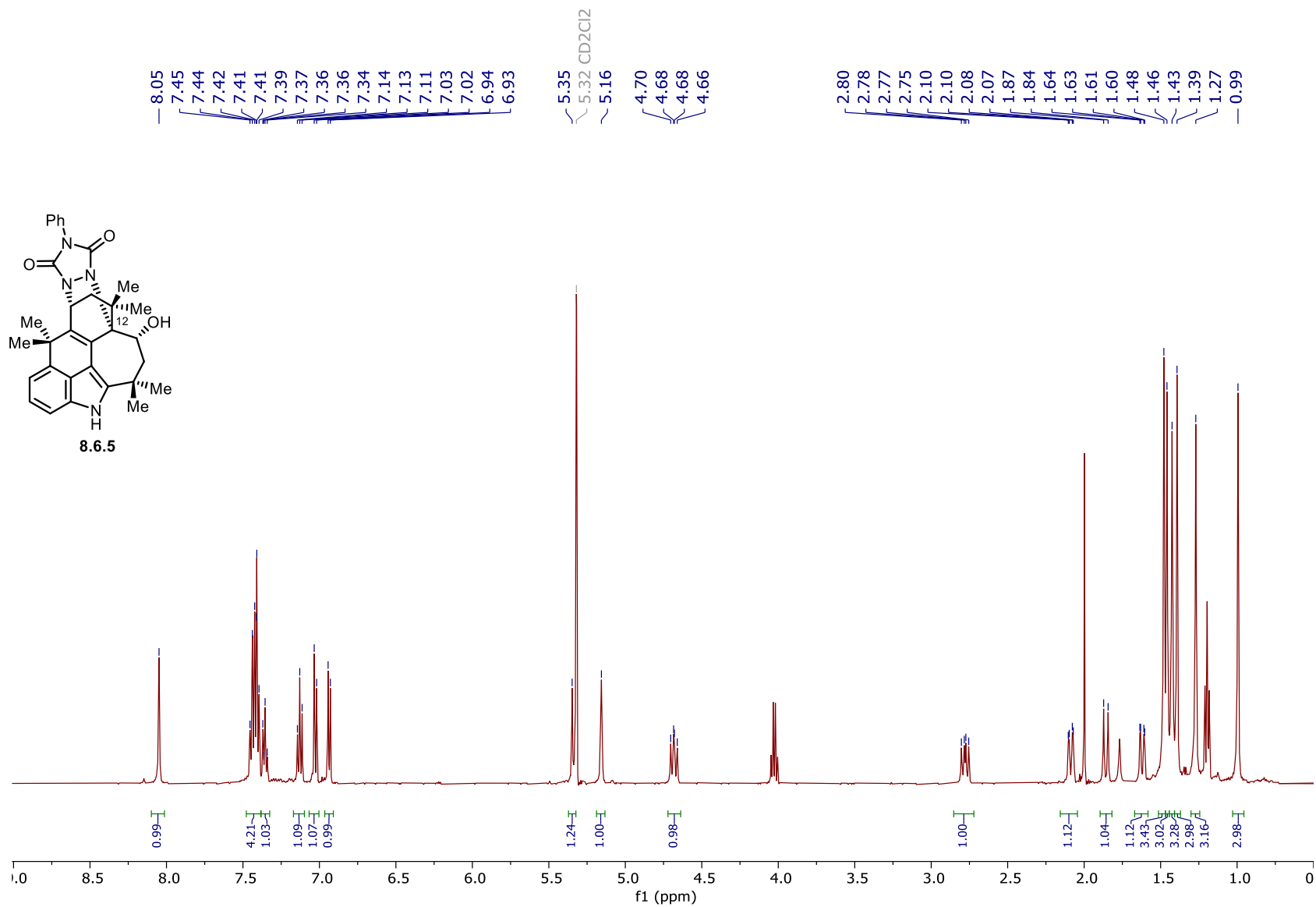


Figure 146. ¹H NMR spectrum of **8.6.5** (500 MHz, CD₂Cl₂).

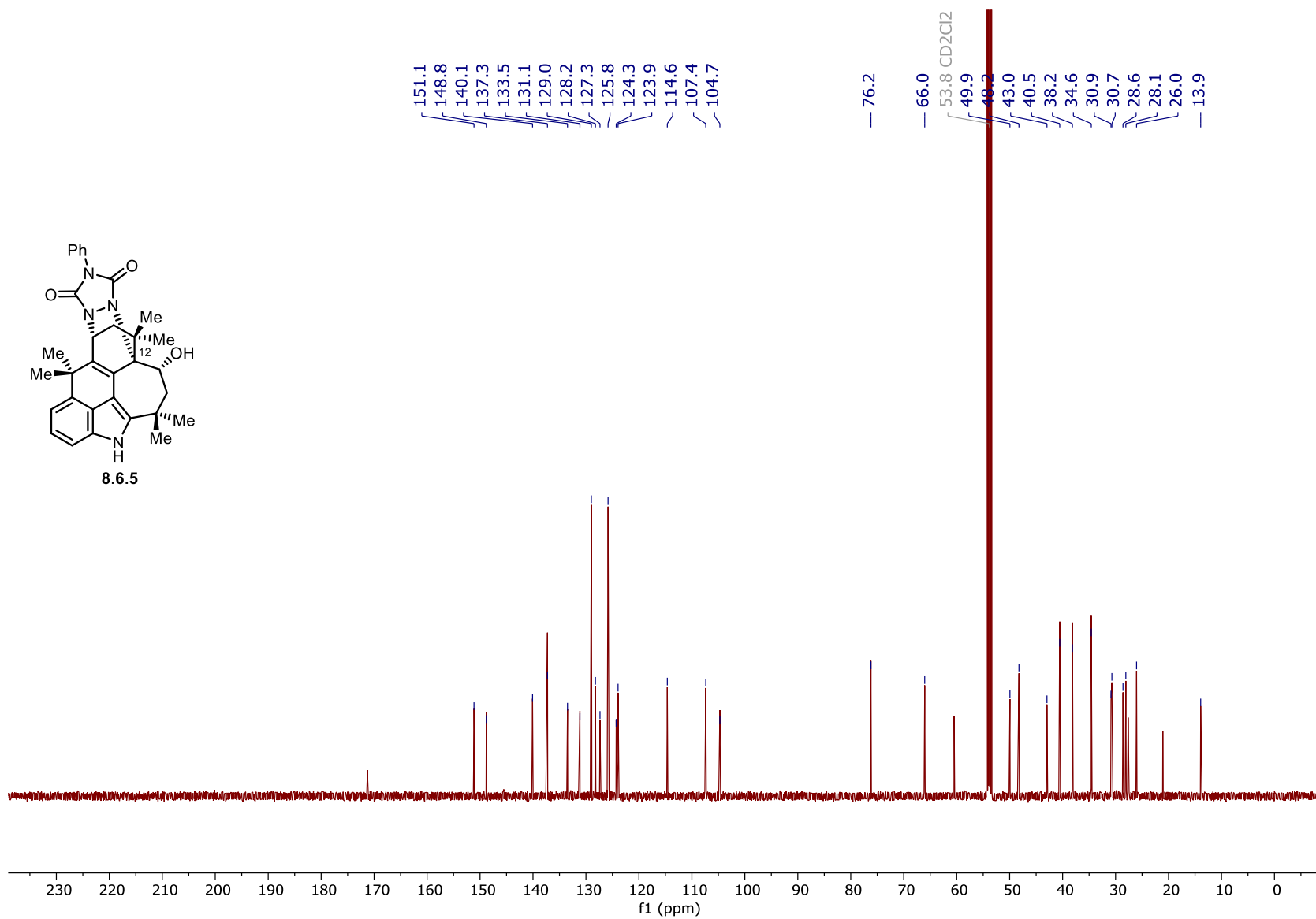


Figure 147. ^{13}C NMR spectrum of **8.6.5** (125 MHz, CD_2Cl_2).

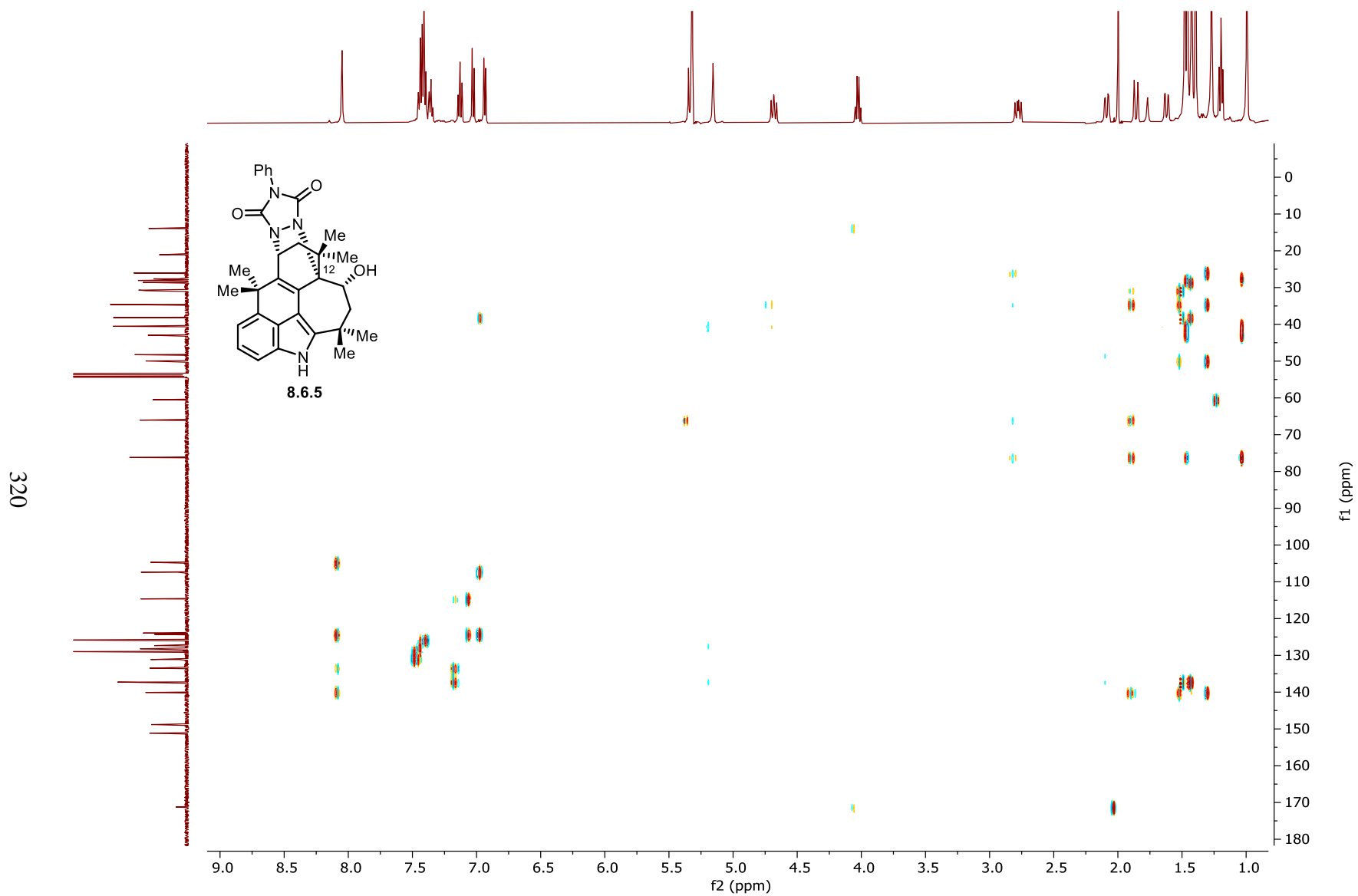


Figure 148. HMBC spectrum of **8.6.5** (CD₂Cl₂).

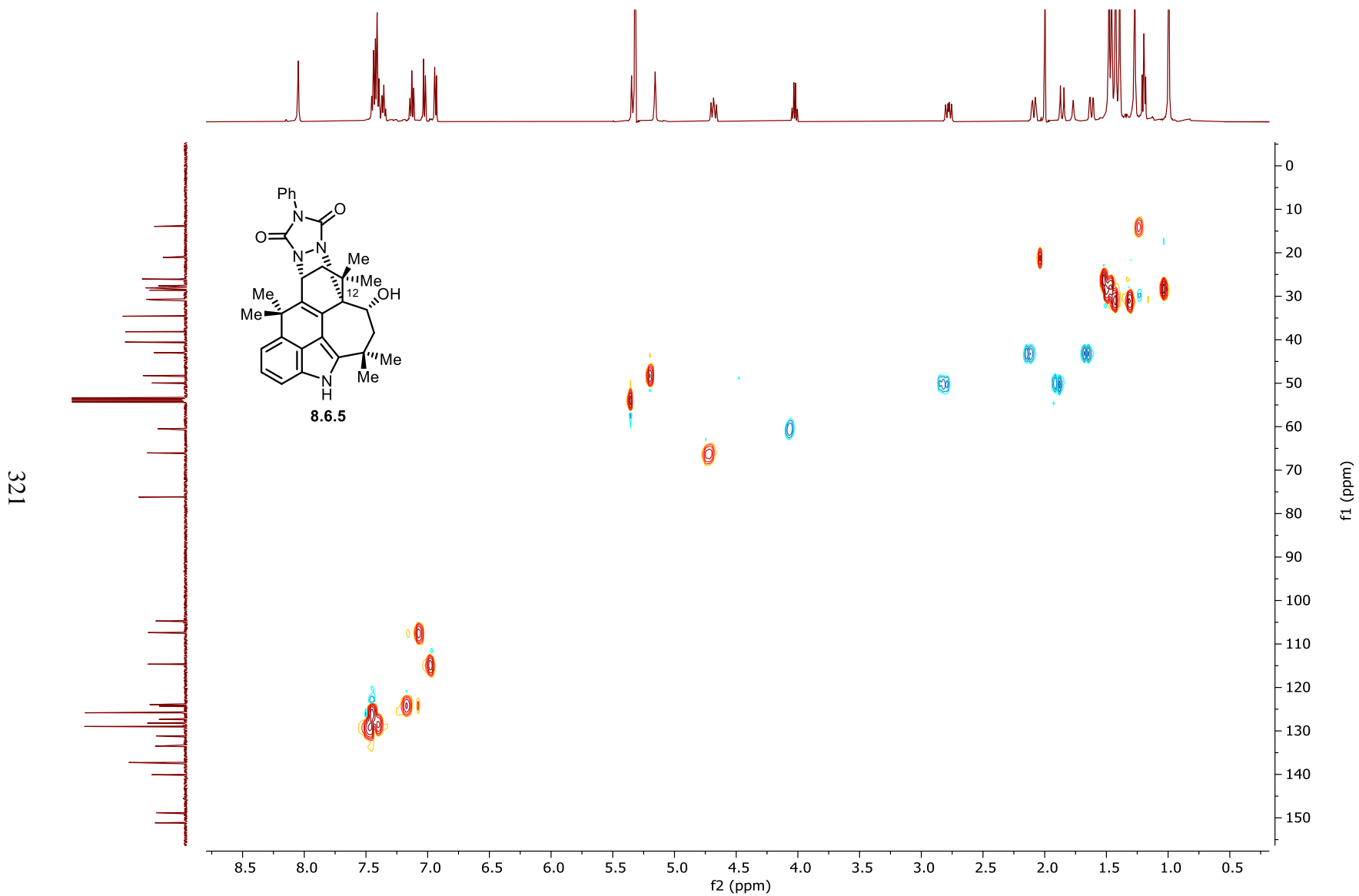


Figure 149. HSQC spectrum of **8.6.5** (CD_2Cl_2).

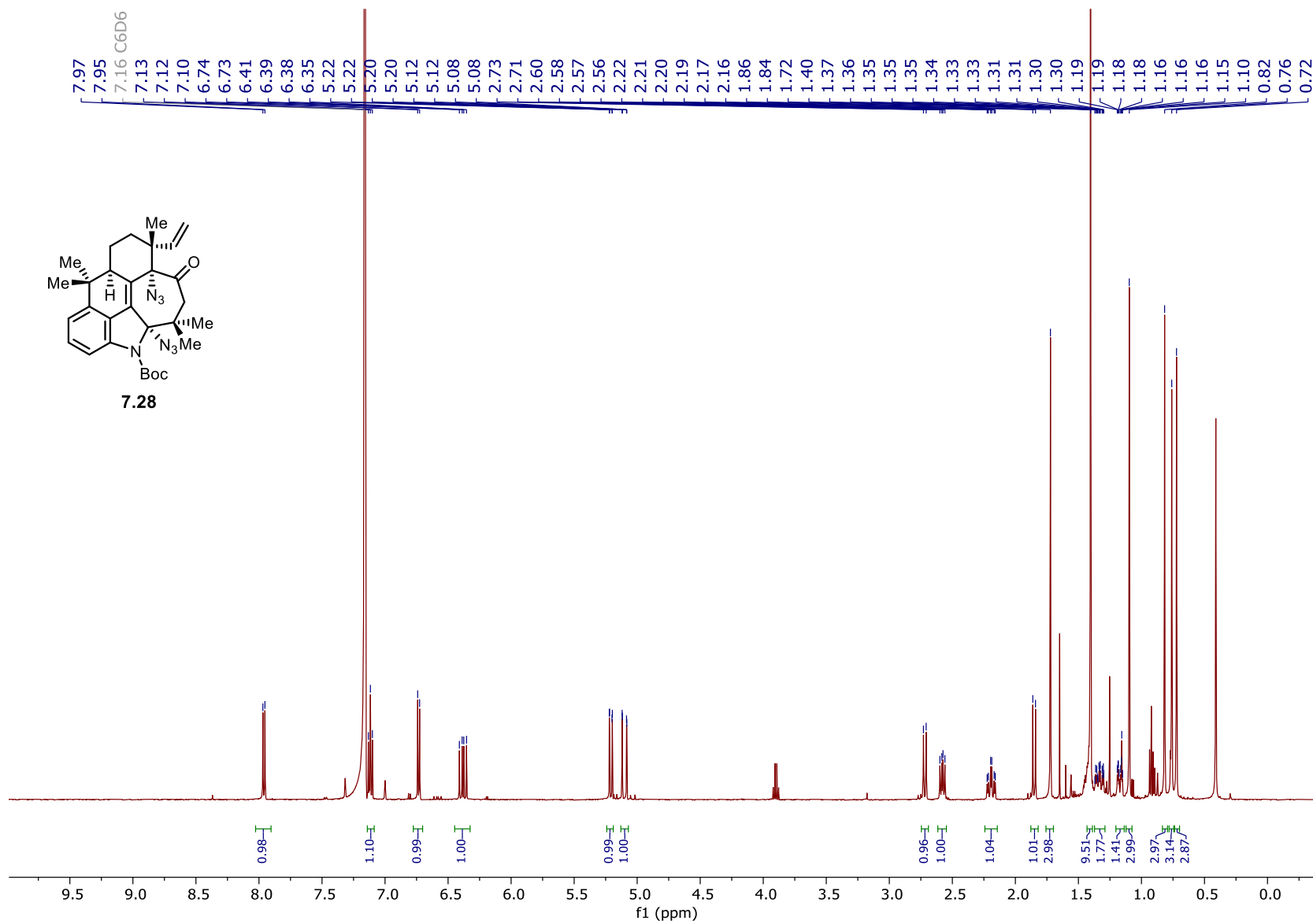


Figure 151. ^1H NMR spectrum of **7.28** (500 MHz, CDCl_3).

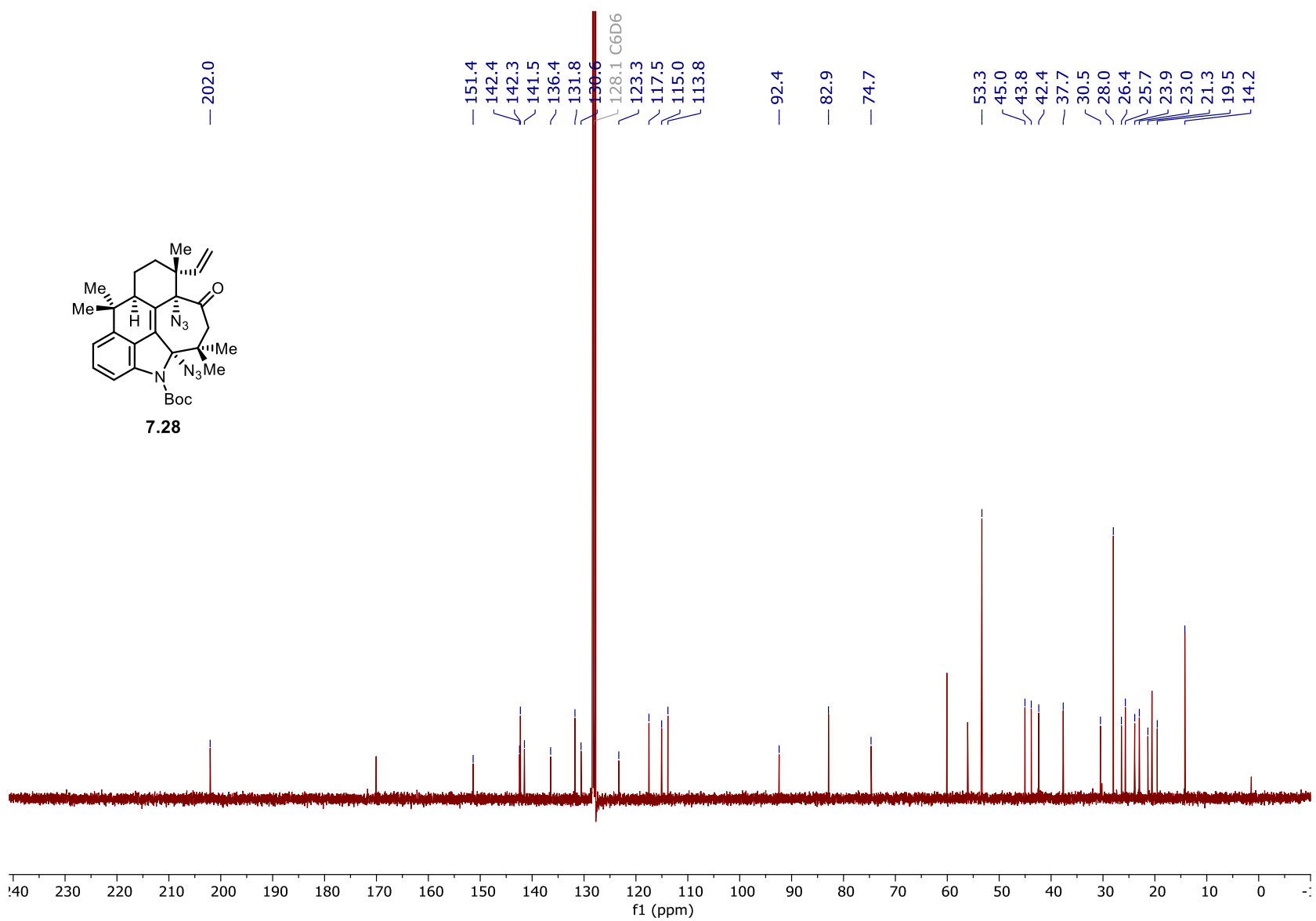


Figure 152. ^{13}C NMR spectrum of **7.28** (100 MHz, C_6D_6).

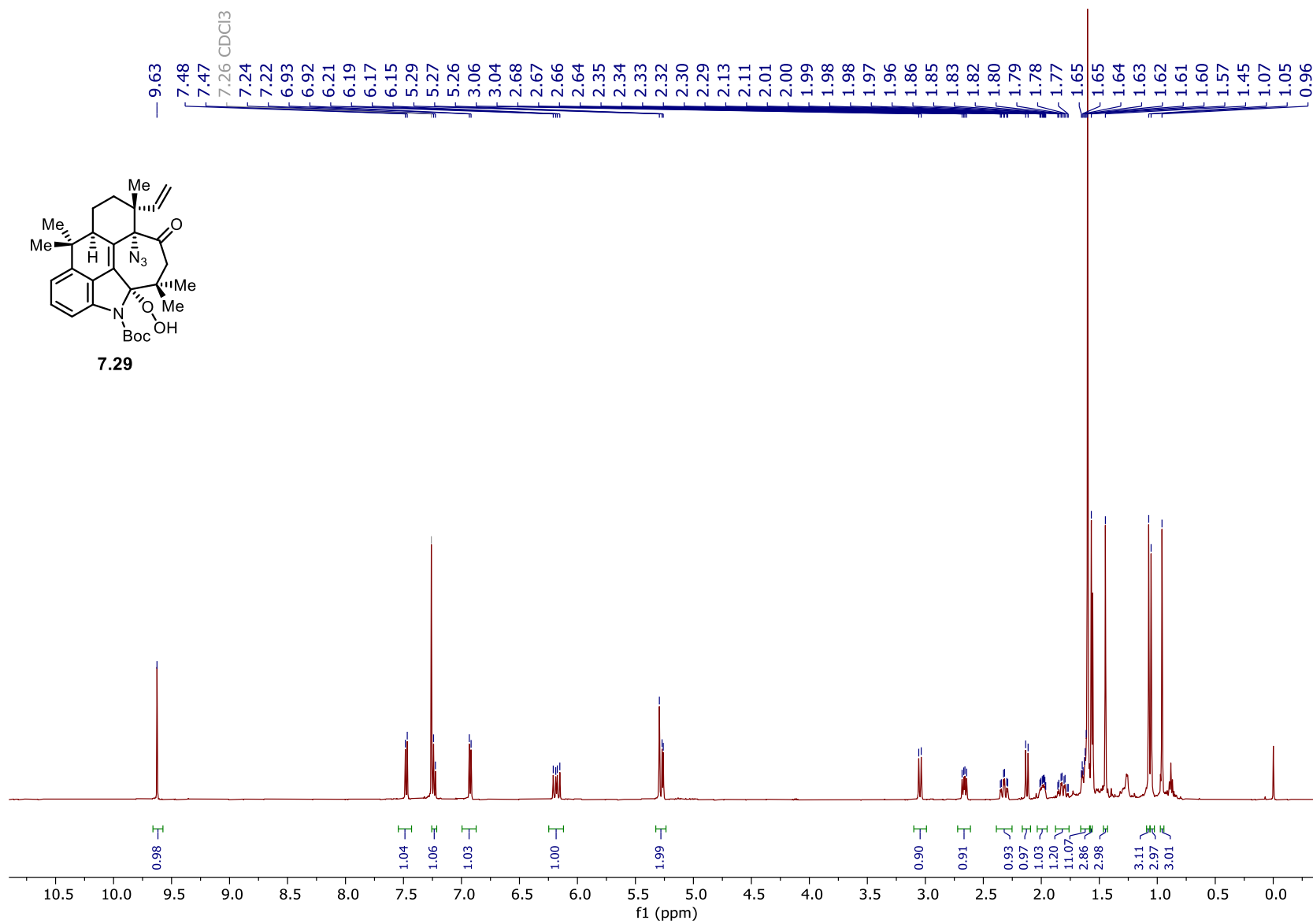


Figure 153. ^1H NMR spectrum of **7.29** (500 MHz, CDCl_3).

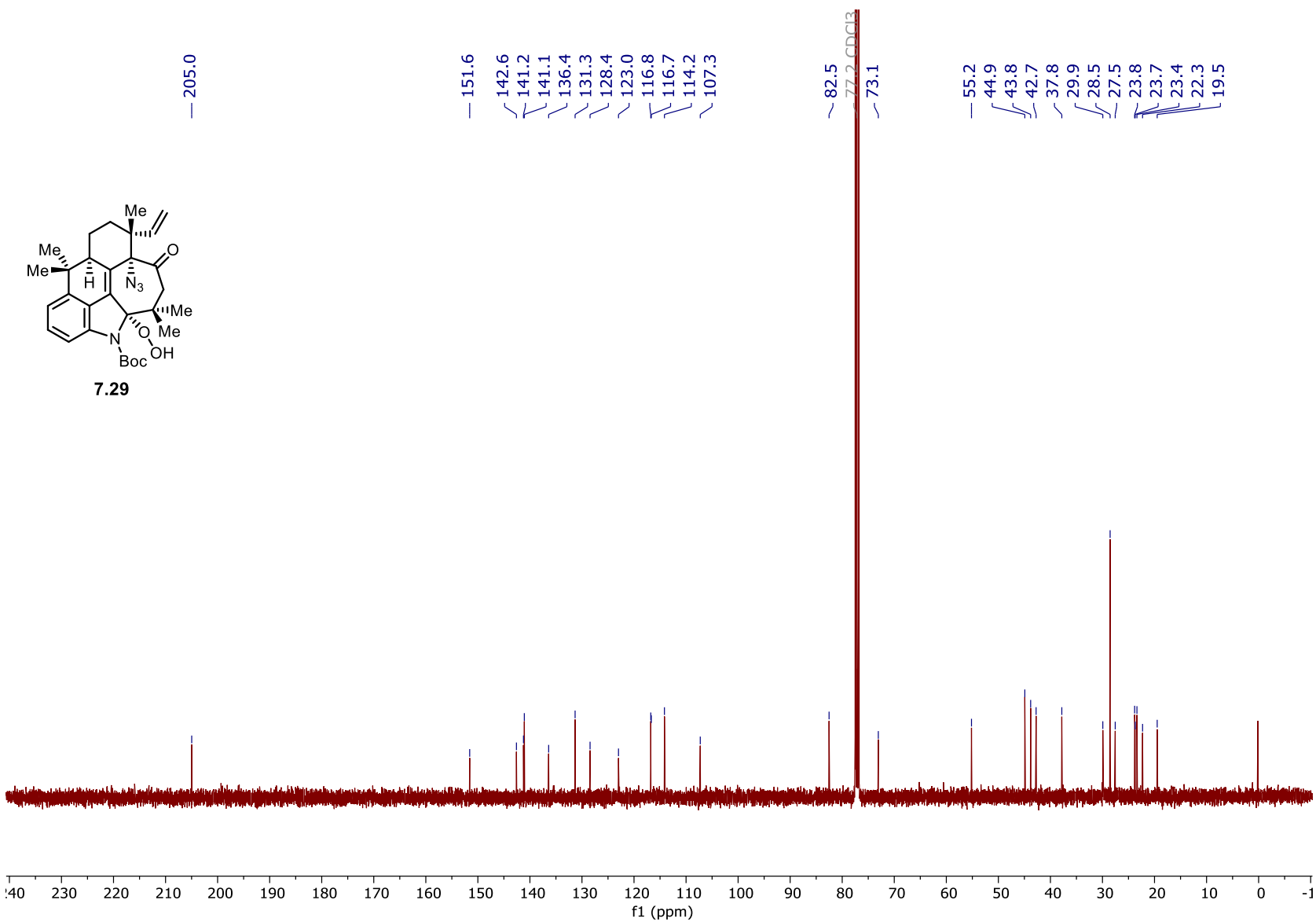


Figure 154. ^{13}C NMR spectrum of **7.29** (100 MHz, CDCl_3).

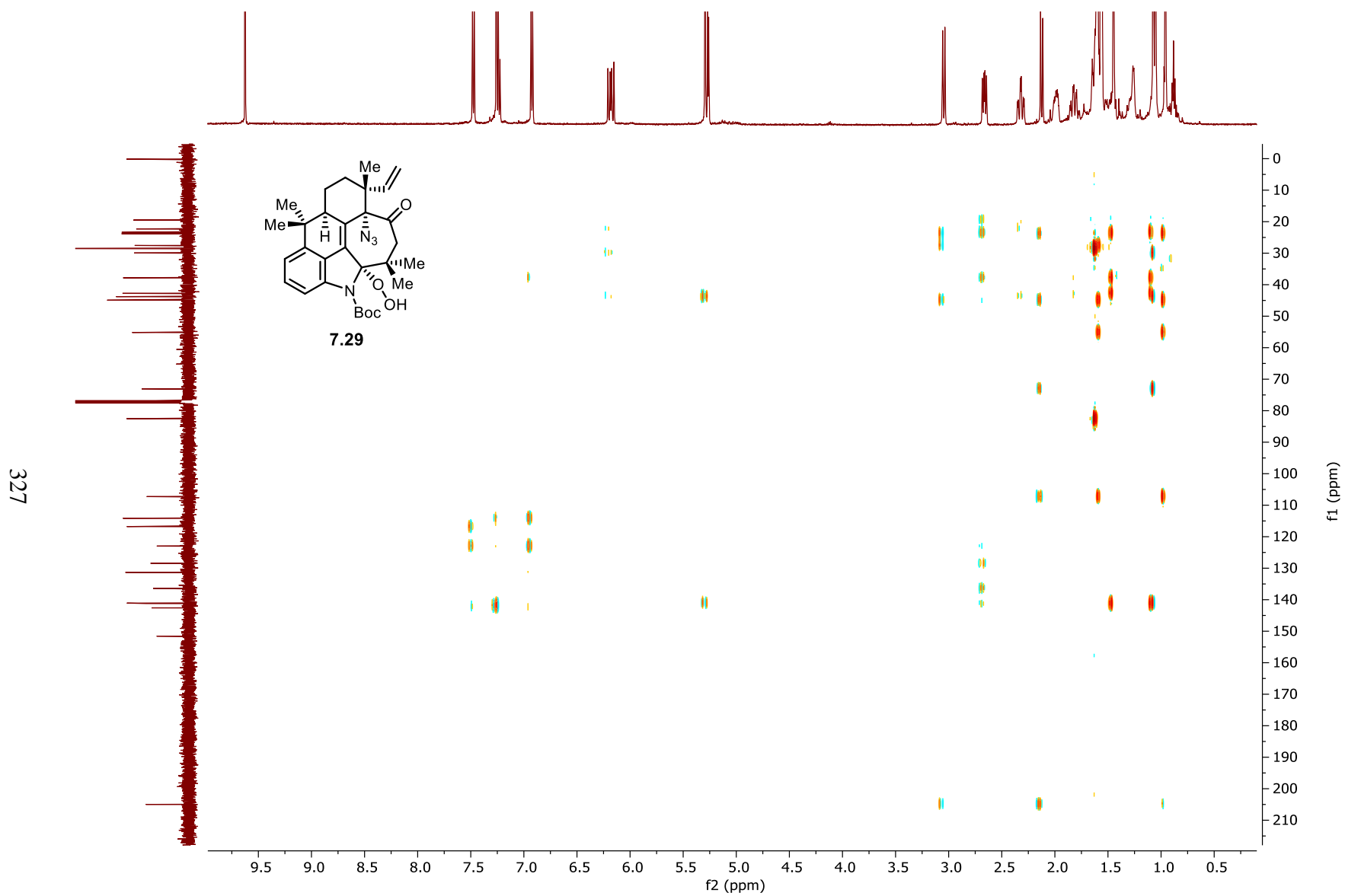


Figure 155. HMBC spectrum of **7.29** (CDCl₃).

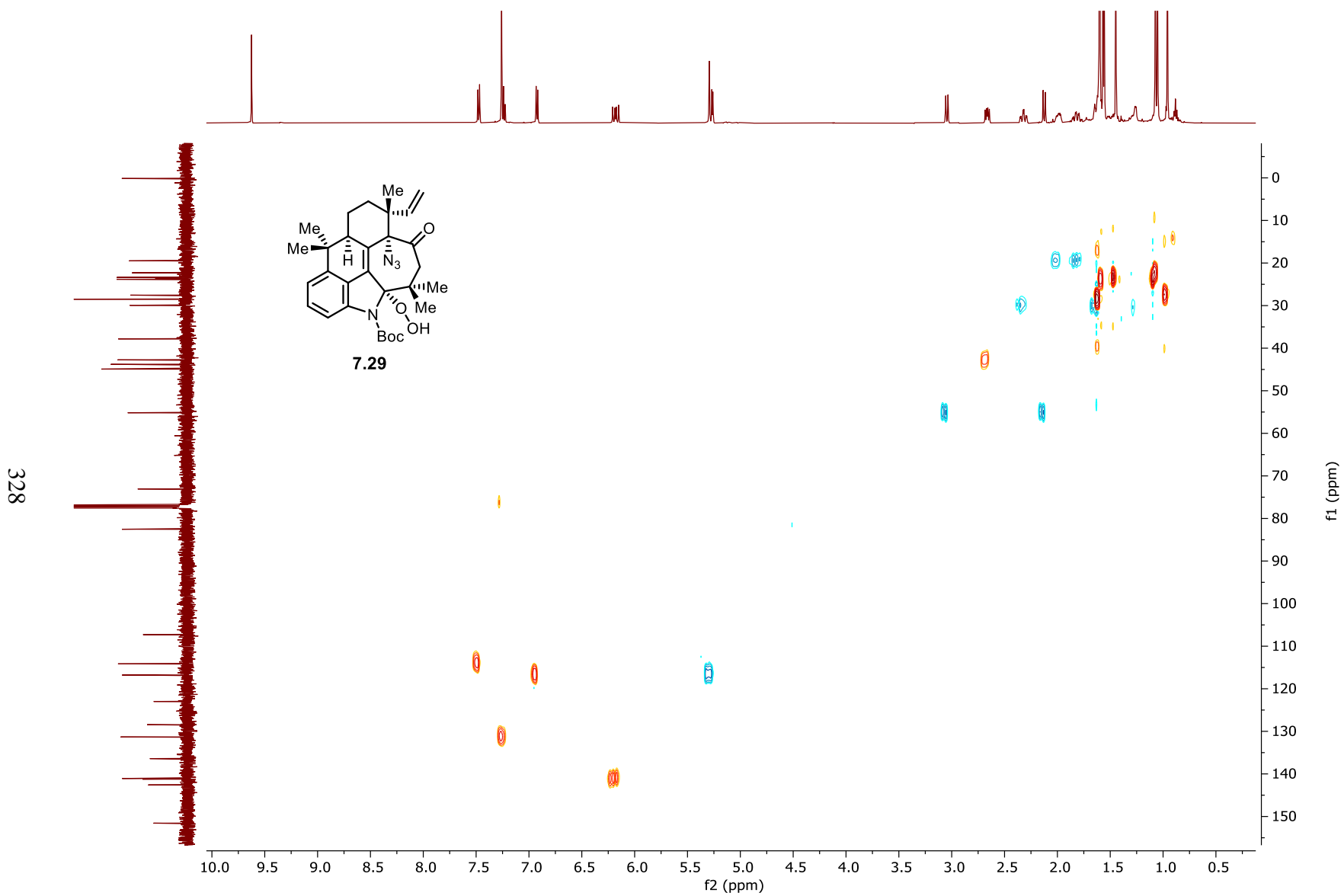


Figure 156. HSQC spectrum of **7.29** (CDCl_3).

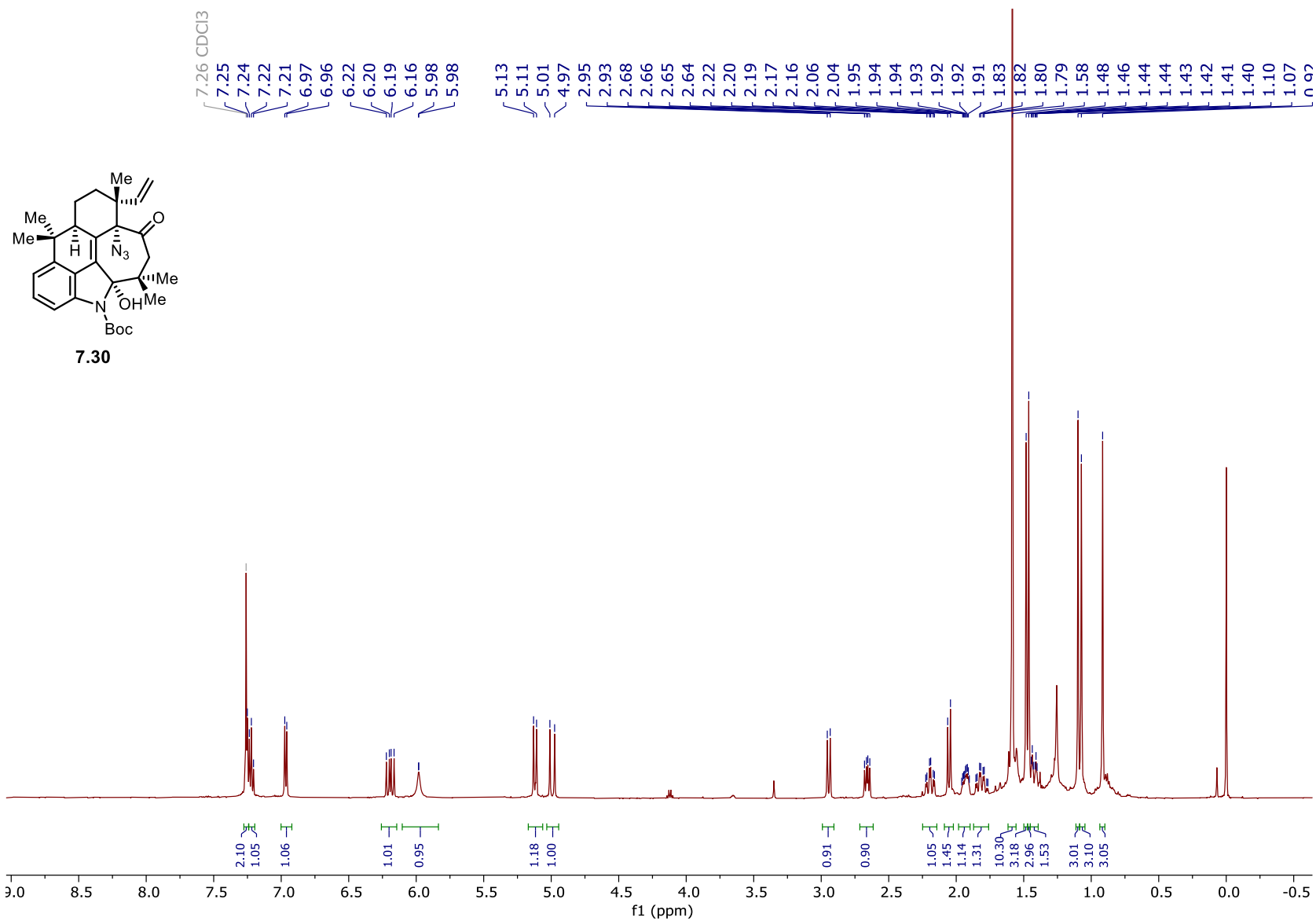


Figure 157. ¹H NMR spectrum of **7.30** (500 MHz, CDCl₃).

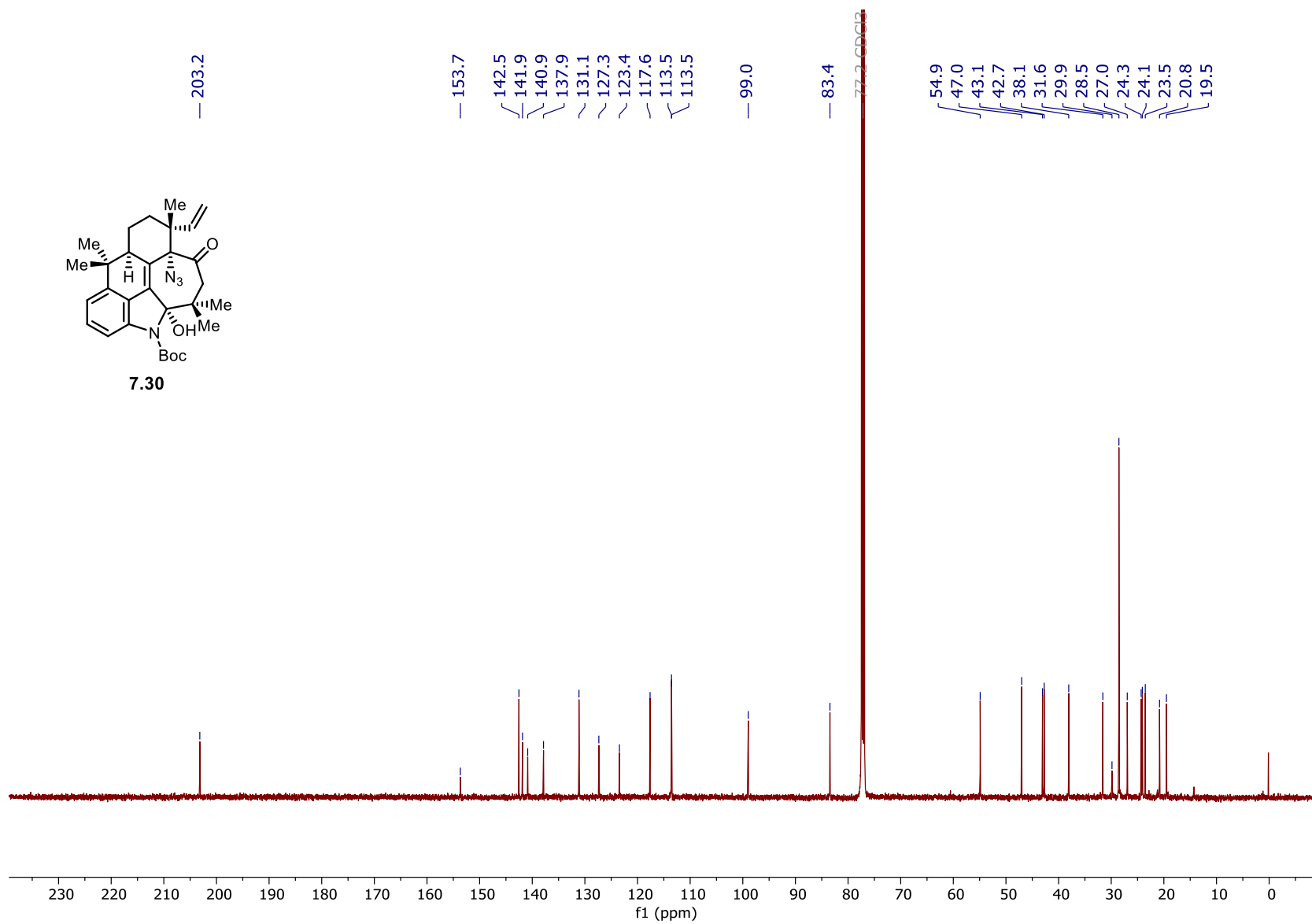


Figure 158. ^{13}C NMR spectrum of **7.30** (125 MHz, CDCl_3).

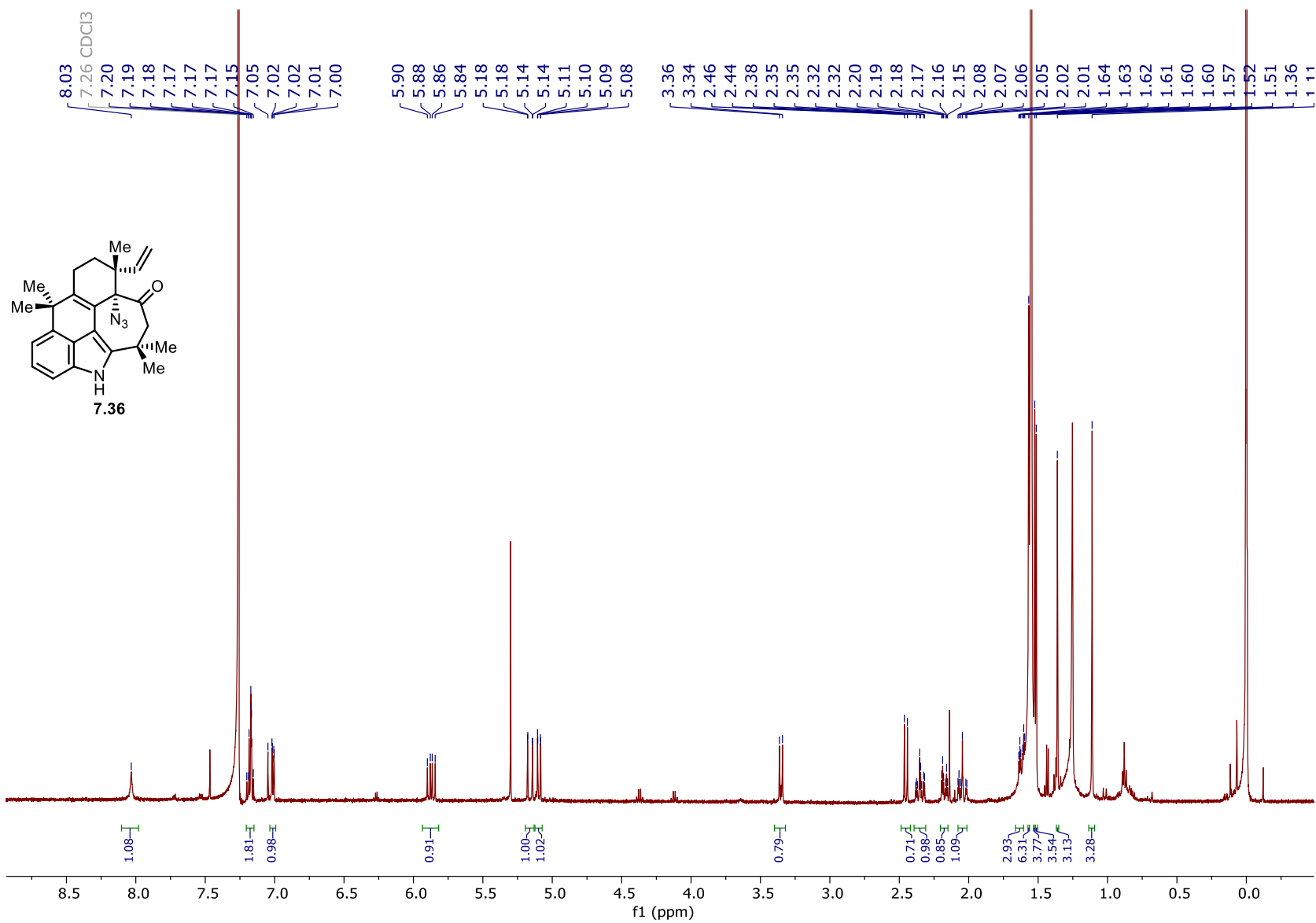


Figure 161. ¹H NMR spectrum of **7.36** (500 MHz, CDCl₃).